ISSN 0861-0509

Acta morphologica et anthropologica (13)

13 • Sofia • 2008
Institute of Experimental Morphology and Anthropology with Museum
Bulgarian Anatomical Society

Contents

Anthropology

Institute of Experimental Morphology and Anthropology with Museum
Bulgarian Anatomical Society

Acta morphologica et anthropologica, 13
Sofia • 2008

EDITORIAL

The 2nd Koprivshtitsa Morphological Days and the 6th National Conference of Anthropology, both with international participation, was held on June 2-4 2006 in Koprivshtitsa town. Organizers of the scientific forum were the Institute of Experimental Morphology and Anthropology at the Bulgarian Academy of Sciences, the Bulgarian Anthropological Society, and the Bulgarian Anatomical Society, and actively supported by the Koprivshtitsa municipality.

The scientific meeting was devoted to the 130th Anniversary of the April Rebellion in 1876 and was led under the patronage of Acad. Ivan Yuhnovski - President of the Bulgarian Academy of Sciences.

More than 130 scientists from Bulgaria, Germany, Russia, Holland and Turkey participated in the conference, 55 reports and 76 posters were presented in the halls of the Koprivshtitsa municipality building.

The conference was opened by the corresponding member Prof. Dr. Yordan Yardanov, Head of the Institute of Experimental Morphology and Anthropology at the Bulgarian Academy of Sciences, President of the Bulgarian Anthropological Society and Bulgarian Anatomical Society.

A welcome address to the participants was delivered by the Mayor of Koprivshtitsa - Mr. Nikola Kamenarov, who honored Prof. Dr. Vassil Vassilev - the Honorary President of the Bulgarian Anatomical Society and Prof. Dr. Yardan Yordanov with Koprivshtitsa Badge of Honour.

On the behalf of the foreign scientists were delivered welcoming speeches by Prof. R. Mesut, Prof. R. Leiser and Prof. E. Godina.

In pursuance of the scientific program had taken part colleagues from the Departments of Anatomy, Histology and Embryology in the Medical Universities, from the Departments, named identically, in the Medical and Veterinary Faculties, Institutes at the Bulgarian Academy of Sciences, the Departments of Biology in the Medical Universities, as well as colleagues from related Departments in Sofia University "St. Kliment Ohridski" and Plovdiv University "Paisii Hilendarski".

The scientific debates and discussions of the reports and posters, as well as, the ideas concerning national scientific projects and such ones with international participation were hold out following the academician and collegial style.

Institute of Experimental Morphology and Anthropology with Museum
Bulgarian Anatomical Society

Acta morphologica et anthropologica, 13
Sofia • 2008

The Role of Gonadal Steroids in Determining Sexual Differences in Expression of C-Fos-Related Antigens in the Rat Striatum

A. Bozhilova-Pastirova, B. Landzhov, L. Malinova, A. Ilieva, W Ovtscharoff

Department of Anatomy and Histology, Medical University, Sofia

Expression the the proto-oncogene product, c-fos protein was studied in the dorsal striatum of male and female rats during postnatal development at 20 and 60 days of age. Morphometric analysis revealed sexual dimorphism in the density of c-fos-immunoreactive neurons in 20-day-old prepubertal and 60-day-old pubertal rats. Females showed higher amounts of c-fos-positive neurons than males. The present results suggest that sex differences in the number of c-fos-positive neurons in the rat dorsal striatum may be related to epigenetic effects of gonadal hormones in pre- and pubertal periods of postnatal development.

Key words: c-fos, dorsal striatum, prepubertal and pubertal age, sex differences, rat.

Introduction

Both age and gender were recognized as factors influencing CNS structure and function [10]. Puberty is the attainment of fertility, a process encompassing morphological, physiological and behavioural development [2]. This dynamic period is characterized by marked changes in the activity and connectivity of the brain [9]. On the other hand, the ability of the variety of physiological [3] and pharmacological stimuli to increase neuronal expression of protooncogene c-fos has led to the suggestion that it might serve as a marker of neuronal reactivity [6]. In the light of the above data, the purpose of the present study was to examine the density of c-fos-immunoreactive neurons in dorsal striatum during the postnatal development in male and female rats.

Material and Methods

We used 6 female and 6 male Sprague-Dawley rats to study the c-fos immunoreactivity in the striatum. Male and female rats were sampled over two nested periods, 20 and 60 days of age, representing prepubertal and pubertal age groups, respectively. Animals were anaesthetized with Thiopental (40 mg/kg b. w.). Transcardial perfusion was done with 4% paraformaldehyde in 0.1 M phosphate buffer, pH 7.2. Coronal

sections were cut on a freezing microtome (Reichert-Jung) at 40 μm. Sections were incubated in polyclonal primary antibody to c-fos (1:1000 in PBS with 0.3% Triton X-100; Santa Cruz Biotechnology, Santa Cruz, CA) for 24 hs. The sections were then incubated for 1h at room temperature in biotinylated anti-rabbit IgG secondary antibody (1:400 in 0.4% TX-PBS; Vector), washed in PBS, and incubated in ABC solution (1:100 in 0.4% TX-PBS; Vectastain Elite, Vector) for 1h. The sections were finally washed in Tris buffer 0.05 M, pH 7.6, and then immersed in 0.03% 3,3'-diaminobenzidine tetrahydrochloride and 0.003% H_2O_2 to visualize the reaction product.

Morphometric analysis was performed using a microanalysis system (primary magnification 40 ´ objective). Data of the entire drawings were entered in the computer program (Olympus CUE-2), recorded automatically and calculated. Data from males and females were compared by Student's t-test. All values are presented as means ± standard error of the mean (S.E.M.).

Results and Discussion

The principal findings in the present study were as follows. First, c-fos-immunohistochemistry allowed us to determine the specific distribution pattern of reactive neurons (positive cells were identified as those expressing a black nuclear reaction product). The outlines of measures for the density of c-fos-immunoreactive neurons and contours were performing using the computer-assisted program. The average number of c-fos-immunoreactive neurons of 20 days old male and female rats was measured and compared with the same measures of the 60 day old rats (Fig. 1).

Second, our data provide the evidence that there are sex differences in the density of c-fos-immunoreactive neurons of the rat striatum at 20 and 60 days of age. Females have greater density of c-fos-immunoreactive neurons than males in all parts in the dorsal striatum (Fig. 1). There is the greater but not significant expression of c-fos protein in the striatum of pubertal female and male than of that of prepubertal males and female (Fig. 1).

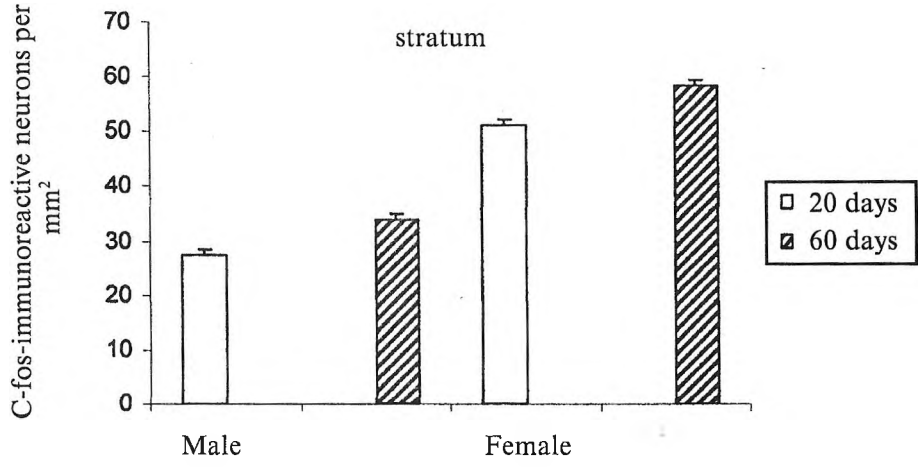

Fig. 1. The number of c-fos-immunoreactive neurons in the dorsal striatum of 20 days and 60 days old male and female rats, $p<0.01$. Values are presented as means ± S.E.M.

These results suggest that sex differences in the density of c-fos-immunoreactive neurons in the dorsal striatum can be related to the epigenetic action of gonadal hormones during the pre-pubertal and pubertal stages of the development. This conclusion corresponds to results that reported such correlation between androgens and expression of different neuroactive substances in various brain regions [1, 2, 4, 5, 7, 8]. However, the exact mechanism, by which sex differences in c-fos-immunoreactivity are settled during the pre- and pubertal development, remains an intriguing question. Our new data emphasize the need to examine the c-fos-immunoreactivity in sectors of the striatum at different days of ages and after experimental manipulations of the hormonal environment.

Acknowledgments. This work was supported by the Council for Science, Medical University, Sofia project (project 46/2005). The authors are grateful to Mrs. D. Brazitsova for her help with computer-assisted measures.

Referenses

1. D'Souza, D.N, R. E. Harlan, M. M. Garcia. Sexually dimorphic effects of morphine and MK-801: sex steroid-dependent and-independent mechanisms. — J. Appl. Physiol., **92**, 2002, 493-503.
2. Ebling, F.J. The neuroendocrine timing of puberty. — Reproduction, **129**, 2005, 675-683.
3. Insel, T. R. Regional induction of c-fos-like protein in rat brain after estradiol administration. — Endocrinology, **126**, 19901849-1853.
4. Ovtscharoff, W., A. Bozhilova-Pastirova, T. Christova. Postnatal development of neurons expressing NADPH-diaphorase and parvalbumin in the parietal cortex of male and female rats. — Acta Histochem., **104**, 2002, 23-28.
5. Polston, E. K., G. Gu, R. Simerly. Neurons in the principal nucleus of the bed nuclei of the stria terminalis provide a sexually dimorphic GABAergic input to the anteroventral periventricular nucleus of the hypothalamus. — Neuroscience, **123**, 2004, 793-803.
6. Robertson, G. S., J.G. Pfaus, L. J., Atkinson, H. Matsumura, A. G. Phillips, H.C. Fibiger. Sexual behavior increases c-fos expression in the forebrain of the male rat. — Brain Res., **564**, 1991,352-357.
7. Stefanova N., A. Bozhilova-Pastirova, W. Ovtscharoff. Sex and age differences of neurons expressing GABA-immunoreactivity in the rat bed nucleus of the stria terminalis. — Int. J. Dev. Neurosci., **16**, 1998, 443-448.
8. Stefanova, N., W. Ovtscharoff. Sexual dimorphism of the bed nucleus of the stria terminalis and the amygdala. Adv. Anat. Embryol. — Cell Biol., **158**, 2000, 1-78.
9. Viau, V., B. Bingham, J. Davis, P. Lee, M. Wong. Gender and puberty interact on the stress-induced activation of parvocellular neurosecretory neurons and corticotropin-releasing hormone messenger ribonucleic acid expression in the rat. — Endocrinology, **146**, 2005,137-146.
10. Zubieta, J. K., R. F. Dannals, J. J. Frost. Gender and age influences on human brain μm-opioid receptor binding measured by PET. — Am. J. Psychiatry, **156**, 1999, 842-848.

Institute of Experimental Morphology and Anthropology with Museum
Bulgarian Anatomical Society

Acta morphologica et anthropologica, 13
Sofia • 2008

Diaphorase Activity Expression in Dissociated Cortical Cultures from Mouse Embryos

A. Dandov, N. Lazarov

Department of Anatomy, Medical Faculty, Thracian University, Stara Zagora

The free radical nitric oxide (NO) is involved in neuromodulation and present in many species. NO has a short life and a high diffusion coefficient, and is generated by NO synthase (NOS). It is interesting when in the ontogenesis NO first appears. We set it as a goal to investigate NO in embryonic neurons in vitro. We established cortical cultures from seventeen-day-old (E-17) mouse brains. On the sixth day the cultures were processed for investigating the NOS marker, nicotinamide adenine dinucleotide phosphate diaphorase (NADPH-d). Our results demonstrated that NADPH-d reactivity is present in many embryonic cortical neurons and is distributed in the perikarya and neurites. A background reaction in the neuroglial cells is also observed. It can be inferred that NO begins its action early in the ontogenesis by its own synthesis. Further investigation is to find out when NO appears in the mouse cortex and what factors activate NOS.

Key words: cortical culture, diaphorase, histochemistry, mouse embryo, nitric oxide synthase.

Introduction

The free radical nitric oxide (NO) is a neural messenger involved in neuromodulation, and present across a large number of animal phyla. Its significance as an important chemical mediator has become apparent only since 1980, when it was first described by Furchgott, and demands a considerable readjustment of our views about neurotransmission and neuromodulation [5]. NO has an important modulatory role on the processing of sensory signals in vertebrates and invertebrates. It has been implicated in the control of neuronal development and of synaptic plasticity in the central nervous system, as well as in appetite and nociception [1, 3, 4].

NO is a molecule with a short life span and a very high diffusion coefficient that readily traverses cell membranes, and thus spreads rapidly around its site of origin. It is generated by the enzyme NO synthase (NOS) from L-arginine, and neurons containing NOS have been found to exist in both vertebrates and invertebrates.

It is still a matter of considerable interest when and where in the ontogenesis NO comes into the group of an already large cast of neurotransmitters and/or modulators. Therefore, in order to answer at least partly this question, we set it as a goal of

this study to investigate the presence of NO in embryonic neurons in a nerve cell culture. To do so, we applied NADPH-diaphorase (NADPH-d) histochemistry, with NADPH-d acting as a marker for NOS. It is very well known now that NADPH-d activity is often used as a marker of NOS localization and this activity has been shown to correspond with the distribution of NOS in nervous systems of both vertebrates and invertebrates.

Materials and Methods

For the present study we used eight seventeen-day-old embryonic (E17) mouse brains, from which were established primary dissociated cortical neuronal cultures. All the procedures described were performed in a laminar flow hood. After a routine dissection of the cortexes, they were thoroughly minced and trypsinized in a 10 ml solution of 2x trypsin-EDTA (Gibco BRL) for exactly 15 min at 37°C in a water bath. The trypsinization process was discontinued by adding 3 ml fetal calf serum (FCS) (Gibco BRL) in 17 ml PBS. The cell preparation was then passed through a fine meshwork (50 μm large pores) to obtain mostly separate cells and further centrifuged at 1.500 rt. for 9 min. The pellets were then gathered in Fischer's medium (for reference cf. 6) containing 5% FCS, re-stirred, and the cell numbers and viability prior to establishing the cultures were assessed using 0.4% Trypan Blue stain (Gibco BRL) and standard hemocytometer counting [6]. The cultures were seeded in ten four-well manufacturer's dishes, preliminarily coated with poly-L-lysine (Sigma Chemicals Co, St. Louis, Mo., USA) and after a starvation period of 24 h, the whole medium was changed and the cultures were then fed on Fischer's modified medium containing 5% FCS on an "every other day" routine. All the cultures were grown in an incubator supplied with 95% air and 5% CO_2.

On the sixth day the cultures were processed for investigating the NOS histochemical marker, NADPH-d. In brief, the cultures were fixed in refrigerated 4% paraformaldehyde, permeabilized in TBS containing 0.3% Triton X-100, and then incubated in a staining solution containing β-NADPH, nitroblue tetrazolium (NBT) and 0.3% Triton X-100 in TBS for 30-60 min at 37°C until the reaction had developed satisfactorily. The cultures were observed under an inverted microscope, photographed with a digital camera, and the images were further processed with the PhotoShop software computer program

Results

Our results clearly demonstrated that NADPH-d reactivity is present in a large population of embryonic cortical neurons, with no intracellular preference. NADPH-d reactivity is well distributed in both the perikarya and the neuritis (Fig. 1). We also observed a steady background histochemical reaction in the neuroglial cells, although in a somewhat weaker manner (Fig. 2).

Discussion

This study focuses on the expression of NOS and its histochemical marker, NADPH-d, in primary dissociated cell cultures from mouse embryonic brains. Our results comply with these obtained by other authors, who also investigated diaphorase ac-

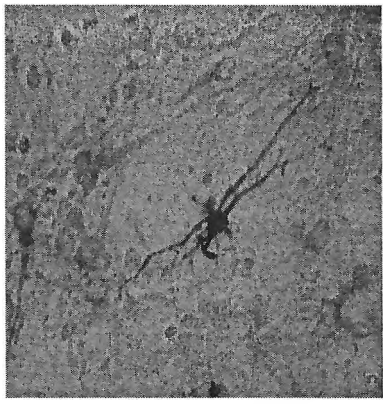

Fig. 1. NADPH-d histochemical reaction in a solitary cortical neuron. The perikaryon and the neuritis are well marked. × 100

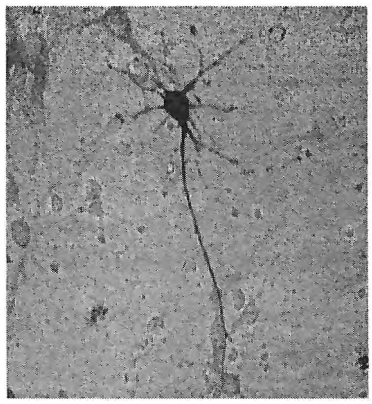

Fig. 2. In the photomicrograph, a steady backdround reaction can be observed against a definitely marked neuron. × 100

tivity in cell culture models [2]. First and foremost, we were able adequately to apply the method of diaphorase histochemistry to neuronal culture models to demonstrate such an expression. From the obtained results it can be inferred that NO begins exerting its neuromodulatory action early in the ontogenesis, at that not through diaplacentar diffusion but via its own proper synthesis in the investigated cells in an *in vitro* situation. NO has been implicated in the control of neuronal development and of synaptic plasticity in the central nervous system, as well as in appetite and nociception, and it is very much possible that it starts exerting its functional impacts rather early in the ontogenesis and facilitates the synaptic development and intercellular communication both in the living embryo and the *in vitro* models. It is still a matter of further investigation to find out at what point precisely NO and its synthesizing enzymes first appear in the mouse cortex *in utero* and what factor activates the genes encoding the expression of NOS.

References

1. Bombardi, C, A. Grandis, R. Chiocchetti, M. L. Lucchi. Distribution of calbindin-D28k, neuronal nitric oxide synthase, and nicotinamide adenine dinucleotide phosphate diaphorase (NADPH-d) in the lateral nucleus of the sheep amygdaloid complex. — Anat. Embryol. (Berl), **211**, 2006, 707-720.
2. Hon, W M, V. J. Chhatwal, H. E. Khoo, S. M. Moochhala. Histochemical method for detecting nitric oxide synthase activity in cell cultures. — Biotech. Histochem., **72**, 1997, 29-32.
3. Fallah, Z. Nicotinamide adenine dinucleotide phosphate-diaphorase (NADPH-d) activity and CB-28kDa immunoreactivity in spinal neurons of neonatal rats after a peripheral nerve lesion. — Iranian Biomed. J., **9**, 2005, 103-110.
4. Chang, H. M., U. I. Wu, T. B. Lin, C. T. Lan, W. C. Chien, W. L. Huang, J. Y. Shieh. Total sleep deprivation inhibits the neuronal nitric oxide synthase and cytochrome oxidase reactivities in the nodose ganglion of adult rats. — J. Anat., **209**, 2006, 239-250.
5. Furchgott, R.F. Endothelium-derived relaxing factor: discovery, early studies, and identification as nitric oxide. — Biosci. Rep., **19**, 1999, 235-251.
6. Schilling, K, M. H. Dickinson, J. A. Connor, J. I. Morgan. Electrical activity in cerebellar cultures determines Purkinjie cell dendritic growth patterns. — Neuron, **7**, 1991, 891-902.

Institute of Experimental Morphology and Anthropology with Museum
Bulgarian Anatomical Society

Acta morphologica et anthropologica, 13
Sofia • 2008

Direct Projections from the Mesencephalic Trigeminal Neurons to the Trigeminal Motoneurons and Interneurons in the Rat

M. Draganov, D. Itzev, N. Lazarov

Department of Anatomy, Faculty of Medicine, Trakia University, Stara Zagora
**Institute of Physiology, Bulgarian Academy of Sciences, Sofia*

The afferent projections of the mesencephalic trigeminal nucleus (MTN), which is a unique structure in the CNS and composed of primary sensory neurons, are well known although the efferent projections still remain unclarified and controversial. Descending projections from the MTN were studied using biotinylated dextran amine as an anterograde tracer. The tracer was injected under pressure unilaterally into the pontine part of the nucleus. The anterograde tracing experiments show the presence of direct projections from mesencephalic trigeminal neurons, located in the caudal part of the MTN, to the motor trigeminal nucleus and to interneurons of the supratrigeminal, intertrigeminal and juxtatrigeminal areas. Our results show that through all these projections the mandibular movement is facilitated.

Key words: mesencephalic trigeminal nucleus, trigeminal motoneurons, anterograde tracing, biotinylated dextran amine, rat.

Introduction

The mesencephalic trigeminal nucleus (MTN) is a unique structure in the CNS, composed of primary sensory neurons. At the pontine level, MTN neurons are situated in the triangle between the locus coeruleus and the medial parabrachial nucleus. At the level of the mesencephalon they border laterally the central periaqeductal gray. Mesencephalic trigeminal neurons innervate the jaw-closing muscles, periodontal ligament and a subset of the extraocular muscles [1]. While the MTN afferent projections in the rat are well studied, little is known about the afferent connections of the nucleus with other brain regions. The presence of direct projections from the MTN to the motoneurons, located in the motor trigeminal nucleus (MoTN) has been studied by different researchers using various tracing techniques [3, 5]. It has been demonstrated that projecting fibers reach the supratigeminal nucleus [2], and also the intertrigeminal and juxtatrigeminal areas [6].

The aim of this study is to describe the efferent projections of mesencephalic trigeminal neurons to the trigeminal motoneurons and interneurons in the rat. After

injecting biotinylated dextran amine (BDA) into the caudal part of the MTN it is possible to follow intensely marked axons from the MTN neuronal perykaria to their peripheral target areas.

Material and Methods

Ten adult Wistar rats of both sexes weighing 280-350 g were used for this study. The animals were anesthetized with Thiopental (Biochemie, GmbH, Kundl, Austria; 25mg/kg b.w.) and then mounted in a stereotaxic frame. Under aseptic conditions small craniotomies were performed. The location of the injection site was precised to the following coordinates according to the rat brain stereotaxic atlas of P a x i n o s and W a t s o n [4]: 0.68 mm posterior to the interaural line and 1.4 mm lateral to the midline. A 10% solution of BDA (m.w. 10,000; Molecular Probes Europe BV, Leiden, The Netherlands) dissolved in phosphate buffer (PB; 0,1M, pH 7.2) was injected under pressure unilaterally with a Hamilton microsyringe (Hamilton Co, Reno, Nevada, USA), while the contralateral side remained intact to serve as a control. At the end of injecting, the microsyringe was held in place for 2 min to insure that the injected BDA had been absorbed into the tissue. Following 6-8 days of survival, the animals were perfused transcardially, first with 100 ml of 0.9 % saline, followed by 400 ml of 4% paraformaldehyde in PB (Merck, Darmstadt, Germany).

The brains were quickly removed and then placed into the same fixative at 4°C for 4 hours. Frozen sections (40 μm of thickness) were prepared on a freezing microtome Cryocut E (Reichert — Jung, Austria) and collected in PB in a free-floating state. The sections were reacted by using the avidin-biotin complex (Vectastain ABC Kit, Vector Laboratories Inc., Burlingame, USA) in PB and then the peroxidase activity was developed in 0,05 M Tris-HCl buffer, pH 7,6 containing 0,012% 3,3 diaminobenzidine tetrahydrochloride (DAB; Sigma) and 0,01% H_2O_2 for up to 15 min. All the sections were mounted onto gelatin-coated glass slides, air-dried and counterstained with Cresylviolet. The slides were viewed with a Zeiss Axioplan 2 light microscope and photographed with an Axiocam MRc digital camera.

Results

After leaving the MTN a bundle of well-marked fibers goes ventrolaterally to the region, situated above the MoTN, called supratrigeminal nucleus, where intensely labeled axons are clearly observed. The fibers pass in the vicinity of the somata of trigeminal interneurons located here (Fig. 1). In the MoTN well marked fibers are seen, spread in its dorsolateral portion, whose collaterals are in direct contacts with the perikarya of large-sized trigeminal motoneurons (Fig. 2). Intensely labelled fibers and terminals are also found in the ipsilateral juxtatrigeminal area, situated below the ventral pole of the MoTN. Furthermore, marked fibers reach the intertrigeminal region, located between the MoTN and the principal trigeminal nucleus.

To verify these projections, we injected BDA in the MoTN and were able to see that all mesencephalic trigeminal neurons along the whole rostrocaudal length of the MTN were labeled. This projection is invariably unilateral (Fig. 3).

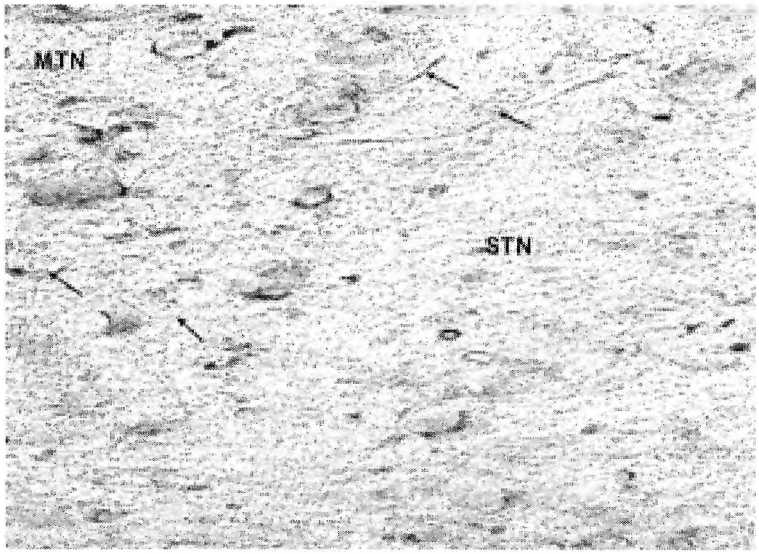

Fig. 1. Microphotograph illustrating the labeled projection fibers (arrows), passing through the supratrigeminal nucleus (STN). × 160

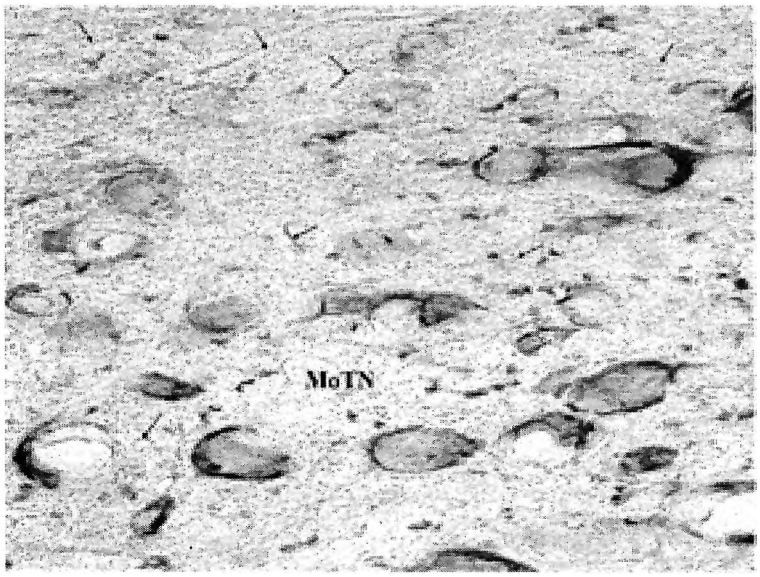

Fig. 2. Anterogradely BDA-labeled fibers (arrows) traveling toward large-sized perikarya in the motor trigeminal nucleus (MoTN). × 400

Discussion

Our results clearly show the presence of a direct projection from the MTN to the MoTN, especially to its dorsolateral part. This portion of the latter is known to contain the cell bodies of motor neurons innervating masticatory and suprahyioid muscles.

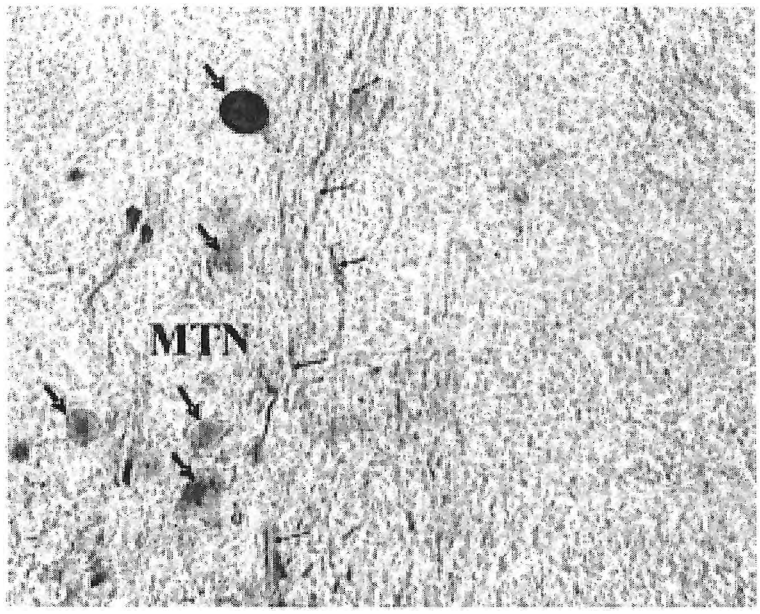

Fig. 3. Retrogradely labeled cell bodies (large arrows) and fibers (small arrows) in the MTN after injecting BDA into the motor trigeminal nucleus. × 400

The masticatory muscle spindle afferents send, via the central axons of the mesencephalic trigeminal neurons, their projections to jaw-closing motoneurons located in the MoTN. In this study we were able to observe numerous intensely labelled projection fibers to the dorsolateral part of the MoTN, where the majority of jaw-closing motoneurons are located. These data correlate well with previous studies, which confirm the presence of labelled fibers also in the supratrigeminal nucleus [3, 5]. It can be inferred from our findings that mesencephalic trigeminal neurons, supplying the jaw-closing muscles, may during mastication activate supratrigeminal neurons, which in turn inhibit trigeminal motoneurons innervating the masticatory muscles.

References

1. Alvarado-Mallart, M. R., C. Batini, C. Buisseret-Delmas, J. Corvizier. Trigeminal representations of the masticatory and extraocular proprioceptors as revealed by horseradish peroxidase retrograde transport. — Exp. Brain Res, **23**, 1975, 167-179.
2. Lorente de Nó R. Contribución al conocimento del nervio trigémino. — In: Libro en Honor de DS Ramón y Cajal: *Trabajos Originales de sus Admiradores y Discipulos Estranjeros y Nacionales.* Madrid,Jaminez y Molina, 1922.
3. Matesz, C. Peripheral and central distribution of fibres of the mesencephalic trigeminal root in the rat. — Neurosci. Lett, **27**, 1981, 13-17.
4. Paxinos, G., C. Watson. The rat brain in stereotaxic coordinates, 4th ed. New York, Academic Press, 1998.
5. Raappana, P., J. Arvidsson. Location, morphology, and central projections of mesencephalic trigeminal neurons innervating rat masticatory muscles studied by axonal transport of choleragenoid-horseradish peroxidase. — J. Comp.Neurol, **328**, 1993, 103-114.
6. Shigenaga, Y., Y. Mitsuhiru, A. Yoshida, C. Qin Cao, H. Tsuru. Morphology of single mesencephalic trigeminal neurons innervating masseter muscle of the cat. — Brain Res, **445**, 1988, 392-399.

Institute of Experimental Morphology and Anthropology with Museum
Bulgarian Anatomical Society

Acta morphologica et anthropologica, 13
Sofia • 2008

Prion Neurodegeneration as Factor for Increasing of Astrocytosis and Microgliosis in CNS

D. Kadiysky, M. Svetoslavova, N. Sales, J.-Ph. Deslys**

Institute of Experimental Morphology and Anthropology with Museum, Bulgarian Academy of Sciences, Sofia
**Laboratoire de NeuroVirologie, Direction: Recherche Medicale, GIDTIP, Commissariat a l'Energie Atomique, Paris*

In order to investigate the cellular basis of gliosis accompanying prion pathology we have selected four zones in mammalian CNS (cortex, thalamus, hippocampus and cerebellum) providing a relatively simple access to the most affected by degeneration brain areas. The intensification of the cellular reactivity of brain cells is an important pathomorphological feature *in situ* contributing for prion disease diagnosis as neuronal loss and spongiosis. Immunohistochemical approaches using specific monoclonal antibodies V9 and 5D4 was performed. The examination of hamster brains affected by experimental scrapie (263K agent strain) was accomplished to determine the extent of the astrocytosis and microgliosis during degeneration. New non-conventional methods for visualizing of the glial reaction in CNS were applied.

Key words: central nervous system (CNS), prion neurodegeneration, astrocytosis, microgliosis.

Introduction

Prion neurodegeneration is result of transmissible, sporadic or hereditary conditions characterized by progressive nervous system dysfunction. Fatal prion diseases or transmissible spongiform encephalopaties (TSE) affect humans (Creutzfeldt-Jacob disease variants, fatal familial insomnia, Gerstmann-Straussler-Scheinker syndrome) and numerous other mammalian species ("mad cow" disease, scrapie, chronic wasting disease, spongiform encephalopathies in cat family etc.). In the course of prion diseases a long incubation period is followed by histopathological changes restricted in CNS. General histopathological signs in CNS during prion degeneration are spongiosis, gliosis or reaction of resident glia, neuronal death, appearance and concentration of pathologic isoform of prion protein (PrPres), and specific amyloid plaque formation.

The cellular reactivity in degenerating brain is registered by morphological methods as a decreasing (for neuronal population) or an increasing (for astroglia and microglia) in the number and density of the brain cells. Glial reaction during prion neurodegeneration has two different basic components: astrocytosis and microgliosis, united in the common neuromorphological phenomenon — *gliosis*.

Recently introduced in prion biology the vimentin immunoreactivity for astrocytes [5, 8] and keratan sulfate immunohistochemistry for ramified microglia [3] were used in this study for evaluation of the extent of gliosis and glial cell density in four brain levels during development of the experimental prion disease.

Material and Methods

Infection of animals: Adult 45-week-old female outbred golden Syrian hamsters were injected intracerebrally into the right hemisphere with 50 µl of 1% w/v brain homogenate from 263K scrapie strain ($2.2 \cdot 10^{11}$ 50% lethal dose/g). Anaesthetized hamsters (injected and controls) were sacrificed at 30^{th}, 70^{th} and 87^{th} days after agent inoculation (incubation period, florid and terminal stages of the prion encephalopathy). The brains were fixed in Carnoy's solution at room temperature overnight. Serial transversal sections 5-7 microns thick were obtained from selected levels using Leica paraffin microtome after embedding in paraffin.

Immunohistochemical localization of the astroglial reaction in CNS: Slides with transversal brain sections from selected regions (5-7 microns thick) were blocked for endogenous peroxidase (H_2O_2/methanol 1:60) and for non-specific IgG tissue binding (20% normal horse serum). Incubation with anti-vimentin monoclonal antibodies (Dako) clone V9 diluted 1:5000 for 24 hours at 4°C was performed the first day. As secondary antibody was used biotinilated anti mouse IgG (1:500 diluted) followed by application of ABC (Vector) kit and diaminobenzidine (DAB) substrate. Controls: whole immunostaining procedure without anti-vimentin antibodies and whole procedure using nonspecific second antibodies.

Visualization of the microglial reaction in CNS by keratan sulfate immunohistochemistry: Commercially available anti-keratan sulfate monoclonal antibodies 5D4 (Calbiochem-San Diego CA), clone5-D-4, isotype IgG1, k, were used for immunohistochemical procedure. Optimal working dilution of monoclonal antibodies was precised as 1:1000 for overnight incubation at 4°C. The next day a procedure, using PicTure Polymer Detection System — a horseradish peroxidase/Fab fragment polymer conjugate (ZYMED), was applied for 45 min at room temperature. DAB substrate kit for peroxidase (VECTOR) was used as diaminobenzidine chromogen source for 5-10 min. Controls: Whole immunostaining procedure without 5D4 mAb and whole procedure with diluted 1:1000 5D4 mAb in PBS containing 100 mg/ml type I and II keratan sulfate in the solution.

Studied CNS regions: cerebral cortex, hippocampus, cerebellum and thalamus.

Results

Immunodensitometric assay for vimentin immunoreactivity was made in the 4 selected regions of the affected by the prion neurodegeneration hamster CNS. In general, astrogliosis demonstrated by the vimentin re-expression during prion pathology is easier to estimate because vim (+) astroglia lacks in adult healthy brain (absolutely negative control!). During the earlier periods of development of prion degenerative disease (florid stage) astrogliosis estimated by the appearance of vim (+) cells is less intensive. It's important to note that during the florid stage of the prion disease scrapie 263K there is regional distribution of the groups of vim (+) astroglia in small foci of gliosis (Fig.1). The distribution of the vim (+) astrocytes in this period could

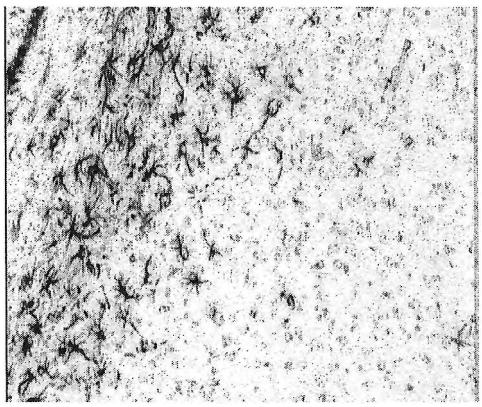

Fig. 1. Astrocytosis - regional distribution of the concentrated in small foci vim (+) astroglia. Thalamic area of affected by scrapie 263K hamster brain. Vimentin immunohistochemistry with *mAb V9.* × 100

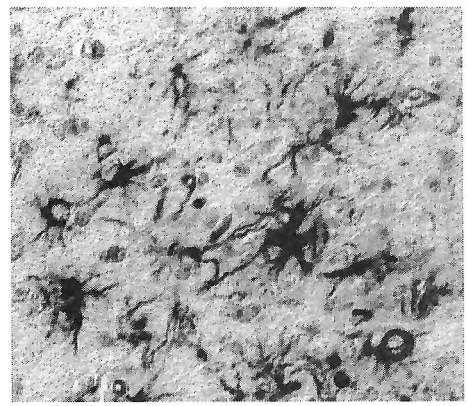

Fig. 2. Large areas of confluent vimentin positive cells during terminal stage of the prion neurodegeneration in hamster brain. × 480

be registered in thalamus, hippocampus and cortex. At 70th day post inoculation (dpi) of the scrapie agent many vim (+) cells were located in deep cortex layers but they were at the same time less prominent in medium layers. Astrocytic morphology of these cells is most evident especially in the cortex ant thalamus. There they had morphological traits of mature hypertrophic astrocytes. Between 70th and 87th dpi vimentin immunoreactivity in thalamus and hippocampus demonstrates 3-5-fold increase forming large areas of positive cells (Fig. 2). Starting from lacking of vim (+) cells in pre-clinic incubation stage (30th day after infection) a progressive increase of astrocytic reaction measured by vimentin immunoreactivity was demonstrated in studied brain areas.

Keratan sulfate immunohistochemical (KS-IHC) visualization of microglial reaction during prion degeneration is more demonstrative in comparison with conventionally used till now lectin methods. 5D4 (+) cells in hamster brain are abundant in cerebral cortex, hippocampus, thalamus and cerebellum of the scrapie-infected hamster brain. The course of the prion neurodegeneration checked by this microglial reactivity in 30th, 70th and 87th dpi changes microglial density in these regions (Fig. 3). A non-essential decrease of the cell density is registered during incubation stage (30th dpi). In the florid (70th day) and terminal (86th day after infection) disease stages we found an essential increase of the density of ramified type 5D4 (+) microglia in the cortex, thalamus, hippocampus and granular layer of the cerebellum. The most of the 5D4 (+) cells have big cell shapes respectively its branching morphology, numerous cytoplasmatic processes and ramified structure. The nuclei are prolonged and relatively small. The cytoplasm is moderately marked by the reaction product in contrast of the strongly positive to keratin sulfate nucleus. Microgliosis during degenerative changes in CNS (estimated by KS-IHC) is co-localized with another histhopathological sign of degeneration — spongiosis (Fig. 4).

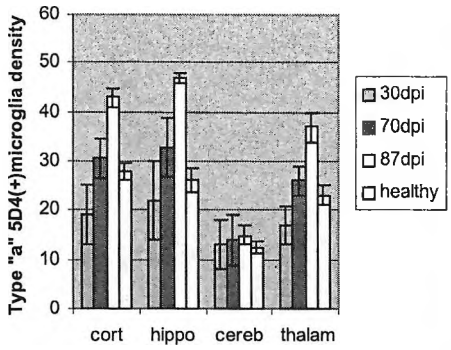

Fig. 3. Profiles of the 5D4(+) microglial reactivity during the course of prion neurodegeneration

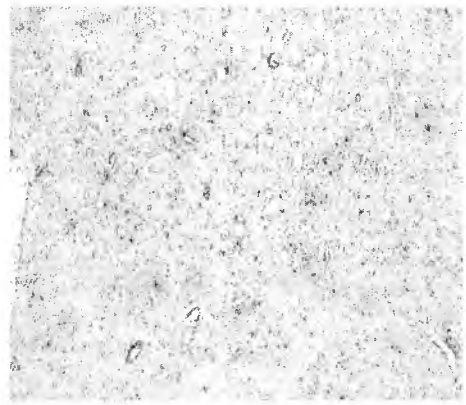

Fig. 4. Parallelism of the cellular reactivity (microgliosis) and spongiosis in the periventricular area of the hamster brain. Terminal stage of experimental scrapie 263K in hamster. Keratan-sulfate immunohistochemistry. × 80

Discussion

Astrogliosis, registered as re-expression *de novo* of vimentin marker in mature CNS during prion neurodegeneration is an additional biological marker of the pathogenesis of transmissible spongiform encephalopathies. This marker is useful not only for diagnostics but for the studies onto neurodegenerative changes. In morphological diagnostics of the prion degenerative diseases now currently is in use simple immunohistochemical detection of GFAP (+) astroglia. We propose and use in this work vimentin as additional marker for demonstration of the gliosis in prion infected brains. Vimentin immunohistochemistry possesses different characteristics and advantages revealing astrogliosis as one of the more important histopathological sign of prion degeneration. The appearance of vim (+) cells does not result from the insult made by intracerebral trauma during agent inoculation suggested earlier [4]. In the prove of this is the fact that in control animals injected with non infected brain vim (+) cells were observed rarely only in the right side of brain around the needle tract.

Microglial reaction, or microgliosis as a regional or local increasing of the microglial concentration, is described in parallel with degenerative changes in prion diseases. A correlation between prion deposition, spongiform degeneration and proliferation of the reactive microglia (microgliosis) is found in some CNS regions — thalamus, pons, cortex etc. [9, 10]. Our present results show a stable correlation between the morphological signs of spongiform degeneration and the relative increasing of reactivity of the 5D4 (+) subgroup of the microglia. Studies by J a n d e r et al. [7] confirm at minimum a large preservation of the 5D4 expression in degenerative lesions in contrast of the lacking of the T-cell-mediated autoimmune inflammation. Microglial activation results brain damage and triggering of the neurodegenerative process in [6]. According to B e r t o l o t t o et al. [2] there is no correlation between cellular activation and expression of the keratan-sulfate epitope from the 5D4 (+) microglia. A possible explanation of the microglial reaction during prion neurodegeneration could be the presumption that microglia can participate in the prion agent clearance and at the same time they act as reservoir [1].

In this study the wider distribution as well as higher density of 5D4(+) microglia and vim(+) astrocytes have been demonstrated with two newly introduced procedures. Immunohistochemistry for keratan sulfate and vimentin epitopes in scrapie-affected CNS is useful additional tool in diagnostics and for morphological approaches of the prion neurodegeneration.

References

1. Baker, C., Z.Y. Lu, I. Zaitzev, L. Manuelidis. Microglial activation varies in different models of Creutzfeldt-Jakob disease. — J. Virol., **73**, 1999, 5089-5097.
2. Bertolotto, A., C. Agresti, A. Castello, E. Manzardo, A. Riccio. 5D4 keratan sulfate epitope identies a subset of ramified microglia in normal central nervous system parenhyma. — J. Neuroimmunol., **85**, 1998, 69-77.
3. Bertolotto, A., B. Katerson, G. Canavese, A. Migheli, D. Schiffer. Monoclonal antibodies to keratan sulfate immunolocalize ramified microglia in paraffin and cryostat sections of rat brain. — J. Histochem. Cytochem., **41**, 1993, 481-487.
4. Calvo, J., A. Carbonell. Co-expression of GFAP and vimentin in reactive astrocytes following brain injury in rats. — Brain Res., **566**, 1991, 333-336.
5. Gomi, H., T. Yokoyama. Mice devoid of GFAP develop normally and are susceptible to scrapie prions. — Neuron, **14**, 1995, 29-41.
6. Heppner, FL., M. Prinz, A. Aguzzi. Pathogenesis of prion diseases: possible implication of microglial cells. — Prog. Brain Res., **132**, 2001, 737-750.
7. Jander, S., M. Schroeter, J. Fischer, G. Stoll. Differential regulation of microglial keratan sulfate immunoreactivity by proinflamatory cytokines and colony-stimulating factors. — Glia, **30**, 2001, 401-410.
8. Lafarga, M., M. T. Berciano. Cytology and organization of reactive astroglia in human cerebellar cortex with severe loss of granule cells: a study on the ataxic form CJD. — Neuroscience, **40**, 1991, 337-352.
9. Liberski, P., A. Bratosiewicz-Wasik, D. C. Gajdusek, P. Brown. Ultrastructural studies of expeimental scrapie and Creutzfeldt-Jacob disease in hamsters. II. Astrocytic and macrophage reaction towards axonal destruction. — Acta Neurobiol. Exp., **62**, 2002, 131-139.
10. Siso, S., B. Puig, R. Varea, E. Vidal, C. Acin, M. Prinz, F Montrasio, J. Badiola, A. Aguzzi, M. Pumarola, I. Ferrer. Abnormal synaptic protein expression and cell death in murine scrapie. — Acta Neuropathol., **103**, 2002, 615-626.

Institute of Experimental Morphology and Anthropology with Museum
Bulgarian Anatomical Society

Acta morphologica et anthropologica, 13
Sofia • 2008

Effect of Radiation with Low Doses Fast Neutrons and High Energy Oxygen Ions on the Rat Choroid Plexus Blood Vessels

V. Ormandjieva

Institute of Experimental Morphology and Anthropology with Museum, Bulgarian Academy of Sciences, Sofia

In the present study the morphometric analysis has been used to investigate the changes of the rat choroid plexus blood vessels. The applied irradiation provoked statistically significant changes in the rat choroid plexus blood vessels. These data provided evidence that the effect on the blood vessels in the delay period after irradiation can be induced in the rat choroid plexus by single doses of 1.0 Gy fast neutrons and oxygen ions. We suggest that these changes may be related with alteration of cerebrospinal fluid secretion and transcellular and absorbtion-transport functions of the rat choroid plexus.

Key words: rat choroid plexus blood vessels, morphometry, low doses of fast neutrons and oxygen ions irradiation.

Introduction

The choroid plexuses are specialized highly vascular anatomycal structures which protrude into the lateral ventricle, as well as in the third ventricle and fourth ventricle. The surface of the choroid plexus consist of numerous villi each covered with single layer of epithelial cells surrounded by vascular connective tissue cells [7]. As a secretory source of vitamins, peptides and hormones for neurons, the choroid plexus provides substances for brain homeostasis [4]. Most blood vessels in the plexus choroideus are wide-calibre (approximately 15 μm) fenestrated capillaries [6]. Irradiation with therapeutic doses may result in the development of early and late effects in normal tissues. Extensive experimental studies have shown a clearly defined association between vascular damage and the development of late radiation effects, however, the exact role played by vascular lesions remains uncertain [3]. The aim of the present study is to investigate the morphometrical changes of the blood vessels of the rat choroid plexus after exposure to low doses of fast neutrons and high-energy oxygen ions irradiation.

Materials and Methods

Three months aged female Wistar rats were exposed to fast neutrons (n=3) to 1.5 MeV at the dose of 1.0 Gy and single dose of 10^4 particles/cm^2 of oxygen ions (n=3). Experiments were performed in the impulsive reactor and the synchrophasotron of the Joint Institute of Nuclear Research in Dubna, Russia. Three months after whole-body irradiation experimental animals and 6 months aged control rats (n=4) were perfused intracardially with 2.5% glutaraldehyde and 2% paraformaldehyde in 0.1 M cacodilate buffer [5]. Extracted choroid plexuses were postfixed in 1% OsO4 and embedded in Durcupan. The semithin sections (1μm) were stained with 1% toluidine blue for morphometric measurment and examined under Light microscope Carl Zeiss Jena.

Morphometric analysis

We obtained morphometric data from the light microscope at 1000 × magnification using a square grid system [9] calibrated for linear measurment in μm and area measurment in μm^2 (625 grid points). We measured the relative number of blood vessels and luminal diameter and area of the blood vessels divided in four subgroups. The luminal diameter was measured as perpendicular distance across the maximum chord axis of each vessels.

Statistical analysis

Results are reported as mean values ± SEM and as relative part in percentage. We evaluated data from control rats and irradiated rats by using the Student's t-test for independent comparisons.

Results

Changes in the relative number of all blood vessels and vessels divided in four subgroups were determined after irradiation with a single dose of 1.0 Gy fast neutrons and oxygen ions in comparison to control rats. These findings are shown in Figures 1 and 2 and Tables 1 and 2. The significant changes three months after fast neutrons irradiation were approximately 13% reduction (p<0.001) in the number of vessels of 5-7 μm in diameter and 33% reduction (p<0.001) in vessels of 7-16 μm in diameter. A significant increase of 32% was seen in the number of large vessels of 16-30 μm

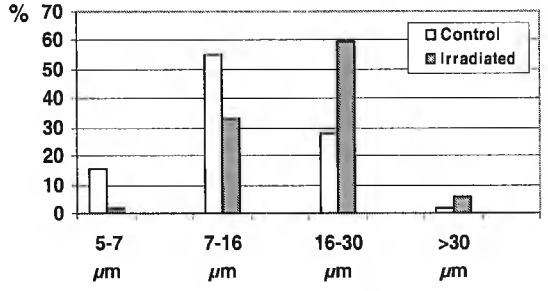

Fig. 1. Comparison of morphometric data of choroid plexus blood vessels of control rats and fast neutrous irradiated rats (% — relative parts)

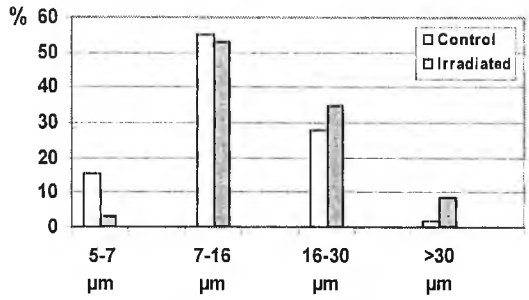

Fig. 2. Comparison of morphometric data of choroid plexus blood vesse of control rats and high-energy oxygen ions irradiated rats (% — relative parts)

($p<0.001$) and 3% in vessels >30 μm in diameter. Similar changes were determinated after irradiation with a single dose of high energy oxygen ions in comparison to control rats: approximately 12% reduction ($p<0.001$) in the number of vessels of 5-7 μm in diameter and 2% reduction in vessels of 7-16 μm in diameter. A significant increase of 7% was seen in the number of large vessels of 16-30 μm ($p<0.01$) and >30 μm (<0.01) in diameter after irradiation with oxygen ions.

Significant changes were not seen in luminal diameter (mean luminal diameter of neutrons irradiated rats — 18.80 ± 0.93 μm and oxygen irradiated rats — 18.87 ± 0.93 μm and mean luminal diameter of control rats — 18.50 ± 0.94 μm) and luminal

T a b l e 1. Morphometric data of choroid plexus blood vessels of control rats and fast neutrons irradiated rats (luminal diameter in μm, luminal area in μm²)

Blood vessels	Control rats		Irradiated rats	
	Luminal diameter ± SEM	Luminal area ± SEM	Luminal diameter ± SEM	Luminal area ± SEM
5–7 μm	7.37±0.24	100.92±2.84	7.50±0.20	87.50±12.50
7–16 μm	11.16±0.41	174.13±10.52	12.64±0.74	168.75±17.10
16–30 μm	21.56±1.26	401.28±30.59	20.56±1.04	369.53±36.45
>30 μm	33.87±1.87	731.25±40.49	34.37±1.76	791.66±40.82
Number of measurments	242	242	159	159

T a b l e 2. Morphometric data of choroid plexus blood vessels of control rats and high-energy oxygen ions irradiated rats (luminal diameter in μm, luminal area in μm²)

Blood vessels	Control rats	Irradiated rats
	Luminal diameter ± SEM	
5–7 μm	7.37±0.24	7.05±0.23
7–16 μm	11.16±0.41	11.55±0.59
16–30 μm	21.56±1.26	21.73±1.62
>30 μm	33.87±1.87	34.73±1.59
	Luminal area ± SEM	
5–30 μm	199.08±17.51	212.22±18.13
Number of measurements	242	148

area (mean luminal area of neutrons irradiated rats — 354.36 ± 26.71 μm^2 and mean luminal area of control rats — 351.89 ± 20.52 μm^2) of all blood vessels.

Discussion and Conclusion

In the present study it was estimated that the relative part of the capillaries, i.e. vessels <16 μm in diameter were 70.66% in control rats, and 34.86% in fast neutrons and 56.34% in oxygen ions irradiated rats. The initial loss of capillaries and the increase in number of larger vessels in plexus choroideus three months after irradiation were consistent with the effects attributed to regeneration in the choroid plexus. Ultrastructural and morphometrical changes were reported previously in the cytoplasm of endothelial cells of fenestrated capillaries and epithelial cells of this experimental model [1, 8]. Most of the choroid plexus epithelial cells exhibited ultrastructural signs of increased absorbing and transport activity. The augmented transport activity was evident from a large number of micropinocytotic vesicles in cytoplasm of the endothelial cells of fenestrated capillaries. This increased intensity of the cellular transport relates, probably, with early post-exposure edema or subserves elimination of toxic substances consequent to radiation exposure. From the morphometric investigation in the previously our study it was established that the nuclear, cytoplasmic and cell area of the light and dark epithelial cells diminished after exposure to fast neutrons. These changes may be indicative of compensatory reactions in the organism following radiation exposure. Experimental study have shown a significant reduction in the number of blood vessels > 16 μm in diameter and atrophy of the choroid plexus epithelial cells only after 25 Gy of X-rays [2, 3].

In conclusion, it can be pointed out that the applied irradiations provoked significant changes in rat choroid plexus blood vessels. These results clearly demonstrate that the effect on blood vessels after irradiation can be induced in the choroid plexus by single dose of 1.0 Gy fast neutrons and oxygen ions. We suggest a hypothesis that the vascular damage is predominant factor leading to development of late effects in irradiated normal tissues.

Refferences

1. Bourneva, V., L. Gitsov, V. Mladenova, B. Fedorenko, R. Kabitsyna, N. Budyonnaya. Morphological changes in rat's brain choroid plexus after exposure to low doses of high energy oxygen ions, fast neutrons and gamma radiation. — Aviakosm. Ekolog. Med., **29**, 1995, 49-52.
2. Calvo, W., J. W. Hopewell, H. S. Reinhold, A. P. van den Berg, T. K. Yeung. Dose-dependent and time-dependent changes in the choroid plexus of the irradiated rat brain. — British J. of Radiology, **60**, 1987, 1109-1117.
3. Hopewell, J. W., W. Calvo, R. Jaenke, H. S. Reinhold, M. E. Robbins, E. M. Whitehouse. Microvasculature and radiation damage. — Recent Results Cancer Res., **130**, 1993, 1-16.
4. Johanson, C., P. McMillan, R. Tavares, A. Spangenberger, J. Duncan, G. Siverberg, E. Stopa. Homeostatic capabilitis of the choroid plexus epithelium in Alzheimer's disease. — Cerebrospinal Fluid Res., **1**, 2004, p. 3.
5. Karnovsky, M. J. A formaldehyde-glutaraldehyde fixative of high osmolarity for use in electron microscopy. — J. Cell Biol., **27**, 1965, 137A.
6. Milhorat, T. H. Structure and function of the choroid plexus and other sites of cerebrospinal fluid formation. — Intern. Rev. Cytol., **47**, 1976, 225-288.
7. Ormandjieva, V. K. Electronmicroscopical and hystometrical investigations of the rat choroid plexus during development and experimental conditions. PhD Thesis, Sofia, 1993.
8. Ormandjieva, V. K. Ageing choroid plexus and experimental models: morphometrical study. — Compt. Rend. Acad. Bulg. Sci., **56**, 2003, 105-110.
9. Weibel, E. R. Selection of the best method in stereology. — J. Microsc., **100**, 1974, 261-269.

Institute of Experimental Morphology and Anthropology with Museum
Bulgarian Anatomical Society

Acta morphologica et anthropologica, 13
Sofia • 2008

Vesicular Amine Transporter VMAT2 in the Gut: from Principal Mechanism to Therapeutic Application

I. Stoyanova

Department of Anatomy, Faculty of Medicine, Thracian University, Stara Zagora

Besides the role of classical neurotransmitter, histamine plays a key role in the immune/inflammatory processes in the gastrointestinal tract. Specific transport proteins pack the amine neurotransmitters into vesicles so that their release can be regulated by neural activity. Recently, two vesicular amine transporters (VMAT1 and VMAT2), essential components of monoaminergic neurons and endocrine cells were identified. In our study we investigated VMAT2 distribution in rat small intestine using immunocytochemical techniques. VMAT2-immunreactivity was found in neurons of the submucosal plexus. Nerve fibres containing VMAT2 were numerous in the submucosal and myenteric plexuses, in the circular muscle layer and around the blood vessels. Some fibres were observed beneath the epithelial cells.

This data provide important information about the amine-handling structures in the gut wall, and neuroendocrine and immune/inflammatory cell functions. Moreover, it raises the possibility for development of new pharmacotherapeutic approach to inflammatory bowel diseases.

Key words: gut innervation, histamine transporters, immunohistochemistry, rat.

Introduction

Besides the function of classical neurotransmitter in the nervous system, the biogenic amine histamine (HIS) also plays a key role in the endocrine and immune/inflammatory system. In the gastrointestinal tract (GIT) HIS is a crucial mediator, and during the last two decades it was discovered to be responsible also for diarrhoea in inflammatory bowel diseases (IBD) and food allergy [1].

HIS-handling cells, like the other amine-handling cells, are characterized by synthesis, accumulation and secretion of the amine, which require amine-synthesizing enzymes, plasma membrane transporters for amine intake, and intracellular transporters, named vesicular amine transporters (VATs), for amine loading from the cytoplasm into secretory or synaptic vesicles [2]. Two structurally related but pharmacologically distinct monoamine transporters are known: VMAT1 and VMAT2 [3]. They act as an electogenic exchanger of protons and monoamines, using a proton electrochemical gradient. Functional analysis showed that the two VATs differ in substrate recognition and inhibition by drugs. [4]. In addition, VMAT1 and VMAT2 differ in their tissue distribution. While in the rat VMAT1 is a principal amine transporter of the PNS and of the neuroendocrine and mast cells, VMAT2 is expressed

predominantly in the neuronal amine-handling cells: serotoninergic, noradrenergic, dopaminergic, histaminergic and adrenergic neurons of the CNS [5].

In both rodent and human, most of the VMAT2 positive nerve fibres are found at the blood vessels' wall and around the enteric ganglia. These fibres represent projections of postganglionic sympathetic neurons, and in the muscle and mucosal layer they are rare. VMAT2 positive neuronal perikarya are very rare or absent in the rodent gut [5].

Despite the fact that the biogenic amine-containing neuronal structures in the enteric nervous system (ENS) were extensively studied, there are still several unanswered questions about their distributional pattern, chemical coding and function. Therefore, we aimed this study to demonstrate the VMAT2-positive elements in the intestinal wall of the rat, and to assess their potential therapeutic implication.

Material and Methods

Specimens from the distal ileum of five rats were investigated with immunocytochemical techniques for detection of VMAT2. The staining was performed using the avidin-biotin method on free-floating sections with primary antibody rabbit anti-VMAT2, for 24 h at room temperature. After rinsing in PBS, sections were incubated with the secondary antibody, biotinylated goat anti-rabbit IgG. After washing the sections, the ABC complex was applied. Following rinsing, peroxidase activity was visualized with the SG chromogen as gray staining of the immunoreactive structures. Finally, sections were dehydrated in a graded series of alcohol and xylene, and embedded in Entellan.

Results

Immunostaining of VMAT2 in specimens of rat distal ileum showed abundant varicose neuronal fibres in all layers of the gut wall. As shown in Fig. 1, VMAT2-immunreactivity was found in single neurons of the submucosal and myenteric plexuses. The immunoreactive fibres clearly marked by the SG were numerous in both plexuses, and they surrounded VMAT2-positive neuronalal perikarya. In addition, we observed a high frequency of VMAT2-positive varicosities in the circular muscle layer and around the blood vessels. In the mucosa there was well expressed VMAT2-immunoreactivity. Some immunolabelled nerve fibres were observed distributed throughout lamina propria. As can be seen in Fig. 2, a large number of VMAT2-containing neuronal processes and terminals were in a close apposition to the intestinal glands, and delineated the glandular epithelial cells.

Discussion

In the present study, we show that the intestinal wall of the rat is well innervated by VMAT2 expressing intrinsing neurons and neuronal fibres. Moreover, it clearly demonstrates abundance of VMAT2-positive neuronal projections into the intestinal musculature and mucosa layers; hence, their function is under monoamine-ergic control.

These data provide important information about the amine-handling neuronal structures in the gut. VATs-staining will enable co-transmitters to be identified, particularly in subtypes of intestinal amine-handling cells. The visualization of the

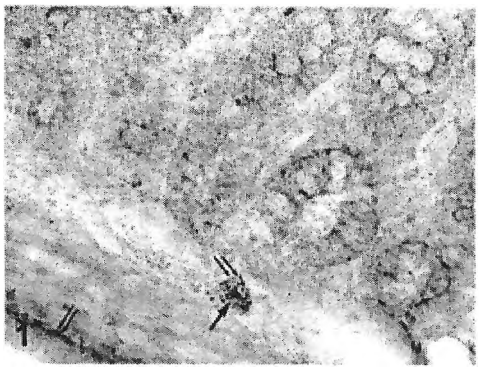

Fig. 1. Photomicrograph of the distal ileum showing VMAT2-positive neuron in the submucosal plexus (arrow). Note the numerous VMAT2-immunoreactive neuronal fibres in both the myenteric and submucosal plexus (double arrows). × 400

Fig. 2. Numerous neuronal projections, stained for VMAT2 in the circular muscle layer and in the submucosis (thick arrows). The glandular epithelium is delineated by VMAT2-containing varicosities (thin arrows). × 400

VMAT2-positive elements of the gut wall provides a potential for their imaging in the clinical context of disorders, related to them. This immunocytochemical method allows an *in situ* exploration of plasticity, regulation, and degeneration of specific sets of amine-handling neurons, and the function of amine-handling inflammatory and immune cells.

The abundance of VMAT2-positive nerve fibres in the intestinal wall and the fact that HIS transporter VMAT2 can be inhibited by substances like ketanserin, reserpin or dicyclohexylcarbodiimide (DCCD), which clock various H^+-translocating enzymes [6], suggest that HIS or VMAT2 antagonists may be used for pharmacological targeting of IBD. Moreover, it raises the possibility for development of new pharmacotherapeutic approach to inflammatory bowel diseases.

References

1. Crowe, S. E., G. K. Luthra, M. H. Perdue. Mast cell mediated in transport in intestine from patients with and without inflammatory bowel disease. — Gut, **41**, 1997, 785-792.
2. Edwards, R. H. The transport of neurotransmitters into synaptic vesicles. — Curr. Opin. Neurobiol., 2,1992, 586-594.
3. Liu, Y., A. Peter, A. Roghani, S. Schuldiner, G. G. Prive, D. Eisenberg, N. Brecha, R. Edwards. A cDNA that suppresses MPP^+ toxicity encodes a vesicular amine transporter. — Cell, **70**, 1992, 549-551.
4. Erickson, J. D., M. K. H. Schafer, T. I. Bonner, L. E. Eiden, E. Weihe. Distinct pharmacological properties and distribution in neurons and endocrine cells of two isoforms of the human vesicular monoamine transporter. — Proc. Natl. Acad. Sci., USA, **93**, 1996, 5166-5171.
5. Weihe, E., L. Eiden. Chemical neuroanatomy of the vesicular amine transporters. — FASEB J., **14**, 2000, 2435-2449
6. Gasnier, B., D. Scherman, J.P. Henry. Dicyclohexylcarbodiimide inhibits the monoamine carrier of bovine chromaffin granule membrane. — Biochemistry, **24**, 1985, 1239-1244.

Institute of Experimental Morphology and Anthropology with Museum
Bulgarian Anatomical Society

Acta morphologica et anthropologica, 13
Sofia • 2008

Serum Ganglioside GT1b Changes in Patients with Multilpe Sclerosis

E. Zaprianova, V. Kolyovska, D. Deleva , E. Sultanov, D. Georgiev**, X. Kmetska***

Institute of Experimental Morphology and Anthropology with Museum, Bulgarian Academy of Sciences, Sofia
** National Center of Radiology and Radiation Protection, Sofia*
*** Specialized Hospital for Active Treatment in Neurology and Psychiatry St. Naum, Sofia*

The relative distribution of ganglioside GT1b was determined in the serum of 52 patients with relapsing-remitting multiple sclerosis (RRMS) during the different stages of the disease and of 30 healthy subjects. There was statistically significant decrease of serum GT1b during the first attack of RRMS when axonal damage and demyelination are present in the central nervous system (CNS). In remission with a long duration, characterized by the occurrence of remyelination, serum GT1b increases twice in comparison to healthy individuals. These findings further support the concept concerning the role of GT1b in mediating the interactions between axons and oligodendrocytes needful for the formation of the myelin sheath and the maintenance of its integrity. Therefore, serum GT1b could be monitored as markers of demyelination and remyelination in the CNS of MS patients.

Key words: ganglioside GT1b, multiple sclerosis, serum, axon-oligodendrocytes interactions.

Introduction

Gangliosides, the most abundant sialyted glycoconjugates in the nervous system, are major cell surface determinants. The brains of higher vertebrates contain at least four major gangliosides: GM1, GD1a, GD1b and GT1b. They occur most prominently in the neuron where they comprise the major type of sialoconjugate in the plasma membrane. Gangliosides are present also in non-cell-associated form in blood, lymph, saliva and other body fluids. The main gangliosides in human blood serum are GM3, GM1, GD1a, GD1b and GT1b.

Gangliosides have been proposed to regulate cellular function including neuronal cell adhesion, transmembrane signalling and cell growth and differentiation. Perhaps the most dramatic interactions between neurons and glia in the central nervous system (CNS) occurs during myelination when oligodendroglial processes must recognize, adhere to, and ensheathe axons. A binding protein specific for neuronal ganglioside GT1b was detected on rat oligodendroglial membrane and it was suggested that GT1b play a role in mediating the interactions between axons and oligo-

dendroglia needful for myelination and maintenance the integrity of myelin sheath [11]. We recently first reported a significant increase of relative portion of GT1b in the brain and in the serum of Lewis rats during myelination [6]. There was an apparent correlation between the GT1b levels in the brain and in the serum during the different periods of myelination.

The disturbance of axon-oligodendroglial interrelationship occurs during demyelination and destruction of neuronal perikaryon, axons and oligodendrocytes. Multiple sclerosis (MS) is a demyelinating disease of the CNS with a considerable social impact. It is the major cause of non-traumatic disability in young adults. Traditionally, it was belived that MS was a primary demyelinating disorder and that neuronal and axonal damage occurred in chronic lesions. However, recent imaging and morphological studies indicate that neuronal loss and axonal injury are hallmarks of early MS [2, 10, 13, 15]. Considerable changes of serum gangliosides in pathological conditions [3, 16] were observed. We demonstrated a significant changes of GM1, GD1a and GM3 gangliosides in the serum of patients with early MS [16].

There is no data concerning serum GT1b variations in MS patients. In this study, the relative distribution of GT1b was determined in the serum of patients with relapsing-remitting multiple sclerosis (RRMS) during their first MS attack and in remission with a long duration.

Materials and Methods

Sera were obtained from 52 patients hospitalized at the Specialized Hospital for Active Treatment in Neurology and Psychiatry St. Naum, Sofia, with clinically definite MS according to Poser's criteria [9] and from 30 healthy subjects. Seven patients were evaluated during their first attack of the disease of what later was definitely diagnosed as RRMS, forty five patients were in remission with a long duration.

Isolation of serum gangliosides was performed by the method of I l i n o v et al. [5]. It includes the following stages: a) dehydration of the sample by azeotropic distillation of the mixture of serum water/n-propanol = 1:10 (v/v); b) total lipid triple extraction with cyclohexane (I), chloroform : methanol =1:1 (v/v) (II), and chloroform: methanol = 1:2 (v/v) (III); c) non-polar lipids removal by preparative TLC with a mobile phase: chloroform : methanol: 0,3 % CaCl2= 30:18:4 (v/v/v); d) elimination of the blood sugar by Sep Pak technique according to W i l l i a m s and M c C l u e r [14]; e) HPTLC of the ganglioside fractions with a mobile phase: chloroform : methanol : 0,1 M sodium lactate = 55:40: 10 (v/v/v).

The spots were visualized by spraying with orcinol reagent followed by local heating at 110°C and the gangliosides were quantified densitometrically. Bovine brain gangliosides (Calbiochem) were used as a test mixture for identification. The Student's test was used to determine statistical differences between the groups using $P<0.05$ as the level of confidence.

Results

The relative percentage of the five major serum gangliosides (GM3, GM1, GD1a, GD1b and GT1b) during different stages of MS and in healthy subjects was recalculated on the basis of the densitograms (Fig. 1). The relative proportion of GT1b decreases from 6.19 % in the healthy subjects to 5.10 % during the first attack of MS. In remission with a long duration ganglioside GT1b content increases twice in compari-

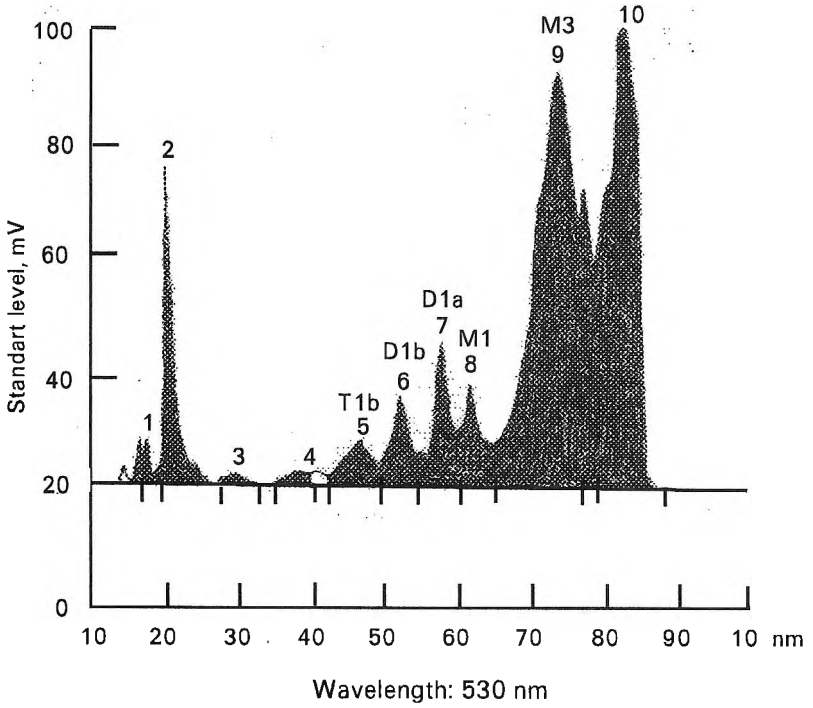

Fig. 1. Densitogram of serum gangliosides of a RRMS patient with a first attack of the disease

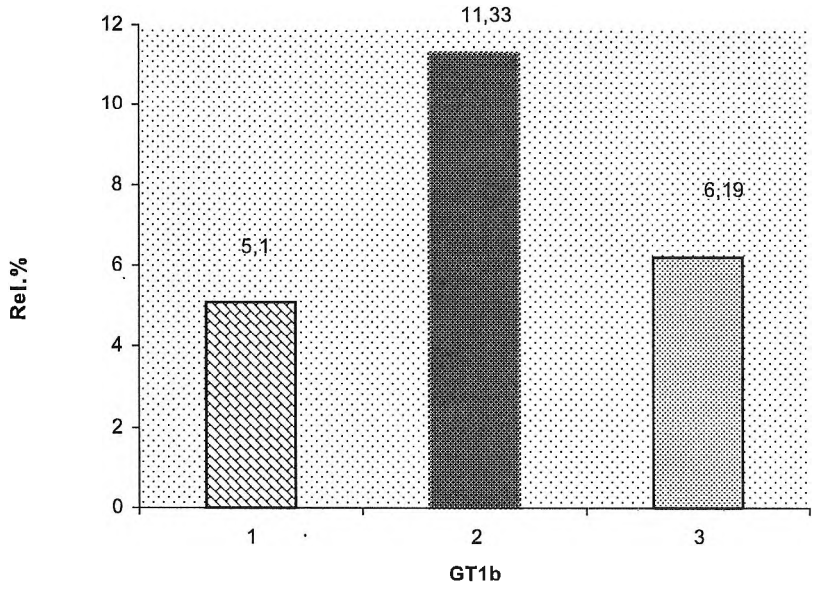

Fig. 2. Diagram of serum ganglioside GT1b of RRMS patients with a first attack of the disease (1), RRMS patients in remission with a long duration (2) and in healthy subjects (3)

Table 1. Relative Percentage of Major Serum Gangliosides in Patients during Different Stages of Relapsing-Remitting MS and in Healthy Subjects

Gangliosides	I group (n=7) M ± SEM	II group (n=45) M ± SEM	III group (n=30) M ± SEM
GT1b	**5.10 ± 1.84**	**11.33 ± 2.04**	**6.19 ± 1.08**

M — mean value; SEM — standard error of mean; I group — RRMS patients with first attack of the disease; II group — RRMS patients in remission with a long duration; III group — healthy subjects;

son to its content in healthy subjects (Fig. 2). The relative portion of GT1b content during different stages of MS and in healthy subjects was statistically significant (P<0.05) (Table 1).

Discussion

In this study the content of ganglioside GT1b was analyzed in the serum of patients with RRMS during different stages of the disease. The results demonstrated in comparison to healthy individuals a statistically significant decrease of serum GT1b during the first attack of RRMS and a twice increase in remission with a long duration.

We could suggest that the decrease of serum GT1b in patients with early MS is connected with the disturbance of axon-oligodendroglia relationships due to axonal damage and demyelination, well demonstrated by the imaging and morphological studies of recent years [1, 2, 4, 7, 12]. In remission with a long duration remyelination may occur in MS [8]. The interactions between axon and oligodendrocytes had to be restored. Since ganglioside GT1b plays a role in mediating these interactions the twice increase of GT1b in the serum of RRMS patients does not seem to be surprising. This finding corresponds well with our previous studies concerning GT1b changes in the brain of Lewis rats with chronic relapsing experimental allergic encephalomyelitis (CREAE) during the early stages of the disease [17]. A significant decrease of relative portion of GT1b was revealed in the brain during the first clinical episode of CREAE, an animal model of RRMS.

In conclusion, the results of this study provide for the first time evidence that serum ganglioside GT1b undergoes statistically significant changes in RRMS patients during their first MS attack and in remission with a long duration. This finding further support the concept concerning the role of GT1b in mediating the interactions between axon and oligodendrocytes, needful for the formation of the myelin sheath and the maintenance of its integrity. Therefore, serum GT1b ganglioside could be monitored as markers of demyelination and remyelination in the CNS of patients with multiple sclerosis.

Acknowledgments: We thank Ginka Zaharieva for exellent technical assistance.

References

1. Casanova, B., M. C. Martinezbisbal, C.Valero, B. Celda, L. Martibonmati, A. Pascual, L. Landente, F. Coret. Evidence of Walerian degeneration in normal appearing white matter in the early stages of relapsing-remitting multiple sclerosis. — J. Neurol., **250**, 2003, 22-28.
2. DeStefano, N., M. Bartolozzi, L. Guidi, M. Stromillo, A. Federico. Magnetic resonance spectroscopy as a measure of brain damage in multiple sclerosis. — J. Neurol. Sci., **233**, 2005, No 1-2 , 203-208.
3. Dyatlovitskaya, E. Blood serum gangliosides and antibodies to gangliosides. — Biokhimiya, **57**, 1992, 1004-1010.
4. Gadea, M., M. C. Martinezbisbal, L. Martibonmati, R. Espert, B. Casanova, F. Coret, B. Celda. Spectroscopic axonal damage of the right locus coeruleus relates to selective attention impairment in early stage relapsing-remitting multiple sclerosis. — Brain, **127**, 2004, Nol, 89-98.
5. Ilinov, P., D. Deleva, S. Dimov, E. Zaprianova. A variant for isolation of serum gangliosides. — J. Liquid Chrom. Rel. Technol., **20**, 1997, No8, 1149-1157.
6. Kolyovska, V., E. Zaprianova, D. Deleva, A. Filchev, E. Sultanov. GT1b ganglioside changes in Lewis rat serum during myelination. — Acta morphol. et anthropol., **12**, 2007, 3-9.
7. Kornek, B., H. Lassman. Neuropathology of multiple sclerosis—new concepts. — Brain Res. Bull., **61**, 2003, Nol, 321-326.
8. Lassman, H. Comparative Neuropathology of Chronic Experimental Allergic Encephalomyelitis and Multiple Sclerosis. — Berlin, Heidelberg, New York, Tokyo, Springer-Verlag, 1983, 135.
9. Poser, C., D. Paty, L. Scheiberg, W. Mc Donald, F. Pavis, G. Ebers, W. Sibly, D. Silberberg, W. Touertellotte. New diagnostic criteria for multiple sclerosis: guidelines for research protocols. — Ann. Neurol., **13**, 1983, 227-231.
10. Sultanov, B. Neuronal and axonal damage in early multiple sclerosis. — Acta morphol. et anthropol., **9**, 2004, 208-210.
11. Tiemeyer, M., Swank-Hill,P., Schnaar, R. A membrane receptor for gangliosides is associated with central nervous system myelin. — J. Biol. Chem., **265**, 1990, 11990-11999.
12. Trapp, B., J. Peterson, J. Mcdonough. Mechanisms of axonal loss and neuronal dysfunction in MS. — Multiple Sclerosis, **10**, 2004, 89-98.
13. Waxman, S.G. Multiple sclerosis as neuronal disease. — Arch. Neurol., **57**, 2000, 22-24.
14. Williams, A., R. McCluer. The use of Sep-Pak C18 cartidges during the isolation of gangliosides. — J. Neurochem., **35**, 1980, 266-270.
15. Yong, V. Prospects for neuroprotection in multiple sclerosis. — Frontiers in Bioscience, **9**, 2004, 864-872.
16. Zaprianova, E., D. Deleva, P. Ilinov, E. Sultanov, L. Christova, B. Sultanov. Serum ganglioside patterns in multiple sclerosis. — Neurochem.Research, **26**, 2001, No2, 95-100.
17. Zaprianova, E., D. Deleva, A. Filchev, V. Kolyovska, B. Sultanov. GT1b ganglioside brain changes in chronic relapsing experimental allergic encephalomyelitis induced in the Lewis rats. — Acta morphol. et anthropol., **10**, 2005, 9-12.

Institute of Experimental Morphology and Anthropology with Museum
Bulgarian Anatomical Society

Acta morphologica et anthropologica, 13
Sofia • 2008

Effects of Somatostatin and Sandostatin® on Guinea-Pig Urinary Bladder Subjected to Experimental Ischemia and Reperfusion

R. Kalfin, F. Pessina, K. Jangyozova, G. Sgaragli**

Institute of Neurobiology, Bulgarian Academy of Sciences, Sofia
**Department of Anatomical, Biomedical and Pharmacological Sciences, University of Siena, Italy*

Somatostatin and its stable analogue Sandostatin® were tested for their capability to protect the intrinsic nerves in an *in vitro* model of guinea-pig whole urinary bladder subjected to ischemia and reperfusion injury. Sandostatin® (1 to 300 nM) and somatostatin (300 nM) improved significantly the response of the bladder to electrical field stimulation (EFS) during reperfusion as compared to untreated control bladders. Both Sandostatin® and somatostatin exhibited significant antiperoxidant activity with a pIC_{50} M values of 7.0 ± 0.6 and 6.7 ± 0.3, respectively, which could eventually underlie their neuroprotective action during reperfusion.

Key words: somatostatin, sandostatin, bladder, ischemia, reperfusion.

Introduction

It is generally accepted that the partial bladder obstruction represents one of the major pathologies of the urinary bladder that leads to chronic post-void residual urine or acute urinary retention followed by progressive contractile failure. A current hypothesis is that bladder decompensation following partial bladder obstruction is directly related to decreased tissue perfusion, resulting in periods of hypoxia and ischemia [3]. It is important to look for substances which could decrease the ischemia-reperfusion induced neuronal damage in detrusor muscle and in such a way to ameliorate the functional disorders of urinary bladder. Somatostatin-14 and particularly its stable analogue, the cyclic octapeptide Sandostatin®, are known to exert cytoprotective activities in peripheral tissues and in neuronal cells. The somatostatin peptides were also shown to afford protection against neuronal damage caused by experimentally induced cerebral ischemia in rats [8]. However, their effect on detrusor nerves subjected to ischemia-reperfusion, has not been established so far. The aim of this study, therefore, is to examine the efficacy of somatostatin and its stable analogue Sandostatin® to counteract the damage suffered by neurons in an *in vitro* model of whole urinary bladder subjected to ischemia and reperfusion.

Materials and Methods

Male Charles River guinea-pigs (350-500 g) were anesthetized with Ketavet and sacrificed by cervical dislocation. The animals were treated in accordance with the European Committee standards concerning the care and use of laboratory animals. The neuroprotective effects of somatostatin and Sandostatin® were studied in an *in vitro* model of whole urinary bladder subjected to ischemia and reperfusion injury as it has been previously described [7].

Results

The response to electrical field stimulation (EFS) declined rapidly in the combined absence of oxygen and substrate (ischemia-like condition), and was abolished within an hour. After reintroduction of normal conditions, the recovery of the response to electrical field stimulation (neurogenic response) in control bladders was poor, reaching in 2 hours a maximum of about 25 % of the initial response (Fig. 1A and 1B). At this time, however, the response of the muscle to carbachol had fully recovered (data not shown). To see if somatostatin and Sandostatin® could partially reduce the nerve damage described above, the peptides have been perfused during ischemia and the first 30 min of reperfusion, as it is supposed that the major damage to the tissue develops not only during ischemia, but also at the beginning of reperfusion when free radicals are being formed intensively. Sandostatin® at 1, 100 and 300 nM improved significantly the EFS-induced contractile response in reperfusion phase, reaching 67.45 ± 5.10 % at 180 min for a concentration of 300 nM, as compared to 54.15 ± 6.85 % in control bladders ($n = 6$, $P < 0.01$) (Fig. 1B). Somatostatin at concentrations of 1 and 100 nM did not exert any effect (Fig. 1A),

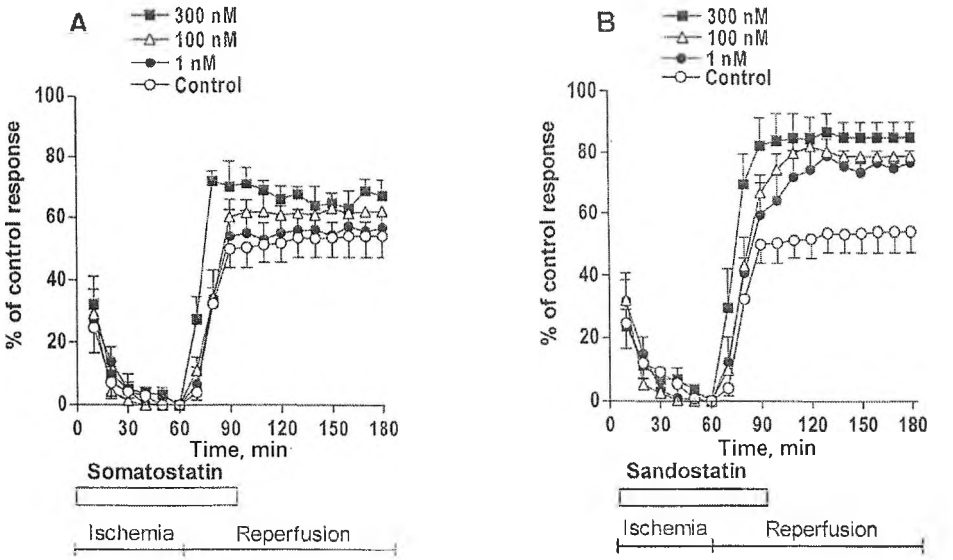

Fig. 1. Electrical field stimulation-induced contractile responses of guinea-pig whole urinary bladder subjected to 60 min of ischemia and subsequent 120 min of reperfusion. Experiments were carried out in the absence or presence of somatostatin (A) or Sandostatin® (B), applied for the first 90 min of the experiment. Results are expressed as mean ± SEM of six experiments in each group

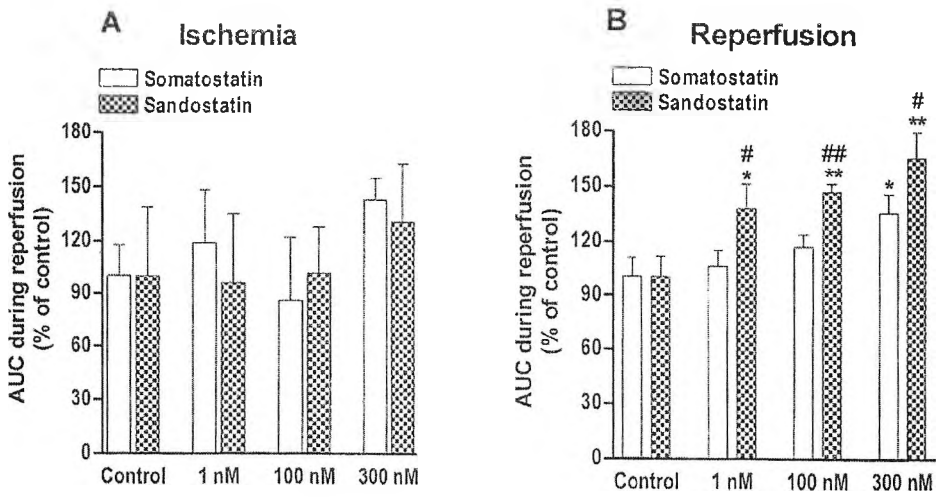

Fig. 2. Electrical field stimulation-induced contractile responses of guinea-pig whole urinary bladder subjected to 60 min of ischemia (A) and subsequent 120 min of reperfusion (B). Experiments were carried out in the absence or presence of somatostatin or Sandostatin®. Results are expressed as mean of area under curve (AUC) ± SEM of six experiments in each group. Differences among groups were evaluated by one-way ANOVA followed by Dunnett's *post hoc* comparison test ($^{*}P < 0.05$ and $^{**}P < 0.01$ versus controls; $^{\#}P < 0.05$ and $^{\#\#}P < 0.01$ versus somatostatin-treated group)

while at 300 nM it increased the recovery of contractile response during reperfusion (Fig. 2B). The antioxidant activity of the peptides was assessed for their capability to prevent linoleic acid peroxidation. Both somatostatin and Sandostatin® exhibited remarkable antiperoxidant activity with a pIC_{50} M values of 6.7 ± 0.3 and 7.0 ± 0.6, respectively (Table 1).

Discussion

Bladder outlet obstruction generally due to prostatic hyperplasia, a common problem in men over 60 years of age, is a major urologic problem that has been the subject of many clinical and experimental studies. The hyperplasia of prostate leads to obstructed micturition, during which occurs periodic bladder ischemia. The latter has been suggested to result in the partial denervation of the detrusor smooth muscle through ischemia and reperfusion injury to the post-ganglionic parasympathetic neurons within the bladder wall [1]. Previous investigations showed that *in vitro* ischemia-like condi-

T a b l e 1. Inhibition of lipid peroxidation

ANTIOXIDANT	IC_{50} (mM) ± SEM	pIC_{50} (mM) ± SEM
DTBHA	0.088 ± 0.006	7.1 ± 0.5
Sandostatin®	0.097 ± 0.011	7.0 ± 0.6
Somatostatin	0.164 ± 0.019	6.7 ± 0.3
Vasoactive intestinal peptide	0.380 ± 0.008	6.4 ± 0.1
BHA	0.428 ± 0.005	6.3 ± 0.4
β-TAG	1.040 ± 0.330	6.0 ± 0.4
Propofol	3.100 ± 0.380	5.5 ± 0.3
β-GLU	9.910 ± 2.480	5.0 ± 0.4

tions were more damaging to the nervous tissue than to the detrusor muscle [6]. Somatostatin-14 and its stable analogue Sandostatin® were shown to ameliorate pancreatic microcirculatory injury and enzyme release after ischemia-reperfusion of the pancreas [4] and to reduce liver and intestinal injury induced by hypoxia/ischemia in rats [5]. In this study we showed for the first time that Sandostatin® counteracts neuronal damage of the whole urinary bladder during reperfusion. The mechanisms by which Sandostatin® protects bladder nerves from reperfusion injury is only a matter of speculation, though a reduction in the amount of somatostatin among loss of other sensory neuropeptides in the obstructed human bladder has been previously described [2]. In the present study, a remarkable antioxidant activity of Sandostatin® has been found, which could underlie its neuroprotective action during reperfusion, when a significant amount of free radicals has been formed. In summary, the pharmacological action of drug Sandostatin® (Novartis), outlined in the present study, may represent a new therapeutic option for the control of functional disorders of the urinary bladder.

Acknowledgements: This study was supported by Grant L-1305/03 (from the National Science Fund, Sofia, Bulgaria), and MF-07/2006 (from Trakia University, Stara Zagora, Bulgaria).

References

1. Brading, A.F. Alterations in the physiological properties of urinary bladder smooth muscle caused by bladder emptying against an obstruction. – Scand. J. Urol., **184**, 1997, 51-58.
2. Chapple, C. R., P. Milner, H. E. Moss, G. Burnstock. Loss of sensory neuropeptides in the obstructed human bladder. – Br. J. Urol., **70**, 1992, 373-381.
3. Greenland, J. E., J. J. Hvistendahl, H. Anderson, T. M. Jorgensen, G. McMurray, M. Cortina-Borja, A. F. Brading, J. Frokiaer. The effect of bladder outlet obstruction on tissue oxygen tension and blood flow in the pig bladder. – BJU Int., **9**, 2000, 1109-1114.
4. Hoffmann, T. F., E. Uhl, K. Messmer. Protective effect of the somatostatin analogue octreotide in ischemia/reperfusion-induced acute pancreatitis in rats. – Pancreas, **12**, 1996, 286-293.
5. Morris, J. B., N. H. Guerrero, E. E. Furth, T. A. Stellato. Somatostatin attenuates ischemic intestinal injury. – Am. J. Surg., **165**, 1993, 676-680.
6. Pessina, F., G. McMurray, A. Wiggin, A. F. Brading. The effect of anoxia and glucose-free solutions on the contractile response of guinea-pig detrusor strips to intrinsic nerve stimulation and the application of excitatory agonists. – J. Urol., **157**, 1997, 2375-2380.
7. Pessina, F., K. Marazova, P. Ninfali, L. Avanzi, S. Manfredini, G. Sgaragli. In vitro neuroprotection by novel antioxidants in guinea-pig urinary bladder subjected to anoxia-glucopenia/reperfusion damage. – Naunyn Schmiedebergs Arch. Pharmacol., **370**, 2004, 521-528.
8. Rauca, C., K. Schafer, V. Hollt. Effects of somatostatin, octreotide and cortistatin on ischaemic neuronal damage following permanent middle cerebral artery occlusion in the rat. – Naunyn Schmiedebergs Arch. Pharmacol., **360**, 1999, 633-638.

Institute of Experimental Morphology and Anthropology with Museum
Bulgarian Anatomical Society

Acta morphologica et anthropologica, 13
Sofia • 2008

Influence of α_2-Agonists and Antagonists on Acetylcholine Release in the Circular Muscle of Rat Jejunum

R. Kalfin, G. Vanneste, R. Lefebvre**

Institute of Neurobiology, Bulgarian Academy of Sciences, Sofia
**Heymans Institute of Pharmacology, Gent University, Gent, Belgium*

The aim of the present experiments was to measure the release of acetylcholine directly from the circular muscle strips of rat jejunum and to investigate α_2-adrenoceptor agonists and antagonists involvement in this release. The selective α_2-adrenoceptor agonist UK-14,304 (1 μM) significantly inhibited electrically evoked release of [^{3}H]-acetylcholine. This effect was prevented by the α_2-adrenoceptor antagonist rauwolscine (2 μM), suggesting that presynaptic α_2-adrenoceptors are present on cholinergic neurons of the rat jejunum. Both basal and electrically-evoked release of acetylcholine were not affected significantly in the presence of rauwolscine or guanethidine, suggesting that in the rat jejunum sympathetic nerves do not modulate acetylcholine release via the inhibitory α_2-adrenoceptors.

Key words: Acetylcholine release, α_2-adrenoceptors, ileum, jejunum.

Introduction

The small intestine belongs to the affected area in human postoperative ileus [4], and rodent models are used to understand the pathogenesis of the disturbed motility in postoperative ileus. In order to study the influence of operative procedures on gastrointestinal motility, it is important to know its exact regulation under normal conditions. The majority of noradrenergic fibres, innervating the gastrointestinal tract, end on intrinsic enteric neurons rather than on smooth muscle cells, and exert their effect by modulating the activity of intrinsic neurons. In general, noradrenergic activity inhibits non-sphincteric gastrointestinal smooth muscle by inhibition of acetylcholine release from intrinsic excitatory cholinergic motor neurons via α_2-adrenoceptors [7]. This has also been shown at the level of the stomach: α_2- or α_2-like adrenoceptors have been shown to be present on postganglionic cholinergic neurons in the dog gastric fundus [6]. The aim of this study, therefore, was to measure acetylcholine release directly and to investigate the influence of α_2-agonists and antagonists on the electrically induced acetylcholine release in the rat jejunum.

Materials and Methods

Male Wistar rats (250-350 g) were used in the experiments. All animals had free access to water and commercially available rat chow. Rats were sacrificed by stunning and subsequent decapitation. The circular muscle preparations of jejunum were prepared as described before [8]. The release of acetylcholine from jejunum smooth muscle strips was measured directly according to the method described before [5].

Results

The results from 13 experiments with control animals are summarized in Fig. 1. Ninety minutes after starting the superfusion, the spontaneous efflux of [^{3}H]-acetylcholine from the strips, preloaded with [^{3}H]-choline-chloride, reached a steady state. The strips were stimulated twice (S_1 and S_2) for 2 min by application of electrical field stimulation (5 Hz, 40 V, 1 ms). The first stimulation started at 5th sample, while the second stimulation started at 27th sample (Fig. 1). The electrical stimulation (S_1 and S_2) significantly increased the release of [^{3}H]-acetylcholine from the smooth muscle strips (Fig. 1). Pretreatment with 3 μM tetrodotoxin prevented the electrically-stimulated release of [^{3}H]-acetylcholine (Fig. 2), suggesting that [^{3}H]-acetylcholine was released from neuronal elements of the intestine. The selective α_2-adrenoceptor agonist UK-14,304 (1 μM), added 7 min before the second stimulation period, did not alter the basal efflux of [^{3}H]-acetylcholine (data not shown). However, UK-14,304 significantly decreased the amount of [^{3}H]-acetylcholine released upon electrical stimulation (Fig. 3). The α_2-adrenoceptor antagonist rauwolscine (2 μM) prevented the inhibition of the electrically evoked release of [^{3}H]-acetylcholine by UK-14,304 (Fig. 3). Since UK-14,304 was dissolved in 100 %

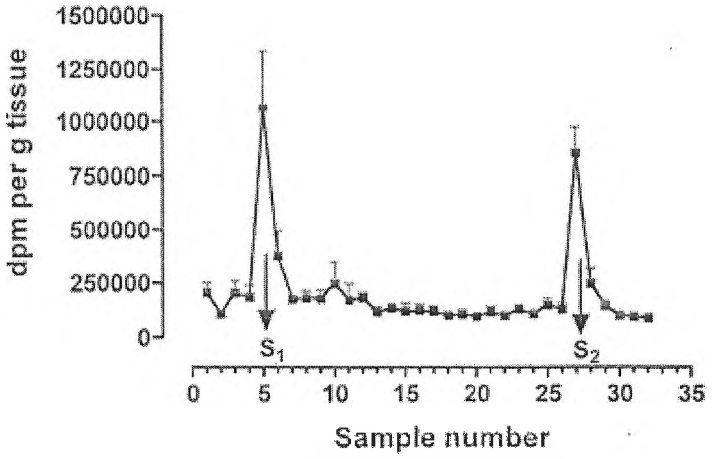

Fig. 1. Spontaneous and electrically-induced release of [^{3}H]-acetylcholine in circular smooth muscle strips from rat jejunum. The strips were stimulated twice (S_1 and S_2) for 2 min by application of electrical field stimulation (5 Hz, 40 V, 1 ms). The first stimulation started at 5th sample (13th min), while the second stimulation started at 27th sample (79th min). Results are expressed as disintegrations per minute (dpm), and normalized to the gram weight of the tissue. The means ± SEM of 13 experiments in the control rats are presented

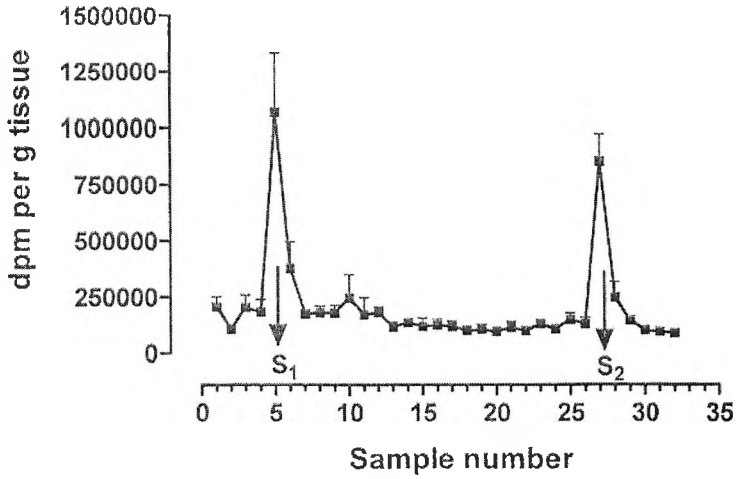

Fig. 2. Effect of tetrodotoxin (TTX) on [^{3}H]-acetylcholine release from circular smooth muscle strips of rat jejunum. The strips were stimulated twice (S_1 and S_2) for 2 min by application of electrical field stimulation (5 Hz, 40 V, 1 ms). Tetrodotoxin (3 μM) was added 10 min (24th sample) before S_2. Results are expressed as disintegrations per minute (dpm), and normalized to the gram weight of the tissue. The means ± SEM of 5 experiments are presented

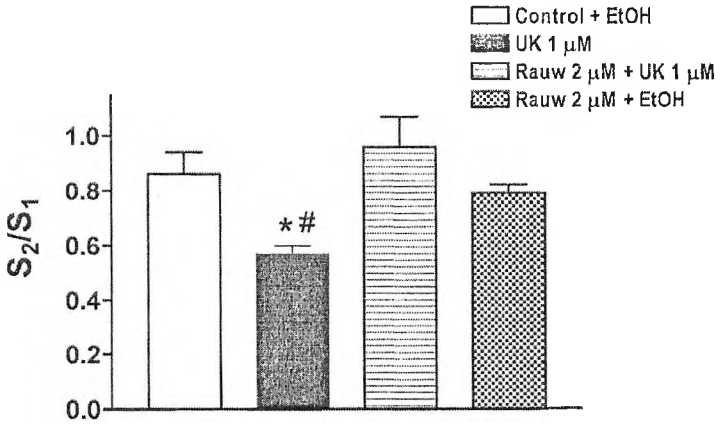

Fig. 3. Effects of UK-14,304 (UK), rauwolscine (rauw), and UK-14,304 in the presence of rauwolscine, on the [^{3}H]-acetylcholine release from circular smooth muscle strips of rat jejunum. The strips were stimulated twice (S_1 and S_2) for 2 min by application of electrical field stimulation (5 Hz, 40 V, 1 ms). The electrically evoked [^{3}H]-acetylcholine efflux is expressed as S_2/S_1 ratio for each muscle strip. Rauwolscine (2 μM, dissolved in distilled water) was added 37 min before S_2, while ethanol (4 μl) or UK-14,304 (1 μM, dissolved in 100 % warm ethanol) were added 7 min before S_2. Each column represents the mean ± SEM (n = 6), $^*P < 0.05$ versus control group; $^\#P < 0.01$ versus rauwolscine + UK-14,304 group

warm (37 °C) ethanol, the same amount of ethanol (4 ml) was added 7 min before the second stimulation to both control and rauwolscine-treated strips.

Discussion

Several investigators have reported that presynaptic inhibitory α_2-adrenoceptors are presented on cholinergic nerves in various gastrointestinal tissues and in other tissues [2]. In this study, the α_2-adrenoceptor agonist UK-14,304 significantly decreased the electrically-induced efflux of [^{3}H]-acetylcholine in the rat jejunum. This inhibitory action of UK-14,304 was completely antagonized by rauwolscine, a selective α_2-adrenoceptor antagonist, indicating that cholinergic nerves of the rat jejunum are also endowed with α_2-adrenoceptors, causing inhibition of transmitter acetylcholine release. To study whether endogenous noradrenaline is able to inhibit acetylcholine release via the presynaptic α_2-adrenoceptors on the cholinergic neurons, we performed experiments also in the absence of guanethidine. Both basal and electrically-evoked release were not lower compared to the release in the presence of guanethidine, suggesting that in rat jejunum sympathetic nerves do not modulate the release of acetylcholine via the inhibitory α_2-adrenoceptors within the experimental conditions and/or that electrical field stimulation does not lead to the release of noradrenaline. This was confirmed when rauwolscine was added between S_1 and S_2: it was without effect on the electrically-evoked release of [^{3}H]-acetylcholine. Also in the guinea-pig ileum and rat trachea [1, 3] no evidence to suggest that endogenous noradrenaline influences acetylcholine release was obtained. In conclusion, our results suggest: i) The presence of presynaptic muscarinic and α_2-adrenoceptors on the cholinergic neurons in the rat jejunum; ii) Endogenous noradrenaline is not inhibiting acetylcholine release via the presynaptic α_2-adrenoceptors.

Acknowledgements: This study was supported by Grant L-1305/03 from the National Science Fund, Sofia, Bulgaria.

References

1. Alberts, P., L. Stjarne. Facilitation, and muscarinic and alpha-adrenergic inhibition of the secretion of 3H-acetylcholine and 3H-noradrenaline from guinea-pig ileum myenteric nerve terminals. — Acta Physiol. Scand., **116**, 1982, 83-92.
2. de Ponti, F., C. Giaroni, M. Cosentino, S. Lecchini, G. Frigo. Adrenergic mechanisms in the control of gastrointestinal motility: from basic science to clinical applications. — Pharmacol. Ther., **69**, 1996, 59-78.
3. Fabiani, M. E., D. T. Dinh, D. F. Story. Interaction of the rennin-angiotensin system, bradykinin and sympathetic nerves with cholinergic transmission in the rat isolated trachea. — Br. J. Pharmacol., **122**, 1997, 1089-1098.
4. Holte, K., H. Kehlet. Postoperative ileus: a preventable event. — Br. J. Surg., **87**, 2000, 1480-1493.
5. Leclere, P. G., R. A. Lefebvre. Influence of nitric oxide donors and of the α_2-agonist UK-14,304 on acetylcholine release in the pig gastric fundus. — Neuropharmacology, **40**, 2001, 270-278.
6. Lefebvre, R. A., J. L. Willems, M. G. Bogaert. Inhibitory effect of dopamine on canine gastric fundus. — Naunyn Schmiedebergs Arch. Pharmacol., **326**, 1984, 22-28.
7. McIntyre, A. S., D. G. Thompson. Review article: adrenergic control of motor and sensory function in the gastrointestinal tract. — Aliment Pharmacol. Ther., **6**, 1992, 125-142.
8. Vanneste, G., P. Robberecht, R. A. Lefebvre. Inhibitory pathways in the circular muscle of rat jejunum. — Br. J. Pharmacol., **143**, 2004, 107-118.

Institute of Experimental Morphology and Anthropology with Museum
Bulgarian Anatomical Society

Acta morphologica et anthropologica, 13
Sofia • 2008

The Muscarinic Cholinergic Receptor-stimulated Signal Transduction Cascade is Affected by Interleukin-1β

*L. Kirazov, M. Gniezdzinska**, E. Kirazov, A. Szutowicz**, R. Schliebs**

Institute of Experimental Morphology and Anthropology with Museum, Bulgarian Academy of Sciences, Sofia
**Paul Flechsig Institute for Brain Research, University of Leipzig, Germany*
***Clinical Biochemistry, Medical University of Gdansk, Poland*

β-amyloid plaque-mediated glial up regulation of the pro-inflammatory cytokine interleukine-1β (IL-1β) has been assumed to contribute to the impairments of cortical cholinergic neurotransmission observed in Alzheimer's disease (AD). To test for this hypothesis two neuroblastoma cell lines, a murine cholinergic septal cell line SN56 and the human SH-SY5Y cell line, were exposed to IL-1β followed by agonist stimulation of muscarinic acetylcholine receptors. By detecting key molecules of both signal transduction cascades (phosphatidyl inositol breakdown, protein kinases, transduction factors, cholinergic enzyme expression) the downstream levels of interaction of both signal cascades should be revealed.

Key words: interleukine-1β, cholinergic signal transduction, Alzheimer's disease.

Introduction

In AD there is increasing evidence that neurotoxicity is mediated also through inflammatory processes. These processes involve activation of microglia by amyloid-β peptide leading to release of pro-inflammatory cytokines including IL-1β among others. Neurotoxic processes mediated by these cytokines may include direct neuronal death by enhancement of apoptosis, decreased synaptic function, and inhibition of hippocampal neurogenesis.

One of the currently held hypothesis is that an inflammatory cycle drives AD pathology [1, 2]. Feedback and feed forward effects of cytokines on glial cells and neurons amplify initial stimuli into rampant runaway responses.

In this study we show that IL-1β affects the cholinergic transduction cascade.

Materials and Methods

Cell culture. Human neuroblastoma SH-SY5Y cells were cultured in Dubelco's modified Eagle's medium. One day after transfer to culture dishes (10^5 cells/dish) the cells were incubated for 8 days with 10 μM trans-retinoic acid.

Culturing of murine. SN56.B5.G4 cells was performed in the same medium and under similar conditions as described for SH-SY5Y cells (for details, see [3]).

Stimulation experiments. Cultured differentiated cells were incubated with varying concentrations of IL-1β for 1 to 24 h as indicated, followed by stimulation of the cholinergic receptors by varying concentrations of the agonist carbachol for 1 h.

Results and Discussion

Effect of IL-1β on the muscarinic acetylcholine receptor (mAChR)-mediated cascade. Preexposure of SN56 cells to IL-1β for one hour did not affect the carbachol-stimulated formation of inositol phosphates (IP; Table 1), but significantly induced the expression of acetylcholinesterase (AChE) activity (Table 2), while cholineacetyltransferase (ChAT) activity was not affected by IL-1β. Interestingly, stimulation of IL-1β-preexposed cells with 1 mM carbachol resulted also in upregulation of AChE activity but to a lower extent as compared to incubations in the absence of carbachol (Tabe 2), indicating interactive mechanisms.

T a b l e 1. Pre-exposure of SN56 and SH-SY5Y cells to IL-1β affects the mAChR-stimulated formation of IP_3

Treatment	Percentage changes of IP_3 level over basal level	
	SN56	SH-SY5Y
100 mM carbachol	328±47	n.d.
1 mM carbachol	187±12	280±48
1 ng/ml IL-1β	n.d.	150±40
1 ng/ml IL-1β + 100 mM carbachol	294±28	n.d.
1 ng/ml IL-1β + 1000 mM carbachol	n.d.	340±49

n.d. — not determined.

T a b l e 2. Pre-exposure of SN56 and SH-SY5Y cells to IL-1b affects the mAChR-mediated up-regulation of activities of AChE and ChAT

Treatment	Percentage changes over basal level			
	SN56		SH-SY5Y	
	AChE	ChAT	AChE	ChAT
1 ng/ml IL-1β for 1 h	42±5	-4±5	19±10	23±33
100 ng/ml IL-1β for 1 h	n.d.	n.d.	18±9	n.d.
100 mM carbachol	n.d.	n.d.	-39±2	n.d.
1 mM carbachol	18±3	-1±4	8±1	13±41
1 ng/ml IL-1β + 1 mM carbachol	21±2	19±10	-1±4	27±13

Effects of mAChR stimulation. Stimulation of SN56 cells with the non-subtype-selective mAChR agonist carbachol resulted in dose-dependent increases in the level of IP_3 (Table 3), as well as in translocation of protein kinase Cα to the membrane fraction (Table 4).

The activities of AChE and ChAT of SN56 cells were increased after stimulation with carbachol, while with increasing concentrations of carbachol the cholinergic enzyme activities in SH-SY5Y cells approached the control levels (Table 5).

The carbachol-mediated effect on cholinergic enzyme activities could not be prevented by blocking the M1-mAChR subtype with pirenzepine. However, the non-

selective mAChR antagonist atropine alleviated them (Table 6) suggesting an effect through the M2-mAChR signaling cascade.

T a b l e 3. Formation of IP_3 following stimulation of SN56 or SH-SY5Y cells with carbachol for 30 min

Carbachol	Percentage increase of IP_3 over basal level	
	SN56	SH-SY5Y
100 mM	330±80	n.d.
1000 mM	186±26	280±51

T a b l e 4. Translocation of proteinkinase Cα to the membrane fraction following stimulation of SN56 or SH-SY5Y cells with carbachol for 30 min

Carbachol	Percentage of translocated protein kinase Cα over basal level	
	SN56	SH-SY5Y
1 mM	5±4	n.d.
10 mM	34±14	n.d.
100 mM	70±10	n.d.
1000 mM	48±4	300±40

T a b l e 5. Changes in the activities of AChE and ChAT following stimulation of SN56 and SH-SY5Y cells with increasing concentrations of mAChR agonists for 60 min

Treatment	Percentage changes over basal level			
	SN56		SH-SY5Y	
Carbachol	AChE	ChAT	AChE	ChAT
1 mM	116±6	80±8	n.d.	n.d.
10 mM	79±16	40±12	n.d.	n.d.
100 mM	78±4	30±10	-31±6	n.d.
1000 mM	32±4	6±3	8±1	13±5
Talsaclidine 50 mM	n.d.	-6±4	19±10	n.d.

T a b l e 6. Changes of the activities of AChE and ChAT following stimulation of SN56 cells with carbachol for 60 min in the presence of various antagonists of mAChR

mAChR drug	Percentage changes of enzyme activity over basal level	
	AChE	ChAT
10 mM carbachol	80±8	n.d.
+25 mM pirenzepine	110±14	51±7
+50 mM atropine	5±4	4±5
+100 mM atropine	142±15	9±8
+25 mM pirenzepine	58±7	-22±14
+50 mM atropine	-18±11	-27±16

Conclusions. Cholinergic enzyme activities are controlled through both M1- and M2-mAChR activation but in opposite directions: induction of enzyme activity is mediated through M2-mAChR, while stimulation of M1-mAChR inhibits or does not af-

fect activity as compared to the control level (Table 5). This was proved by the stimulation of cells with the M1-mAChR-specific agonist talsaclidine, which kept the cholinergic enzyme activities suppressed (Table 5).

These presented data strongly support the suggestion that chronic IL-1β exposure interferes with the muscarinic cholinergic receptor-mediated signaling cascade which may contribute to the cholinergic deficits in AD.

References

1. M c G e e r, E. G., P. L. M c G e e r. The importance of inflammatory mechanisms in Alzheimer's disease. — Exp. Gerontol., **33**, 1998, 371-378.
2. M c G e e r, P. L., E. G. M c G e e r. Inflammation of the brain in Alzheimer's disease: implications for therapy. — J. Leukoc. Biol., **65**, 1999, 409-415.
3. J a n k o w s k a, A., B. M a d z i a r, M. T o m a s z e w i c z, A. S z u t o w i c z. Acute and chronic effects of aluminium on acetyl-CoA and acetylcholine metabolism in differentiated and nondefferentiated SN56 cholinergic cells. — J. Neurosci. Res., **62**, 2000, 615-622.

Institute of Experimental Morphology and Anthropology with Museum
Bulgarian Anatomical Society

Acta morphologica et anthropologica, 13
Sofia • 2008

In Vivo Modulation of Catecholamines Release from Cortex and Hippocampus by Vasoactive Intestinal Peptide

M. Lazarova, R. Kalfin, P. Mateeva, L. Mateva, S. Petrov*, V. Lozanov**

Institute of Neurobiology, Bulgarian Academy of Sciences, Sofia
**Department of Chemistry and Biochemistry, Medical University, Sofia*

The aim of this work was to collect data regarding *in vivo* effects of vasoactive intestinal peptide (VIP), administered locally through the microdialysis probe, on catecholamines release from the cortex and hippocampus. Studies were performed in awake, male Wistar rats by means of transversal microdialysis technique and high-performance liquid chromatography (HPLC). VIP (0.1 to 10 nM) decreased in a dose-dependent manner the release of endogenous dopamine in cortex, while in hippocampus its effect on catecholamines release was stimulatory. Our results suggest that VIP affects dopaminergic neurotransmission both in hippocampus and cortex, probably via two different mechanisms.

Key words: VIP , dopamine, cortex, hippocampus, microdialysis.

Introduction

Vasoactive intestinal peptide (VIP) is a 28-amino acid peptide. It is widely distributed in the central and peripheral nervous system, showing rich profile of biological activities - from neurotransmission to neuromodulation and neurotrophic properties. The cerebral cortex and hippocampus have the highest ratio of VIP immunoreactive neurons and VIP receptors. VIP has potential to be used in therapy of Parkinson's disease (PD) because of its potent antioxidant, antiinflammatory and neuroprotective activity [4, 2]. However, there are not enough data regarding effects of VIP on dopaminergic neurotransmission in normal and PD animal models. In order to study the action of VIP in Parkinson's disease model, it is important to know its effect under normal conditions. The aim of this study, therefore, was to investigate the effect of VIP *in vivo* on catecholamines (dopamine, norepinephrine and epinephrine) release in hippocampus of freely moving rats. In additional experiments effect of VIP on dopamine release in rat cortex has been investigated.

Materials and Methods

Adult male Wistar rats (250-300 g) were housed on a 12 h/12 h light/dark cycle at a constant temperature and free access to food and water. The rats were anaesthetized

with chloral hydrate (400 mg/kg i.p.) and placed in stereotaxic apparatus. Microdialysis tubes (molecular weight cut-off 15 000 Da) were inserted transversally into hippocampus (AP — 3.3 mm posterior from the bregma and H +3.3 mm) or cortex (AP — 1.0 mm posterior from the bregma and H +2.0 mm). One day after surgery, the inlet of the microdialysis probe was connected to a microperfusion pump and perfused with Ringer solution at a constant rate of 2 μl/min. After 1 h stabilization period, during which the animals were perfused without collecting the dialysate, samples were collected at 40-min intervals. After collecting the first four samples to measure the basal outflow, drugs (dissolved in Ringer solution) were administered locally through the dialysis membrane for 80 min. Dialysates, derived from hippocampus, were analyzed for dopamine, norepinephrine and epinephrine using high-performance liquid chromatography apparatus with fluorescent detector. Separation was achieved on a column Hypersil C18 bonded phase, 5 μM particle size (Hewlett-Packard). Data acquisition and processing were carried out with program DataApex (Czech Republic). The peak area of the external standard was used to quantify the sample peak. At the end of experiment the rats were anaesthetized with chloral hydrate (800 mg/kg, i.p.) and sacrificed by decapitation. The brain was rapidly removed and placed in a vial containing 10 ml of 9 % formaldehyde solution in phosphate buffer. Three days later thin hippocampal or cortical slices were cut to verify the position of the dialysis membrane. Data obtained from rats in which the dialysis membrane was positioned outside of the cortical or hippocampal brain structure were discarded (< 5 %).

Results and Discussion

After 60 min recovery period basal extracellular levels of dopamine, norepinephrine and epinephrine in microdialysis perfusate from hippocampus were 6.68 pmol/40 min, 5.90 pmol/40 min and 15.84 pmol/40 min, respectively. Basal level of dopamine in cortex was 2.98 pmol/40 min. Catecholamine levels remained relatively constant from one collection period to the next through each experiment (up to 6th hour for hippocampus, and up to 8th hour for cortex). In cortex VIP (0.1, 1 and 10 nM) was applied for 80 min locally through microdialysis probe. The neuropeptide induced dose-dependent decrease in extracellular dopamine levels, the most effective concentration being 0.1 nM VIP (Fig. 1). The maximum decrease by 65.59 % was observed about 80 min after VIP administration (Fig. 1A). On the contrary, applied locally through microdialysis membrane in hippocampus, VIP (0.1, 1 and 100 nM) induced an increase of extracellular dopamine, norepinephrine and epinephrine levels (Fig. 2). The maximum increase of 59.61 % and 38.19 % for dopamine and epinephrine, respectively, was observed at concentration of 1 nM VIP (Figs. 2A, 2B). VIP (100 nM) enhanced the norepinephrine release by 108.04 %, while after 1 nM VIP the increase was only 26.11 % as compared to the controls (Fig. 2C). There are not enough data in the literature regarding interaction between dopaminergic and VIPergic neurotransmitter systems, but a suggestion that VIP facilitates the dopamine metabolism in the brain has been made [3]. Our results suggest that VIP can modulate dopamine neurotransmitter system in hippocampus and cortex. We observed different effects of VIP on dopamine release in those structures: in hippocampus VIP provoked an increase in extracellular catecholamine levels, including dopamine, while in cortex the peptide decreased the release of dopamine. In the cortex VIP exhibits over 70 % co-localization with acetylcholine and 30 % co-localization with γ-aminobutyric acid (GABA) [1], while in hippocampus one third to one

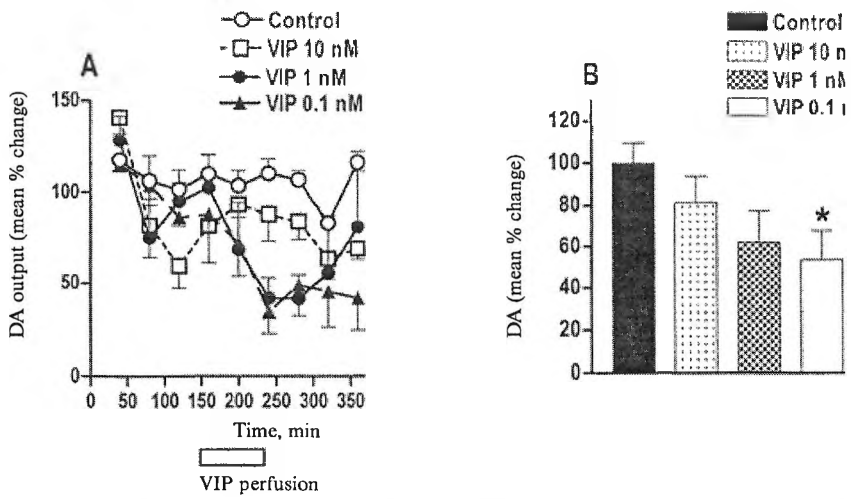

Fig. 1. Effect of vasoactive intestinal peptide (VIP) on dopamine (DA) release from cortex of freely moving rats. Dialysate samples were collected every 40 min. The release of DA was expressed as per cent change over the mean of the first three basal samples. VIP (0.1, 1 and 10 nM) was administered for a period of 120 min after collection of the first three basal samples (A); Bars in Fig. 1B represent mean percent change of area under the curve in Fig. 1A, calculated from time 160 min to time 360 min. Results are expressed as mean ± SEM of at least four experiments in each group. Differences among groups were evaluated by Student's t-test, $*P < 0.05$ versus control

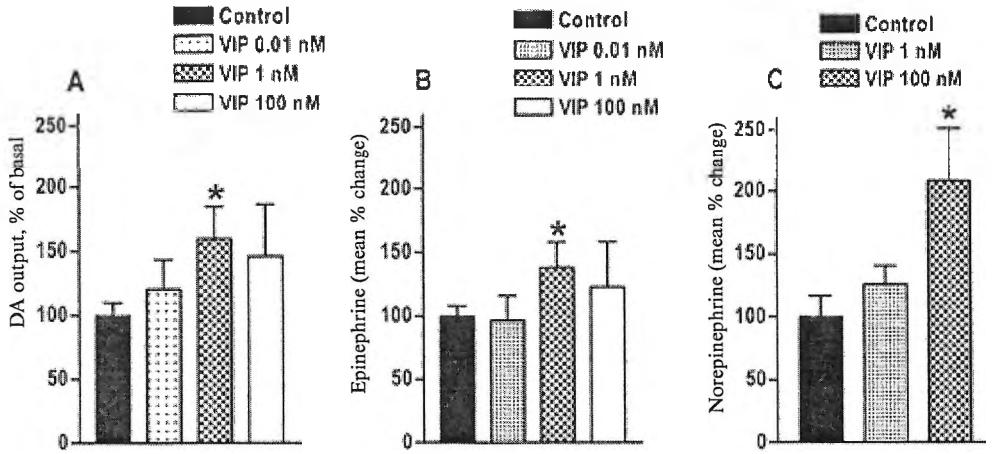

Fig. 2. Effect of vasoactive intestinal peptide (VIP) on dopamine (A), epinephrine (B) and norepinephrine (C) release from hippocampus of freely moving rats. Dialysate samples were collected every 20 min. The release of catecholamines was expressed as per cent change over the mean of the first four basal samples. VIP (1 and 100 nM) was administered for a period of 40 min after collection of the first four basal samples. Results are expressed as mean ± SEM of at least four experiments in each group. Differences among groups were evaluated by Student's t-test, $*P < 0.05$ versus control

half of the VIP-ergic neurons contain only GABA and/or cholecystokinin [5]. Taken together, the above-mentioned data and our results suggest that probably two different mechanisms underlie the effect of VIP on dopamine release in rat hippocampus and cortex.

Acknowledgements: This study was supported by National Science Fund, Sofia, Bulgaria (Grants MU-L-1502/05 and L-1305/03).

References

1 Bayraktar, T., J. F. Staiger, L. Acsady, C. Cozzari, T. F. Freund, K. Zilles. Co-localization of vasoactive intestinal polypeptide, gamma-aminobutyric acid and choline acetyltransferase in neocortical interneurons of the adult rat. — Brain Res., **757**, 1997, 209-217.

2. Delgado, M., D. Ganea. Neuroprotective effect of vasoactive intestinal peptide (VIP) in a mouse model of Parkinson's disease by blocking microglial activation. — FASEB J., **17**, 2003, U568-585.

3. Itoh, S., G. Katsuura, A. Takashima. Effect of vasoactive intestinal peptide on dopaminergic system in the rat brain. — Peptides, **9**, 1988, 315-317.

4. Offen, D., Y. Sherki, E. Melamed, M. Fridkin, D. E. Brenneman, I. Gozes. Vasoactive intestinal peptide (VIP) prevents neurotoxicity in neuronal cultures: relevance to neuroprotection in Parkinson's disease. — Brain Res., **854**, 2000, 257-262.

5. Sloviter, R. S. Decreased hippocampal inhibition and a selective loss of interneurons in experimental epilepsy. — Science, **235**, 1987, 73-76.

Institute of Experimental Morphology and Anthropology with Museum
Bulgarian Anatomical Society

Acta morphologica et anthropologica, 13
Sofia • 2008

Lipid Composition of Mitochondrial Membrane in Ischemic Rat Brain

E. Petrova, A. Dishkelov, E. Vasileva

Institute of Experimental Morphology and Anthropology with Museum, Bulgarian Academy of Sciences, Sofia

In this study, we report lipid changes in brain mitochondria in a rat model of cerebral ischemia. We found an increase of total phospholipids, cholesterol, glycolipids and free fatty acids (FFAs) with the largest increase of the cholesterol and glycolipids — 14 and 6 times the control values, respectively. These changes indicate a disturbance of lipid metabolism and may be interpreted as a physiological adaptive response to ischemia.

Key words: lipids, cerebral ischemia, mitochondria, rat brain.

Introduction

It has been established that alterations in lipid metabolism are key event that contributes to neuronal death in cerebral ischemia [4]. The studying of pathogenic mechanisms on brain subcellular level is of great interest because membranes and membrane-associated enzymes have a crucial role in energy metabolism. The relationship between the membrane lipid environment and its intrinsic enzymes is well documented in mitochondrial membranes [2]. It is known that mitochondria are responsible for the energy state of the cell. The reduced supply of oxygen during ischemia results in ATP depletion in brain, loss of ion homeostasis, changes in calcium metabolism and release of free radicals [9, 11].

The aim of the present investigation is to evaluate the level of phospholipids, cholesterol, glycolipids and free fatty acids in mitochondrial membrane in rat model of cerebral ischemia.

Materials and Methods

Three-month-old male Wistar rats were used in the experiment. Animals were subjected to cerebral ischemia according to the model of S m i t h et al. [12] with minor modifications. Mitochondrial subcellular fraction was isolated according to the method described by Venkov [13]. Lipids were extracted according to the technique

described by K a t e s [14]. The content of cholesterol and FFAs was determined by gas chromatography as we previously described [6, 7]. The content of total glycolipids was determined according to H a m i l t o n et al. [3]. Total phospholipids were determined by the method of B a r t l e t t [1]. Glycolipid and phospholipid classes were separated by thin-layer chromatography. The Perkin-Elmer scanning spectrophotometer was used to estimate the concentration of migrated spots.

The data were analyzed with Student's t-test.

Results and Discussion

In our study we examined the ischemia-induced changes of four lipid classes in rat brain mitochondria. The total phospholipid content was increased by 6% (from 36.6±0.05 to 38.75±0.16 mg/g/ml, $p<0.001$). The total cholesterol increased 14-fold (from 0.54±0.07 to 7.4±0.17 mg/g/ml, $p<0.001$). Ischemia caused a 41% increase in the content of total FFAs (from 35.67±0.2 to 50.25±0.1 mg/g/ml, $p<0.001$). The content of total glycolipids rose 6-fold (from 0.48±0.05 to 2.88±0.09 mg/g/ml, $p<0.001$). The changes in the percentage of individual phospholipids, sterols, glycolipids and FFAs are given in Fig. 1, 2, 3 and 4, respectively.

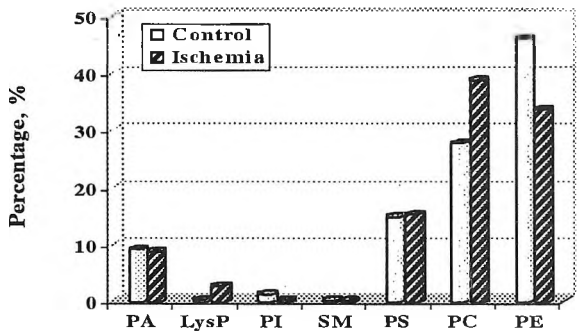

Fig. 1. Changes of the phospholipid content in brain mitochondria after cerebral ischemia. PA — phosphatidic acid, SM — sphingomyelin

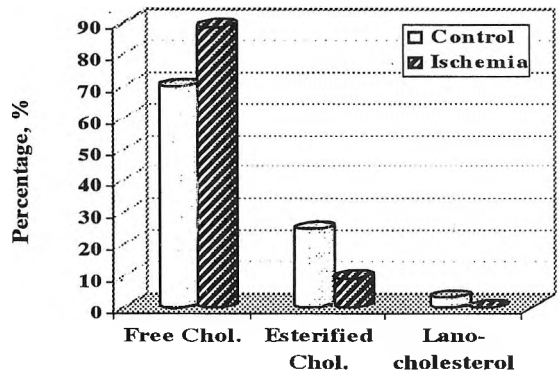

Fig. 2. Changes of the cholesterol content in brain mitochondria after cerebral ischemia

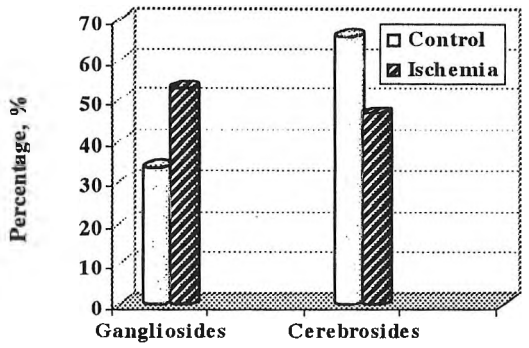

Fig. 3. Changes of the glycolipid content in brain mitochondria after cerebral ischemia

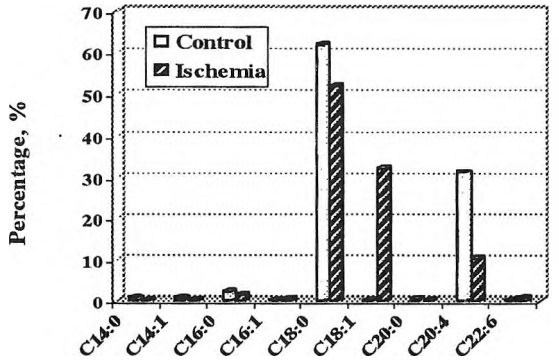

Fig. 4. Changes of the free fatty acid content in brain mitochondria after cerebral ischemia

The content of phosphatidylserine (PS), phosphatidylcholine (PC) and lysophospholipids (LysP) was increased which was most pronounced in LysP — more than 8-fold. The concentration of phosphatidylethanolamine (PE) and phosphatidylinositol (PI) was decreased by 23% and 70%, respectively. Probably the mitochondrial Ca^{2+}-dependent phospholipase A_2 is responsible for the mitochondrial membrane damage, because there are data about its involvement in the turnover of membrane phospholipids and in the process of Ca^{2+} release from mitochondria [8]. PE and PC accounted for 72% of the total phospholipids and it can be suggested that the high amount of unsaturated molecular species in their composition make them appropriate substrates for mitochondrial phospholipase A_2.

The concentration of the free and esterified cholesterol was increased 17-fold and 5-fold, respectively. Probably the hydrolysis of phospholipids disturbs the integrity of the membrane which leads to the release of active cholesterol that can easily be esterified with fatty acid. The high concentration of sterol esters can apparently be explained with a role of the ester to serve as a carrier and storage site for the otherwise toxic free fatty acids [10].

The content of gangliosides and cerebrosides increased 9-fold and 4-fold, respectively. Gangliosides are considered neuroprotectors [5] and the high content may be interpreted as a defensive and compensatory mechanism against the ischemic shock.

The concentration of $C_{16:0}$ and $C_{18:0}$ was increased by 5% and 18%, respectively. The content of $C_{20:0}$ and $C_{20:4}$ was decreased by 80% and 18%, respectively. A notable observation was the accumulation of $C_{16:1}$ and $C_{18:1}$. We found $C_{22:6}$ too, which appears to be a neuroprotector.

In conclusion, our results reveal that the ischemic process disrupts to a great extent the lipid metabolism in brain mitochondria. These changes are probably associated with impaired energy metabolism and may indicate the disturbances in lipid biosynthesis.

Acknowledgment: This study was supported by the National Science Fund of Bulgaria (NSFB) under Contract MU-L-1512/05.

References

1. Bartlett, G. R. Phosphorus assay in column chromatography. — J. Biol. Chem., **234**, 1959, No3, 466-468.
2. Daum, G. Lipids of mitochondria. — Biochim. Biophys. Acta, **822**, 1985, 1-42.
3. Hamilton, P. B. A spectrometric determination of glycolipids. — Anal. Chem., **28**, 1956, 557-565.
4. Lipton, P. Ischemic cell death in brain neurons. — Physiol. Rev., **79**, 1999, 1431-1568.
5. Mahadik, S. P., S. K. Karpiak. Gangliosides in treatment of neural injury and disease. — Curr. Trends Rev., **15**, 2004, No4, 337-360.
6. Petrova, E., A. Dishkelov, E. Vasileva. Changes of the cholesterol content in rat brain subcellular fractions in experimental model of cerebral ischaemia. — Compt. Rend. Bulg. Acad. Sci., **58**, 2005, No7, 839-842.
7. Petrova, E., A. Dishkelov, L. Venkov, E. Vasileva. Changes in free fatty acids in rat brain subcellular fractions after cerebral ischemia. — Acta Morphol. et Anthropol., **11**, 2006, 9-16.
8. Pfeiffer, D. R., P. C. Schmid, M. C. Beatrice, H. H. O. Schmid. Intramitochondrial phospholipase activity and the effects of Ca^{2+} plus N-ethylmaleimide on mitochondrial function. — J. Biol. Chem., **254**, 1979, 11485-11494.
9. Rabin, O., J. Deutsch, E. Grange, K. D. Pettigrew, M. C. J. Chang, S. I. Rapoport, A. D. Purdon. Changes in cerebral acyl-CoA concentrations following ischemia-reperfusion in awake gerbils. — J. Neurochem., **68**, 1997, 2111-2118.
10. Ramsey, R. B., A. N. Davison. Steryl esters and their relationship to normal and diseased human central nervous system. — J. Lipid Res., **15**, 1974, 249-255.
11. Siesjö, B. K., F. Bengtsson. Calcium fluxes, calcium antagonists, and calcium-related pathology in brain ischemia, hypoglycemia and spreading depression: a unifying hypothesis. — J. Cereb. Blood Flow Metab., **9**, 1989, 127-140.
12. Smith, M. -L., G. Bendek, N. Dahlgren, I. Rosén, T. Wieloch, B. K. Siesjö. Models for studying long-term recovery following forebrain ischemia in the rat. 2. A 2-vessel occlusion model. — Acta Neurol. Scand., **69**, 1984, 385-401.
13. Венков, Л. Получаване на обогатени фракции на елементи, изграждащи нервната тъкан. — Съвр. пробл. невроморфол., **11**, 1983, 1-60.
14. Кейтс, М. Техника липидологии. М., Мир, 1975. 322 с.

Institute of Experimental Morphology and Anthropology with Museum
Bulgarian Anatomical Society

Acta morphologica et anthropologica, 13
Sofia • 2008

Morphological Expression of Antiphospholipid Syndrome

Mary Gantcheva

Department of Dermatology, Medical Faculty, Sofia

We reviewed the histopathological findings of skin lesions of 18 patients with Antiphospholipid syndrome. The cutaneous manifestations were as follows: livedo reticularis, pseudovasculitis lesions, livedoid vasculitis-like ulcers, thrombophlebitis, cutaneous gangrene and necrosis. Investigating these different skin markers of the disease we were searching for a specific finding, which could be typical for the disease. However, a constant and characteristic feature was occlusive vasculopathy, leading to vascular thrombosis of dermal and subcutaneous vessels. It was demonstrated in all specimens from these quite different skin lesions.

Key words: Antiphospholipid syndrome, Livedo reticularis, Livedo vasculitis, morphology, histopathology.

Introduction

Antiphospholipid syndrome (APS) is a relatively "young" syndrome and a multisystem disease. Clinically it is characterized by venous and arterial thromboses, recurrent fetal losses, accompanied by moderate thrombocytopenia in the presence of positive lupus anticoagulant (LA), elevated anticardiolipin antibodies (aCL), or both of them. Patients suffering from this syndrome have to undergo one clinical test plus one laboratory test during the course of the disease. Laboratory findings produced by two consecutive blood analyses at 3 month intervals should confirm the clinical picture.

APS may arise as a primary disease in patients who have no clinical or laboratory evidence of another pathologic condition: primary APS, or may be associated with other diseases: secondary APS. Secondary APS is often associated with systemic lupus erythematosus. However, APS may develop in the context of autoimmune diseases, malignancies, drug induced and infectious diseases. LA recognize lipid-bound (human) prothrombin [1]. In this way they inhibit the phospholipid-dependent coagulation reactions [2]. ACL are directed towards β2-Glycoprotein I (β2-GPI) bound to an anionic lipid surface [3]. They are detected by solid phase ELISA or by radioimmunoassay systems employing cardiolipine as coated antigen.

The skin lesions of APS are quite heterogenous. The most characteristic clinical sign is a persistent cyanotic mottling of the skin, affecting the extremities and the

trunk which is known as livedo reticularis. Vasculitic lesions, skin infarcts, ulcerations of different types, thrombophlebities, peripheral gangrene and widespread necrosis are other dermatological aspects of the disease [4].

We reviewed the histopathological findings of different skin lesions in 18 patients with APS, hoping to find a specific morphological feature.

Materials and Methods

We have studied the histopathological findings in 18 patients with APS, diagnosed according to clinical and laboratory criteria. Patients with the skin manifestation of livedo reticularis were four. Their skin biopsies were performed on either the "holes" of the netlike pattern (i.e., the clinically apparent normal skin in the center of the circle segments) or on the "net" itself (i.e., the discolored red or bluish peripherial border segments). Five patients presented pseudovasculitis lesions: macules, nodules and purpura. Edema and erythema were the signs of thrombophlebitis in two cases. The biopsies from these seven patients were performed from the lesions. Five specimens were taken from the edge of the livedoid vasculitis-like ulcers located on the lower portion of the legs, from the edge of gangrenous lesions located on the finger and on a toe in two other cases. All the histological findings were studied of hematoxylin-eosin staining.

Results

On the peripheral discoloured segments only dermal vessels hyperplasia was present. The biopsies from the centers of the circles were normal or show signs of occlusion-microthrombus in dermal capillaries without vasculitis (Fig. 1). Biopsy from vasculitis-like lesions (subcutaneous nodule) demonstrated thrombosed medium-size vessel surrounded by many small vessels (Fig. 2). Histopathological findings of macula on fingers that clinically were in early stages of development showed hemorrhage and prominent dermal edema. Thromboses were seen in both arteries and veins through-

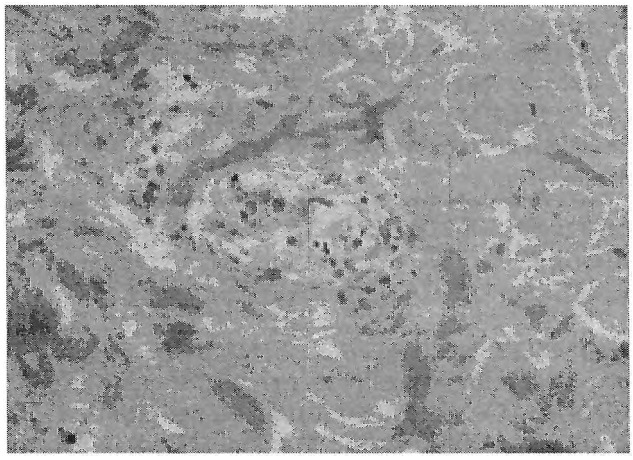

Fig. 1. Microthrombus in dermal vessel. × 300

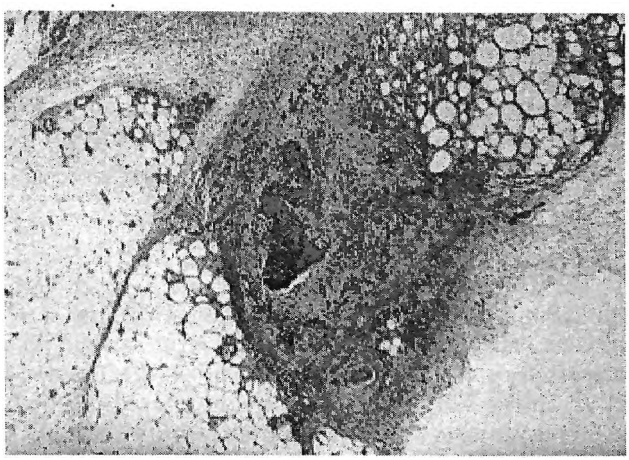

Fig. 2. Mediumsized vessel with thrombosis surrounded by many small vessels. × 150

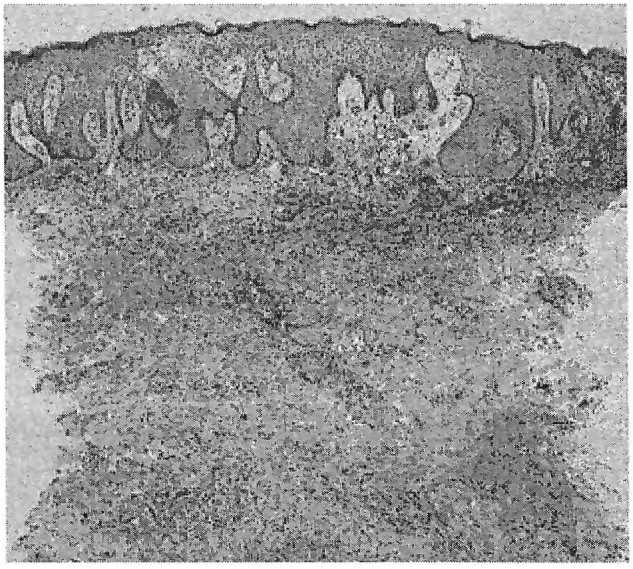

Fig. 3. Prominent dermal edema with disruption of the epidermis from derma. Extensive hemorrhage in papillary derma with thrombosis in vessel. × 15

out the dermis and into the subcutaneous fat (Fig. 3). Lesions that have been present for days showing vascular thrombosis with reactive vascular proliferation and a mild inflammatory infiltrate (Fig. 4). Histological findings from less acute lesions were with thrombosis and fibrinoid deposits in vessels lumens. There were erythrocyte extravasations in fresh lesions and prominent lymphoplasmocytic infiltrate in whole derma (Fig. 5). The specimens from skin gangrene showed non-inflammatory throm-

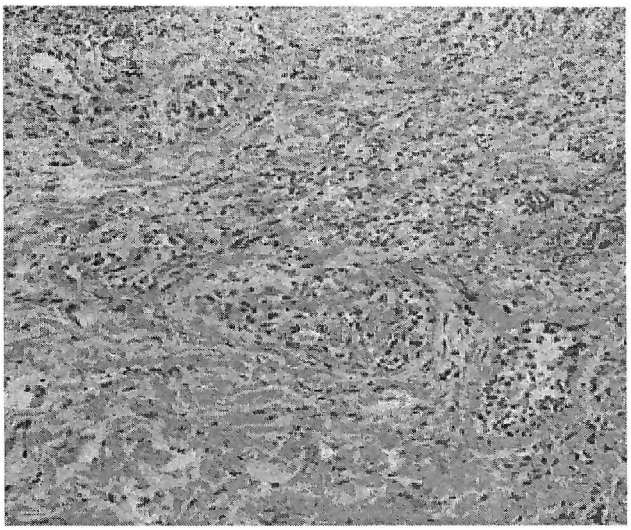

Fig. 4. Thrombosis in the vessels with reactive endothelial proliferation and edema of the endothelial cells. Extensive erythrocyte extravasation. × 150

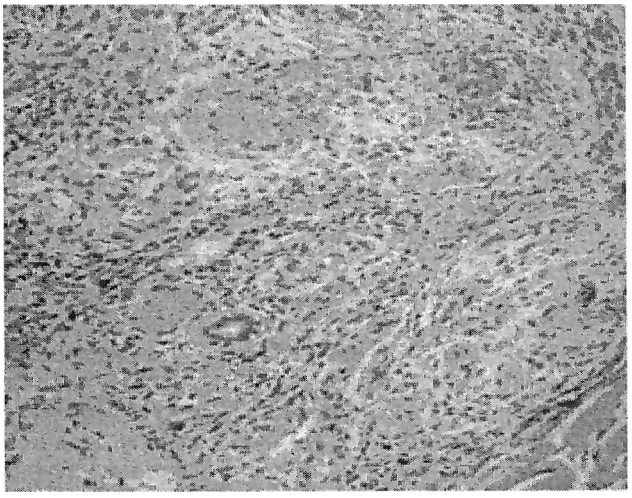

Fig. 5. Thrombosis and fibrin deposits in vessel lumens, erythrocyte extravasation, lymphocytic infiltrate. × 150

bosis of small dermal vessels surrounded by collagen necrosis. In one of the thrombophlebitic biopsy thrombosis was associated with vascular lymphocytic inflammation. Hyalinizing segmental vasculitis with fibrinoid deposits around vessels and thrombosis within were seen in biopsies performed from livedoid vasculitis-like ulcers (Fig. 6). There were no evidence of leucocytoclasia in all five cases.

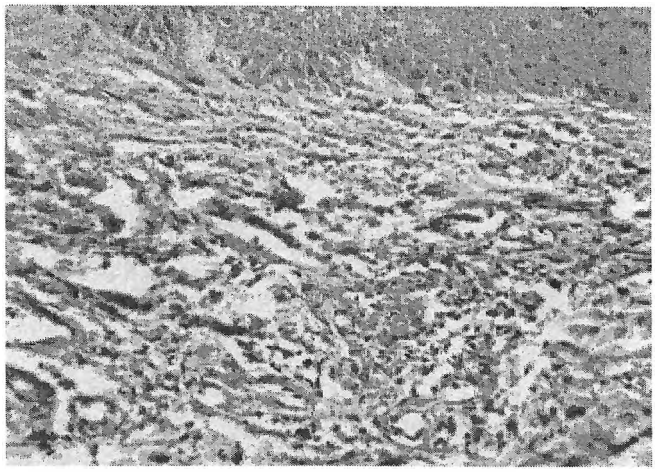

Fig. 6. Hyper and parakeratosis, acantosis, swollen endotel and hyalinization of the vessels, fibrinoid deposits in the lumen vessels and thrombosis within. × 150

Discussion

The main clinical manifestation associated with APS is thrombosis. It occurs in venous and in arterial blood vessels. Leg vein thrombosis and pulmonary emboli are the most frequent events of venous APS related thromboses. Transient ischemic attacks and cerebral infarction are the most frequent arterial damage in arterial APS related thromboses. However, thrombosis has been recorded in almost every vessel of the human body. It was initially thought that only large and medium vessels were affected. It has recently become evident that small vessels might also be involved. Therefore, many diverse clinical manifestations resulting from vascular occlusions in the liver, adrenal glands, lungs, heart, kidney, eyes may be present in APS.

Cutaneous manifestations of APS are extremely diverse and heterogeneous, ranging from minor symptoms to life threatening conditions [5]. We could summarize that the process thrombosis is a constant and characteristic feature in all these skin lesions which were minimal and non traumatic like livedo reticularis, and serious and dangerous, like cutaneous gangrene and necrosis. Discrete lesion on the skin as erythema, edema and purpura could be very important sign and the first clinical sign of a thrombotic disease, leading to extensive skin manifestations. Hyalinizing vasculitis, which is typical for livedo vasculitis must be included in the spectrum of vasoocclusive vasculopathy and could be a marker for underlying thrombooclusive process, such as APS.

In conclusion, we have demonstrated that in very different skin lesions, vascular thrombosis could be found and this should alert the physicians to think for this rare and in some cases catastrophic disease—APS.

References

1. Bevers, E., M. Galli, T. Barbni. Lupus anticoagulant Ig's are not directed to phospholipids only, but to a complex of lipid-bound human prothrombin. — Thromb Haemost., **66**, 1991, 623-629.
2. Galli, M., G. Finazzi, E. Bevers. Kaolin-clotting time and Dilute Russell's Viper Venom Time distinguish between prothrombin-dependent and β2-Glycoprotein I-dependent antiphospholipid antibodies. — Blood, **86**, 1995; 617-623.
3. Galli, M., P. Comfurius, C. Massen. Anticardiolipin antibodies directed not to cardiolipin but to a plasma protein cofactor. — Lancet, **335**, 1990, 1542-1544.
4. Grob, J., J. Bonerandi. Cutaneous manifestations associated with the presence of the Lupus anticoagulant: a report of two cases and review of the literature. — J. Am. Acad. Dermatol., **15**, 1986; 211-219.
5. Gantcheva, M. Dermatological aspects in antiphosphoilipid syndrome. — Int. J. Dermatol., **36**, 1997, 173-180.

Institute of Experimental Morphology and Anthropology with Museum
Bulgarian Anatomical Society

Acta morphologica et anthropologica, 13
Sofia • 2008

Ultrastructural Features of the Different Zones of the Menisci

M. Kalniev, N. Vidinov, K. Vidinov

Department of Anatomy and Histology. Medical University, Sofia

The aim of our study was to present in detail that the meniscus is a heterogeneous, whose structure is depending on the different functional demands from the different zones. The investigations were performed upon menisci of the knee joints of Wistar rats. A light microscopy and transmission electronic microscopic observation were used. We made a new division of the zones of the meniscus: 1. A Superficial sliding zone (SSZ). 2. A Transitional sliding zone (TSZ). 3. A Superficial pressure zone (SPZ). 4. A Transitional pressure zone (TPZ). 5. A Central zone (CZ). 6. A Zone of fusion (ZF). 7. A Parameniscal zone (PZ). We pay attention to the SSZ and the CZ because these zones were more energetic than the others.

Key words: meniscus, proteoglycans, collagen, chondroblasts, fibroblasts.

Introduction

The menisci are different depending on the type of cells and the intercellular matrix. The menisci are built on following zones: a sliding zone (upper and lower), a pressure zone (in the middle), a tense zone (in the periphery) [8] and a parameniscal zone [11]. These zones have heterogeneous structure especially as far as the intercellular matrix is concerned. The pressure zone is built on a hyaline cartilage; the sliding zone is built on a fibrocartilage. The tense zone has a fibrous connective tissue [4]. This structure is formed in connection with the mechanical functions of the meniscus. These functions depend on the meniscus' viscoelastic properties and the interaction between the macromolecules of the tissue (collagen, proteoglycans) and water [6, 7, 3]. There are contradictory investigations about cytoarchitectonics, the collagen and the proteoglycans in the different zones of the meniscus. Some authors claim, the regions that are subjected to tense forces are fibrous and contain fibroblasts. The regions subjected to pressure forces are more "hyalinizates" and contain chondroblasts [2, 5, 6, 10].

Transmission electron microscopy shows, that on the surface of the meniscus there is an amorphous layer covering it [1]. The question of the precise division of the meniscus is not completely resolved. A full ultrastructural characterization of the cells in the different zones of the normal meniscus has not done.

Material and Methods

The materials of the investigation were menisci of the knee joints of 20 Wistar rats. The fixation was carried out by glutaraldehyde and formalin. The samples were investigated by routine light microscopy after staining in Mason, Azan, alcian blue, hematoxylin-eosin and microscopy and Van Gieson. Routine transmission electron microscopy was used.

Results

We made a new division of the zones of the meniscus: 1. A Superficial sliding zone (SSZ). 2. A Transitional sliding zone (TSZ). 3. A Superficial pressure zone (SPZ). 4. A Transitional pressure zone (TPZ). 5. A Central zone (CZ). 6. A Zone of fusion (ZF). 7. A Parameniscal zone (PZ). We pay attention to the SSZ and the CZ, because these zones were more energetic than the others.

The light microscopic examination of the meniscus showed, that SSZ was narrowly stripe, which lateral passed to the PZ, medial to the ZF, downwards to the TSZ. The articulations surface above the zone is completely smoothly. The relief of the SSZ depends of the prolongated bodies of the cells of the superficial layer and the bundles of thick collagen fibers situated between them. The cells from this zone were fibroblasts. They were prolonged and were situated parallel to the articulation surface. These cells had developed granular endoplasmic reticulum, which sometimes was approximately 2/3 of the cells' volume. At the same time they had developed Golgi complex and lysosomes (Fig. 1). The lysosomes of the chondroblasts of the articular cartilage were observed comparatively rarely. The examination with Safranin O showed comparatively few proteoglycan complexes situated uniformly in the intercellular matrix. The CZ was built on rare situated large, light, blistered cells. These

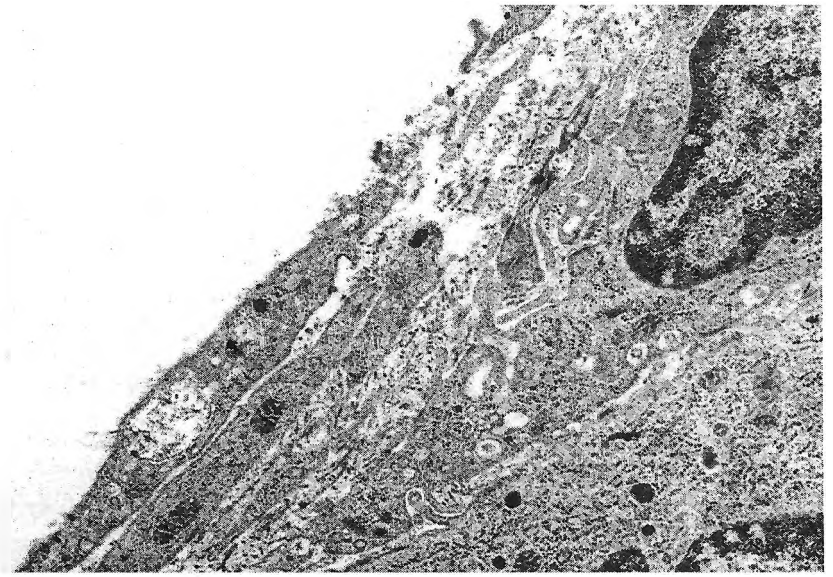

Fig. 1. Cells from the superficial sliding zone. × 10 000

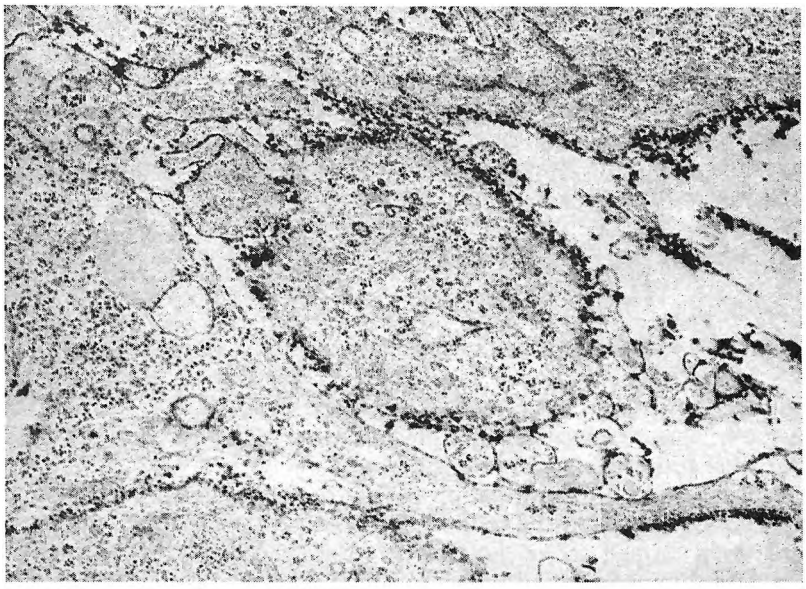

Fig. 2. Cells from the central zone. There is a big concentration of proteoglycans in the territorial matrix. × 10 000

cells had cytoplasm with few organelles (mainly separately cisterns GER). The intercellular space was filled with fine collagen network type II and proteoglycan complexes. They were more in the territorial matrix than the teritorial matrix (Fig. 2). There were matrix vesicles in the matrix of the CZ without clear marks of calcification. These vesicles were single or filled considerable part of the intercellular space.

Discussion

The meniscus is a heterogeneous, whose structure is depending on the different functional demands from the different zones. SSZ has ultrastructural characterization that resembles the tangential layer of the articular cartilage [9]. The fact that the cells are fibroblasts shows us the presence of intensive collagen synthesis, which depends on the considerable tense forces in this zone. The evidence for the above-mentioned is the electron microscopic characterization of the collagen type I. The distribution of the proteoglycan complexes, however, shows for severe friction forces at the same time. The conclusion is that SSZ is metabolic the most actively in response to the increased functional requirements. A CZ manifests reinforced processes of degeneration and calcification. A cause for the above-mentioned is the necessity of opposition to the increased pressure forces at the time of growth.

Further investigation of the ultrastructural organization ought to be done in connection with the important role of the menisci for the biomechanics of the knee joint. It is known that the injuries of the menisci are the most frequent injuries of the soft tissues of the knee.

References

1. Ghadially, F. N., J. M. Labonde, J. H. Wedge. Ultrastructure of normal and torn menisci of the human knee joint. — J. Anat., **136**, 1983, 773-779.
2. Gillard, G. S., H. C. Reilly, P. G. Bell-Booth, M. H. Flint. The influence of mechanical forces on the glycosaminoglycan content of the rabbit flexor digitorum profundus tendon. — Connect. Tissue Res., 7, 1979, 37-46.
3. Helio Le Graverand, M. P., Y. Ou, Y. Schield, L. Barclay, D. Hart, T. Natsume, J. B. Rattner. The cells of the rabbit meniscus: their arrangement, interrelationship, and morphological variations on cytoarchitecture. — J. Anat., **198(Pt 5)**, 2001, 525-535.
4. Kalinev, M., N. Vidinov. Ultrastructural investigation of the menisci of the knee joints in rats. — In: 11th Congress of Anatomists, Histologists and Embryologists. Sofia 1993.
5. Mow, V. C., M. H Halmes, W. M. Lai. Fluid transport and mechanical properties of articular cartilage: a review. — J. Biomech., **17**, 1984, 377-394.
6. Myers, E. R., W. Zhu, V. C. Mow. Viscoelastic properties of articular cartilage and meniscus. — In: Collagen: Chemistry, Biology and Biotechnology, (Ed. M.E. Nimni) vol. II, Boca Raton, FL. CRC Press, 1988, 268-288.
7. Proctor C. S., M. Schmidt, R. R. Whipple, M. A. Kelly, V. C. Mow. Material properties of normal medical bovine meniscus — J. Orthop. Res., 7, 1989, 771-782.
8. Sick, H., P. Ring, Ch. Ribat Koritke. — Compt. Rend. Ass. Anat., **143**, 1969, p. 1565.
9. Vidinov, N. Development of Articular Cartilage. Ultrastructural and Histochemical Investigation. Dissertation, 1981.
10. Vogel, K. G., M. Paulsson, D. Heinegard. Specific inhibition of type I and type II collagen fibrogenesis by the small proteoglycan of tendon. — Biomech. J.,**223**, 1984, 587-597.
11. Wladimirov, B., A. Welisarov. Changes in structure of menisci in various functional states of the knee joint in dogs. — Anat Anz., **135**, 1974, p. 327.

Institute of Experimental Morphology and Anthropology with Museum
Bulgarian Anatomical Society

Acta morphologica et anthropologica, 13
Sofia • 2008

Missing Single or Double Peripheral Microtubules in Amniote Axonemes

M. Markova, Ts. Marinova

Department of Biology, Medical Faculty, Medical University of Sofia

Despite the universality of the axonemal structure, exceptions of the 9+2 pattern are normal for some eukaryotes and are often found in pathology. We studied the ultrastructure of thymic epithelial cilia of the snake *Coluber jugularis* and compared their axonemes to the diversity found in human teratozoospermic ejaculates. In the *Coluber* epithelial cilia, one or more peripheral doublets were sometimes replaced by single microtubules in the absence of other structural peculiarities. In the human pathological flagella, missing single peripheral microtubules were rarely seen and were always associated with other axonemal defects. We conclude that the single peripheral microtubules observed in some snake cilia could be a normal variation of axonemal structure in lower amniotes.

Key words: axoneme, ultrastructure, single peripheral microtubules.

Introduction

The axoneme consisting of 9 peripheral doublets and 2 central microtubules (9+2) is almost universal for eukaryotic cilia and flagella. However, exceptions are found to be normal for some organisms [1], and a diversity of axoneme peculiarities can be found in pathological cases [2]. We performed an electron microscopic study of snake thymic epithelial cilia and the variations found in their ultrastructure were compared to the diversity of abnormal human sperm axonemes.

Materials and Methods

The snake species studied by us was *Coluber jugularis* Laur, found in the region of Zlatni Pyassatsi. Thymus specimens were obtained by dissection. For comparison, teratozoospermic human ejaculates were used as a source of very diverse axonemal variants. Thymus samples and washed sperm cells were processed for routine transmission electron microscopy as described in [3]. Briefly, they were fixed with glutaraldehyde, postfixed with OsO_4, dehydrated, embedded in resin and sectioned.

Results

Most axonemes of thymic epithelial cells of *C. jugularis* were standard 9+2. However, one or more peripheral doublets were sometimes replaced by single microtubules (Fig. 1). No other peculiarities in the axonemal structure were observed.

In the pathological human spermatozoa, one or more missing whole peripheral doublets were often found. However, missing single peripheral microtubules were rarely seen and were always associated with other axonemal defects, such as displaced, partially disintegrated or entirely missing peripheral doublets (Fig. 2).

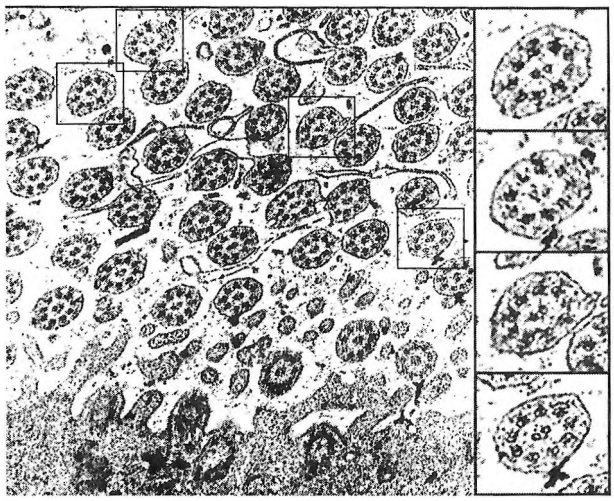

Fig. 1. *Coluber jugularis* thymic epithelial cilia in cross-section (× 15 000). Examples of axonemes with single peripheral doublets are indicated and shown as magnified insets (× 30 000)

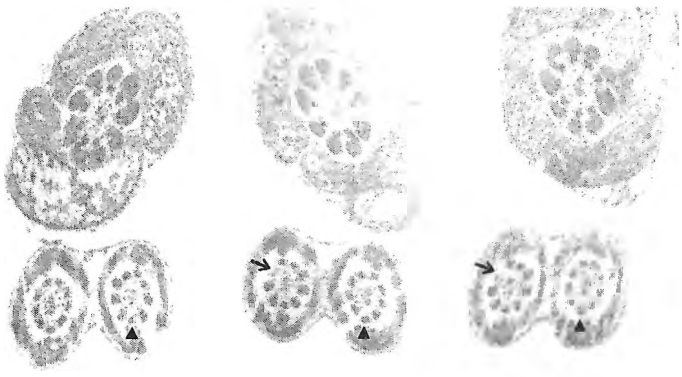

Fig. 2. Serial cross-sections of an abnormal bent or double sperm tail from a patient with teratozoospermia (× 26 000). One of the peripheral doublets is replaced by a single microtubule (arrowheads). Another peripheral doublet seems to disintegrate along the tail (arrows)

Discussion

Although the 9+2 pattern is strikingly universal among eukaryotes, variations are sometimes found in specific ciliary or flagellar structures. Single peripheral microtubules are normal for the cilia of some flatworm larvae, where the axoneme begins with the typical 9+2 structure but only single microtubules extend to the medial and distal regions [5]. We observed single peripheral microtubules in some thymic epithelial cilia of the snake *Coluber*, for which we found no literature reports concerning axonemal structure. Single peripheral microtubules, among other more common defects, were reported in cilia of human endometrial neoplastic cells [2]. However, we did not observe them in abnormal cilia of mouse thymic epithelial cells with oncornaviruses, although supernumerary central microtubules and peripheral triplets instead of doublets were common in the ciliary axonemes [4]. Even in the very diverse human teratozoospermic sperm axonemes, single peripheral microtubules were found rarely and always in the presence of other anomalies. In conclusion, missing single peripheral microtubules in the absence of other structural peculiarities are not typical for human axonemal pathology. This makes it probable that the single peripheral microtubules observed in some snake cilia are a normal variation of axonemal structure in lower amniotes.

Acknowledgements. We thank Dr. Krasimir Kosev for providing the snake specimens.

References

1. Dallai, R., P. Lupetti, G. Osella, B. A. Afzelius. Giant sperm cells with accessory macrotubules in a neuropteran insect. — Tissue Cell, **37**, 2005, 359-366.
2. Gould, P. R., L. Li, D. W. Henderson, R. A. Barter, J. M. Papadimitriou. Cilia and ciliogenesis in endometrial adenocarcinomas. An ultrastructural analysis. — Arch. Pathol. Lab. Med., **110**, 1986, 326-330.
3. Marinova, T. T., M. D. Markova, R. K. Stanislavov. Distribution of vimentin in abnormal human spermatozoa. — Andrologia, **28**, 1996, 287-289.
4. Marinova, Ts. Ts., N. I. Valkov. Ultrastructural characteristics of the cytoskeleton in thymus epithelial cells with oncornaviruses. — CR Acad. Bulg. Sci., **37**, 1984, 533-535.
5. Xylander, W. E. R. A presumptive ciliary photoreceptor in larval *Gyrocotyle urna* Grube and Wagener (Cestoda). — Zoomorphology, **104**, 1984, 21-25.

Institute of Experimental Morphology and Anthropology with Museum
Bulgarian Anatomical Society

Acta morphologica et anthropologica, 13
Sofia • 2008

Morphological Changes in the Smooth Muscle Cells of the Valvular Sinus Wall in Essential Varicosis

*M. Minkov, G. Marinov, V. Knyazhev**

Department of Anatomy, Histology and Embryology
* *Clinic of Vascular Surgery, Prof. Paraskev Stoyanov Medical University, Varna*

The investigations cover the operative material taken from 60 patients aged between 18 and 62 years during the surgical interventions. The electron microscopic data demonstrate that in the valves during the initial stage of valvular cusps' reduction the first and most common alterations in the smooth muscle cells (SMCs) of the valvular sinus wall are established in the mitochondria. They present with a congestion of the mitochondrial matrix, disorganization of the crests and loss of the crest-like structure of the mitochondria. In the morphologically inferior valves presenting with advanced valvular cusps' reduction there exist not only alterations in the mitochondrial complex but also changes related to the degeneration and destruction of the cells.

Key words: vein, valves, varicosis, TEM, smooth muscle cells.

Introducton

Valvular dysfunction is a fundamental reason for venous hypertension and stasis in the superficial venous system of the lower extremities. In case of venous hypertension, the blood pressure that is exerted on the valvular cusp during the valve closure is transmitted not only to the little valvular axle but also to the wall of the valvular sinus. It seems logically to assume that the venous hypertension and the hypoxia would induce early changes in the morphology of SMCs of the valvular sinus wall.

The objective of the present work is to study the morphological changes of the SMCs of the valvular sinus wall of the great saphenous vein (VSM) during the development of the essential varicosis by using of the methods of transmission electron microscopy (TEM).

Material and Methods

The investigations of the venous valvular complex during the development of the essential varicosis of the VSM were performed on an operative material taken from

60 patients age between 18 and 62 years during the surgical interventions. The material was put into a fixer such as 3% or 4% solution of glutaraldehyde in 0,1M phosphate buffer at pH 7,4. The selected regions were processed after a routine procedure for TEM examination. After a careful inspection of the semi-thin sections some representative areas were chosen from which ultra-thin sections were prepared. The sections were observed by using JEM 7A and OPTON transmission electron microscopes.

Results

The electron microscopic data show that in the valves during the initial stage of valvular cusps' reduction, the first and most common changes in the SMCs of the valvular sinus wall are established in the mitochondria. They possess the shape typical of them and are surrounded by an internal and an external membrane that lose their contours at certain places as the spaces limited by them fuse with the intracellular matrix (Fig. 1). The inner space limited by the internal membrane is filled-up with a non-homogenous matrix that, at certain places, demonstrates a high electron microscopic density. The crests typical of this space that are formed by their inner membrane strongly decrease. The greater part of the mitochondria loses their crest-like structure as a few disorganized crests can be established in single mitochondria only. Along with the changes in the ultrastructure of the mitochondria in the SMCs of the valvular sinus wall described above some multivesicular bodies as well as events of alteration of the type of myelin degeneration can be found out (Fig. 2).

Fig. 1. Valvular sinus wall of a morphologically inferior valve.
TEM, × 30 000

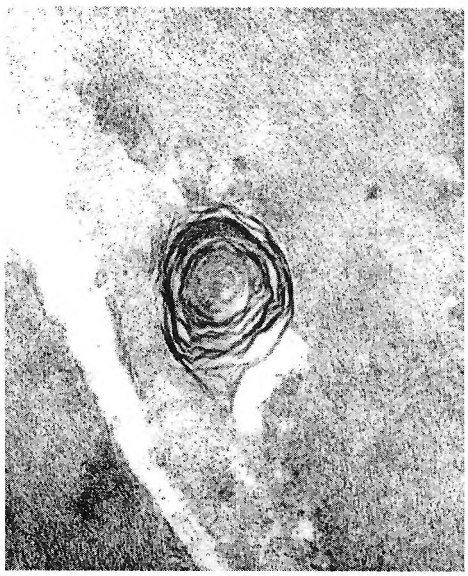

Fig. 2. SMC in the sinus wall of a morphologically inferior valve. TEM, × 30 000

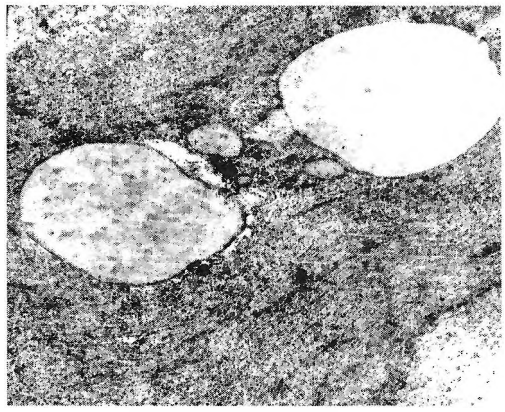

Fig. 3. Morphologically inferior valve presenting with advanced valvular cusps' reduction. Valvular sinus wall. TEM, × 30 000. SMC and vacuoles of different size and content

Along with the progression of the varicose process in the morphologically inferior valves presenting with advanced reduction of the valvular cusps, the SMCs appear to be predominantly alone among an abundant fibrous mass and are united in bundles in rare cases only. In them, one can establish not only alterations in the mitochondrial complex but also changes related to the degeneration and destruction of the cells. One observes vacuoles of different size and content (Fig. 3) as well as sequestration of the regions of SMC destruction.

Discussion

The changes established in the mitochondria of the SMCs of the valvuar sinus wall resemble the analogous findings in the extravalvular regions of the varicose veins already reported by Marinov and Vankov [1]. That is why we accept that the mechanisms of origin of the morphological changes in the SMCs of the valvular sinus wall are, in principle, similar to those that cause varicose changes in the extravalvular areas. In the mitochondria, the metabolism of a series of amino acids, fatty acids and other substances is accomplished in addition to the oxidative phosphorization [7]. The variety of the functional opportunities makes the mitochondria sensitive to the hypoxia of the venous wall.

The enhancement of the tissue compression on the intramural vessels in the venous wall with the valves in advanced stage of valvular cusps' reduction will block the blood circulation in them that, on its part, will increase the hypoxia and the manifestations of degeneration and destruction related to it. Michels et al. [2, 3, 4, 5] and Michels [6] argue that the influence of venotropic drugs on the mitochondrial respiratory chain provides a rational explanation of the therapeutic effects of the drugs of this class. They are capable of increasing the vascular tone and to reduce the capillary permeability. In fact, their targets are the complexes of the mitochondrial respiratory chain, and they preserve the production of ATP during hypoxia.

References

1. Marinov, G., V. Vancov. Early changes of the smooth muscle cells (SMC) and extracellular matrix in the wall of varicose veins. — Verh. Anat. Ges. Anat. Anz., **84**, 1991, Suppl. 168, 99-100.
2. Michiels, C., T. Arnould, D. Janssens, K. Bajou, I. Geron, J. Remacle. Interactions entre les cellules endothéliales et les cellules musculaires lisses apres activation par l'hipoxie. Une étiologie possible de la maladie veineuse. — Phlébologie, **48**, 1995, 141-149.
3. Michiels, C., T. Arnould, D. Janssens, J. Remacle. Importance des cellules endothéliales et de l'hypoxie dans le développement des veines variqueuses: effect de ginkor fort. — Phlébologie, **48**, 1995, 150-154.
4. Michiels, C., J. Remacle, N. Bonaziz. Endothelium and venotropic drugs in chronic venous insufficiency: a review. — Phlebology, **17**, 2002, 145-150.
5. Michiels, C., N. Bonaziz, J. Remacle. Role of the endothelium and blood stasis in the appearance of varicose veins. — Int. Angiol., **21**, 2002, 1-8.
6. Michiels, C. Role of the respiratory activity of vascular endothelial mitochondria in the pathophysiology of CVI. — Phlebolymphology, **39**, 2003, 105-112.
7. Кръстев, Л., И. Вълков, Р. Райчев, Х. Прокопанов. Основи на ултраструктурната патология. София, Медицина и физкултура, 1982. 231 с.

Institute of Experimental Morphology and Anthropology with Museum
Bulgarian Anatomical Society

Acta morphologica et anthropologica, 13
Sofia • 2008

Structure of Pericapillary Space of Adrenal-Gland Sinusoid Capillaries

A. Petrova

Department of Anatomy, Histology and Embryology, Prof. Paraskev Stoyanov Medical University, Varna

Adrenal gland of white Wistar rats was studied by transmission electron microcopy (TEM). The pericapillary space was manifested at single places only along the sinusoid capillaries and contained extraendothelial cell elements of connective tissue nature, reticulin fibrils and bundles of elastic microfibrils. As a rule, a continuous basal membrane on the surface of the vascular pole of the parenchymatous cells in the adrenal cortex could be observed. This could be related with the presence of microvilli and processi. In the adrenal medulla, the basal membrane strictly followed the cellular surface facing the sinusoid capillary that was smooth and with small invaginations. A basic qualitative difference between the capillaries of both adrenal parts was established. Microvilli and processi of parenchymatous cells in the pericapillary space and the wall of the sinusoid capillaries in the cortex were observed while such relationships were lacking in the medulla.

Key words: adrenal gland, sinusoid capillaries, pericapillary space, TEM.

Introduction

Transcapillary exchange within the adrenal gland includes not only the movement of substances related to the trophics of the glandular parenchyma but also a series of hormones related to the specific functions of the gland. This exchange depends on the structure of the sinusoid capillaries as well as on the relations of the glandular cells towards the capillary wall that includes the structural peculiarities of the pericapillary space, too. Literature data about the structure of the pericapillary space are scanty and contradictory [1-4, 6].

Material and Methods

We studied the adrenal gland of white rats of Wistar breed. We made use of a conventional electron microscopic technique: glutaraldehyde, osmium tetraoxide, durcopan, uranyl acetate, lead citrate. Microscope JEM 7A.

Results

The pericapillary space of the sinusoid capillaries of the adrenal gland is located between the endothelial basal membrane and the surface of the parenchymatous cells or their basal membrane in case of its existence. Our observations show that when the parenchymatous cell is firmly attached to the capillaries by a smooth surface there is one basal membrane only situated between both cells with a thickness of about 30 nm (Fig. 1a). It is separated from the surface of the endothelial cell by a narrow subendothelial space with a width of 30-40 nm. As it can be observed the thickness of the only basal membrane common for both cells corresponds to the thickness of the endothelial basal membrane. When the surface of the parenchymatous cell moves away from the endothelium the basal membrane remains in unchanged relationships with the latter; sometimes but not always, a basal membrane can occur on the distant surface of the parenchymatous cell. The absence of a parenchymatous basal membrane could be related to the presence of processi and microvilli of the glandular cell. In the dilatations of the pericapillary space, there are fibrillary elements, pericapillary cells, processi and microvilli of the parenchymatous cells (Fig. 2). Here, as a comparatively rare component, the basal processi of the endothelial cells are also located. The fibrillary elements occur at a restricted stretch. In most cases, it deals with small bundles of reticulin fibrils. More significant accumulations are established in the neighbourhood to the pericapillary cells rich in filamentous material. Elastic elements can be very rarely observed. No typical elastic fibres presenting with a shaped elastin component of amorphous appearance can be found out. The pericapillary cellular elements repre-

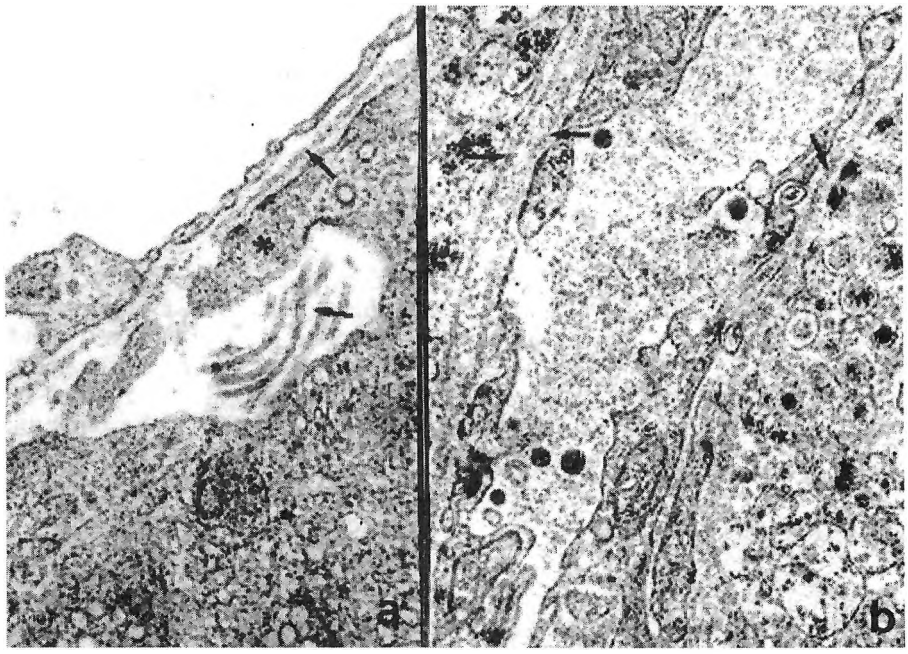

Fig. 1. Electron micrograph of rat adrenal gland
a — adrenal cortex, × 20 000; b — adrenal medulla, × 20 000

Fig. 2. Adrenal cortex. × 20 000

sent multipotent cells of connective tissue nature with a secretory, motor, and phagocytary function. (Their detailed cytological characteristics have been described in another paper of ours [5]). The main part of the content of the pericapillary space is represented by the microvilli and processi of the parenchymatous cells, some of them penetrate into the lumen of the vessel.

The pericapillary space of the sinusoid capillaries in the medulla is located between the endothelial basal membrane and the basal membrane of the parenchymatous cells; which is permanent and strictly follows the surface of the cell (Fig. 1b). The pericapillary space is absent comparatively often and at a considerable stretch. In these regions, the parenchymatous cells closely attach to the capillary wall being separated from the endothelial cells by a common basal membrane thus it deals with a different degree of fusion of both membranes, i.e., of the endothelial and the parenchymatous one. The surface of the medullary cells facing the sinusoid capillary is smooth and with small invaginations of the cytolemma. In the pericapillary space, there are fibrillary and cellular elements which, in principle, do not differ from these in the cortical part of the gland.

Discussion

The results disprove the general validity of some additional signs incorporated into the classification characteristics of the capillaries of the endocrine organs, namely, the uninterrupted layer of periendothelial elements, parenchymatous basal membrane as an obligatory external borderline of the pericapillary space, and microvilli of the parenchymatous cells [3, 4, 6].

Our data demonstrate that in the cortical part of the gland, the parenchymatous basal membrane occurs as an exception and there are no microvilli in the pericapillary space of the medulla.

We establish a basic qualitative difference between the capillaries of both parts of the gland. It concerns the interrelationships of the sinusoid capillaries with the parenchymatous cells. We observe microvilli and processi of the parenchymatous cells in the pericapillary space and the wall of the sinusoid capillaries in the cortical part and absence of such relationships in the medullar one.

References

1. Enrico, A. Lo spazio pericapillare nell gliandole endokrin. — Arch. Ital. Anat. Embriol., **80**, 1975, 37-56.
2. Kikuta, A., O. Ohtani, T. Mukakami. Three-dimensional organization of the collagen fibrillar framework in the rat adrenal gland. — Arch. Histol. Cytol., **54**, 1991, 133-144.
3. Mori, M., T. Onoe. Electron microscopic study on capillary endothelial cells of the adrenal cortex. — Tohoku J. Exp. Med., **93**, 1967, 301-315.
4. Nakamura, K. Adrenal vasculature and RE cells. — Rec. Adv. Res., **14**, 1974, 38-51.
5. Petrova, A., V. Vancov. Fine structure of the pericapillary cells in the adrenal gland as regard to their function. — Verh. Anat. Ges., **76**, 1982, 403-404.
6. Шахламов, В. А. Каппиляры. Москва, 1971.

Institute of Experimental Morphology and Anthropology with Museum
Bulgarian Anatomical Society

Acta morphologica et anthropologica, 13
Sofia • 2008

Ultrastructural Peculiarities in the Stroma of the Thyroid Gland with Struma Nodosa

*K. Vidinov, N. Vidinov, M. Kalniev**

Department of Endocrinology and Gerontology, Medical University
**Department of Anatomy, Medical University, Sofia*

The follicules of the thyroid gland are surrounded by connective tissue stroma, which is not well investigated. To fulfill our aim we studied ultrastructurally the operative tissue from Struma nodosa patients. We compared fibroblasts next to active thyrocytes and those near epithelial cells with low activity. Our results point out in stages of thyroid activity the follicular cells show hypertrophy endocytosis complex lysosome activities. The fine basal lamina can be seen. In the fibroblasts from the septum larger and deformed GER, bigger Goldgy apparatus, and number of primary lysosomes can be seen. In the extracellular matrix we found an increased amount of collagen bundles type I as well as proteoglycans. The connective tissue of II group was larger in the septums and in the interlobular space. The number of hypertrophical cells enlargement. The fibroblast from these group were activated with large GER, inormaly large Goldgy complex and lysosomes.

Key words: stroma, thyroid gland, ultrastructure.

The follicules of the thyroid gland are surrounded by connective tissue stroma in which blood and lymphatic vessels are situated. There are many investigations concerned the thyrocytes of the thyroid gland [1, 2, 3, 9, 10], but there are no investigations about connective tissue elements in the gland.

Purpose

Our purpose is to follow the electron microscopical alterations in the connective tissue stroma between the thyroid follicules. To fulfill our aim we studied ultrastructurally the operative tissue from Struma nodosa patients. We compared fibroblasts next to active thyrocytes and those near epithelial cells with low activity.

Material and Methods

In order to do so we used material from 23 patients surgically operated for Struma nodosa (I group) and 4 patients operated for Hashimoto disease [II group]. The

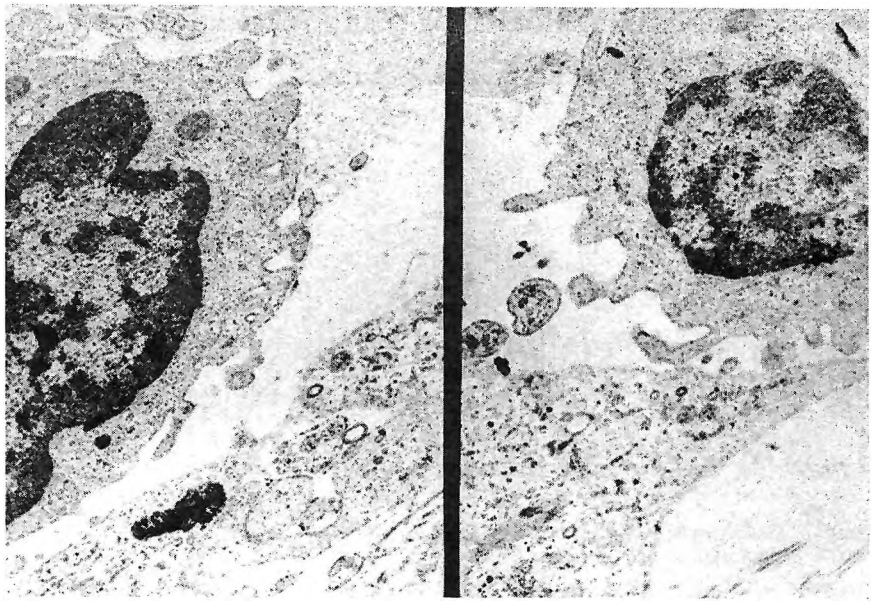

Fig. 1. Cells of I group. A larger and deformed GER and number of primary lysosomes can be seen in them. × 12 000

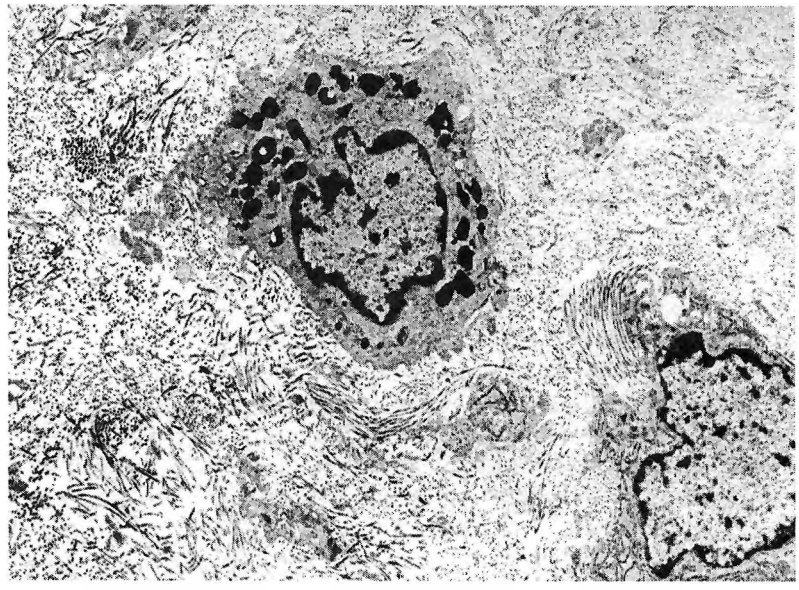

Fig. 2. Cells from II group. The fibroblast from these group were activated with large GER, large Goldgy complex and many complex lysosome. × 8400

materials were used for light microscopical investigations staining with hematoxilin-eosin and by Masson. Electron microscopical investigations was made by standard electron microscopy as well as Safranin O staining [8].

Results

The follicules of the thyroid gland from the I group were with very different size. The connective tissue stroma was a thin layer in the septa of the follicules and as a group of cells in the interlobular space. Our results point out in stages of thyroid activity the follicular cells show hypertrophy endocytosis complex lysosome activities. The fine basal lamina can be seen. In the fibroblasts from the septum larger and deformed GER, bigger Goldgy apparatus, and number of primary lysosomes can be seen (Fig.1). In the extracellular matrix we found an increased amount of collagen bundles type I as well as proteoglycans. The connective tissue of II group was larger in the septums and in the interlobular space. The number of hypertrophical cells enlargement. The fibroblast from these group were activated with large GER, abnormally large Goldgy complex and lysosomes (Fig. 2).

Conclusion

The results from the ultrastructural findings have to be considered in regard to the participation of the connective tissue in the gland metabolic changes (5, 6, 7) and in the alterations of the epithelial cells [4].

References

1. Beamont, A., P. Fragu.Ultrastructural changes in rat thyroid gland during iodine deficiency. — Bioll. Cell, **54**, 1985, 177-180.
2. Chen, H., D. Hayakawa, S. Emura. Effects of ethanolol on the ultrastructure of the hamster thyroid cells. — Histol. Histopathol., **15**, 2000, 469-474.
3. Davidson, N. Ultrastructure of thyroid C cells in sheep treated with vit D3. — J.Vet. Med Sci., **53**, 1991, No5, 921-927.
4. Hoang-Vu, C., G. Barabant, A. Leitolf, H. Von Muhlen. Functional and morphological changes of the thyroid gland following 5 days of pulsative TRH stimulation in male rats. — Journal of Endocrinology, **146**, 1995, 339-348.
5. Kniec, B. Histoenzimatic investigations of the thyroid gland of guinea pig. — In: Proc. 33 Conference of the Polish Histochemical Soc.
6. Lawson, V., F. Carrick. Morphology of thyroid in coastal and noncoastal population of the koala in Queensland. — General and Comparative Endocrinology, **110**, 1998, 295-306.
7. Lee, T., S. Kuo, T. Yah. Reversible systolic heart failure in hyperthyroidism. — Am. J. Med. Sci., **312**, 1996, 246-248.
8. Shepard, N., N. Mitchel. The location of proteoglycans by light and electron microscopy using Safranin O. — J. Ultruct. Res., **54**, 1976, 451-460.
9. Shin, W., B. Aftalion, E. Hotchkiss, E. Shenkman. Ultrastructure of a primary fibrosarcoma of the human thyroid gland. — Cancer, **44**, 1979, 584-591.
10. Werthington, B., C. Enwonwu. Functional variations in the ultrastructure of the thyroid gland in malnutrished infant monkeys. — Am. J. Clin. Nutrition, **28**, 1975, 66-75.

Institute of Experimental Morphology and Anthropology with Museum
Bulgarian Anatomical Society

Acta morphologica et anthropologica, 13
Sofia • 2008

Ultrastructural Characteristics of the Connective Tissue Elements in PVR and PDR

C. Vidinova, N. Vidinov, K. Michailova*

Clinic of Ophthalmology, Military Medical Academy, Sofia
Department of Anatomy, Medical University, Sofia

Diabetic retinopathy (PDR) and Proliferative vitreoretinopathy (PVR) are characterized by the formation of fibrous epiretinal membranes (ERMs) at the vitreoretinal interface that are due to the excessive proliferation, migration and differentiation of several cell types and they are causes of blindness. Much investigated PVR is still poorly understood. Its pathological mechanisms are not yet very clear. Similar pathological changes occur at the end stage of Proliferative diabetic retinopathy.
The purpose of our study was to compare the ultrastructure of the epiretinal membranes in PVR with those of the proliferations in PDR patients. The results from our investigations showed that in the membranes of the patients with PVR mainly two types of cells prevailed: the elongated fusiform-shaped, fibroblasts and the retinal pigment epithelial cells. Occasionally transitional forms with mesenchymal origin, glial cells and macrophages were seen in the membranes. In the proliferations of PDR patients we found significant differences. The main cell types comprising these membranes unlike PVR were: macrophages, fibroblasts, glial cells and other elements of the blood. In contrast to the previous group pigment epithelial cells were very rare to find. In these fibrovascular proliferations different types of capillaries were seen embedded in the fibrous tissue.

Key words: ultrastructure, PVR, PDR.

Introduction

One of the most common causes for ablations retinae are Diabetic retinopathy (PDR) and Proliferative vitreoretinopathy (PVR). PVR is characterized by the formation of fibrous epiretinal membranes (ERMs) at the vitreoretinal interface that are due to the excessive proliferation, migration and differentiation of several cell types [1, 5, 6, 8]. They usually tend to contract and provoke tractional retinal detachments, leading to impairment of the visual acuity and often blindness. Much investigated PVR is still poorly understood. Its pathological mechanisms and risk factors are not yet very clear.

Similar pathological changes occur at the end stage of Proliferative diabetic retinopathy, which is one of the major causes of blindness all over the world [10, 11]. It usually affects young people with type I diabetes and its hallmarks are the neovascular proliferations in the posterior pole, often related with bleeding, retinal tractions and visual loss.

Purpose

The purpose of our study was to compare the ultrastructure of the epiretinal membranes in PVR with that of the proliferations in PDR patients.

Material and Methods

In our prospective study 32 patients, 21 with PVR CP 1-4 and 11 with PDR were included. All of them after undertaking a precise ophthalmologic examination were operated with pars plana vitrectomy. During the operation proliferative tissue was collected and used for transmission and scanning electron microscopy according to the routine techniques.

Results

The results from our investigations showed that in the membranes of the patients with PVR (CP 1-4) mainly two types of cells prevailed: the elongated fusiform-shaped, fibroblasts and the retinal pigment epithelial cells. Occasionally transitional forms with mesenchymal origin, glial cells and macrophages were seen in the membranes. The cells were usually situated close to one another and the connections between them were strong, the so called "tight junction" type. The retinal pigment epithelial cells (RPE) were either among the fibroblast-like or in clusters. They were more or less cubuoid or oval in shape. Various amounts of electron microscopically dense granules, with average size — melanin granules were seen in the cell cytoplasm. In the extracellular matrix we observed collagen bundles with different length —

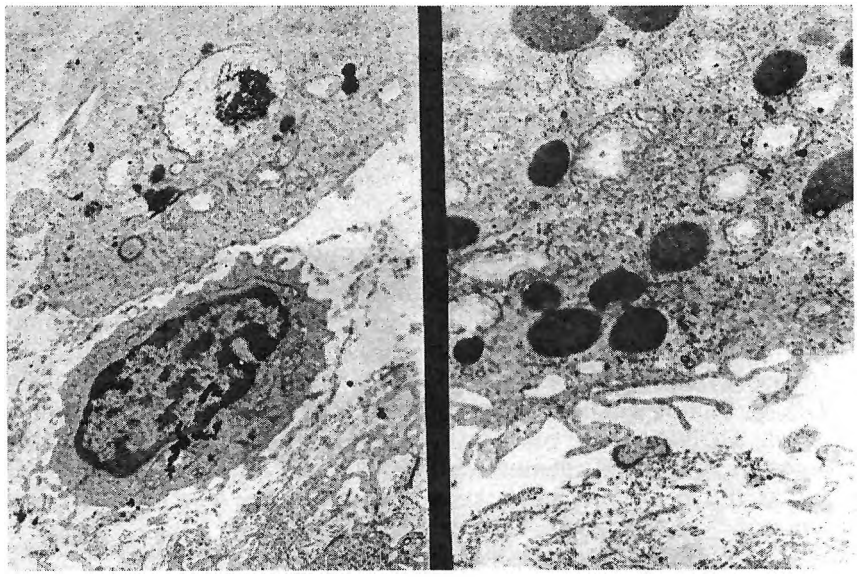

Fig. 1. Macrophages from PVR-membranes. There are many complex lysosomes and phagosomes. × 10 000

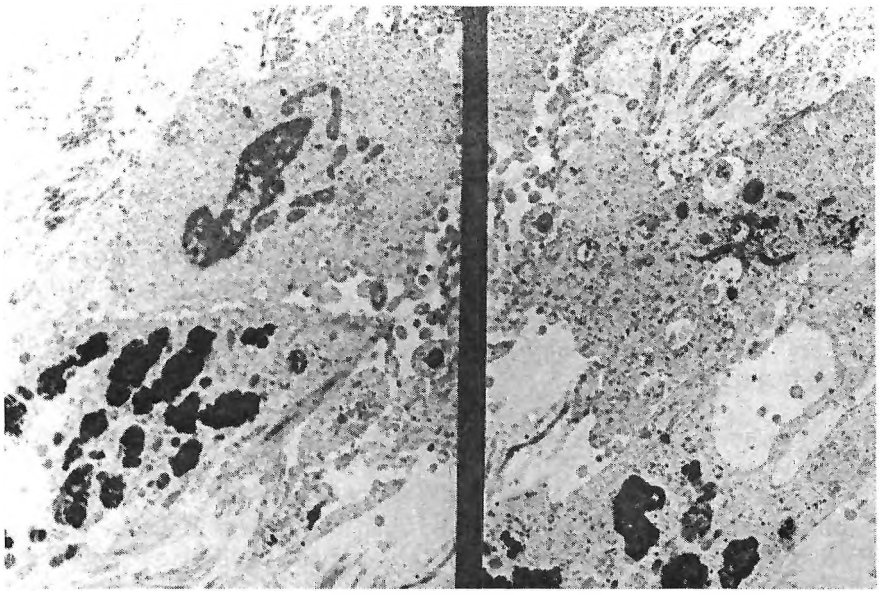

Fig. 2. Cells from PDR membranes. Degenerated fibroblasts and pigment cells can be seen. × 10 000

mainly type II collagen. In the proliferations of PDR patients we found significant differences. The main cell types comprising these membranes unlike PVR were: macrophages, fibroblasts, glial cells and other elements of the blood. In contrast to the previous group pigment epithelial cells were very rare to find. In these fibrovascular proliferations different types of capillaries were seen embedded in the fibrous tissue. They were generally two types: young — with a small lumen, no basal lamina, thin layer of fenestrated endothelial cells, and the mature capillaries with a medium size lumen — comprised of thin layer endothelial cells, developed basal membrane, containing formal elements of the blood.

Discussion

Our results point out that the proliferative tissues in PVR and PDR differ considerably in their cellular and extracellular content. This to a certain extent is expected as the pathogenesis of the two illnesses differs considerably. While in PVR mainly processes of cell migration, cell dedifferentiation and proliferation are having a key role in the pathogenesis, in PDR the triggering mechanism is the formation of the new vessels (2, 3, 4). That is why PVR membranes in their cytoarchitecture are richer of fibrous elements, migrated RPE cells and cells undergoing transdifferentiation (5, 7, 9). On the other hand, in PDR membranes fibrous tissue follows the developing new vessels and is richer of elements typical for the blood: macrophages, segment nuclear leucocytes etc.

References

1. Ayo, S. H., R. Radnik. W. F. Glass II, J. A. Garoni, E. R. Rampt, D. R. Appling, J. R. Kreisberg. Incresed extracellular matrix synthesis and mRNA in mesangial cells grown in high-glucose medium. — Am. J. Physiol., **260**, 1991, F185-F191.
2. Balian, G., E. M. Click, P. Bornstein. Location of a collagen binding domain in fibronectin. — J. Biol. Chem., **255**, 1980, 3234-3236.
3. Cagliero, E., T. Roth, S. Roy. Characteristics and mechanisms of high glucose-induced overexpression of basement membrane components in cultured endothelial cells. — Diabetes, **40**, 1991, 102-110.
4. Casaroli Marano, R. P., S. Vilaro. The role of fibronectin, laminin, vitronectin and their receptors on cellular adhesion in PVR. — Invest. Ophthalmology Vis. Sci., **35**, 1994, 2791-2801.
5. Charteris, D. Proliferative vitreorethinopaty: pathology, surgical managment, and adjunctive treatment. — British J.Ophtalm., **79**, 1995, 953-960.
6. Hiscott, P. S., I. Grierson, D. McLeon. Natural history of fibrocellular epiretinal membranes: a quantitative, autoradiographic, and immunohistichemical study. — British J. Ophtalmol., **69**, 1985, 810-823.
7. Hiscott, P. S., I. Grierson, C. J. Trombetta, A. H. S. Rahi, J. Marshall, D. McLeon. Retinal and epiretinal glia: An immunohistochemical study. — British .J. Ophthalmol., **68**, 1984, 698-707.
8. Kampik, A., K. Kenion, R. Michels, W. Green, Z. Criz. Epiretinal and vitreous membranes: Comparative study of 56 cases. — Arch. Ophthalmol., **99**, 1981, 1445-1454.
9. Koteliansky, V. E., M. A. Glukhova, M. V. Bejanian. A study of the structure of fibronectin. — Eur. J .Biochem., **119**, 1981, 619-624.
10. Pillat, M., A. Kapetanios, G. Donati, M. Redard. TGF-bl, TGF-b receptorII and ED-A fibronectin expression in myofibroblast of vitreoretinopathy. — IOVS, **41**, 2000, 2336-2342.
11. Sayon, R., E. Cagliero, M. Lorenzi. Fibronectin overexpression in retinal microvessels of patients with Diabetes. — Invest. Ophth. Vis. Science, **37**, 1996, p. 2.

Institute of Experimental Morphology and Anthropology with Museum
Bulgarian Anatomical Society

Acta morphologica et anthropologica, 13

Morphological Alterations in Rat Testis during Aging

M. Bakalska, N. Atanassova, E. Pavlova, Y. Koeva, B. Nikolov*

Institute of Experimental Morphology and Anthropology with Museum, Bulgarian Academy of Sciences BAS, Sofia
**Department of Anatomy, Histology and Embryology, Medical University, Plovdiv*

The present study aimed to investigate dynamic of the changes in rat aging testis using specific immunohistochemical markers. Aging of the testis is manifested by germ cells (GCs) loss, reduced responsiveness of Sertoli cells (SCs) to androgens and suppression of steroidogenesis in Leydig cells (LCs). Thickened basal lamina and vessel wall proved by immunohistochemistry for α-smooth muscle actin are indicative for disturbed communication between seminiferous epithelium (SE) and interstitium as well as altered testicular trophic during ading.

Key words: Sertoli cells, Leydig cells, spermatogenesis, aging testis.

Introduction

The functions and histology of the testis during development and in the adults are well described but the effects of aging on the testis have not been as intensively studied. Aging of the testis is accompanied by loss of germ cells (GCs) leading to a decline sperm production [3]. Studies by C h e n et al. [1] have shown that the production of testosterone (T) per Leydig cells (LCs) is reduced with aging, but the numbers of LCs per testis do not change, suggesting that changes to individual cells account for reduced serum T levels. The abnormalities and loss of SCs seen in aging testis are probably involved in disruption of Sertoli cells—germ cells communications. Aging of seminiferous epithelium (SE) is associated with thickening of basal lamina that created an additional barrier for nutrient and regulatory factors form the interstitium [4]. The precise mechanisms underlain the alterations in aging testis remain unknown yet. In this respect **the objective** of the present study was to investigate dynamic of the changes in rat testis using specific immunohistochemical markers and to characterize relationships between different testicular cell types during aging.

Materials and Methods

Testes from Lewis rats were sampled at different ages (2, 7, 12, 15, 18 and 21 months), fixed in Bouin's, embedded in paraffin and cult into 5 μ. Immunohistochemistry was performed for: 1) α-smooth muscle actin using mouse Mo Ab (Sigma, UK) in dilution 1:5000); 2) 3β-hydroxy steroid dehydrogenase (3β-HSD) using rabbit Poly Ab (1:1000) kindly provided by Professor I. Mason, Edinburgh University; 3) Androgen receptor (AR) using rabbit Poly Ab (Santa Cruz Biotechnology, USA) diluted 1:200. Measurement of seminiferous tubule (ST) diameter was carried out.

Results

The seminiferous epithelium of the rats of 2 to 12 months of age exhibited intact spermatogenesis with all the steps of germ cell development. By 18 months of age, both normal and altered tubules were observed (not shown). At 21 months tubules with regression of SE were predominantly present. Some germ cells sloughed off into the lumen. The altered tubules were smaller in size, with a thickened basement membrane and a disrupted spermatogenesis. Quantitative analysis of ST diameter demonstrated significant and progressive age-related reduction by 15-30% (Fig. 1).

Between 2-6 months, the basal lamina of the ST was visualized as a thin layer. At the age of 12-18 months, the basal lamina is thicker, with irregular contour. Immunohistochemical study showed positive reaction for β-smooth muscle actin in basal membrane of the ST and peritubular myofibroblasts, as well (Fig. 2A). Strong

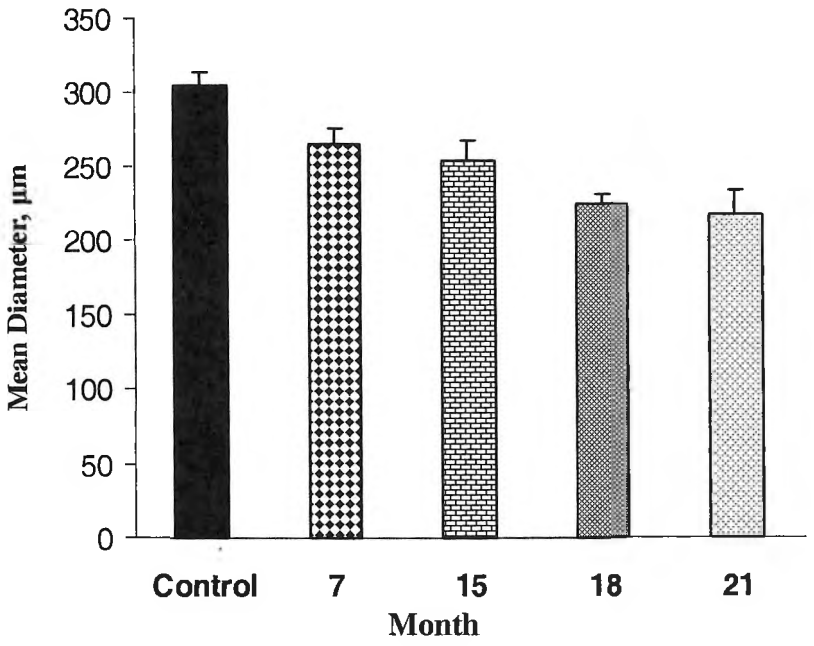

Fig. 1. Progressive age-related reduction in mean diameter of seminiferous tubules (μm). Data represent mean value ± SE. All data are significant compared to control

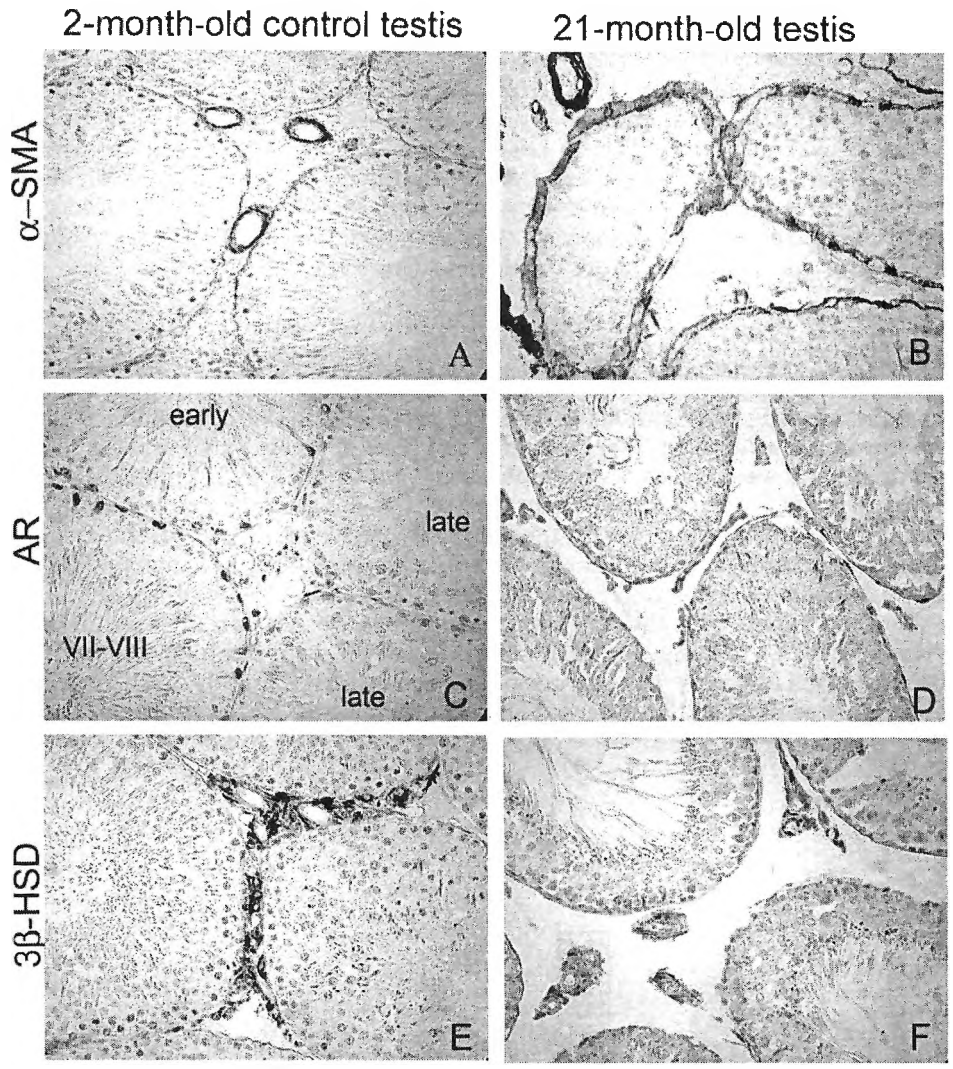

Fig. 2. Immunohistochemical visualization of α-smooth muscle actin (A, B); Androgen receptor (C, D); 3β-HSD (E, F) of 2-month-old control and 21-month-old aging rat testis. × 400

immunoreactivity was found in the testis of 21 months of age (Fig. 2B). Intense reaction was seen in the thickened wall of small blood vessels in the interstitium.

Normally, Androgen receptor (AR) is localized in the nuclei of Sertoli cells, Leydig cells, peritubular cells but not in germ cells. There was a stage specific pattern of immunoexpression of AR in SCs with maximal staining in stages VII-VIII of the spermatogenic cycle and lowest intensity in late (IX-XIV) stages (Fig. 2C). During aging we observed decrease in immunoreactivity of AR in the testicular cell types and there was lack of stage specificity in SCs at age of 21 months (Fig. 2D).

The interstitium of aging testes appeared to increase in size without any evidence for LCs hyperplasia. This appearance was simply a consequence of age-re-

lated tubular regression. Immunoexpression of 3β–HSD (marker for steroidogenic activity of LCs) was greatly reduced at age of 21 months compared to 2-month-old control (Fig. 2 E, F).

Discussion

In present study we investigated the influence of aging on the main cell types in rat testis. Our findings of a reduction of tubular diameter confirmed results by W a n g et al. [9] reporting significant age-related decrease in tubular volume, diameter and length and luminal volume. It is known that lamina propria displays pronounced changes in the period of aging that involved peritubular cells and intercellular matrix. [5, 6]. The thickening of the basement membrane in aging rats and humans was coincidental with changes in the blood-testis barrier and germ cells depletion [3, 6]. Our results for intense reaction in thickened basal lamina and vessel wall are indicative for disturbed communication between SE and interstititum as well as altered testicular trophic during aging. Androgens are especially important for maintenance of spermatogenesis in adulthood [2, 7] and their effects on GCs are mediated via androgen receptor localized in Sertoli cells. In our study we observed that the reduced AR immunoreactivity in SCs first occurred in androgen dependent stage (VII-VIII) and loss of stage specificity probably is associated with the functional alterations (decreased responsiveness to androgens) in SCs [8]. It is likely that SCs from aging testis are unable to provide adequate support for germ cells and to respond to selective signal from them. The abnormalities and loss of SCs seen in the adding testis might be responsible for disruption of the blood-testis barrier [3, 5] and germ cell depletion.

Our findings of reduced immunoexpression of 3β-HSD are indicative for suppressed steroidogenic activity of aging LCs that correlate with data for reduced serum T levels. According to Z i r k i n and C h e n [10] the reduced ability of aging LCs to produce T might be caused by events occurring outside or inside these cells that impinge upon them involving accumulation of free radicals. In rats, aging is associated with a decline in serum LH levels, suggesting that the reduced T production probably is due to chronic understimulation of LCs by LH [1]. The mechanism by which suppression of steroidogenesis results in a delay or prevention of age-related reductions of LCs ability to produce T remains uncertain [10].

In conclusion, our data suggest that altered trophic of seminiferous epithelium that occurred with aging is associated with decreased LC steroidogenesis and reduced androgen signalling in SCs.

References

1. C h e n, H., M. P. K a r d y, B. R. Z i r k i n. Age-related decreases in Leydig Cell testosterone production are not restored by exposure to LH in vitro. — Endocrinology, **143**, 2002, 1637-1642.
2. H e i n l e i n, C. A., C. C h a n g. Androgen Receptor (AR) coregulators: An overview. — Endocrine Rev., **23**, 2002, 175-200.
3. L e v y, S., V. S e r r e, L. H e r m o, B. R o b a i r e. The effects of aging on the seminiferous epithelium and the blood-testis barrier of the Brown Norway rat. — J. Androl., **20**, 1999, 356-365.
4. N i p k e n, C., K.W r o b e l. A quantitative morphological study of age-related changes in the donkey testis in the period between puberty and senium. — Andrologia, **29**, 1997, 149-161.
5. P a n i a g u a, R., M. N i s t a l, F. S a e z. Ultrastructure of the aging human testis. — J. Electron Microsc. Tech., **19**, 1991, 241-260.

6. R i c h a r d s o n, L., H. K l e i n m a n, M. D y m. Altered basement membrane synthesis in the testis after tissue injury. — J. Androl., **19**, 1998, 145-155.
7. R o y, A., Y. L a v r o v s k y, C. S o n g, S. C h e n, M. J u n g. Regulation of androgen action. — Vitam. Horm., **55**, 1999, 309-352.
8. S y e d, V., N. H e c h t. Selective loss of Sertoli cell and germ cell function leads to a disruption in Sertoli cell-germ cell communication during aging in the Brown Norway rat. — Biol. Reprod., **64**, 2001, 107-112.
9. W a n g, C., A. L e u n g, A. S i n h a - H i k i m. Reproductive aging in the male Brown Norway rat: a model for the human. — Endocrinology, **133**, 1993, 2773-2781.
10. Z i r k i n, B., H. C h e n. Regulation of Leydig Cell steroidogenic function during aging. — Biol. Reprod., **63**, 2000, 977-981.

Institute of Experimental Morphology and Anthropology with Museum
Bulgarian Anatomical Society

Acta morphologica et anthropologica, 13
Sofia • 2008

Mast Cell Intercellular Interactions of Involuting Infantile Hemangiomas

Vesselin Belovejdov, Dorian Dikov, Penka Stefanova**, Victoria Sarafian****

Department of General and Clinical Pathology, Medical University, Plovdiv, Bulgaria
**Centre Hospitalier de Lagny-Marne-La-Valle, Service d'Anatomie et de Cytologie Pathologiques, France*
***Clinic of Pediatric Surgery Medical University, Plovdiv, Bulgaria*
****Department of Biology, Medical University, Plovdiv, Bulgaria*

Mast cell intercellular interactions are presented in the present article as well as their significance in infantile hemagioma (IH) involution. The influence of mast cells (M) upon endothelial cells, fibroblasts and myofibroblasts and the processes associated with endothelial thrombosis, microthrombosis, together with stromal hyalinosis and fibrosis recognizes the leading role of mast cells in tumor regression phenomenon.

Key words: Mast cells, hemangionas, endothelial cells, stromal cells, apoptosis.

Introduction

Infantile hemangiomas (IH) are the most common tumors in early childhood, whose molecular pathogenesis still remains unclear [1]. Recent hypothesis [2] suggest block of endothelial development in early development, hence suppressed proliferation and initiation of regression.

Many reports show presence of mast cells M in vascular proliferations. The interaction of M from one side and endothelium with fibroblasts from the other is a complex and reciprocal process [10], which leads to involutive changes in IH presented with hyalinosis and fibrosis. Mediators of M play certain role in this process too [6].

Piling up data for IH, together with the investigations on M, related to angiogenesis, tissue remodelling and fibrosis, evoke further questions still waiting to be answered.

Material and Methods

Ten IH are fixed in 10 % neutral formalin and embedded in paraffin. Tissue cuts (5 μm) are stained with hematoxyline and eosin and toluidine blue.

Tissue from 3 of the IH has been selected for ultrasrtucture and samples achieved by routine tissue processing (each 0,05 μm in thickness) have been inspected on electron transmission microscope "Phillips" CM 12 /STEM.

Results

Stained with hematoxyline and eosin MC present with centrally placed nuclei and evenly distributed chromatin. The cytoplasm is intensively pinkish, appreciating well its composition from bright granules. The toluidine blue staining provides a better vision of M and particularly of their granules in the cytoplasm, as well as in the stroma after cellular degranulation and in close proximity with stromal cells and blood vessels.

Most of the mast cells are located close to capillaries and stromal cells. The endothelium of the capillaries demonstrates apoptotic change — pyknosis of the nuclei (Fig. 1). On ultrastructure nuclear debris and lipofuscin granules are readily seen (Fig. 2). Some

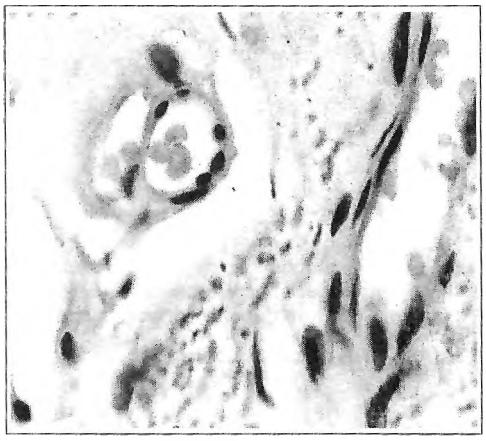

Fig. 1. Endothelial apoptosis (arrow) and mast cells (arrowhead). HE, × 200

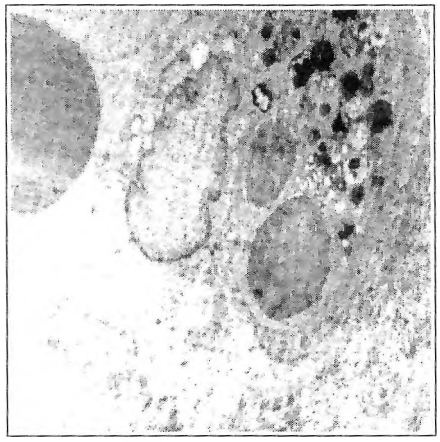

Fig. 2. Nuclear endothelial apoptotic debris. Electron microscopy. × 8000

Fig. 3. Microthrombosis (arrow) and mast cells (arrowhead). HE, × 400

Fig. 4. Two types mast cells — oval (arrowhead) and elongated (arrow). HE, × 200

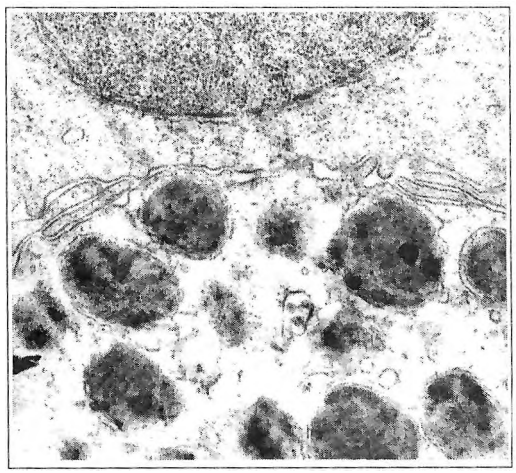

Fig. 5. Mast cell rich in granules in immediate proximity to stromal cell and finger-like cytoplasmatic protrusions between two cell types. Electron microscopy. × 18 000

Fig. 6. Mast cells (arrowhead) and stromal cells and perivasal hyalinosis (arrow). HE, × 400

of the capillaries close to the Ms display thrombotic aggregates and microthrombosis (Fig. 3). Expressed hyalinosis surrounds many of the blood vessels (Fig. 4).

Electron microscopy demonstrates the abundance of secretory granules in the cytoplasm of the mastocytes neighboring stromal cells. In cells intercellular regions, in between the cellular membrane of closely opposed cells, a finger-like cytoplasmic projections are seen (Fig. 5).

The stroma shows fibrosis, inflammatory cells, fibroblasts, myofibroblasts — the cytoplasm of the latter being rich in profiles of rough endoplasmic reticulum and myofilaments. Pinocytic vesicles are also present.

The observed mast cells display two morphological varieties— the classical "oval" and elongated (Fig. 6).

The underneath tissue shows inflammatory reaction.

Discussion

Phases of IH development (evolution) are dependent on changes in stroma and endothelium. Important role in the vascular changes has been attributed to apoptois. Nuclear pyknosis of endothelium is its earlier change. On ultrastructure nuclear debris and lipofuscin granules are readily seen (direct and indirect apoptotic features), as were shown in some of our previous works [4, 5].

Some of the capillaries in involuting IH display thrombotic aggregates and microthrombosis close to apoptotic endothelium, which suggests their relation with programmed cell death.

Next to endothelium in apoptosis, multiple mast cells are found which further puts their role in the above mechanism, a phenomenon already described by H a s a n et al. [7].

The interaction between endothelium and M is a complex and reciprocal process, not solely dependent on apoptosis. In view of this, large numbers of M are seen close to capillaries, even corresponding with the endothelium. Such a proximity is

not by chance—M survive lacking exogenous factors in an endothelium medium which suggests that endothelium compensates these factors in their "lifetime" [9].

Significant numbers of M are found in late stages of IH when fibrosis and hyalinosis prevail, which suggests M influence on these two processes as well. In proof of that are the ultrastructural cytoplasmic outpouching of M and neighboring stromal cells in involuting IH, similar to those depicted by D e t h l e f s e n et al. [3]. They can be accepted as contact expression, activating collagen synthesis of the stroma.

Other morphological expression of such functional influencing is probably the M changed appearance. Some of the M are different from the common oval shape. These elongated M are found alongside the classical M situated to stromal cells. The first description of the two M forms in both proliferative and involuting phases of IH belongs to P a s y k et al. [11]. It has been suggested that this change explains different functional capacities: M a k l o u f and I s h a k [8].

In conclusion — the present study demonstrates the morphological changes in IH. They are mainly related to M and M-cellular interactions which supports the thesis for the great importance of these multifunctional cells in IH regression.

References

1. B r u c k n e r, A. L., I. J. F r i e d e n. Hemangiomas of infancy. — J. Am. Acad. Dermatol., **48**, 2003, 477-493.
2. D a d r a s, S. S., P. E. N o r t h., J. B e r t o n c i n i, M. C. M i h m, M. D e t m a r. Infantile hemangiomas are arrested in an early developmental vascular differentiation state. — Modern Pathol., **17**, 2004, 1068-1079.
3. D e t h l e f s e n, S. M., J. B. M u l l i k e n, J. G l o w a c k i. An ultrastructural study of mast cell interactions in hemangiomas. — Ultrastruct. Pathol., **10**, 1986, 175-183.
4. D i k o v, D.I., J. R o l a n d, F. P. C h a t e l e t, C. C y w i n e r - G o l e n z e r. An autopsy study of the prostate in acquired immunodeficiency syndrome: evidence for excessive apoptosis and intracytoplasmic epithelial inclusions. — Arch. Pathol. Lab. Med., **122**, 1998, 875-879.
5. D i k o v, D. I., F. P. C h a t e l e t. In situ hybridization determination of the heterophagocytic origin of type 2B prostate epithelial lipochrome pigment granules: histochemical and ultrastructural correlates. — Folia Med. (Plovdiv), **43**, 2001, 13-16.
6. G a r b u z e n k o, E., A. N a g l e r, D. P i c k h o l t z, P. G i l l e r y, R. R e i c h, F. X. M a q u a r t, F. L e v i - S c h a f f e r. Human mast cells stimulate fibroblast proliferation, collagen synthesis and lattice contraction: a direct role for mast cells in skin fibrosis. — Clin. Exp. Allergy, **32**, 2002, 237-246.
7. H a s a n, Q., B. M. R u g e r, S. T. T a n, J. G u s h, P. F. D a v i s. Clusterin/apoJ expression during the development of hemangioma. — Hum. Pathol., **31**, 2000, 691-697.
8. M a k h l o u f, H. R., K. G. I s h a k. Sclerosed hemangioma and sclerosing cavernous hemangioma of the liver: a comparative clinicopathologic and immunohistochemical study with emphasis on the role of mast cells in their histogenesis. — Liver, **22**, 2002, 70-78.
9. M i e r k e, C., M. B a l l m a i e r, U. W e r n e r, M. P. M a n n s, K. W e l t e, S.C. B i s c h o f f. Human endothelial cells regulate survival and proliferation of human mast cells. — J. Exp. Med., **192**, 2000, 801-811.
10. M i e t t i n e n, M., M. S a r l o m o - R i k a l a, J. L a s o t a. KIT expression in angiosarcomas and fetal endothelial cells: lack of mutations of exon 11 and exon 17 of C-kit. — Modern Pathol., **13**, 2000, 536 -541.
11. P a s y k, K. A., W. C. G r a b b, G. W. C h e r r y. Ultrastructure of mast cells in growing and involuting stages of hemangiomas. — Hum. Pathol., **14**, 1983, 174-181.

Institute of Experimental Morphology and Anthropology with Museum
Bulgarian Anatomical Society

Acta morphologica et anthropologica, 13
Sofia • 2008

IFN-γ Colony-Stimulating Activity and *In Vitro* Effects on Neopterin Synthesis and Tryptophan Degradation

Y. Gluhcheva, E. Zvetkova, G. Konwalinka, D. Fuchs**

Institute of Experimental Morphology and Anthropology with Museum, Bulgarian Academy of Sciences
** Medical University, Innsbruck, Austria*

IFN-γ stimulated *in vitro* hematopoietic (erythroid and myeloid) colony formation by cultured human CD34+ hematopoietic progenitor cells, as well as their neopterin production and tryptophan degradation. Elevated neopterin (NP) concentrations in the liquid layer of the semi-solid agar cultures corresponded to enhanced hematopoietic colony formation, decreased amounts of tryptophan (Try) and increased kynurenine concentrations. When the quantitative changes of both substances — neopterin and tryptophan, were compared, they showed linear statistical relation. Neopterin concentrations — compared to kynurenine/tryptophan ratio, gave exponential relation.

Key words: human CD34+ hematopoietic progenitor cells, semi-solid agar cultures, IFN-γ, neopterin production, tryptophan degradation.

Introduction

IFN-γ stimulates *in vitro* not only hematopoiesis but also the production and/or degradation of some biologically-active substances such as neopterin, kynurenine, tryptophan, etc. [1-3, 8]. Recent data [6, 7] suggested a correlation between tryptophan degradation and neopterin synthesis in cases of different neurodegenerative diseases. Positive correlation between NP and K/T is found in cases of anemia, HIV infection and some autoimmune diseases [4].

The aim of the study was to determine the *in vitro* colony-stimulating activity of IFN-γ on human CD34+ hematopoietic progenitor cells and the statistical relation between the concentrations of neopterin and tryptophan in the liquid layer of the semi-solid agar cultures.

Material and Methods

Human purified and enriched CD34+ hematopoietic progenitor cells (isolated from mobilized peripheral blood of myeloma patient) were cultured in semi-solid agar

cultures in IMDM — supplemented with SCF, IL-3, erythropoietin /Epo/ (called recombinant cocktail — RC) or with 20% Agar-stimulated leukocyte conditioned medium (Agar-LCM). IFN-γ was added to both experimental systems at a single dose — 5000 U/ml or at doses 200 and 400 U/ml, applied every second day. CD34+ hematopoietic cell cultures were incubated for 14 days at 37°C in humidified air of 5% CO_2. After incubation cell colonies and clusters were stained with May-Grünwald-Giemsa and observed by light microscope. The liquid overlayers of agar cultures were used for measuring neopterin and tryptophan concentrations. NP concentrations were determined by ELISA (ELItest®Neopterin Screening — BRAHMS Diagnostica, Berlin, Germany). *In vitro* tryptophan concentrations and kynurenine amounts respectively, were measured by HPLC [5]. Regression analysis was applied for determining the statistical relation between neopterin and trytophan concentrations in both experimental systems (hematopoietic cells cultured in RC and/or Agar-LCM).

Results

The addition of different doses IFN-γ to the semi-solid agar cultures stimulated hematopoietic (erythroid and myeloid) colony and cluster formation by purified and enriched human CD34+ progenitor cells growing in RC and Agar-LCM (Tables 1, 2).

T a b l e 1. Total number of hematopoietic colonies formed by purified CD34+ human progenitor cells

Culturing conditions	Controls	5000 U/ml IFN-γ - once	400 U/ml/ IFN-γ 2d	200 U/ml/ IFN-γ 2d
Agar-LCM	75	106	93	92.5
RC	89	100.5	122.75	118.5

T a b l e 2. Total number of hematopoietic colonies formed by enriched CD34+ human progenitor cells

Culturing conditions	Controls	5000 U/ml IFN-γ - once	400 U/ml/ IFN-γ 2d	200 U/ml/ IFN-γ 2d
Agar-LCM	60.2	85	100.75	99.75
RC	120	177	174.75	169.25

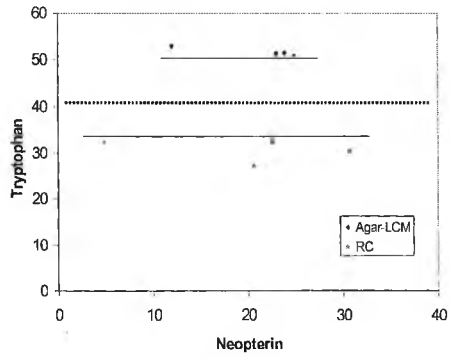

Fig. 1. Relation between neopterin production and tryptophan degradation by cultured *in vitro* purified CD34+ hematopoietic progenitor cells

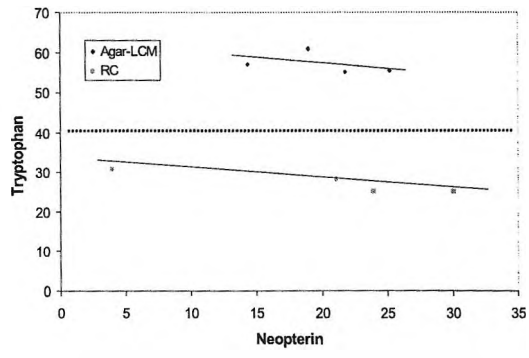

Fig. 2. Relation between neopterin production and tryptophan degradation by cultured *in vitro* enriched CD34+ hematopoietic progenitor cells

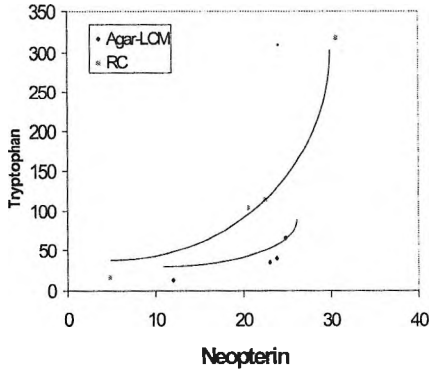

Fig. 3. Relation between neopterin production and kynurenine/tryptophan (K/T) ratio by cultured *in vitro* purified CD34+ hematopoietic progenitor cells

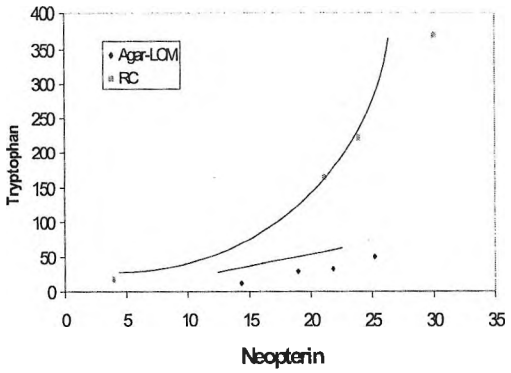

Fig. 4. Relation between neopterin production and kynurenine/tryptophan (K/T) ratio by cultured *in vitro* enriched CD34+ hematopoietic progenitor cells

When compared the concentrations of both biologically-active substances — NP and Try, a linear statistical relation was determined (Figs. 1, 2). The relation was exponential, when the logarithmic values of tryptophan/kynurenine (K/T) ratio and NP concentrations was compared (Fig. 3, 4). The enhanced colony formation under the *in vitro* influence of IFN-γ, corresponded to lower Try concentrations and elevated amounts of NP in the liquid layers of cultures.

Discussion

IFN-γ stimulated the *in vitro* formation of erythroid and myeloid colonies in both agar culture systems used — RC and Agar-LCM. The effects of the cytokine are better expressed when the CD34+ hematopoietic progenitor cells were cultured in RC where more erythroid colonies were obtained. The culture medium Agar-LCM enhanced myeloid (granulocyte/macrophage) cell proliferation, differentiation and colony formation. IFN-γ stimulated hematopoietic cell NP production and Try degradation in both culture systems. Our results are in agreement with those of W i r l e i t n e r et al. [7], showing in liquid cultures that increased NP concentrations correspond to decreased amounts of Try. The statistical correlation between the concentrations of both biologically-active substances — NP and Try is possibly due to simultaneous enzyme activation of GTP cyclohydrolase I (for neopterin production) and IDO (for tryptophan degradation) by IFN-γ, as is shown by T a y l o r et al. [3] for macrophages.

Conclusions

IFN-γ stimulates *in vitro* human CD34+ hematopoietic progenitor cell proliferation, differentiation and colony formation in semi-solid agar cultures. The cytokine activates the *in vitro* production of biologically-active substances — neopterin and kynurenine, used as biochemical markers for cellular activation. The quantitative relations determined between cellular NP synthesis and Try degradation may be used to predict the *in vitro* concentrations of either one of these substances.

References

1. Mellor, A. L., D. B. Keskin, T. Johnson, P. Chandler, D. H. Munn. Cells expressing indoleamine 2,3 dioxygenase inhibit T cell responses. — J. Immunol., **168**, 2002, No8, 3771-3776.
2. Shiohara, M., K. Koike, T. Nakahata. Synergism of interferon-γ and stem cell factor on the development of murine hematopoietic progenitors in serum-free culture. — Blood, **81**, 1993, No6, 1435-1441.
3. Taylor, M. W., G. Feng. Relationship between interferon-γ, indoleamine 2,3-dioxygenase, and tryptophan catabolism. — FASEB J., **5**, 1991, No11, 2516-2522.
4. Weiss, G., K. Schroecksnadel, V. Mattle, C. Winkler, G. Konwalinka, D. Fuchs. Possible role of cytokine-induced tryptophan degradation in anaemia of inflammation. — Eur. J. Haematol., **72**, 2004, No2, 130-134.
5. Widner, B., E. R. Werner, H. Schennach, H. Wachter, D. Fuchs. Simultaneous measurement of serum tryptophan and kynurenine by HPLC. — Clin. Chem., **43**, 1997, No12, 2424-2426.
6. Widner, B., M. Ledochowski, D. Fuchs. Interferon-γ-induced tryptophan degradation: neuropsychiatric and immunological consequences. — Curr. Drug Metabol., **1**, 2000, No2, 193-204.
7. Wirleitner, B., G. Neurauter, K. Schroecksnadel, B. Frick, D. Fuchs. Interferon-γ-induced conversion of tryptophan: immunologic and neuropsychiatric aspects. — Curr. Med. Chem., **10**, 2003, No16, 1581-1591.
8. Wachter, H., D. Fuchs, A. Hausen, G. Reibnegger, E. R. Werner. Neopterin as a marker for activation of cellular immunity: immunologic basis and clinical application. — Adv. Clin Chem., **27**, 1989, 81-141.

Institute of Experimental Morphology and Anthropology with Museum
Bulgarian Anatomical Society

Acta morphologica et anthropologica, 13
Sofia • 2008

Interactions between FGF2 and TGFβ-family Members in Control of the Onset of Mouse Spermatogenesis

Y. Martinova

Institute of Experimental Morphology and Anthropology with Museum, Bulgarian Academy of Sciences, Sofia, Bulgaria

The effect of different TGFβ-family members, namely TGFβ1, activin, inhibin, Mullerian inhibitory substance (MIS) — holo MIS, N- and C-terminal domains, on the onset of mouse spermatogenesis in presence of FGF2 was studied. 2-day-old mouse testes were cultured 24 hours in vitro in DMEM supplemented with maximally stimulating dose of FGF2 and different TGFβ family members. DNA synthesis in quiescent mouse spermatogonia was detected by means of immunocytochemistry using Cell proliferation kit (Amersham). It was registered that TGFβ1, inhibin, holo MIS and C-terminal domain of MIS down-regulate FGF2-stimulated germ cell proliferation while activin and N-terminal domain of MIS were not effective. The obtained results show that interactions between FGF2 and TGFβ family members play a key role in controlling the onset of mouse spermatogenesis.

Key words: growth factors, mouse spermatogenesis.

Introduction

Factors regulating the proliferation of spermatogonial stem cells and thereby providing the lineage of germ cells required to generate enormous number of sperm, are the object of intensive studies lately. In adult testes the progenitor stem cells are the source for mitotically proliferating spermatogonia and in turn the differentiating spermatocytes and spermatids [1]. It is suggested that FSH together with local growth factors are involved in the renewal of male germ cell proliferation. In immature testis few days before and after birth prospermatogonial cells enter nonmitotic quiescent phase. About day 3-4 after birth in mouse testis quiescent spermatogonia undergo nearly coordinately a series of cell divisions and this event marks the onset of spermatogenesis. Previously we showed that FGF2, LIF and TGFβ family members are involved in regulation of the onset of rat spermatogenesis [3, 4]. In the present paper we present a data about the interactions between FGF2 and TGFβ family members, namely inhibin, activin, TGFβ1, MIS (holo MIS, N- and C-terminal domains) in control of the onset of mouse spermatogenesis.

Material and Methods

2-day-old mice testes were cut into 2 segments, placed on permeable celloidine membranes and cultured in organ culture dishes, containing DMEM, supplemented with 2% BSA and 5-bromo-2-deoxyuridine (BrdU) (negative control). In positive controls the medium was supplemented additionally with FGF2: maximal effective dose of 1 ng/ml. In experimental groups in addition to FGF2, the medium was supplemented with different doses inhibin, activin, TGFβ1, holo MIS, N- or C-terminal domains of MIS. The explants were cultured 24 h, immersed in OCT compound, snap-frozen and cryosectioned at 5 μm. Detection of BrdU incorporation was achieved immunocytochemically by using Cell proliferation kit (Amersham). Labelled germ cell nuclei were counted and dose-response curves were prepared.

Results

In the testis of immature mouse spermatogonial cells are situated centrally in the seminiferous cords. After culturing of 2-day-old mouse testes 24 hrs in presence of maximally stimulating dose of 1ng/ml FGF2, the percentage of proliferating spermatogonial cells increases up to 50% (Fig 1A). The effect of different doses of TGFb family members (inhibin, activin, TGFβ1, MIS) applied in combination with 1ng/ml FGF2 showed that inhibin, TGFβ1, holo MIS and C-terminal domain of MIS

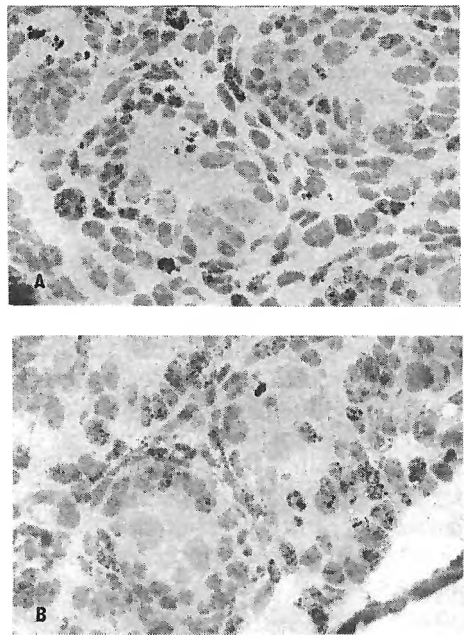

Fig.1. Light micrographs of stained frozen sections prepared from 2-day-old mouse testes after incubation 24 hrs with BrdU in presence of 1 ng/ml FGF2 (A) — positive control, or in presence of 1ng/ml FGF2 and 100ng/ml inhibin (B). × 100

down-regulate FGF2-stimulated spermatogonial proliferation. According to prepared dose-response curves (not shown), the percentage of labelled germ cells decreases up to negative controls — about 10% (Fig. 1B).

Discussion

We have shown previously that activin, together with FGF2 and LIF may positively regulate spermatogonial proliferation in mammalian testis [3]. These data support the finding about the expression of activin IIB receptors on type A spermatogonia in prepubertal testes [2]. The suppressive effect of holo MIS and C-terminal domain on FGF2-stimulated spermatogonial proliferation confirm the suggestion that C-terminal domain is the active one but not N-terminal. It is known that MIS concentration decreases during puberty and coincides with rapid germ cell proliferation stimulated by other growth factors including FGF2. In addition FGF2 stimulates Leydig cell steroidogenesis which positively regulate germ cell proliferation. In addition to MIS, an opposite relationship exists between TGFβ1 and Inhibin on one side and FGF2 from the other side. Thus interactions between TGFβ family members and FGF2 participate actively in control of the onset of mouse spermatogenesis.

References

1. Bellve, A. R. The molecular biology of mammalian spermatogenesis. — Oxford Rev. Reprod. Biol., **1**, 1979, 159-261.
2. Manova, K.,V. De Leon, M. Angeles, S. Kalantry, M. Giarre, L. Attisano, J. Wrana, R. Bachvarova. mRNAs for activin receptors II and IIB are expressed in mouse oocytes and in the epiblast of pregastrula and gastrula stage mouse embryos. — Mech. Dev., **49**, 1995, 3-11.
3. Martinova, Y., D. Nikolova, A. Bellve. Mullerian inhibitory substance down-regulates Seminiferous growth factor — stimulated rat prospermatogonial cell proliferation in vitro. — Acta morphol. Anthropol., **6**, 2001, 45-50.
4. Nikolova, D., Y. Martinova, M. Seidensticker, A. Bellve. Leukaemia inhibitory factor stimulates prospermatogonial stem cell proliferation. — Reprod. Fertil. Develop., **9**, 1997, 717-721.

Institute of Experimental Morphology and Anthropology with Museum
Bulgarian Anatomical Society

Acta morphologica et anthropologica, 13
Sofia • 2008

Immunocytochemical Localization of Antigen Involved in Sperm-Zona Pellucida Interaction

*M. Mollova, Y. Martinova**

Institute of Biology and Immunology of Reproduction "Acad. K.Bratanov", Bulgarian Academy of Sciences, Sofia
**Institute of Experimental Morphology and Anthropology with Museum, Bulgarian Academy of Sciences, Sofia*

Previously we have produced Mab 4B12 which recognized a surface membrane-associated protein located in the acrosome portion of the boar capacitated spermatozoa with role in a primary sperm-zona pellucida binding. The objective of the present study is to determine the tissue specificity of Mab 4B12 cognate antigen. The reaction of Mab 4B12 against saline extracts of boar reproductive and somatic organs was examined by indirect ELISA and immunoperoxidase technique. The ELISA results showed a dose-depended reaction of the antibody with testis as well as with caput, corpus and cauda epididymis, but not with somatic extracts used. Immunocytochemical analysis of paraffin-embedded somatic and reproductive boar tissue showed positive reaction on Leydig cell cytoplasm as well as on elongated spermatids. In the epididymis positive reaction was observed on the apical epithelium cells and on the spermatozoa in the lumen. Somatic tissue sections studied as well as HEP-2 cells were negative in immunoperoxidase test. The results showed tissue specificity of the 4B12 protein with possible doublet secretion in the testis and epididymis, proposing its significance in the fertilization.

Key words: sperm-egg interaction, monoclonal antibody, sperm antigens.

Introduction

Fertilization in mammals involves a series of specific interactions between ligand and receptor molecules on complementary gametes [6, 7]. In the majority of species these molecules are located on the limiting surfaces of spermatozoa and egg; in the case of spermatozoa, specifically on the plasma membrane overlying the acrosomal domain and in the case of eggs, on the zona pellucida (ZP) [5]. The identification of sperm receptors and the complementary molecules to which they bind in the zona pellucida is of a great importance for studying mechanisms of gamete recognition and initial binding processes during the first steps of fertilization.

Previously we produced a series of monoclonal antibodies (Mabs) against boar capacitated sperm [2] and we found Mab 4B12 to recognize a surface membrane-associated protein localized on the acrosomal portion of capacitated sperm, shared by

different animal species. In addition we showed protein 4B12 is not connected with sperm motility and secondary sperm-ZP binding as well as with acrosome reaction of spermatozoa, either spontaneous or induced [4]. The results from biological experiments demonstrated that protein 4B12 participates in the primary binding of sperm to ZP [3]. The present study was aimed on tissue specificity of Mab 4B12 cognate antigen.

Material and Methods

Tissue specificity of the 4B12 protein was studied by means of enzyme linked immunosorbent assay (ELISA) and immunocytochemistry. The reactivity of Mab 4B12 against boar reproductive and somatic organs as well as against somatic cell line HEP-2 was examined. Boar capacitated spermatozoa ($1\text{-}5 \times 10^6$) as positive control, boar seminal plasma as negative control (diluted 1:1 in bicarbonate coating buffer pH 9.6) or saline extracts (1mg/ml protein) of boar reproductive (testis and epididymis-caput, corpus and cauda) and somatic (spleen, stomach, kidney, muscle, lung, intestines, colon, liver, lymph node, heart) organs in PBS were coated onto PVC 96-well U-bottomed microtitre plates (Costar Ltd., USA) and the procedure for ELISA reported earlier [1] was applied. The optical density was read at Titertek ELISA reader at 492 nm. Pieces of the same tissues were fixed and embedded in paraffin. Tissue sections (5 μm) after deparaffinization and dehydratation as well as smears of HEP-2 somatic cell line were stained by immunoperoxidase technique. Endogenous peroxidase activity was blocked by incubation in 1.2% H_2O_2 in medium for 10 min. The non-specific binding was blocked by 5% normal goat serum. The tissues and smears were incubated with Mab 4B12 (culture supernatant) overnight at 4°C and with HRP- conjugated goat anti- mouse IgG at dilution 1:80 for 60 min. The reaction was developed with 0.1% DAB in the presence of 0.02% H_2O_2. The sections were counterstained with Harris's hematoxilyn and observed on Zetopan microscope (Reichert, Vienna, Austria). Control probes were examined using supernatant of nonspecific monoclonal antibody — Mab 3G2 against melanoma associated antigens.

Results and Discussion

ELISA of Mab 4B12 with saline extracts of boar somatic organs showed negative reaction. Strong concentration-dependent reaction of Mab 4B12 with positive control (boar capacitated spermatozoa) and no reaction with negative control (boar seminal plasma) was observed. A weak positive reaction with an antigen from stomach only was registered (Fig. 1). The ELISA results with saline extracts of reproductive organs showed a dose-depended reaction of the antibody with testis as well as with caput, corpus and cauda epididymis, the reaction being weakly exposed in comparison with control capacitated spermatozoa (Fig. 2). The tissue specificity of 4B12 protein was further confirmed by immunocytochemical analysis of paraffin-embedded sections of the boar somatic and reproductive tissues. In the testis weak staining of the Leydig cell cytoplasm as well as of elongated spermatids was detected (Fig. 3). In the epididymis weak positive reaction was observed on the apical epithelium cells as well as on the spermatozoa in the lumen (Fig. 4). Somatic tissue sections used were negative. The data that Mab 4B12 did not stain HEP-2 cells in immunoperoxidase test confirmed the lack of appreciable cross reactivity of antibody with antigenic determinants on somatic tissues.

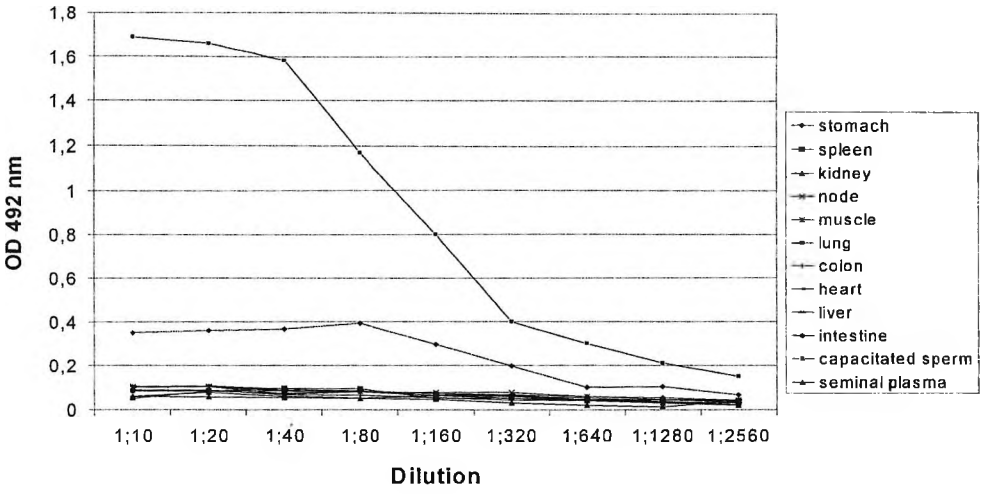

Fig.1. Negative reaction of Mab 4B12 with saline extracts of somatic tissues in ELISA is registered. Strong dose-depended reaction with positive control (capacitated spermatozoa) and weak positive reaction with an antigen from stomach only was observed

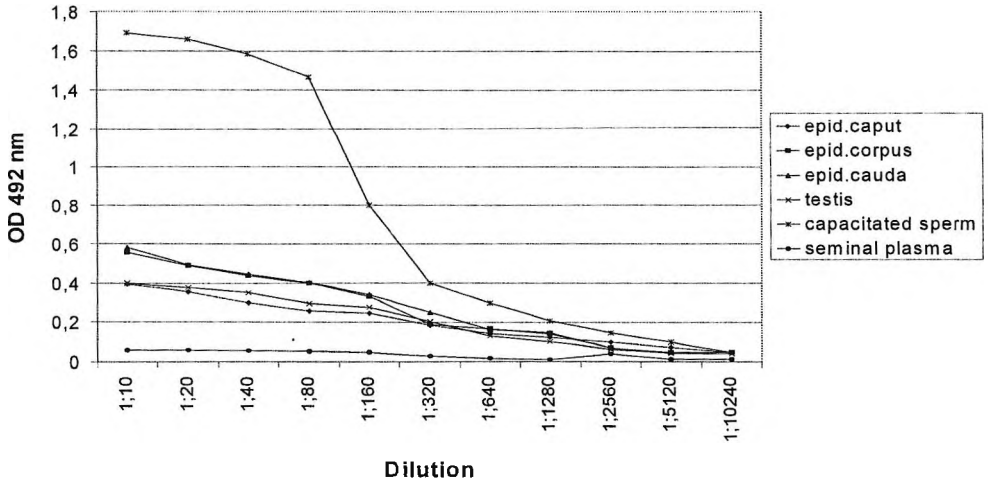

Fig.2. Dose-depended positive reaction of Mab 4B12 with saline extracts of boar reproductive tissues (testis and caput, corpus and cauda epididymis) is seen, the reaction being weakly exposed in comparison with positive control (capacitated spermatozoa)

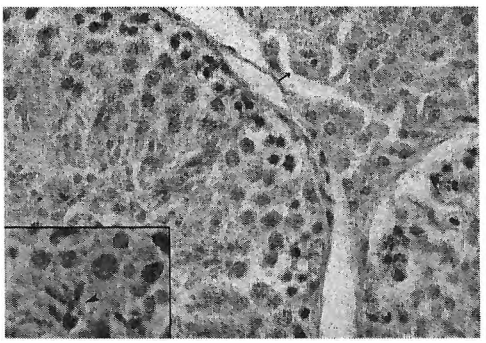

Fig. 3. Immunocytochemical analysis of boar reproductive tissues (testis) with Mab 4B12: labelling of the Leydig cell cytoplasm (arrow) as well as of the elongated spermatids was detected (arrowhead). × 480

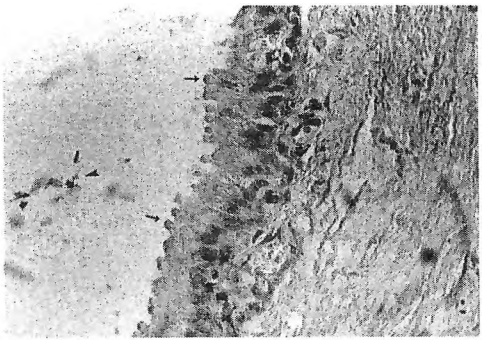

Fig. 4. Immunocytochemical analysis of boar reproductive tissues (cauda epididymis) with Mab 4B12: labelling of the apical epithelium cells (arrows) as well as of the caudal spermatozoa in the lumen was observed (arrowhead). × 320

The results on the positive, although weak reaction of Mab 4B12 with the testis and the epididymis but not with somatic tissues, obtained after the application of two different methods, suggest that the corresponding antigen seemed to be an intrinsic cell membrane protein secreted by Leydig and epididymal cells and connected with sperm maturation. Positive reaction of Mab 4B12 with both reproductive tissues and capacitated sperm may result from an unmasking and/or transformation of ligand (s) that is already present in the sperm and becomes accessible to antibody after plasma membrane modifications accompanying sperm capacitation. It is possible that 4B12 corresponding antigen is secreted by Leydig cells, transported to the Sertoli cell cytoplasm and bound to the sperm cell membrane during their terminal differentiation stage. The immunocytochemical staining of Leydig cells as well as of epididymal epithelial cells together with positive reaction of Mab 4B12 with an antigen from extracts of the reproductive organs tested in ELISA gives ground to assume doublet secretion of the antigen in the testis and epididymis, proposing its significance in the fertilization process.

References

1. Kyurkchiev, S., Tz. Surneva-Nakova, M. Ivanova, L. Nakov, E. Dimitrova. Monoclonal antibodies to porcine zona pellucida that block the initial stages of fertilization. — J. Reprod. Fertil., **18**, 1988, 11-16.
2. Mollova, M., G. Atanasova, S. Kyurkchiev, M. Ivanova, J. Peknicova. Monoclonal antibodies reacting against capacitated but not with freshly ejaculated boar spermatozoa. — AJRI, **36**, 1996, 301-308.
3. Mollova, M., R. Nedkova, M. Ivanova, T. Djarkova, J. Peknicova, S. Kyurkchiev. Role of a capacitation-related protein on some sperm functional parameters. — Folia Biologica (Praha), **48**, 2002, 232-236.
4. Nedkova, R., M. Mollova, M. Ivanova, S. Kyurkchiev. Effect of Mab 4B12 against capacitated boar spermatozoa on spontaneous and induced acrosome reaction. — 3rd Balkan Congress on Andrology, June 6-8, 2002, Sofia.
5. Parry, R. V., P. J. Barker, R. Jones. Characterization of low Mr zona pellucida binding proteins from boar spermatozoa and sminal plasma. — Molecular Reproduction and Development, **33**, 1992, 108-115.
6. Wassarman, P. M. Profile of a mammalian sperm receptor. — Development, **108**, 1988, 1-17.
7. Yanagimachi, R. Mammalian Fertilization. — In: The Physiology of Reproduction (Eds.E. Knobil and J. Neill). New York, Raven Press, 1994, 189-317.

Institute of Experimental Morphology and Anthropology with Museum
Bulgarian Anatomical Society

Acta morphologica et anthropologica, 13
Sofia • 2008

Erectile Dysfunction in Men in Reproductive Age

B. Nanova

Department of Anatomy, Histology and Embryology, Medical University "Prof. Dr Paraskev Stoyanov", Varna

One of the enumerate reasons for sexual insecurency in a man and in a couple as a whole is the erectile dysfunction.We have the idea to examine ejaculates to determine the main characteristics of sperm and morphologically to investigate the biopsies of men with vascular disturbances such as idiopathic varicocele and testicular torsio.Material was received from testicular biopsies of 18 men in reproductive age and the applying of new modern apparatus-γ-chamber scintigraphy and echography in men with erectile dysfunction as idiopathic varicocele, trauma and torsio testis enrich the diagnostic possibilitites in andrologic practice.The different ethiological factors lead to one type morphological alterations in both testes, that are expressed with:trsansitional changes — hypospermatogenesis, desorganisation of germ cells, intratubular cessation of maturation. Peritubular matrix reacts to pathogenic factors with increasing amount of fibrous elements of matrix components.

Key words: erectile dysfunction, idiopathic varicocele, torsio.

Introduction

The reproduction of the population is a basic demographic index for each nation. Exsisting in Bulgaria and in many European countries unfavourable tendencies on basic demographic indexes as bearing, lethality, growth of the population, put the problem of human reproduction of a social significance. According to our data and findings, searching the facts for structural and functional changes characterizing the man in different ages in ontogenic aspect, show different characteristical specificities, that give us the reason to limit and differ corresponding age groups: early childhood, childhood, puberty, postpuberty, reproductive and sexual period of mature man, adult men — this period goes with partial androgenic deficiency (PADAM) and period of "aging man" — in this period andropause is in fact.

Aim of the study

We aimed to study morphological changes in testicular tissue that occur in pathological process such as erectile dysfunction in patients with vascular alterations: varicocele, torsio and trauma testis.

Material and Methods

Material was received from testicular biopsies of 18 men with varicocele, torsio and trauma testis. **Methods** – examination of local status of the patients:examining the external genitals in standing position; examining the external genitals in laying position.

Sperm analysis – including all sperm indexes: – volume of the ejaculates;number of the spermatozoa in 1 ml; speed of the sperm; motility; vitality test of spermatozoa; PH of the ejaculates; fructose in ejaculates; cells in ejaculates; light microscopy examination of ejaculates.

Special methods – noninvasive: testicular echography**semiinvasive** [9]; testicular scintigraphy (conventional and γ-chamber scintigraphy); **invasive:** Dopler's angiography of the penis, testicular biopsy.

We used classical histological technique for examination of testicular biopsies. Material was fixed in Bouen and then paraffine sections were prepared. Haematoxyline- eosine staining was applied, as other stainings as well — according to Masson, Azan, Gommory, etc. To distinguish the changes that occur in testicular peritubular matrix we used classical immunohistochemistry and slides were incubated with monoclonal antibodies against collagen type IV, desmin, α-SMA.

Results

In men with idiopathic varicocele are affected testicular veins "plexus pampiniformis". The reason for varicocele is genetic weakness of the vein's vessel wall. The idiopathic varicocele is a reason for surgical intervention after diagnosis because the main effect is to prevent break of spermatogenesis and sexual depression with following hormonal treatment. Scrotal hypothrophy and disturbed spermatogenesis are observed (Fig. 1). Proliferation of collagen fibres affected the elements of funiculus spermaticus, mainly musculus cremaster is in fact.

The torsion and trauma testis are the critical sitiations of so called acute scrotum and need an emergency surgical intervention-detrocvation to 4th hour of torsion to 180 degrees. If the surgical treatment comes late a difinative morphological alterations even of contralateral testis are observed as a reason of autoimmune processes and this aqired orhidopexy. The degree of testicular lesions correspond to the time and duration of the pathogenic factors. Pathohistological findings show adequate alterations in both testes. Hypospermatogenesis, dezorganization of germ cells are observed (Fig. 2, 4). Sertoli cells are enlarged prominating in the lumen of seminiferous tubules and tubules are with diminished lumen (Fig. 1). Around Leydig cells proliferation of connectiove tissue elements is observed (Fig. 3, 6, 7).Torsion or trauma testis is the situation of acute scrotum needing emergency surgical intervention. Affected circulation and irreversible changes lead soon to disappearance of seminiferous epithelium (germ cells) (Fig. 3).Germinal aplazia is in fact (Fig. 3). Changes are observed in Sertoli cells, the lumen is abnormally enlarged and the reason is changes in normal development of germ cells. The reason for destractive alterations in basal membrane is the fact that myofibroblasts are dislocated, degenerate and we can not observe them (Fig. 3, 4, 5, 7). In the interstitum we found local increasing of the number of Leydig cells (Fig. 7). The relationships between the basic elements of haematotesticular barrier are affected and changes of Leydig cells cause influence on autocrine and paracrine regulation of spermatogenesis.

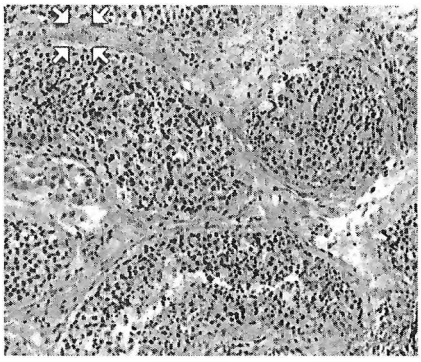

Fig. 1. Testicular biopsy. Idiopathic varicocele.Hypoispermatogenesis. Dezorganization of germ epithelium. Peritubular fibrosis. Haematoxyline-Eosine staining. × 200

Fig. 2. Testicular biopsy. Torsio testis. Hypospermatogenesis. Oligosoospermia II-III degree. Proliferation of collagen fibres in testicular peritubular matrix.Haematoxyline-Eosine staining. × 300

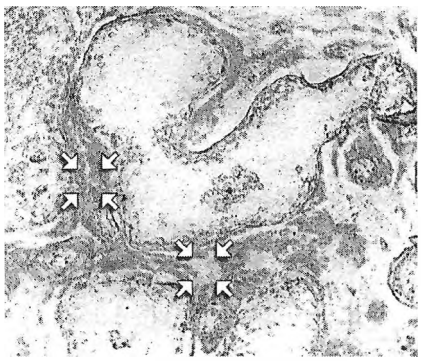

Fig. 3. Testicular biopsy. Azoospermia. Immunohistochemistry. Monoclonal anti-collagen type IV antibody. Possitive immune staining. × 400

Fig. 4. Testicular biopsy. Oligozoospermia III dg. Possitive immunostaining for alpha smooth muscle actine. Anti-alpha smooth muscle actine antibody. × 250

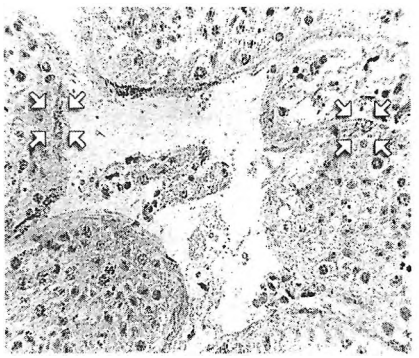

Fig. 5. Testicular biopsy. Oligoastenozoospermia III dg. Possitive immunostaibning for desmine and strong immune reaction in basal membrane and in the wall of blood vessels in testicular interstitium. × 300

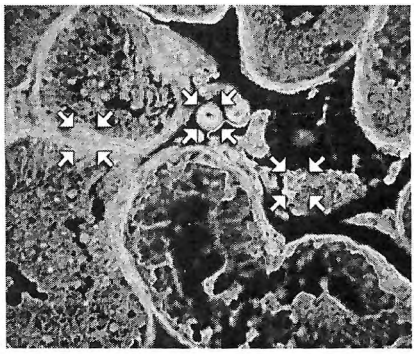

Fig. 6. Testicular biopsy. Strong immune reaction for alpha smooth muscle actine in peritubular tissue, around blood vessels and in testicular interstitium. Direct immunofluorescence. × 250

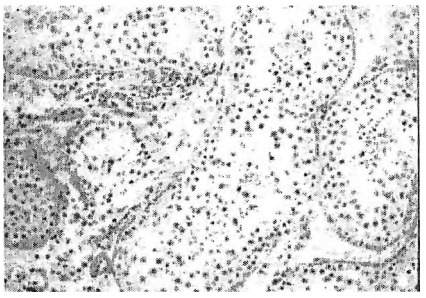

Fig. 7. Testicular biopsy. Testicular torsion (12th hour). Diminished lumen of seminiferous tubules, fractured basal membrane,dislocation of myofibroblasts, local proliferation of Leydig cells. Haematoxyline-Eozine staining. × 250

Discussion

Deseases leading to haematodynamic alterations affected male gonads related to male infertility and sexual problems take a real important place in androgenic and sexologic practice. Usually affected men are young (20-50 years old, in reproductive age). Testicular microvasculature is still not enough examined mainly in men with fertile problems. The most common diseases with vascular changes leading to erectile dysfunction are: idiopathic varicocele, priapismus, torsio testis, induratio penis plastica.

According to data in literature stress and intensification of life as some congenital alterations in male reproductive system cause troubles in human fertility [3,5]. Mainly in standing for a long period of time, walking, physical training or sexual excitement, patients with idiopathic varicocele have some troubles. Echography shows increasing the size of left testicular vein, the scrotum, does not show any assimetry. Enlarging of the veins are not observed. During the last stages of the disease clinical changes lead to pathohistological once of testicular tissue-hypospermatogenesis, disorganization of germ cells and intratubular cessation of maturation on the level of late spermatids, and the changes affect both testes. Some authors find changes in ultrastructure such as affected spermatogenesis-cessation of the maturation is in fact and they observed late spermatids [1, 4, 5]. Because of the defect of condensation of the chromatin a nuclear vacuole is formed and it takes place more than the half of the nuclear volume of the spermatid. This, on the one hand, will lead to damage of other stages of the cell differentiation and, on the other, will cause changes in the structure of the spermatozoa (so called teratozoospermia), [5, 6]. We comment this as a result of metabolic changes in spermatogenesis.

In men with torsio and trauma testis we have in mind cases with open and closed trauma, acute haemodynamic testicular changes and complications after herniotomy. The basic pathogenic mechanisms are direct testicular trauma, or acute disturbances in haemodynamics as a reason of affected circulation.While testicular torsion is incidently occurred as a disturbance of haemodynamics. In most patients schurgical intervention (detorquation) was done after 48th hour of torsion. This late surgical intervention we can explain with taking not seriously and critically the situ-

ation and the need of emergency surgical treatment. In all cases even in such when detorquation was done after 12 hour of torsion pathohistological findings show changes in both testes- germinal aplasia, Sertoli cell syndrome [6, 7, 8]. Peritubular tissue shows increasing of the fibrous elements of peritubular matrix,dislocation of myofibroblasts and in some places they cannot be observed [7]. On some places of testicular interstitium a local proliferation of Leydig cells is observed [2, 5]. Some authors [2, 4, 7, 8] give us information for ultrastructural changes — deformation and folding and thiked basal membrane. [5, 8] discussed about affected haematotesticular barrier and we support this facts with our data for dislocated myofibroblasts that we observed in our cases. Something more paralelly with morphological studies we provide examination of sperm and sperm analysis shows in severe cases aspermia. All this we can comment with severe irreversible changes in ipsilateral testes (morphological and functional alterations) followed by adequate changes in contralateral testes as an autoimmune answer. Changes in testicular interstitum — in number of Leydig cells lead to paracrine and endocrine changes in spermatogenesis.

Conclusions

Idiopathic varicocele in all ways need surgical treatment after correct diagnosis, because leads to disturbed spermatogenesis, sexual problems and depression, testicular torsion and trauma as situations of "acute scrotum" needing adequate surgical treatment as soon as possible (till 4th hour of torsion), as well.

References

1. Alberts, B., D. Bray, J. Lewis, M. Raff, K. Roberts, J. D. Watson. Molecular biology of the cell. Third Eddition, Inc, New York — London, 1994.
2. Burrow, M., M. Cough. Billateral absence of tesis. — Lanset, 1970, 366-367.
3. Motta,P. Microscopy of reproduction and development:a dynamic approach. — In: Medicina Scienze (Ed. A. Delfino). Roma-Milano.
4. Кънчева, Л., Й. Мартинова, Д. Цветков. Електронномикроскопски проучвания на тестикуларна тъкан при мъжки инфертилитет. — Акушерство и гинекология, **23**, 1984, No 5, 445—449.
5. Нанов, З. Клинико-морфологични проучвания на мъжкия инфертилитет (канд. дис.). София, 1996, 1—128.
6. Нанов, З. Ембриология на човека — анатомия, тератология и клиника. София, Знание, 2003, 1—237.
7. Нанова, Б. Проучване на тестикуларен перитубуларен матрикс на човек в норма и патология и на плъх в условия на експеримент (морфологични, хистохимични, имунохистохимични и хормонални методи на изследване (канд. дис.), София, 2005, 1—55.
8. Рускова, Ц., М. Карапандов, Д. Цветко. Клинична андрология. София, Медицина и физкултура, 1982.
9. Цветков, Д., Л. Саломбашев, П. Трингов. Възможността на функционалната сцинтиграфия при някои заболявания на тестисите. — Хирургия, **34**, 1981, №3, 262—274.

Institute of Experimental Morphology and Anthropology with Museum
Bulgarian Anatomical Society

Acta morphologica et anthropologica, 13
Sofia • 2008

Estrogen-Induced Abnormalities in Rat Germ Cell Development during Puberty

*E. Pavlova, N. Atanassova, R. Sharpe**

Institute of Experimental Morphology and Anthropology with Museum, Bulgarian Academy of Sciences, Sofia
** MRC, Human Reproductive Sciences Unit, Edinburgh, UK*

The present study aimed to characterize the estrogen effect on different stages of germ cell development in tandem with Sertoli cell support to defined germ cell types. Neonatal treatment with diethilstilboestrol (DES) or GnRH-antagonist (GnRHa) exerted similar negative effects on spermatogonia (Sg), whereas spermatocytes (Sc) were more affected by DES compared to GnRHa. Among the spermatogonia, more differentiated types intermediate (In) and B-Sg underwent more pronounced changes than A-Sg. In the population of spermatocytes, leptotene and zygotene stages were most sensitive to hormonal manipulation and the effect of DES was more severe than that of GnRHa. DES caused retardation of testis development at puberty and suppressed spermatogenesis acting on differentiation of Sg, initiation and proceeding of meiosis via direct and indirect mechanisms. Differential effect of DES and GnRHa on Sg and Sc and their subtypes demonstrated differential sensitivity of mitotic and more advanced meiotic stages of spermatogoenesis to neonatal hormonal disbalance.

Key words: estrogens, androgens, spermatogenesis, Sertoli cells, testis.

Introduction

Exposure to estrogens during neonatal life is reported to cause delayed development of the testis and permanent impairment of spermatogenesis in adulthood that adversely affects total germ cell (GC) and Sertoli cell (SC) populations [2]. Neonatal administrations of estrogens suppressed FSH production at the time when this hormone is essential for initiation of spermatogenesis at puberty. For that reason the negative effect of estrogens were attributed to suppression of gonadotropin secretion during the treatment that results in inhibition of testosterone (T) production by Leydig cells, as well [1].

The effect of estrogens, in particular DES, on different steps of germ cell differentiation was not investigated. In this respect **the aim** of the present study was to characterize the estrogen effect on different stages of germ cell development in tandem with Sertoli cell support to defined germ cell types that would reveal their differential sensitivity to DES. These data would elucidate our understanding about the mechanisms via which estrogens regulate particular phases of spermatogenesis and to evaluate the importance of estrogens, androgens and gonadotrophins.

Material and Methods

We used experimental model for manipulation of neonatal hormonal environment by treatment with DES-10 μg or DES-0.1 μg (2-12 day); GnRH antagonist -10mg/kg (2 and 6 day); co-administration of 10 μg DES and 200 μg T-propionate. In situ detection of germ cell apoptosis by TUNEL method [5] and subsequent 121-point counting using clock-face sampling of 25 fields (3025 p) [2] were applied. We estimated absolute nuclear volume (ANV) of SC, total GC (TGC), spermatogonia (A-Sg, In and B-Sg) and spermatocytes including preleptotene (Pl), leptotene and zygotene (L+Z) and pachytene (Ph), as well as the ratios of GC/SC. Comparison of the different parameters of the various treatment groups was made using Student's t- test.

Results and Discussion

On day 18 in the control group GC development proceeds to the late pachytene stage of meiotic prophase-I. The lumen was observed in most seminiferous tubules. There were seen single apoptotic cells.

Both the neonatal administration of DES-10 or GnRHa induced pronounced structural changes involving elevation of GC apoptosis and retardation of lumen formation (Figs. 1, 2). Quantitative analysis revealed that both treatments caused 3-fold reduction of spermatogonial ANV than control whereas ANV of Sc was decreased 10 times by DES-10 and 6 times by GnRHa (Fig. 3). Differences between mean values of DES-10 and GnRHa were significant that implied the direct estrogen action on meiotic germ cells. Co-administration of DES-10 with T partially prevented negative estrogen effects on Sg and Sc. There was a milder effect of 100-fold lower dose of DES-0.1 on the investigated parameters of spermatogenesis. The similarities in the action of high levels of estrogen and those induced by GnRHa (both treatments inhibit T-production by Leydig cells; [4]) indicate that gonadotrophin suppression is involved in indirect mechanism of action of DES.

The function of SCs to support GCs, known as efficiency of spermatogenesis, was evaluated by estimation of ANV of GCs per unit SC ANV (Fig. 4). The ratio of TGC/ SC decreased in larger extent in DES-10 (50 % reduction than control) compared to GnRHa group (30%). The differences between mean values of DES-10 and GnRHa were significant. The SC supporting capacity to Sg and Sc was affected by treatment with DES-10 or GnRHa. The direct estrogen action is evident at ratio Sc/ SC but not Sg/SC, similarly to ANV of Sc and Sg. Spermatogenic efficiency remained in a normal range in experimental group of DES-0.1 and DES-10+T. The ratio Sg/SC is unaffected and that of Sc/SC is lower by 25-35% but not significantly different compared to control. These data suggest direct action of low estrogen levels on GCs (Sg and Sc) rather than indirect mechanism via SCs and their supporting function. Sertoli and germ cells were reported to express ER-β [3] and the direct adverse effect of high estrogen levels on functional maturation of SCs was demonstrated by Sharpe et al. [5].

The differential sensitivity of different types Sg and Sc to neonatal hormonal manipulation was shown in Fig. 5 and 6. Exposure to DES-10 or GnRHa caused more pronounced changes in advanced types of spermatogonia — ANV of types In+B-Sg were reduced by 80% than control whereas that of A-Sg decreased non significantly by 35%. Among the Sc, L-Z stages were most sensitive to different hormonal treatments and the effect of DES was significantly more severe than those of GnRHa (13-fold and 8-fold decrease of ANV respectively). In support of this sug-

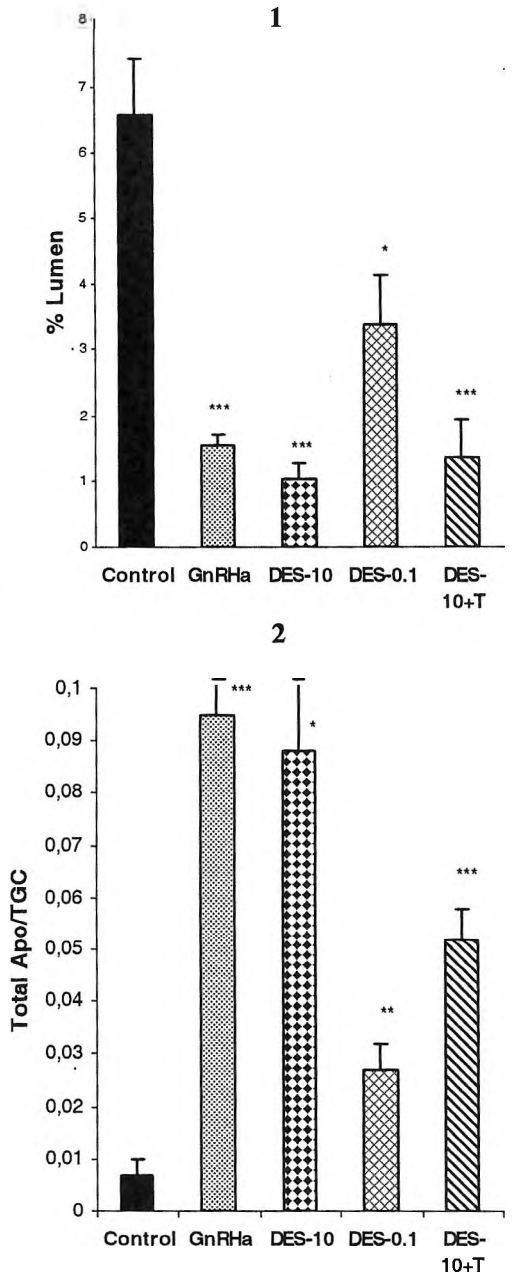

Figs. **1-4**. Quantification of spermatogenesis on day 18 of control and neonatally treated rats with GnRHa, DES-10 μg, DES-0.1 μg or co-administration of DES-10 μg and 200 μg T including Lumenal per cent volume (Fig. **1**); Apoptotic index (Fig. **2**); Absolute Nuclear Volume (mm^3) of GC types (Fig. **3**); Absolute Nuclear Volume of GC types per unit SC nuclear volume (Fig. **4**). Data represent mean value ± SE (* $p< 0.05$; ** $p< 0.01$; *** $p< 0.001$). TGC- Total Germ cells

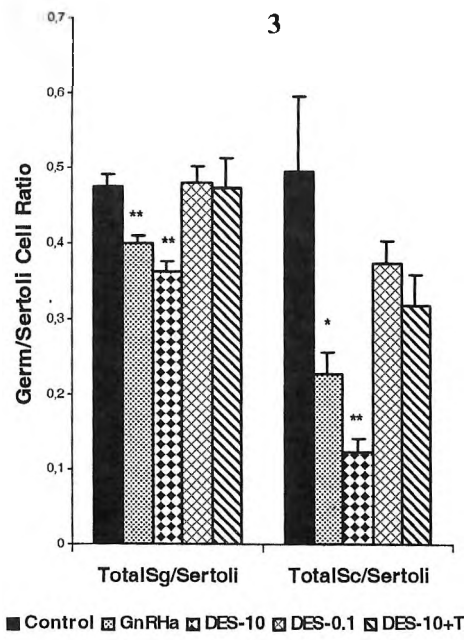

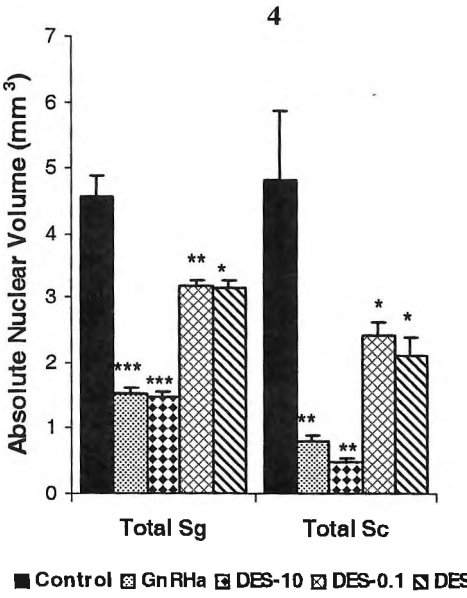

Figs. **1-4**. Quantification of spermatogenesis on day 18 of control and neonatally treated rats with GnRHa, DES-10 µg, DES-0.1 µg or co-administration of DES-10 µg and 200 µg T including Lumenal percent volume (Fig. **1**); Apoptotic index (Fig. **2**); Absolute Nuclear Volume (mm^3) of GC types (Fig. **3**); Absolute Nuclear Volume of GC types per unit SC nuclear volume (Fig. **4**). Data represent mean value ± SE (* $p< 0.05$; ** $p< 0.01$; *** $p< 0.001$).

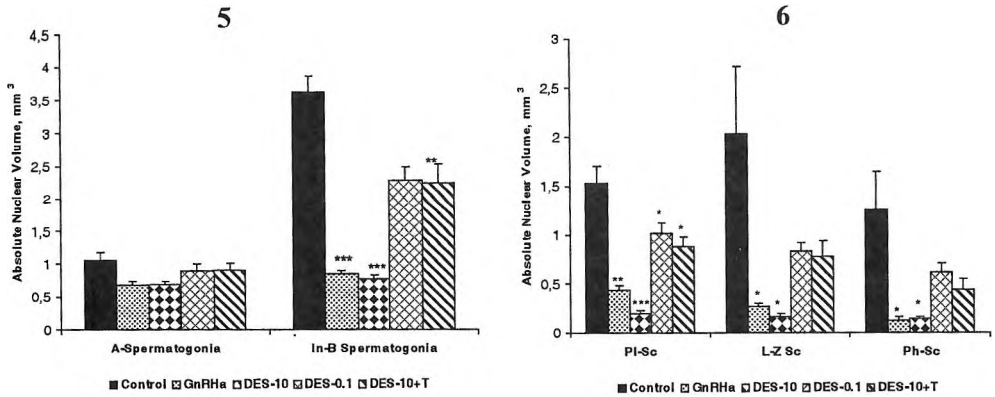

Figs. **5-6**. Quantification of Absolute Nuclear Volume (mm^3) of subtypes of spermatogonia (Fig. **5**) and spermatocytes (Fig. **6**) on day 18 of control and neonatally treated rats with GnRHa, DES-10 μg, DES-0.1 μg or co-administration of DES-10 μg and 200 μg T. Data represent mean value ± SE (* $p< 0.05$; ** $p< 0.01$; *** $p< 0.001$)

gestion are the data for combined treatment of DES-10+T. There was a lesser restoration effect of T-therapy toward L-Z stages (40% of control value) compared to that of Pl-Sc (60% of control value).

Conclusion

DES and GnRHa exerted similar negative effects on Sg, whereas Sc were more effected by DES compared to GnRHa. Among the Sg, more differentiated types In+B-Sg underwent more pronounced changes than A-Sg. In the population of Sc, L-Z stages were most sensitive to hormonal disbalance and the effect of DES was more severe than those of GnRHa. DES caused retardation of testis development at puberty and suppressed spermatogenesis acting on differentiation of Sg, initiation and proceeding of meiosis via direct and indirect mechanisms. Differential effect of DES and GnRHa on Sg and Sc and their subtypes demonstrated differential sensitivity of mitotic and meiotic stages of spermatogoenesis to neonatal hormonal manipulation.

References

1. Arai, Y., T. Mori, Y. Suzuki, H. A. Bern. Long-term effects of perinatal exposure to sex steroids and diethylstilbestrol on reproductive system of male mammals. — Int. Rev. Cytol., **84**, 1983, 235-268.
2. Atanassova, N., C. McKinnell, M. Walker, K. J. Turner, J. S. Fisher, M. Morley, M. R. Millar, N. P. Groome, R. M. Sharpe. Permanent effect of neonatal estrogen exposure in rats on reproductive hormone levels, Sertoli cell number and the efficiency of spermatogenesis in adulthood. — Endocrinology, **140**, 1999, 5364-5373.
3. Saunders P. T. K., J. S. Fisher, R. M. Sharpe, M. R. Millar. Expression of estrogen receptor beta (ERb) occurs in multiple cell types, including some germ cells, in the rat testis. — J. Endocrinol., **156**, 1998, R13-R17.
4. Sharpe, R. M. The "oestrogen hypothesis" — where do we stand now? — Int. J. Androl., **26**, 2003, 2-15.
5. Sharpe, R. M., N. Atanassova, C. McKinnel, P. Part, K. J. Turner, J. S. Fisher, J. B. Kerr, N. P. Groome, S. Mcpherson, M. R. Millar, P. T. K. Saunders. Abnormalities in functional development of the Sertoli cells with diethylstilbestrol: a role of estrogens in Sertoli cell development? — Biol.Reprod., **59**, 1998, 1084-1094.

Institute of Experimental Morphology and Anthropology with Museum
Bulgarian Anatomical Society

Acta morphologica et anthropologica, 13
Sofia • 2008

Beta-actin Expression in the Developing Small Intestine of Rat Embryos and Newborns

N. Penkova, I. Koeva, P. Atanasova, G. Baltadjiev

Department of Anatomy, Histology and Embryology, Medical University, Plovdiv

The primitive gut tube — archenteron is composed of tissues coming from both embryonal layers — endoblast and mesoblast. Endoblastic epithelium taping of the foregut lumen is surrounded by a layer of mesenchyme cells coming from the splanchnopleura of the mesoblast. Cell signalling between both embryonal sources plays a critical role in the coordinating processes and organogenesis of the foregut and its elements [4]. The aim of the present work was to follow beta-actin immunohistochemical expression in the differentiating endoblast and mesoblast derivatives in the developing rat gastrointestinal tract during late embryogenesis and in newborns. Material from 20 rat embryos (18^{th} gestation day) and fragment from the gastrointestinal tract of 10 newborn rats were investigated immunohistochemically (beta-actin). There were dynamic changes in the beta-actin expression in the differentiating small intestine..These dynamic changes suggest probable interaction of induction between consistent differentiating mesoblast and endoblast during both studied periods.

Key words: beta-actin, small intestine, endoblast, mesoblast.

Introduction

The primitive gut tube — archenteron is composed of tissues coming from both embryonal layers — endoblast and mesoblast. Endoblastic epithelium taping of the foregut lumen is surrounded by a layer of mesenchyme cells coming from the splanchnopleura of the mesoblast. Cell signalization plays a crucial part in the processes of coordination and organogenesis of the primitive gut tube and its derivatives [4]. Beta-actin is one of the three isoforms of the globular G actin that composes the actin microfilaments in the eucariotic cells. Despite the presence of slight differences in the sequence and properties of the three isoforms all G-actin isoforms — alfa, beta and gamma are assembled into microfilaments and are essentially identical in the majority if tests performed *in vitro* [1]. The double localization of beta-actin: in the contractile and cytoskeletal structures gives us a reason to search for its expression in the both types of differentiating cells — epithelial and smooth muscle. The aim of the present study is to follow beta-actin immunochistochemical expression in the differentiating endoblast and mesoblast derivatives in the developing rat small intestine during late embryogenesis and in newborns.

Material and Methods

The study is carried out on material from 20 rat embryos in the 18th gestation day and fragments of small intestine of 10 newborn rats. The material for immunochistochemical study of beta-actin is fixed in Buen's solution for 24 hours. Paraffin sections are investigated by the ABC method with primary antibody for beta-actin (rabbit polyclonal antibody Actin H — 196 Santa Cruz Biotechnology USA) dilution 1:500 at 4°C for 12 hours. Beta-actin is visualized as brown-colored granules.

Results

The lumen of the small intestine of the 18-day-old rats is coated with pseudostratified columnar endoblast epithelium situated on top of a thick mesenchyme layer. Prolonged endoblast cells are observed in the periphery of the mesenchyme. They are arranged in a circular fashion — in 2 or 3 lines. The expression of beta-actin is localized predominantly in the periphery of the mesenchyme. The cytoplasm of the myoblast cells is filled with brown coloured fine granulation. The expression of beta-actin in the epithelium cells is weaker while the weakest expression is in the undifferentiated mesenchyme cells (Fig. 1). The intestinal villi of the newborn are parallel and close to each other. They have a thin basal part and a widening central part. The covering epithelium is columnar and single-layer. In between the villi there is a small number of shallow crypts. The muscular coat is composed of spindle shaped smooth muscle cells arranged in thick layers in different directions. The immunohistochemical expression of beta-actin is dynamic. The reaction in the smooth muscle layers is positive but it is stronger in the covering epithelium. Unlike the embryonal small intestine the apical surface of the epithelium cells of the newborns is filled with a well expressed layer of fine brown granules (Fig. 2).

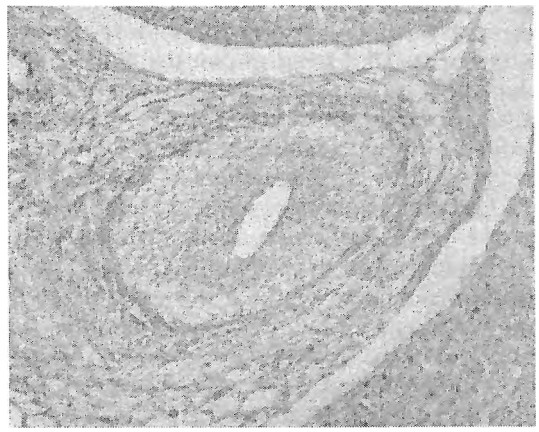

Fig. 1. Small intestine of an 18-day-old embryo of a rat. Positive immunohistochemical expression of beta-actin in the myoblast cells. Weaker expression in the covering endoblast. × 20

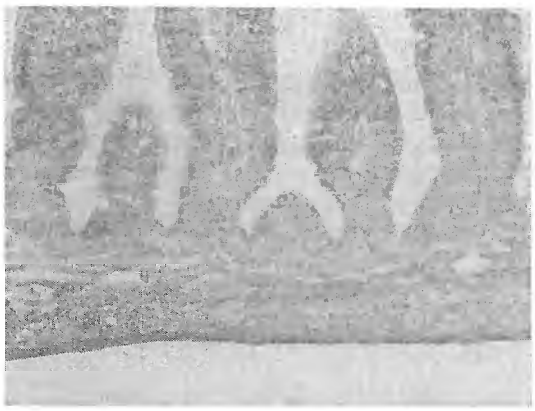

Fig. 2. Small intestine of a newborn. Immunohistochemical expression of beta-actin in the apical part of the cells of the columnar absorptive epithelium. × 20

Discussion

Smooth muscle cells contain both isoforms of actin — smooth muscle alfa-actin and cytoskeletal beta-actin. D r e w et al. (1991) determine that those isoforms are present proportionately in every actin microfilament of the smooth muscle cells from swine stomach [2]. The mesenchyme cells from the small intestine of rat embryos in the 18th gestation that we study are in a process of differentiation into contractile cells. The expression of beta-actin suggests that contractile actin filaments are being formed in the mesenchyme that is differentiating in smooth muscle cells. During its development we confirm that the endoblast of the 18-day-old embryos is pseudostratified while the epithelium of the newborns is single-layered and columnar. The expression of beta-actin in the embryo epithelium is weak while in newborns it is clearly manifested. A thick layer of brown granules are formed in the apical surface of the epithelium cells. That suggests that the epithelium cells already have well shaped microvilli that are filled with actin filaments. This is confirmed by M a u n o u r et al. (1988) who trace the villin expression in the forming microvillus surface of the absorptive cells in the developing small intestine of the rat [3]. The study of beta-actin in two different types of developing tissues in two successive stages enables us to confirm that there are dynamic changes in its expression in time as well as in localization. The expression in mesenchyme is leading in the 18-day-old embryos while it is weaker in the endoblast. The expression of beta-actin in newborns is already weaker in the smooth muscle cells while in the covering epithelium it is well manifested. This dynamics suggests inducing reactions between successively differentiating endoblast and mesenchyme. T h e o d o s i o u et al. (2003) has confirmed that in tissue cultivation of early gut endoblast with non-gut mesoblast induces smooth muscle cell differentiation. Intestinal mesoblast is cultivated with stomach endoblast which induces the formation of microvilli that are specific of intestinal absorptive epithelium [5].

Conclusion

Beta-actin can be used as a marker for the differentiation of the endoblast and splanchnic mesoblast of the small intestine. Beta-actin in the mesenchyme that derives from the splanchnic mesoblast gives information for the formation of contractile structures in the differentiating smooth muscle cells. In the epithelium that derives from the endoblast beta-actin shows the differentiation of the covering absorptive cells. Dynamic changes are present in the expression of beta-actin in time as well as in localization. This dynamics is probably a reflection of the successive inducing reactions between the differentiating tissues of mesoblast and endoblast.

References

1. Bárány, M., J. Barron, L. Gu, K. Bárány. Exchange of the actin-bound nucleotide in intact arterial smooth muscle. — J. Biol. Chem., **276**, 2001, 48398-48403.
2. Drew, JS., C. Moos, R. Murhy. Localization of isoactins in isolated smooth muscle thin filaments by double gold immunolabeling. — Am. J. Physiol., **260**, 1991, C1332-40.
3. Maunoury, R., Robine, E. Pringault, C. Huet, JL. Guenet, JA. Gaillard, D. Louvard. Villin expression in the visceral endoderm and in the gut angle during early mouse embryogenesis. — The EMBO Journal, **7**, 1988, 3321-3329.
4. Romalho-Santos, M., D. Melton, A. McMahon. Hedgehog signals multiple aspects of gastrointestinal development. — Development, **127**, 2000, 2767-2772.
5. Theodosiou, N., C. Tabin. Wnt signaling during development of the gastrointestinal tract. — Developmental Biology, **259**, 2003, 258-271.

Institute of Experimental Morphology and Anthropology with Museum
Bulgarian Anatomical Society

Acta morphologica et anthropologica, 13
Sofia • 2008

In Vitro Manipulation Influence on Embryogenesis

E. Sapundzhiev

Faculty of Veterinary Medicine, University of Forestry, Sofia

This review summarizes the consequences of biotechnological used methods for farm animal reproduction such as multiple ovulation and embryo transfer (MOET), in vitro embryo production (IVEP) after oocyte and zygote collection and culture, cloning by nuclear transfer (NT) and transgenesis (TG) such as freezing of sperms (SF), oocytes (OF) and embryos (EF).

There is evidence that MOET and IVEP can result in a recipient of deleterious side-effect commonly known as the large offspring syndrome (LOS). On the other hand, NT may lead to incompletely reprogramming of the transferred genome. Also TG may constitute an additional set of factors that may negatively affect the expression of the transgene and the concomitant synthesis and release of a protein. The freezing programmes for SF, OF and EF harmful cell membranes and viability after thawing has specific tolerance depending on animal species.

It is suggested that the introduction of biotechnology methods into farm animal husbandry should be carefully used and monitored animals used in experiments or routinely treated must be accompanied with a comprehensive analyzing protocol.

Key words: biotechnology, in vitro manipulation, embryogenesis.

Introduction

The aim of this study is to provide further information on the consequences of biotechniques employed in farm animal breeding. Biotechnological experiments on animals have been considerably expanded. That has produced a positive effect on the development of scientific findings, but it has also recorded some negative consequences on the animal's ontogenesis (2, 24, 29, 30). In Bulgaria biotechnological approaches and in vitro manipulations involved are applied in limited mainly for experimental needs [22].

Materials and Methods

In the animal reproduction the following biotechnologies have been routinely applied — multiple ovulation (MO), oestrus cycle synchronisation (OCS), oocyte collection (OC), in vitro embryo production (IVEP), and the subsequent embryo transfer (ET) to suitable recipients. Simultaneously like an extra niche cloning approaches using nuclear transfer (NT) and transgenesis (TG) are being developed but they are

still in process of development and are being applied largely for experiments. Furthermore cryogenic techniques for a long-term preservation of gametae, zygotae and preimplantation embryos are used for sperm freezing (SF), oocyte freezing (OF) and embryo freezing (EF) in liquid nitrogen at a temperature of — 196°C.

Results and Discussion

Biotechnologies IVEP and ET have been broadly adapted in the breeding programmes of advanced countries. However, the existing data suggest that biotechnologies in use lead to asynchronisation of folliculogenesis [10], chromosome aberration [11], oogenesis and hormonal disfunction [12], asynchronisation of the uterus cycle and embryogenesis [13], prolonged pregnancy with signs of uterus distonya [24]. According to researchers after induced MO a total of 27 - 45 % of the embryos have abnormal karyotype and are expected to be eliminated before, during or after implantation [11].

Recently a convincingly evidence has been collected and showed that a newborn weight of IVEP obtained calves is on 30% over 50 kg in comparison with in vivo controls at birth [29, 30]. Besides offspring cows and sheep by IVEP are less active and avital at the same time. Also increasing the percentage of anomalies of hydroalantois and congenital malformations including abnormal limbs and vertebral column are detected [12]. The observed anomalies were summarized as a large offspring syndrome (LOS) of these animals [30]. Furthermore in calves obtained by IVEP signs of embryogenetic disorders in various organs — heart, liver, kidneys, and adrenal glands have been reported, as well as usual postnatal deviations [7, 25]. Anomalies related to overweight body at birth are explained with the demetilation of the recombinant gene IGF2 [15[. For the LOS escape the evaluation criteria and effective reliable morphological control of foliculogenesis, gametes and embryos must be strictly observed. It also seems that the added at in vitro culture serum, hormones and inhibitors are impact factors on the genome or cellular mitochondria that visibly change the intracellular metabolism which needs constant parameters [4].

Manifestation of LOS symptoms after NT can be connected with common manipulations by objects but also with factors specifically dependent on NT [3]. First the nucleus of the donor somatic cell must past through the process of genetic reprogramming which is connected to transforming the origins of the gene expression characteristic of the donor cell to one specific of early embryo development. This process may be incomplete and leads to unsuitable origins of gene expression. Secondly NT involves exposure to reconstructed oocytes of different oblique stimulations aiming to facilitate the fusion between the nucleus and the recipient cytoplasm as electric shock or treating with various protein inhibitors [5]. These stimulants can lacerate the epigenetic modifications or transcripted genes. Theoretically in any procedure or in any stage of the subsequent processes when carrying out manipulations embryo development, fetus features and the newborn can be affected [27].

A transgenic animal contains genome in which DNA from exogenous source has been introduced by experimental manipulation. In the beginning the application of this technique was focused on studying the genetic factors related to human disease development [8]. Lately TG focused on animals because it aimed at improving farm animal productivity [6, 28]. Congenital malformations and a high rate of prenatal mortality have been reported in transgenic experiments carried out on cows using microinjection [26]. Readings of transgenic lambs and calves obtained through NT also show high rates of prenatal mortality and distinct prenatal and neonatal pathology and immunity disorders [19].

The cryobiological approaches of gametes, zygotes and preimplantation embryo freezing have a selective effect on the viability of the thawed objects [18]. Considerable and more fundamental research has been conducted for freezing male gametes of different kinds of animals. It permits to introduce the technologies on a massive scale mainly in cattle and sheep breeding [1, 9]. It was established that female gametae in different stages of the gametogenesis are more frost-tender and suffer relatively a lower percentage (15%) undergoing freezing and thawing procedures [20, 23]. The claims that meiotic maturing oocytes are more susceptible to the damaging effect of the cryogenic factors forced researchers to focus their efforts on objects with reconstructed diploid genome and the cells are divided by mitosis [7]. Our results of embryo freezing show that the crystal structure of the frozen water damage not only the membrane components in the cell but also biopolymers with protein, lipid and carbonhydrate content (Fig. 1). Under deep frozen condition to −196°C in liquid nitrogen only some physician-chemical reactions are going on and it is considered that they have no practical impact on the cell genome [21]. Whether this is also true of the long-term storage is an issue still to be proved by the future when the objects stored in the cryobanks will be used [22]. Over the last few years contrary to the conventional freezing methods vitrification of the biological object is being employed more convincingly [9, 14, 16]. But in this method they are still looking for the optimal ratio between the concentration of the cryoprotectant used and the time present in the cell. The high cryoprotectant concentration inhibits metabolism and creates conditions for membrane lesion [17].

Conclution

The current research presents convincing evidence according to which after particular interference in ontogenesis of farm animals different anomalies occur in embryogenesis being reflected in the postnatal development as well. Therefore it must be

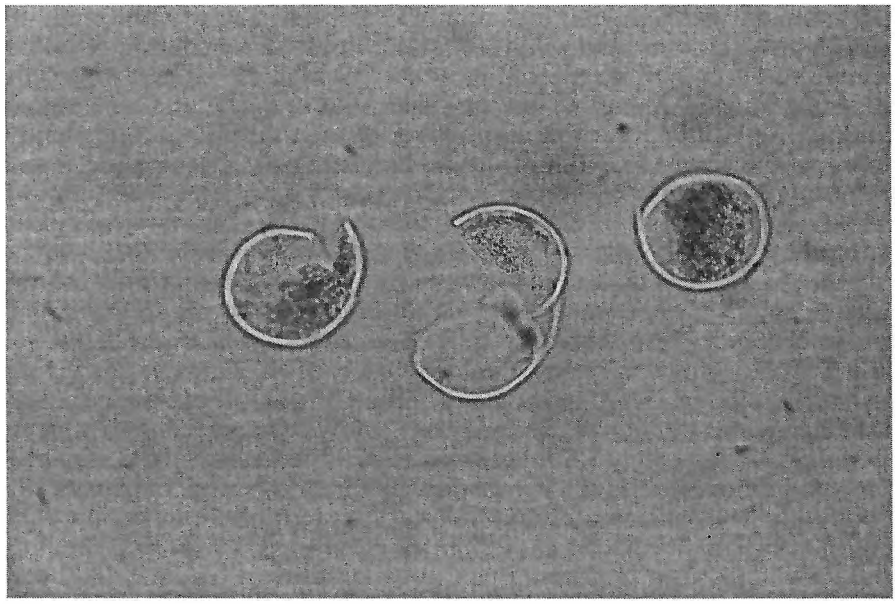

Fig. 1. Damaged frozen-thawed sheep embryos after long-term storage. Native, × 400

concluded that employed reproductive biotechnologies on farm animals should be carefully introduced by monitoring of their condition. The data including the total number of animals and treated groups, their observed normal and pathological status as well as some paraclinic and clinic prenatal and neonatal parameters of the development should be summarised in comprehensive protocol. The obtained results should be systematically analyzed so that it could be scientifically used for experiments and routine biotechnical approaches employed in animal reproduction.

References

1. Backman, T., Bruemmer, J. E., Graham, J. K., Squires, E. L. Pregnancy rates of mares inseminated with semen cooled for 18 hours and then frozen. J. Anim. Sci., **82**, 2004, 690-694.
2. Bower, C., M., Hansen. Assisted reproductive technologies and birth outcomes: overview of recent systematic reviews. — J. Reproduction Fertility and Development, **17**, 2005, No3, 329-333.
3. Brower, V. Cloning improvements suggested. — Nature Biotechnology, **16**, 1998, p. 809.
4. Carroll, J. Coordinating the transition from egg to embryo in mammals. — J. Reprod. Fertil. Develop., **16**, 2004, 9-10.
5. Colman, A. Somatic nuclear transfer in mammals: Progress and applications. — Cloning, **1**, 2000, 185—200.
6. Farin, C. E., P. W. Farin and J. A. Piedrahita. Development of fetuses from in vitro produced and cloned bovine embryos. — J. Anim. Sci., **82**, 2004, 53-62.
7. Fogarty, N. M., W. M. C. Maxwell, J. Eppleston, G. Evans. The viability of transferred sheep embryos after long-term cryopreservation. — J. Reprod. Fertil. Develop., **12**, 2000, No2, 31-37.
8. Gordon, J. W. nimal reproduction. — Genetic enhancement in humans. Science, **283**, 1999, 2023-2024.
9. Hafez, E.S.E. Animal reproduction — In: Reproduction in Farm Animals. Philadelphia., Lea & Febiger, 1993, 405-557.
10. Hyttel P., H. Callesen, T. Greve. Ultrastructural features of preovulatory oocyte maturation in superovulated cattle. — J. Reprod. Fertil., **76**, 1986, 645-656.
11. Karwasky, S. J., P. K. Basrur, R. B. Stubbings, P. J. Hansen, W. A. King. Chromosomal abnormalities in bovine embryos and their influence on development. — J. Biol. Reprod., **54**, 1996, 53-59.
12. Kruip T. A. M., M. M. Bevers, B. Kemp. Environment of oocytes and embryo determines health of IVP offspring. — Theriogenology, **53**, 2000, 611-618.
13. Kruip T. A. M., C. Van Reenen. New biotechnicues and their consecuences for farm animal welfare. — J. Reprod. Dom. Anim., **35**, 2000, 247-252.
14. Kuleshova, L. Birth following vitrification of a small number of human oocytes. — Hum. Reprod. **14**, 1999, 3077-3079.
15. Lau, M. M. H., Liu Bhatt, C. E. H. Steward Ziying, H. Rotwei, P. C. L. Stewart. Loos of imprinted IGF2/cation independent mannose 6-phosphate receptors results in fetal overgrowth and perinatal lethality. — Genes Dev., **8**, 1994, 2953-2963.
16. Lane M. et al. Vitrification of mouse and human blastocysts using a novel cryoloop container-less technique. Fertil. Steril., **72**, 1999, 1073-1078.
17. Massip, A., F. Van der Swalmen, P. Ectors. Pregnancies following transfer of cattle embryos preserved by vitrification. — Cryo-Letters, **7**, 1986, 270-273.
18. Mazur, P. Freezing of living cells. Am. — J. Physiol., **247**, 1984, No3, 125-142.
19. McCreath, K. J., J. Howcroft, H. S. Campbell, A. Colman, A. E. Schnieke, A. J. Kind. Production of gene-targeted sheep by nuclear transfer from cultured somatic cells. — Nature (Lond.), **405**, 2000, 1066-1069.
20. Quinn P., C. Barros, D. G. Whittingham. Preservation of hamster oocytes. — J. Reprod. Fert., **66**, 1982, 161-168.
21. Rall, W. F, D. S. Reid, C. Polge. Analysis of slow warming injury of mouse embryos by cryomicroscopic and physiochemical methods. — Cryobiology, **21**, 1984, 106-121.
22. Sapundzhiev, E. Cryobank introduction for endangered animals in Bulgaria. IV — Int. Conf. ESDAR, Prague, P. 2000, 1-6.
23. Sapundzhiev, E. Cryopreservation mammalian oocytes in liquid nitrogen. PhD Thesis. Czechoslovakian Academy of Sciences, 1986.
24. Seidel, G. E. The future of transgenic farm animals. — In: Transgenic Animals in Agriculture. Wallingford, CAB International, 1999, 269-282.

25. Sinclair, K. D., T. G. McEvoy, E. K. Maxfield, C. A. Maltin, L. E. Young, I. Wilmut, P., Broadbent J., and J. J. Robinson. Aberrant fetal growth and development after *in vitro* culture of sheep zygotes. — J. Reprod. Fertil., **116**, 1999, 177-186.
26. Van Reenen, C. G., T. H. Menwissen, H. Hopster, K. Oldenbroek, T. H. Kruip, H. J. Blokhuis. Transgenesis may affect farm animal welfare. —J. Anim. Sci., **79**, 2001, No7, 1763-1779.
27. Van Wagtendonk-de Leeuw, A. M., E. Mullart, A. P. W. de Roos, J. S. Merton, J. H. G. den Daas, B. Kemp and L. de Ruigh. Effects of different reproduction techniques: AI, MOET or IVP, on health and welfare of bovine offspring. — Theriogenology, **53**, 2000, 575-597.
28. Wall, R. J. Transgenic livestock: progress and prospects for the future. — Theriogenology, **45**, 1996, 57-68.
29. Wilson, J. M., J. D. Williams, K. R. Bondioli, C. R. Looney, M. E. Westhusin and D. F. McCalla. Comparison of birth weight and growth characteristics of bovine calves produced by nuclear transfer (cloning), embryo transfer and natural mating. — Anim. Reprod. Sci., **38**, 1995, 73-83.
30. Young, L. E., K. D. Sinclair and I. Wilmut. Large offspring syndrome in cattle and sheep. — Rev. Reprod., **3**, 1998, 155-163.

Institute of Experimental Morphology and Anthropology with Museum
Bulgarian Anatomical Society

Acta morphologica et anthropologica, 13
Sofia • 2008

Morphological Changes in the Skin Caused by Influence of Dialyzable Lymphoid Cell Extracts

A. Arnaudov

Department of Human Anatomy and Physiology, Faculty of Biology, University of Plovdiv "P. Hilendarski", Plovdiv

A study has been made of the morphological alterations in the skin of guinea pigs, intracutaneously injected with dialyzable lymphocytic extracts with molecular weight of 20 kDa and 10 kDa. It has been found out that the application of the extracts causes various alterations, involving enhancement of vascular permeability in the skin. The morphological basis of alterations is mononuclear infiltration in the dermis. The extracts, obtained from peripheral lymphoid organs, cause more strongly expressed erythrodiapedesis, and the extracts, obtained from blood leucocytes, cause stronger exudation. The substances, causing the skin alterations are with molecular mass £10 kDA.

Key words: leucocytes, ultrafiltration, skin, lymphoid organs.

Leucocytes contain over 200 low-molecular substances of various physicochemical and biological properties [2]. With a view to the prospects of using these substances in immuno- and chemotherapy, the tests on the composition of leucocytic populations of animals and human continue. In 1980 Gottlieb et al. [3] demonstrated the ability of a dialyzable extract of leucocytes from peripheral human blood, after being intracutaneously injected, to cause local inflammatory reaction, morphologically similar to allergic skin reaction of protracted type. Using chromatographic equipment, the authors managed to isolate substances, causing the effects above — substances with molecular weight under 3500 Da.

An interesting question from a theoretical point of view is whether such substances as above are also contained in the leucocytes of other species and in the leucocytes of the lymphoid tissue.

The goal of the present study is to determine whether the extracts of leucocytes from various animal species also contain low-molecular substances with similar effect.

Material and Methods

Test animals. For the obtaining of leucocytic extracts we used rabbits, bred in laboratory conditions.

Cells. We prepared cellular suspensions in apyrogenic distilled water from leucocytes of peripheral blood, splenocytes and cells of lymph nodes with concentration of 7.5×10^8 cells/ml.

Obtaining of low-molecular extracts of leucocytes

We obtained the extracts, using the *Lawrence*'s method via cryolisis of the leucocytic suspensions [6]. We put the extracts to ultrafiltration, using the method described earlier by us [1]. Membrane filters with permeability of 20 kDa and 10 kDa respectively were used.

We determined the protein content in the ultrafiltrates via *Hartree's* method, using beef serum albumin as standard [4].

Test on the effect of leucocytic extracts on the skin morphology at intracutaneous application

We injected strictly intracutaneously a dose of 0.1 ml, equivalent to 7.5×10^7 cells of the obtained extracts to a depilated area on guinea pigs. At the 3rd and 24th hour following the injection we recorded the skin reaction:

A. Macroscopically

— erythema (degree of hyperemia and intensity);

— skin induration (difference in the thickness of the skin flap compared to a symmetric area).

B. Microscopically — we determined the type of the tissue reaction, using skin samples, obtained via biopsy at the 3rd and 24th hour following the application. The biopsic tissue pieces were treated according to the classical histological methods, described by R o m i e s [7].

Results and Discussion

The protein content in the obtained extracts is shown in Table 1.

T a b l e 1. Protein contents (mg/ml) in the rabbit's lymphoid cell extracts

Origin of the leucocytes	20 k Da ultrafiltrate	10 k Da ultrafiltrate
Peripheral blood	0.82	0.66
Lymph nodes	2.43	1.09
Spleen	5.10	1.32

As you can see, the extracts are with low protein content, due to which, when injected, they do not cause reactions, related to their species specificity.

Skin macroscopic alterations, caused by the injected leucocytic extracts — skin induration and erythema, are shown in Table 2.

T a b l e 2. Skin alteration in guinea pigs caused by injecting of leucocytes and lymph cells extracts

Origin of the leucocytes	Alterations after 3 hours		Alterations after24 hours	
	20 k Da ultrafiltrate	10 k Da ultrafiltrate	20 k Da ultrafiltrate	10 k Da ultrafiltrate
Peripheral blood	10.3/2.1 *	10.3/1.8	10.0/2.0	10.1/1.6
Lymph nodes	10.8/2.2	10.5/2.2	10.5/2.0	10.3/1.9
Spleen	10.7/2.2	10.5/2.1	10.5/2.1	10.4/1.8

10.5/2.1=diameter of the erythema (mm)/induration of the skin (mm)

It is evident from the results obtained that the intracutaneous application of leucocytic extracts, obtained both from peripheral blood and from peripheral lymphoid organs, cause macroscopic alterations of the skin in the form of erythema with size of more than 1 cm and skin induration of the order of 1.6 - 2.2 cm. The obtained values of these alterations are the highest for the 3rd hour after the injection. They remained up to the 24th hour, although the values recorded then were lower for all types of extracts. The extracts obtained from spleen and lymph nodes cause more distinct alterations in comparison with the extracts obtained from peripheral blood. There were not found reliable differences in the results, obtained via 20 kDa and 10 kDa ultrafiltrates, on the basis of which we can conclude that the active substances, causing the skin alterations, have molecular mass $\leq$ 10 kDa. The availability of these substances in leucocytes of circulating blood as well as in leucocytes of peripheral lymphoid organs proves that they can be found in these cells during different stages of their development. Histological testing of skin samples taken from the place of extracts injection showed various alterations, which resemble the morphological finding, observed at allergic reaction of protracted type:

- Hyperplasia and vacuolar dystrophy of epidermis;
- Edema in papillary layer of the dermis;
- Erythrodiapedesis and mononuclear infiltration as well as swelling of the collagenic fibres were found in the reticular layer of the dermis.

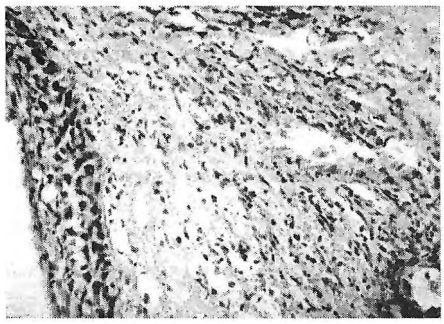

Fig. 1. Edema, mononuclear infiltrations end erythrodiapedesis in the dermis. HE, × 40

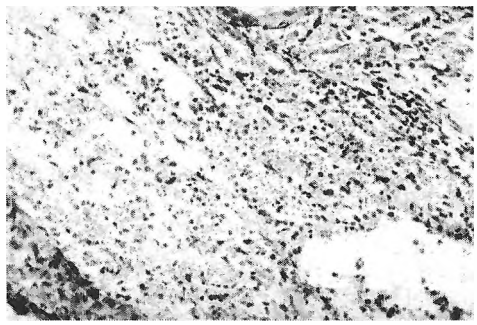

Fig. 2. Erythrodiapedesis, lymphoid cell infiltration. Swelling of the collagen fibres *in stratum reticulare* in the dermis. HE, × 40

These alterations were caused by all three types of extracts. A mononuclear infiltration in the dermis was observed with all three extracts (independently of the origin and molecular mass of the cells), while the other alterations manifested themselves in a different degree, depending on the origin of the lymphocytes: The extracts obtained from peripheral blood cause alterations, in which the edema and hyperplasia of the epidermis are more strongly expressed. The extracts obtained from spleen and lymph nodes cause more expressed erythrodiapedesis in the dermis. Obviously, the leucocytes of circulating blood contain substances, causing stronger exudative processes, whereas the cells of peripheral lymphoid organs produce substances, causing more expressed diapedesis. In contrast to the results, obtained from G o t t l i e b et al. (3), who had found out mainly mononuclear infiltration in the dermis, we showed that the extracts, obtained from the rabbit, when injected intracutaneously, caused other skin alterations as well. Therefore, depending on their species origin, the different leucocytic extracts contain substances of different activity.

The obtained various finding (alterations in the epidermis as well as in both layers of the dermis) calls for further tests, which to differentiate the effect of the individual types of leucocytes on the formation of the determined morphological alterations. To a great extent this will answer the question whether these effects are a pharmacological or immunological phenomenon (passive transfer of anaphylaxis of protracted type, discovered by Landsteiner et Chase [5].

Conclusions

1. 3 hours later, the leucocytic dialysates (ultrafiltrates) of the rabbit induce alterations in the skin, owing to the enhanced vascular permeability for blood cells and fluids. These alterations remain up to the 24th hour.
2. Morphological basis of the skin alterations is the mononuclear infiltration in the dermis. The ultrafiltrates, obtained from spleen and lymph nodes cause more expressed erythrodiapedesis, whereas the extracts, obtained from peripheral blood cause alterations with more expressed exudation.
3. The substances, causing these alterations have molecular mass < 10 kDa. They are found in leucocytes with different degree of differentiation.

References

1. Arnaudov, At., N. Tziporkov. Study on peripheral lymphoid origins from antigen-stimulated animals. — Homo (Univ. Plovdiv "P. Hilendarski" Publsh.), **39**, 2003, No 6, 65-72.
2. Fudenberg, H., H. Fudenberg. Transfer factor: Past, present and future. — Annu. Rev. Pharmacol. — Toxicol., **29**, 1989, 475-516.
3. Gottlieb, A. A., G. Maziarz, N. Tamaki, S. Sutcliffe. The effect of dializable products from human leucocyte extracts on cutaneous delayed hypersensitivity response. — Journal Immunol., **124**, 1980, 885-892.
4. Hartree, E. A modification of the Lowry method that give a lineal photometric responce. — Anal. Biochemistry, **48**, 1972, 442-447.
5. Landsteiner, K., M. Chase. Experiments on transfer of cutaneous sensitivity to simple chemical compounds. —Proc. Soc. Exp. Biol. Med., **49**, 1942, 688-690.
6. Lawrence, H. S. Transfer factor. Advances in Immunology, v.11. — In: Academic Press, New York, 1969, 195-266.
7. Romeis, B. Microskopische Technik. München-Wien R. Oldenbourg Verlag, 1968.

Institute of Experimental Morphology and Anthropology with Museum
Bulgarian Anatomical Society

Acta morphologica et anthropologica, 13
Sofia • 2008

Immunomodulatory Activities of Zygacyne Isolated from *Veratrum nigrum*

M. Cholakova, E. Georgieva, N. Kostova,*
M. Bratanov, V. Christov, E. Nikolova*

Institute of Experimental Morphology and Anthropology with Museum, Bulgarian Academy of Sciences, Sofia
** Institute of Organic Chemistry with Centre of Phytochemistry, Bulgarian Academy of Sciences, Sofia*

Veratrum species are well known for their pharmacological properties. Some of them reduce high blood pressure, inhibit Sonic hedgehog (Shh) signaling during the gastrulation-stage of embryonic development and provoke malformations in several animal species. We tested zygacine isolated from *Veratrum nigrum* on murine bone marrow colony formation and two tumor lines K-562 and LSCC-SF(Mc29) It was found that zygacine activated bone marrow precursor cells and had different dose dependent effect on tumor lines.

Key words: zygacine, lymphocyte proliferation, bone marrow cells, tumor lines.

Introduction

Veratrum species are well known for their pharmacological properties. Extracts of several *Veratrum* plants have been used for treatment of various health disorders as toothache, herpes and hypertension. The steroidal alkaloids cyclopamine and jervine are shown to be primarily responsible for the malformations in several animal species. They are potent teratogens that inhibit Sonic hedgehog (Shh) signaling during gastrulation stage of embryonic development [1]. The steroidal alkaloid cyclopamin acts as inhibitor of P-gp-mediated drug transport and multi drug resistance [2]. Rubijervine possesses antimicrobial and antifungal activity [3]. Here we report for isolation of zygacine from *Veratrum nigrum* and first examine its immunomodulatory activity in mouse.

The aim of the present study was to explore the in vitro influence of this steroidal alkaloid on the formation of bone-marrow cells cultures and its activity on cells of two tumor line K-562 and LSCC-SF(Mc29).

Material and Methods

Plant material

Roots and rootage of *Veratrum nigrum* L. (Liliaceae) were collected in September 2005 from the Vratsa mountain, Bulgaria. Zygacine was isolated according the meth-

ods proposed of Atta - Ur - Rahman and preparative thin layer chromatography. The structure of alkaloid was elucidationed on the basis of NMR assay.

Bone-marrow agar cultures

Bone-marrow was isolated from femur bone by washing the internal bone cavity with RPMI 1640 containing 10% fetal calf serum. Cells were adjusted to 5×10^5 cells/ml and were distributed to plastic Petri dishes. The alkaloid was added in concentrtations 8, 16 and 33 μg/ml. After 7 days of incubation 37°C, 5% CO_2, 98% humidity the samples were dried and stained with Giemsa. The number of the colonies were observed under light microscope. Supernatant from fibroblast cell line 3T3 served as a positive control.

Proliferation of K-562 and LSCC-SF(Mc29) cell lines.

Veratrum alkaloid was added at concentrations 25, 12.5, 6.25, 3.125, 1.56, 0.78, 0.39 and 0.19 μg/ml to 1×10^4 cells. The samples were incubated for 24 h at 37°C, 5% CO_2, 98% humidity. For the last 16-18h of the culture 1 μCi [^{3}H]-thymidine was added to each culture. The cells were harvested with cell harvester. The cells were count in scintillation counter (Beckman). The [^{3}H]-thymidine incorporation was expressed as counts per minute (cpm). All samples were in triplicates and the results are shown as average value for each triplicates.

Results and Discussion

Until now the alkaloid zygacyne was not reported about *Veratrum nigrum*. Its immunomodulatory activity was not investigated.

In Figs. 1 and 2 bone marrow agar cultures from mice treated with zygacine and a positive control / supernatant from fibroblast cell line 3T3/ are presented.

They show that the alkaloid have a stimulatory effect on bone-marrow progenitory cells and stimulate formation of bone-marrow colony compared with the control /supernatatant from fibroblast cell line 3T3/.

Some Veratrum alkaloids have been identified for their anticancer effect. We tested zygacine's effect toward two tumor lines K-562 and LSCC-SF(Mc29)

The results are presented in Figures 3 and 4.

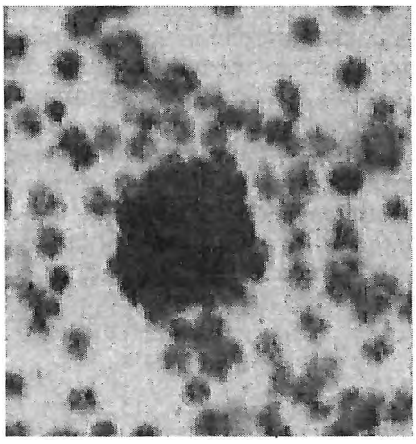

Fig. 1

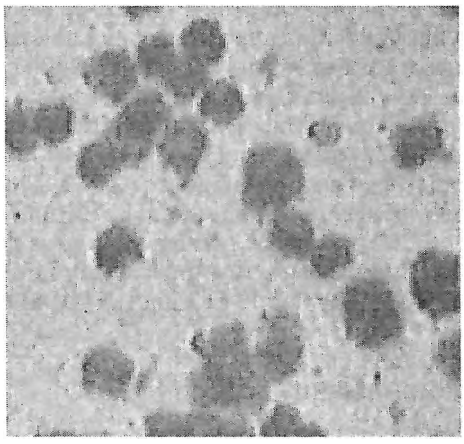

Fig. 2

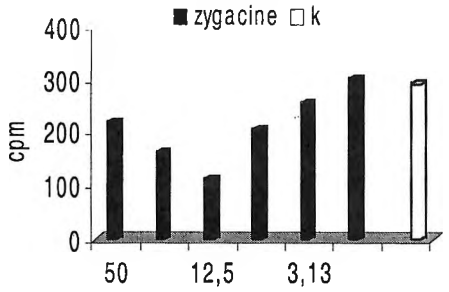

Fig. 3

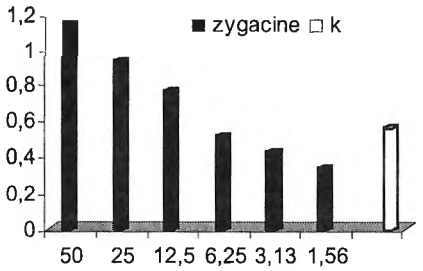

Fig. 4

They show that the zygacine with the exception of concentration 0.19 mg/ml was toxic toward the cells of K-562. It decreased thymidine incorporation into tumor cells in all used concentration. In the case of LSCC-SF(Mc29) the alkaloid's activity is dose-depended. In high concentration zygacine stimulated proliferation of tumor cells but in low concentration it suppress cells proliferation.

Acknowledgement. This work was financially supported by grant ML-SS-1406 of Ministry of Education and Science, Bulgaria.

References

1. Incardona, J., W. Gaffield, R. Kapu, H. Roelink. The teratogenic Veratrumalkaloid cyclopamine inhibits Sonic hedgehog signal transduction. — Nature, **406**, 2000, 1005-1009.
2. Lavie, Y., T. Harel-Orbital, W. Gaffield, M. Liscovitch. Inhibitory effect of steroidal alkaloids on drug transport and multidrug resistance in human cancer cells. — Anticancer Research Mar-Apr; **21(2A)**,2001, 1189-94.
3. Khalid, A., E. Sayed, D. Chuck. Microbial Transformation of Rubijervine. — Tetrahedron, **59**, 2003, 5743-5747.

Institute of Experimental Morphology and Anthropology with Museum
Bulgarian Anatomical Society

Acta morphologica et anthropologica, 13
Sofia • 2008

Epithelial Cells and Macrophages of Aged Human Thymus Possess IGF-I Immunoreactivity

Ts. Marinova, D. Petrov, S. Philipov**, D. N. Angelov****

Department of Biology, Medical University, Sofia
**Department of Surgery, Medical University, Sofia*
***Department of General and Clinical Pathology, Medical University, Sofia*
****Anatomical Institute, University of Cologne, Germany*

The presence and distribution of insulin-like growth factor I (IGF-I) immunoreactivity in the aged human thymus were investigated both at light and electron microscopic levels. IGF-I immunoreactive cells were observed in the structurally preserved regions of the chronic involuted thymus. Presenting novel data for presence of IGF-I immunopositive epithelial cells and macrophages, we conclude that the aged human thymus is still capable to govern some "beneficial" microenvironment events, including IGF-I signalling mechanisms. The latter might be involved in the local regulation of T cell development and plasticity of thymocytes-epithelial cells interactions during aging.

Key words: IGF-I immunoreactivity, human thymus, chronic involution.

Introduction

Accumulating evidence shows that adult mammalian thymic cells express insulin-like growth factor I (IGF-I) immunoreactivity [1, 2]. Astonishingly, despite the generally acknowledged roles of IGF-I in the ontogeny [1, 7, 8], generation and survival of T-cells [3, 6, 10], little is known about the exact time course of IGF-I occurrence during the age-related thymic involution and the decline of immunoreactivity [4, 5, 9].

This is why, in the present study we concentrated our efforts to perform a detailed temporo-spatial analysis of IGF-I expression in the aged human thymus.

Material and Methods

Specimens from thymuses of old (aged 66-82 years) (n=14) and young (aged 2-27 years) (n=10) individuals were obtained from autopsy and thoracic surgery cases, and examined immunocytochemically at light and transmission electron microscopic level. The thymuses collected have had no pathological disorders. Three kinds

of antibodies (Ab), namely: Anti-human monoclonal IGF-I Ab (UBI/Biomol, Hamburg, Cat. Nr. 05-172); Anti-Pan cytokeratin monoclonal Ab (C 1801, Sigma Chemical Co.) and Anti-CD 14 monoclonal Ab (UCH-M1, sc-1182, Santa Cruz Biotechnology) were used. The immunoreactivity of IGF-I, cytokeratin and CD14 was studied.

Indirect immunoperoxidase staining, immunogold transmission electron microscopy and immunogold-silver staining procedures were applied [9, 11]. To define the nature of the thymic cell types which expressed IGF-I we stained serial tissue sections with Anti-cytokeratin Ab and Anti-CD14 Ab which reacted with epithelial cells and monocyte/macrophages, respectively (according to the manufacturer's instructions). Control experiments (negative and positive controls) were carried out in parallel. Labomikroscop Axioskop 20 (Fb Carl Zeiss Opton) and electron microscope Hitachi H500 were used.

Results

Thymuses from young individuals showed lobulated structure, distinct corticomedullary junction and prominent Hassall's corpuscles in the medulla. Aged thymuses displayed a large mass of adipose tissue containing scattered islands composed of epithelial cells, lymphocytes and reticular connective tissue. Most of the epithelial cells were organized into a framework that provided support for lymphoid cells.

Young thymus. All types of medullary epithelial cells, some subcapsular epithelial cells and macrophages displayed strong IGF-I immunoreactivity. Especially those medullary epithelial cells that were located in close proximity to the Hassall's corpuscles were very strongly positive (Fig. 1). They possessed IGF-I immunoreactivity with granular appearance diffusely distributed within the cytoplasm.

Aged thymus. IGF-I immunoreactivity was also present in the adult thymus. However, the immunocytochemical data showed a decreased amount of immunopositive epithelial cells and macrophages an attenuated IGF-I expression (Figs. 2, 3, 4). The cytoplasm of epithelial cells was only moderately immunopositive. The

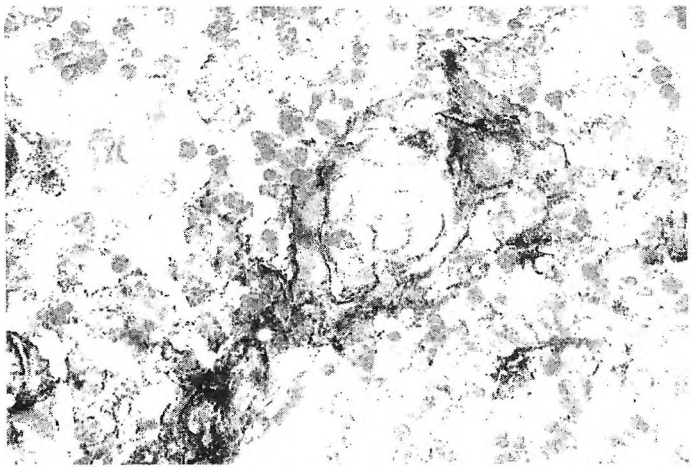

Fig. 1. Young human thymus (21 years old male) — strong IGF I-immunopositive medullary epithelial cells, immunoperoxidase staining, Mayer's hemalaun counterstaining). × 1000

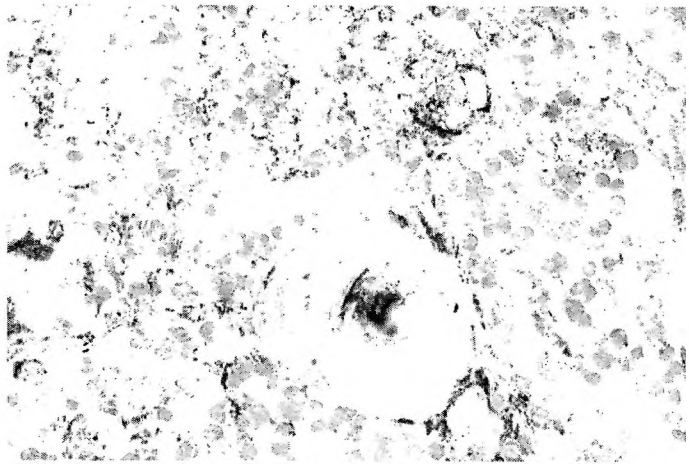

Fig. 2. Aged human thymus (69 years old male)-attenuated IGF I immunoreactivity of medullary epithelial cells around to Hassall's corpuscle; immunoperoxidase staining; Mayer's hemalaun counterstaining. × 1000

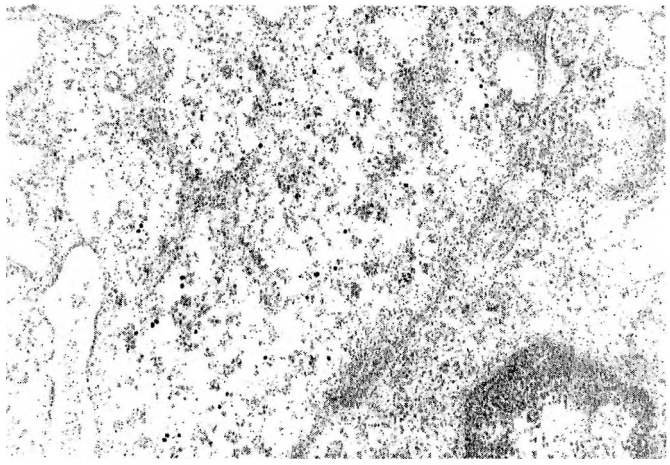

Fig. 3. Aged human thymus (69 years old male) — IGF I-gold granule complexes with cytoplasm localization in part of immunopositive medullary epithelial cell; immunogold transmission electron microscopy. × 26 000

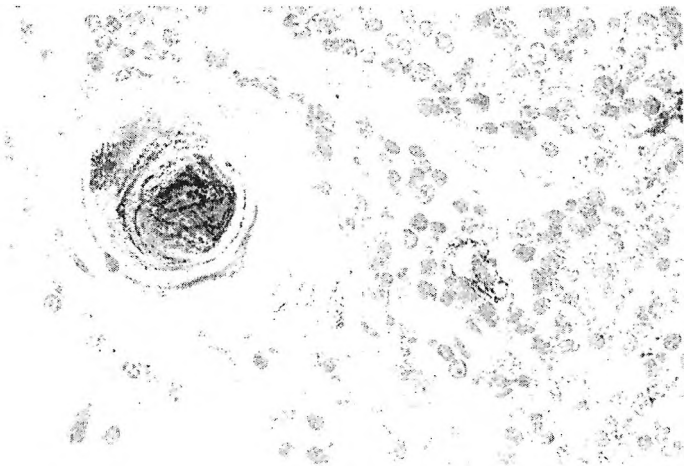

Fig. 4. Senile human thymus (77 years old male) — single IGF I-immunopositive medullary epithelial cells and Hassall's corpuscle with central immunopositive part; immunoperoxidase staining; Mayer's hemalaun counterstaining. × 1000

labelling intensity of the Hassall's corpuscles was heterogeneous. The detailed analysis by electron microscopy showed cytoplasm localization of the IGF I-gold granules complexes in the thymic epithelial cells and macrophages.

Discussion

The present study is the first attempt to investigate the presence and distribution of IGF-I immunopositive epithelial cells and macrophages at both light and electron microscopic levels during the chronic involution of human thymus. Our results are in good correlation with literature data about the immunocytochemical characteristics of animal thymic cells [1, 3, 10].

We found that the age-involuted human thymus retains IGF-I immunoreactivity in its structurally preserved regions. Most probably, the aged human thymus is still capable to govern some "beneficial" microenvironment events, including IGF-I signalling pathways [2, 7] that might be involved in the local regulation of T cell development and in the plasticity of thymocytes-epithelial cells interactions during aging.

References

1. De Mello-Coelho, V., D. M. S. Villa-Verde, D. A. Farias de Oliveira, M. M. de Brito, M. Dardenne, W. Savino. Functional insulin-like growth factor-1/insulin-like growth factor-1 receptor-mediated circuit in human and murin thymic epithelial cells. — Neuroendocrinology, 75, 2002, No2, 139-150.
2. Garcia-Suarez, O., M. Perez-Perez, A. Germana, I. Esteban, G. Germana. Involvement of growth factors in thymic involution. — Microsc. Res. Tech., 62, 2003, No6, 514-523.

3. G e e n e n, V. The thymus insulin-like growth factor axis: involvement in physiology and disease.- Horm. Metab. Res., **35**, 2003, 11-12, 656-663.
4. G o y a, R. G., F. B o l o g n a n i. Homeostasis, thymic hormones and aging. — Gerontology, **45**, 1999, 174-178.
5. H a y n e s, B. F. The human thymus during aging. — Immunol. Res, **22**, 2001, 253-261.
6. H i n t o n, P. S., C. A. P e t e r s o n, E. M. D a h l y, D. M. N e y. IGF I alters lymphocytes survival and regeneration in thymus and spleen after dexamethasone treatment. — Am. J. Physiol., **274**, 1998, No4Pt2, 912-920.
7. L i, L., H. C. H s u, G. E. W i l l i a m, C. R. S t o c k a r d, K. J. H o, P. L o t t, P. A. Y a n g, H. G. Z h a n g, J. D. M o u n t z. Cellular mechanism of thymic involution. — Scand. J. Immunol., **57**, 2003, No5, 410-422.
8. K e l l e y, K. W. From hormones to immunity: the physiology of immunology. — Brain, Behavior, and Immunity, **18**, 2004, 95-113.
9. M a r i n o v a, T., K. V e l i k o v a, S. P h i l i p o v, I. S t a n k u l o v, G. C h a l d a k o v, L. A l o e. Cellular localization of NGF and NGF receptors in aged human thymus. — Folia Biol. (Praha), **49**, 2003, 160-164.
10. M o n t e c i n o - R o d r i g u e z, E., R. C l a r k, K. D o r s h k i n d. Effects of insulin-like growth factor administration and bone marrow transplantation of thymopoiesis in aged mice. — Endocrinology, **139**, 1998, 4120-4126.
11. V o n G a u d e c k e r, B., M. D. K e n d a l l, M. A. R i t t e r. Immuno-electron microscopy of the thymic epithelial microenvironment. — Microsc. Res. Tech., **38**, 1997, 237-249.

Institute of Experimental Morphology and Anthropology with Museum
Bulgarian Anatomical Society

Acta morphologica et anthropologica, 13
Sofia • 2008

ABH Histo-Blood Group Antigens are Differentially Expressed in Involuted Human Thymus

*V. Sarafian, Ts. Marinova**

Department of Medical Biology, Medical University, Plovdiv,
**Department of Medical Biology, Medical University, Sofia*

Although ABH histo-blood group antigens (HBGA) have a wide tissue distribution, their role in pathological conditions is still disputable. The present work examines the expression pattern of ABH HBGA in the process of aging of human thymus. Glands from senile and young individuals were studied by routine histology and immunohistochemistry. Involuted thymus exhibited scattered epithelial cells (EC), positive for HBGA. Endothelial cells of blood vessels and erythrocytes were always immunopositive. Only single lymphocytes possessed HBGA. The epithelial framework reorganization during senile thymus involution involves differential expression of ABH antigens. In the gland of young individuals, in contrast with senile thymus, all lymphocyte populations and the Hassall's corpuscules expressed HBGA. The reduced reactivity for ABH antigens in the lymphocytes of the senile gland might reflect the damaged communication between these two cell types. New evidence for differential expression of HBGA in thymic ontogeny is presented.

Key words: histo-blood group antigens, thymus, involution, aging.

Introduction

ABH histo-blood group antigens (HBGA) are glycoproteins present in different cell types apart from red blood cells [3]. It is believed that they participate in cell differentiation [8], cellular adhesion [11], cancer metastasis and angiogenesis [5]. The epithelial cells (EC) comprising the thymocyte microenvironment play an important role in the ontogeny of the thymus [9]. The thymus undergoes age-related, physiological involution during normal human development [1, 4]. We present a new outlook on the expression pattern of ABH HBGA in senile thymus related to the process of aging.

Material and Methods

Normal thymus glands with no pathological alterations were taken from autopsy samples of senile (aged 65-80 years; n=10) and young (aged 2-16 years, n=8) individuals (Department of General and Clinical Pathology, Medical University, Sofia,

Bulgaria). The blood group phenotype was determined by direct agglutination. The study was approved by the Ethics Committee of the hospital. Routine microscopy was performed prior to the immunohistochemical study. The indirect immunoperoxidase technique with the universal LSAB-2 kit (DAKO) with chromogen AEC was carried out on paraffin sections according to previously described protocols (12). As primary antibodies were used monoclonal antibodies with defined specificity to human HBGA A and B (BulBio; Cat. N: 780001, 780002). Negative and positive controls were examined in parallel. Specific reactivity for EC in positive controls was evaluated on serial sections by anti-pancytokeratin antibody (Sigma Chemical Co; Cat. N: C1801). Immunoreactivity was assessed by a semiquantitative scale ranging from (3+) to (—).

Results

A complete match between blood group phenotype and tissue immunoreactivity for HBGA was detected. Senile thymus exhibited large areas of adipose tissue containing scattered EC and lymphocytes. Stromal EC, positive for HBGA, revealed different size, morphology and intrathymic localization. Endothelial cells of blood vessels and red blood cells were intensely stained for HBGA (Fig. 1). Almost no Hassall's corpuscules (HC) were detected in the medullar part of the involuted gland. Only single scattered lymphocytes possessed HBGA.

In control normal thymus from young individuals the lobulated structure of the gland was preserved. EC were organized as a supporting framework for lymphoid cells. HBGA were discovered in endothelial cells and erythrocytes. EC were also positive for ABH antigens. In contrast with senile thymus, most lymphocyte popula-

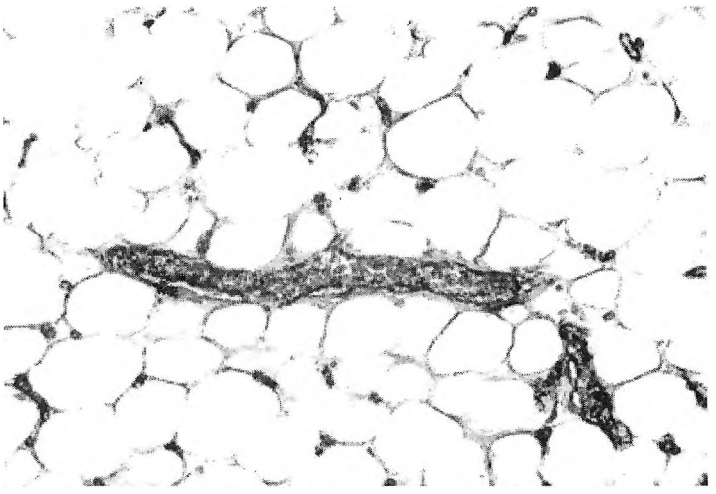

Fig. 1. Expression of HBGA B in erythrocytes and endothelial cells of thymic capillaries in senile human thymus (78-year-old male). Single stromal EC positive for HBGA B. Biotin-streptavidin-peroxidase technique. × 400

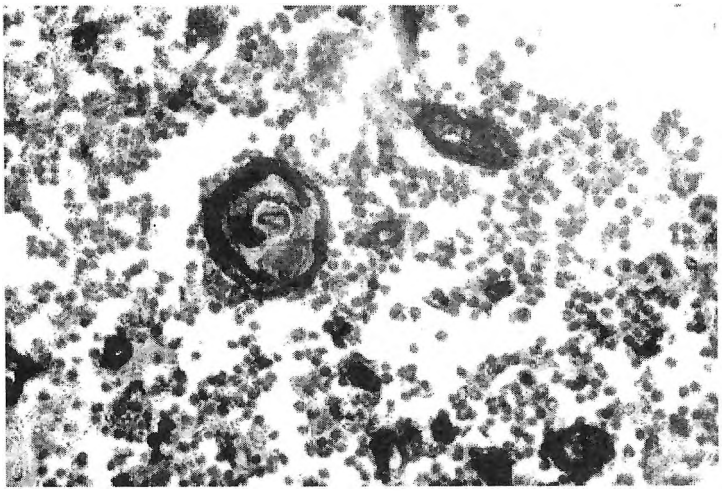

Fig. 2. Expression of HBGA A in Hassall's bodies, single lymphocytes and EC in young normal human thymus (6-year-old boy). Biotin-streptavidin-peroxidase technique. × 630

tions in the gland of young individuals expressed HBGA but with varying intensity. Lymphocytes in close proximity to hyperexpressing HC were strongly positive, while those near to the scattered immunoreactive EC revealed low staining intensity (Fig. 2).

Discussion

Our study indicates that in both aged and young thymus glands a permanent reactivity for HBGA was detected in endothelial cells of blood vessels and in red blood cells. That immunostaining pattern served as a positive internal control, as these cell types are known to be constantly positive in normal human tissues [6, 7].

It has been suggested that the blood group related antigen Le-Y may be associated with intercellular adhesion between lymphocytes and high endothelial venules in lymphoid organs [10]. Interestingly, our observations reveal that ABH HBGA are preserved in aged human thymus, although demonstrating a different pattern of reactivity compared to young individuals. We have detected previously HBGA A in desmosomal contacts between cortical EC and in zones of close contacts between thymic EC and lymphocytes [8]. It is quite possible that these glycoproteins serve as adhesion molecules in human thymus. Although the number of EC diminish in the course of involution, those which are still present in the senile thymus preserve their HBGA. The epithelial framework reorganization in aged human thymus possibly involves a differential expression of ABH antigens as shown in the present study. Probably these molecules are required by thymic EC to maintain the reduced but important crosstalk with lymphocytes during involution. Alternatively, lymphocytes also need HBGA, as most of them express ABH molecules in the young thymus. The diminished reactivity for ABH antigens in the lymphocytes of aged thymus might reflect the impaired communication between these two cell types.

The number of HC in the senile thymus was quite reduced because of the involution process. Almost none of them was immunopositive in contrast with the in-

tensely stained HC in the young gland. As these structures are regarded as components providing developing thymocytes with signals to ensure their proper functional maturation (2), HBGA might be part of these signalling molecules.

Our study presents new immunohistochemical evidence for differential expression of ABH antigens during age-related human thymus involution in reorganized EC and in single lymphocytes. These glycoproteins might be implicated in the complex cellular interactions during the ontogeny of the thymus gland.

Acknowledgement: The study was supported by Grant N:1/2002 from the Medical University, Sofia, Bulgaria and by Grant N:01/2005 from the Medical University, Plovdiv, Bulgaria. The authors thank Dr. I. Goranova and Dr. S. Philipov from the Department of General and Clinical Pathology, Medical University of Sofia, for providing the thymus specimens.

References

1. Bodey, B., B. Jr. Bodey, S. E. Siegel, H. E. Kaiser. Involution of the mammalian thymus, one of the leading regulators of aging. — In Vivo, **11**, 1997, 421-440.
2. Bodey, B., B. Jr. Bodey, S. E. Siegel, H. E. Kaiser. Novel insights into the function of the thymic Hassall's bodies. — In Vivo, **14**, 2000, 407-418.
3. Clausen, H., S. Hakomori. ABH and related histo-blood group antigens; immunochemical differences in carrier isotypes and their distribution. — Vox Sang., **56**, 1989, 1-20.
4. Haynes, B. F. The human thymus during aging. — Immunol. Res., **22**, 2001, 253-261.
5. Kannagi, R., M. Izawa, T. Koike, K. Miyazaki, N. Kimura. Carbohydrate-mediated cell adhesion in cancer metastasis and angiogenesis. — Cancer Sci., **95**, 2004, 377-384.
6. Oriol, R., R. Mollicone, P. Coullin, A-M. Dalix, J-J. Candelier. Genetic regulation of the expression of ABH and Lewis antigens in tissues. — AMPIS Suppl., **100**, 1992, 28-38.
7. Ravn, V., E. Dabelsteen. Tissue distribution of histo-blood group antigens. — APMIS, **108**, 2000, 1-28.
8. Sarafian, V., T. Marinova, H. Taskov. Blood group antigen A is localized in zones of intercellular contacts in human foetal thymus. — Compt. Bulg. Acad. Sci., **48**, 1995, 101-104.
9. Takacs, L., T. Marinova. The ontogeny of the human thymic epithelial specific antigens as defined by monoclonal antibodies. — Thymus, **15**, 1990, 147-152
10. Tanegashima, A., I. Ushiyama, K. Nishi, H. Yamamoto, T. Fukunaga. Tissue-specific expression of Le(Y) antigen in high endothelial venules of human lymphoid tissues. — Glycoconj. J., **16**, 1999, 809-819.
11. Telen, M. Erythrocyte adhesion receptors: blood group antigens and related molecules. — Transfus. Med. Rev., **19**, 2005, 32-44.
12. Tomova, E., A. Popov, V. Sarafian. Expression of human blood group antigens A and B in kidney and lung of some vertebrates. — Folia Biologica, **49**, 2001, 251-257.

Institute of Experimental Morphology and Anthropology with Museum
Bulgarian Anatomical Society

Acta morphologica et anthropologica, 13
Sofia • 2008

Cytotoxic and Antiproliferative Activities of a Newly Synthesized Mixed Ligand Cobalt (II) Complex on Tumor Cell Lines

R. Alexandrova, A. Vacheva, I. Todorova, Y. Martinova, E. Nikolova*, E.-M. Mosoarca**, R. Tudose**, O. Costisor***

Institute of Experimental Pathology and Parasitology, Bulgarian Academy of Sciences, Sofia
**Institute of Morphology and Anthropology with Museum, Bulgarian Academy of Sciences, Sofia*
***Institute of Chemistry Timisoara of the Romanian Academy of Sciences*

The aim of this study was to evaluate cytotoxic and antiproliferative activities *in vitro* of a newly synthesized mixed ligand Co(II) complex $Co_2(BAMP)py_2Cl_4$ (BAMP = N,N′-bis(4-antipyrylmethyl)-piperazine, py = pyridine). The permanent cell lines LSCC-SF(Mc29) (transplantable chicken hepatoma induced by the myelocytomatosis virus Mc29) as well as 8 MG-BA (human glioblastoma multiforme) were used in the experiments. The effects of the compound on cell viability and proliferation were studied by neutral red uptake cytotoxicity test, colony-forming assay and autoradiography.

Key words: cobalt, Mannich bases, pyrazolone, cytotoxic/antiproliferative activity, tumor cell lines.

Introduction

Cobalt is one of the most important trace elements in the world of animals and humans. In the form of vitamin B12 (cobalamin) this metal plays a number of crucial roles in many biological functions. Thus, cobalamin is necessary for DNA synthesis, formation of red blood cells, maintenance of the nervous system, growth and development of children. There is evidence to support the role of cobalt in immune processes. A variety of cobalt containing compounds have been proved to possess antineoplastic activity [1, 2]. It was found in our previous investigations that some Cu(I, II), Co(II), Fe(II, III) and Ni(II) complexes with Mannich type ligands - N,N′-bis(4-antipyrylmethyl)-piperazine (BAMP) and N,N′-tetra-(antipyryl-1-methyl)-1, 2-diaminoethane (TAMEN), exhibited cytotoxic and antiproliferative effects on several human and animal tumor cell lines [3, 4, 5]. In order to continue the investigations in this field the aim of the study presented here was to evaluate the antitumor activity *in vitro* of a newly synthesized mixed ligand cobalt (II) complex - $Co_2(BAMP)py_2Cl_4$, containing the above-mentioned Mannich base BAMP as well as pyridine as a coligand.

Material and Methods

The mixed ligand cobalt (II) complex $Co_2(BAMP)py_2Cl_4$ was dissolved in dimethylsulfoxide (DMSO, Serva) and then diluted in culture medium. The final concentration of DMSO in the stock solution of the compound (10 mg/ml) is 10%. The permanent cell lines LSCC-SF(Mc29) (transplantable chicken hepatoma induced by the myelocytomatosis virus Mc29) and 8 MG BA (human glioblastoma multiforme), were used in the experiments. Cells were grown as monolayer cultures in a combination (1 : 1, vol. : vol.) of medium H-199 and Minimum Essential Medium (Appli-Chem, Germany), supplemented with 5-10% fetal bovine serum (Cambrex, Belgium), 100 U/ml penicillin and 100 mg/ml streptomycin. The cytotoxic and antiprolifetative effects of the compound were studied by neutral red uptake cytotoxicity test, colony-forming assay and autoradiography as it was previously reported [4, 5]. Statistical differences between control and treated groups were assesses using one-way analysis of variance (ANOVA) followed by Dunnett post-hoc test.

Results and Discussion

The data obtained about antitumor activity of $Co_2(BAMP)py_2Cl_4$ *in vitro* are summarized in Table 1. LSCC-SF(Mc29) chicken hepatoma cells were found to be more sensitive to cytotoxic and antiproliferative effects of the compound tested than 8 MG BA human glioblastoma cells. Applied at concentrations ranging from 1 to 200 μg/ml the BAMP ligand did not reduce significantly the viability and proliferation of tumor cells examined.

Independently tested, DMSO (administered at the same concentrations as in the solutions of the compound examined) had no significant cytotoxic effect the viability of the treated cells was > 94% ($P > 0.05$) as compared to the control.

The antitumor [1, 2, 5] and antimicrobial [7, 8] activities of different cobalt compounds have been reported. It was found in our previous investigations that cobalt (II) complexes with N,N′-bis(4-antipyrylmethyl)-piperazine (BAMP) - Co(BAMP)-$(NCS)_4$ and $Co_2(BAMP)Cl_4$, possessed more pronounced cytotoxic and antiproliferative properties than the complexes of the same metal with N,N′-tetra–(antipyryl-1-methyl)-1,2-diaminoethane (TAMEN) — $Co_2(TAMEN)Cl_4$ and $Co_2(TAMEN)$-$(NCS)_2$ [8]. In this study we report for the first time data about antitumor potential *in vitro* of a newly synthesized mixed ligand Co(II) complex $Co_2(BAMP)py_2Cl_4$, containing not only Mannich base BAMP but also pyridine as a coligand. The results

T a b l e 1. Effect of $Co_2(BAMP)py_2Cl_4$ on viability and proliferation of tumor cells

	LSCC-SF(Mc29)	8 MG BA
Inhibitory concentration 50[a] (IC_{50}, μg/ml) established by Neutral red uptake cytotoxicity assay, determined after 48 h cell treatment with the complex examined	45	100
Concentrations (μg/ml) that inhibit colony-forming ability of tumor cells, determined after 14 day cell cultivation in the presence of of $Co_2(BAMP)py_2Cl_4$	≥ 50	≥ 75
Per cent of ^3H thymidine-labelled cells as compared to the control after 48 h cell treatment with the compound tested	$60.23 \pm 3.54^{**}$	$70.53 \pm 4.28^{*}$

[a] The concentrations producing 50% reduction of neutral red uptake; data represent mean ± SEM ($^{*}P < 0.05$; $^{**}P < 0.01$)

obtained revealed that this complex expressed time- and concentration-dependent cytotoxic and antiproliferative effects on chicken and human tumor cells used as model systems in the experiments. $Co_2(BAMP)py_2Cl_4$ was found to be much more active as a cytotoxic agent as compared to the previously tested Co(II) complexes with BAMP and TAMEN. Thus, inhibitory concentration 50 (IC_{50}, the concentration producing 50% reduction of neutral red uptake) of $Co_2(BAMP)py_2Cl_4$ for LSCC-SF(Mc29) was calculated to be 45 μg/ml after 48 h treatment whereas IC_{50} for $Co(BAMP)(NCS)_4$, $Co_2(BAMP)Cl_4$ and $Co_2(TAMEN)Cl_4$ were 87, 100 and 98 μg/ml, respectively. Cobalt (II) complexes examined in the study presented here as well as in our previous experiments differ from each other in ligand (BAMP, TAMEN or BAMP + pyridine) and anion (NCS^-, Cl^-). Each of these components (ligands and anions) influences in different way physico-chemical and biological properties of the complexes obtained which could explain the differences in their antitumor effects.

Acknowledgement: Supported by Grant CC 1402/2004, National Scientific Council, Bulgarian Ministry of Education and Science as well as by a bilateral project between Institute of Experimental Pathology and Parasitology, Bulgarian Academy of Sciences, and Institute of Chemistry Timisoara of the Romanian Academy of Sciences.

References

1. Alexandrova R., R. Tudose, E. Arnaudova, O. Costisor, L. Patron. Cobalt. — Exp. Pathol. Parasitol., 7, 2004, No2, 3-14.
2. Alexandrova, R., E. Nikolova. Metals as potential anticancer agents. — J. Bulg. Acad. Sci., **1**, 2004, 19-23.
3. Alexandrova, R., G. Rashkova, T. Popova, R. Tudose, S. Slavov, E.-M. Mosoarca, O. Costisor. Investigations on cytotoxic activity of three copper complexes with Mannich type ligands. — Exp. Pathol. Parasitol., **8**, 2004, No2, 93-98.
4. Alexandrova, R. I., G. Rashkova, S. Slavov, E. Nikolova, M. Kirilova, G. Miloshev, E. M. Mosoarca, R. Tudose, O. Costisor. Cytotoxic and antiproliferative effects in vitro of iron complexes with Mannich type ligands. — In: The Proceedings of 5th International Symposium on Trace Elements in Human: New Perspectives (Eds. S. Ermidou-Pollet, S. Pollet). Athens, Greece, 2005, 242-250.
5. Alexandrova, R., T. Popova, G. Rashkova, S. Slavov, M. Alexandrov, M. Kirilova, G. Miloshev, Y. Martinova, E. Nikolova, D. Culita, L. Patron. Study on antitumor and antimicrobial effects of Zn(II), Cu(II), Co(II) and La(III) complexes with cholic acid in vitro. — In: The Proceedings of 5th International Symposium on Trace Elements in Human: New Perspectives (Eds. S. Ermidou-Pollet, S. Pollet), Athens, Greece, 2005, 233-241.
6. Alexandrova, R., G. Rashkova, T. Popova, R. Tudose, E. M. Mosoarca, S. Slavov, O. Costisor. Preliminary investigations on cytotoxic activity of four nickel (II) complexes with Mannich type ligands on virus-induced tumor cell lines. — Acta Morphol. Anthropol., **11**, 2006, 60-85.
7. Varadinova, T., S. Shishkov, M. Panteva, P. Bontchev. Effect of complexes of cobalt with aminoacids on on the replication of herpes simplex virus type 1 (HSV-1). — Metal Based Drugs, **3**, 1996, 149-154.
8. Alexandrova, R., T. Popova, G. Rashkova, S. Slavov, R. Tudose, E.-M. Mosoarca, O. Costisor. Cytotoxic and antimicrobial effects in vitro of four cobalt (II) complexes with mannich type ligands. — In: The Proceeding of Scientific Conference "10 Years Faculty of Veterinary Medicine" Forest Technical University, 2005, 304-311.

Institute of Experimental Morphology and Anthropology with Museum
Bulgarian Anatomical Society

Acta morphologica et anthropologica, 13
Sofia • 2008

Influence of EGF on Gut Development in Mice

E. Georgieva, Y. Martinova, M. Cholakova, R. Todorova, M. Dimitrova, M. Bratanov, E. Nikolova

Institute of Experimental Morphology and Anthropology with Museum, Bulgarian Academy of Sciences, Sofia

The stimulation of enterocytes with growth factors in organ culture have great importance for the structural and functional study of the gut mucosa and could ensure understanding of the basic aspects of intestinal epithelium cells differentiation in early stages of postnatal development. We studied enzyme activity of lactase and alkaline phosphatase and carried out electron microscopy studies of enterocytes of newborn mice. We established that EGF promotes morphological and functional development of the murine small intestine and affects the growth and development of gastrointestinal tract.

Key words: small intestine, SEM, EGF, enzymes.

Introduction

Human and mammals colostrums contain bioactive substances called "growth modulators" [1]. The last include growth factors, some of which can directly influence the newborn metabolism after gut absorption and promote the growth and differentiation of different tissues [2].

One of the most prominent growth factors in colostrum, by means of quantity is EGF. It is considered in the literature as the main activator in human milk, which stimulates cell division and migration, induces gene expression of mucus enzymes and different peptides, stimulates gut regeneration at necrotizing entherocolitis and mucus inflammation, regulates enzyme activity.

The aim of the presence study was to determine the influence of the EGF on small intestinal development in murine organ culture by means of enterocytes morphology and alkaline phosphatase and lactase enzyme activity.

Materials and Methods

Organ culture: The newborn mice Balb/c were used to isolate the small intestine. The explants were cultivated from 24h to 96h in culture medium RPMI 1640 containing 10% fetal bovine serum at 37°C, 5% CO_2 and 100% humidity. We added 50 ng/ml EGF per well, except for the control specimen, which were cultivated without growth factor.

Scanning electron microscopy: The specimen were fixed in 2.5% glutaraldehyde containing 0.4M Na-caccodylate. The explants were post-fixed in 1% osmium tetraoxide. The specimens were prepared for observation with scanning electron microscope (JEOL JSM 35).

Enzyme histochemistry: The specimen were embedded in tissue freezing medium and were cryo cut to obtain 10 μm thin sections. We prepared substrate media for two enzymes:

Alkaline phosphatase activity: The substrate medium consisted of 0.5mM menadiol diphosphate disodium salt (substrate), 1 μg/ml NBT (nitroblue tetrazolium) and 0.005mM methoxyphenazine methasulfate in 0.1M Tris/HCl, pH 9.2. The incubation lasted 15 min at 37°C.

Lactase activity: The substrate medium consisted 0.5mM 5-bromo-4-chloro-1-indoline-β-D-galaktopyranoside (substrate), 1mg/ml NBT, 0.005mM methoxyphenazine methasulfate in 0.1M Citrate buffer, pH 6.0. The incubation lasted 2 h at 37°C.

Results

Scanning electron microscopy: Characteristic for the early stage of the morphogenesis of intestinal villi is their finger-like shape, upright to the gut lumen. The cells are typically polygonal like hive facets (Fig.1), they are arranged tightly to each other like pavement, and only in some spots loose cell junctions could be observed. The microvilli are well shaped and cover entire striated apical cell surface.

In control samples the enterocytes are not well distinguished, their polygonal shaped is not well structured and cell junctions cannot be well observed (Fig. 2).

Enzyme activity examination: *Alkaline phosphatase* is a marker for differentiated intestinal villous cells and usually is localized at the apical membrane of the cells *in vivo*.

We have observed that in duodenum explants cultivated for 96h have enterocytes, which gave reaction for presence of alkaline phosphatase (Fig. 3). In the figure it makes an impression that the enzyme is localized predominantly on the top of the villi and the cells are more poorly stained in the crypt direction. This effect is connected with cell differentiation stage.

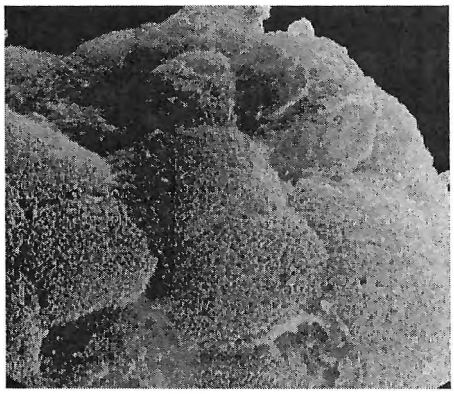

Fig. 1. Explants from duodenum, cultivated with EGF for 72h. Originally × 3900

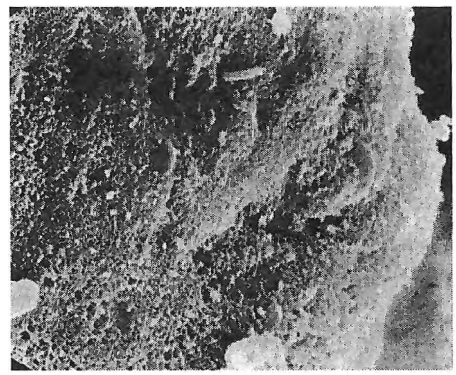

Fig. 2. Explants from duodenum, cultivated without EGF for 72h. Originally × 3900

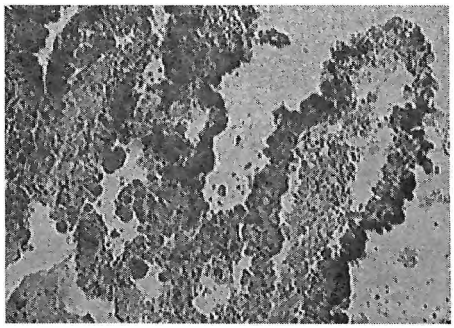

Fig. 3. Alkaline phosphatase: duodenum cultivated with colostrum for 96h. Originally × 100

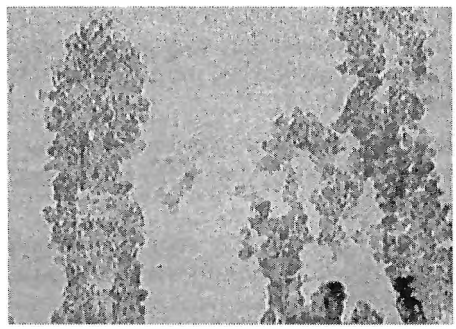

Fig. 4. Alkaline phosphatase: duodenum cultivated without colostrum for 96h. Originally × 100

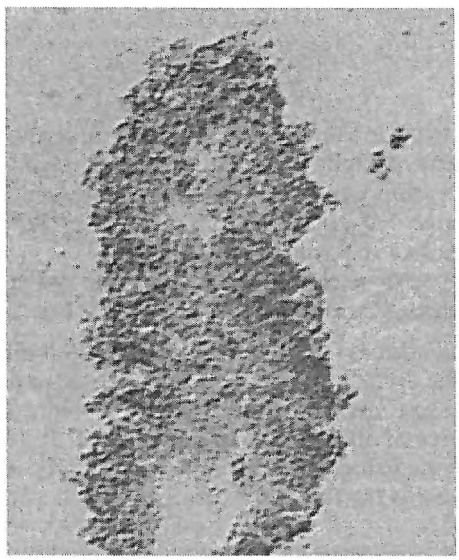

Fig. 5. Lactase: Jejunum cultivated and stimulated with EGF for 72h. Originally × 400

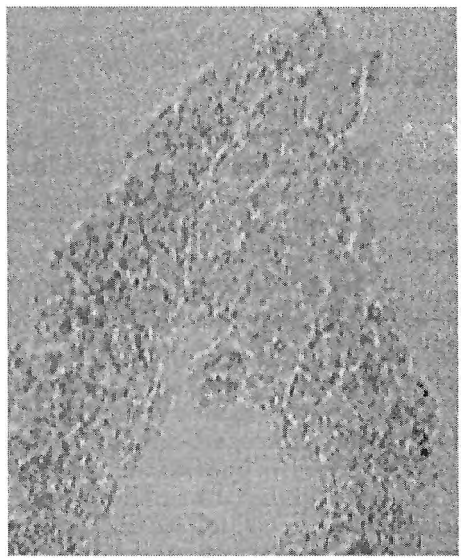

Fig. 6. Lactase: Jejunum cultivated and stimulated without EGF for 72h. Originally × 400

The control samples are slightly stained which is distinctive feature for lower enzyme activity. This trend is also observed in the explants from jejunum and ileum cultivated 48-72 h respectively. In control samples only separate cells display presence of enzyme (Fig. 4).

Lactase: in explants from duodenum and jejunum, cultivated for 48-72 h respectively (Fig. 5), reveal well expressed enzyme activity in contrast to controls (Fig. 6), in which single cells show enzyme presence.

The maturation stage in newborn gut is related to changes in lactase activities and the latest is determined solely by gut mucosal growth and differentiation changes. The diminishing in lactase absorption could play a crucial role in development of food intolerance, effect that occurs frequently in premature infants.

Discussion

The results of the present study indicate that EGFR-signalling has an important function in regulating the newborn gut crypt/villous axis and goblet cell maturation during the organ culture. The newborn mouse gut in organ culture showed many developmental similarities to those grown *in vivo*. Early intestinal villous development *in vitro* indicates an anterior-posterior pattern of regionally specific epithelial differentiation. Moreover the clustering of proliferative epithelial cells to intervillous crypt region in the proximal small intestine during organ culture stimulates normal gut maturation in which the intestinal epithelium organizes into proliferative crypt region and terminal differentiated villi with characteristic for them enzymes.

We have shown that exogenous EGF produces a complex pattern of *in vitro* growth effect on newborn mouse gut. The effects are regionally distinct as EGF 50 ng/ml affect small intestinal growth. Although we have not directly demonstrated how exogenous EGF has access to its cognate receptor on the intestinal epithelium, the observed biologic effects of exogenous EGF on newborn mouse gut growth and development indicate that significant receptor-ligand interaction had occurred [3].

The EGFR-signalling system regulate the growth and maturation of the embryonal and newborn small intestine to crypt-villous axis. This mechanism has potential application in necrotizing entherocolitis therapy that affect severely premature infant [4].

Acknowledgements. This work was financially supported by grant TKL-1609/06 of Ministry of Education and Science, Bulgaria.

References

1. Bust, J. P. Bioactive factors in milk. — Arch. Pediat., **5**, 1998,298-306.
2. Cummins, A. G., F. M. Thompson. Effect of breast milk and weaning on epithelial growth of the small intestine in humans. — Gut, **5**, 2002, 748-754.
3. Murphy, M. S. Growth factors and the gastrointestinal tract. -- Nutr., **10**, 1998, 771-774.
4. Abud, H. E., N. Watson, J. K. Heath. Growth of the intestinal epithelium in organ culture is dependent of EGF signalling. — Exp. Cell Res., **2**, 2005, 252-262.

Institute of Experimental Morphology and Anthropology with Museum
Bulgarian Anatomical Society

Acta morphologica et anthropologica, 13
Sofia • 2008

Influences of Probiotic "Biomilk" on Indomethacin-induced Oxidative Injuries of Some Tissues

M. Georgieva, G. Bekyarova, M. Gabrovska***

Department of Preclinical and Clinical Pharmacology and Biochemistry, Prof. Paraskev Stoyanov Medical University of Varna
** Department of Pathophysiology, Prof. Paraskev Stoyanov Medical University of Varna*
***Department of Anatomy, Histology and Embryology, Prof. Paraskev Stoyanov Medical University of Varna*

The effect of probiotics Biostim LBS (Biomilk) and LBB of pure culture on ulcerogenesis in Indomethacin-induced oxidative stress by means of a model of Indomethacin-induced ulcer in white male rats was studied. Indomethacin was subcutaneously injected in a dose of 20 mg/kg bw 4 hours prior to taking for examination the biopsy material such as blood, liver and brain. Both probiotics Biostim LBS and LBB were introduced per sondam in a dose of 1600 mg/kg bw for 30 consecutive days prior to modelling the Indomethacin-induced ulcers. Malonyldialdehyde (MDA) as a marker of lipid peroxidation was examined in plasma, liver and brain homogenate. The results from the morphometric study of gastric lesions were presented as index of lesions. Indomethacin caused the formation of numerous lesions and haemorrhages and enhanced MDA level in plasma and tissues. Both probiotics Biostim LBS and LBB introduced for 30 days restrict the lipid peroxidation and protect the gastric mucosa from Indomethacin ulcerogenic action.

Key words: Biostim LBS, Indomethacin, gastric ulcer, index of lesions.

Introduction

Indomethacin is a NSAID widely used in the treatment of rheumatoid arthritis, collagenoses etc. and possesses a manifested ulcerogenic effect [9]. It has been proved that it suppresses prostaglandins' synthesis and thus their antiacid and gastroprotective properties. This is accompanied by the occurrence of mucosal lesions, haemorrhagic erosions and delay of reparation processes [3]. There exist data about the involvement of free-radical processes in indomethacin-induced ulcers [10].

Probiotics stimulate the growth and development of bifidum and lactobacilli [2]. There are data about the antioxidant activity of lactic acid bacteria [1, 4, 5]. A protective effect of probiotics containing such bacteria has been established in experimental stress- and alcohol-induced ulcerogenesis as well as in patients with ulcer disease [7].

The objective of the present study is to establish the effect of the probiotic Biostim LBS (Biomilk) containing livecells of *Lactobacillus bulgaricus*, proteins, fats, carbohydrates, minerals and vitamins as well as the effect of LBB-pure culture of *Lactobacillus bulgaricus* on ulcerogenesis in Indomethacin-induced oxidative stress.

Materials and Methods

The study covered white male Wistar rats weighing 180-200 g who were maintained at free access to standard food and water. The animals were divided into 6 groups with 7 animals each: group I — controls, distilled water for 30 days; group II — Indomethacin on the last day of experiment; group III — Biostim LBS for 30 days; group IV — LBB for 30 days; group V — Biostim LBS for 30 days + Indomethacin on the last day of experiment and group VI — LBB for 30 days + Indomethacin on the last day of experiment.

Indomethacin (Fluka Chemie, Switzerland) in the shape of suspension in distilled water and Tween-80 was chosen as an ulcerogenic agent with pro-oxidative action and subcutaneously injected in a dose of 20 mg/kg bw. Stomachs were taken for examination 4 hours after Indomethacin administration under ethereal narcosis. A morphometric investigation of gastric lesions was performed and the results were presented as indez of lesions. Malonyldialdehyde (MDA) as a marker of lipid peroxidation after the method of P o r t e r [8] was estimated in blood plasma, liver and brain homogenates.

Results and Discussion

Indomethacin treatment induced the formation of numerous lesions and haemorrhages. The index of lesions in this group was highest (Fig. 1). Independent

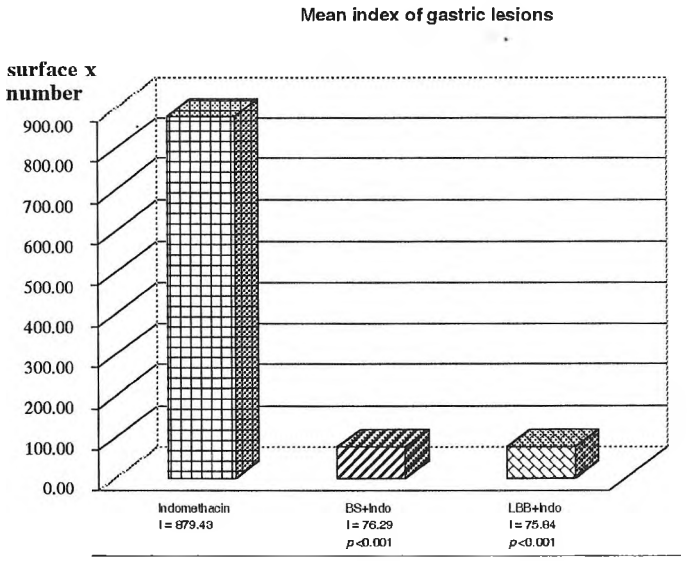

Fig. 1. Mean index of gastric lesions in Indomethacin-treated rats in a model of Indomethacin-induced ulcerogenesis

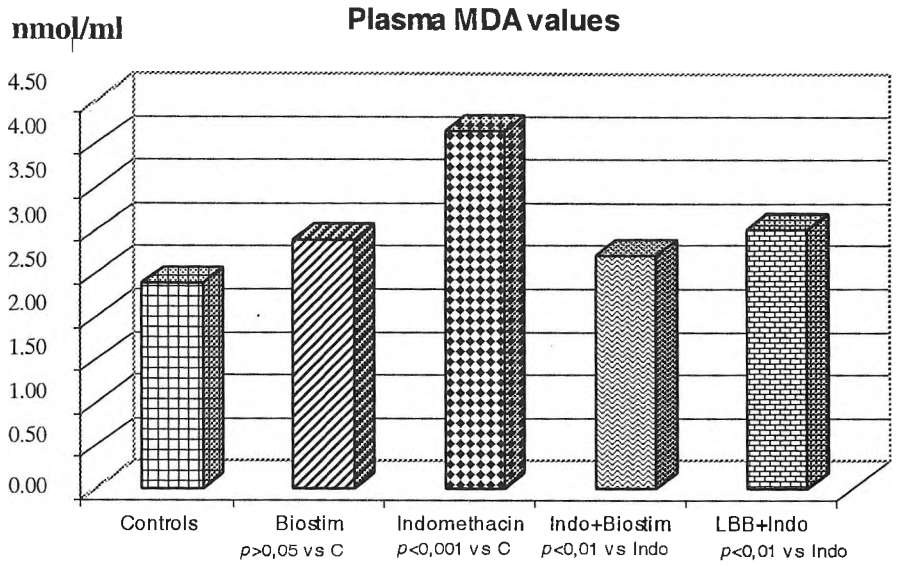

Fig. 2. Plasma MDA values

chronic treatment with Biostim LBS and LBB did not cause any ulcer formation at all. The probiotics Biostim LBS and LBB introduced for 30 days strongly protect the gastric mucosa against the ulcerogenic action of Indomethacin.

MDA in plasma

In the animals treated Biostim LBS or LBB only MDA values did not differ significantly from these of the controls ($p>0,05$). Indomethacin treatment caused a significant ($p<0,001$) MDA increase in plasma as compared with that of the controls. MDA in plasma reduced in the groups with Biostim LBS+Indomethacin and LBB+Indomethacin in comparison with the group with Indomethacin only ($p<0,01$) (Fig. 2).

MDA in liver homogenate

In the animals treated with Biostim LBS or LBB only MDA values in liver tissue did not differ significantly from these of the controls ($p>0,05$). Indomethacin treatment caused a significant ($p<0,01$) MDA increase in liver homogenate as compared with that of the controls. In the liver homogenate, MDA values reduced significantly ($p<0,01$) in the animals of the groups with Biostim LBS+Indomethacin and LBB+Indomethacin when compared with these with Indomethacin only (Fig. 3).

MDA brain homogenate

In the animals treated with Biostim LBS or LBB only MDA values in a homogenate from brain tissue did not differ significantly from these of the controls ($p>0,05$). Indomethacin treatment caused a significant ($p<0,001$) MDA increase in brain homogenate as compared with that of the controls. In the brain homogenate, MDA values reduced significantly ($p<0,01$) in the animals of the groups with Biostim LBS+Indomethacin and LBB+Indomethacin when compared with these with Indomethacin only (Fig. 4).

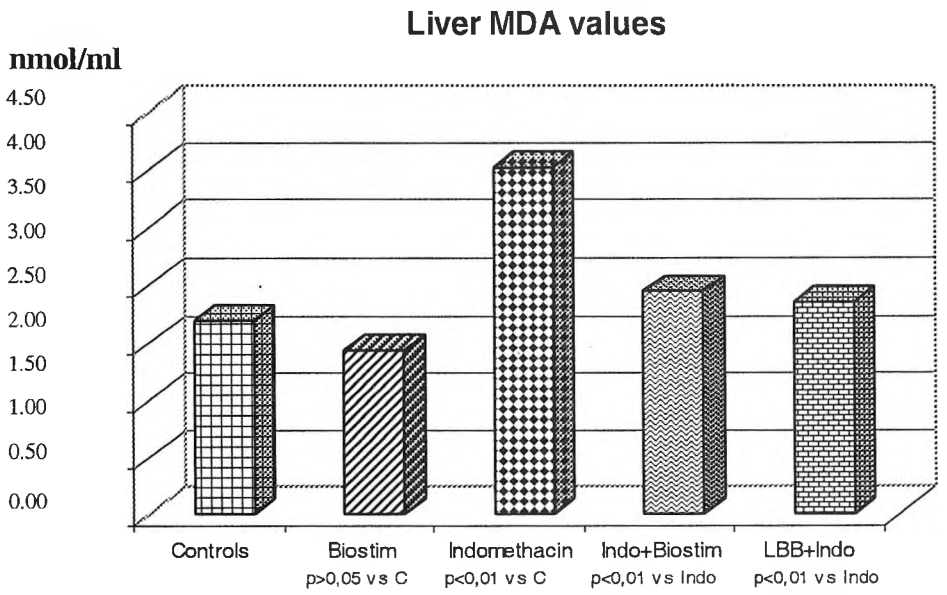

Fig. 3. Liver MDA values

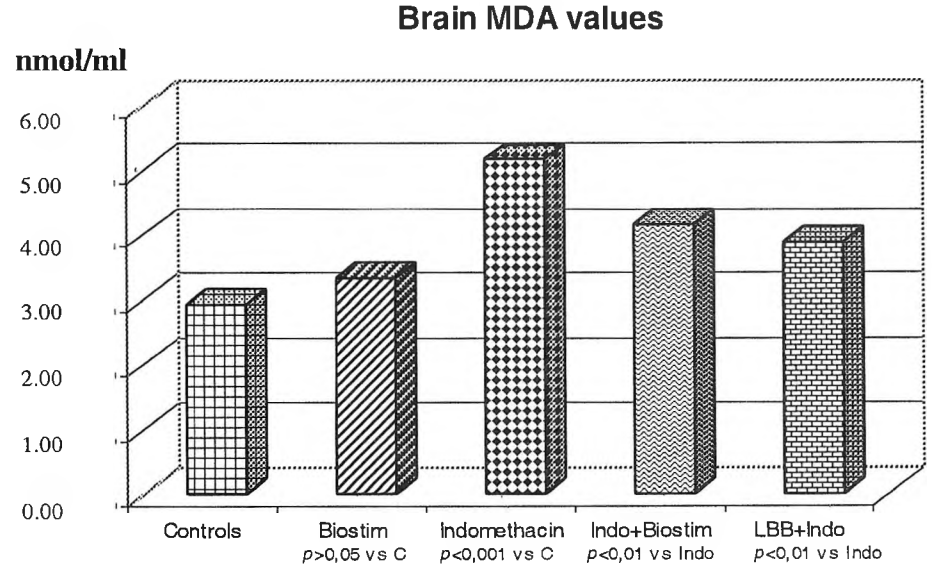

Fig. 4. Brain MDA values

Indomethacin causes MDA elevation in plasma along with that in liver and brain homogenate that allows the assumption of oxidative stress involvement. In the groups with Biostim LBS (Biomilk)+Indomethacin and LBB+Indomethacin these

parameters were favourably influenced upon. It is known that lactic acid bacteria possess an antioxidant activity [5, 6]. It is possible that the protective action of the probiotics Biostim LBS and LBB on the gastric mucosa is due to the restriction of lipid peroxidation. It stresses that MDA as a marker of this peroxidation in liver and brain decreases to a greater extent in the group of LBB+Indomethacin than in that of Biostim LBS + Indomethacin. LBB representing a pure culture with a greater amount of live cells of *Lactobacillus bulgaricus* proved to exert a stronger effect in the examined organs than Biostim LBS. Probably, the antioxidant activity is determined by the number of live cells of *Lactobacillus bulgaricus*. The resent results have shown that there exists a parallelism between the degree of the antioxidative effect and the number of live cells of *Lactobacillus bulgaricus*.

In stress-induced gastric ulcers a protective effect of alpha-lactalbumin has been established. The authors assume that this antiulcerogenic activity is due to the stimulated prostaglandin synthesis [9, 10, 11].

Based on the aforementioned data we could draw the conclusion about the clionical significance of the chronic application of both Biostim LBS (Biomilk) and LBB in Indomethacin-provoked pathology of the gastric mucosa that corresponds with the data of other authors about the protective properties of these probiotics against stress- and ethanol-induced ulcer.

References

1. Bay, B. H., Y. K. Lee, B. K. Tan, E. A. Ling. Lipid peroxidative stress and antioxidative enzymes in brains of milk-supplemented rats. — Neurosci. Lett., **277**, 1999, 127-130.
2. Havenaar, R., J. H. J. Huis in't Veld. Probiotics: a general view. The lactic acid bacteria. — In: The Lactic Acid Bacteria in Health and Disease (Ed. B. J. B. Wood). London, Elsevier Applied Science, 1992, 1, 71-151.
3. Hawkey, C. J. Nonsteroidal anti-inflammatory drug gastropathy. — Gastroenterology, **119**, 2000, 521-535.
4. Kaizu, H., M. Sasaki, H. Nakajima, Y. Suzuki. Effect of antioxidative lactic acid bacteria on rats fed a diet deficient in vitamin E. — J. Dairy Sci., **76**, 1993, 2493-2499.
5. Lin, M. Y., C. L. Yen. Antioxidative ability of lactic acid bacteria. — J. Agric. Food Chem., **47**, 1999, 1460-1466.
6. Madsen, K. L. The use of probiotics in gastrointestinal disease. — Can. J. Gastroenterol, **115**, 2001, 817-822.
7. Matsumoto, H., Y., Shimokawa, Y., Urhida, T., Toida, H., Hayasawa. New biological function of bovine alpha-lactalbumin: protective effect against ethanol — and stress-induced gastric mucosal injury in rats. — Biosci. Biotechnol. Biochem., **65**, 2001, 1104-1111.
8. Porter, N. A., J. Nixon, R. Isaac. Cyclic peroxides and the thiobarbituric assay. — Biochim. Biophys. Acta, **441**, 1976, 506-512.
9. Rostom, A.,. C. Dube, G. Wells, P. Tugwell, V. Welch, E. Jolicoeur, J. McGowan. Prevention of NSAID-induced gastroduodenal ulcers (Review). — Cochrane Database Syst. Rev., **4**, 2000, CD 002296.
10. Sugimoto, N., N. Yoshida, T. Yoshikawa, et al. Effect of vitamin E on aspirin-induced gastric mucosal injury in rats. — Dig. Dis. Sci., **45**, 2000, 599-605.
11. Vilaichone, R. K., V. Mahachai, S. Tumwasorn. Inhibitory effect of Lactobacillus acidophilus on Helicobacter pylori in peptic ulcer patients: in vitro study. — J. Med. Assoc. Thai., **85**, 2002, S79-S84.

Institute of Experimental Morphology and Anthropology with Museum
Bulgarian Anatomical Society

Acta morphologica et anthropologica, 13
Sofia • 2008

Influence of the "Biostim LBS" Probiotic on Morphological Liver Changes in Experimentally Induced Hepatotoxicity

M. Georgieva, E. Softova, M. Gabrovska**, N. Alexandrov***, N. Manolov*****

Department of Preclinical and Clinical Pharmacology and Biochemistry, University of Varna
** Department of General and Clinical Pathology, University of Varna*
***Department of Anatomy, Histology and Embryology,*
University of Varna, Prof. Paraskev Stoyanov Medical
****Department of Toxicology and Allergology, Military Medical Academy of Sofia*
*****Clinic of Vascular Surgery, St. Anna University Hospital of Varna*

The effect of chronic treatment with probiotic Biostim LBS containing the original *Lactobacillus bulgaricus* on morphological hepatic changes in an experimental model of carbon tetrachloride (CCl_4) induced hepatotoxicity was studied. Male white Wistar rats were treated with Biostim LBS in doses of 800 and 1600 mg/kg once daily for 30 consecutive days. CCl_4 was administered during the two last days in a dose of 0,2 mL/kg. On the 31th day material from the liver was taken for histological examination. The application of Biostim LBS favorably influences upon the necrotic changes in the liver induced by the hepatotoxic agent CCl_4.

Key words: Biostim LBS, carbon tetrachloride, liver morphology, hepatoprotection.

Introduction

Probiotics are immunomodulatory bacteria in the gastrointestinal tract that protect their host [4, 6]. The probiotic Biostim LBS (Biomilk) combines live cells of *Lactobacillus bulgaricus*, milk proteins, fats, carbohydrates, natural vitamins, minerals and pectin. The milk products containing lactobacilli proved to exert favourable effects in liver and biliary tract diseases of toxic, bacterial and viral nature [3, 5, 9].

The purpose of this study is to establish the effect of chronic treatment with the probiotic Biostim LBS in different dosages on the morphological liver changes in an experimental model of carbon tetrachloride (CCl_4) induced hepatotoxicity.

Materials and Methods

Male Wistar rats weighing at an average of 250±10 g were used to examine the influence of Biostim LBS. Biostim LBS was administered dissolved ex tempore in distilled water in doses of 800 and 1600 mg/kg bw rat, per sondam, once daily for 30 consecu-

tive days. CCl_4 was applied two days long per sondam in a dose of 0,2 mL/kg bw as 10% solution in sunflower oil.

According to the kind of treatment, the animals were divided into 6 groups with 7 animals each: I group — Biostim LBS 800 mg/kg; II group — Biostim LBS 1600 mg/kg; III group — CCl_4; IV group — Biostim LBS 800 mg/kg and CCl_4; V group — Biostim LBS 1600 mg/kg and CCl_4; VI group — untreated controls.

The animals from groups four and five were initially treated for 30 days with Biostim similarly to those of groups one and two as during the last two days of experiment they were given CCl_4. The animals were anaesthesized and decapitated 24 hours after the last CCl_4 administration.

Material from the liver was taken for histopathological examination, fixed in 5% neutral formaline and Carnoy's solution. Five paraffin sections were stained with hematoxylin eosin (HE), impregnated with silver, after Gomori for reticular fibres' proof and with PAS reaction under and without control of alpha-amylase after McManus for glycogen proof.

Results

Morphological liver changes in animals treated with the probiotic Biostim LBS in doses of 800 mg/kg and 1600 mg/kg (groups I and II)

The examination of the liver revealed a completely preserved histological structure of the organ and no differences in comparison with the controls (Fig. 1).

Morphological liver changes in animals treated with CCl_4 (group III)

There were large areas of coagulation necrosis affecting the hepatocytes from the central and intermediary parts of the hepatic lobules. At numerous places, the ne-

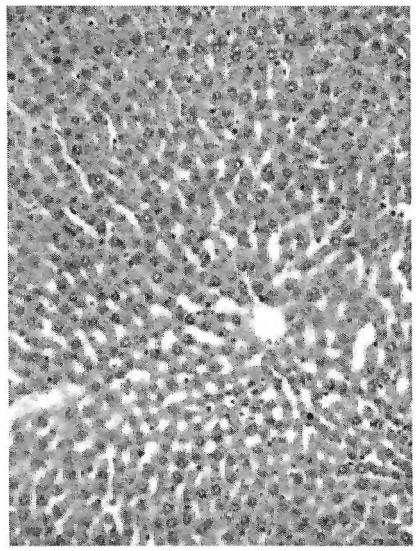

Fig. 1. Liver of an animal treated with Biostim LBS in doses of 800 mg/kg and 1600 mg/kg. × 160

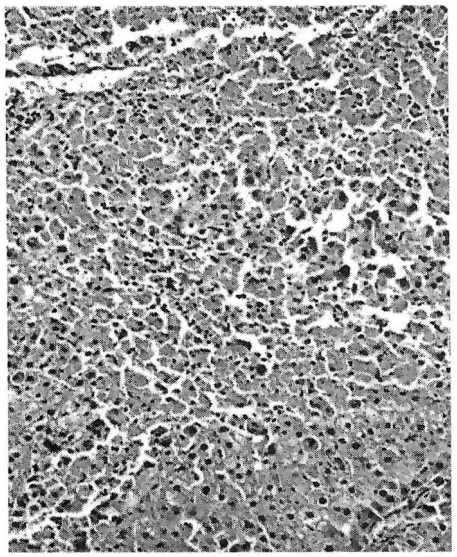

Fig. 2. Liver of an animal treated with CCl_4. Large areas of coagulation necrosis beginning from the central parts of the lobules and tending to merging of the necrotic zones. Lymphocytes and single leukocytes around necrotic hepatocytes. HE, × 200

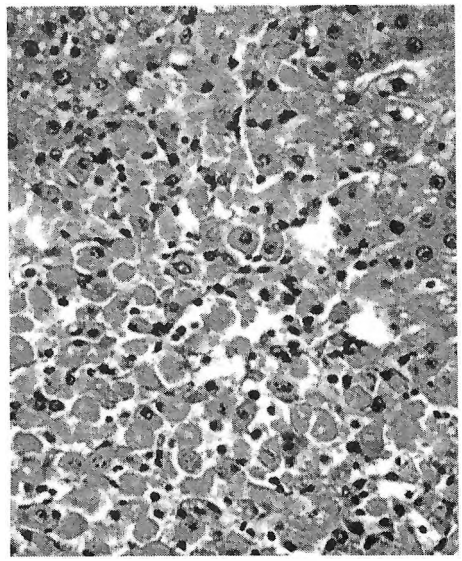

Fig. 3. Liver of an animal treated with CCl_4. Kunselmann's bodies in foci of necrosis. In the periphery there are preserved hepatocytes with hydropic and fatty degeneration. HE, × 400

crotic zones merged and thus the so-called 'bridge necroses' were formed (Fig. 2). In some lobures there were hepatocytes with still preserved cellular membrane but with swallen or picnotic nuclei along with absence of glycogen in the cytoplasm. At this place, amidst the necrotic masses, "free Kunselmann's bodies" could be observed (Fig. 3). Reticular fibres were destroyed.

Morphological liver changes in animals treated with the probiotic Biostim LBS in a dose of 800 mg/kg bw and CCL_4 (group IV)

Only in one animal of this group there was a coagulation necrosis in the central parts of the hepatic lobules and of a smaller size of the affected regions. In all the rest animals there was no coagulation necrosis at all. The alterations being considerably less expressed in comparison with those of the animals treated with CCL_4 only were characterized with a hydropic degeneration manifested to a different extent but in some lobules only — of balloon degeneration (Fig. 4). There were hepatocytes with microvesicular steatosis in the cytoplasm, too.

Morphological liver changes in animals treated with the probiotic Biostim LBS in a dose of 1600 mg/kg bw and CCL_4 (group V)

The application of the preparation in this dosage exerted a manifested hepatoprotective effect in CCL_4 treated animals. On the one hand, there was a considerable reduction of the surface of affection in the hepatic lobules. On the other hand, the comparison with the animals pre-treated with the probiotic Biostim LBS in a dose of 800 mg/kg impressed through the less outlined lesion of the liver parenchyma. It was

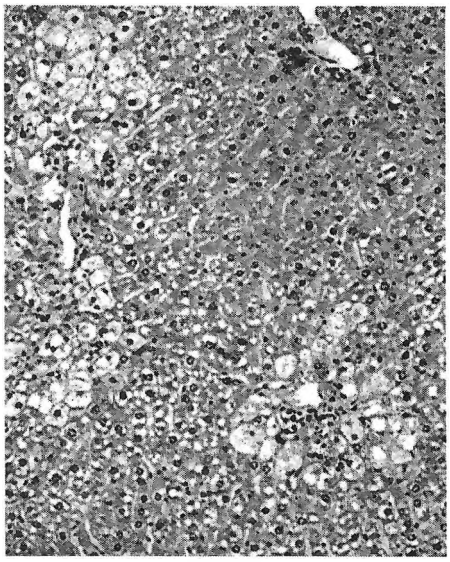

Fig. 4. Liver of an animal treated with Biostim LBS (800 mg/kg bw) and CCl_4. In the hepatocytes of some lobules there is hydropic up to balloon degeneration. There is no coagulation necrosis. bafatty droplets. HE, × 200

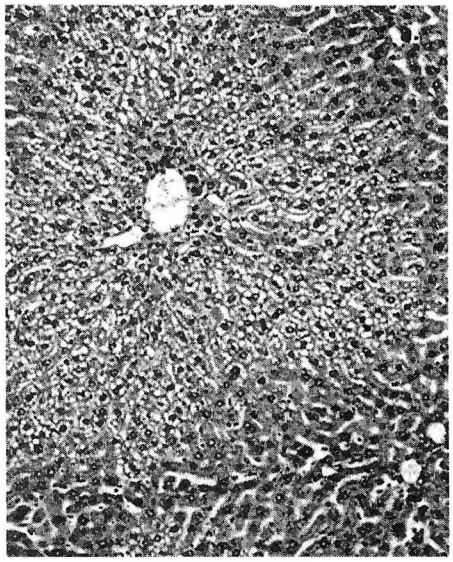

Fig. 5. Liver of an animal treated with Biostim LBS (1600 mg/kg bw) and CCl_4. Hydropic degeneration in the hepatocytes from the central and, partially, from the intermediary area of the lobule. In the periphery there are hepatocytes with small-droplet fatty degeneration. HE, × 200

manifested by the development of a vacuolar, partially, up to hydropic degeneration of the hepatocytes from the central and, partially, from the intermediary areas of the lobules (Fig. 5). Around these parts, at places, hepatocytes with small-droplet fatty degeneration could be observed. Necrotic changes and balloon degeneration in the hepatocytes that were observed in other groups were missing. The amount of the glycogen granules was comparatively regularly distributed in the cytoplasm of the cells. The kind of the reticular fibres did not differ from that of the control, untreated animals.

Discussion

In toxicology, acute poisoning with CCL_4 are a concrete example of a dramatic disturbance of the balance between the free radical peroxidation of the lipids and the antioxidant capacity of the organism [2,10].

The biotransformation of CCL_4 in the liver generates free radicals. The formed free radicals CCL_3^+ act on the organism in two main directions: first, they immediately damage the different enzymatic systems and first of all the oxygenases CYP 450 and second, that deserves the greatest attention the free radicals CCL_3^+ unlock the processes of free radical peroxidatioon of unsaturated faty acids. New radicals RO_2^+ and hydrogen peroxides ROON formed from the aforementioned fatty acids lead to structural and functional changes in different biological membranes. Next follows a displacement of the oxidative links, disturbace of the integrity of the cellular membranes, exudation of intracellular proteolytic enzymes and apoptosis [2, 10].

The probiotic Biostim LBS containing *L. bulgaricus* protects the liver from the damaging action of CCL_4. This is, most probably, a result from the inhibition of lipid peroxidation and stimulation of the cellular antioxidant system [1, 7, 8].

There are literature data about the antioxidant effect of probiotics containing lactobacilli. The authors establish that lactic acid bacteria clean the eractive oxygen radicals, possess helating capacity for metal ions, realize enzyme inhibition and possess a reduction activity. Milk proteins containing in the lactic acid products enhance the concentrations of glutathione in the liver. The glutathione is important for the detoxication of endogenic and exogenic carcinogens and free radicals as well as it regulated the immune function [11, 12].

Conclusion

The data from the present investigation demonstrate that the probiotic Biostim LBS administered in definite dosages exterts a hepatoprotective effect in acute hepatic toxicity in rats induced by CCL_4. Preliminary treatment with this probiotic leads to reduction of the severity of the degenerative and necrotic changes in the liver caused by CCL_4 and of the size of the area of the necrotic alterations as well. Our data confirm the clinical significance of the chronic application of Biostim LBS in hepatic diseases such as viral hepatitis, in ethanol-induced liver damage and in experimental hepatotoxicity as well.

References

1. Bay, B. H., Y. K. Lee, B. K. Tan, E. A. Ling. Lipid peroxidative stress and antioxidative enzymes in brains of milk-supplemented rats. — Neurosci. Lett., **277**, 1999, 127-130.
2. Boll, M., L. W. Weber, E. Becker, A. Stampfl. Mechanism of carbon tetrachloride-induced hepatotoxicity. Hepatocellular damage by reactive carbon tetrachloride metabolites. — Z. Naturforsch. (C), **56**, 2001, 649-659.
3. Bounous, G., S. Baruchel, J. Falutz, P. Gold. Whey protein as a food supplement in HIV-seropositive individuals. — Clin. Invest. Med., **16**, 1993, 204-209.
4. Havenaar, R., J. H. J. Huis in't Veld. Probiotics: a general view. The lactic acid bacteria. — In: The Lactic acid Bacteria in Health and Disease (Ed. B. J. B. Wood). London, Elsevier Applied Science, 1992, 1, 71-151
5. Heller, K. J. Probiotic bacteria in fermented foods: product characteristics and starter organisms.— Am. J. Clin. Nutr., **73**, 2001, S374-S379.
6. Ivanova, I., M. Jenova. Preventive role of liophilic dairy products "Bulgaricum" and "Biostim". — Cancer Lett., **114**, 1997, 93-95.
7. Kaizu, H., M. Sasaki, H. Nakajima, Y. Suzuki. Effect of antioxidative lactic acid bacteria on rats fed a diet deficient in vitamin E. — J. Dairy Sci., **76**, 1993, 2493-2499.
8. Lin, M. Y., C. L. Yen. Antioxidative ability of lactic acid bacteria. — J. Agric. Food Chem., **47**, 1999, 1460-1466.
9. McIntosh, G. H., G. O. Regester, R. K. Le Leu, P. J. Royle, G. W. Smithers. Dairy proteins protect against dimethylhydrazine-induced intestinal cancers in rats. — J. Nutr., **125**, 1995, 809-816.
10. Perez-Trueba, G. Protective effect of Gossypitrin on carbon-tetrachloride-induced *in vivo* hepatotoxicity. — Redox Rep., **8**, 2003, 215-221.
11. Wu, D., S. N. Meydani, J. Sastre, M. Hayek, M. Meydani. *In vitro* glutathione supplementation enhances interleukin-2 production and mitogenic response of peripheral blood mononuclear cells from young and old subjects. — J. Nutr., **124**, 1994, 655-663.
12. Yamauchi, A., E. T. Bloom. Requirement of thiol compounds as reducing agents for IL-2-mediated induction of LAK activity and proliferation of human NK cells. — J. Immunol., **151**, 1993, 5535-5544.

Institute of Experimental Morphology and Anthropology with Museum
Bulgarian Anatomical Society

Acta morphologica et anthropologica, 13
Sofia • 2008

Influence of Probiotics on Histopathological Liver Alterations in Experimental Hypercholesterolemia

M. Georgieva, E. Softova, M. Gabrovska**, P. Borisova, N. Manolov****

Department of Preclinical and Clinical Pharmacology and Biochemistry,
Prof. Paraskev Stoyanov Medical University of Varna
** Department of General and Clinical Pathology, Prof. Paraskev Stoyanov Medical University of Varna*
***Department of Anatomy, Histology and Embryology,*
Prof. Paraskev Stoyanov Medical University of Varna
****Clinic of Vascular Surgery, St. Anna University Hospital of Varna,*
Prof. Paraskev Stoyanov Medical University of Varna

The effect of chronic treatment with probiotic Biostim LBS containing the original *Lactobacillus bulgaricus* on liver morphology in hyperlipidemia was studied. Biostim LBS (800 mg/kg bw and 1600 mg/kg bw), Biostim LBS-1 (1600 mg/kg bw) and cholesterol (0,7 mL/100 g) were administered once daily for 30 consecutive days in male Wistar rats. Liver specimens were taken on the 31st day for histological analysis. Steatogenic diet induced fatty degeneration in the hepatocytes that underwent involution after Biostim LBS treatment in a dose of 800 mg/kg bw without complete normalization. The application of Biostim LBS and Biostim LBS-1 in a dose of 1600 mg/kg bw completely restored the hepatocytes. These probiotics possess regenerative and protective properties concerning lipid degeneration. There is no reliable statistical difference between the effects of both probiotics.

Key words: Biostim LBS, cholesterol, fatty degeneration, hepatocytes.

Introduction

There is evidence that Lactobacilli, including *Lactobacillus bulgaricus*, exert favourable effects concerning the prevention and treatment of various gastrointestinal diseases, including colon cancer. They reduce the risk of cardiovascular diseases, possess an immunomodulatory, antiallergic and X-ray protective action at absent teratogenic effect [1, 4, 6, 7, 11].

Probiotic Biostim LBS is a low-lactose, moderately fatty and dry milk product while probiotic Biostim LBS-1 is a low-lactose, fat-free and dry milk product. Both probiotics are obtained through lactic-acid fermentation from ecologically pure cow milk. They contain live cells of *Lactobacillus bulgaricus*, milk proteins, fats, carbohydrates, natural vitamins, minerals, and pectin. They do not contain, however, preservatives and genetically manipulated microorganisms at all.

The purpose of the present study is to establish the effect of a chronic treatment with the probiotic Biostim LBS containing the original *Lactobacillus bulgaricus* on the morphological liver alterations in experimentally induced hyperlipidemia.

Materials and Methods

The study covered 42 white male Wistar rats weighing initially 250±10 g bw. They were maintained under conditions of room temperature and free access to standard food and water.

According to the treatment module, the animals were divided into 8 groups of 6 animals each as the substances were introduced per sondam.

Group I — Biostim LBS 800 mg/kg bw; Group II — Biostim LBS 1600 mg/kg bw; Group III — Biostim LBS-1 1600 mg/kg bw; Group IV — cholesterol 0,7 ml/100 g; Group V — Biostim LBS 800 mg/kg bw and cholesterol; Group VI — Biostim LBS 1600 mg/kg bw and cholesterol; Group VII — Biostim LBS-1 1600 mg/kg bw and cholesterol; Group VIII — pure controls, not treated at all.

Two types of Biostim LBS were used. The animals were given Biostim LBS (800 mg/kg bw and 1600 mg/kg bw) and Biostim LBS-1 (1600 mg/kg bw) once daily for 30 consecutive days. These doses were selected to match the recommended doses in humans. The control animals were given physiological saline. Both probiotics were solved ex tempore in distilled water. Cholesterol was administered into the stomach by a soft tube in a dose of 0,7 ml/100 g (1,5% cholesterol dissolved in sunflower oil) for 30 consecutive days.

On the 31st day, material was taken from rat liver and processed after a standard paraffin method. Some livers were cut by cryostat to prove the fats. Eight-mkm thick sections were stained with hematoxylin-eosin, oil-red (for fats), PAS reaction with Schiff's reagent for glycogen and Gomori for reticular fibres.

Results

The application of an steatogenic diet resulted in a fatty degeneration in the hepatocytes from central and intermediary areas of the hepatic lobules (Fig. 1, 2). These alteration underwent an involution to a great extent after the application of Biostim LBS in a dose of 800 mg/kg bw (Fig. 3) without any complete restoration. However, the administration of both Biostim LBS and of Biostim LBS-1 (Fig. 4) in a dose of 1600 mg/kg bw led to a complete fading away of the changes as the appearance of the hepatocytes could not be distinguished from that of the controls (Fig. 5).

Discussion

The lipid lowering effect of the sour milk (yoghourt) is related to the increased content of lactic-acid bacteria in the gastrointestinal tract. These bacteria ferment the carbohydrates from the food that are difficult to digest. Such a fermentation results in an increased production of short-chain fatty acids that reduce the concentration of circulating cholesterol either through inhibition of liver cholesterol synthesis, or through cholesterol redistribution from plasma to the liver. Besides the increased bacterial activity in the intestines leads to enhanced bile acid deconjugation. These deconjugated bile acids cannot be well absorbed by the gastrointestinal mucosa and

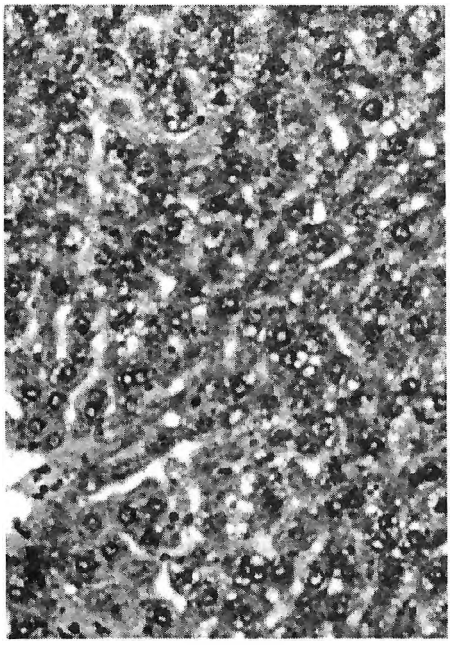

Fig. 1. Liver of an animal on steatogenic diet. Small and merging fatty droplets in the hepatocytes of the hepatic lobule. HE, × 250

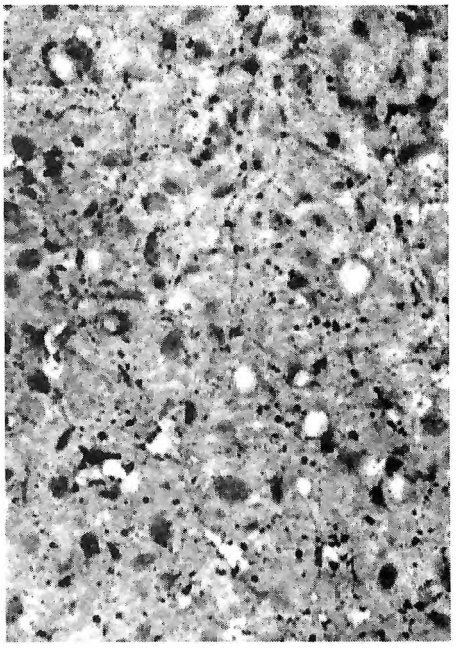

Fig. 2. Liver of an animal on steatogenic diet. Staining with oil-red for fats. × 400

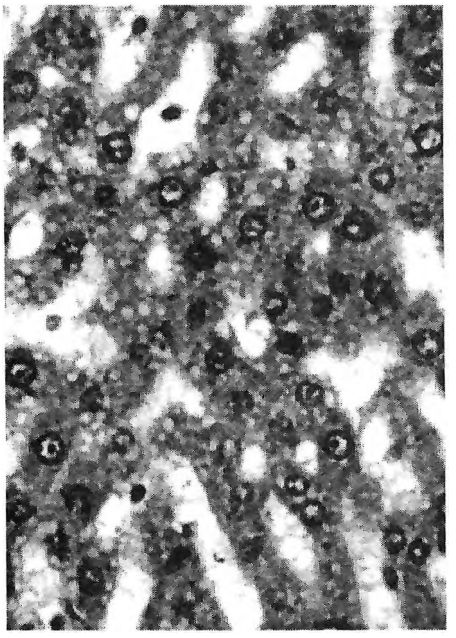

Fig. 3. Liver of an animal on steatogenic diet given Biostim LBS (800 mg/kg bw). In some hepatocytes there are scattered fatty droplets. HE, × 400

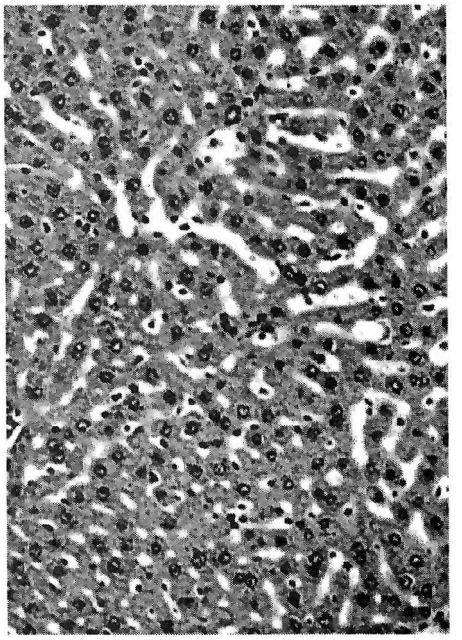

Fig. 4. Liver of an animal on steatogenic diet given Biostim LBS and Biostim LBS-1 (1600 mg/kg bw). Complete restoration of the changes after probiotic application. In the cytoplasm of the hepatocytes there are no fatty droplets at all. HE, × 250

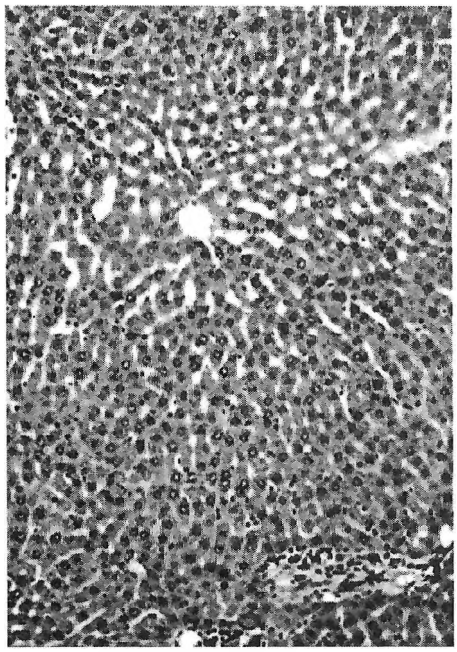

Fig. 5. Liver of a control animal. Preserved histological structure. HE, × 160

are liberated [9]. Therefore, the cholesterol as a bile acid precursor is used to a greater extent for de novo synthesis of the bile acids. Other authors report that the investigations on animals and humans show a moderate hypocholesterolemic action of lactic acid products containing strains of *Lactobacillus* and *Bifidobacteria* [8]. Besides the inhibition of the absorption of exogenous cholesterol by the small intestine either through bile acid deconjugation and influencing upon cholesterol metabolism, or through direct cholesterol assimilation by the bacterial cells has been supposed. The mechanisms for serum lipid lowering have been suggested in other in-vitro and in-vivo investigations. In-vitro experiments by some authors [2, 5, 10] demonstrate that intestinal lactic acid bacteria are capable of assimilate and bind both cholesterol and bile acids. It is known that serum cholesterol values decrease when the probiotics suppress the intestinal bile acid resorption as cholesterol catabolism is stimulated in the liver [3].

Conclusion

The probiotics Biostim LBS and Biostim LBS-1 possess regenerative properties concerning hepatocytes and protect the liver from lipid degeneration caused by the steatogenic diet. There is no reliable statistical difference between the effects of both probiotics.

References

1. Donchev, N., R. Enikova. Antitumor effect of dietary regiments including sour-milk products fermented by original Bulgarian strains.— Biotechnology, **1**, 1992, 43-47.
2. Grundy, S. M. Treatment of hypercholesterolemia by interference with bile acid metabolism. — Arch. Intern. Med., **130**, 1972, 638-648.
3. Hashimoto, H., K. Yamazaki, F. He, M. Kawase, M. Hosod, A. Hosono. Hypocholesterolemic effects of *Lactobacillus casei* subsp. casei TMC 0409 strain observed in the rats fed cholesterol contained diets. — Anim. Sci. J., **72**, 1999, 90-97.
4. Heller, K. J. Probiotic bacteria in fermented foods: product characteristics and starter organisms. — Am. J. Clin. Nutr., **73**, 2001, S374-S379.
5. Hosono, A., H. Otani, N. Yasuih, M. Watanuki. Impact of fermented milk on human health: cholesterol-lowering and immunomodulatory properties of fermented milk. — Anim. Sci. J., **73**, 2002, 241.
6. Huis in't Veld, J. H. J., R. Havenaar. Selections criteria and application of probiotic microorganisms in man and animal. — Microecol. Ther., **26**, 1997, 43-58.
7. Ivanova, I., M. Jenova. Preventive role of liophilic dairy products "Bulgaricum" and "Biostim". — Cancer Lett., **114**, 1997, 93-95.
8. Pereira, D. I., G. R. Gibson. Effects of consumption of probiotics and prebiotics on serum lipid levels in humans. — Crit. Rev. Biochem. Mol. Biol., **37**, 2002, 259-281.
9. St-Onge, M. P., E. R. Farnworth, P. J. Jones. Consumption of fermented and nonfermented dairy products: effects on cholesterol concentrations and metabolism. — Am. J. Clin. Nutr., **71**, 2000, 674-681.
10. Xiao, J. Z., S. Kondo, N. Takahashi, K. Miyaji, K. Oshida, A. Hiramatsu, K. Iwatsuki, S. Kokubo, A. Hosono. Effects of milk products fermented by *Bifidobacterium longum* on blood lipids in rats and healthy adult male volunteers. — J. Dairy Sci., **86**, 2003, 2452-2461.
11. Георгиева, М., Н. Александров, А. Белчева. Изследване на пробиотика „Биос-

Institute of Experimental Morphology and Anthropology with Museum
Bulgarian Anatomical Society

Acta morphologica et anthropologica, 13
Sofia • 2008

Leukocyte Cytochemistry and Hematometric Indices in Chronic Heroin Addicts

Y. Savov, E. Zvetkova, I. Sainova, Y. Gluhcheva, N. Antonova, I. Ivanov*, E. Bichkidjieva, I. Ilieva*

Institute of Experimental Morphology and Anthropology with Museum – Bulgarian Academy of Sciences, Sofia
** Institute of Mechanics and Biomechanics – Bulgarian Academy of Sciences*

The influence of diacetylmorphine (heroin) on white blood cell morphological/functional characteristics and some hematometric indices — leukocyte count (WBC), differential leukocyte count, granulocyte/lymphocyte ratio, whole blood viscosity (WBV) as well as some cytological/cytochemical changes of polymorphonuclears (granulocytes) from the peripheral blood of chronic heroin addicts has been investigated, comparing data to those of healthy individuals. The role of WBC and some morphological/cytochemical changes in granulocytes of chronic heroin abusers has been discussed as factors for the elevated WBV, the acute allergic states and the high sensitivity of heroin addicts to bacterial and viral infections.

Key words: chronic opiate (heroin) addicts, hematometric indices, whole blood viscosity, leukocyte count, leukocyte cytology/cytochemistry.

Introduction

Narcotics such as morphine, diacetylmorphine (heroin) etc., influence white blood cells changing morphological and functional characterisctics of leukocytes, as well as blood viscosity and hematometric indices of drug abusers [4, 5, 7, 9, 14, 15, 19]. Recent studies [14] show an increase in monocyte, neutrophil and eosinophil counts in drug abusers compared to healthy individuals. C h a r u v a s t r a and E h r m a n n [3] find positive correlation between elevated number of eosinophils and intravenous drug use. The *aim* of the study is to investigate leukocyte hematometric indices — white blood cell count (WBC — g/l) and differentiation count (%), granulocyte/lymphocyte ratio (Gr/Ly), mean whole blood viscosity (WBV) as well as some cytological/cytochemical characteristics of polymorphonuclears (granulocytes) in chronic opiate users, comparing data to those of healthy individuals.

Material and Methods

Whole blood heparinized samples from 15 chronic heroin addicts (3 female and 12 male - mean age 26.53 ± 7.34 years, HIV-seronegative, under methadone mainte-

nance therapy), obtained from the Bulgarian National Center for Addictions, were studied. Blood samples were collected in heparinized tubes and rheological measurements were completed within 3 hours after blood preparation. Whole blood viscosity (WBV) was measured at 37°C using a rotational viscometer Contraves Low Shear 30 (Switzerland) with the standard measuring system MS1/1, at a steady flow over a shear rate range of 0.0237 s^{-1} to 128.5 s^{-1}. The results were compared with a control group of 19 healthy individuals (9 female and 10 male; mean age — 34.84 ± 4.06 years). White blood cell hematometric indices — white blood cell count (WBC) and granulocyte/lymphocyte ratio were analyzed by automated cell counter. Cytological characteristics of granulocytes were examined by May-Grünwald-Giemsa technique and by the cytochemical method for cytoplasmic cationic proteins [23]. Student's t-test for determining differences in the mean values of the parameters examined at level of significance $p<0.05$ was used. Relationships between leukocyte parameters and WBV were evaluated using simple correlation coefficient r. Statistical analysis was done on MATLAB 6.5.

Results

The results from total white blood cell count (g/l) showed differences in leukocyte number of chronic heroin addicts (6.89 ± 1.86) and healthy individuals (7 ± 1.2). Based on the total WBC, the granulocyte/lymphocyte ratio (Gr/Ly) is 1.8 for the drug users, versus 1.7 — for healthy donors (Fig. 1). Differential leukocyte count (%) also showed changes in the granulocyte/lymphocyte ratio of drug users compared to that of healthy donors: increased ratios (1.8) were determined in cases of drug abuse, versus 1.6 — in healthy individuals (Fig. 2). Mean whole blood viscosity (WBV) values of the investigated group of heroin abusers were elevated compared to these of healthy persons and the elevation was statistically significant at higher shear rates (γ=20.4 s^{-1}, p=0.1; γ=94.5 s^{-1}, p=0.05). Statistical correlation between granulocyte differential count (%) and WBV at low shear rates was also determined. Our cytological/cytochemical data showed changes in the condensation and distribution of the nuclear chromatin in granulocytes: unevenly dispersed and distributed nuclear DNP - containing irregularly condensed spots of chromatin, were obtained in neutro-

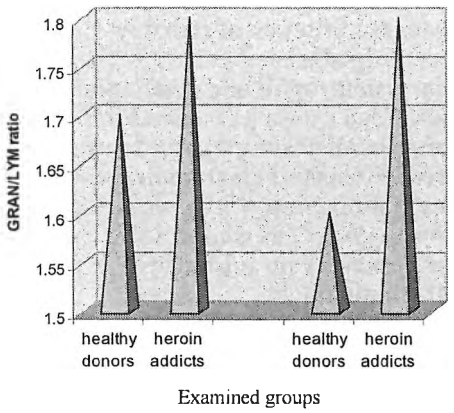

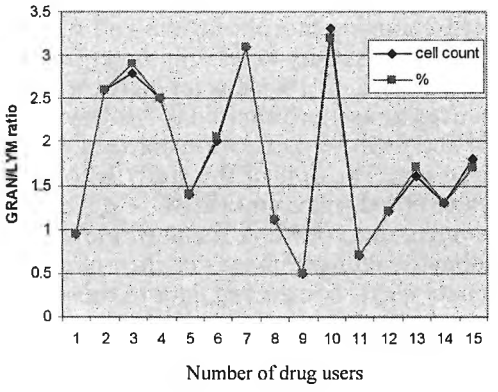

Figs. 1, 2. Granulocyte/lymphocyte ratios in heroin abusers and healthy donors

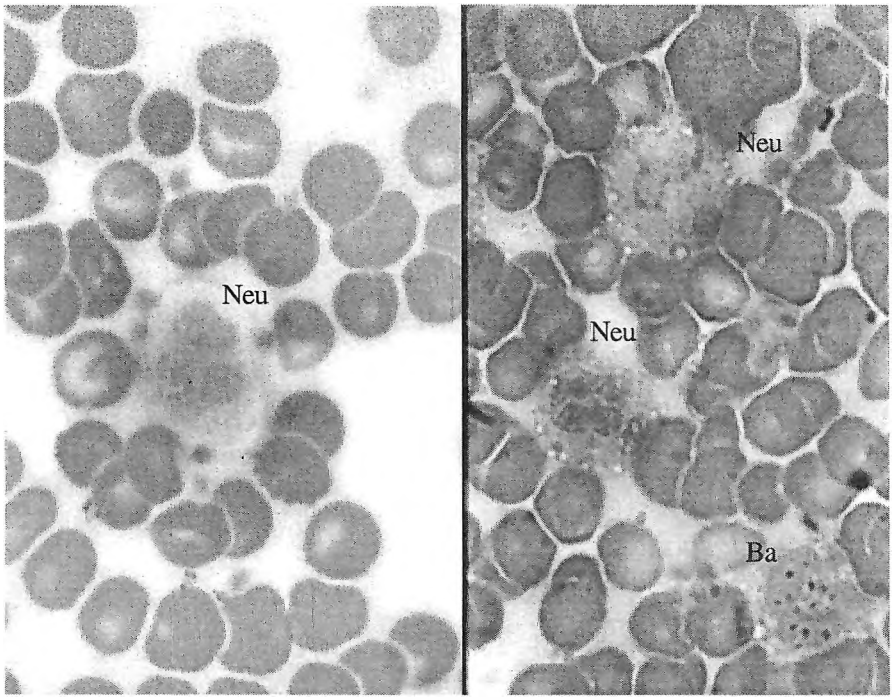

Figs. 3, 4. Neutrophils (Neu) and one basophil (Ba) from the peripheral blood smears of chronic heroin addicts. Changes in the condensation and distribution of DNP in the nuclear chromatin and reduced quantity of cytoplasmic granules, containing cationic proteins could be seen in neutrophils; the cytoplasmic granules of basophil were partially degranulated. × 450

phils and eosinophils of chronic heroin addicts (Figs. 3—6). Low quantity of cytoplasmic granules and diffusely stained cationic proteins are visible in the neutrophils from peripheral blood of heroin abusers (Figs. 3, 4). Abundant fast-green positive granules, containing large amount of cationic proteins, could be seen only in the cytoplasm of eosinophils as well as in a population of eosinophil-like neutrophils (Figs. 5, 6). The percentage of partially degranulated basophils (Fig. 4) is often higher in the peripheral blood of chronic heroin abusers, compared to data of the control group.

Discussion

The reduced total number of leukocytes, increased granulocyte/lymphocyte ratio as well as decreased quantity of cationic protein-containing granules in neutrophils correlate with data [6, 14] for the high sensitivity of heroin addicts to bacterial and viral infections. It is well known fact [9, 16, 22] that narcotics lead to a significant decrease in the phagocytic index and chemotaxis of granulocytes, as well as to the reduced production of superoxide anions (O_3, H_2O_2, NO) which is independent of the co-existance of HIV-infection in drug addicts. On the other hand, the abundant amount of cationic protein-containing cytoplasmic granules in the eosinophilic granulocytes may contribute to the acute allergic states as eosinophilic aseptic arachnoiditis, acute eosinophilic pneumonia, pulmonary edema, urticaria, asthma, etc., often

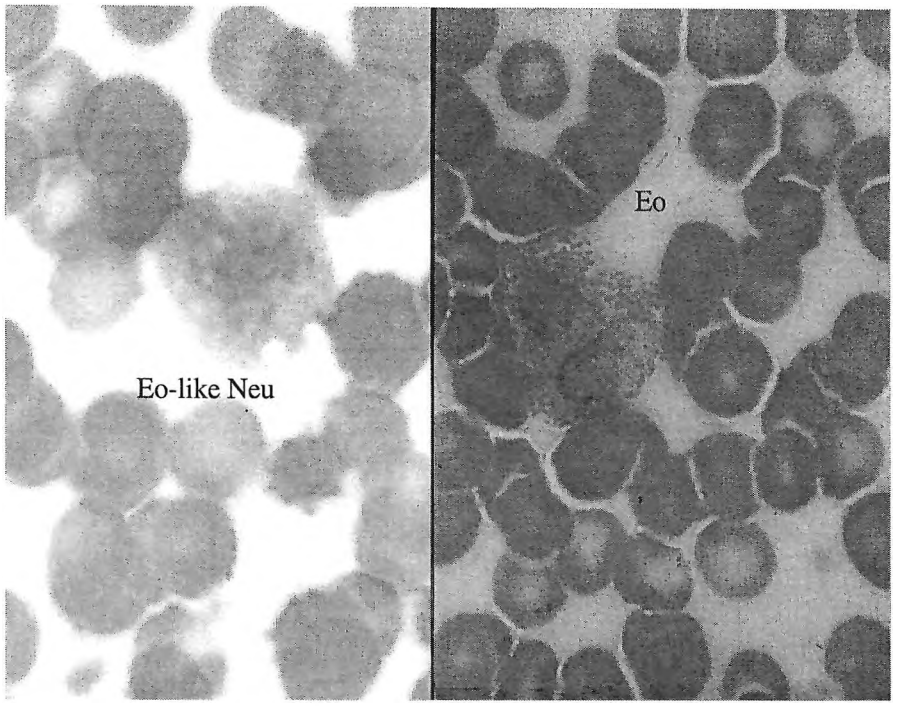

Figs. 5, 6. Eosinophil (Eo) and eosinophil-like neutrophil (Eo-like Neu) containing abundant cytoplasmic granules with large amount of basic cationic proteins in peripheral blood smears of chronic heroin abusers. × 450

observed in heroin addicts [2, 8, 12, 13, 17, 19]. Our data that partially degranulated basophils are frequently seen in blood smears of drug abusers are in agreement with those of other researchers [1, 10, 18] about the increased number of tissue mast cells leading to anaphylactoid reactions, typical for drug addiction. There are speculations about the relationship between white blood cell count (WBC) and blood viscosity: prevails the opinion that not only the hematocrit, hemoglobin and RBC, but also WBC and platelet count could affect WBV [11]. In our previous experimental studies [21] we hypothesized that changes in RBC (macrocytic anemia) are main factors for elevated WBV, but the role of WBC and morphological/cytochemical changes in granulocytes of chronic heroin addicts should be also considered and evaluated. In this regard the statistical correlation obtained between granulocyte differential count (%) and WBV at low shear rates is important. The influence of chronic heroin use on the proliferation and differentiation of early myeloid precursor cells in bone marrow has been studied [20], but the effect should be further examined.

References

1. Barke, K. E., L. B. Hough. Opiates, mast cells and histamine release. — Life Sci., **53**, 1993, No18, 1391-1399.
2. Brander, P. E., P. Tukiainen. Acute eosinophilic pneumonia in a heroin smoker. — Eur. Respir. J., **6**, 1993, 750-752.

3. Charuvastra, V., M. Ehrmann. Six-month follow-up of eosinophil counts in veteran heroin addicts. — Ann. Allergy, **34**, 1975, No1, 15-18.
4. Fecho, K., D. T. Lysle. Heroin-induced alterations in leukocyte numbers and apoptosis in rat spleen. — Cell. Immunol., **202**, 2000, No2, 113-123.
5. Fineschi, V., R. Cecchi, F. Centini, L. P. Reattelli, E. Turillazzi. Immunohistochemical quantification of pulmonary mast cells and post-mortem blood dosages of tryptase and eosinophil cationic protein in 48 heroin-related deaths. — Forensic Sci. Int., **120**, 2001, No3, 189-194.
6. Friedman, H., C. Newton, T. W. Klein. Microbial infections, immunomodulation, and drugs of abuse. — Clin. Microbiol. Rev., **16**, 2003, No2, 209-219.
7. Galante, A., A. De Luca, A. Pietroiutsi, F. Tiratterra, E. Benincasa, B. Domenici, C. Baldelli, C. Valenzi. Effects of opiates on blood rheology. — J. Toxicol. Clin. Toxicol., **32**, 1994, No4, 411-417.
8. Ghodse, A. H., J. S. Myles. Asthma in opiate addicts. — J. Psychosom. Res., **31**, 1987, No1, 41-44.
9. Gutierrez, J., M. C. Maroto, G. Piedrola. Granulocyte abnormalities in parenteral drug-addicts. The influence of HIV infection. — Allergol. Immunopathol. (Madr.), **17**, 1989, No5, 251-255.
10. Hakim, T. S., M. M. Grunstein, R. P. Michel. Opiate function in the pulmonary circulation. — Pulm. Pharmacol., **5**, 1992, No3, 159-165.
11. Ho, C. H. White blood cell and platelet counts could affect whole blood viscosity. — J. Chin. Med. Assoc., **67**, 2004, No8, 394-397.
12. Hogen Esch, A. J., S. van der Heide, W. van den Brink, J. M. van Ree, D. P. Bruynzeel, P. J. Coenroads. Contact allergy and respiratory/mucosal complaint from heroin (diacetylmorphine). — Contact Dermatitis, **54**, 2006, No1, 42-49.
13. Hughes, S., P. M. Calverley. Heroin inhalation and asthma. — BMJ, **297**, 1988, No6662, 1511-1512.
14. Islam, S. N., K. J. Hossain, M. Kamal, M. Ahsan. Serum immunoglobulins and white blood cells status of drug addicts: influence of illicit drugs and sex habit. — Addict. Biol., **8**, 2004, No1, 27-33.
15. Lazzarin, A., L. Mella, M. Trombini, C. Oberti-Foppa, F. Franzetti, G. Mazzoni, M. Galli. Immunological status in heroin addicts: effects of methadone maintenance treatment. — Drug Alcohol Depend., **13**, 1984, No2, 117-123.
16. Mazzone, A., I. Mazzucchelli, G. Fossati, D. Gritti, M. Fea, G. Ricevuti. Granulocyte defects and opioid receptors in chronic exposure to heroin or methadone in humans. — Int. J. Immunopharmacol., **16**, 1994, No11, 959-967.
17. McLelland, J. The mechanism of morphine induced urticaria. — Arch. Dermatol., **122**, 1986, No2, 138-139.
18. Rook, E. J., A. P. van Zanten, W. van den Brink, J. M. van Ree, J. H. Beijnen. Mast cell mediator tryptase levels after inhalation or intravenous administration of high doses pharmaceutically prepared heroin. — Drug Alcohol Depend., 2006.
19. Rossetti, A. O., K. Meagher-Villemure, F. Vingerhoets, P. Maeder, J. Bogousslavsky. Eosinophilic aseptic arachnoiditis. A neurological complication in HIV-negative drug-addicts. — J. Neurology, **249**, 2002, No7, 884-887.
20. Roy, S., S. Ramakrishnan, H. H. Loh, N. M. Lee. Chronic morphine treatment selectively suppresses macrophage colony formation in bone marrow. — Eur. J. Pharmacol., **195**, 1991, No 3, 359-363
21. Savov, Y., N. Antonova, E. Zvetkova, Y. Gluhcheva, I. Ivanov, I. Sainova. Whole blood viscosity and erythrocyte hematometric indices in chronic heroin addicts. — Clin. Hemorheol. Microcirc., **35**, 2006, No1-2, 129-133.
22. Tubaro, E., C. Santiangeli, L. Belogi, G. Borelli, G. Cavallo, C. Croce, U. Avico. Methadone vs morphine: comparison of their effect on phagocytic functions. — Int. J. Immunopharmacol., **9**, 1987, No1, 79-88.
23. Zvetkova, E. B., I. B. Zvetkov. A cytological method for the simultaneous staining of nucleoproteids and some cathionic proteins. — Acta Histochem., **57**, 1976, No1, 1-13.

Institute of Experimental Morphology and Anthropology with Museum
Bulgarian Anatomical Society

Acta morphologica et anthropologica, 13
Sofia • 2008

Enzyme Histochemical Expression of Lipoprotein Lipase (LPL) in Renal Blood Vessels in Dogs Fed a High-Calorie Diet

P. Yonkova, P. Atanassova, A. Vodenicharov, M. Andonova***

Department of Veterinary Anatomy, Histology and Embryology, Faculty of Veterinary Medicine, Trakia University, Stara Zagora
**Department of Anatomy, Histology and Embryology, Medical University, Plovdiv*
***Department of General and Clinical Pathology, Faculty of Veterinary Medicine, Trakia University, Stara Zagora*

The enzyme lipoprotein lipase (LPL) is synthesized and secreted by adipocytes, myocytes, mammary gland epithelium etc. and is transported to the endothelium of capillaries. LPL is the main lipolytic enzyme participating in the intravascular metabolism of lipoproteins. In the present study, two groups of dogs were used — experimental (obese) and control (non-obese). Immediately after euthanasia, specimens from the renal blood vessels were obtained from both groups. The enzyme histochemical reaction (according to Gomori, 1952) was performed on fresh cryostat sections and by the Tween method, positive expression of LPL in the wall of renal blood vessels in dogs fed a high-calorie diet, was evidenced. In the three vascular layers in control animals, no LPL expression was observed.

Key words: lipoprotein lipase, obesity, high-calorie diet, dogs.

Introduction

Lipoprotein lipase (LPL) is an enzyme that is synthesized and secreted by adipocytes, myocytes (especially cardiomyocytes), the epithelium of lactating mammary gland and other cells. It is transported to the endothelial surface of blood vessels where it exerts its effect. The function of LPL is to hydrolyze triacylglycerols (TAG) from chylomicrons, very low and intermediate density lipoproteins from the luminal side of capillary endothelium [5, 6].

P e n t i k ä i n e n et al. [6] detected LPL in the endothelial cells of capillaries and arteries. K o j a m a et al. [4] reported about endothelial lipase (EL) that is synthesized and secreted mainly by vascular epithelium as a new member of the lipase gene family. Genetically, endothelial lipase is 44% identical to lipoprotein lipase and 41% identical to hepatic lipase according to H i r a t a et al. [1].

LPL expression is immunohistochemically evidenced in the intima, subendothelium, smooth muscle cells and the adventitia of arterial wall [2, 4, 8]. This

shows that subendothelially secreted LPL is not stored in stromal cells where it exerts its functions. In the ischaemic zone of the myocardium throughout sudden death of geriatric dogs, LPL reduction is observed [11, 12].

Mutations in LDL receptors result in a dominant autosomal disease — family hypercholesterolaemia [13, 14]. Mice with severe LPL deficiency die 24 hours after birth. LPL deficiency is also reported in cats and minks. The genetic lack of LPL causes a significant hyperchylomicronaemia, increased plasma TAG concentrations, acute pancreatitis that could be life-threatening [3]. In men such deficiency is encountered in 3-7% of the population [9].

S u s a n n e et al. [10] show that LPL has either a pro- or anti-atherogenic effect depending on its localization. Arterial LPL has a considerable proatherogenic function as it increases the accumulation of intra- and extracellular lipids into the intima [6]. On the contrary, the capillary endothelial LPL is clearly antiatherogenic via its antidyslipidaemic effect [9]. In dogs with moderate and severe atherosclerotic lesions of the aorta, coronary and renal arteries, a significant immunohistochemical expression of the enzyme in endothelial cells, the media, smooth muscle cells and macrophages has been observed. Positive signals for the enzyme were not detected in normal arteries [8]. J o n a s s o n et al. [2] observed the highest LPL amount in smooth muscle cells of blood vessels in vessels affected by atherosclerotic lesions as well as in unaffected arteries. Therefore the authors assumed that vascular smooth muscle cells were the biggest source of LPL.

The aim of the present study was to follow out the enzyme histochemical expression of LPL in renal blood vessels in dogs, fed a high-calorie diet.

Material and Methods

Two groups of dogs — experimental and control were used. The experimental dogs (n=3) had an initial body weight of 12.8667 ± 1.4305 kg. For 90 days, each dog received a daily ration of 400 g canine dry food "Jambo Dog" (Gallisman S. A., Bulgaria) supplemented with 10g/kg b.w. lard, in order to induce experimental obesity. By the end of the high-calorie diet intake, the dogs weighed 16.5417±1.6734 kg. The control group (n=2) weighed 13.654±3.315 kg. Their daily ration consisted of 310 g canine dry food "Jambo Dog" (Gallisman S. A., Bulgaria).

Immediately after the euthanasia of the dogs from both groups, specimens from renal blood vessels (arteries and veins) were obtained. The enzyme histochemical reaction was performed on fresh cryostat sections for detection of positive expression of lipoprotein lipase in vascular walls according to Gomori (1952). The reaction was based upon the Tween method consisting in the deposition of insoluble calcium soaps at the sites of enzyme activity that are further converted to lead soaps and finally, in lead sulfide precipitates. On ready preparations, these precipitates appeared as clusters of dark-brown granules [7].

Results and Discussion

The performed enzyme histochemical studies showed a strong positive expression of LPL in renal blood vessel wall in dogs fed the high-calorie diet. The reaction was detected as presence of dark brown granules — lead sulfide precipitates.

A positive LPL enzyme histochemical expression was observed in the wall of all renal blood vessels in dogs from the experimental group. Positive LPL reaction was

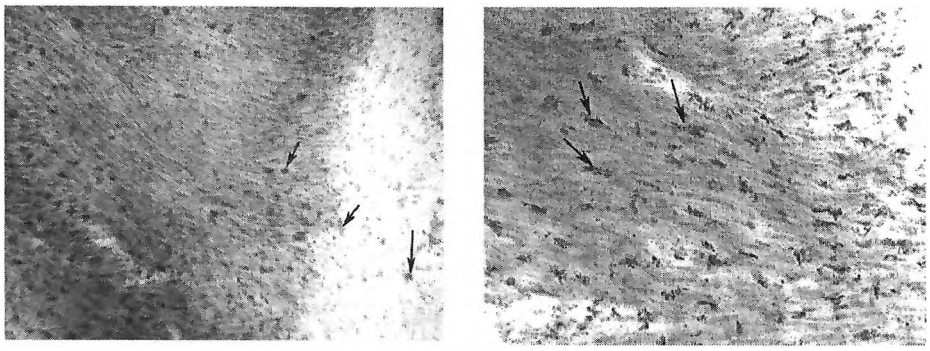

Fig. 1. LPL expression in *Tunica intima* (1a, × 40) and in smooth muscle cells in *Tunica media* (1b, × 100) of dog's renal arteries (arrows)

Fig. 2. LPL expression in the wall of the dog's renal veins (arrows). × 20

detected in the *Tunica intima* of arteries (Fig. 1) and veins (Fig. 3). It was strongly expressed in vascular endothelium.

A similar reaction was observed in connective tissue cells of the subendothelium as well as in sebaceous cells, whose counts were higher as a result of obesity.

In the *Tunica media*, a positive LPL expression was also observed. It was however, the most strongly expressed in smooth muscle cells of arteries (Fig. 2).

Single cells of the adventitia also exhibited a positive LPL reaction. The observations on control dogs revealed no expression of the enzyme in all three blood vessel layers.

As a result of performed studies, it was found out that the high-calorie diet provoked a strong enzyme histochemical expression of LPL in the renal blood vessels of dogs. These data of ours correlate to a certain extent to the results of S a k o et al. [8] for a considerable immunohistochemical LPL expression in the cytoplasm of endothelial cells, smooth muscle cells, of macrophages in the subendothelium, the intima and the media in dogs with lesions of the aorta, the coronary and renal arteries.

We stated that the enzyme histochemical LPL reaction was the strongest in the smooth muscle cells of renal vascular *Tunica media* in the dog. J o n a s s o n et al. [2] had also observed the biggest LPL amount in smooth muscle cells of blood vessels,

both with atherosclerotic lesions and unaffected. This allowed assuming that the greatest source of LPL in blood vessels were vascular smooth muscle cells.

Taking into consideration the proved proatherogenic function of LPL as an enzyme, participating directly or indirectly in the intimal lipoprotein metabolism, augmenting the accumulation of intra- and extracellular lipids into the intima [10], we consider that most probably, the observed enhanced LPL reaction in canine renal blood vessels due to the high-calorie diet, was one of morphological features, perhaps early and prognostic, of atherosclerotic alterations in the wall of these vessels, occurring with obesity.

References

1. Hirata, K., L. Dichek, A. Cioffi, Y. Choi, J. Leeper, L. Quintana, G. Kronmal, A. Cooper, T. Quertermous. Cloning of a unique lipase from endothelial cells extends the lipase gene family. — J. Biol. Chem., **274**, 1999, 14170-14175.
2. Jonasson, L., G. Bondjers, G. K. Hansson. Lipoprotein lipase in atherosclerosis: its presence in smooth muscle cells and absence from macrophages. — Journal of Lipid Research, **28**, 1987, 437-445.
3. Kawashiri, M., D. Rader. Gene therapy for lipid disorders. — Curr. Control Trials Cardiovasc. Med., **1**, 2000, No2, 120-127.
4. Kojama, Y., K. Hirata, T. Ishida, Y. Shimokawa, N. Inoue, S. Kawashima, T. Quertermous, M. Yokoyama. Endothelial lipase modulates monocyte adhesion to the vessel wall. — J. Biol. Chem., **279**, 2004, 54032-54038.
5. Marks, B., A. Marks, C. Smith. Lipid metabolism. — In: Basic Medical Biochemistry, a Clinical Approach. Baltimor, Williams and Wilkins, 1996, 487-544.
6. Pentikäinen, M., R. Oksjoki, K. Öörni, P. Kovanen. — Lipoprotein lipase in the arterial wall. — Arteriosclerosis, Thrombosis and Vascular Biology, **22**, 2002, p. 211.
7. Pearse, A. Lipases, lipases methods. — In: Histochemistry Theoretical and Applied. London, J.& A. Churchill, Ltd., 1960, 472-475, 888-889.
8. Sako, T., E. Uchida, Y. Kagawa, K. Hirayama, T. Nakade, H. Taniyama. Immunohistochemical detection of apolipoprotein A-I and B-100 in canine atherosclerotic lesions. — Vet. Pathol., **40**, 2003, No3, 328-331.
9. Semenkovich, F., T. Coleman, A. Daugherty. Effects of heterozygous lipoprotein lipase deficiency on diet-induced atherosclerosis in mice. — Journal of Lipid Research, **39**, 1998, 1141-1151.
10. Susanne, C., N. Bissada, F. Miao, L. Miao, A. Marais, H. Henderson, P. Steures, J. McManus, R. LeBoeuf, J. John, P. Kastelein, M. Hayden. Plasma and vessel wall lipoprotein lipase have different roles in atherosclerosis. — Journal of Lipid Research, **41**, 2000, 521-531.
11. Vik-Mo, H., P. Moen, O. Mjos. Myocardial lipiproteins lipase activity during acute myocardial ischemia in dogs. — Horm. Metab. Res., **14**, 1982, No2, 85-88.
12. Williams, K. Coronary arteriosclerosis with myocardial atrophy in a 13-year-old dog. — Veterinary Pathology, **40**, 2003, 695687.
13. Попов, Ч. Биохимия. София,Земиздат, 1992, 236-260.
14. Сиракова, И., Л. Сираков. Рецептори и клетки. София, Медицина и физкултура, 1989, 141—145.

Institute of Experimental Morphology and Anthropology with Museum
Bulgarian Anatomical Society

Acta morphologica et anthropologica, 13
Sofia • 2008

Application of the Therapy Method with Left-rotating Circularly Polarized Light in the Medical Practice

*J. Stoyanov, I. Tanev**

Department of Anatomy, Medical Faculty, Thracian University, Stara Zagora
**Department of Physics and Biophysics, Medical Faculty,*
Thracian University, Stara Zagora

There have been no data for the application of left-rotating circularly polarized light as a therapeutical method in the medical literature until nowadays. We have designed a device that uses the method of Frennel for obtaining circularly polarized light and have tested it through implementing it clinically. We found that the therapeutic method with left-rotating circular polarized light can be applied widely and successfully in the medical practice for the treatment of diseases of the locomotory apparatus, the respiratory, digestive and cardiovascular systems as well as for disorders of psycho-emotional nature. The method is an excellent mode for the treatment of stress. It includes local application of left-rotating circularly polarized light and projecting regular geometric figures on the palm skin or back side of the hand with a certain color. These figures have a differing harmonious impact on the human organism.

Key words: left-rotating circularly polarized light, light therapy, bio-information.

Introduction

The shaft of light contains a huge number of elementary rays and in any of them the vector of the electric field oscillates in its own plane. If the particular plane of oscillation is different, we obtain ordinary and unpolarized light. If the rays are situated in near vicinity, we obtain partly polarized light, and if they coincide completely in the same plane only there is linearly-polarized light. There is another type of polarization when this vector rotates in a definite direction around the axis of light distribution with a frequency that is equal to the frequency of the light wave. If during this rotation the vector of the electric field does not change its magnitude, there is circularly polarized light. If the vector changes its magnitude, there is elliptic polarized light. Depending on the rotating direction of this vector, we can differentiate left and right rotating polarized light.

The light, especially plane-polarized, has medicinal effect on skin diseases, wounds, etc. [3]. In medicine the visible and ultraviolet rays are used for photo-therapy and photo-dynamic therapy to initiate reactions of synthesis and polymerization [1]. The infrared rays have a calorific affect on the tissues. They penetrate

only a few centimeters into the tissues and heat them up and this way set into motion the system for thermoregulation [2].

The plane-polarized light is used for the examination of optical active substances, in polarizing microscopes, in television sets with a flat screen for localizing the lines of internal pressure, etc. [5].

Materials and Methods

Most of the light sources (lamps, the flame and the sun) radiate unpolarized light. Plane-polarized light is obtained in: a/ reflection and refraction of ordinary light on the borderline between two transparent dielectrics - for example air/ water. The level of polarization of the reflected light depends on the angle of incidence and at the angle of Bruster it becomes 100%; b/ refraction of ordinary light from special, double- refracting crystals (calcite, tourmaline and gerapatit). At the moment of refraction, the falling ray is divided into two plane-polarized rays. These are the crystals used for polirizers (the Nikol's prism, polaroids) — the optical elements for obtaining plane-polarized light through double refraction. A classical way for obtaining circularly polarized light is via the so-called "polar meter of Stocks" that consists of a light filter, a polarizer and a quarter- wave lamella, all of them consecutively positioned [6]. The light filter must be interferential to obtain a very narrow passage range. The quarter-wave lamella has the thickness equal to one fourth of the nanometer (nm) and is made of mica. The disadvantage of this device is that for any wave length (for any used filter) an appropriate quarter-wave lamella that is very hard must be used, so we use an achromatic quarter-wave compensator designed for the first time by F r e n n e l [6].

Operating mechanism

The method of electromagnetic-resonance impact of the circularly polarized light on the human organism uses visible rays with a wavelength from 380 nm to 760 nm. It is known that the skin is a big receptor field and the human organism is built up of proteins. It is also known that protein molecules have a spiral form. The ray of circularly polarized light spreads in the form of a spiral. All the types of proteins, without any exception, are optically active as they rotate the plane of polarized light to the left at definite angle [4]. This is a universal property and therefore we choose the use of left-rotating circularly polarized light as a therapy method. On affecting a definite skin region with the above-described radiation, the protein structures acquire an electromagnetic resonance. Membrane proteins, free nerve endings, potential dependent Na+, Ka+, Ca++ canals that are built of proteins and can absorb a few alternative conformations react. These limited conformational changes in the proteins lead to alterations in their functional activity. A specific action potential is created that corresponds to the wavelength. It reaches the central nervous system (CNS) along the afferents where it provokes a reaction in some of its structures: the motor neurons, sustantia lateralis intemedia, the reticular formation and the limbic system. Effectors responses are developed and along the efferents they reach the skeletal, the smooth and the cardiac muscular tissues, the internal organs, the glands and blood vessels. Thus information is passed to the CNS as we create a differing harmony corresponding to the various systems. This can be achieved when we project the electro-

magnetic resonance radiation with a definite wavelength on a certain skin region in combination with regular geometric figures. The period of time of exposure is from 10 to 12 minutes which is enough for the healthy harmonic effects to develop.

Results

Observed healthy effects

1. Impact on the physical activity-positive effect on the skeletal muscles- increase or decrease in the muscular tone, depression and elimination of myalgia, contracture, or muscule fatigue.
2. Impact on the smooth muscular tissue: spasmolytic or tonic effect;
3. Stabilizing of cardiac activity
4. Effective results in: astheno-vegetative conditions, state of agitation, insomnia, seasonal disorders, depression, and emotional breakdowns.
5. Analgetic effect
6. Anti-inflammatory effect in processes of non-infectious nature (for example: of traumatic origin). Resolution of oedemas.

Results from successfully accomplished treatment

Arthrosis of lumbar vertebrae accompanied with monolateral or bilateral radiculitis - 12 cases; Discal hernia (L4, L5) - 10 cases; Arthrosis of cervical vertebrae accompanied with radiculitis - 10 cases; Osteophytes - 8 cases; Coxarthrosis - 12 cases; Gonarthritis - 8 cases; Periarthritis - 6 cases; Epycondylitis - 8 cases; Tendinitis - 13 cases; Plexitis - 9 cases; Inflammation of the paranasal sinuses (chronic suppurative inflamed) - 18 cases; Migraine - 8 cases; peptic ulcer disease - 8 cases; Chronic colitis - 5 cases; Chronic Cholecystitis - 8 cases; Hypertension - 14 cases; Astheno-vegetative conditions - 12 cases; Depression - 2 cases.

Using this method no undesirable side effects such as erythema, irritation, edema, or nociceptia are developed since the harmful impact of the infrared and ultraviolet rays is avoided. We evaluated the reports from the implemented treatment. Some of the patients were sent by colleagues at the Medical Faculty to the Thracian University. After the treatment the same professionals noted the results from the implemented treatment in examination reports of the patients.

Discussion

The advantage of the described method to other phototherapeutical methods is due to its impact mechanism. It does not rely on penetrating tolerance of the rays deeply in the tissues depending on the different wavelength. Most importantly, the frequency of vibrating of left-rotating circularly polarized light is transferred through the resonance to the protein structures that oscillate with their own vibration frequency and this is transferred in depth as well as along the nerves. Thus the colors combined with regular geometric figures have a harmonizing impact on the CNS, psycho- emotional conditions and then in a nerve- reflecting way to all organs in different systems of the human organism.

The human organism is a complex informational and energetic structure. Through bringing harmonic information in it, the desired results on an individual's state of health can be achieved.

Conclusion

The left-rotating circularly polarized light has a strong biological activity. It is a method that can be used to send information to the CNS and as the result we can change the psychoemotional and physical state of a person. The electromagnetic resonance radiation is an excellent vitalizing mode that can significantly increase the life expectancy at a reasonable application. The method can be used as an efficacious curative approach independently as well as in combination with pharmacotherapy of modern medicine.

References

1. Aetna, American Medical Association, 2004.
2. Glasgow, P.D., I.D. Hill, A.M. McKevitt, A.S. Lowe, D. Baxter. Low intensity monochromatic infrared therapy: a preliminary study of the effects of a novel treatment unit upon experimental muscle soreness. — Laser's Surg. Med., **28**, 2001, 33-39.
3. Гачева, Й. Физикална терапия, С., Медицина и физкултура, 1993.
4. Дамянова, Л. Химия. С., НИ, 1987, с. 366
5. Николова, Н. Физика с основи на биофизиката. С., ЗИ, 1984.
6. Рвачев, В. П. Методы оптики светорассеивающих сред в физике и биологии. Минск, Издательство БГУ, 1978.

Institute of Experimental Morphology and Anthropology with Museum
Bulgarian Anatomical Society

Acta morphologica et anthropologica, 13
Sofia • 2008

New Synthetic Fluorescent Substrate for Histochemical Localization of the Enzyme Dipeptidyl Peptidase II on the Base of 1,8-Naphthalimides

R. Todorova, I. Ivanov, M. Dimitrova*

Institute of Experimental Morphology and Anthropology with Museum, Bulgarian Academy of Sciences, Sofia
** Faculty of Biology, St. Kl. Ohridsky University of Sofia, Sofia*

A novel fluorescent substrate L-Lys-L-Ala-6-hydrazido-N-hexyl-1,8-naphthalimide for the histochemical visualization of activity distribution of Dipeptidyl peptidase II is proposed. By now, a fluorescent determination of the DPP II activity is realized only in cell homogenates and cultivated cells, whereas fluorescent method for the enzyme localization in tissue sections is missing. The results of our work show that the new method permits precise localization and visualization of dipeptidyl peptidase II in tissue sections from several Wistar rat organs.

Key words: Dipeptidyl peptidase II, 1,8-naphthalimide derivatives, fluorescent histochemical methods, synthetic fluorescent substrates.

Introduction

Dipeptidyl peptidase II (DPP II; EC 3.4.14.2) belongs to serine peptidases family. Biochemical investigations show the lysosomal localization of the enzyme. Preferably, DPP II catalyzes the liberation of dipeptides, with lysine, phenylalanine or leucine at the N-terminal, and alanine or proline at penultimate position [2] from tripeptides, oligopeptides and from synthetic substrates at pH 5.5. The enzyme activity is inhibited by protonated Tris [3].

Here we propose a novel histochemical fluorescent substrate L-Lys-L-Ala-6-hydrazido-N-hexyl-1,8-naphthalimide (Lys-Ala-HHNI) for Dipeptidyl aminopeptidase II and use the substrate, based on 1,8-naphthalimide compound, to investigate the distribution of the enzyme activity in rat kidney, small intestine, colon and epididymis.

Materials and Methods

*Synthesis of N-hexyl-6-hydrazino-1,8-naphthalimide(HHNI).*The fluorochrome HHNI was synthesized as follows: Acenaphthene (Merck, Germany) was brominated by N-

bromo succinimide in dimethylformamide. The obtained 6-bromo acenaphthene was oxidized to 6-bromonaphthalanhydride by a standard procedure with sodium dichromate in acetic acid. The last compound was coupled with hexylamine by boiling it in absolute ethanol for 12 hours to give 6-bromo-N-hexyl-1,8-naphthalimide. The fluorochrome — HHNI was obtained from the brom-containing compound and hydrazine monohydrate in dimethylsulphoxide at 60°C using potassium fluoride as auxiliary reagent and tetrabutyl ammonium sulfate as a catalyst by a novel procedure, which will be published elsewhere. *Synthesis of the substrate.* The DPP II substrate — L-Lys-L-Ala-6-hydrazido-2-hexyl-1,8-naphthalimide (Lys-Ala-HHNI) was synthesized in two steps: First HHNI was coupled with Boc-Ala-OH (Bachem, Switzerland) by the well known N,N,N',N'-Tetramethyl-O-(benzotriazol-1-yl)uronium tetrafluoroborate (TBTU) procedure. The Boc-protection was cleaved in 4N HCl/dioxane. Then the obtained L-Ala-HHNI.HCl was coupled with Boc-Lyz(Boc)-OH (Bachem, Switzerland) again by the TBTU-method. The Boc-protection was cleaved as above and the substrate was obtained as dihydrochloride salt.

Tissue treatment and incubation. Mature male Wistar rats were decapitated under ether anesthesia. Pieces of kidney, small intestine, colon and epidydimis were removed and fixed in 2% formaldehyde in 0.1 M cacodylate buffer, pH 7.0 for 18 hrs. at +4°C. After that, the pieces were washed in Holt solution for 24 hrs. and frozen in liquid nitrogen. Ten μM sections were cut on cryotome Reichert Jung (Nussloch, Germany) at —25°C and mounted on gelatinized glass slides. The sections were covered with 0,5 % celloidin for one minute at room temperature and incubated in solutions, consisting of 0,5 mM substrate (Lys-Ala-HHNI) and 1 mg/ml aromatic aldehyde (piperonal), dissolved in 0.1 M phosphate buffer, pH 5.5. The incubation lasted 30-60 min at 37°C. The samples were post-fixed in 4 % neutral formaline and embedded in glycerol-jelly. Control sections were incubated in buffered aldehyde (in the absence of substrate) or in the full substrate medium supplied with 50 mM Tris.

The sections were studied under fluorescent microscope OPTON IM 35 with filter combination G 546 FT 580 LP 590. The photos were made on Konica Minolta (Japan) VX 200 colorful films.

Results and Discussion

DPP II is thought to play important role in the breakdown of some oligopeptides such as substance P and casomorphin [1]. The enzyme has certain requirements to substrate peptide sequence. It hydrolyzes Lys-Pro and Ala-Pro peptide derivatives, but shows higher specificity to Lys-Ala substrates. Besides, Dipeptidyl peptidase IV co-reaction is avoided by using Lys-Ala substrates. Therefore, we synthesized Lys-Ala derivative of 6-hydrazino-N-hexylamine-1,8-naphthalimide as fluorescent substrate for DPP II.

By newly developed substrate and histochemical method based on it, we managed to determine DPP II activity in rat kidney, small intestine (duodenum, jejunum, ileum), colon and epididymis. Non-specific staining was not observed in control sections, lacking the substrate. Single fluorescent granules were scare in the sections, inhibited by Tris.

For kidney, short incubation period was needed. The enzyme was localized in epithelial cells of the convoluted tubules. There was no reaction in the glomeruli (Fig. 1). We found that, the DPP II activity was higher in the convoluted tubules near to the medulla than in this, which are far off it. DPP II showed high activity levels in small intestine too. We did not observe enzyme activity differences between duodenum, jejunum and ileum. DPP II was localized in the entherocites (Fig. 2). At prolonged incubation, there was a weak Dipeptidyl peptidase IV co-reaction in ileum

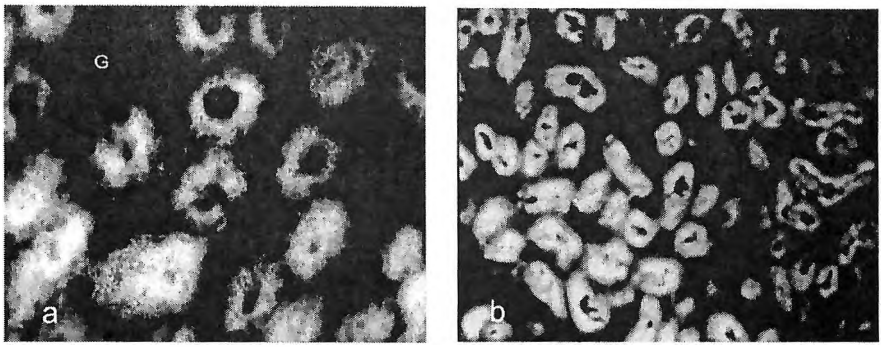

Fig. 1. Kidney. DPP II activity in epithelial cells of convoluted channels
a — No DPP II activity in glomeruli (G), × 500; b — Higher activity in the convoluted channels near to the medulla, × 200

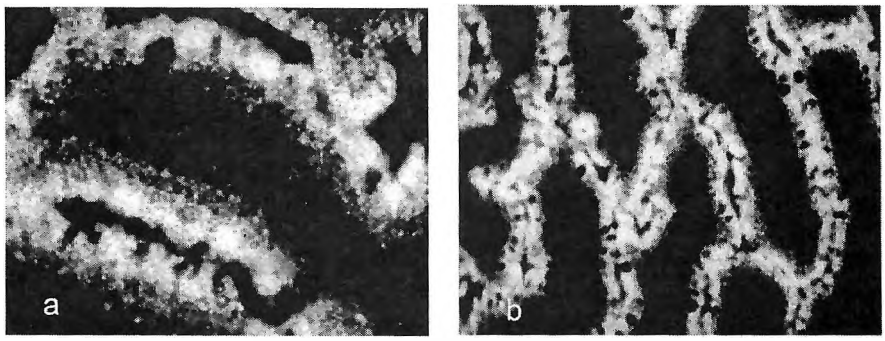

Fig. 2. Small intestine (jejunum). Strong reaction for DPP II in the entherocytes.
a — × 500; b — × 200

Fig. 3. Epididymis. DPP II in the principal and basal cells of the channels. × 500

(not shown here). Dipeptidyl peptidase II reaction in colon was missing. The DPP II activity was comparatively lower in epididimys and the incubation period had to be longer (60 min). Granular histochemical pattern which, probably corresponds to lysosomal localization of the enzyme was obtained. DPP II activity was observed exactly in the principal and basal cells of the channels (Fig. 3).

The results of our work demonstrate that 6-hydrazino-N-alkyl-1,8-naphthalimides are proper for substrate synthesis, and histochemical method based on them is appropriate for localization of the lysosomal peptidase DPP II. The newly proposed fluorescent histochemical substrate for DPP II can be used for further investigations of the enzyme activity distribution.

Acknowledgments: This work was supported by the Bulgarian National Science Fund of Ministry of Education and Science. Grant No MUL-1505/05.

References

1. Hisazumi, A., L. Yao-Hua, Y. Yamamoto, Y. Haneda, M. Nishi, R. Kikkawa. Immunohistochemical Localization of Dipeptidyl Peptidase II from the Rat Kidney and Its Identity with Quiescent Cell Proline Dipeptidase. — J. Biochem., **129**, 2001, 279-288.
2. Lojda, Z., R. Gossrau, T. H. Schiebler. A laboratory manual. — In: Enzyme Histochemistiy. New York, Springer, 1979, 169-170.
3. Maes, M., A. Lambeir, K. Gilany, K. Senten, P. Van der Veken, B. Leiting, K. Augustyns, S. Scharpé, I. De Meester. Kinetic investigation of human dipeptidyl peptidase II (DPPII)-mediated hydrolysis of dipeptide derivatives and its identification as quiescent cell proline dipeptidase (QPP)/dipeptidyl peptidase 7 (DPP7). — Biochem. J., **386**, 2005, 315-324.

Institute of Experimental Morphology and Anthropology with Museum
Bulgarian Anatomical Society

Acta morphologica et anthropologica, 13
Sofia • 2008

Anthropology

Physical Development of Plovdiv Students

*E. Andreenko, S. Mladenova**

University of Plovdiv, Boilogical Faculty Deptartament of Human Anatomy and Physiology
** University of Plovdiv, Branch Smolyan, Deptartament of Natural Mathematical Science*

The purpose of the present study is to determine the somatometric status of young men and women, students from the city of Plovdiv by characterizing the specificity of their physical development and determining the differences in the body stature and the individuals of both sexes. Object of the study are 136 clinically healthy individuals (88 girls and 48 boys), students from different majors of the University of Plovdiv, at the average age of 20-21 years. The data of 9 basic somatometric indicators, 7 body proportions and indexes have been analyzed, as well as their distribution by categories according to the rubrics generally accepted in anthropology. Statistically significant intersexes differences were established according to all body length indicators, diameters and circumferences of body. More information about significant intersexes differentiation, provide the features for body weight and dimensions (absolute and relative) of the upper body part.

Key words: anthropometry, proportions, categories, students.

Introduction

Human ontogenesis is a long and versatile process, which stages are characterized with processes different in their strength and nature. One of the external expressions of these features, are the body dimensions and proportions typical for a specific moment. Body measurements provide possibility the growth and development of individuals throughout different age periods to be controlled [1, 3, 5], analysis of the social variants to be conducted [2, 3], the effectiveness of activities to be inspected, stimulating health and working capacity of population [4]. The purpose of the present study is to determine the somatometric status of young men and women, students from the city of Plovdiv by characterizing the specificity of their physical development and determining the differences in the body stature and the individuals of both sexes.

Material and Methods

Object of the study are 136 clinically healthy individuals (88 girls and 48 boys), students from different majors of the University of Plovdiv, at the average age of 20-21 years. A standard anthropometric instrumentarium had been used. The data of 9 basic somatometric indicators, 7 body proportions and indexes have been analyzed, as well as their distribution by categories according to the rubrics generally accepted in anthropology. The data are statistically processed.The authenticity of the obtained results was checked by means of ANOVA — tukey test for independent extract of significance level $p \leq 0{,}05$.

Results

The average values of investigated features and their proportions of both sexes are presented in Table 1. The percentage distribution of the investigated students by cat-

T a b l e 1. Metrical data abaut the investigated features and their proportions

Lengths and Body Weight					
Features	**Female students, *n*=88**	**Male students, *n*=48**	**Difference**		**ANOVA-Tukey HSD test**
	Mean / SD	**Mean / SD**	**Absolute (cm)**	**%**	
Stature, cm	**162.85** 6.30	**178.02** 6.39	15,17	8.52	0.000 *
Body weight, kg	**57.06** 9.30	**77.97** 13.14	20,91	26.82	0.000*
Trunk length, cm	**47.43** 2.80	**53.30** 3.15	5,87	11.01	0.000*
Lower extremity length (troh.), cm	**82.81** 4.46	**89.76** 4.63	6.95	7.74	0.000*
Chest Circumference and Body Diameters					
Features	**Female students, *n*=88**	**Male students, *n*=48**	**Difference**		**ANOVA-Tukey HSD test**
	Mean / SD	**Mean / SD**	**Absolute (cm)**	**%**	
Chest ircumference-pause, cm	**75.09** 7.17	**90.61** 9.95	15.52	17.13	0.000*
Transversal chest diameter, cm	**23.56** 2.45	**27.82** 2.58	4.26	15.31	0.000*
Sagital chest diameter, cm	**15.84** 2.31	**19.71** 2.80	3.87	19.63	0.201
Biakromial diameter, cm	**31.83** 2.60	**37.66** 2.79	5.83	15.49	0.000*
Bicristal diameter, cm	**26.38** 2.60	**28.61** 2.71	2.23	7.79	0.000*
Body proportions, %					
Proportions and indexes	**Female students, *n*=88**	**Male students, *n*=48**	**Difference**		**ANOVA-Tukey HSD test**
	Mean / SD	**Mean / SD**	**Absolute (cm)**	**%**	
(TRL / S) x 100	**29.34** 2.11	**29.93** 1.25	0.59	1.97	0.120
(LEL / S) x 100	**50.84** 2.9	**50.41** 1.85	0.43	0.85	0.234
(CC / S) x 100	**46.15** 4.56	**50.87** 5.00	4.72	9.28	0.000*
(BAD / S) x 100	**19.55** 1.53	**21.16** 1.53	1.61	7.61	0.000*
(BCD / S) x 100	**16.20** 1.49	**16.06** 1.36	0.14	0.87	0.644

Abbreviations: Stature — S, Trunk length — TRL, Lower extremity length — LEL, Chest circumference — CC, Bicristal diameter — BCD, Biakromial diameter — BAD

Table 2. Distribution according to the proportion of the investigated features, %

1. Distribution according to the proportion of lower extremity's length- Brugsch's rubrics

Categoty		Male students		Female students	
		n	%	*n*	%
short	x - 50.4	25	52.08	36	40.91
middle	50.5 – 52.9	16	33.34	47	53.41
long	53.0 - x	7	14.58	5	5.68

2. Distribution according to the proportion of trunk length- Brugsch's rubrics

Categoty		Male students		Female students	
		n	%	*n*	%
short	x - 27.9	3	6.25	21	23.86
middle	28.0 - 29.9	22	45.83	43	48.78
long	30.0 - x	23	47.92	24	27.27

3. Distribution according to the proportion of Chest circumference- Brugsch's rubrics

Categoty		Male students		Female students	
		n	%	*n*	%
narrow	x - 50.9	25	52.08	77	87.5
middle	51.0 – 55.9	18	37.5	7	7.95
wide	56.0 - x	5	10.42	4	4.55

4. Distribution according to the Biacromial diameter's proportion -Brugsch's rubrics

Categoty	Male	Male students		Female	Female students	
		n	%		*n*	%
narrow	x - 22.0	17	35.42	x – 21.5	71	80.68
middle	22.1 -23	15	31.25	21.6 – 22.5	15	17.05
wide	23.1 - x	14	29.17	22.6 - x	2	2.27

5. Distribution according to the Bicristal diameter's proportion -Brugsch's rubrics

Categoty	Male	Male students		Female	Female students	
		N	%		N	%
narrow	x – 16,5	34	70,83	x – 17,5	77	87,5
middle	16,6 – 17,5	9	18,75	17,6-18,5	5	5,68
wide	17,6 - x	5	10,42	18,6 - x	6	6,82

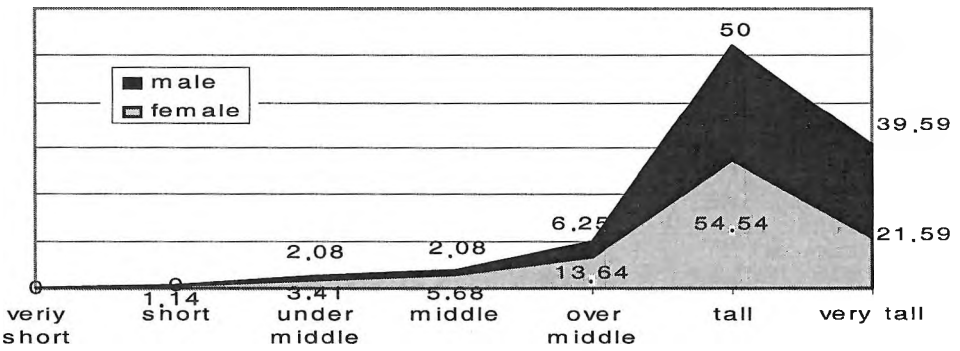

Fig. 1. Distribution according to the Stature - Martin's rubrics, %

egories according to generally accepted rubrics is presented in Table 2. The absolute values for stature, weight and lengths of body (trunks length and lower extremity length) are reliably higher among men. The percentage distribution of the individuals of both sexes according to the rubrics generally accepted in Anthropology by Martin. R for the stature is presented in the Fig. 1.

The results show that the prevailing multitude of young men and women are individuals of high stature having height significantly over the middle one (54.54 % in young women and 50.00 % in young men). The average values of the proportions

of trunk length and lower extremity length of both sexes are statistically insignificant. We established more essential differences in percentage distribution of the individuals by categories.

Among the rubrics of Brugsh the prevailing part of men have short lower extremities (52.08 %) and long (47.92 %) or middle trunk (45.83 %). The larger part of women has middle trunk (48.78 %) and middle lower extremity (53.41 %).

The absolute values of chest circumference and diameters of body are reliably higher among men (excluding the sagital diameter). According to Brugsh's rubrics the larger part of men has narrow chest and narrow pelvis. Regarding shoulder width the distribution is almost equal in the three of the categories — narrow, middle and wide shoulders. Among women the distribution of the larger part is in the following categories — narrow chest, narrow shoulders and narrow pelvis.

Generalize results of the our investigation we can indicate that they are in regular and quite normal biological — all investigated somatometric features are with larger values in young men than young women. More interesting to us is to establish which of the investigated features the differences between two sexes are more clear. The results show (Fig. 2) that the young men and women differ significantly in their body weight and the features characterizing the proximal body part (shoulder width, chest circumference, transversal chest diameter) and differ not so significantly in the features characterizing the distal body part (pelvis) and the linear dimensions - trunk length, lower extremities length and their proportions.

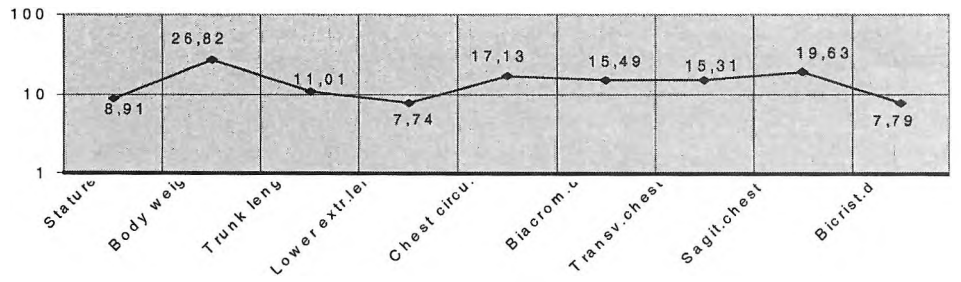

Fig. 2. Degree of intersexual differences about the investigated features, %

Conclusions

1. A characteristics of the basic somatometric status of young men and women, students from Plovdiv University at the age 20-21 years was made. Statistically significant intersexes differences were established according to all body length indicators, diameters and circumferences of body excluding the sagital diameter. More information about significant intersexes differentiation, provide the features for body weight and dimensions (absolute and relative) of the upper body part.

2. Young men are with high and very high statute according to the standards of the European population, with shorter lower extremities and with middle to long trunk. In the body configuration there are combined: a narrow pelvis, proportionally smaller chest circumference with slight predominance of narrow and middle shoulders over the wide shoulders. Young women are tall in respect of the height according to the standards of the European population, with middle lower extremities and middle trunk according to the length. They are with narrow shoulders and a narrow pelvis.

3. The general evaluation of physical development, body stature and proportionality of body made of Plovdiv students contributes for supplementing the total anthropometric characteristics of young men and women from Bulgarian population at the beginning of 21st century.

References

1. Atanassova-Timeva, N. Anthropometrical characteristic of Bulgarian students at the beginning of 21st century. — Proceedings of the Balkan scientific conference of biology in Plovdiv (Bulgaria). 2005, 82-101.
2. Rebato, E. Nutritional status by socioeconomic level in an urban sample from Bilbao. — Amer. J. Human Biology, **13**, 2001, 5, 668-678.
3. Младенова, С. Динамика на растежа и развитието на деца и подрастващи от Смолянски регион и влияние на социално-икономически фактори върху техния морфологичен статус. (канд. дис.) 2003. 151 с.
4. Начева, А., Е. Лазарова. Връзка между подкожната мастна тъкан и вида физическа активност на индивида. — Journal of Anthropology, **2**, 1999, 68-77.
5. Христов, И., Т. Матев, Я. Буков, Г. Балтаджиев, Н. Йотова. Антропометрична характеристика на български и гръцки студенти-мъже от ВМИ Пловдив. — Journal of Anthropology, **2**, 1999, 41-49.

Institute of Experimental Morphology and Anthropology with Museum
Bulgarian Anatomical Society

Acta morphologica et anthropologica, 13
Sofia • 2008

Kinetic Evaluation of Some Daily Activities

C. Bozer, B. S. Cigali, E. Ulucam

Faculty of Medicine, Department of Anatomy, Trakya University, Edirne, Turkey

The reaction force from the ground is called the ground reaction force (GRF). The GRF is important external force acting upon the human body in motion and we use this force as propulsion to initiate and to control our movements.

We have measured the GRF on the foot by using an insole system and evaluated the net forces acting on the foot during unobstructed level walking and stepping over obstacles with the opinion that rarely is the path of walking perfectly level and clear.

As a result, unobstructed level walking and stepping over obstacles data showed statistically significant differences particularly for Fmax1 and Tmax1 variables.

Key words: kinetics, ground reaction force, level walking, obstacle.

Introduction

Walking is one of the most basic forms of human motion. The basic unit of walking is the gait cycle, which is typically recorded from the time one foot strikes the ground until that episode recurs and starts the next, repeating cycle [14].

Biomechanics is the study of normal mechanics (kinetics and kinematics) in the musculoskeletal system by analyzing forces and their effects on anatomical structures. And kinetics studies the relationship between the forces acting on a body and the changes they produce in the motion of the body. Kinetics concentrates on the study of forces associated with motion using force plates, pressure platforms and/or inshoe sensors providing a direct description/orientation of foot posture. The basic principles of kinetics are Newton's three laws of motion. Newton's third law, the law of action and reaction (to every action there is an equal and opposite reaction), is very important for the study of gait and other aspects of biomechanics. This law relates the forces interacting between the foot and the floor as always being equal and opposite. In other words, the action to the ground is always accompanied by a reaction from it. The unit of force is Newton (N) that is defined as the force necessary to accelerate a mass of 1 kg by 1 ms^{-2}. Forces in walking can be internal (such as muscle activity, ligamentous constraint or friction in muscles and joints) or external (such as ground reaction forces created from external loads) [1, 3, 9, 10, 12, 15].

The reaction force from the ground is called the ground reaction force (GRF). The GRF is important external force acting upon the human body in motion. We use

this force as propulsion to initiate and to control our movements. The GRF is represented by three perpendicular directions: forward, lateral and vertical. The GRF is counteracted and controlled by the function of the lower limb muscles which, in conjunction with the bones, joints and tendons of the foot, controls the kinetic progression of foot with the ground [1, 14].

Rarely is the path of walking perfectly level and clear. Commonly, during walking a person is confronted with a course consisting of obstacles of various heights, widths, depths and compositions like water, mud, drainage, sidewalks, stairs, doorsteps etc.

We have measured the forces of ground reaction on the foot by using an insole system and evaluated the net forces acting on the foot during unobstructed level walking and stepping over obstacles.

Materials and Methods

Ten able-bodied young adult subjects (5 males — 5 females) aged between 19 and 24 were taken place in this study. The Medical Ethical Committee of Trakya University Faculty of Medicine Hospital approved the study and the subjects signed an informed consent.

Subjects wore boot-like designed flat shoes of Zebris© with insole-mats inserted in them. Subjects were asked first to walk at their natural rhythm and then cross the obstacles which is 0 cm height from the ground (sticky tape) and 2 cm height (doorstep), across the 8 m long gait laboratory walkway. They were not asked to restrict their movement, including arm swing. After a few trials of familiarization, the ground reaction forces were recorded from both sides by Zebris 3D Motion Analysis System©. For each subject at least three individual trials were collected. This system has insole mats connected to an analog to digital converter by a cable adapter. Vertical GRF is sampled continuously at 60 Hz. Data converter was connected to a computer to enable the time versus force graphics to be seen while the subject was walking. Data from hind foot, middle foot, forefoot lateral side and forefoot medial side were recorded separately in the same steps. The hind foot is from 0% to 30%, midfoot is from 30% to 60% and forefoot is from 60% to 100% of the foot length. The forefoot divides equally into forefoot lateral and forefoot medial sides. Each of these foot areas are represented with a time versus force graphic in the report paper and it is possible to convert the data as a text file to process in a worksheet program. The maximum value of each kinetic curve was extracted for each subject's leading limb (limb crossing the obstacle first) of selected step (Fig. 1).

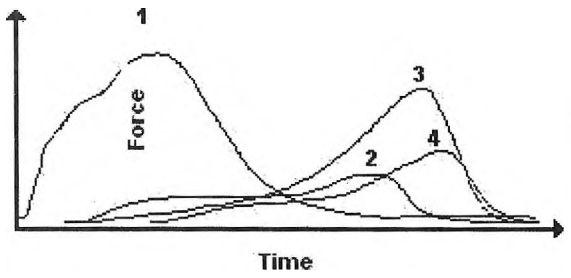

Fig. 1

The force-time data were normalized to body weight in order to compare force magnitudes across subjects independent of body mass. Fmax1 - Tmax1, Fmax2 — Tmax2, Fmax3 — Tmax3 and Fmax4 — Tmax4 variables are for the hind foot, midfoot, forefoot lateral side and forefoot medial side respectively (Fig. 2).

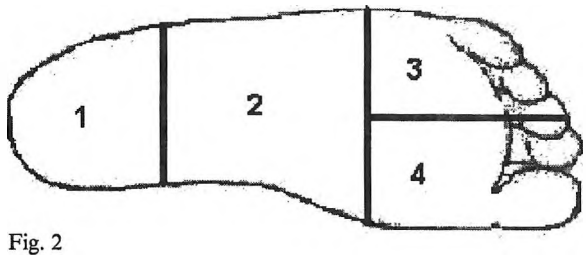

Fig. 2

Descriptive statistics were calculated for accordance to normal distribution. It is tested with a One-Sample Kolmogorov — Smirnov test. The statistics were compared with the use of a one-way analysis of variance (ANOVA) and a post-hoc Bonferroni t test. ANOVA was used to see if there are differences between level walking, stepping over 0 cm and stepping over a doorstep. Bonferroni t test was used for evaluation of differences between the walks. Significance level was set at $p < 0.05$.

Results

All subjects adapted their gait easily and naturally to the obstacles. None of them showed any difficulties in performing the task. Unobstructed level walking, stepping over 0 cm and stepping over a doorstep data showed statistically significant differences particularly for Fmax1 and Tmax1 variables (Table 1).

Fmax1 and Tmax1 values were significantly different between unobstructed level walking and crossing over the doorstep (p=0.030 for Fmax 1 values and p=0.000 for Tmax1 values). Also, Tmax1 values between unobstructed level walking and crossing over 0 cm obstacle was significantly different (p=0.035<0.05). There was no significant difference in other force and time values between the tests.

Discussion and Conclusion

In this basic study about human gait analysis, we see that different conditions affect gait. According to the results; in crossing over the doorstep, the GRF on the hind foot region increases and the time needed to reach maximum GRF shortens accord-

T a b l e 1. Differences of time and force values between unobstructed level walking, crossing over 0 cm and crossing over the doorstep. The units are "N/kg" for force and "ms" for time.
(Statistically significant differences are marked in bold, p<0.05)

Test	Fmax1±SD	Tmax1±SD	Fmax2±SD	Tmax2±SD	Fmax3±SD	Tmax3±SD	Fmax4±SD	Tmax4±SD
Level Walking	**5.05±0.71**	**0.20±0.04**	1.06±0.33	0.43±0.13	2.82±0.94	0.62±0.60	2.69±0.81	0.65±0.49
0 cm	5.47±0.93	**0.16±0.05**	1.13±0.44	0.35±0.14	3.07±1.27	0.62±0.89	2.49±1.17	0.64±0.08
Doorstep	**5.79±0.84**	**0.14±0.04**	1.11±0.04	0.36±0.14	2.91±1.06	0.62±0.05	2.72±1.01	0.63±0.06

ing to unobstructed level walking. Also, in crossing over the doorstep maximum GRF time shortens according to crossing over a 0 cm obstacle. In normal human gait, foot's first contact surface with the ground is the heel which is named as "initial contact" in gait terminology. So we can say, the heel of the leading foot exerted greater force during the initial contact phase, and the time to reach the maximum point of this force shortens in obstacle crossing. These findings are consistent with earlier literature [2, 4-8, 11, 13, 16].

The foot is critical to an understanding of the mechanics of gait, as the foot often affects the normal motion pattern of the entire lower extremity. Alterations of normal foot mechanics can adversely influence the normal functions of the ankle, knee, hip and even the back. Measurement of GRF can be used to assess the loads to which the human body is subjected in normal activities like walking, stepping over obstacles, stair ascent and descent, running, sports etc. Measurement of GRF with insole systems is useful and advantageous because there is no constraint on foot placement and it is possible to measure several consecutive strides during gait and it provides detailed information specific to each region of the foot sole.

References

1. Abboud, R. J. Relevant foot biomechanics. — Curr. Orthop., **16**, 2002, 165-179.
2. Austin, G. P., G. E. Garrett, R. W. Bohannon. Kinematic analysis of obstacle clearance during locomotion. — Gait Posture., **10**, 1999, 109-120.
3. Ayyappa, E. Normal human locomotion, part 2: motion, ground reaction force and muscle activity. — J.P.O., **19**, 1997, 49-60.
4. Begg, R. K., W. A. Sparrow, N. D. Lythgo. Time-domain analysis of foot-ground reaction forces in negotiating obstacles. — Gait Posture., 7, 1998, No2, 99-109.
5. Chen, H. C., J. A. Ashton-Miller, N. B. Alexander, A. B. Schultz. Stepping over obstacles: gait patterns of healthy young and old adults. — J. Gerontol., **46**, 1991, No6, 196-203.
6. Chen, H. L., T. W. Lu. Comparisons of the joint moments between leading and trailing limb in young adults when stepping over obstacles. — Gait Posture., **23**, 2006, No1, 69-77.
7. Chou, L. S., L. F. Draganich. Stepping over an obstacle increases the motions and moments of the joints of the trailing limb in young adults. — J. Biomech., **30**, 1997, No4, 331-337.
8. Cigali, B. S., E. Ulucam, A. Yilmaz, M. Cakiroglu. Comparison of asymmetries in ground reaction force patterns between normal human gait and football players. — Biol. Sport., **21**, 2004, 241-248.
9. Cordero, A. F., H. J. F. M. Kopman, F. C. T. van der Helm. Use of pressure insoles to calculate the complete ground reaction forces. — J. Biomech., **37**, 2004, 1427-1432.
10. Katoh, Y. Biomechanical analysis of foot function during gait and clinical applications. — Clin. Orthop. Rel. Res., **177**, 1983, 23—33.
11. Lu, T. W., H. L. Chen, S. C. Chen. Comparisons of the lower limb kinematics between young and older adults when crossing obstacles of different heights. — Gait Posture., **23**, 2006, No4, 471-479.
12. Panjabi, M. M., A. A. White. Biomechanics in the musculoskeletal system (1st Edition), Pennsylvania, Churchill Livingstone, 2001.
13. Patla, A. E., S. Rietdyk. Visual control of limb trajectory over obstacles during locomotion: effect of obstacle height and width. — Gait Posture., **1**, 1993, 45-60.
14. Pease, W. S., B. L. Bowyer, V. Kaydan. Human Walking. — In: Physical Medicine & Rehabilitation: Principles and Practice (Eds. J. A. DeLisa, B. M. Gans, 4th edition). Philadelphia, Lippincott Williams & Wilkins, 2005.
15. Rosenbaum, D., H. P. Becker. Plantar pressure distribution measurements. Technical background and clinical applications. — J. Foot Ankle Surg., **3**, 1997, 1-14.
16. Sparrow, W. A., A. J. Shinkfield, S. Chow, R. K. Begg. Characteristics of gait in stepping over obstacles. — Hum. Mov. Sci., **15**, 1996, 605-622.

Institute of Experimental Morphology and Anthropology with Museum
Bulgarian Anatomical Society

Acta morphologica et anthropologica, 13
Sofia • 2008

The Evaluation of Ground Reaction Force (GRF) Graphics Acquired During Some Daily Activities

B. S. Cigali, C. Bozer, E. Ulucam

Faculty of Medicine, Department of Anatomy, Trakya University, Edirne, Turkey

Due to the gravity, we constantly maintain contact with the ground, and in this process, interactions occur between the body and the ground. According to Newton's 3rd Law of Motion (Law of Reaction), for every action, there is an equal and opposite reaction. The reaction force exerted to the body by ground is specifically called the ground reaction force (GRF). Measuring the GRF with insole mats is more useful and objective than the force platforms. In this method, it is possible to get data from more than one step in one single trial.

Our purpose in this study was to demonstrate the gait graphics taken from some daily activities and to evaluate the GRF during stair ascent and descent.

The data taken from the measurements of 10 subjects' (5 males, 5 females) stair ascent and descent were analyzed and discussed.

Key words: ground reaction force, stair ascent, descent.

Introduction

Walking is one of the complex movements of human and its basic component is gait. In last twenty years, gait analysis has become a method of diagnosis and follow up for patients with gait disorders. In the meantime, gait analysis has developed with kinematics and kinetics. Kinematics means the science of movement. In this kind of analysis you can measure positions, velocities, and accelerations of body segments. In another words, angular displacements of the joints can be measured. In kinetic analysis, force measurements are possible. According to Newton's 3rd Law of Motion (Law of Reaction), for every action, there is an equal and opposite reaction. When a human body is contact with the ground, a force is exerted to the body as a reaction by the ground. Due to the gravity, we constantly maintain contact with the ground, and in this process, interactions occur between the body and the ground. The reaction force supplied by the ground is specifically called the ground reaction force (GRF), which is basically the reaction to the force the body exerts on the ground [1, 5]. The GRF, along with the weight, is an important external force. When a person stands still, this ground reaction force is equal to the person's mass multiplied by the gravitational acceleration (F = m.g). For a typical person of 80 kg weight, this reaction will be (80 x 10) 800 N. GRF has three component vectors in vertical, medial-lateral and ante-

rior-posterior planes. Vertical force is generated by the vertical acceleration of the body and is of highest magnitude. The GRF is commonly measured by force-platforms and insole mats. Force platforms are more common in movement laboratories but they have some disadvantages that patients must target the platform and they have to place the foot only once in one trial. Otherwise, it is hard to get clear data. The second method is the insole mats, which can be set into a shoe or a booty-like shoe. In measurement of GRF with insole systems, there is no constraint on foot placement and it is possible to measure several consecutive strides during gait and it provides detailed information specific to each region of the foot sole. So, it is more objective than the force platforms.

In this study, our purpose is to demonstrate the gait graphics taken from some daily activities and to evaluate the GRF during stair ascent and descent.

Materials and Methods

Five males (mean age 20.4 ± 2.1 yr; mean mass 73.6 ± 8.7 kg) and five females (mean age 19.8 ± 0.8 yr; mean mass 54.2 ± 4.4 kg) were informed about the procedure and accepted to participate in this study. They were all right-handed. Subjects wore boot-like designed flat shoes of Zebris© with insole-mats inserted in it and were required to ascend and then descend the 4 steps stair model at natural speed. After a few trials of familiarization, the ground reaction forces were recorded from both sides by Zebris 3D Motion Analysis System©. This system has insole mats connected to an analog digital converter by a cable adaptor. Its sampling rate was 60 Hz. Data converter was connected to a PC to enable the time versus force graphics to be seen while the subject was walking. Data from heel (1), midfoot (2), forefoot lateral side (3), and forefoot medial side (4) were recorded separately in the same steps. The heel was from 0% to 30% and midfoot from 30% to 60% to foot length. The forefoot was from 60% to 100% and this part was divided into the lateral and medial forefoot regions equally. Each of these areas is represented with a time versus force graphic in the report paper. The peak forces (Fmax1, Fmax2, Fmax3, and Fmax4) are the maximum force values normalized by dividing with body weight in each corresponding area. The time between reaching the peak force and initial contact in each corresponding area (Tmax1, Tmax2, Tmax3, and Tmax4) were recorded for every step on stairs in milliseconds (ms).

In statistical analysis, Man - Whitney U test was applied for gender differences. And Kruskal — Wallis test was applied to test the differences between the steps.

Results

The mean fmax and tmax values of all steps during stair ascent and descent were given in table 1 and table 2 (Tables 1, 2). And in Table 3, mean values of fmax and tmax for all 40 steps were presented (Table 3). The differences between the stair ascent and descent were found for Fmax1, Tmax1, Fmax2, Tmax2, Tmax3 and Tmax4 values. In this comparison we did not find any differences in between Fmax3 and Fmax 4 values. Again, during stair ascent only Fmax3 values were different ($p<0,05$) and during stair descent Tmax3 and Tmax4 values were different ($p<0,05$).

T a b l e 1. Mean values of fmax and tmax for all areas and for both sex during stair ascent. Tmax2 in step I and fmax2, tmax2, and fmax3 in step II differs (p<0,05)

			StepI		StepII		StepIII		StepIV	
	sex	*n*	mean	std	mean	std	mean	std	mean	std
fmax1	f	5	4.95	1.68	4.01	0.96	3.96	1.21	3.17	1.58
	m	5	3.08	2.06	4.27	2.74	2.82	2.11	2.21	1.44
tmax1	f	5	0.27	0.09	0.23	0.14	0.25	0.16	0.4	0.22
	m	5	0.17	0.05	0.22	0.14	0.29	0.19	0.31	1.23
fmax2	f	5	1.22	0.4	**1.41**	0.50	0.91	0.50	1.05	0.36
	m	5	0.8	0.56	**0.66**	0.23	0.85	0.55	0.72	0.50
tmax2	f	5	**0.67**	0.18	**0.55**	0.24	0.55	0.20	0.59	0.28
	m	5	**0.31**	0.15	**0.29**	0.15	0.21	0.03	0.54	0.22
fmax3	f	5	3.13	1.02	**3.50**	1.26	2.59	0.90	2.09	1.35
	m	5	2.39	0.66	**1.89**	.95	1.71	0.79	0.93	0.83
tmax3	f	5	0.8	0.22	0.70	0.21	0.68	0.24	0.66	0.24
	m	5	0.56	0.19	0.58	0.12	0.55	0.23	0.63	0.30
fmax4	f	5	1.87	0.69	2.53	1.33	2.27	0.96	2.62	1.37
	m	5	1.96	0.86	2.25	1.06	2.34	1.20	1.28	0.61
tmax4	f	5	0.73	0.19	0.62	0.28	0.64	0.20	0.51	0.19
	m	5	0.59	0.17	0.51	0.27	0.56	0.24	0.37	0.31

T a b l e 2. Mean values of fmax and tmax for all areas and for both sex during stair descent, there are no statistically differences between female and male data

			StepI		StepII		StepIII		StepIV	
	sex	*n*	mean	std	mean	std	mean	std	mean	std
fmax1	f	5	2.43	0.78	3.05	1.29	2.74	2.31	1.82	1.21
	m	5	1.90	1.35	2.50	2.14	1.45	1.42	1.69	1.40
tmax1	f	5	0.14	0.05	0.17	0.10	0.14	0.03	0.18	0.16
	m	5	0.18	0.07	0.18	0.05	0.16	0.04	0.23	0.20
fmax2	f	5	1.28	0.58	1.55	0.44	1.11	0.51	1.47	0.51
	m	5	0.86	0.39	1.47	0.93	1.07	0.44	1.31	0.96
tmax2	f	5	0.13	0.03	0.11	0.03	0.18	0.13	0.11	0.02
	m	5	0.19	0.05	0.14	0.04	0.15	0.34	0.17	0.15
fmax3	f	5	2.11	0.82	2.56	0.93	2.40	0.59	2.74	0.75
	m	5	2.12	0.72	2.30	0.69	2.66	0.40	2.05	0.76
tmax3	f	5	0.38	0.24	0.19	0.17	0.19	0.28	0.15	0.21
	m	5	0.37	0.24	0.26	0.29	0.22	0.25	0.07	0.04
fmax4	f	5	2.47	0.42	2.80	1.44	2.69	0.73	2.51	1.71
	m	5	3.08	1.04	3.01	1.01	3.12	1.36	1.62	0.48
tmax4	f	5	0.59	0.11	0.33	0.24	0.27	0.28	0.15	0.04
	m	5	0.56	0.23	0.32	0.28	0.38	0.26	0.16	0.15

T a b l e 3. Mean values of fmax and tmax for all areas and for all steps

	During	*n*	Mean	Std
fmax1	ascent	40	3.56	1.84
	descent	40	2.20	1.51
tmax1	ascent	40	0.27	0.15
	descent	40	0.17	0.1
fmax2	ascent	40	0.95	0.49
	descent	40	1.27	0.61
tmax2	ascent	40	0.46	0.24
	descent	40	0.15	0.07
fmax3	ascent	40	2.28	1.19
	descent	40	2.37	0.7

Продължение на табл. 3

tmax3	ascent	40	0.65	0.22
	descent	40	0.23	0.23
fmax4	ascent	40	2.14	1
	descent	40	2.55	1.1
tmax4	ascent	40	0.57	0.24
	descent	40	0.35	0.25

Discussion and Conclusion

There are statistically differences of Tmax2 values in step 1 and Fmax2, Tmax2, Fmax3 values in step 2 between female and male subjects. There are no differences in all other data. As a conclusion, kinetic characteristics of men and women gait according to GRF are similar to each other. As expected, most of the values are different between stair ascent and descent [2, 3]. Because, during ascent, the gait starts with the heel contact, then continues with midfoot and forefoot. But during stair descent, it starts with the forefoot and continues with midfoot and heel.

Comparing the steps gives more evidence for the neuromuscular control of the gait and the characteristics of exceeding an obstacle [4, 7]. In our study we used a wooden model of standard home stairs including 4 steps. The surfaces of the steps are natural and not slippery. It is seen that, while subjects ascend the stairs, the fmax1 values tend to decrease from 1st step to 4th step. This means heel contact is getting slighter as the subjects repeat the movement. In another words, contractions of the muscles which provide the stability of body against GRF during the contacts with the ground were regulated in optimum level. This is one of the most important components of gait control. In a neuromuscular problem such as diabetes mellitus or neuropathies, it would be difficult to resist the GRF and regulate the muscle contractions especially for the braking mechanism in gait. Beside this, it is also known that the peak forces are higher in climbing an obstacle than level walking [6].

If we compare all the steps during ascent and descent together, it is seen that Fmax1 is the highest and then Fmax3, Fmax4 and Fmax2 are in sequence. It means that, the highest force is exerted on the heel, then in sequence, on the lateral forefoot, medial forefoot and midfoot. These results are also same with the level walking.

References

1. Christina, A. K., P. R. Cavanagh. Ground reaction forces and frictional demands during stair descend: effects of age and illumination. — Gait Posture, **15**, 2002, 153-158.
2. Heller, M. O., G. Bergmann, G. Deuretzbacher, L. Durselen, M. Pohl, L. Claes, N. P. Haas, G. N. Duda. Musculo-skeletal loading conditions at hip during walking and stair climbing. — J. Biomech., **34**, 2001, 883-893.
3. Reiner, R., M. Rabuffetti, C. Frigo. Stair ascent and descent at different inclinations. — Gait Posture., **15**, 2002, 32-44.
4. Salsich, B. G., J. H. Brechter, C. M. Powers. Lover extremity kinetics during stair ambulation in patients with and without patellofemoral pain. — Clin. Biomech., **16**, 2001, 906-912.
5. Stacoff, A., C. Diezi, G. Luder, E. Stussi, I. A. K. Quervain. Ground reaction forces on stairs, effects of stair inclination and age. — Gait Posture., **21**, 2005, 24-38.
6. Taylor, W. R., M. O. Heller, G. Bergmann, G. N. Duda. Tibio-femoral loading during human gait and stair climbing. — J. Orthop. Res., **22**, 2004, 625-632.
7. Wu, W. L., P. J. Huang, C. H. Lin, W. Y. Chen, K. F. Huang, Y. M. Cheng. Lower extremity kinematics and kinetics during level walking and stair climbing in subjects with triple arthrodesis or subtalar fusion. — Gait Posture., 2004 (in press).

Institute of Experimental Morphology and Anthropology with Museum
Bulgarian Anatomical Society

Acta morphologica et anthropologica, 13
Sofia • 2008

The Artistic Anatomically Examination of the Turkish Women's Heights and Some Body Proportions

S. Cikmaz, A. Yilmaz, R. Mesut

Faculty of Medicine, Department of Anatomy, Trakya University, Edirne, Turkey

In this study, we tried to examine the body proportions of Turkish women according to the artistic anatomy and how the change of lengths of the parts that form the body effect the body height.

495 female students with a 20,7 mean age participated in our study. They had no orthopaedic and physical defect and were being educated in Trakya University Medical Faculty. The Harpenden anthropometer was used in measurements. The distances, mean values, standard deviations, proportions to body height and correlation coefficients in our study are these respectively: 1) Basion-vertex (body height): 159.86cm ± 4.97, 2) Basion-gnathion: 136.25cm ± 4.39, %84.20, 0.89, 3) Basion-acromiale: 130.92cm ± 4.4 %80.95, 0.81, 4) Basion-suprasternale: 127.50 ± 3.30, %79.83, 0.81, 5) Basion-thelion: 112.08 ± 4,44, %56.14, 0.8, 6) Basion-omphalion: 94.08cm ± 3.03, %59.56, 0.80, 7) Basion-iliospinale: 87.40cm ± 2.85, %55.77, 0.75, 8) Basion-trochanterion: 79.58cm ± 1.59, %50.59, 0.67, 9) Basion-symphysion: 77cm ± 3.21, %50.02, 0.67, 10) Basion-gluteale; 67.50cm ± 2.81, %44.62, 0.67, 11) Basion-dactylion: 60.58cm ± 1.69, %37.94, 0.55, 12) Basion-tibiale: 41.08cm ± 2.71, %24.77, 0.45, 13) Basion-sphyrion: 7.83cm ± 0.62, %4.80, 0.28.

Key words: Artistic anatomy, anthropology, proportion.

Introduction

Artistic anatomy is a subspecialty of anatomy which, through all works of art, aims at describing the movement and shape of human body, placing its different parts correctly and exploring the ways of describing the changes caused by movements at the best, by utilizing various proportion and separation plans [1, 9, 12].

Within 5000 years' time, artists have examined the human body, which has been a subject for their works, from a geometrical perspective and have come to realize that there are various proportions between the parts of the body. Later on, they have standardized these proportions and tried to set the rules that they would use in their own works of art. Since the early ages, these proportions introduced by the scientists and artists have been called "CANON", and the unit measurement of each canon has been called "module". In many canons, parts of the body such as the length of the foot, the head, the face, the 3rd finger of the hand have been used as modules.

The oldest and the most important studies unifying the art and the anatomy, were conducted by Leonardo Da Vinci, while in the scientific sense, it was French anatomist Dr. Paul Richer who handled these studies. Dr. Richer presented his findings in his book "Anatomie Artistique". Besides, he is noteworthy for his researches on the women's body [2, 4, 6, 8, 9, 11].

In this study, we have aimed at examining the body proportions of Turkish women in terms of artistic anatomy and in what amount the change in the lengths of the parts forming the body effects the height of a person.

Material and Methods

Our study has been carried out on 495 female students, studying at the Faculty of Medicine, Trakya University, whose mean age is 20,7, with no orthopaedic and physical disabilities. Harpenden anthropometer was used in measurements. Measurements and findings have been listed by women assistants in tables prepared beforehand.

We have utilized the anthropological landmarks in the measurements providing the basis for our study. However, for some of the height measurements, we have used surface anatomy landmaks which are not utilized in anthropology, but preferred in plastic anatomy. In normal anatomic position, the distance between the foot basis and anthropological points has been measured (Fig. 1):

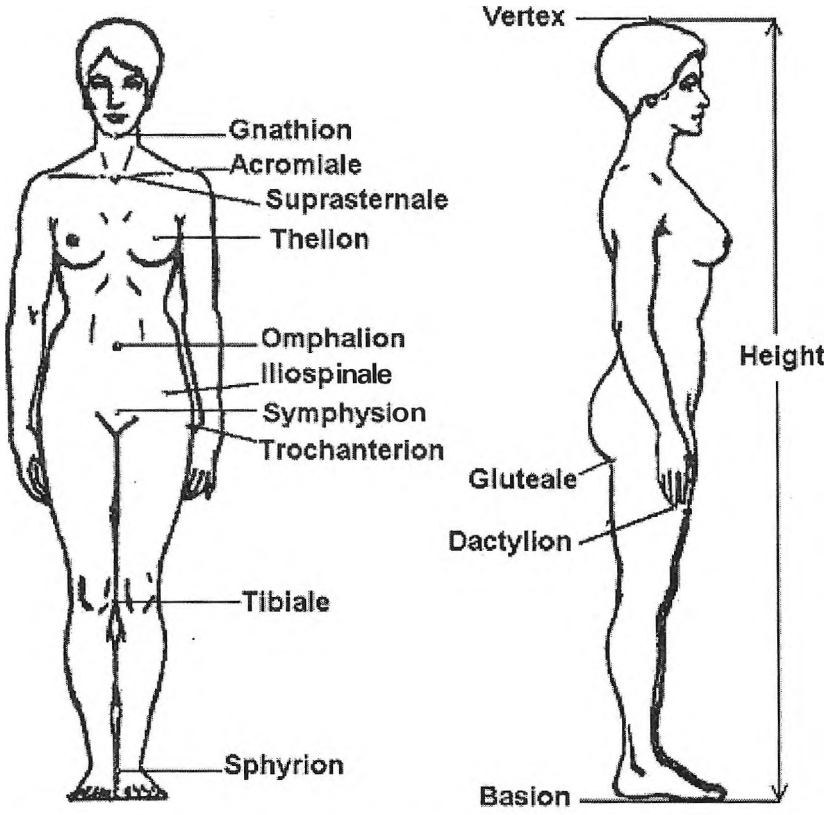

Fig. 1. Anthropological points that are used in measurements

Vertex: In anatomic position, its the highest point of the head.
Gnathion: The midline point of the bottom edge of Mandibula.
Acromiale: The point matching Angulus acromii.
Suprasternale: Midpoint of incisura jugularis sterni.
Thelion: Midpoint of Papilla mammae.
Omphalion: Upper midpoint of the navel.
Iliospinale: The point matching Spina iliaca anterior superior.
Trochanterion: The highest and the most lateral point of Trochanter major.
Symphysion: The highest point of Symphysis pubis.
Gluteale: Midpoint of Plica glutealis.
Dactylion: Matches the tip of the longest finger.
Tibiale: The highest point of Condylus medialis tibae.
Sphyrion: The lowest point of Malleolus medialis [5, 7].

Results

After recording the measurements of 495 female students with a mean age of 20,7 in the forms prepared beforehand, we have calculated, for each distance, the arithmetic average of the group, standard deviations, their ratios to the stature and their correlation quotients. We have shown the results in table 1.

T a b l e 1. In our research, the height of women, on whom measurements have been made, the standard deviation, their rate to the height and the correlation quotients have been shown

Measure's	Measured values (cm)	SD (±)	The proportion to body height (%)	Correlation (r)
Basion-vertex	159.86	4.97		
Basion-gnathion	136.25	4.39	84.2	0.89
Basion-acromiale	130.92	4.42	80.95	0.81
Basion-suprasternale	127.5	3.3	79.93	0.81
Basion- thelion	112.08	4.44	70.11	0.83
Basion-omphalion	94.08	3.03	59.56	0.8
Basion-iliospinale	87.4	2.85	55.77	0.75
Basion-trochanterion	79.58	1.59	50.59	0.67
Basion-symphysion	77	3.21	50.02	0.67
Basion-gluteale	67.5	2.81	44.62	0.68
Basion-dactylion	60.58	1.69	37.94	0.55
Basion-tibiale	41.08	2.71	24.77	0.45
Basion-sphyrion	7.83	0.62	4.8	0.28

Discussion

Since every individual has a different body type, it is inevitable that the anthropometric measurements yield different results. The reason to this is that socioeconomic conditions such as the place where a person lives, his life style and eating habits have

Table 2. Data of the other researchers (cm)

Measure's	Inan, A. [12], n=20263	Yildiz, Z. et al. [7]. Mean value of age, 22-35, n=100	Kahraman, G. et al. [8]. Mean value of age, 20-35, n=200
Basion-vertex	152.2	161.79	162.64
Basion-gnathion	-----	------	141.57
Basion-trochanterion	-----	82.54	------

an impact on the growth period. Consequently, this fact should not be neglected when comparing the data acquired through measurements.

In our study, 495 female student with a mean age of 20.7 have been involved and their average height has been found to be 159.86 cm. When we compare this result to the previous researches on women, a parallelism in the results of Yildiz et al. and Kahraman et al. demonstrated; it is much more than the height that A. Inan tested in 1937 with 20263 women. We assume that the reason Kahraman and his friends found longer distances than our data represents the reason for the the difference in height that creates a disadvantage for other researchers [3, 4, 11].

The focus of our study is the effect of some parameters on height. Given this assumption, we have examined the correlation between the average values of some body parts and the average height. As a results of the correlation analysis, we have found that the parts that affect the height most are gnathion, acromion, suprasternale, mamillare, omphalion, iliospinale.

A correlation between the height and sphyrion, %4,80 of the average height and tibiale length, %24,77 of the average height does not exist. There is a medium correlation between the height and trochanterion and symphysion bony landmarks (for trochanterion r = 0,67, for symphysion r=0,67) which are the other points of lower extremity. This shows that on the stature, thigh of the lower extremity is more important than leg.

In the landmarks on the upper body (omphalion, mamillare, suprasternale and acromiale), the correlation increases when moving towards the top. These results show that on the stature, axial skeleton system plays a more important role.

The correlation of the gnathion height which is %84,20 of the stature is of the greatest degree with 0,89.

In conclusion, the average stature of Turkish women today, increases much more rapidly compared to the past, contributed the most by the upper body, and a little bit less by thigh distances. In appearance, Turkish women have short legs and long upper bodies.

References

1. Dere, F., O. Oguz. Artistik Anatomi. Adana, Nobel Tip Kitabevi, 1996, 11-20.
2. Gurun R, O. Kuran. Yüzle Ilgili Anatomik Olçumler ve Orantəlar. — Yeni Symposium, **2**, 1991, 59-66.
3. Inan, A. Turkiye Halkinin Antropolojik Karakterleri ve Turkiye Tarihi, Turk Irkinin Vatani Anadolu. Ankara, TTK Basimevi, 1947.
4. Kahraman, G., T. Pestemalci. Turk Kadinlarinda Ust Ekstremite'ye Ait Bazı Olcum ve Oranlar. — Morfoloji Dergisi, **9**, 2001, №2, 30-33.
5. Mesut, R., M. Yildirim. Insan Vucudunda Antropolojik ve Yuzeyel Bulu$_3$ Noktalari. — Istanbul, Beta Basim Yayim Dagitum A.S., 1989.

6. Muftuoglu, A., Y. Tuna, R. Terzi, F. Vural, S. Selvili. Eriskin ve Yeni Doganlarda "Splanchnocranium" Yuzolcum ve Oranları. — Okmeydanı Hastanesi Bulteni, 4, 1987, No3,173-178.
7. Ozer, K. Antropometri. Sporda Morfolojik Planlama. — Istanbul, Kazanci Matbaasi, 1993.
8. Soyluoglu, A. I. Yetiskin Turk Kadin ve Erkeklerinde Bazı Bas Olçüm ve Oranları. Uzmanlik Tezi, Istanbul, 1990.
9. Taskinalp, O., R. Mesut. "Boy-Beden" Iliskisine Esas Bazı Antropometrik Orantilar. — T.U. Tip Fakultesi Dergisi, 8-10, 1991-1993, (Bilesik sayi), 1-8.
10. Yildirim, M., O. Taskinalp, G, Kahraman. Yetiskin Turk Erkeklerinde Boy ile Bazı El ve Ayak Olcumleri Arasənda Somatometrik Iliskiler. — Trakya Universitesi Tip Fakultesi Dergisi, 5, 1988, No1, 75-81.
11. Yildiz, Z., G. Kahraman, A. Muftuoglu. Turk Kadinlarənda Alt Ekstremite Olcumlerinin Birbirlerine ve Diger Vucut Olcumlerine Gore Oranlari. — Cerrahpasa Tip Fakultesi Dergisi, 24, 1993, 207-212.
12. Чоканов, К. Пластична анатомия. София, НИ, 1994, 370-395.

Institute of Experimental Morphology and Anthropology with Museum
Bulgarian Anatomical Society

Acta morphologica et anthropologica, 13
Sofia • 2008

The Influence of Environmental Factors on Growth and Development in Humans

E. Godina, I. Khomyakova, L. Zadorozhnaya

Institute and Museum of Anthropology, Moscow State University

2,106 girls and 2,169 boys from 7 to 17 were investigated in 2002-2004 in three urban settlements of the Saratov region: the town of Khvalynsk, and the cities of Saratov and Balakovo. The whole area, particularly the location of Khvalynsk, is characterized by iodine deficiency. The program included about 30 anthropometric measurements, evaluation of developmental stages of secondary sexual characteristics, and information on menarcheal age by the status quo method. For the analysis all data were standardized, and further comparisons were made irrespective of age groups. The significance of differences was assessed by one-way ANOVA. The Khvalynsk children are the smallest in body height and weight with the age of menarche for girls being 13 years 5 months. In Balakovo and Saratov the corresponding figures were identical: 13 years 2 months. Secular changes in Khvalynsk and Saratov children are discussed as compared to the literature.

Key words: ecology, growth and development, Russian children, environmental adaptation, secular trend.

Introduction

The growth process is determined by interactions of endogenous genetical factors (so called "determinants"), endogenous paragenetic factors ("stimulators") and exogenous environmental factors — "modificators" [3]. In this last group the following factors could be named: biogeographical (climate, seasonality, etc) social-economic (parental education and professional qualification, income, socioeconomic family status, living conditions, etc), psychological, anthropogenic and others [7].

One of the powerful natural factors influencing the processes of growth and development is the content of iodine in the environment. It affects growth via thyroid hormones. Approximately 1.5 billion people on our planet are affected by this condition [1]. Iodine deficiency causes the enlargement of the thyroid gland (goiter), the impairment of its functioning, deterioration of physical and mental health and development of serious diseases.

In Russia huge territories are characterized by iodine deficiency. One such territory is the Saratov oblast (region). In the soil of this area, particularly in Khvalynsk rayon, iodine levels are significantly low: 0.78 mkg/kg $\pm$ 0.32 versus normal values of 5-7 mkg/kg [5]. There is a deficit of other trace elements, such as Cu, Co, Zn with additional effects on thyroid deficiency.

Materials and Methods

The data were collected in 2002-2004. 2,106 girls and 2,169 boys from 7 to 17 were investigated cross-sectionally in three urban settlements of the Saratov region differing in the degree of iodine deficiency and in socio-economic development. The town of Khvalynsk (group 1) has only 15,000 inhabitants, does not have any industries and is very close to rural areas judging by the lifestyle of the population. One of the important characteristics of this area is the high degree of iodine deficiency. The median of ioduria in children of prepubertal age is 24 mkg/l [10].

In the cities of Balakovo (group 2) and Saratov (group 3) the same indicators are correspondingly 42.9 and 32.4 mkg/l, which can be considered a moderate iodine deficiency [10]. At the same time, the three localities differ in their degree of urbanization and industrialization: the city of Balakovo, population 220,000, is highly industrialized and has a nuclear power station; the city of Saratov, population around 1,000,000, is the regional capital and is highly industrialized. About 78 % of all investigated subjects were Russians; 4 % were Ukranians and Byelorussians; 86 % were born in the geographical localities where they were studied.

Anthropometric program included a large number of anthropometric measurements taken according to the standard techniques [6,4]. The children were measured during or immediately after school-hours; an age group consisted of children whose age falls within the interval $\pm$ 6 months of the whole year (e.g., 7-year olds: from 6.5 to 7.49, etc.).

The body mass index (BMI) of the studied subjects was calculated as weight (kg) divided by height $(m)^2$.

Besides anthropometric measurements, stages of secondary sexual characteristics were assessed. Breast development, axillary and pubic hair for girls; age at menarche was evaluated by the status quo method. Voice mutation, nipple enlargement, axillary and pubic hair and a number of other indicators were assessed for boys.

The *questionnaire* contained information on parental profession and education, family income, number of children in the family, birth order, birth weight and length of the individual investigated.

To follow *secular changes*, literary data from the 1920s, 1950s and 1960s were used.

Statistics: The data obtained were standardized and Z-scores were calculated. The significance of differences was assessed by a Scheffe test (one-way ANOVA). Principal component analysis, canonical analysis was used. Data analysis was conducted with Statistica 6 software. For the secondary sexual characteristics, the median age of their development was calculated from accumulated frequencies graphs.

Results

Khvalynsk children, both boys and girls, were smaller in stature and weight if compared to their peers from the two bigger cities. However in chest circumference they are either bigger (boys) or equal (girls). In BMI Saratov children are ahead of their counterparts from Khvalynsk and Balakovo in prepubertal age but in later ages have the same or even smaller mean values.

In such measurement as leg length, the children in Khvalynsk are the shortest: e.g., in 17-year-old males of Khvalynsk, Balakovo and Saratov the corresponding mean values are 94.71, 96.05 and 96.61 cm; in females — 85.76, 89.76 and 87.72 cm. During the whole growth period the children of Khvalynsk have smaller values of biacromial and bigger values of biiliac diameter, though the differences are not sta-

tistically significant. Interpopulation comparison of skinfold thickness in boys shows a clear gradient of increasing their values in the order Khvalynsk-Balakovo-Saratov. Among girls, Balakovo females at certain ages and for certain skinfolds (subscapular, triceps) exceed their counterparts from the two other localities.

In skinfold thickness there is a definite decrease of values in the boys and girls of Khvalynsk; the level of significance varies for different skinfolds from $p<0.001$ to $p\leq0.02$. In Balakovo girls the values of biceps and forearm skinfolds are lower than in their counterparts from Saratov ($p\leq0.001$).

Thus, it can be concluded that the degree of differences between the three groups studied varies: the children from Balakovo in some traits are close to their peers from Khvalynsk, and in some other traits to those of Saratov. There are also some gender differences in variations of growth parameters.

Besides morphological parameters, characteristics of sexual maturation were also studied. Khvalynsk children of both sexes are characterized with the highest values of those indices, i.e. with a delayed process of sexual maturation. For Balakovo children there are trends of both later and earlier maturation, depending on the gender of the children. Balakovo boys have an intermediate position in terms of sexual maturation between the other two groups; while girls for some characteristics display even earlier ages than the girls of Saratov. The major marker of sexual maturation — age at menarche — is the same for the girls studied in Balakovo and Saratov (13 years 2 months) and 3 months later in Khvalynsk (13 years 5 months).

Discussion

The results show that the children of Khvalynsk and Saratov are clearly differentiated from each other. Balakovo children in some way are closer to the Khvalynsk group. This is rather unexpected as both Balakovo and Saratov are big cities and one could expect a similarity in the parameters of children's growth.

In terms of iodine deficiency, Khvalynsk is the town most severely affected by this adverse factor, while both Balakovo and Saratov are characterized with only a moderate degree of iodine deficiency.

Observed variations can also be explained by socio-economic differences in the three populations. Though Khvalynsk is a local district center, in terms of urbanization and economic development it is much less advanced than Balakovo or Saratov. The number of families where parents have a higher education is much lower here, while the number of families with several children is higher. At the same time, in Khvalynsk there is a high level of parental unemployment and mortality.

Balakovo is a relatively young city; its development was closely connected with the construction of a nuclear power station and its functioning. That is why about 40 years ago the city became a center of local migration from adjacent rural areas. We think that this might be one of the reasons why the children of Balakovo are in some ways closer to their peers from Khvalynsk than those from Saratov. It may also explain why we did not find the usual gradient of increase of body parameters parallel to the population increase.

Saratov is a large industrial city with a population almost equal to 1,000,000. It is a city with a long and important history. In the early 20th century, long before the revolution of 1917, it was one of the most developed cities of the Russian Empire, a center of trade and industry, of highly developed agriculture.

According to our results, it is characterized by the largest values of growth parameters in children and adolescents and stability of population structure.

Because the children of Saratov were measured several times during the 20th century we were able to compare our results with historical data [11].

While stature was increasing during those years, such traits as weight, chest circumference and BMI are characterized by negative changes, which are more clearly expressed in girls of older ages. At the same time, girls are also characterized by negative changes in such traits as pelvic breadth.

These results coincide with those obtained early for a young Moscow generation. It was shown that there were important changes towards more leptosomic (from Greek *leptos* — narrow, *soma* — body) morphotypes in young males and females living in Moscow [8, 2].

In sexual maturation there were typical changes towards early ages from 1929 to 2004. Thus, the median menarcheal age has changed from 14 years 5 months in 1929 to 13 years 5 months in 1959, and 13 years 2 months in 2004.

For Khvalynsk children it was possible to follow certain secular changes comparing the results of the present study with the data by Kakorina and Tcheplyagina [9] who examined Khvalynsk children in 1991. For the past decade there were some negative changes in body dimensions both for boys and girls. Even stature decreased significantly for an 11-year period: from 163.7 to 160.85 cm for 15-year-old girls, and from169.4 to 166.28 for 15-year-old boys. The reason for such a decrease may be the negative socio-economic changes in Khvalinsk after "perestroika".

Acknowledgements. The work was supported by the Russian Foundation of Basic Research, grants NoNo 05-06-80390-a, 05-06-80907-a; and Russian Foundation of Humanities Research, grant No 04-06-00260-a.

References

1. Bogin, B. A. Patterns of Human Growth. 2nd ed. Cambridge, Cambridge University Press, 1999.
2. Godina, E. Z., Y. Yampolskaya. Recent secular growth changes in Moscow schoolchildren. — Anthrop. Kozl., **45**, 2004, 51-57.
3. Malinowski, A. Auksologia. Rozwoj osobniczy czlowieka w ujeciu biomedycznym. Zielona Gora, 2004.
4. Weiner, J. S., J. A. Lourie. Human Biology. A Guide to Field Methods. Edinburgh, Blackwell Scientific Publ. Oxford, 1969.
5. Болотова, Н. В. Эндемический зоб у детей (этиология, клиника, прогноз). Дис. док. мед. наук. Саратов, СГМУ. 1995.
6. Бунак, В. В. Антропометрия. М., 1941.
7. Година, Е. З., Н. Н. Миклашевская. Экология и рост: влияние факторов окружающей среды на процессы роста и полового созревания человека. В сб.: Рост и развитие детей и подростков. Итоги науки и техники. Сер. Антропология. Т.3. М., ВИНИТИ, 1989, 77—134.
8. Година, Е. З., И. А. Хомякова, О. А. Гиляров а, Л. В. Задорожная, А. Л. Пурунджан. О современной направленности эпохальных сдвигов (по материалам изучения показателей роста и развития московских детей и подростков). — В: Материалы Конгресса Педиатров России (Москва, 16-18 февраля 1999 г.). М., 1999, 113—114.
9. Какорина, Е. П., Л. А. Щеплягина. Физическое развитие детей школьного возраста 6-15 лет. Хвалынский район Саратовской области. — Материалы по физическому развитию детей и подростков городов и сельских местностей Российской Федерации. Выпуск 5. М., 1998. 100—101.
10. Свинарев, М. Ю. Клинико-эпидемиологические особенности йодного дефицита у детей (диагностика лечение, профилактика). — Дис. докт. мед. наук М., 2002.
11. Соловьева, В.С. Материалы по половому созреванию подростков Саратова. — Вопросы антропологии, **11**, 1962, 81—95.

Institute of Experimental Morphology and Anthropology with Museum
Bulgarian Anatomical Society

Acta morphologica et anthropologica, 13
Sofia • 2008

Basic Dimensions and Proportions of the Head between 7 to 17 Years of Age

Z. Filcheva, N. Kondova

Institute of Experimental Morphology and Anthropology with Museum, Bulgarian Academy of Sciences, Sofia

The presented results are a part of a large anthropological study on schoolchildren aged 7-17 from Sofia. The age-dependent of five basic dimensions and four indices characterizing the cerebral part of the head have been followed up. 3640 individual measurements — 1787 for the boys and 1853 for the girls have been taken. A differing type of growth of the basic head sizes in both sexes has been recorded. Even as early as the age of 7 years the sexual differences are clearly expressed in all head features. A tendency towards debrachycephalization has been detected.

Key words: cerebral part of the head, growth velocity, sexual differences, secular changes, debrachycephalization.

Introduction

Head size growth is closely linked to brain development. Human brain starting from its embryonic development surpasses the development of the other organs. In newborns the human brain represents 25% of its weight in adults, while in children at 10 years of age it is 95% [4]. Due to this fact the skull reaches final values much earlier than the other parts of the skeleton. The brain part is thus formed earlier than the facial one. In accordance with that the cerebral part sizes of the head as opposed to that of the facial cranium are expected to reach the values of the adult individuals earlier. The **aim** of the present study is to trace the dynamics of the changes in the basic dimensions and proportions of the cerebral part of the head between ages 7 and 17, to register the growth velocity of the features under study, to asses the sexual differences and to look for secular changes in the studied features at the end of the past century and at the beginning of the present century.

Material and Methods

Schoolchildren from 5 Sofia schools aged from 7 to 17 years were the subject of an in-detail anthropological study. A total of 3640 individual measurements — 1787 for the boys and 1853 for the girls during the period from 1993 to 2001 were carried out

after the classical method [1]. The changes in five basic sizes and four indices of the head combined in the age groups 7-9, 9-11, 11-13, 13-15 and 15-17 years were followed up and analyzed (Tables 1, 2). The growth velocity of the features under study is calculated after the formula (X2—X1)*100/(X2+X1), where X1 is the mean value from the preceding year and X2 — that from the next year of the study. The statistical significance of the sexual differences is checked by the Student's-criterion ($P<0.05$). They are quantitatively estimated by the help of the relative index of sexual differences (ISD) expressed in index units (IU) and is calculated after the formula 2*(Xз-Xэ)*100/(Xз+Xэ) [5].

Results and Discussion

The boys at the age between 7 and 13 years and only the 7-year-old girls are with a medium length of the head. After this age the heads are long. Between the ages of 7 through 17 both sexes display narrow heads (Table 1). According to the data on the head index both sexes are mesocephal. The transversal fronto-parietal index defines the boys in all age groups as mesometop. Only the girls between the 7 and 13 years of age belong to that category. After that age they are hypermesometop. According to the long-height index of the head both sexes in all age groups are hypsicephal. The wide-height index defines both sexes between the ages of 7 to 17 as metriocephal. Between the ages 15 and 17 years the boys are akrocephal and the girls remain at the metriocephal-acrocephal border (Table 2). The sexual differences are most clearly expressed in all head features studied as early as the age of 7 years ($P<0.05$). It has

Table 1. Age changes in the basic head measurements

Feature	Age (years)	Boys			Girls			t-test	ISD
		n	*X*	SD	*n*	*X*	SD		
Head length	7	182	179.01	6.13	178	174.93	5.87	6.45	2.30
	9	189	181.78	6.16	182	177.30	5.65	7.30	2.50
	11	183	182.60	6.20	205	178.49	5.83	6.70	2.28
	13	166	183.92	6.03	186	180.64	5.36	5.37	1.80
	15	124	187.38	6.62	138	181.70	6.03	7.23	3.08
	17	118	189.75	6.46	138	180.67	6.53	11.15	4.90
Head breadth	7	182	141.78	5.38	178	137.06	4.44	9.09	3.38
	9	189	144.40	5.06	182	140.09	4.56	8.62	3.03
	11	183	144.91	4.92	205	140.42	4.76	9.11	3.15
	13	166	145.43	5.10	186	141.59	4.76	7.28	2.68
	15	124	145.96	5.41	138	141.33	5.15	7.08	3.22
	17	118	147.48	5.25	138	141.74	4.66	9.18	3.97
Frontal breadth	7	182	100.68	3.67	178	98.65	3.38	5.46	2.04
	9	189	103.37	3.76	182	101.28	3.38	5.64	2.04
	11	183	104.39	3.89	205	102.83	3.51	4.13	1.51
	13	166	106.22	3.90	186	105.08	3.68	2.81	1.08
	15	124	108.07	4.18	138	106.14	3.72	3.93	1.80
	17	118	109.71	3.88	138	106.29	3.60	7.27	3.17
Auricular head height	7	182	118.29	6.39	178	113.58	6.70	6.82	4.06
	9	189	121.18	6.93	183	115.35	7.08	8.02	4.93
	11	183	120.03	9.13	205	115.05	6.86	6.02	4.24
	13	166	118.87	8.28	184	113.71	7.48	6.09	4.44
	15	124	126.32	10.49	138	120.15	8.34	5.23	5.01
	17	118	129.43	8.95	136	120.15	7.00	9.10	7.44
Head circumference	7	182	526.25	14.82	178	516.65	12.89	6.56	1.84
	9	189	536.40	14.02	182	528.25	12.77	5.86	1.53
	11	183	541.82	14.44	205	538.09	15.18	2.48	0.69
	13	166	549.02	15.62	186	549.03	14.97	0.01	0.00
	15	124	562.01	17.71	138	553.15	15.30	4.30	1.59
	17	118	571.03	15.91	138	554.30	15.87	8.33	2.97

T a b l e 2. Age changes in the basic head indices

Feature	Age (years)	Boys			Girls		
		n	*X*	SD	*n*	*X*	SD
Head index	7	182	79.29	4.01	178	78.43	3.53
	9	189	79.52	3.89	182	79.09	3.56
	11	183	79.46	3.92	205	78.75	3.62
	13	166	79.16	3.75	186	78.44	3.31
	15	124	77.98	3.76	138	77.87	3.84
	17 .	118	77.81	3.72	138	78.54	3.70
Transversal fronto-parietal index	7	182	71.07	2.84	178	72.02	2.47
	9	189	71.63	2.63	182	72.34	2.62
	11	183	72.07	2.55	205	73.28	2.62
	13	166	73.07	2.50	186	74.26	2.58
	15	124	74.10	2.91	138	75.16	2.80
	17	118	74.44	2.69	138	75.03	2.61
Long-height index of the head	7	182	66.14	3.91	178	64.97	3.83
	9	189	66.72	4.22	182	65.12	4.04
	11	183	65.90	5.04	205	64.48	3.73
	13	166	64.68	4.70	184	62.96	4.10
	15	124	67.47	5.78	138	66.20	5.09
	17	118	68.23	4.36	136	66.52	3.87
Wide-height index of the head	7	182	83.50	4.66	178	82.92	5.08
	9	189	83.99	5.16	182	82.42	5.18
	11	183	83.03	6.20	205	81.99	5.07
	13	166	81.77	5.50	184	80.38	5.67
	15	124	86.63	7.51	138	85.08	6.14
	17	118	87.83	6.14	136	84.82	5.54

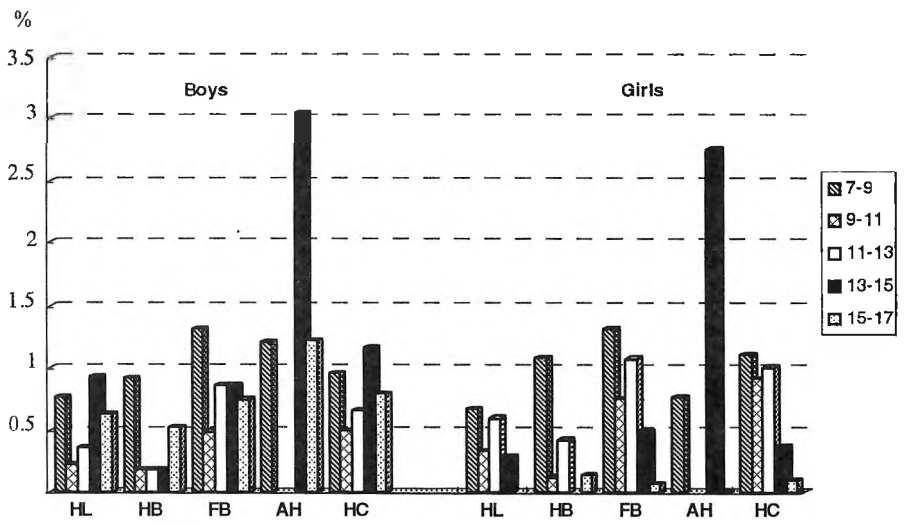

Fig. 1. Growth velocity in the basic head measurement

been established by the help of (ISD) that they are greatest in the auricular head height and smallest in the head circumference. Growth velocity in the boys for most of the features is most intense between ages 13 and 15. In the case of the girls the growth between 7 and 9 years is most accelerated for all features excepting for the auricular head height. In them a second peak of growth — between the years of 11 to13 is observed (Fig. 1). At the age of 7 years the head sizes in both sexes represent

between 87.9% and 93.8% of the values for adult individuals from Sofia while in the case of the 17-years old these are already between 94% and 100% (National programme "Anthropological characteristics of the Bulgarian people", 1989/1999, unpublished data).

The secular changes of the basic head sizes and the head index compared to data from anthropological studies at the beginning and the 1970-ies of the past century have been traced [8, 9]. A tendency to brachycephalization expressed in the head length growth and diminution of the head breadth has been established. R. S t o e v and Y. Y o r d a n o v [3] have observed a decrease of the head index in adult Bulgarians born after 1950. The tendency to debrachycephalization has been established by foreign authors as well [2, 6, 7]. The changes in the head circumference are most weakly pronounced as compared to 1970 [9]. Its mean values in the 17-year old persons are quite close to those from the present study. St. V a t e v [8] has found a significantly smaller head circumference.

Conclusion

During the period between 7 and 17 years of age heads of medium length to long ones, narrow, of medium height to high with a forehead of medium breadth and mesocephalic shape are typical for both sexes. In the boys for the most of the features the growth velocity is highest between the ages of 13 and 15 years and in the girls it is highest between the years of 7 to 9. The sexual differences in all features of the head under study are clearly outlined as early as 7 years of age. A tendency towards debrachycephalization is registered.

References

1. M a r t i n, R., K. S a l l e r. Lehrbuch der Anthropologie in sistematischer Darstellung, Bd. I. Stuttgart, Gustav Fischer Verlag, 1957, 363-371, 385-429.
2. Š t e f a n č i č, M., P. L e b e n - S e l j a k. Growth of head and face in children from Ljubljana during adolescence: mixed longitudinal study. — Antropološki zvezki, 4, 1996, 73-85.
3. S t o e v, R., Y. Y o r d a n o v. Secular trend in Bulgaria — In: Secular Growth Changes in Europe, Budapest, Eötvös Univ. Press, 1998, 65-73.
4. T a n n e r, J., M. Growth at adolescence. Oxford, Blackwell Scientific Publications, 1962.
5. W o l a n s k i, N. Function of the extremities and other influence on the asymmetric structure of body in children and young persons from different environmental conditions. — Acta Med. Auxologica, IV-1, 1972, 3-11.
6. Z e l l n e r, K., U. J a e g e r, K. K r o m e y e r - H a u s c h i l d. Das Phänomen der Debrachykephalisation bei Jenaer Schulkindern. — Anthrop. Anz., 56, 1998, No4, 301— 312.
7. Z e l l n e r, K., K. K r o m e y e r - H a u s c h i l d, J. S t a d l e r, U. Y a e g e r. Ergebnisse der Untersuchung ausgewhlt Kopfmaße bei Jenaer Kindern. — Anthrop. Anz., 57, 1999, No2, 147-163.
8. В а т е в, Ст. Антропология на българите. С., 1939, 38—49.
9. Я н е в, Б., П. Щ е р е в, П. Б о е в, Ф. Г е н о в, Д. С е п е т л и е в, И. П о п о в, Б. З а х а р и е в. Физическо развитие, физическа дееспособност и нервно-психическа реактивност на населението. С., Медицина и физкултура, 1982.

Institute of Experimental Morphology and Anthropology with Museum
Bulgarian Anatomical Society

Acta morphologica et anthropologica, 13
Sofia • 2008

Sexual Development of Boys and Girls Aged 14-18 Years, Studying at Different Types of Schools

Zh. Hristov, T. Stoev, S. Savov

Medical University, Plovdiv

On the basis of a large-scale examination of the psycho-emotional condition of students, a pilot survey has been carried out for assessment of the sexual development in three types of schools (secondary production-oriented school, secondary school of general education (Roma children) and a sports school).

The survey analyzes results of three periods — 1978, 1988 and 2004. Several things have been established: the manifestation of the secondary sex characteristics, through 8 indexes in boys and 6 indexes in girls, the influence of the biological development on the degree of manifestation of the sex characteristics, time and factors affecting the occurrence of the first menstruation and the first ejaculation, on the beginning of the first sexual contacts, etc.

Dependencies between the morphological indexes and the degree of sexual development have been sought through plural correlation. What impresses is that today's youth show a more accelerated sexual development which does not always correspond with their socialization in the contemporary society.

Key words: physical, biological, sexual development, harmonious and disharmonious type, acceleration, retardation.

The attempt to make a periodization of the ontogenic development of the individual is a complex task, because it is necessary to specify the influence of many factors, which for their part do not play one and the same role in the different stages and do not provide one and the same informativeness. Questions grow more complex since when considering the norm of an individual index we should take into account that an organism's systems do not develop synchronously.

In this connection the individual differences in the speed of the physical and sexual development and the discrepancy between the biological and calendar age of children require a differentiated approach with regards to the fact that the maximum acceleration of growth often (but not always) is connected with the development of the reproductive system.

Lately we have been witnessing the much earlier occurrence of the primary and secondary sex characteristics in both sexes.

A number of observations indicate that sexual maturation plays a significant role in developing the motorics, for increasing the individual motive and func-

tional characteristics, for the purposefulness of the personality and the frequent occurrence of a discrepancy between the biological and social maturity of the individual.

Material and Methods

Within the framework of a large-scale research connected with assessment of the psycho-emotional condition of students of the 14-18 age bracket, a pilot poll survey and examination were carried out on the basic indexes characterizing the degree of sexual maturity with the two sexes in the indicated age groups. A total 212 boys and 236 girls, evenly distributed according to sex and age, were included in the survey. The survey was carried out in schools of different profiles in Haskovo and Plovdiv districts.

The characteristics of the observation units were: manifestation of the secondary sex characteristics in both sexes; relation between the degree of the biological development and the manifestation of the secondary sex characteristics; time of occurrence of the first menstruation and its nature; time of the first ejaculation; beginning of sexual contacts; relation between the sexual maturation and the morphological indexes; specification of the influence of certain factors on sexual maturation.

The assessment of the manifestation of the secondary sex characteristics was carried out in accordance with a modification of ours of the Zeller method in rating marks from 1 to 5, different for the individual characteristics. Boys were observed for 8 sex characteristics which in terms of the maximum number of rating marks give a total of 28. Girls were observed for 6 characteristics, giving the maximum rating mark of 22.

We determined the biological age by means of skeletometric methods, while the assessment of the morphological indexes — through the accepted anthropometric methods.

We sought plural correlation dependencies between the individual indexes providing objectiveness of the conclusions reached.

Results

The manifestation of the sex characteristics was traced in different types of schools, and the data obtained were compared to other researches of ours from 1978 and 1988. (Table 1)

Analyzing the results of the manifestation of the secondary sex characteristics in the three age periods (1978,1988,2004), we should point out that 2004 saw a stronger manifestation of the secondary sex characteristics with boys at the age of 14, 15 and 16 years, after which no significant differences with the other periods were established. A similar tendency has been witnessed with girls, with the stability of the rating marks reached as early as the age of 16 years.

We tried to find out the influence of the degree of biological maturity on the manifestation of the secondary sex characteristics for the three periods under examination (Tables 2 and 3).

The data from the two tables show a direct relation between the degree of the biological development and the manifestation of the secondary sex characteristics as they are significant in both sexes between accelerated, retarded and normally developed.

T a b l e 1. Manifestation of the secondary sex characteristics in boys and girls aged 14-18 years (total rating mark) in 1978, 1988 and 2004

Age, years	Total rating mark											
	Boys						Girls					
	1978		1988		2004		1978		1988		2004	
	X	SD	X	SD	X	SD	X	SD	X	SD	X	SD
14	17.25	1.69	17.15	1.90	18.32	1.59	15.21	1.45	15.13	1.30	16.21	1.43
15	21.47	1.73	20.55	1.73	22.27	1.74	17.47	1.53	17.11	1.26	18.03	1.58
16	23.11	1.84	23.02	1.35	23.78	1.51	18.52	1.61	18.33	1.41	18.80	1.71
17	24.60	1.81	24.73	1.49	24.83	1.77	19.70	1.58	19.61	1.38	19.86	1.53
18	24.96	1.84	25.11	1.44	25.31	1.53	19.87	1.64	19.97	1.39	20.35	1.64

T a b l e 2. Manifestation of the secondary sex characteristics (rating marks) with boys in different degree of biological development

Age, years	Periods								
	1978			1988			2004		
	Acceleration	Normal Development	Retardation	Acceleration	Normal Development	Retardation	Acceleration	Normal Development	Retardation
14	18.9	16.5	14.3	19.3	16.1	13.9	19.7	17.1	15.7
15	21.7	19.4	17.5	21.5	19.3	16.3	22.3	20.2	18.4
16	23.6	22.1	19.9	23.9	22.2	18.5	23.8	22.7	20.3
17	25.6	24.9	22.1	24.8	24.6	21.7	24.9	23.1	22.9
18	25.8	25.0	23.7	25.9	25.3	24.9	25.7	24.9	24.1

T a b l e 3. Manifestation of the secondary sex characteristics (rating marks) with girls in different stages of biological development

Age, years	Periods								
	1978			1988			2004		
	Acceleration	Normal Development	Retardation	Acceleration	Normal Development	Retardation	Acceleration	Normal Development	Retardation
14	15.4	14.5	11.5	15.9	14.7	10.9	16.1	15.3	12.2
15	17.4	15.9	13.2	17.9	16.8	13.8	17.9	16.4	14.1
16	19.1	17.3	15.1	19.3	17.9	15.9	20.1	17.5	16.7
17	20.5	19.7	17.3	20.6	19.8	17.7	20.7	20.1	18.3
18	21.2	20.7	19.4	21.5	20.6	20.4	21.1	20.4	19.8

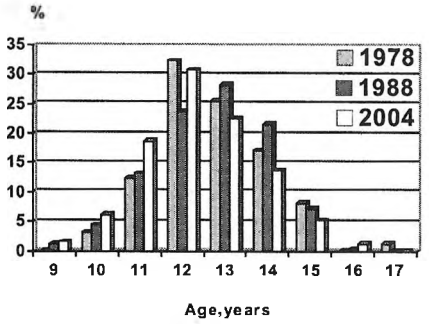

Fig 1. Age of occurrence of first menstruation in schoolgirls 14-18 years studied in 1978, 1988 and 2004

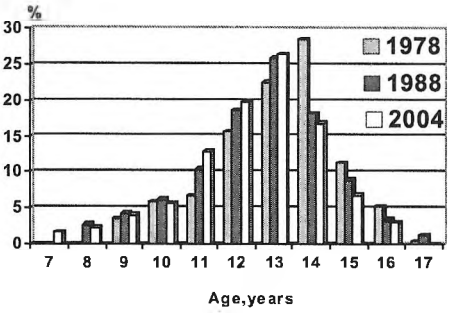

Fig. 2. Age of occurrence of first ejaculation in schoolboys 14-18 years studied in 1978, 1988 and 2004

The time of occurrence of the first menstruation in girls is influenced by a number of factors. With the recipients examined by us it was established that during the periods under examination it is different (Fig. 1).

It has been proved that the average age of occurrence of the first menstruation in the examined girls is 12.74 years ± 1.24, and with girls from the secondary production-oriented schools it is manifested at 12.75 years ± 1.28, while in Roma children - 12.53 ± 1.37, and in the sports school — 12.53 ± 1.37.

The time of occurrence of the first ejaculation in boys during the years of the three examined periods is as follows: 1978 — 12.8±1.19; 1988 — 12.9±1.7; 2004 — 12.5±1.24 (Fig. 2).

Of all the boys examined in 2004, 31.28% had their ejaculation earlier, in the mean norm the figure was 54.19 and another 14.53 had their ejaculation later. In its nature, in 10.32% of the boys it is manifested through pollution, while in 89.68% it is caused by masturbation. It should be stressed that during the mentioned year ejaculation was ascertained with nearly 8% of the schoolboys under 10 years of age.

The beginning of sexual contacts with boys and girls was specified through a poll in 2004 (Fig. 3).

We looked for the relation between the sexual development and morphological indexes. Through a plural regression between the final height, the height in recent years, BMI and puberty development it has been proved that there exist low correlation relations, except for those during the 14th and 15th years.

A number of factors influencing sex maturation were witnessed during the general examination of 874 students of both sexes aged 14-18 years: type of nervous system, system of values, influence of the social, family and school environment, the psycho-emotional tension and depression, the health status, mode of life, etc.

Conclusions

1. An increase in the rating marks of manifestation of the secondary sex characteristics in 2004 in comparison with 1978 and 1988 was proved, with the manifestation influenced by the degree of biological development.
2. The time of occurrence of the first menstruation and ejaculation comes much earlier as a result of the influence of a number of factors.

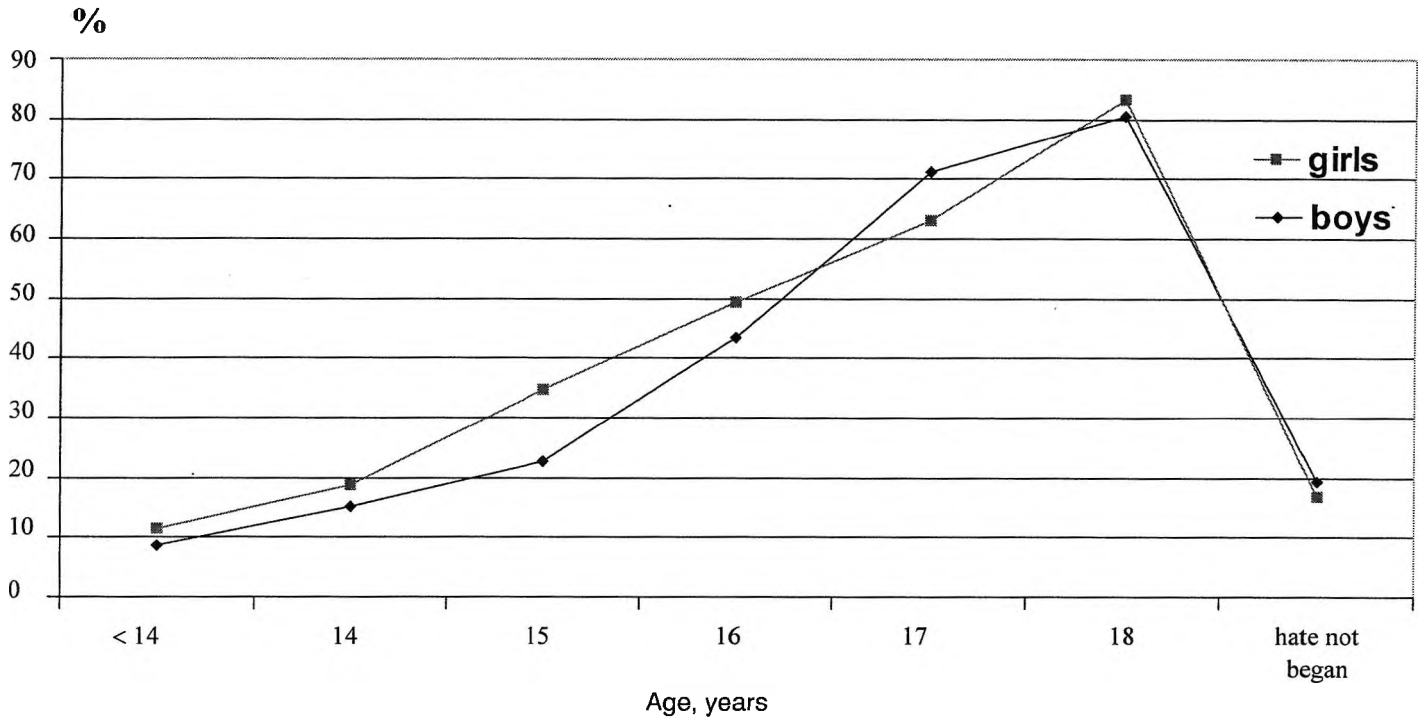

Fig. 3. Percentage of school children 14-18 years of age studied in 2004, who have began having sexual contacts

3. In recent years sexual contacts start much earlier with girls as compared to boys and have their peak between 15 and 16 years. This necessitates the implementation of a purposeful prophylactic activity, the aim being to curb them.

References

1. Bernhord, W., C. Glockler. New investigations on the question of secular acceleration of permanent dentition. — Morph. ANTH., **81**, 1995, 111-123.
2. Hauspic, R. S. Secular changes in growth and maturation: an update. — Acta paed. Suppl., **423**, 1997, 20-27.
3. Helm, P. L. Groeulud. A halt in the secular trend towards earlier menarche in Denmark. — Acta Obst. et Gynecolog. Scandinav., 77, 1998, 198-200.
4. Liestoel, K. Height, weight and menarcheal of schoolgirls in Oslo: an update. — Amm. Hum. Biol., **22**, 1995, 199-205.
5. Savov, S. Sex maturity in boys and girls actively engaged in Sport. Sixth Bal.congr.of sport medicine — CV-T., 1988, 184-188.
6. Tryggvadott, L. A decline and a halt in mean age at menarche in Iceland. — AMM hum. biol., **21**, 1994, 179-185.
7. Мартиросов, З. Г. Половой диморфизъм некоторых морфо-функциональных показателей — М. Теории и прак. физ. култ., **4**, 1997, 24—27.
8. Савов, С. Особености в половото съзряване при момичета и момчета, активно занимаващи се със спорт. — В: Сб.науч.конф.Адаптационных изменения огранизма и физических нагрузов. Kaunas Litva, 1996, 122—128.
9. Станчев, З., Н. Страшимирова. Пубертет у момчетата. Поява на вторични полови белези и физическо развитие. С., МФ, 1981.
10. Стоев, В., З. Станчев. Спорт и пубертет. С., МФ, 1981, с. 167.

Institute of Experimental Morphology and Anthropology with Museum
Bulgarian Anatomical Society

Acta morphologica et anthropologica, 13
Sofia • 2008

Secular Changes in Body and Head Dimensions in Bulgarian and Russian Children

M. Nikolova, E. Godina, V. Akabaliev***

Department of Human Anatomy and Physiology, University of Plovdiv
**Institute of Anthropology, University of Moscow*
***Medical University of Plovdiv*

The purpose of this research is to study the effect of secular processes on body and head and face dimensions of Bulgarian and Russian children and adolescents. The results indicate that in the case of Moscovite children in the last decade of the 20th c. there is a stabilization of stature and a trend towards astenization and gracialization. In the case of the children from Plovdiv, at the end of the 20th and the beginning of the 21st century, there continue to be positive changes in the basic somatometric parameters. In both populations the secular changes in the head and face parameters are related to debrachycephalization and leptoprosopnosis.

Key words: secular changes, body and head dimensions, children.

Introduction

The morphological aspects of secular processes are most fully reflected in the numerous studies of children and adolescents. They include mainly long-term consequences of the effect of acceleration [retardation] on the child's growth and development. One such consequence is the astenization of the constitution of the children, causing deteriorated physical condition and increase of chronic sickness rate.

Secular changes in body parameters are complemented by changes in head and face parameters. The main direction of these changes in most cases is brachycephalization and debrachycephalization. Information concerning this appears in a number of European countries [1, 4, 5, 8].

The purpose of the present research is to study the secular phenomena among Bulgarian and Russian children and adolescents and their effect on body, head and face dimensions.

Material and Methods

The subjects of the research are children and adolescents aged 7-17 from Plovdiv and Moscow. The Russian children were studied in 1996-1999 (1153 girls and 1152

boys). The Bulgarian children were studied in 2000-2002 (910 girls and 920 boys). The anthropometric programs for both sample groups include a wide range of body, head, and face dimensions taken by means of the classical method of M a r t i n - S a l l e r [3].

The present study focuses on 3 body dimensions — height, weight, chest circumference and 4 cephalometric dimensions: length and breadth of the head, morphological height and breadth of the face. For the analysis of the secular changes, data was used of children and adolescents from Moscow measured in the 70's and 80's, and of children from Plovdiv, measured in the 60's and the 80's. The data has been statistically processed, considering the significance of differences by tlcriteria of Student.

Results and Discussion

The growth process in Moscovite children and adolescents in terms of stature show that most considerable secular changes occurred in the 70's and 80's; whereas in the 90's the growth rate is stabilized despite a preserved trend toward a positive longitudinal growth (Fig. 1).

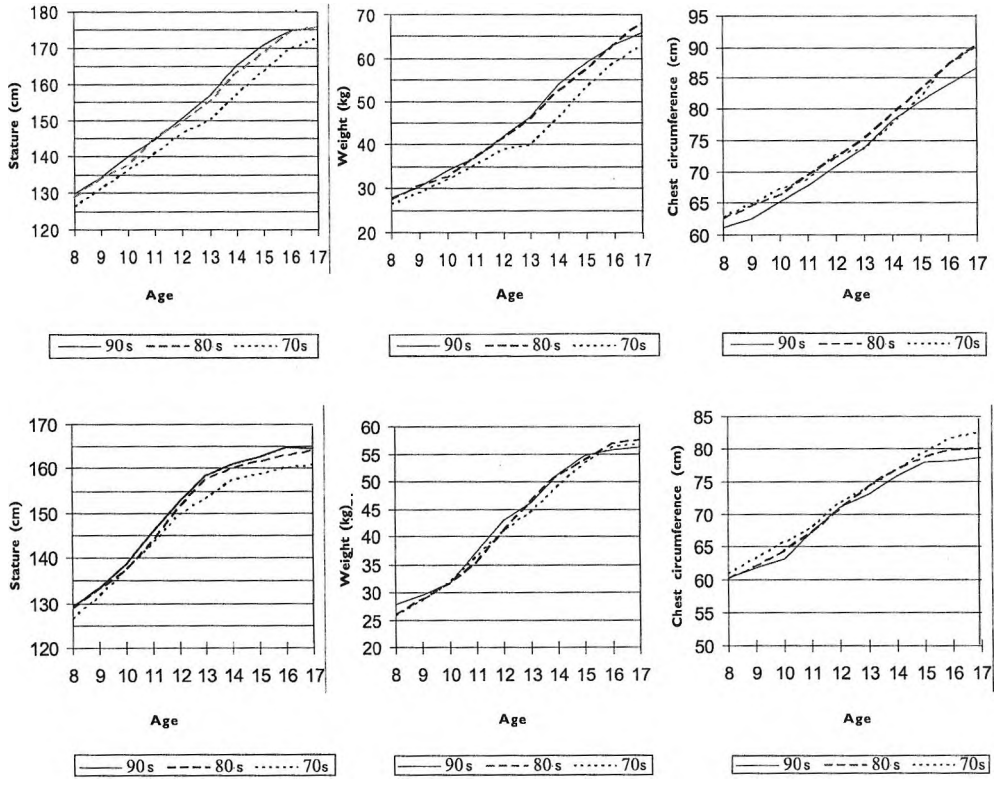

Fig. 1. Secular changes in children from Moscow

The changes in the weight have also a positive sign and are reliable ($p<0.0001$) among boys studied in the 70's and the 80's. Secular weight changes among girls are not statistically significant in the three samples (Fig. 1).

Unlike the case with the stature and weight, the chest circumference has significantly lower values in the children and adolescents studied in the 90's as compared to the parameters in the same age group registered in the studies in the 70's and 80's. A similar trend in the dynamics of the development of the chest cage is confirmed by other authors [2, 9].

The situation, however, with the children and adolescents from Plovdiv is quite different. As seen in Fig. 2, the secular changes have a positive sign for all the three basic somatometric parameters. In one of our previous articles about the characteristics of the growth processes in different ethnoterritorial groups of children and adolescents, two distinct varieties in the course of the growth process were distinguished: "western" — with a tendency towards astenization of the stature and decreasing acceleration and "south-eastern" with continuing acceleration [7]. The children and adolescents from Moscow belong to the first group, their peers from Plovdiv belong to the second, e.g. both groups are at different stages of microevolutionary transformations.

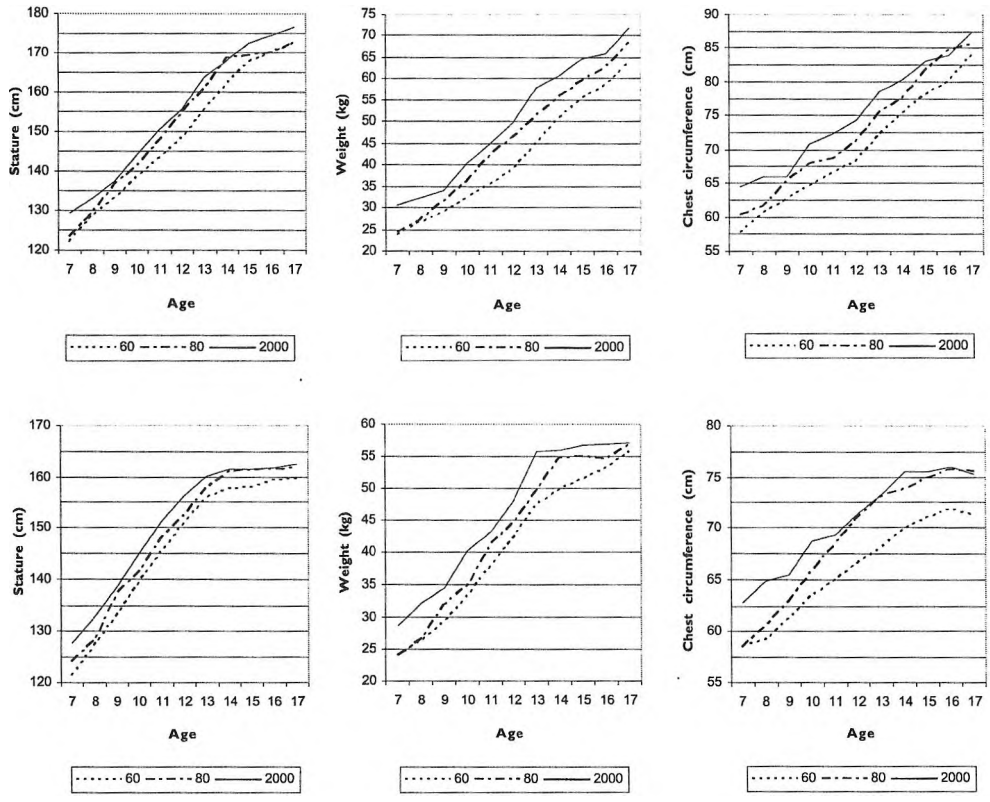

Fig. 2. Secular changes in children from Plovdiv

The secular changes in the body parameters are also complemented by the processes of brachy and debrachycephalization. In both populations an increase in the head length and the morphological height of the face is observed — for a period of 30-40 years with 4-9 mm depending on the age group, which corresponds to a difference in the stature of 4-9 cm. The breadth parameters of the head and face on the whole remain at the level of that in the 60's.

It is well known that there is a direct correlation between longitudinal head and face parameters and the stature. This fact indirectly shows that the possible reason for the changes of the parameters is the correlation of the age dynamics with the general growth processes. The changes in the mean values of the longitudinal head and face dimensions are reflected on the shape of the two divisions of the head. As shown in Tables 1 and 2, in both populations the changes in time are towards decrease of the measurements of the head index and increase in the face index. In the case with the children from Moscow, there is a stabilization of the stature, which shows that the morphological changes in the head proportions are not entirely due to acceleration changes. In the case with the children from Plovdiv, the processes occur together with ongoing positive changes of body parameters.

T a b l e. 1. Secular changes in the head and face index of children from Moscow

Age	Head index						Face index			
	boys			*girls*			*boys*		*girls*	
	1940's	*1960's*	*1990's*	*1940's*	*1960's*	*1990's*	*1960's*	*1990's*	*1960's*	*1990's*
7	84.0	84.9	82.2	82.9	83.7	80.7	79.0	91.2	77.5	90.9
8	83.3	84.1	80.7	82.8	84.4	79.9	77.8	92.1	78.4	91.9
9	84.0	83.0	80.9	83.1	84.7	80.0	78.4	93.4	77.9	92.4
10	82.5	84.0	81.3	83.3	83.7	80.7	77.6	91.5	78.1	92.4
11	82.6	83.5	80.1	83.0	83.8	80.9	77.0	90.3	77.6	91.3
12	82.3	84.0	80.9	83.1	83.0	81.0	77.3	90.6	77.5	90.5
13	82.7	83.7	80.0	82.0	83.4	79.6	76.8	91.5	92.0	90.6
14	83.6	82.2	80.3	82.5	83.1	80.2	75.8	92.0	76.7	91.1
15	83.1	82.6	80.0	82.9	83.8	80.7	75.4	91.6	77.1	90.8
16	82.9	82.7	79.2	82.5	83.4	79.6	75.8	92.0	77.1	89.6
17	82.2	81.9	80.0	82.9	83.1	81.8	75.5	91.3	77.3	88.9

T a b l e 2. Secular changes in the head and face index of children from Plovdiv

Age	Head index						Face index					
	boys			*girls*			*boys*			*girls*		
	1960's	*1980's*	*2000's*	*1960's*	*1980's*	*2000's*	*1960's*	*1980's*	*2000's*	*1960's*	*1980's*	*2000's*
7	82.76	81.59	77.51	82.62	80.23	79.14	81.09	83.76	95.03	79.77	84.15	95.22
8	82.23	80.29	79.63	82.78	79.06	80.57	81.64	85.15	94.95	81.14	84.17	96.27
9	82.14	80.87	80.23	82.39	80.17	80.18	82.29	86.27	96.98	81.38	83.60	95.47
10	81.78	81.28	79.48	82.46	79.93	80.01	82.39	86.65	98.89	81.55	85.21	96.29
11	81.45	81.14	79.50	81.73	80.79	79.80	83.14	92.19	97.06	82.25	87.85	94.06
12	81.74	82.20	78.14	81.83	81.22	78.65	83.38	95.17	94.23	82.94	95.93	96.40
13	81.59	81.12	78.18	81.68	81.32	79.36	83.58	96.52	95.87	82.79	94.88	94.43
14	81.30	80.07	79.02	81.58	81.78	79.18	84.34	94.73	95.88	82.99	93.28	93.52
15	80.79	81.77	79.01	81.70	82.26	79.22	85.42	93.90	96.75	83.76	93.47	95.54
16	80.74	82.65	78.16	81.40	80.60	78.42	84.91	92.96	94.56	82.42	93.22	92.05
17	81.02	80.82	78.84	81.70	80.78	80.65	84.67	93.07	93.44	82.69	95.71	92.93

Conclusion

The growth curves of the basic somatometric parameters in the two populations show that they are at different stages of micro-evolutionary transformations. In the last decade of the 20th century the children and adolescents from Moscow show a certain stabilization of the stature, the beginnings of negative changes in weight and reliable decrease of chest circumference, especially in the case of girls. The children and adolescents from Plovdiv, at the end of the 20th century and the beginning of the 21st century, still have positive changes in stature, weight and chest circumference.

Secular changes in the shape of the head and face show that both populations after the 90's exhibit certain debrachycephalization and increase of leptoprosopnosis.

The time-related changes in both body parts in children from Moscow occur independently, whereas in the case of the children from Plovdiv, the transformations are more synchronized.

Acknowledgements: This study was supported by the National Fund of Scientific Research, Bulgarian Ministry of Science and Education, grant No B 1404/2004.

References

1. Gyenis G. Rapid change of head and face measurements in university students in Hungary. — Anthrop. Anz., **52**, 1994, 149-158.
2. Jaeger, U., K. Kromeyer-Hauschild. Growth studies in Jena, Germany: Changes in thoracic measurements between 1975 and 1995. — Amer.J.Hum.Biol., **11**, 1999, 786-792.
3. Martin, R., K. Saller. Lehrbuch der Anthropologie in sistematischer Darstellung. T. I. Stuttgart, Gustav Fischer Verlag, 1957, 273-395.
4. Zellner, K., U. Jaeger, K. Kromeyer-Hauschild. Das Phnomenon der Debrachykephalisation bei Jenaer Schulkindern. — Anthrop. Anz., **56**, 1998, No4, 301-312.
5. Zellner K., K. Kromeyer-Hauschild, J. Stadtler, U. Jaeger. Ergebnisse der Untersuchung ausgewählter Kopfmaße bei Jenaer Kindern. — Anthrop. Anz., **57**, 1999, No2, 147-163.
6. Година, Е. З., А. Л. Пурунджан, И. А. Хомякова. Эпохальная трансформация размеров тела и головы у московских детей и подростков как критерий микроэволюционных процессов. — В: Народы России. Антропология, 2 (Под. ред. Т.И.Алексеевой), М., 2000, 305—330.
7. Година, Е. З., А. Л. Пурунджан, И. А. Хомякова, М. И. Николова. Особенности процессов роста у детей и подростков Болгарии,Польши и России. Korektywa I kompensacja zaburzen w rozwoju fizycznym dzieci i mlodziezy, tom I (pod redakcja K.Gorniak). Biala Podlaska, 2005, 129—140.
8. Хомякова, И. А., Е. З. Година, Л. В. Задорожная, А. Л. Пурунджан. Морфологические особенности головы и лица у детей и подростков Московского региона. — В: Народы России. Антропология., 1. (Под. ред. Т. И. Алексеевой), М., 1998, 95—113.
9. Ямпольская, Ю. А. Физическое развитие школьников — жителей крупного мегаполиса в последние десятилетия: состояние, тенденции, прогноз, методика кринин-оценки. Автореф. дис. труд. М., 2000. 76 с.

Institute of Experimental Morphology and Anthropology with Museum
Bulgarian Anatomical Society

Acta morphologica et anthropologica, 13
Sofia • 2008

Characteristics in the Dynamics of Physical Development of Students Aged 14-18 Years

T. Stoev, Zh. Hristov, S. Savov

Medical University, Plovdiv

Certain characteristics have been traced in the individual development of students of the two sexes aged 14-18 years in two surveys carried out with an interval of 20 years. Making use of different methods an assessment has been made of the degree of development and the related alterations of the basic morphological, functional and motive indexes.

It is stressed that as a phenomenon acceleration has been on the wane in recent years which affects the total body sizes, the changes in the vegetative functions and motive activity. It is pointed out that the type of acceleration and retardation processes — harmony and disharmony, should be taken into consideration when assessing the different types of indexes of the individual.

Key words: physical, biological and psycho-emotional development.

An organism's physical development is a complex biological process the regulation of which is affected by a number of endo- and exogenic factors. They result in quantitative and qualitative alterations, in an organism's morpho-functional indexes, taking place at different speed and continuance.

The influence of the secular trend and the acceleration in growth is being taken into account in the past decades and this changes the general somatic appearance of the individual persons and of the entire population.

The indicated characteristics in the development of the individual explain the emerging "sensitive" critical periods during which the individual development is characterized by a specific set of the most efficient factors of the environment, which combined with the genetic preconditions reveal an organism's biological potential in the best way.

The interest of anthropologists in the connection between structure and function is justified because defining the ideal model of physical fitness always corresponds with an optimal structure.

Material and Methods

The results from the alterations in the basic medico-biological indexes of the students in the 14-18-year age bracket have been compared during two four-year peri-

ods (1980-1984; 2000-2004) from Plovdiv and Haskovo districts. 243 boys and 198 girls were observed during the first period, while in the second one - 296 boys and 212 girls, evenly distributed in the abovementioned age groups.

The characteristics of observation of the units were distributed in several groups: assessment of the degree of development; alteration in the basic morphological indexes; alteration in the functional indexes; assessment of the motive activity.

The assessment of the degree of biological maturity was carried out by means of $R_{\bar{e}}$ and skeletometric methods in the first period and through skeletometric methods in the second period.

The standard anthropometric methods were used to assess the morphological indexes, while the functional indexes were assessed by means of tests and apparatus methods. The motive activity was assessed through tests characterizing the basic motive qualities and coordination capabilities of the individual.

The annual growth in the individual types of indexes and the general growth for the periods under examination were traced. This provided for an opportunity to highlight certain characteristics of the development and its more precise prognostication.

The data from the surveys have been presented in numerous tables and diagrams.

Results

To assess the degree of development we used the correlation between the calendar and biological age and the degree of alteration in the individual indexes.

The deviations from the norm of the biological development in relation to acceleration and retardation in the two sexes in the periods under examination were traced. It has been proved that the variation width of the differences is the biggest with boys of over 14 years. With girls it begins considerably earlier, yet certain changes are observed in this period. The analysis of the data shows that during the 2000-2004 period the deviations were less well manifested as compared to the first period under examination, which testifies to a halt and a decrease in acceleration as a phenomenon. (Figs. 1 and 2).

Tracing the type of acceleration and retardation in the compared periods shows that it changes differently with boys and girls. During the first period 95.78% пf the boys and 91.87% пf the girls showed a harmonious type of acceleration. During the second period these figures were respectively: 96.05% and 95.54%. In assessing the retardation for the first period 90.37% пf the boys and 88.32% пf the girls showed a harmonious type of retardation, while in the second period the figures were 96.29% and 94.97% respectively.

What impresses is that with girls the harmonious type of retardation decreases in the second period, while the disharmonious one increases. As far as boys are concerned, both types of retardation increase in the second period under examination.

The puberty leap with the accelerated boys takes place in a saltatory mode, for a short period of time and has its peak before 15 years. With the normally developed boys it is witnessed in the 16th year too, but is not too well manifested. With retarded boys the puberty leap is even, does not show a pronounced peak and has a longer duration.

As for the accelerated girls over 14 years of age a continuation of the earlier reached peak is witnessed after which the development starts to descend. The normally developed girls mark a peak in the puberty leap in their 14th year and the height increases though at a less acceleration speed. With retarded girls the puberty leap has a plateau-like acceleration of an even nature and longer duration.

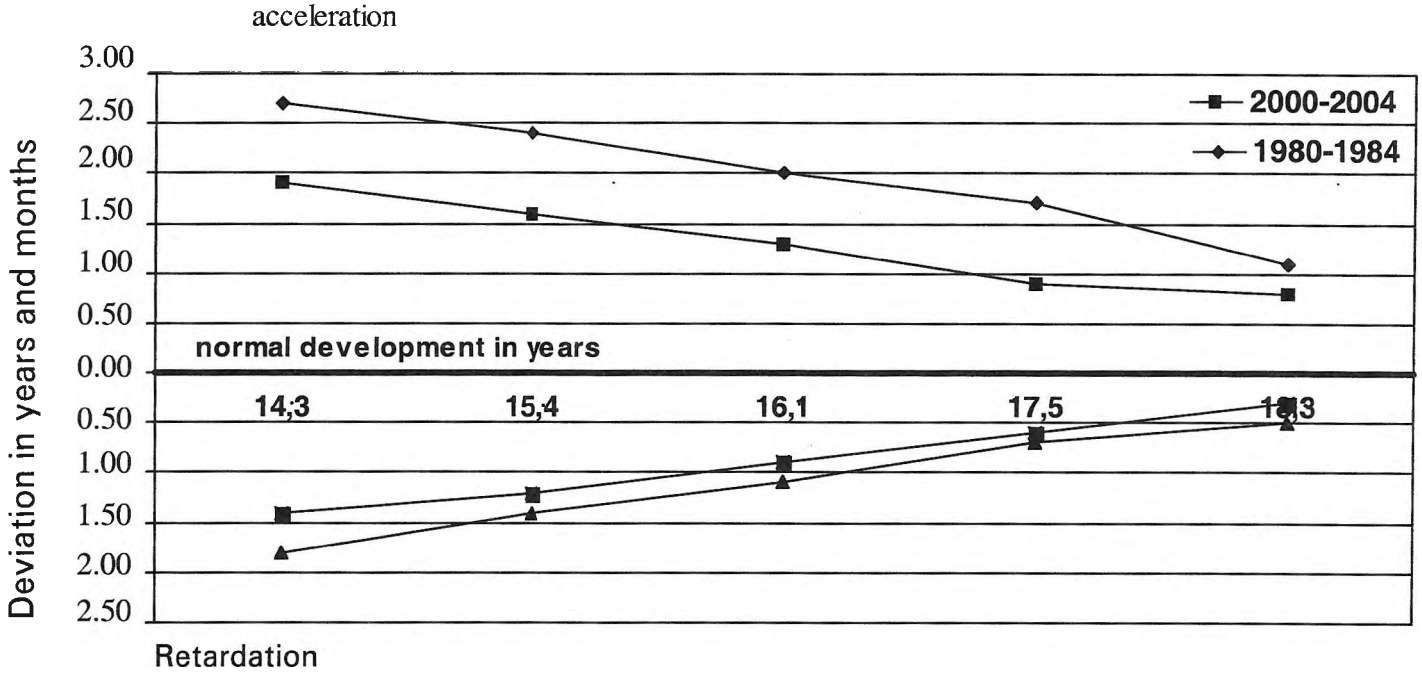

Fig. 1. Degree of biological maturity of boys 14-18 years of age studied in the periods 1980-1984 and 2000-2004 (in years and months)

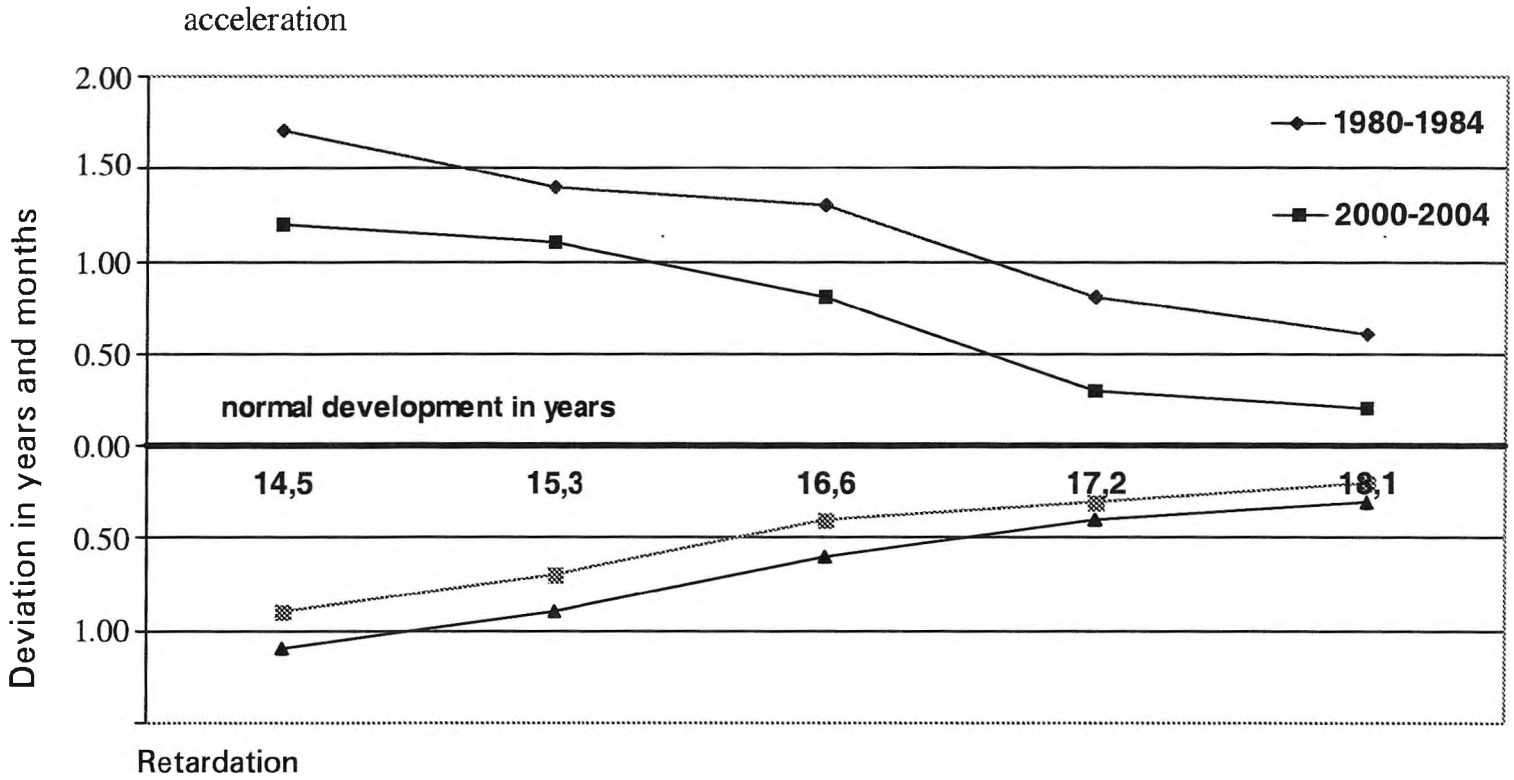

Fig. 2. Degree of biological maturity of girls 14-18 years of age studied in the periods 1980-1984 and 2000-2004 (in years and months)

Both surveys testify to one and the same data concerning body proportions. The children of an earlier maturation have a relatively longer torso, shorter limbs, wider diameters of the chest and chest measurements. This is used for a purposeful selection in sports, art and some other professions.

There also exist differences concerning the vegetative indexes of children with a different biological development. Most often they are connected with changes in the pulse frequency, the cystologic, diastolic and pulse blood pressure, with the speed of the blood flow, the stroke and minute volume of the heart, the use and absorption of oxygen, the power supply, economization of the vegetative functions, etc.

The harmonious and disharmonious types of acceleration and retardation show different adaptive reactions to the cardio-respiratory system and the homeostatic regulative reactions.

The morphological status of children in the different stages of biological maturation influences the dynamics of growth of the motive and coordination capabilities which is most clearly seen between 13-14 and 15 years of age. This plays an important role in assessing the planning of the educational and training load and for forecasting the high sports breaks.

Conclusions

- The overall assessment of the growth and development should always take into consideration the degree of the biological maturation and the way it runs.
- The results of the two surveys (with an interval of 20 years) show a lull and decrease in acceleration as a phenomenon.
- Nearly 1/3 of the normal population shows an accelerated or retarded development of organism as a whole, or of one or several of its indexes.
- No statistically significant differences between the participants surveyed by us and the Bulgarian population with regard to height and the body mass have been established.
- The nature of an individual's development influences the functions of the individual systems and of organism's motive activity.

References

1. Deryabin, B. E. Miometry in anthropology. — In: Anthropology. M., 2004, 835-849.
2. Procopes, M. Secular trends body size and proportions and their biological meaning. — Stud. Hum. Ecology, **6**, 1998, 37-61.
3. Pades, C., F. Johnston. Secular trends factors on the morphological and functional characteristics childen in Portugal. — Amm.Hum.Biol., **26**, 1999, 287-298.
4. Rostak, M., H.S.Wtolarezuk. Secular changes of massiveness of body structure in children of Lodz. — M. Anthropologi, **2**, 674-685.
5. Schroeder, G. Talend und Sporttypologie. — Med. Sport., **9**, 1998, 284-289.
6. Василев, С. В. Основы возрастной и конституциональной антропологии. М.,1996. с. 327.
7. Кузма, В. Р. Некоторые особености физического развитие детей и подрастков на современном этапе. Здяраву реблека Мат. конф. педиат., России. 2002, 201-217.
8. Никитюк, Б. А. Акцелерация развитие детей и ее последствия. — В: Алма Ата сб. докл. 1999, 176—193.
9. Савов, С. Лонгитудинални проучвания върху възрастовата динамика и надеждност на медико-биологичните критерии в развитието. С., 1989, ДД-316.
10. Стоев, В., З. Станчев. Спорт и пубертет. София, МФ, 1981, с. 167.
11. Халдеева, Н. И. Антропометрическое разнообразие и опыт его анализа. — М. сб. Эколог. и демограф.человека, **3**, 2004, 112—113.

Institute of Experimental Morphology and Anthropology with Museum
Bulgarian Anatomical Society

Acta morphologica et anthropologica, 13
Sofia • 2008

Some Upper Extremity Proportions in the Young Turkish Male Adults

O. Taskinalp, R. Mesut, L. Elevli

Trakya University, Faculty of Medicine, Department of Anatomy, Edirne, Turkey

In this study our aim was to investigate the relationships of the lengths of the upper extremity parts to their circumferences in the Turkish male adults. 532 male students who were studying at the Trakya University Faculty of Medicine in the period 1986-1993 participated in our study. We found the arm length as 34.82±2.55 cm, the forearm length as 24.94±2.16 cm and the hand length as 18.92±1.5 cm while the circumference values for the arm, the forearm and the hand were 26.87±2.81 cm, 25.95±1.85 cm and 20.79±1.11 cm, respectively. The arm circumference/arm length ratio was 69.21%, the forearm circumference/forearm length ratio was 104.04% and the hand circumference/hand length ratio was 109.88%. Considering these values while the arm circumference/arm length ratio was approximately 2/3 the forearm and the hand circumferences were higher than their lengths.

Key words: anthropometry, upper extremity, circumference.

Introduction

The history of the studies concerned with the human body begins from the time of Hippocrates. These studies which were for scientific purposes formerly became artistically oriented during the Renaissance so that they were inspirational for many artists. The artists such as Polykleitos, Lysippos, Guyaume, Vitruvius, Michelangelo and Paul Richer worked on the theme of the human body and created such masterpieces that are admired by the society even today [1, 2, 3, 12]. "The Scientific Rule" was used in the measurements concerned with the human formerly [1, 3], then Fritsch found "The Fritsch Rule" improving on this. Physical anthropologists used these rules to reveal the racial differences [5] in their studies. They considered that there were many proportions in the human body while they were doing those studies.

The measurements of the different parts of the human body and the ratios between these measurements became commercially useful as well as they have been in arts as a consequence of developing technology. Those measurements and ratios which are especially important in the clothing and automotive fields differ between the societies. With this regard we believe that the results of our study will be useful for the Turkish clothing industry.

Material and Methods

We conducted our study in the anthropometry laboratory in the Depatment of Anatomy of the Trakya University, Faculty of Medicine. 532 male students who were studying at the Faculty of Medicine between the years 1986-1993 participated in our study. All the measurements were done by the same researcher at the same time of the day. A ruler fixed to the wall, a pelvimeter and a tape measure made of cloth, all with milimetric scales were used in the study. All the data were recorded using forms prepared before and they were analyzed statistically in the NCSS programme.

Upper extremities are the parts of the body with the greatest mobility and connected to the upper lateral sides of the trunk by the shoulder joint. In the anatomical terminology extremities are called as membrum or member but the preferred term is extremities [6, 7, 8, 9]. Anatomically upper extremity is divided into three parts; the arm, the forearm and the hand. These parts are seperated from each other with the shoulder, cubital and wrist joints, respectively [8, 9, 10, 11].

We first determined the anthropologic landmarks before the measurements we have done on the upper extremity. Then we performed our measurements from these points. Our measurements and the anthropologic landmarks we used in these measurements are below [3, 4]:

1. **Arm length:** The distance between the acromion (acromiale) and the radiale.
   Acromion: The highest lateral process of the processus acromialis.
   Radiale: The highest point of the lateral border of the caput radii.
2. **Forearm length:** The distance between the radiale and the stylion.
   Stylion: The lowest point of the processus styloideus radii.
3. **Hand length:** The distance between the radiale and the dactylion.
   Dactylion: The lowest point of the middle finger.
4. **Arm circumference:** The measurement taken from the widest part of the arm.
5. **Forearm circumference:** The measurement taken from the widest part of the forearm.
6. **Hand circumference:** The masurement taken from the widest part of the palm of the hand.

Results

The length, the circumference and the circumference/length ratios of the parts of the upper extremity are shown in Table 1.

Discussion and Conclusion

In our literature review we encountered length measurements on the upper extremity. However, we could not find any article concerned with the circumference measurements and the length/circumference ratios.

T a b l e 1. The lengths, the circumferences and the circumference/length ratios of the parts of the upper extremity

Upper extremity part	Length, cm	Circumference, cm	Circumference/length ratio, %
Arm	34.82±2.55	26.87±2.81	69.21
Forearm	24.94±2.16	25.95±1.85	104.04
Hand	18.92±1.5	20.79±1.11	109.88

We found the arm length as 34.82 cm, the forearm length as 24.94 cm and the hand length as 18.92 cm. Kahraman found these lengths as 32.21 cm, 25.2 cm and 19.51 cm, respectively while these values were 32.48 cm, 24.22 cm and 20.97 cm in Muftuoglu's study [5]. In a study conducted in USA these lengths were 28.20 cm, 25.1 cm and 19 cm, respectively. When we compare our arm length values were significantly different from the US based study while the differences were lower with the Kahraman's and Muftuoglu's studies [1, 5]. But the differences between the forearm lengths were minimal [2, 3, 5, 7].

The arm circumference/arm length ratio was 69.21% while these values were higher than 100% for the forearm and the hand. We could not make any comparison for these data as there are no previous data in the literature. We think that the reason for the ratio higher than 100% is related to the structure of the extremities and the population's inactivity in sports.

Considering the hand we think that the ratio higher than 100% is related to the anatomical structure and this ratio is not much prone to a high degree of variability.

References

1. Kahraman, G. Yetiskin Türk Kadin ve Erkeklerinde Ust Ekstremite Olcumleri ve Oranlari. Istanbul, Uzmanlik Tezi, 1988.
2. Lumley, J.S.P. Surface Anatomy. — In: The Anatomical Basis of Clinical Examination. International Student Edition (Second Edition). Edinburgh, London, Churchill-Livingstone, 1966, 55-84.
3. Mesut, R., M. Yildirim. Insan Vucudunda Antropolojik ve Yuzeyel Bulus Noktalari. Istanbul, Beta Basim Yayim Dagitim A.S., 1989, 51-60.
4. Mesut, R., M. Yildirim. Disseksiyona Yonelik Topografik Anatomi. T.2.Ekstremiteler. Istanbul, Beta Basim Yayim Dagitim A.S., 1995, 11-23.
5. Muftuoglu, A. Yetiskin Türk Erkeklerinde Bazi Vucut Olculeri ve Aralarindaki Oranlar. İstanbul, Uzmanlık Tezi. 1981.
6. Ozer, K. Antropometri, Sporda Morfolojik Planlama. Istanbul, Kazanci Metbaasi, 1993, 44-46, 133.
7. Pestemalci, T., G. Kahraman. Türk Erkeklerinde Ust Ekstremiteye Ait Bazi Olcumler ve Oranlar. — Morfoloji Dergisi, 9, 2001, No2, 37-40.
8. Saran, N. Antropoloji. Inkilap Kitabevi, Istanbul, 1993.
9. Sinnatamby, C. S. Last's Anatomy, Regional and Applied (Tenth Edition). Edinburgh, London, Churchill-Livingstone, 1999, 35-36.
10. Taskinalp, O. Yetiskin Türk Kadin ve Erkeklerinde Aksiyal Vucut Caplari ve Cevreleri. Edirne, Uzmanlik Tezi, 1989.
11. Zeren, Z., I. Eralp. Kisa Topografik Anatomi (Dorduncu Baski). Istanbul, Sermet Matbaasi, 1972.
12. Чоканов, К. Пластична анатомия. София, НИ, 1994, 370—395.

Institute of Experimental Morphology and Anthropology with Museum
Bulgarian Anatomical Society

Acta morphologica et anthropologica, 13
Sofia • 2008

The Achieved Growth of Basic Anthropometrical Features and Their Proportionality in Newborn Infants Compared to Respective Data in Adults

I. Yankova

Institute of Experimental Morphology and Anthropology with Museum, Bulgarian Academy of Sciences, Sofia, Bulgaria

The aim of the study is to assess the achieved growth of basic anthropometrical features and their proportionality at birth, compared to the anthropometrical status in adults. The anthropological investigation of 110 fullterm newborn boys and 109 fullterm newborn girls was carried out during 2001 in Sofia. The metrical data about five basic body sizes at birth and 4 indexes, giving information about proportionality between separate body parts are presented. The newborn boys have bigger sizes of the studied features, while the relative shares of these features compared to the final sizes in adults are bigger in newborn girls. The gender differences in absolute sizes of the anthropometrical features at birth are better marked compared to these about indexes of body proportionality. The results obtained characterize quantitatively the forthcoming changes after birth for proportionality between the lengths of torso and lower extremities and between the upper and lower extremities lengths.

Key words: anthropometrical features, proportionality, growth, fullterm newborns, adults.

Introduction

The basic characteristics of physical development in newborn infants are important indicators for their health state at birth, for the specificity of prenatal development, as well as, for the prognosis of future harmoniously body development of the child [1, 2, 4, 5]. The purposeful anthropological investigations for the determination of body maturity and body proportionality at birth could give information for these characteristics.

The **aim** of the present study is to assess the achieved growth of basic anthropometrical features and their proportionality at birth, compared to the anthropometrical status in adults.

Material and Methods

A detailed anthropological investigation of 219 fullterm clinically healthy newborn infants (110 boys and 109 girls) was carried out during the period of April-May 2001

in the ward of Neonatology at II[nd] Hospital of Obstetrics and Gynecology "Sheynovo"— Sofia. The anthropometrical measurements were taken using the Martin-Saller's classical methods [3], in a lying position of the child, from the right side of the body.

In this report we present the metrical data about five features, which reflect basic body sizes at birth and 4 indexes, giving information about body shape and proportionality between separate body parts.

To assess the achieved growth at birth we used not published till now data from the National Anthropological Program (NAP) of the IEMAM — BAS about mature Bulgarian population (30-40 years) from Sofia at the end of the 20[th] century.

Results

The assessment of physical development is led in two directions — in relation to the body sizes and about the proportionality between separate body parts and segments.

Comparative assessment of basic body sizes

The obtained metrical data of the basic body sizes are presented in Table 1 and Fig. 1.

The newborn boys have bigger sizes of five directly measured anthropometrical features, which show that even at birth the tendency of gender differences for body sizes that are typical for adults is marked. The biggest absolute differences between both genders of newborns are established for the stature (4.2 mm), and the smallest — for the lower extremities' length (0.6 mm).

Notwithstanding the metrical priority for boys, the relative shares of each five anthropometrical feature compared to the final sizes in adults are bigger in the newborn girls. The achieved growth of these features by them varies between 24.04 per cent and 34.64 per cent, and by boys — between 22.62 per cent and 32.02 per cent. The torso length for both genders is nearest to the final sizes at birth as the girls have priority over the boys with 2.62 per cent. The biacromial breadth and stature are the following features in newborn girls that achieved 30.0 per cent and more from the final sizes in adult women. In the newborn boys the achieved growth of these features is already under 30.0 per cent. The growth of their biacromial breadth up to birth is lower with 2.8 per cent than in girls, and of their stature with 1.95 per cent. The newborns from both genders have smallest relative shares about upper and lower extremities' length compared to their sizes in adults. For the upper extremities' length and the lower extremities' length the girls have priority over boys with 1.79 per cent and 1.42 per cent respectively.

T a b l e 1. The absolute values and relative shares of body sizes in newborn infants compared to the respective data in adults

Features	Fullterm newborns						Adults (30-40 years old)			
	Boys (n = 110)			Girls (n = 109)			Males (n = 230)		Females (n = 271)	
	X	SD	% from adults	X	SD	% from adults	X	SD	X	SD
1. Stature	505.5	14.9	29.22	501.3	16.5	31.17	1730.0	64.9	1608.1	58.1
2. Torso length	172.9	9.0	32.02	173.6	8.6	34.64	540.0	30.6	501.2	27.2
3. Biacr. breadth	119.9	7.0	29.30	118.0	6.3	32.10	409.2	22.3	367.6	18.1
4. Upper extr.length	210.4	9.1	27.53	207.2	7.9	29.32	764.2	39.5	706.6	33.2
5. Lower extr.length	220.8	8.3	22.62	220.2	7.9	24.04	976.3	53.5	915.8	43.7

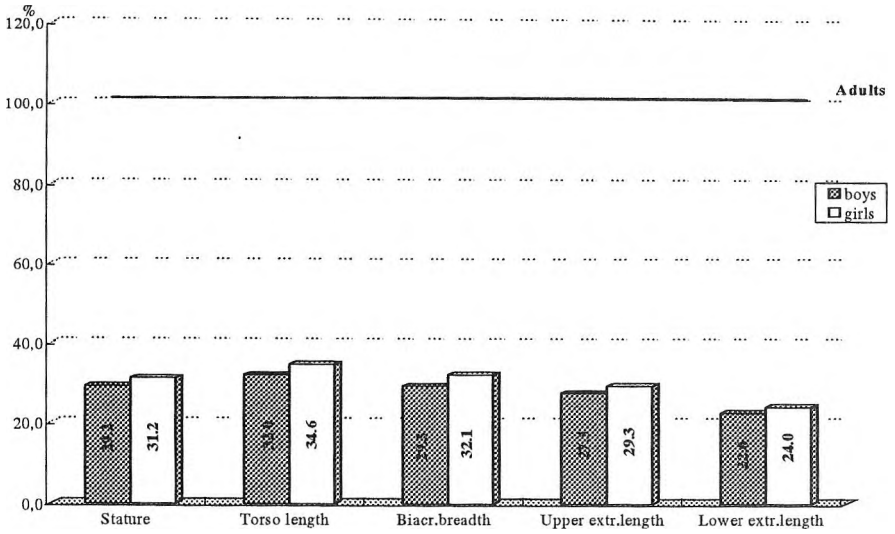

Fig. 1. The achieved growth of basic anthropometrical features in newborn infants compared to the final sizes in adults

Comparative assessment of body proportionality

In this study we make an attempt to characterize quantitatively the differences between body proportionality at birth and body proportionality in adults (Table 2, Figs. 2, 3).

The gender differences of the achieved body proportionality at birth are lower, compared to these in the absolute sizes of the anthropometrical features. The biacromial breadth proportion in newborn infants from both genders is nearest to the same one in adults. This result shows that at birth the proportionality between both sizes of shoulder girdle and stature is already formed.

The biggest differences between newborn infants and adults are established for the ratio lower extremity length/torso length. The relative length of lower extremities at birth is quite lower (about 30.0 per cent) than it is in adults and the formation of their proportionality continues during the following stage of postnatal ontogenesis. The torso length related to stature is about 10.0 per cent bigger at birth, compared to this in adults. The data from interextremities index show that the upper and lower

T a b l e 2. Body proportionality in both newborns and adults — comparative assessment

Indexes	Fullterm newborns						Adults (30-40 years old)			
	Boys (n = 110)			Girls (n = 109)			Males (n = 230)		Females (n = 271)	
	X	SD	% from adults	X	SD	% from adults	X	SD	X	SD
1. Torso length proportion	34.20	1.42	109.62	34.63	1.39	110.99	31.2	1.5	31.2	1.5
2. Biacr. breadth proportion	23.73	1.20	100.13	23.56	1.21	102.88	23.7	1.2	22.9	1.1
3. Interextremities index	95.33	3.61	121.75	94.17	2.98	121.98	78.3	2.9	77.2	2.8
4. Lower extr.length / Torso length	127.94	6.19	70.76	127.07	6.23	69.54	180.80	-	188.72	-

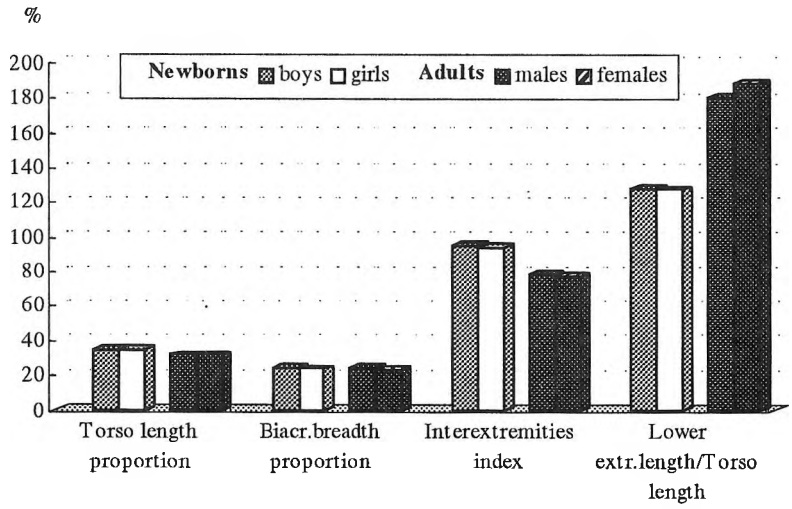

Fig. 2. Gender differences in the body proportionality

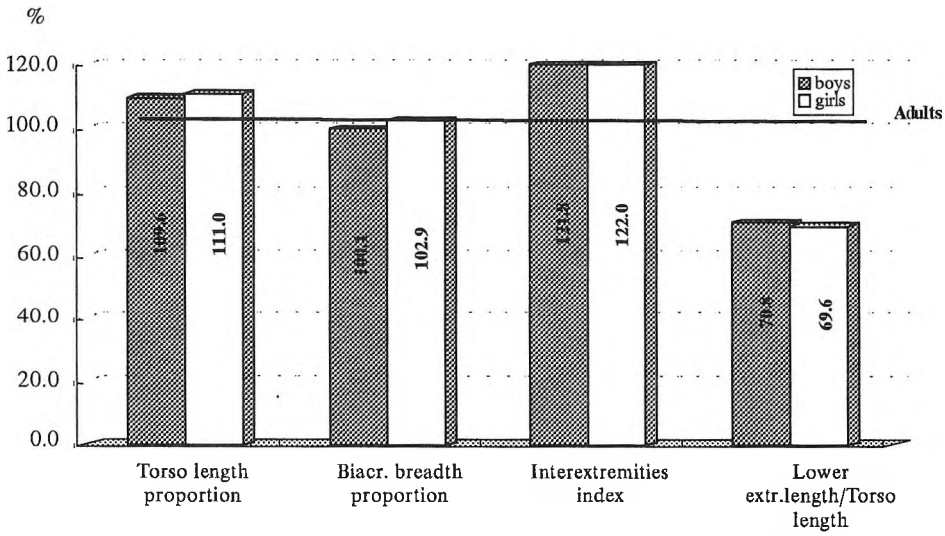

Fig.3. Body proportionality in newborn infants compared to the proportionality in adults

extremities' length have similar values at birth, while in adults the upper extremities' length is smaller with 20.0 per cent and more from the lower extremities' length.

The changes of body proportionality after birth show tendencies to increment of the relative length of lower extremities, compared to the torso length approximately by 30 per cent; to decrement of the relative torso length, compared to the stature approximately by 10 per cent and to a change of the proportion of both extremities lengths, in order to reach their proportionality in adults.

Conclusions

- The newborn boys have bigger sizes for the five studied anthropometrical features of physical development than newborn girls;
- The newborn girls have bigger relative shares of the same features compared to the final sizes in adults;
- The gender differences in absolute sizes of the anthropometrical features at birth are better marked compared to these differences in the indexes of body proportionality;
- The results obtained characterize quantitatively the forthcoming changes after birth for proportionality between the lengths of torso and lower extremities and between the upper and lower extremities lengths.

References

1. Falkner, F., J. M. Tanner. Human Growth — 2nd Edition. New York and London, Plenum Press, 1987, 1-537.
2. Johnston, P. The newborn child. Edinburgh, Vulliamy's Churchill Livingstone, 1994, 29-32.
3. Martin, R., K. Saller. Lehrbuch der Anthropologie in sistematischer Darstellung. Bd. I. Stuttgart, Gustav Fischer Verlag, 1957, 322-324.
4. Tanner, J. M., R. H. Whitehouse, M. Takaishi. Standards from birth to maturity for height, weight, height velocity, and weight velocity: British children, 1965. I. — Arch. Dis. Child., 41, 1966, 454-471.
5. Бобев, Д, Е. Генов. Педиатрия. 2000.

Institute of Experimental Morphology and Anthropology with Museum
Bulgarian Anatomical Society

Acta morphologica et anthropologica, 13
Sofia • 2008

Relevance of the Antique Canons to the Contemporary Turkish Males

A. Yilmaz , R. Mesut

Trakya Universty, Faculty of Medicine, Department of Anatomy, Edirne, Turkey

106 male students and research assistants without any orthopaedic problems and studying in different departments of Trakya University took part in our study which we determined the body proportions of young Turkish men and searched the congruity of the results with the antique canons.

The measurements of the subjects were performed in our "Laboratory of Anthropometry". Harpenden anthropometer was utilized in these measurements. We were obliged to include the empirical points defined by the artists in addition to the established anatomical structures in the anthropometric guidelines.

Testing the compatibility of the oldest four Canons (The Ancient Egyptian Canon; The New Egyptian Canon; The Greek Canon; The Roman Canon) to the young Turkish men is the aim of our study.

Key words: Artistic anatomy, anthropology, body proportion.

Introduction

All civilizations that have existed so far have treated the human body by their own social understanding and culture [2]. In the ancient and the new Egyptian (Ptolemaic) art closely related to religious beliefs and legends, men figures are illustrated as wide shouldered, narrow hipped and thin waisted.

In the ancient Greek art which represents a more sophisticated level, beauty, virtue, independence, love and immortality themes were embodied in the human figures.

In the plastic arts, the Romans pursuing the apprehension inherited from the Greeks, meant to embody the martial force and discipline by the magnificient statues of their commanders and emperors that they are proud of [11]. During this period known as the Antique Age, the Egyptian, Roman and Greek artists tried to fix the human body as an ideal shape and to make it systematic by setting some rules [9].

Material and Methods

150 male students and research assistants without any orthopaedic problems and studying in different departments of Trakya University took part in our study. Regional differences and socioeconomical factors were not taken into consideration.

All of the parameters were measured on our all subjects. But as our intention was not to find the anthropometric values of a randomly-selected population, we had to make a selection. As our emphasis was on artistic criteria, the very tall and the very short and the very weak and the very fat subjects were not comprised into the statistical analysis. Those who were below 18 years and over 30 years of age were not comprised either. So, the data obtained from 44 subjects were not included in the statistical calculations. Considering these criteria, a total of 106 students and research assistants (36 from Faculty of Medicine, 16 from Kırklareli Undergraduate School of Health Sciences and 54 from Undergraduate School of Physical Education and Sports) whose mean age 22,4 years were included in our study.

The measurements of the subjects were performed in our laboratory of anthropometry. When measurements were done the subjects were required to undress, with the exception of a slip, for the measurements to be done. Harpenden anthropometer was utilized in our measurements. We were obliged to include the empirical points defined by the artists in addition to the established anatomical structures in the anthropometric guidelines. In the first stage of our study we have defined experimentally those points which are not included in the scientific literature and are anatomically ambiguous ("collum femoris", "cubitale", "plica carpalis distalis", "suprapatellare", "midpatellare", "infrapatellare"). We have assigned the parameters mentioned below using the measurements based on these anthropologic and empirical points (Fig. 1) [4, 10]: 22 metric measurements were done on our each subject and their arithmetic mean and standard deviation were calculated. The topic we were

T a b l e 1. Proportions and equations of the antique canons

I- Proportions

Ancient Egypt Canon	B-V / FL	6,33
New Egypt Canon	B-V / MFL	19
Greek Canon (Polykleitos)	B-V / HW	20
	HL / HW	2
	FH / HW	2
	Om-Sy / HW	2
	FL / HW	3
	Acr-Ol / HW	4
	Ol-Pha / HW	4
	St-Sy / HW	6
	B-SupP / HW	6
Roman Canon (Vitruvius)	B-V / HH	8

II- Equations

Greek Canon (Polykleitos)	MidP-Om = Om -Por
	BID = B-MidP = MidP-CF = CF-St
Roman canon (Vitruvius)	B-V = Armspan
	BID = Cub-Dac = 2*(Ax-Cub)

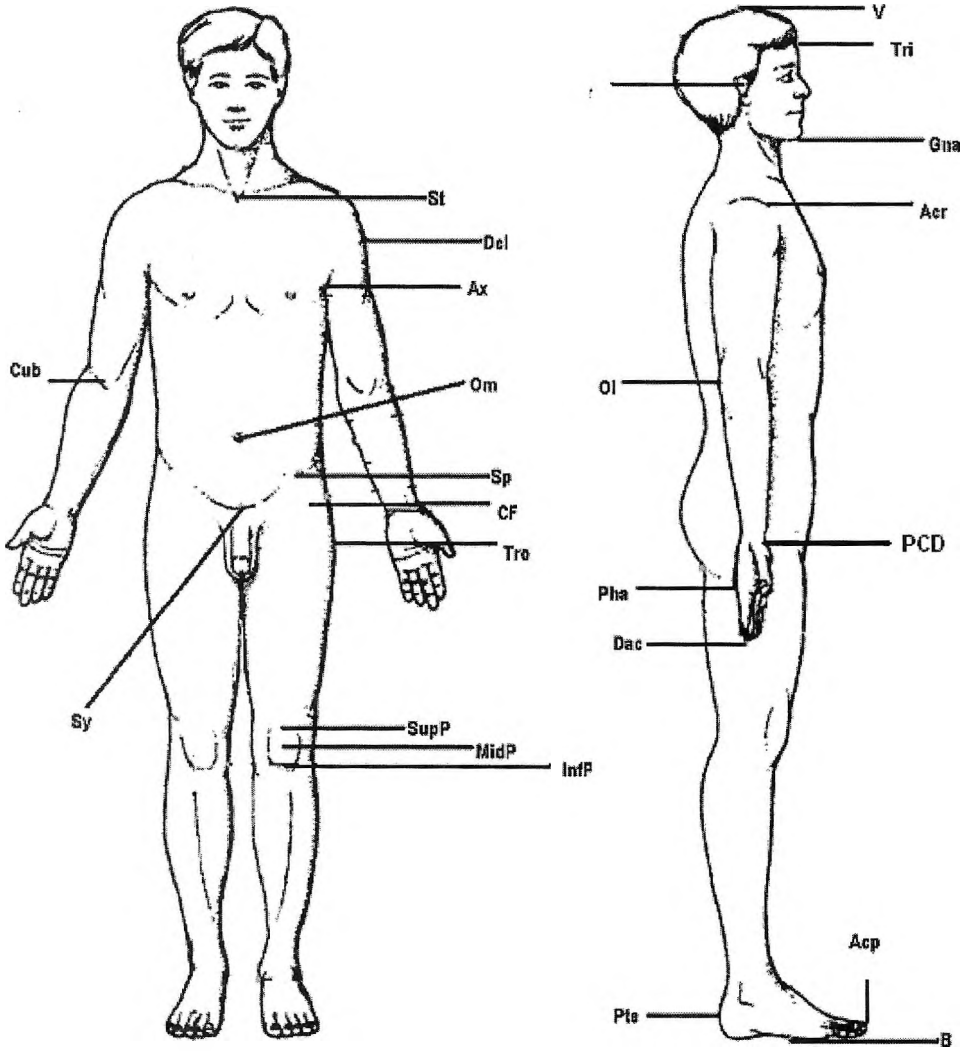

Fig. 1. Anthropological and artistic points
V—vertex; Tri—Trichion; Por—porion; Gna-Gnathion; St—sternale; Del—deltoidale; Acr—acromiale; Ax—axillare; Ol—olecranon; Cub—"cubitale"; Om—omphalion; Sp—spinale; Sy—symphysion; CF—"collum femoris"; PCD—"plica carpalis distalis"; Tro—trochanterion; Pha—phalangion; Dac—dactylion; SupP—suprapatellare; MidP—midpatellare; InfP—infrapatellare; Pte—pternion; Acp—acropodion; B—basion

T a b l e 2. Comparison of our subjects with Antique Canons

Features	Ancient Egypt	New Egypt	Greek Canon	Roman canon
B-V / FL	6.0±0.6	****	****	****
B-V / MFL	****	19.6±1.4	****	****
B-V / HW	****	****	21.6±1.8	****
HL / HW	****	****	2.0±0.3	****
FH / HW	****	****	2.0±0.0	****
Om-Sy / HW	****	****	2.5±0.5	****
FL / HW	****	****	3.0±0.9	****
Acr-Pha / HW	****	****	4.3±0.0	****
Ol-Dac / HW	****	****	4.3±0.3	****
St-Sy / HW	****	****	6.7±0.0	****
B-SupP /HW	****	****	6.1±0.9	****
B-V / HH	****	****	****	7.2 ±0.5

T a b l e 3. The percentage ratios of each of the segments in Polykleitos' equations to the stature

Parameter	Our subject (n=106)	Difference, %
MidP-Om/Body height(%)	32.0	100
Om-Por/ Body height (%)	32.7	101.
BID/ Body height (%)	25.5	100.
B-MidP/ Body height (%)	28.2	109.
MidP-CF/ Body height (%)	25.1	100
CF-St/ Body height (%)	28.	112.8

T a b l e 4. The percentage ratios of each of the parameters in "Vitruvius' equations" to the stature

Parameter	Our subject n=106	Difference, %
Body Height (cm)	175.6	
Armspan (cm)	180.8	+% 3.1
Body Height/Armspan	0.7	
BID/ Armspan (%)	25.1	100.0
Cub-Dac/ Armspan (%)	25.1	100.4
2*(Ax-Cub)/ Armspan (%)	27.6	110.9

focused on was the proportions and equations defined by the Egyptian artists, Polykleitos and Vitruvius.

The results we obtained from our subjects are shown in the Tables 2, 3, 4.

Discussion

"Module" concept in the artistic anatomy was created in the ancient times. In our study the modules utilized in the four canons we put emphasis on were FL (foot length); MFL (middle finger length); HW (hand width); HH (head height). We have determined the values of the modules mentioned above in a metric scale. There were some data published on the anthropometric measures of Turkish men albeit they were scattered. Despite methodological differences we compared our data with the ones published before. We found the stature/foot length ratio 6.60 which was specified as 6.33 in the ancient Egyptian Canon, the first canon we reviewed for compatibility to the young Turkish men. Although we have encountered many studies on foot length during our literature review none of these studies examined the relationship between this parameter and stature.

In Yildirim, Kahraman and Yildiz's studies the values they obtained were very close to each other and higher than ours [3, 7, 8] . Based on the studies conducted in the last decade we observed that the stature/foot length ratio was in a decremental trend although it was higher than the value (6.33) accepted by the ancient Egyptian artists. According to the artists who use the middle finger length as the determinant of stature. Stature/middle finger length ratio is 19:1. This ratio is 19.96:1 in our study. During our literature review we saw that only Yildirim and Kahraman studied on these ratios. The results they reported, 16.67 and 16.83, respectively were significantly different from ours [6, 7]. This difference appears to be due to the middle finger length measurement method they utilized. The percentage of the middle finger length to the stature is 5.0% in the young Turkish men which was 5.2% according to the Egyptian artists. It can be argued that the Turkish young men have shorter fingers according to the Egyptian artistic criteria.

We observed that all of our subjects did have higher values when we examined the ratios described by the eminent artist Polykleitos. These results were within our expectations as Turks have narrower and longer shaped hands. The most significant differences were in the ratios of upper extremity lengths to the hand width. In our literature review we observed that all the segments used in the ratios were examined seperately but as they were not examined as a whole we could not make any comparison with our data.

In the fourth canon we reviewed for compatibility to the young Turkish men, the Roman (Vitruvian) Canon, the stature was acknowledged as being equal to eight times the head height. In our study the stature/head height ratio was 7.82 for the Turkish men. Muftuoglu (1990) reported this value as 7.28 before [5]. We can conclude that the head height has a higher increment than the stature while it does not comply with Vitruvius' description in the young Turkish men.

In our study we also analysed the compatibility of the equations described by Polykleitos and Vitruvius to the young Turkish men. We observed that the MidP-Om and Om-Por distances that Polykleitos used in his dual equation were very close to each other in the young Turkish men as well. We observed that the young Turkish men don't comply with the quartet equation that Polykleitos described and the longest segment belongs to body. We think that it is not a surprising result for Turks who have a macroskelic shape.

We observed that the armspan length is higher than the stature in the young Turkish men. In their study in 2001 Cikmaz et al. reported that 72% of their subjects had higher armspan length [1]. Another equation proposed by Vitruvius is the triple equation which is concerned with the shoulder width and upper extremity. The shoulder width and the forearm length including the hand which must be equal to 25% of the armspan length were close to each other but the last parameter of the triple equation, the double arm length was longer. As arm length is longer than the expected this may be the basis for the armspan to be longer than the stature.

References

1. Cikmaz, S., A. Yilmaz, R. Mesut. Artistik anatomi acisindan Turk erkeklerinde Vitruvius karesi ve esitlikleri. VI. Ulusal Anatomi Kongresi. 3-7 Eylul 2001. Edirne.
2. Hogarth, B. Sanatsal Anatomi. Istanbul, Troya Yayincilik, 1994,11-21.
3. Kahraman, G., Y. Z. Yildiz, T. Pestamalci, M. Yildirim. Turk erkeklerinde ust ekstremiteye ait bazı olcum ve oranlar. — Trakya Univ. Tip. Fak. Derg., **12**, 1995, No1, 7-20.
4. Mesut, R., M. Yildirim. İnsan Vücudunda Antropolojik ve Yuzeyel Bulus Noktalari. Istanbul, Beta Yayim Dagitim A.S., 1989, 13-72.
5. Muftuoglu, A, R. Gurun. Yetiskin Turk Erkeklerinde Bazı Vucut Olcumleri ve Aralarindaki Orantilar. — Yeni Symposium Derg, **3**, 1990, 54-60.
6. Turgut, H. B., A. Anil, T. Peker, C. Pelin, C. Barutcu. 17-25 yas grubunda boy, el ve ayak olcumleri arasindaki iliskinin incelenmesi. — Morfoloji Dergisi, 6, 1998, No1, 36-41.
7. Yildirim, M., O. Taskinalp, G. Kahraman. Yetiskin Turk Erkeklerinde Boy ile Bazi El ve Ayak Olculeri Arasında Somatometrik Iliskiler. — T.U.Tip Fakultesi Dergisi, 5, 1988, No1, 75-81.
8. Yildiz, Z. Y., G. Kahraman, A. Muftuoglu. Turk toplumundaki erkek bireylerin alt ekstremite olcumlerinin birbirlerine ve diger vucut olcumlerine göre oranları. — Cerrahpaka Tip. Fak. Derg., **24**, 1993, 213-218.
9. Yucebas, C. Çagdas Turk resminde insan figuru. Istanbul, Uzmanlik tezi, 2002.
10. Йорданов, Й. Наръчник по антропология. София, Унив. изд., 1997, 150—158.
11. Колев, Б. История на изкуството. София, Техника, 1973, 23—118.

Institute of Experimental Morphology and Anthropology with Museum
Bulgarian Anatomical Society

Acta morphologica et anthropologica, 13
Sofia • 2008

Sexual Differences and Reached Growth of Cephalometric Features in Children at the Age between 3 and 6 Years

Y. Zhecheva

Institute of Experimental Morphology and Anthropology with Museum, Bulgarian Academy of Sciences, Sofia

The aim of the work is to characterize the sexual differences of cephalometric features in children from Sofia at the age between 3 and 6 years and to assess the reached growth for single features regarding the same ones in adult persons. The metrical data about 7 basic cpehalometric features in 640 children (320 boys and 320 girls) aged 3 — 6 years are investigated. Boys have bigger head measurements than girls but girls come more close to the final measurements for the respective features in adult women. Most close to the final size is the head length, while the morphological face height had to gain much more, i.e. the face is awaited to become longer.

Key words: children, head measurements, sexual differences, reached growth.

Introduction

During the period of growth and development for the single body parts and organs occur alterations characteristic with different for both sexes velocity and scope [1]. The cephalometric features are among the anthropological characteristics that change quickly during childhood [5]. For instance the head height at birth is relatively big being 1/4 part from the entire stature of the newborn, at 6 years it is 1/6 part of the stature, and in adult individuals it is already 1/8 part of it [3].

The aim of the work is to characterize the sexual differences of cephalometric features in children from Sofia at the age between 3 and 6 years and to assess the reached growth for single features regarding the same ones in adult persons.

Material and Methods

The data presented are part of a detailed transversal anthropological study carried out in seven kindergartens in Sofia City (June 2004 — May 2005). Totally 640 children (320 boys and 320 girls) aged 3-6 years are investigated.

The metrical data about 7 basic cephalometric features are computed statistically by the variation analysis [4].

The comparative assessment about strength of sexual differences was made on the base of relative Index Units (IU) that are elaborated by Wolanski's [2] index of relative inter-group differences, called in this case the Index of Sexual Differences (ISD).

$$ISD = 2 \times [(\bar{x}_1 - \bar{x}_2) \times 100] / (\bar{x}_1 + \bar{x}_2), \text{ where } \bar{x}_1 = \bar{x}_{boys}, \bar{x}_2 = \bar{x}_{girls}$$

The degree of sexual differences' expression is categorized by the cut off points at P_{25} and P_{75}, which are evaluated on the base of ISD data for the investigated features during the entire studied period. The sexual differences are of a ***low degree expression*** when the index is up to

1.54 IU (P_{25}); from 1.55 IU till 3.18 IU (P_{75}) they are of a ***middle degree expression***; and over 3.18 IU — of a ***high degree expression***.

For the assessment of the reached growth about each cephalometric feature towards its measurement in adults are used data for adult Bulgarian population (30 - 40 years) reported in the National Anthropological Program elaborated in the IEMAM, BAS.

T a b l e 1. Cephalometric characterization of the children and adults

Age	♂							♀							Intersexual differences		
	n	$\bar{x}$	SD	SEM	V	min	max	n	$\bar{x}$	SD	SEM	V	min	max	Abs. diff.	t-test	ISD
Head circumference																	
3	80	506.9	11.8	1.3	2.3	482	537	80	491.0	13.4	1.5	2.7	460	518	15.9	8.0**	3.19
4	80	508.7	13.5	1.5	2.7	475	550	80	501.2	15.0	1.7	3.0	460	545	7.5	3.2*	1.48
5	80	519.1	11.1	1.2	2.1	488	545	80	508.8	13.7	1.5	2.7	485	555	10.3	5.2**	2.00
6	80	523.6	12.0	1.3	2.3	500	550	80	511.8	12.1	1.4	2.4	482	540	11.8	6.2**	2.28
30-40	236	579.2	16.3	1.1	2.8	540	625	276	552.0	16.2	1.0	2.9	512	597	-	-	-
Head length																	
3	80	174.2	5.7	0.6	3.3	162	187	80	167.7	5.7	0.6	3.4	155	180	6.5	7.2**	3.80
4	80	174.2	5.8	0.6	3.3	160	189	80	171.7	6.2	0.7	3.6	150	191	2.5	2.6*	1.44
5	80	177.9	5.5	0.6	3.1	165	191	80	174.0	6.8	0.8	3.9	159	194	3.9	4.0**	2.22
6	80	180.0	6.0	0.7	3.4	165	191	80	174.7	6.0	0.7	3.4	153	188	5.3	5.5**	2.99
30-40	236	190.6	6.7	0.4	3.5	170	215	276	180.3	5.8	0.4	3.2	165	195	-	-	-
Head breadth																	
3	80	137.6	4.6	0.5	3.4	126	152	80	134.4	4.6	0.5	3.5	121	148	3.2	4.4**	2.35
4	80	140.3	5.0	0.6	3.6	129	158	80	136.4	5.2	0.6	3.8	127	157	3.9	4.7**	2.82
5	80	142.6	5.0	0.6	3.6	130	153	80	138.0	5.4	0.6	3.9	128	157	4.6	5.7**	3.28
6	80	142.6	5.1	0.6	3.6	133	155	80	138.2	5.0	0.6	3.6	116	149	4.4	5.3**	3.13
30-40	236	156.9	6.1	0.4	3.9	139	172	276	148.6	5.5	0.3	3.7	133	164	-	-	-
Minimal frontal breadth																	
3	80	97.8	3.8	0.4	3.9	90	107	80	95.5	3.5	0.4	3.6	84	106	2.3	3.9**	2.38
4	80	99.1	4.0	0.4	4.0	90	113	80	97.9	3.6	0.4	3.7	90	109	1.2	2.0*	1.22
5	80	100.5	4.0	0.4	4.0	92	110	80	98.8	4.3	0.5	4.3	87	117	1.7	2.5*	1.70
6	80	101.4	4.0	0.4	3.9	92	114	80	100.0	3.7	0.4	3.7	87	109	1.4	2.4*	1.39
30-40	236	114.5	5.1	0.3	4.4	97	131	276	109.2	5.1	0.3	4.7	97	124	-	-	-
Bizygomatical breadth																	
3	80	112.2	4.5	0.5	4.0	105	127	80	109.7	3.8	0.4	3.5	100	119	2.5	3.9**	2.25
4	80	114.3	4.6	0.5	4.0	102	132	80	112.9	5.0	0.6	4.4	104	133	1.4	1.8	1.23
5	80	117.6	4.9	0.6	4.2	106	132	80	113.7	4.5	0.5	3.9	100	127	3.9	5.3**	3.37
6	80	119.0	5.0	0.6	4.2	108	136	80	115.9	4.3	0.5	3.7	102	127	3.1	4.3**	2.64
30-40	236	143.5	5.6	0.4	3.9	130	157	276	134.6	4.7	0.3	3.5	122	149	-	-	-
Bigonial breadth																	
3	80	85.9	4.8	0.5	5.6	76	99	80	85.1	3.7	0.4	4.4	77	95	0.8	1.1	0.94
4	80	89.4	4.5	0.5	5.0	79	104	80	87.8	4.4	0.5	5.0	78	101	1.6	2.1*	1.80
5	80	91.1	4.8	0.5	5.3	79	102	80	88.4	4.7	0.5	5.3	80	107	2.7	3.5**	3.00
6	80	92.9	4.3	0.5	4.6	85	108	80	89.8	5.3	0.6	5.9	76	104	3.1	4.0**	3.39
30-40	236	109.8	6.3	0.4	5.8	93	130	276	101.7	5.2	0.3	5.2	90	118	-	-	-
Morphological face height																	
3	80	94.1	5.1	0.6	5,4	82	111	80	90.4	4.8	0.5	5.3	80	102	3.7	4.8**	4.01
4	80	96.1	5.5	0.6	5,7	85	115	80	95.2	5.1	0.6	5.3	82	107	0.9	1.0	0.94
5	80	100.3	5.0	0.6	4,9	91	120	80	96.0	4.5	0.5	4.7	85	106	4.3	5.7**	4.38
6	80	101.3	5.5	0.6	5,4	84	112	80	99.1	4.7	0.5	4.8	84	108	2.2	2.7*	2.20
30-40	236	126.2	7.2	0.5	5,7	104	149	276	116.5	5.9	0.4	5.0	104	136	-	-	-

*P< 0,05; ** P< 0,001

T a b l e 2. Reached growth in children towards cephalometric measurements in adults (%)

Age	Head. Circumf.		Head length		Head breadth		Min. frontal breadth		Bizygomat. breadth		Bigonial breadth		Morph. face height	
	Boys	Girls	Boys	Girls	Boys	Girls	Boys	Girls	Boys	Girls	Boys	Girls	Boys	Girls
3	87.5	88.9	91.4	93.0	87.7	90.4	85.4	87.5	78.2	81.5	78.2	83.7	74.6	77.6
4	87.8	90.8	91.4	95.2	89.4	91.8	86.6	89.7	79.7	83.9	81.4	86.4	76.1	81.7
5	89.6	92.2	93.3	96.5	90.9	92.9	87.8	90.5	82.0	84.4	83.0	87.0	79.5	82.4
6	90.4	92.7	94.4	96.9	90.9	93.0	88.6	91.6	83.0	86.1	84.6	88.2	80.2	85.0

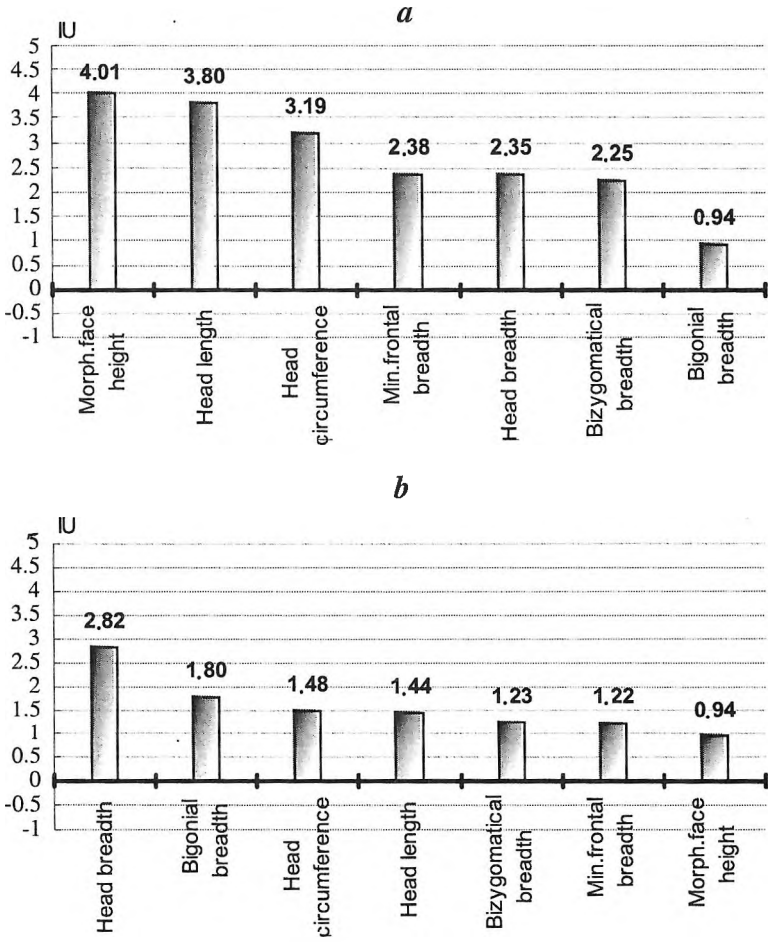

Fig. 1. Sexual differences according to ISD data presented in descendent order: *a* — in 3 years old children; *b* — in 4 years old children

Results

During the entire period of investigation the boys have bigger head measurements than girls, like the directions of sexual differences in adults are. The established sexual differences are statistically significant in all ages, while only in 3 from 28 comparative couples such significance is missing.

For each age group are made descendent formulae according to the data for ISD, by which an idea whether the metrical differences are strongest or slightest in the head parts between both sexes could be gotten.

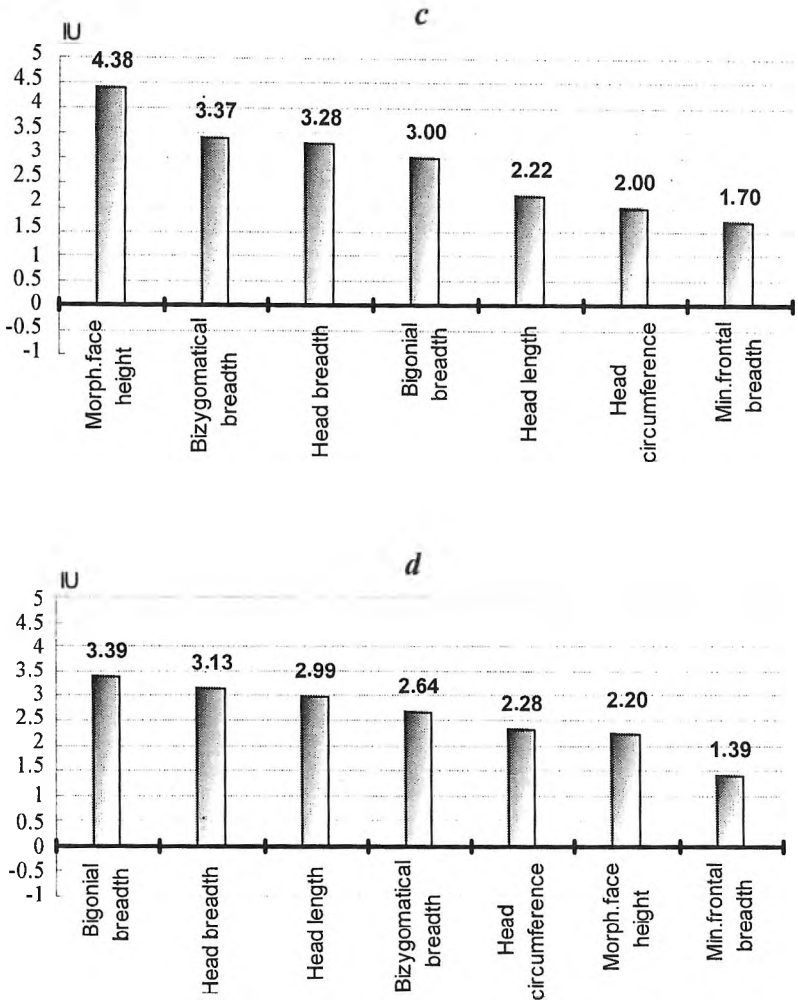

Fig. 1. Sexual differences according to ISD data presented in descendent order: *c* — in 5 years old children; *d* — in 6 years old children

At 3 years of age the sexual differences are strongly expressed in the morphological face height, head length and head circumference. Concerning the upper face breadths and head breadth, the metrical dominance in boys is of a middle degree and the sexual differences of the mandible breadth are most slightly expressed.

Descendent formulae: Morphological face height (4,01 IU — high) > Head length (3,80 IU — high) > Head circumference (3,19 IU — high) > Minimal frontal breadth (2,38 IU — middle) > Head breadth (2,35 IU — middle) > Bizygomatical breadth (2,25 IU — middle) > Bigonial breadth (0-,94 IU — low).

At 4 years of age the sexual differences are smallest being of middle and low expression's degree. They are better marked in the head breadth and the bigonial breadth, and less — in the morphological face height.

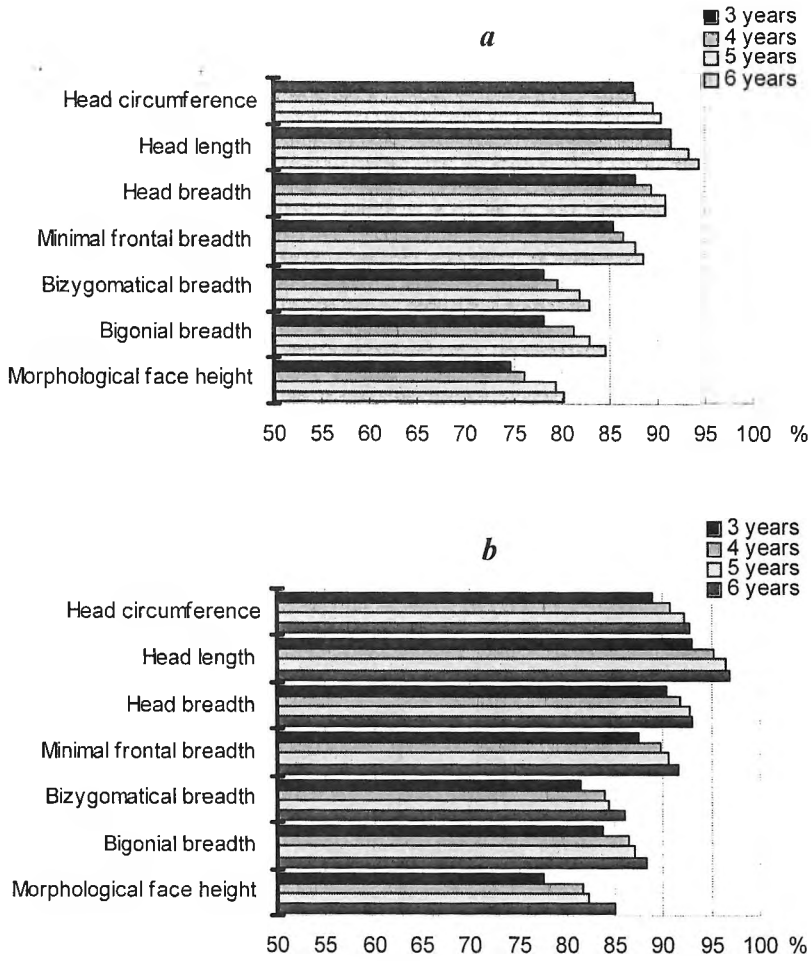

Fig. 2. Reached growth in children towards cephalometric measurements in adults: *a* — in boys; *b* — in girls

Descendent formulae: Head breadth (2,82 IU — middle) > Bigonial breadth (1,80 IU — middle) > Head circumference (1,48 IU — low) > Head length (1,44 IU — low) > Bizygomatical breadth (1,23 IU — low) > Minimal frontal breadth (1,22 IU — low) > Morphological face height (0,94 IU — low).

At 5 years of age the sexual differences are of a high and middle degree expression. For the morphological face height, bizygomatical breadth and head breadth the differences between both sexes are strongly expressed, while for the rest ones — they are middle expressed.

Descendent formulae: Morphological face height (4,38 IU — high) > Bizygomatical breadth (3,37 IU — high) > Head breadth (3,28 IU — high) > Bigonial breadth (3,00 IU — middle) >Head length (2,22 IU — middle) > Head circumference (2,00 IU — middle) > Minimal frontal breadth (1,70 IU — middle).

At 6 years of age interesting are the sexual differences of bigonial breadth, which occupies the first place in the descendent formulae. This fact shows that in the 6 years old children are observed beginnings of sexual differences concerning the face form in mandible area, which in adult menis markedly more massive and angular-shaped.

Descendent formulae: Bigonial breadth (3,39 IU — high) > Head breadth (3,13 IU — middle) > Head length (2,99 IU — middle) > Bizygomatical breadth (2,64 IU — middle) > Head circumference (2,28 IU — middle) > Morphological face height (2,20 IU — middle) > Minimal frontal breadth (1,39 IU — low).

Assessment of the reached growth in separate ages towards cephalometrical measurements in adults

The general evaluation of the reached growth for cephalometric features in children aged between 3 and 6 years towards the respective measurement in adults shows that for all investigated age groups, as well as, for the seven features girls have gained bigger relative share of the final sizes in adult women than the boys have. The head length came most close to the final size in adults concerning the four age groups and both sexes, while the morphological face height had to gain much more being far removed from the final size in adults.

Conclusions

1. Ever since 3 to 6 years of age boys have bigger head measurements than girls, making the sexual differences looks like the ones in adults.
2. Notwithstanding the metrical priority for boys, the girls during the investigated period come more close to the final measurements for the respective features in adult women.
3. The head measurements of brain shape as a whole outstrip in their development the face measurements concerning both sexes and the four age groups. Most close to the final size is the head length, while the morphological face height had to gain much more, i.e. the face is awaited to become longer.

References

1. Gerver, W. J. M., R. De Bruin. Pediatric Morphometrics. Utrecht, Netherlands, 1996.
2. Wolanski, N. A symmetria ciala czlwieka i jet zmiennosc w swiette funkcji konczyn. — Przegl. Anthrop., **23**, 1957, 461-464.
3. Бобев, Др., Е. Генев. Педиатрия. С., 2000.
4. Димитров, Б., Н. Янев. Вероятности и статистика. С., Университетско издателство „Св. Климент Охридски", 1998.
5. Кондова, Н., Зл. Филчева. Възрастови промени в кефалометричната и кефалоскопична характеристика на софийски деца в периода 7—11 години. — Journal of anthropology, **2**, 1999, 117—124.

Institute of Experimental Morphology and Anthropology with Museum
Bulgarian Anatomical Society

Acta morphologica et anthropologica, 13
Sofia • 2008

The Comparison of Bone Mineral Density with Body Mass Index in Postmenopausal Women

Özlen Karabulut, E. Savaş Hatipoğlu

Department of Anatomy, Faculty of Medicine, Dicle University, Diyarbakır, Turkey

The aim of this study was to determine whether there is any relationship between bone mineral density (BMD) and body mass index (BMI) in postmenopausal women. For this reason, 180 women who referred to Diyarbakır Bilim Medicine Center, for measuring bone mineral density, were taken into the study. Bone mineral density was assessed by Dual Energy X-ray Absorptiometey (DEXA) from femur and lumbar 2-4 vertebra areas. In addition, age, weight and height of all cases were reported. The mean age of all cases was 57.95 ± 6.38 years. The average height was 159.60 ± 3.59 cm. The average weight was 71.86 ± 10.91 kg. Body mass index was calculated for each case. The average body mass index and standard deviation was 28.28 ± 4.04.

At the end of the study, a significant relation was found between body mass index and bone mineral density at femur and lumbar 2-4 vertebra areas. A significant reverse correlation was found between age decades and bone mineral density in all areas. Also a significant reverse correlation was found between age decades and body mass index.

Key words: Body mass index, Bone mineral density.

Introduction

Osteoporosis is a major health problem, which affects millions of postmenopausal women worldwide. Reduction of bone characterizes osteoporosis, which results in the disruption of the bony architecture. Osteoporosis affects more than 75 million in the USA, Europe and Japan alone, and the morbidity and mortality of osteoporosis related fractures is so enormous that it is causing major economic concerns [2, 10]. Body weight is considered a strong predictor of bone mineral density (BMD). This study was designed to estimate one of the determinants of bone mineral density, the body mass index (BMI). Body weight can be related to height by calculating the index (BMI, kg/ m^2) which serves to distinguish overweight from normal body weight and between normal body weight and energy deficiency. It has been suggested that the optimum BMI range for women ranges between 18.7 and 23.8 [8] and a bone scan is recommended if BMI found 19 [7]. Regardless of body weight women tend to be concerned with their weight which in turn influences eating habits, dieting and physical activity [6].

Among many factors which are implicated in the development of osteoporosis female population is hypovitaminosis D, multiparity and prolonged lactation. The

identification of factors that influence bone mass has important implications for the design of appropriate strategies to prevent or treat osteoporosis in elderly males and females. The diagnosis of osteoporosis is currently based on measurement of BMD using dual energy X-ray absorptiometry(DEXA). The aim of this study was to determine the relation between BMD and BMI.

Materials and Methods

This was a randomized study carried out in Diyarbakır Bilim Medical Center. The participants were 180 postmenopausal women between ages 45-70. Bone mineral density (BMD) scans were performed with DEXA scanner. Bone mineral density was measured from the femur neck and lumbar spine L2-L4 using DEXA and was expressed in g/cm^2 in assessment of results currently two different scores. Z-score is the ratio of the difference between the assessed BMD and the average BMD of this age, and the standard deviation of the population. T-score is the ratio of the difference between the assessed BMD and the average BMD of the young adult population, and the standard deviation of young adult population. The scores were also expressed in g/cm^2. For T-score we accept the range between (—1 and 1) as normal results, (—1 and —2.5) as osteopeni and the values under (—2.5) as osteoporosis. We measured the weight and height of the patients anthropometrically BMI was calculated according to the Formula weight (g)/height (cm^2). The participants divided in four groups according to their age decades. The groups of ages were 45-49, 50-59, 60-69, 70. We compared body mass index with the bone mineral density of femur and lumbar spine. The data were assessed by the descriptive statistical tests, Posthoc test and Pearson correlation tests in SPSS for Windows programme.

Results

The youngest parcipitant was 45, the oldest was 70 years old. The average age was 57.95 and its standard deviation was 6.38. The highest was 176 cm, the shortest was 150 cm. The average height was 159.60 cm with 3.59 standard deviation. The heaviest was 98 kg and the lightest was 48 kg. The average weight and its standard deviation was 71.86±10.91 kg. The greatest body mass index was 39.83, the lowest was 19.58. The average BMI was 28.28 ± 4.04. In comparison of variables body mass index and lumbar spine bone mineral density, we found the results $r = 0.381$.

The increase in body mass index was found in correlation with the increase in lumbar spine bone mineral density.

Bone mineral density of femur neck another weight bearing site similarly shows positive correlation with body mass index ($r = 0.454$)

Our results support there is a strong positive correlation between bone mineral density and body mass index (Table 1).

Discussion

Osteoporosis is the most common bone metabolism disease. Advanced age is one of the most important determinants of the disease and the mean lifespan gets longer and elderly population will increase nearly 40 % in recent years. The fractures, the most common complication of the disease makes it a common public health prob-

Table 1. The comparison of body mass index and bone mineral density of lumbar spine and femur neck according to the age groups

Ages	BMI	Lumbar spine BMD	Femur neck BMD	*p*
45-49	28.94±4.36	1.107±0.17	1.047±0.13	>0.05
50-59	28.84±3.98	1.061±0.19	0.948±0.13	>0.05
60-69	27.42±4.02	0.930±0.15	0.837±0.13	>0.05
70	26.57±4.03	0.856±0.17	0.860±0.13	>0.05

lem [4]. Age, gender, height, weight, body mass index, physical activity, the geographic position are important factors for the prevalence of the disease [3]. Body size had a major influence on the magnitude of the areal BMD difference between elderly males and females at the femoral neck but also at other sites (e.g., at hip and spine), and found that the magnitude of sex difference, likewise, was reduced after adjustment for weight [11]. BMD distribution with ageing differs at different skeletal sites in both males and females. Elderly people of both sexes experiencing different levels of bone loss at various skeletal sites with ageing may account for the different BMD distribution [1]. The risk for males and females is very similar about 50 years but between 50 and 75 years females have two times much more risk. The bone loss after menopause period is the major risk factor [9]. In our study we found ageing as a risk factor for postmenopausal women. The results suggest that the strong effect of weight on bone mineral density is due to load on weight bearing bones. The sex difference is unexplained but may be due to adipose tissue production of estrogen in women after menopause [5]. Underweight women have less subcutaneous fat compared to normal and overweight women and since it is assumed that inactive vitamin D and estrogen are stored in subcutaneous fat, it serves as a minor energy reserve as well as a storage place for vitamin D. As vitamin D is fat soluble, lack of fat may lead to insufficient levels of vitamin D for bone formation during a particular period. Salamone et al. determined positive correlation between bone mineral density and lean body mass not with fatty mass in perimenopausal women [13]. Reid et al. found fatty mass as a determinant of bone mineral density in only women not in men [12]. Ageing females experience two phases of bone loss whereas ageing males experience only one. An accelerated phase of predominantly cancellous bone loss initiated by menopause is the result of the loss of the direct restraining effect of estrogen on bone turnover [9].

References

1. Dennison, E., C. H. Eastell Fall, S. Kellingray, P. J. Wood, C. Cooper. Determinants of bone loss in elderly men and women. — Osteoporosis Int., **10**, 1999, 384-391.
2. Duncan, H. Regional Osteoporosis. Primer on the metabolic bone diseases and disorders of mineral metabolism. — In: An official publication of the American Society for Bone and Mineral Metabolism Research. New York, Raven Pres Ltd., 1993, 248-250.
3. Effors, L, E. Allander, J. Kanis. The variable incidence of hip fracture on Southern Europe: The MEDOS Study. — Osteoporosis Int., 4, 1994, 253-263.
4. Eryavuz-Saridoğan, M. Osteoporozun tanımı ve sınıflandırılması. — In: Modern Tıp Seminerleri, Sayı 19 (Ed. Y. Gökçe-Kutsal). Ankara, Güneş Kitabevi Ltd. Şti., 2001, 1-5.

5. Felson, D. T., Y. Zhang, M. T. Hannan, J. J. Anderson. Effects of weight and body mass index on bone mineral density in men and women: The Framingham Study. — J. Bone. Miner. Res, **2**, 1993, 567-573.
6. Field, A. E., Jr. Camargo, C. B. Taylor, C. S. Berkey, S. B. Roberts, G. A. Colditz. Peer, parent and media influences on the development of weight concerns and frequent dieting among preadolescent and adolescent girls and boys. — Pediatrics, **107**, 2001, No1, 54-60.
7. Genant, H. K, C. Cooper, G. Poor, I. Reid, G. Ehrlich, J. Kanis, B. E. Nordin, E. Barrett-Connor, D Black, J. P. Bonjour, B. Dawson-Hughes, P. D. Delmas, J. Dequeker, S. Ragi Eis, C. Gennari, O. Johnell, C. C. Johnston, E. M. Lau, U. A. Liberman, R. Lindsay, T. J. Martin, B. Masri, C. A. Mautalen, P. J. Meunier, N. Khaltaev. Interim report and recommendations of the world health organization task-force for osteoporosis. — Osteoporosis Int., **10**, 1999, No4, 259-264.
8. James, W. P., P. J. Francois. The choice of cut-off point for distinguishing normal body weights from underweight or 'chronic energy deficiency' in adults. — Eur. J. Clin. Nut., **48**, 1994, (Suppl. 3), 179-184.
9. Kanis, J. A., O. Wohnell, B. Gullberg, E. Allander, G. Dilşen, C. Gennari. Evidence for efficacy of drugs affecting bone metabolism in preventing hip fracture. — Bric. Med. J., **305**, 1992, 1124-1128.
10. Kleerekoper, M., L. V. Avioli. Evaluation and treatment of postmenopausal osteoporosis. — In: Primer on the metabolic bone diseases and disorders of mineral metabolism (Ed. M.J. Favus, 2nd Edition). New York, Lipincott-Raven, 1993, 223-229.
11. Looker, A. C., T. J. Beck, E. S. Orwoll. Does body size account for gender differences in femur bone density and geometry. — J Bone Miner. Res, **16**, 2001, 1291-1299.
12. Reid, J. R., J. D., Plank, M. C. Evans. Fat mass is an important determinant of whole body bone density in premenopausal women but not in men. — J. Clin. Endocrinol. Metab., **75**, 1992, 779-782.
13. Salamone, L. M., N. Glynn, D. Blac, R. S. Epstein, L. Palermo, E. Meilahn. Body composition and bone mineral density in premenopausal and early perimenopausal women. — Bone. Mineral. Res., **10**, 1995, 1762-1768.

Institute of Experimental Morphology and Anthropology with Museum
Bulgarian Anatomical Society

Acta morphologica et anthropologica, 13
Sofia • 2008

Somatotype at the Growing up Period between 7 and 17 Years of Age

A. Nacheva, L. Yordanova, P. Borissova

Institute of Experimental Morphology and Anthropology with Museum, Bulgarian Academy of Sciences, Sofia

The aim is to be elaborated a somatotype characterization of schoolchildren aged between 7 and 17 years that are representatives of a growing up Bulgarian generation living between the 20th and 21st centuries, and to be established the inter-sexual and inter-age differences during this growing up period as for the integral somatotype, so for its three components. On the base of 10 anthropometrical features for the 7-17 years old schoolchildren (1851 boys and 1787 girls) is elaborated a somatotypological characterization by the method of Heath-Carter. It is established that between 7 and 17 years the mean somatotype of the investigated adolescents from both sexes is relatively constant and doesn't change its belonging to the respective somatotype group as a whole. The separate somatotype components, however, change their values in the ages, most tangible after 13 and 14 years. These changes reflect the differences between both sexes concerning their body composition and body forms associated with the maturation of the children.

Key words: somatotype, schoolchildren, sexual differences, age differences.

Introduction

"...The somatotype represents physically every person as an entity. It points to us the importance of this "entity" and the unique morphological individuality of every person. Once again that every body part or an organ, even a cell are connected and depend on this "entity", termed somatotype" [1, 2, 3]. According to the method of Heath-Carter could be distinguished 13 somatptypes, four variants to Endomorph, Mesomorph and Ektomorph group respectively, and one Central somatotype. The somatotype in children and adolescents has been examined in Bulgaria basically in connection with sports during the 70s and 80s of the past century [4, 5].

The aim is to be elaborated a somatotype characterization of schoolchildren aged between 7 and 17 years that are representatives of a growing up Bulgarian generation living between the 20th and 21st centuries, and to be established the inter-sexual and inter-age differences during this growing up period as for the integral somatotype, so for its three components.

Material and Methods

The somatotype characterization is made on the base of data from a detailed mixed (longitudinal and transversal) anthropological investigation of 7-17 years old schoolchildren from Sofia lead during the period 1993-2001. For the assessment of somatotype are used the anthropometrical data from measurements of 3638 individuals (1851 in girls and 1787 in boys) distributed into 11 age groups for both sexes. The somatotype diagnosis is made according to the methods of Heath-Carter. Because of the mixed character of the study, the statistical analysis of the metrical data is made by the method of weighted mean value.

Results

General notion about the somatotype characterization in schoolchildren between 7 and 17 years of age gives the mean somatotypes (Table 1). The results display that: in **boys** — till 10 years of age the mean somatotype is from the Mesomorph group, at 11 and 12 years — the mean somatotype is Central and from 13 till 17 years it is a boundary type Mesomorph-Ectomorph; at **girls** the diversity of mean somatotypes is greater for the investigated period. At 7 and 8 years it is a Mesomorph-Ectomorph, at 9 and 10 years — a Central one, at 11 and 12 years the mean somatotype is a boundary type Endomorph-Ectomorph and between 13 and 17 it is constantly an Ectomorph-Endomorph.

For the determination of somatotype diversity in the studied adolescents is analyzed the frequency of the 13 somatotypes in the separate ages (Table 2). Concerning the **Endomorph** somatotypes group for both sexes during the entire studied period the Mesomorphic Endomorph prevail (between 9,9% and 38,5%), its frequency being considerably bigger in girls. In them after 11 years the Ectomorphic Endomorph is presented well, while in boys it misses. The somatotypes from **Mesomorph** group was found more often in boys from all ages, the most high frequency being around 20% for 7 and 8 years old boys. In the girls the frequency of Mesomorph somatotypes is under 10% for the period between 7 and 11 years predominantly. From the **Ectomorph** somatotypes group in boys most frequent is the Mesomorphic Ectomorph — markedly between 14 and 17 years (up to 28,2%), slightly expressed in girls. This somatotype is under 10% till 13 years of age. In girls more frequently were found the Endomorphic Ectomorph and the Endomorph-Ectomorph. The **Central**

T a b l e 1. Mean somatotypes between 7 and 17 years of age

Boys		Age	Girls	
component values En M Ec	mean somatotype		mean somatotype	component values En M Ec
3.32 – 4.45 – 2.79	Endomorphic Mesomorph	7	Mesomorph - Endomorph	3.99 – 3.92 – 3.10
3.25 – 4.38 – 3.21	Balanced Mesomorph	8	Mesomorph - Endomorph	3.99 – 3.93 – 3.38
3.28 – 4.13 – 3.33	Balanced Mesomorph	9	Central somatotype	4.03 – 3.55 – 3.56
3.28 – 4.23 – 3.50	Balanced Mesomorph	10	Central somatotype	3.94 – 3.56 – 3.80
3.28 – 3.91 – 3.70	Central somatotype	11	Endomorph - Ectomorph	4.09 – 3.21 – 3.83
3.51 – 3.99 – 3.71	Central somatotype	12	Endomorph - Ectomorph	4.29 – 2.98 – 3.81
3.31 – 4.08 – 3.92	Mesomorph - Ectomorph	13	Ectomorphic Endomorph	4.55 – 2.99 – 3.92
3.18 – 3.90 – 4.29	Mesomorph - Ectomorph	14	Ectomorphic Endomorph	4.89 – 2.90 – 4.14
3.31 – 3.96 – 4.14	Mesomorph - Ectomorph	15	Ectomorphic Endomorph	5.13 – 2.85 – 3.89
3.02 – 3.91 – 4.16	Mesomorph - Ectomorph	16	Ectomorphic Endomorph	5.00 – 2.95 – 3.74
3.19 – 4.05 – 3.90	Mesomorph - Ectomorph	17	Ectomorphic Endomorph	5.17 – 2.96 – 3.66

T a b l e 2. Somatotype's frequency (%) between 7 and 17 years of age

Years of age – boys											Somatotype	Years of age – girls										
7	8	9	10	11	12	13	14	15	16	17		7	8	9	10	11	12	13	14	15	16	17
9.9	14.3	21.8	22.2	24.9	24.0	24.4	21.0	21.0	15.2	16.1	**Mesomorphic Endomorph**	29.4	28.0	33.3	33.7	32.8	33.7	35.3	30.4	29.7	35.2	38.5
0	0	0	0	0.6	1.2	1.2	1.4	0.8	0.8	0.8	**Ectomorphic Endomorph**	0.6	0.5	2.7	3.2	5.4	6.3	11.4	16.7	25.4	17.2	21.5
0.6	1.1	1.1	1.1	2.2	3.5	0.6	1.4	1.6	0.8	2.5	**Balanced Endomorph**	6.8	5.5	7.1	4.8	8.3	14.2	13.0	13.0	13.0	14.1	14.1
12.7	6.9	6.4	7.9	9.4	8.8	6.7	2.9	5.6	5.3	5.1	**Mesomorph - Endomorph**	11.9	11.0	9.3	7.0	5.9	1.6	1.6	2.2	1.4	2.3	1.5
22.1	11.6	13.3	7.4	5.0	4.7	6.1	4.3	6.5	6.8	10.2	**Endomorphic Mesomorph**	8.5	7.7	2.7	3.2	0.5	1.6	1.1	0	1.4	0	0
12.2	15.9	12.8	12.2	6.1	8.2	8.5	5.1	6.5	10.6	10.2	**Ectomorphic Mesomorph**	2.3	1.6	1.1	1.6	0	0	0	0.7	0	0	0
21.5	19.0	9.6	10.1	8.3	6.4	6.1	7.2	6.5	5.1	5.9	**Balanced Mesomorph**	9.0	4.9	4.4	4.3	1.0	0	0.5	0	0	0	0.7
12.7	13.8	9.0	13.8	9.4	9.4	11.6	9.4	8.1	12.1	11.9	**Ectomorph - Mesomorph**	8.5	9.3	3.3	5.9	2.9	1.1	0.5	0	1.4	0.8	0
0	0	0.5	0	0.6	2.9	2.4	3.6	16	3.0	2.5	**Endomorphic Ectomorph**	2.8	2.2	7.1	7.0	14.2	11.6	16.3	15.2	13.0	13.3	11.1
3.9	9.5	13.3	14.8	22.7	19.3	20.1	29.0	28.2	27.2	23.7	**Mesomorphic Ectomorph**	7.3	6.6	7.7	7.0	4.9	2.1	4.3	0.7	0	0	0.7
2.2	2.6	4.3	5.3	6.6	4.1	6.1	6.5	10.5	6.8	9.3	**Balanced Ectomorph**	6.8	12.1	11.5	13.9	11.8	14.7	6.5	6.5	2.2	3.9	2.2
0.6	0	1.1	0.5	0	0.6	1.2	1.4	0	0.8	0	**Endomorph - Ectomorph**	0.6	1.6	3.3	3.7	6.9	7.9	6.0	10.1	7.2	10.2	7.4
1.7	5.3	6.9	4.8	4.4	7.0	4.9	6.5	3.2	4.5	1.7	**Central**	5.6	8.8	6.6	4.8	5.4	5.3	3.3	4.3	5.1	3.1	2.2

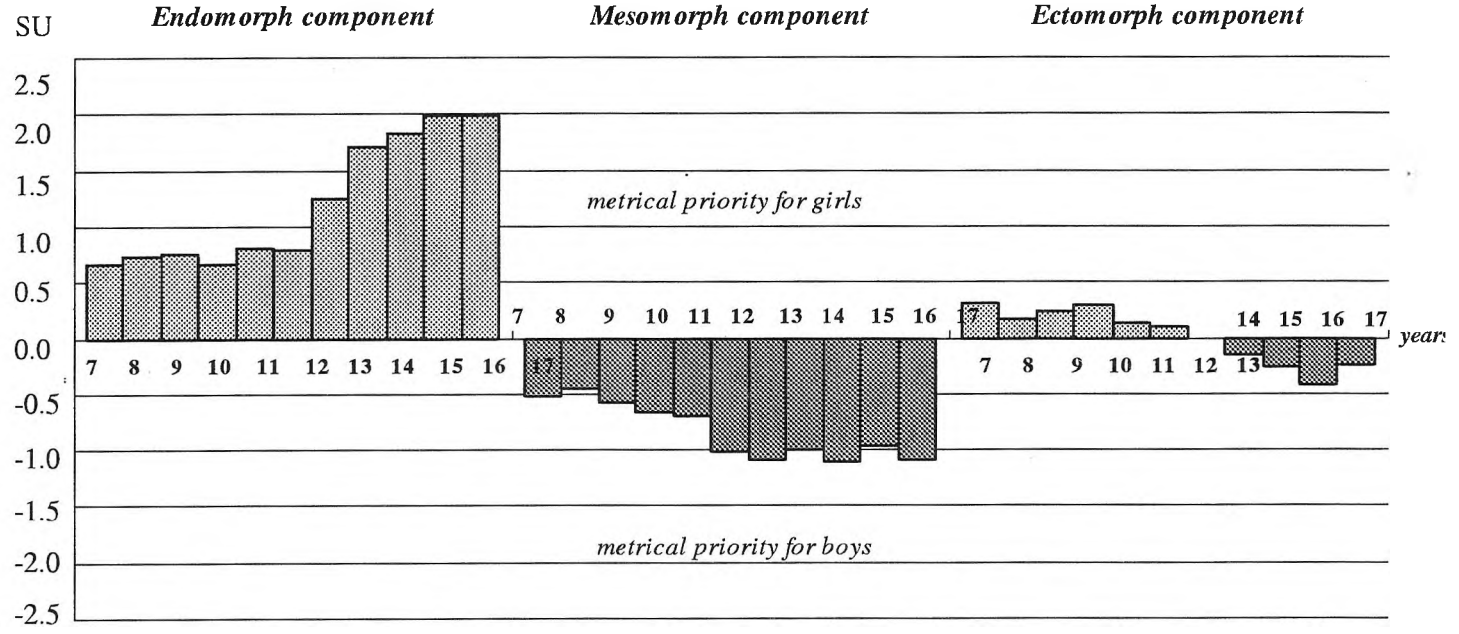

* the negative sign shows metrical priority for boys

Fig. 1. Sex and age differences in the values of somatotype components

somatotype frequency is relatively low for both sexes, and during the youth it could be found more rarely.

Against the base of relatively slight changes of the mean somatotype between 7 and 17 yeras, the values of separate somatotype component change themselves considerably (Table 1, Fig. 1). For all ages between 7 and 17 years the **Endomorph** component have bigger values in girls, the sexual differences being better expressed (up to 2 SU) after the 14 year, i.e. at the end of their puberty and post puberty ages. The **Mesomorph** component throughout the whole period under study has bigger values in boys. The sexual differences are better expressed from the 13 year on, when the Mesomorphy in boys is round or over 1 SU greater. Nevertheless that during the entire studied period the sexual differences of the values for **Ectomorph** component are comparatively small, the age differences are indicative of the specificity for both sexes transformation of body composition and body forms, which transformation is connected with the sexual maturity. Till 13 years of age the girls are more Ectomorphic, i.e. they are more lengthened. At 14 years boys and girls have equal values of the Ectomorph component (round 4 SU), and between 14 and 17 years, the Ectomorphy is already greater in boys that illustrate the formation of a more lengthened forms in them characteristic for the adult man.

Conclusions

The mean somatotype of the investigated adolescents from both sexes is relatively constant and doesn't change its belonging to the respective somatotype group as a whole; during the entire studied period, boys are more Mesomorphic and less Endomorphic, while girls — the opposite more Endomorphic and less Mesomorphic.

In contrast to the unchangeable mean somatotype, the separate somatotype components change their values most tangible after 13 and 14 years of age. These changes reflect the specific for both sexes changes in body composition and body forms connected with their sexual maturation: in boys after 13 year the Mesomorphy increase more markedly and less but specific — the Ectomorphy; for girls most characteristic is the increment of Endomorphy after 14 years of age.

References

1. Carter L., B. Heath. Somatotyping — development and applications. Cambr. Univ. Press. 1990, 1-449.
2. Carter L., J. Parizkova. Changes in somatotypes of European males between 17 and 24 years. — Amer. J. of Physical Anthrop., **48**, 1978, 4-251.
3. Heath, B., L. Carter. Growth and somatotype patterns of Manus children, territory of Papua and New Guinea. Amer. J. of Physical Anthrop., **35**, 1971, 49-67.
4. Захариева, Е., М. Тотева. Сравнителна соматотипна характеристика на висококвалифицирани състезателки по джудо и художествена гимнастика. — Въпр. на физ. култура, **7**, 1986.
5. Тотева, М. Соматотипология в спорта. София, НСА, 1992, 1—338.

Institute of Experimental Morphology and Anthropology with Museum
Bulgarian Anatomical Society

Acta morphologica et anthropologica, 13
Sofia • 2008

Some Circumferential Measurements of the Body and Limbs in Children with Type 1 Diabetes Mellitus

A. Baltadjiev, S. Sivkov, N. Kaleva, T. Shabanova*, G. Baltadjiev*

Department of Anatomy, Histology and Embryology, Medical University
**Department of Pediatrics, University Hospital Sveti Georgi, Plovdiv*

The aim of the present study was to determine some circumferential measurements as indirect indices for deposition and distribution of fat tissue in children with type 1 diabetes mellitus. The examined patients were children with type 1 diabetes mellitus divided into the following age groups: 45 boys aged 4-12 years, 50 boys aged 12.01-18 years, 46 girls aged 4-12 years, 53 girls aged 12.01-18 years. Healthy children (250) were divided into same groups. The following six measurements were taken from each child: circumference of the arm, forearm, waist, hip, thigh and leg. In the boys aged 4-12 years the circumference of the leg was smaller in the diabetic than in the healthy boys. In the boys aged above 12 years the circumferences of the arm and waist were statistically smaller in the diabetic than in the healthy boys. Girls aged 4-12 years showed no statistically significant difference between patients and controls. In the girls aged above 12 years the waist, hip and thigh circumference were significantly greater in the diabetic patients. In between-gender comparison the diabetic girls above the age of 12 showed greater waist and thigh circumference than the same age diabetic boys. No difference was found in the other measurements. In the age group 4-12 years the waist/hip ratio was greater in the diabetic than in the control children. In the 12-18-year-old girls the patients had greater ratio than the controls, while in the boys of the same age group the ratio was greater in the controls than in the patients.

Key words: type 1 diabetes mellitus, circumference measurements, body, limb, anthropometry.

Introduction

Metric examinations of the body and limb circumferences are essential for evaluation of the risk and development of type 1 diabetes mellitus [5].The great prognostic role of the waist, hip and thigh circumference measurements and the ratio between them are especially mentioned [1, 2, 4].

Aim

The aim of the present study was to determine some circumferential measurements as indirect indices for deposition and distribution of fat tissue in children with type 1 diabetes mellitus.

Material and Methods

Children (boys and girls) with type 1 diabetes mellitus treated with insulin by individual schemes were included in the study.

The boys were divided into two groups: group 1 aged from 4 to 12 years (45 children of mean age 9 years and 7 months) and group 2 aged from 12.01 to 18 years (50 children of mean age 15 years and 8 months). The girls were also divided into two groups: group 1 from 4 to 12 years (45 children of mean age 8 years and 9 months) and group 2 from 12.01 to 18 years (53 children of mean age 15 years and 2 months).

Six circumferential measurements were taken: arm, forearm, waist, hip, thigh and leg. Waist/hip ratio was determined. Analogous measurements were done in 250 healthy children divided into the same age groups. They were used as a control group.

The results obtained were analyzed with statistical programmes SPSS 11.0 and INSTAT. The level of significance was determined as low ($p>0.05$), moderate ($p=0.04$-0.001) and high ($p<0.001$).

Results and Discussion

Boys aged from 4 to 12 years

In this age group moderate statistical difference was found only in the circumferential measurements of the leg between the studied and control group ($p=0.04$-0.001).

Boys aged from 12.01-18 years

This age group presents with between-group difference of moderate statistical significance in the waist circumference ($p=0.04$-0.001) and between-group difference of low statistical significance ($p>0.05$) in the arm circumference.

Girls aged from 4 to 12 years

In this age group no statistically significant between-group difference was found in any of the circumferential measurements.

T a b l e 1. Circumferential measurements in diabetic and healthy boys aged 4-12 years

Variables	Diabetic patients			Healthy subjects		
	N	Mean	SD	N	Mean	SD
Arm	45	19.44	2.79	65	19.88	2.62
Forearm	45	19.71	2,21	65	19.76	1.92
Waist	45	60.85	7.76	65	58.91	5.98
Hip	45	71.87	9.47	65	71.10	6.41
Thigh	45	39.51	6.53	65	40.83	5.10
Leg	45	27.13	4.05	65	28.46	3.26

T a b l e 2. Circumferential measurements in diabetic and healthy boys aged 12-18 years

Variables	Diabetic patients			Healthy subjects		
	N	Mean	SD	N	Mean	SD
Arm	50	24.02	2.94	61	25.26	3.56
Forearm	50	24.19	2.41	61	24.45	2.69
Waist	50	68.68	13.21	61	71.93	7.09
Hip	50	87.78	8.91	61	89.08	7.26
Thigh	50	48.07	5.72	61	48.65	5.53
Leg	50	33.40	3.58	61	34.40	3.83

T a b l e 3. Circumferential measurements in diabetic and healthy girls aged 4-12 years

Variables	Diabetic patients			Healthy subjects		
	N	Mean	SD	N	Mean	SD
Arm	46	19.78	2.93	70	20.03	2.79
Forearm	46	19.72	1.74	70	19.50	2.19
Waist	46	58.64	6.32	70	57.81	6.34
Hip	46	70.67	8.52	70	73.16	7.39
Thigh	46	40.78	5.32	70	41.86	5.41
Leg	46	27.59	3.80	70	28.53	3.41

T a b l e 4. Circumferential measurements in diabetic and healthy girls aged 12-18 years

Variables	Diabetic patients			Healthy subjects		
	N	Mean	SD	N	Mean	SD
Arm	53	24.29	2.81	65	23.72	2.80
Forearm	53	23.32	1.91	65	22.66	2.29
Waist	53	69.55	7.63	65	66.02	6.76
Hip	53	91.99	7.09	65	89.70	7.13
Thigh	53	52.34	5.16	65	49.95	5.26
Leg	53	33.95	3.13	65	34,11	3.47

T a b l e 5. Waist/hip ratio in diabetic and healthy children

Groups	Boys aged 4-12 years	Boys aged 12-18 years	Girls aged 4-12 years	Girls aged 12-18 years
Diabetic patients	84.67	79.24	83.00	75.60
Healthy subjects	82.86	80.75	79.00	73.60

Girls aged from 12.01-18 years

Moderate statistically significant difference in the hip and thigh circumferences was found between the diabetic patients and control subjects (p=0.04-0.001). Statistically significant difference was found in the waist circumference (p<0.001). This relationship was mentioned by other authors, too [1].

Between-gender comparison of the circumferential measurements

Besides the above-mentioned comparisons we compared the circumferential measurements between boys and girs divided into two groups: below 12 years and above 12 years of age. Children above the age of 12 showed moderate statistical difference in the hip circumference (p=0.04-0.001) which was significantly greater in girls. In the same age group moderate statistical significance was found in the thigh circumference (p=0.04-0.001), which was significantly greater in girls. No statistically significant differences were found in the remaining measurements. These findings accord with those reported by other authors [1, 2, 3, 6].

Conclusions

1. In the girls with type 1 diabetes mellitus aged from 4 to 12 years the circumferential measurements of the leg are statistically smaller than those in the healthy girls.
2. In the boys with type 1 diabetes mellitus above the age of 12 the circumferential measurements of the arm and waist are statistically smaller than those in the healthy girls.

3. In the girls of 4-12 years of age the difference in none of the circumferential measurements shows statistically significant difference between patients and healthy subjects.
4. In the girls above the age of 12 the waist, hip and thigh circumferences are significantly greater in diabetic than in the healthy children.
5. In between-gender comparison of the circumferential measurements in the diabetic patients the waist and thigh circumferences are significantly greater in the girls than in the boys above the age of 12. No statistically significant differences are found in the other measurements.
6. Waist/hip ratio is greater in diabetic than in the healthy boys and girls aged from 4 to 12 years. In the 12-18-year-old girls the index is also greater in the patients than in the healthy controls, while in the 12-18-year-old boy the healthy children show greater index than the patients.

Acknowledgements: This study was supported by the National Fund of Scientific Research, Bulgarian Ministry of Science and Education, grant No B 1404/2004

References

1. Betts P., J. Mulligan, P. Ward. Increasing body weight predicts the earlier onset of insulin-dependant diabetes in childhood: testing the "accelerator hypothesis". — Diabet Med., **22**, 2005 Feb, No2, 144-151.
2. Codner, E., A. Barrera, D. Mook-Kanamori, R.A. Bazaes, N. Unanue, X. Gaete, A. Avila, F. Ugarte, I. Torrealba, V. Perez, E. Panteon, F. Cassorala. Ponderal gain, waist-to-hip ratio, and pubertal development in girls with type-1 diabetes mellitus. — Pediatric Diabetes, **5**, 2004, 182-189.
3. Ferrante, E., G. Pitzalis, A. Vania, P. DeAngelis, R. Guidi, L. Fontana, L. Ferrante, M. Cervoni, G. Multari. Nutritional status, obesity and metabolic balance in pediatric patients with type 1 diabetes mellitus. — Minerva Endocrinol., **24**, 1999, No2, Jun, 69-76.
4. Ingberg, C.M., S. Sarnblad, M. Palmer, E. Schvarcz, C. Berne, J. Aman. Body composition in adolescent girls with type 1 diabetes. — Diabet Med., **20**, 2003 Dec, No12, 1005-11.
5. Kibirige, M., B. Metcalf, R. Renuka. Testing the accelerator hypothesis: the relationship between body mass and age at diagnosis of type 1 diabetes. — Diabetes Care, **26**, 2003 Oct, No10, 2865-2870.
6. Knerr, I., J. Wolf, T. Reinehr. The "accelerator hypothesis": relationship between weight, height, body mass index and age at diagnosis in a large cohort of 9,248 German and Austrian children with type 1 diabetes mellitus. — Diabetologia, **48**, 2005, 2501-2504.

Institute of Experimental Morphology and Anthropology with Museum
Bulgarian Anatomical Society

Acta morphologica et anthropologica, 13
Sofia • 2008

Interrelationships between Different Functional Asymmetries in Bulgarian Right-, Mixed-, and Left-Handers

G. Karev

Institute of Experimental Morphology and Anthropology with Museum, Bulgarian Academy of Sciences, Sofia

A suggestion exists that the left types of Arm folding and Hand clasping witness for a latent left-handedness. In the light of our previous investigations, if this were true, the majority of the Bulgarian population would be latently left-handed, which is not the case. As far as none of the lateralized preferences Arm folding and Hand clasping showed interrelation with handedness, the suggestion that the left types of these preferences are symptoms of any hidden left-handedness should be categorically rejected.

Highly significant interdependences are established between handedness and footedness, handedness and eyedness and footedness and eyedness. Bearing in mind our previous findings that each of these asymmetries depends very much on the CIFS (Cumulative index of familial sinistrality), it could be hypothesized that functional cerebral asymmetry is under strong genetic influence and that the separate functional asymmetries are partial demonstrations of much more generalized and genetically controlled cerebral mechanisms.

Key words: folding, clasping, handedness, footedness, eyedness.

Introduction

It was found in our previous study, performed on 2100 healthy Bulgarians that the left types of the lateralized preferences Arm folding and Hand clasping prevail in males, in females and in both sexes jointly, all the three mentioned differences being highly significant [5]. The aim of the present study was to establish the presence or the lack of interdependence between the handedness and the two lateralized preferences and, on the other hand, between the three examined functional asymmetries: handedness, footedness and eyedness.

Material and Methods

A sample of 870 apparently healthy secondary school students was studied. The sample comprised 264 right-, 246 mixed- and 360 left-handers, each handedness

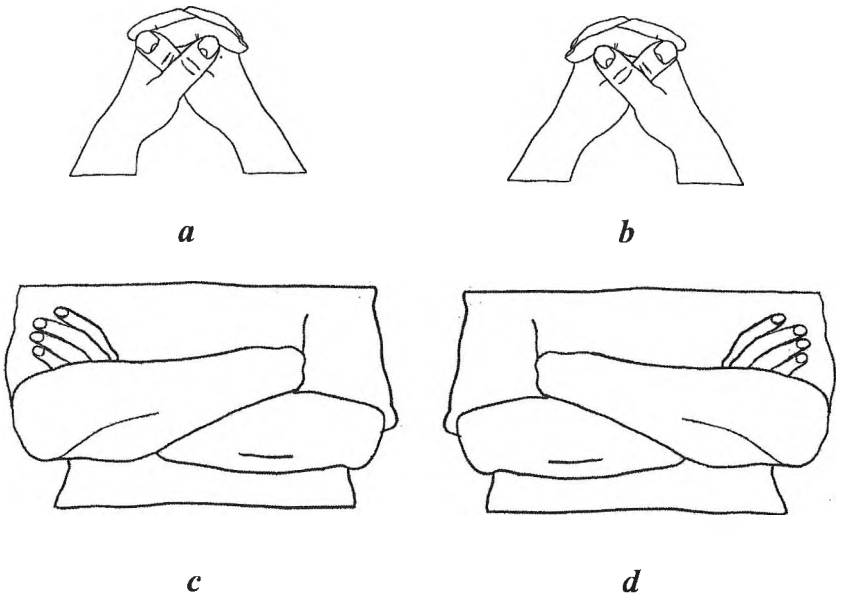

Fig.1. Hand clasping (top): left type, (*a*), and right type, (*b*). Arm folding (bottom): right type, (*c*), and left type, (*d*)

category including equal numbers of males and females. Handedness of each person was determined accordingly to C h a p m a n and C h a p m a n [1], footedness in accordance with C h a p m a n et al. [2] and eyedness as described by G u r and G u r [4] and G o r i n i a and E g e n t e r [3]. Lateralized preferences Arm folding and Hand clasping were examined using the procedures of W i e n e r [8], L e g e u b e [6] and L e g e u b e and M a r t i n e z - F u e n t e s [7], as it is shown in Fig. 1.

Results

Relationships between handedness and the lateralized preferences were looked for using three (handedness categories) X two (types of each preference) contingency tables. The results of these evaluations (Arm folding, males: $chi^2 = 2.414$, d.f. = 2, $p < 0.5$; females: $chi^2 = 5.2$, d.f. = 2, $p < 0.1$ and Hand clasping, males: $chi^2 = .39$, d.f. = 2, $p < .9$; females: $chi^2 = .66$, d.f. = 2, $p < .75$) showed categorically the lack of interdependence between handedness and the two lateralized preferences in both sexes.

Further, the sample was distributed in a 3 (handedness categories) X 3 (footedness categories) contingency table. The chi^2 — testing revealed a strong connection between the two examined lateralities ($chi^2 = 422.59$, d.f. = 4, $N = 870$, $p < .001$). Similarly, the simultaneous distribution of the sample on the three handedness and the two eyedness categories revealed a strong interrelation between these two lateralities ($chi^2 = 127.01$, d.f. = 2, $N = 870$, $p < .001$). And, finally, such a strong connection was established between footedness and eyedness ($chi^2 = 100.97$, d.f. = 2, $N = 870$, $p < .001$).

Discussion

A suggestion exists that the left types of Arm folding and Hand clasping witness for a latent left-handedness. Our previous results [5] showing a considerable prevalence of the left types of these preferences in Bulgarians gave an evidence against the mentioned suggestion. If the latter were true, the majority of the Bulgarian population would be latently left-handed; evidently, such is not the case. The results of the present study give evidences in the same direction. As far as none of the lateralized preferences Arm folding and Hand clasping showed interrelation with handedness, the suggestion that the left types of these preferences are symptoms of any hidden left-handedness should be categorically rejected.

Highly significant interdependences are established between handedness and footedness, handedness and eyedness and footedness and eyedness. Bearing in mind our previous findings that each of these asymmetries depends very much on the CIFS (Cumulative index of familial sinistrality), it could be hypothesized that functional cerebral asymmetry is under strong genetic influence and the separate functional asymmetries are partial demonstrations of much more generalized and genetically controlled cerebral mechanisms.

Conclusion

Our results show that the suggestion that left types of the lateral preferences witness for a hidden left handedness should be categorically rejected. Handedness, footedness and eyedness are significantly interrelated, probably due to a general genetic determination.

References

1. Chapman, L. J., J. P. Chapman. The measurement of handedness. — Brain and Cognition, **6**, 1987, 175-183.
2. Chapman, J. P., L. J. Chapman, J. J. Allen. The measurement of foot preference. — Neuropsychologia, **25**, 1987, 579-584.
3. Gorinia, I., D. Egenter. Intermanual coordination in relation to handedness, familial sinistrality anfd lateral preferences. — Cortex, **36**, 2000, 1-18.
4. Gur, R. E., R. C. Gur. Sex differences in the relations among handedness, sighting-dominance and eye-acuity. — Neuropsychologia, **15**, 1977, 585-590.
5. Karev, G. B. Arm folding, hand clasping and dermatoglyphic asymmetry in Bulgarians. — Anthrop. Anz., **51**, 1993, 69-76.
6. Legeube, A. Hand clasping: etude anthropologique and genetique. — Bull. Soc. Roy. Belge Anthrop. Prehistor., **78**, 1967, 81-107.
7. Legeube, A., A. Martinez-Fuentes. Etude genetique du mode de croisment des bras. — Acta Genet. Med. Gemellol., **20**, 1971, 267-283.
8. Wiener, A. S. Observations on the manner of clasping the hands and folding the arms. — Amer. Natur., **66**, 1932, 365-370.

Institute of Experimental Morphology and Anthropology with Museum
Bulgarian Anatomical Society

Acta morphologica et anthropologica, 13
Sofia • 2008

Forensic and Anthropological Expertise and Verification of the Bulgarian Formulas for Stature Prediction by the Long Bones (A Case Report)

D. Radoinova

Department of Forensic Medicine, Varna University of Medicine, Varna, Bulgaria

We present forensic-anthropological expert case by bone remains with complete and final identification of 21-year-old girl as well as Bulgarian formulae verification for stature assessment by long bones. The comparison to the Troter-Gleser and Ninnis formulae proves the Bulgarian formulae accuracy.

Key words: forensic-antropological expertise, bulgarian stature formulae by long bones.

At the Department of Forensic Medicine, Varna University of Medicine, annually a total of 30-35 expertises of bones and bone remains are performed, comprising about 9.8% of all autopsies. Person identification is different in forensic medicine as compared to other sciences for its importance as evidence in court. For this, very strict rules of performing this type of investigation should be followed, including methodological excellence and repeatability of results.

The following order of steps in performing bone expertise is typical: determination of species (i.e. human) nature of the remains, gender, age, height, and race. Then, the cause of death is determined. The answers to these questions are important as they will direct the future actions of the investigating officials.

The **aim** of the present paper is to demonstrate a forensic case in which a precise identification of personality was achieved. This allows a complete forensic analysis of the bones and verification of the Bulgarian formulas for height determination by the long bones, as their precision is compared to other formulas.

The case:

On 28 July 2005, in a deep gully in the region of the village of Oreshak (Varna district), bone remains were discovered, nearby a small river. The spot was indicated by a witness who claimed he had seen a girl (to whom the bones supposedly belonged) being thrown in the river, in February 2005. The skull was partially sunk in water, and along the shore most of the skeleton bones were dispersed.

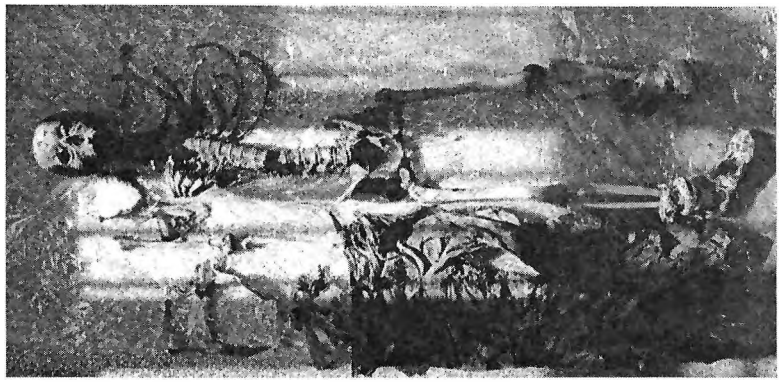

Fig. 1. Discovered bones

Fig. 2. Skull with lower jaw

At the inspection, the following bones were collected (Fig. 1.): skull (including part of the vertebral column attached to it), and the lower jaw. The skull was intact, without mechanical injuries. Only the stylloid processes were broken. Remains of soft tissues and a lot of dirt under the temporal arches as well as in the orbitas were found. The skull was heavy, the first 4 vertebrae attached to it. The lower jaw was completely separated from the skull (Fig. 2.). It was intact, the lower incisors had fallen off post mortem, but their alveolar cavities were intact, deep and with sharp contours. The right humerus was with a missing head and unevenly broken proximal end. Among the vertebral column bones, partially separated were L_1 to L_4 vertebrae, while L_5 was attached to the sacrum. The two ilial bones were completely separated. The upper part of the wing of the right ilial bone was unevenly gnawed. The ribs were intact; their cartilage segments connecting them to the sternum were missing as well as the sternum itself.

Fig. 3. Right foot

Near the lower pat of the sacrum, bikini were found which aided the identification. The left scapula had a broken distal part of the acromion. The right radius was intact without changes. The left femur was with partially gnaws joint surfaces at the knee side. The right tibia and fibula were with unevenly gnawed proximal edges. Distal from the ankle, the right foot had preserved soft tissues, upon which stockings and socks were found. This foot had on it a sport shoe, its soft tissues were partially mummified and partially macerated (Fig. 3.). The length of the right foot was 22 cm. The left shoe was discovered separately, removed from the foot.

The left tibia and fibula were discovered, their proximal edges being gnawed. The bones of the left foot were all missing.

Dry leaves and soil were sealed to most of the discovered bones. No signs of lifetime disease or traumatic processes were identified.

The bones were arranged in an anatomical order. By their morphological appearance (structures, joint surface, etc.) was established that they were human, belonging to a single individual.

The skull with the vertebra attached to it was placed in water for maceration, and subsequently opened. The brain was well preserved, showing grayish or sometimes reddish spots. However, the identification of particular disease or traumatic processes was not possible. Along the inner surface of the top part of the skull, the two anterior cranial fosse and the anterior part of the skull base was observed a black-colored contamination, which was removed in water.

Subsequent histological analyses and a reaction for iron were not sufficiently informative.

The following parameters were defined:

I. Identification signs of gender.

Descriptive or metric parametes of the skull and the seat. The skull was relatively small, gracile, with weakly developed occipital relief. The sinusoid processes were visibly small, the end of the cheekbone did not continue beyond the external auditory orifice. The forehead was convexed outward, the relief over the eyebrows was well-developed. The chin was oval, the lower jaw was thin, gracile, and the man-

dibular angle was over 90 degrees. The orbitas were round. These are features are typical for the female gender.

The metric features were processed with the Russian anthropological program "Anthropolog" with the following results: for female gender — reliably female (2 features), probably female (10 features); for male gender: reliably male (1 feature), probably male (1 feature), undefined gender (11 features).

Based on the descriptive and metric parameters the skull was concluded to be female, Caucasian. The seat was also with female features.

II. Identification signs of age.

The skull was heavy also after maceration. The teeth formula was defined as follows: the nuclei of the wisdom-teeth were not seen, upper right 6th tooth has a small stopping of amalgama, the lower central incisor teeth have fallen off post mortem, the rest of the teeth were without changes. During lifetime, the teeth had been in a very good condition, with wearing out of enamel 1st degree. The cranial sutures along the internal surface of the skull roof were almost accrete, while along the external surface — not accrete.

III. Determination of stature.

We measured the left tibia (32.8 cm; within physiological limits), the left femur (40.8 cm), the right ulna — 22.8 cm (maximal lengths).

The height was determined by the following formulas: (i) according to the **Trotter—Gleser** formula, the height was determined to be 154.2 cm (by the femur length), 155.1 cm (by the ulnar length) or 154.9 cm (by the tibial length); (ii) according to the **Nainis** formula, the height was determined to be 154 cm (by the tibial length); (iii) according to the formulas for the Bulgarian population of **Radoinova** — regression equations, nomograms and computer programming - the height was determined to be 158,6 cm (by the tibial length). **With a reliability of 99.9% the true height of the dead girl is in the range of 152.5-163.5 cm.**

According to the data acquired by her personal identification card and school datasheet, the girl's height had been **160 cm**. Thus, the difference between the projected difference in height from the Bulgarian formulas to those of Trotter—Gleser formula is over 3 cm, while to those of Nainis — 4,6 cm.

The precise identification of the girl was made by constant (general) signs — gender, age, etc. as well as by concomitant signs — clothes, underwear, shoes. No special signs were found. The definitive determination of the identity was done by DNA analysis, which resulted in 0.99986 identities as compared to tissues from her parents.

The cause of death could not be determined.

Summary of the expertise: • All investigated bones are of human origin and belong to a single individual. • The descriptive and metrical parameters of the skull and seat demonstrate that the remains belong to a woman. • According to the teeth, cranial sutures and the rest of the bones, the bone age was defined to be in the range of 18-25 years. • The height as determined by the tibial length with the Bulgarian formulas was found to be 158,6 cm. With a reliability of 99.9% the true height of the dead girl is in the range of 152.5-163.5 cm. According to the data acquired by her personal identification card and school datasheet, the girl's height had been **160 cm**. • No special identification signs were found on the investigated bones. • No lifetime traumatic or disease changes of the bones were identified. • The edges of some of the bones were missing, gnawed post mortem by animals. • The appearance of the bones (heavy, with low amounts of preserved tissues, parts of cartilage and wizened ligaments), including the presence of dry leaves on them, suggested that death had

occurred more than an year ago. • The cause of death was not possible to be determined because of the lack of traumatic or disease changes of the bones. • Probable identification was done based on general and concomitant signs. • The definitive identification was done by DNA analysis.

Conclusions

1. Investigating bones in forensic medicine is always advisable, even if only general signs are being determined.
2. At the lack of traumatic or disease changes of the bones the cause of death is usually impossible to be determined.
3. The general (constant) and specific (not constant) signs as well as the concomitant signs have differential informative value in each particular case.
4. Their integration directs the individual identification. DNA analysis should also be performed if possible.
5. The Bulgarian formulas and nomograms of stature are considerably more precise as compared to other available formulas: these of Trotter—Gleser and Nainis.
6. The time of death is usually defined by approximation in broad boundaries.

References

1. Burns, K. R. Forensic Anthropology Training Manual. New Jersey, Prentice Hall, 1999, 198-204.
2. Knight, B. Simpson's Forensic Medicine.9th ed. New York, Arnold, 1993, 35-39.
3. Nafte, M. Flesh and bone. Durham, North Carolina, Carolina Academic Press. 2002, 117-132.
4. Йорданов, Й., Д. Радойнова. Съдебномедицинска остеологична експертиза. — В: „Престиж офис ООД", 2003, 125—137.

Institute of Experimental Morphology and Anthropology with Museum
Bulgarian Anatomical Society

Acta morphologica et anthropologica, 13
Sofia • 2008

Dermatoglyphics of Bulgarian Females — Finger and Palm Ridge Count

S. Tornjova-Randelova, P. Borissova, D. Paskova-Topalova

Institute of Experimental Morphology and Anthropology with Museum, Bulgarian Academy of Sciences, Sofia

The aim of the present study is to characterize the finger and palm ridge count on both hands of representative excerpt in healthy Bulgarian women. Subject of the study are the dermatoglyphic prints taken from both hands of 1270 Bulgarian females from 116 settlements in the country. Descendent formulae about ridge count of fingers and palm interdigital areas are elaborated. The investigated individuals are distributed according to the summed finger and summed palm ridge count, and according to the total finger and total palm ridge count. The results presented in this work complement the entire dermatoglyphic characterization of the Bulgarian population and could be used as a norm in the dermatoglyphic investigations of patients with different inborn and inherited diseases.

Key words: dermatoglyphics, finger ridge count, palm ridge count, Bulgarian women.

Introduction

The finger and palm ridge count is a quantitative dermatoglyphic feature. In Bulgaria exist data only about finger and palm ridge count of healthy individuals from Northeast Bulgaria [5] and about some control groups of healthy persons when patients suffering from different diseases were investigated [6, 7]. That's why, in the elaboration of the National program "Anthropological characterization of the Bulgarian population" realized in the Department of "Anthropology" in IEMAM, BAS, a dermatoglyphic study of the population was carried out, as well.

The aim of the present study is to characterize the finger and palm ridge count on both hands of representative excerpt in healthy Bulgarian women.

The results about ridge count of healthy Bulgarian men are presented in separate paper [4].

Material and Methods

Object of the study are the dermatoglyphic prints for both hands of 1270 healthy women from 116 settlements in the country. The finger and palm ridge count is

elaborated according to the methods of P e n r o s e [2] and H o l t [1]. Variation statistical analysis is applied too, and for the bilateral differences is used the t-criterion of Student at $P < 0.05$.

Results and Discussion

Finger ridge count. The highest mean ridge count is established for I digit on right hand, and the lowest — for II digit on left hand (Table 1). The descendent formula for right hand is I > IV > V > III > II. For the left hand the first and second positions exchange themselves, but the ridge count difference is only 0.21 — IV > I > V > III > II. The results obtained correspond to the high frequency of whorls and loops on the I and IV digits, as well as, to the high frequency of arches on the II one [3]. The mean ridge count is higher on each finger in right. Statistically significant is the bilateral difference about I, II and IV digits ($P < 0.05$).

The mean summed ridge count in the right hand is considerably higher compared to the left hand ($t = 4.11$) ($P < 0.01$). Higher is the summed ridge count in right at 63.6% of the females, and in left — at 31.7% of them, while lowest is the per cent (4.6%) of women having equal summed ridge count on both hands. The results obtained correspond to those published by Holt for 240 females — 66.7%, 28.3% and 5.0% respectively [1].

T a b l e 1. Statistical parameters of the ridge count on single fingers and Total ridge count in Bulgarian females

Statistics	Right hand						Left hand						Total both hands
	I	II	III	IV	V	I-V	I	II	III	IV	V	I-V	I-X
n	1184	1220	1234	1228	1229	1113	1227	1207	1226	1204	1201	1115	1012
$\bar{x}$	15.99	11.07	11.22	14.98	11.85	64.78	14.01	10.37	10.76	14.22	11.53	60.67	125.52
S	5.85	6.73	5.76	5.82	5.21	23.22	5.92	6.83	6.20	5.90	5.04	24.09	46.58
Sx	0.17	0.19	0.16	0.17	0.15	0.70	0.17	0.20	0.18	0.17	0.14	0.72	1.46
v	36.58	60.79	51.30	38.85	43.97	35.84	42.26	65.86	57.62	41.49	43.71	39.71	37.11
min	0	0	0	0	0	0	0	0	0	0	0	0	0
max	30	29	27	30	28	122	31	32	29	28	26	116	237

The distribution of women after the summed ridge count on I-V digit shows that most are the females who have ridges from 71 till 80 ones in right, a distribution that doesn't tally with the calculated mean value ($x — 64.78 \pm 0.70$), which falls in the previous interval 61-70 ridges. In left again most are the women having summed ridge count of I-V digit in the interval 71-80 ridges, but the mean value falls nearly to the initial limit of the previous interval ($x — 60.67 \pm 0.72$). The frequency distribution of summed ridge count is moved in left, i.e. negatively skewed for both hands. The non-normality is better expressed in the left hand compared with the right one (Fig. 1).

The Total finger ridge count in both hands (TFRC) for the investigated females is 125.52 ± 1.46. The distribution of the individuals is again asymmetrical, moved in left. Most are the cases into the interval 141-160 ridges, which don't tally with the mean value for TFRC (Fig. 2).

Similar are the results presented by H o l t [1] from a study held out in 1955 about 825 women from England and by K a r e v [5] in 1979 about 1065 Bulgarian females from Northeast Bulgaria. The negative skewness in the frequency distribution is accepted by H o l t as an indicator for the influence of comparatively small genes number over TFRC determination. In the case when big number of genes has

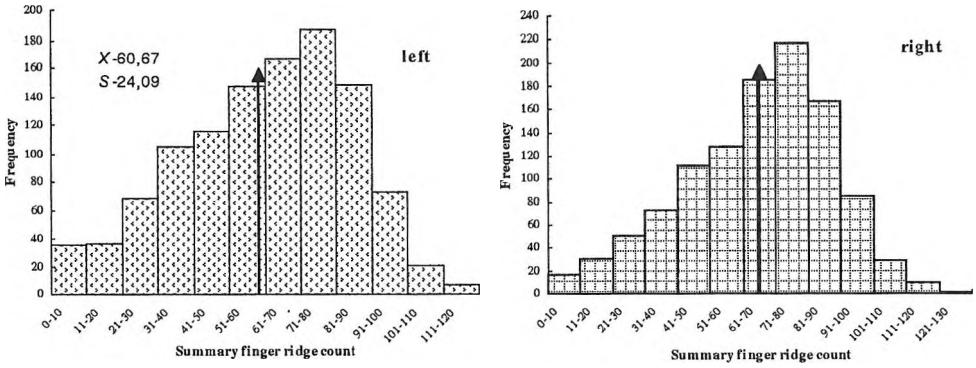

Fig. 1. Distribution of the individuals according to their summary finger ridge count

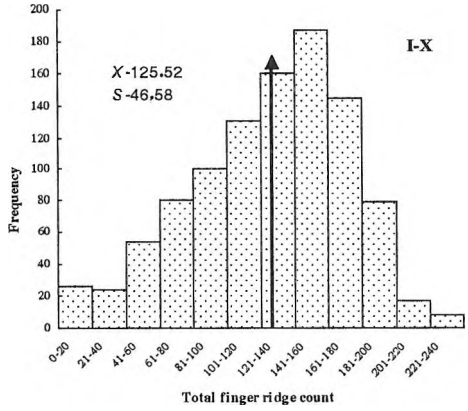

Fig. 2. Distribution of the individuals according to their Total finger ridge count

an appreciable effect on the TFRC determination, the curve of frequency distribution had to be similar to the Gaussian one [1].

Palmar ridge count. Richest of papillary ridges on both hands is the II Interdigital Area (IA) (between finger triradii ***a*** and ***b***), followed in descendent order by IV IA (***c-d***) and III IA (***b-c***). The mean ridge count ***a-b*** is higher for the left hand compared to the right one, while vice versa the ridge count ***c-d*** is in favor for the right hand. Both differences are statistically significant at $P < 0.05$ (Table 2).

T a b l e 2. Statistical parameters of the palmar interdigital ridge count and Total ridge count in Bulgarian females

Statistics	Right hand				Left hand				Total both hands
	a-b	b-c	c-d	a-d	a-b	b-c	c-d	a-d	a-d
n	1178	1129	1128	1084	1184	1108	1097	1061	997
x	36.14	24.75	33.98	95.22	37.12	24.91	33.32	95.61	191.70
S	5.66	5.37	5.76	12.79	5.50	5.23	5.77	12.45	24.18
Sx	0.16	0.16	0.17	0.39	0.16	0.16	0.17	0.38	0.77
v	15.66	21.70	16.95	13.43	14.82	21.00	17.32	13.02	12.61
min	18	8	11	57	17	9	13	60	124
max	61	40	51	140	60	44	50	143	282

The summed ridge count for the three IA in right ***a-d*** vary from 57 till 140 ridges, and in left — from 60 till 143 ridges. The mean values are respectively 95.22 ± 0.39 for the right hand and 95.61 ± 0.38 for the left one. The difference is very small (0.39) and not significant statistically, but yet it exerts probably an influence on the percentage distribution of the individuals according to the ridge count for both hands separately. Equal ridge count for both hands have 5.8% of the women, by 49.3% the ridge count is higher in left, and by 44.8% - in right.

The distribution of females after the summed ridge count ***a-d*** shows that most of them fall into the interval of 91-100 ridges on both hands. These results coincide with the established mean values. The frequency distribution of the summed palmar ridge count is nearly symmetrical in contrast to those of the summed finger ridge count (Fig. 3).

The mean value of Total palmar ridge count (TPRC) for both hands is 191.70 ± 0.77. The minimal TPRC is 124 ridges and the maximal one is 282 ridges. The frequency distribution of the women according to their TPRC is nearly symmetrical, slightly moved in left (Fig. 4).

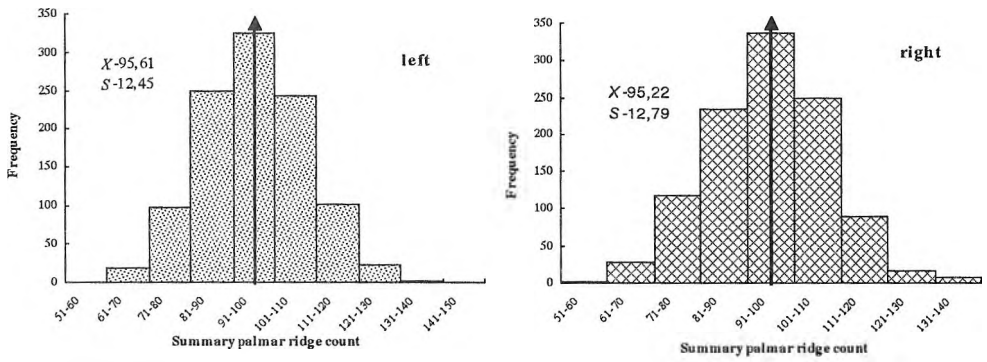

Fig. 3. Distribution of the individuals according to their summary palmar ridge count

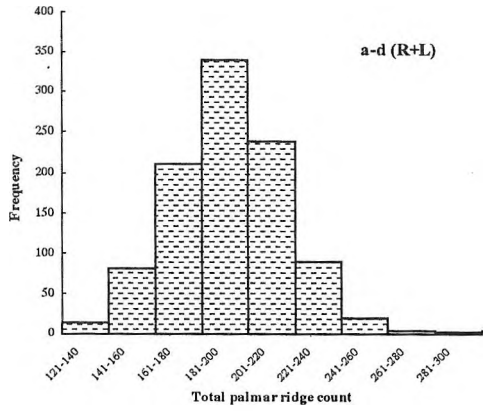

Fig. 4. Distribution of the individuals according to their Total palmar ridge count

Conclusion

The data in present investigation complement the results of previous studies about other dermatoglyphic features in representative excerpt of Bulgarian males and females published by us, being an important contribution to the complete notion about dermatoglyphic status of the Bulgarian population. At the same time they could be used as a norm in the clinical and medico-anthropological studies with theoretical and scientific applied purpose.

References

1. Holt, S. The Genetics of Dermal Ridges. Illinois, Charles C. Thomas, Springfield, 1968, 195 p.
2. Penrose, L. S. Memorandum on Dermatoglyphic Nomenclature. — Birth Defects Original Article Series, **4**, 1968, No3, 1-12.
3. Tornjova-Randelova, S., D. Paskova-Topalova. Dermatoglyphics in Bulgarians — Finger Patterns. — Acta Morphol. et Anthropol., **6**, 2001, 137-143.
4. Tornjova-Randelova, S., P. Borissova, D. Paskova-Topalova. Quantitative Characterization on the Dermatoglyphics of the Fingers and Palms of Male Bulgarians. — Acta Morphol. et Anthropol., 12, 2006, (in press).
5. Карев, Г. Нормален дерматоглифски статус на българите от Североизточна България (канд. дис.). С., 1979. 216 с.
6. Сивков, С. Сравнително антропологично проучване на шизофренно болни от гледна точка на невроонтогенетичната хипотеза за шизофренията (канд. дис.) Пловдив. 2000. 140 с.
7. Торньова-Ранделова, С. Дерматоглифика при здрави деца и деца със зрителна, слухова и интелектуална недостатъчност (канд. дис.). С,. 1986. 214 с.

Institute of Experimental Morphology and Anthropology with Museum
Bulgarian Anatomical Society

Acta morphologica et anthropologica, 13
Sofia • 2008

Anthropometrical Characterization and Sexual Differences of the Mandible Bone

N. Atanassova-Timeva

Institute of Experimental Morphology and Anthropology with Museum, Bulgarian Academy of Sciences, Sofia

The aim of the present investigation is to make a detailed anthropometrical characterization of the mandible bone in skeleton material of individuals from both genders and to determine the sexual differences. The research includes 128 mandibles of adults divided according to their sex into two groups (each group subsumes 64 bones). The absolute metrical differences between both genders are with priority for males concerning all linear features, and for both angles the priority is for females. The sexual differences are biggest for the branch height and they are slightest for the profile angle. The mandible front width and the profile angle vary within wide limits for each bone.

Key words: mandible bone, anthropometrical characterization, sexual differences, categorization.

Introduction

From the literature review [1, 5, 6] we established that in Bulgaria the purposeful anthropological investigations of the mandible bone in skeleton material are not enough and they are orientated predominantly towards bone asymmetry and teeth measuring. The metrical data for mandible bone are scanty, especially for its profile angle.

The aim of the present work is to make a detailed anthropometrical characterization of the mandible bone in skeleton material of individuals from both genders and to determine the sexual differences.

Material and Methods

The investigation includes 128 mandible bones of adults divided according to their sex into two groups (each group subsumes 64 bones). The methods of M a r t i n - S a l l e r [2] and J. J o r d a n o v [7] are applied. In the present paper the data about 8 basic features of mandible bone are discussed: mandible angle width and front width, projectional length, height in symphysis, height and smallest width of the branch, mandibular and profile angle. The distribution by the categories of A l e k -

s e e v-D e b e t z [4] is applied. It was forced to initiate additional categories for some of the features — "hyper small" (for height in symphysis and branch smallest width) and "hyper large" (for mandible front width and projectional length). The data are statistically processed by variation analysis.

The valuation of sexual differences is made by the absolute metrical differences and their relative share, as well as by their standardization according to the Index of relative inter-group differences of W o l a n s k i [3]. This index is applied to determine the sexual differences and it is called Index of Sexual Differences (ISD). Its values submit the sexual differences to the Relative Index Units (IU).

$$ISD = 2 \times [(\bar{x}_{males} - \bar{x}_{females}) \times 100] / (\bar{x}_{males} + \bar{x}_{females}).$$

The *t*-criterion of Student at $P<0.05$ is used to determine the authenticity of the established sexual differences.

Results and Discussion

Valuation of sexual differences' extend

The absolute metrical differences between both genders are with priority for males concerning all linear features (Table 1). All differences are statistically significant with the exception of this of mandible front width. Biggest difference between both genders is observed about branch height. Concerning both measured angles the priority is for females, as the difference is statistically significant only for the mandibular angle.

The values of ISD are graphically presented in Fig. 1. Values of ISD, which are equal to zero, show absence of sexual differences; the positive values display relative priority for males, and the negative ones — for females. The sexual differences are biggest for the branch height, followed by the height in symphysis. Closely values of ISD have the next features: branch smallest width and mandible projectional length, as well as mandible angle width and mandibular angle. The rest two features (mandible front width and profile angle) have slightest sexual differences. This fact probably shows that these both measurements do not depend on the sexual appurtenance of individual.

T a b l e 1. Biostatical characterization of the absolute mandible measurements and sexual differences

	Males							Females							Sexual differences		
	n	$\bar{x}$	SD	SEM	*V*	min	max	*n*	$\bar{x}$	SD	SEM	*V*	min	max	Absolute difference	t-test	ISD
Mandible angle width	58	100.12	6.18	0.81	6.17	86.0	113.5	56	95.88	5.92	0.79	6.18	85.0	113.0	4.24	3.75*	4.33
Mandible front width	60	45.12	2.49	0.32	5.52	40.0	54.0	64	44.53	2.51	0.31	5.64	40.0	53.0	0.59	1.32	1.32
Mandible length-projectional	64	87.47	4.66	0.58	5.32	79.0	98.0	64	82.36	4.36	0.54	5.29	71.5	91.0	5.11	6.41*	6.02
Mandible height in symphysis	64	32.69	2.83	0.35	8.66	28.0	39.0	64	29.23	3.30	0.41	11.29	20.0	35.0	3.46	6.37*	11.18
Mandible branch height	64	64.23	4.38	0.55	6.83	52.0	73.5	64	56.94	5.02	0.63	8.82	46.5	69.5	7.29	8.75*	12.03
Mandible branch smallest width	64	31.66	2.69	0.34	8.48	24.5	37.5	64	29.49	2.46	0.31	8.32	24.0	34.0	2.17	4.76*	7.08
Mandibular angle	64	120.51	5.83	0.73	4.83	106.0	134.5	64	125.53	6.81	0.85	5.42	109.5	141.5	-5.02	4.48*	-4.08
Profile angle of mandible	64	85.48	5.94	0.74	6.95	68.0	99.0	64	86.19	7.47	0.93	8.67	65.0	106.0	-0.71	0.59	-0.82

— Priority for females
* $P<0.05$

T a b l e 2. Distribution of the investigated mandible bones by categories

Category	Rubrics	Males		Category	Rubrics	Females	
		n	%			*n*	%
Mandible angle width							
Very small	*79-90*	3	5,17	*Very small*	*74-85*	2	3,57
Small	*91-96*	11	18,97	*Small*	*86-90*	8	14,29
Medium	*97-103*	25	43,10	*Medium*	*91-97*	25	44,64
Large	*104-109*	15	25,86	*Large*	*98-102*	13	23,21
Very large	*110-121*	4	6,90	*Very large*	*103-114*	8	14,29
Mandible front width							
Very small	*37,8-42,1*	9	15,00	*Very small*	*36,5-40,7*	3	4,70
Small	*42,2-44,6*	16	26,67	*Small*	*40,8-43,1*	18	28,12
Medium	*44,7-47,3*	26	43,33	*Medium*	*43,2-45,7*	22	34,38
Large	*47,4-49,8*	8	13,33	*Large*	*45,8-48,1*	18	28,12
Very large	*49,9-54,2*	1	1,67	*Very large*	*48,2-52,4*	2	3,12
Hyper large	*54,3-x*	-	-	*Hyper large*	*52,5-x*	1	1,56
Mandible length-projectional							
Very small	*64-70*	-	-	*Very small*	*61-66*	-	-
Small	*71-74*	-	-	*Small*	*67-70*	-	-
Medium	*75-79*	3	4,69	*Medium*	*71-75*	6	9,38
Large	*80-83*	11	17,19	*Large*	*76-79*	9	14,06
Very large	*84-90*	38	59,37	*Very large*	*80-85*	36	56,25
Hyper large	*91-x*	12	18,75	*Hyper large*	*86-x*	13	20,31
Mandible height in symphysis							
Hyper small	*x-23,5*	-	-	*Hyper small*	*x-21,2*	2	3,13
Very small	*23,6-28,6*	2	3,12	*Very small*	*21,3-25,8*	8	12,50
Small	*28,7-31,4*	25	39,06	*Small*	*25,9-28,3*	10	15,62
Medium	*31,5-34,5*	19	29,69	*Medium*	*28,4-31,2*	29	45,31
Large	*34,6-37,3*	12	18,75	*Large*	*31,3-33,7*	14	21,88
Very large	*37,4-42,4*	6	9,38	*Very large*	*33,8-38,3*	1	1,56
Mandible branch height							
Very small	*45-53*	1	1,56	*Very small*	*40-48*	5	7,81
Small	*54-58*	7	10,94	*Small*	*49-52*	8	12,50
Medium	*59-63*	19	29,69	*Medium*	*53-57*	24	37,50
Large	*64-68*	26	40,62	*Large*	*58-61*	18	28,13
Very large	*69-77*	11	17,19	*Very large*	*62-70*	9	14,06
Mandible branch smallest width							
Hyper small	*x-24,7*	2	3,13	*Hyper small*	*x-23,1*	-	-
Very small	*24,8-29,5*	9	14,06	*Very small*	*23,2-27,6*	14	21,88
Small	*29,6-32,1*	32	50,00	*Small*	*27,7-30,0*	27	42,18
Medium	*32,2-35,2*	13	20,31	*Medium*	*30,1-32,9*	14	21,88
Large	*35,3-37,8*	8	12,50	*Large*	*33,0-35,3*	9	14,06
Very large	*37,9-42,6*	-	-	*Very large*	*35,4-39,8*	-	-
Mandibular angle							
Very small	*100-111*	5	7,81	*Very small*	*104-115*	4	6,25
Small	*112-117*	15	23,44	*Small*	*116-121*	16	25,00
Medium	*118-124*	27	42,19	*Medium*	*122-128*	24	37,50
Large	*125-130*	16	25,00	*Large*	*129-134*	14	21,87
Very large	*131-142*	1	1,56	*Very large*	*135-146*	6	9,38

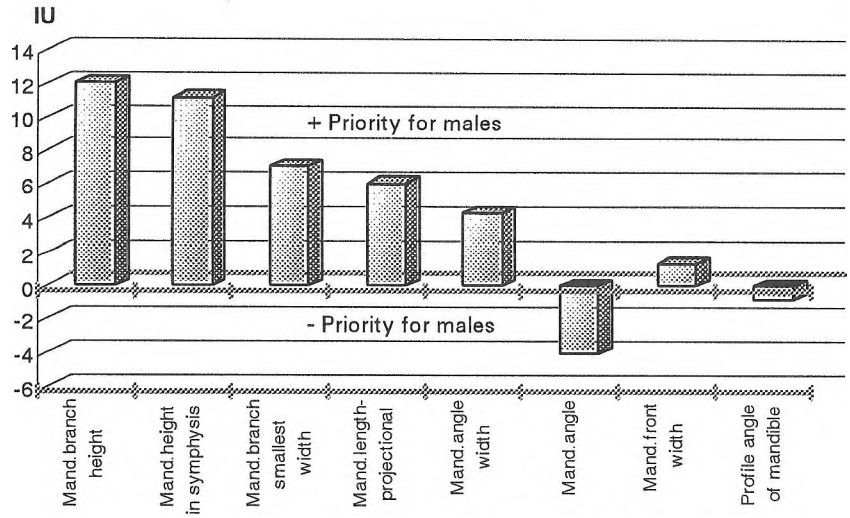

Fig. 1. Sexual differences (ISD data)

Distribution of the investigated mandible bones by categories (Table 2)

Mandible angle width (measurement 66 by Martin–Saller) — concerning both genders the mandibles having "medium angle width" prevail. Lowest is the per cent of the cases, which belong to the category "very small".

Mandible front width (measurement 67 by Martin–Saller) — for both genders the majority of the mandible bones refers to the category "medium". Lowest is the per cent, coming into the category "very large". In female gender there is one case for which the value of this measurement exceed the limits of category "very large" and respectively it was assigned to the category "hyper large".

Mandible length-projectional (measurement 68 by Martin–Saller) — the investigated mandible bones are distinguished for comparatively "large" projectional length. Concerning both genders, the bones with "very large" length prevail. Relatively high is the per cent of the cases that refer to the category "hyper large". For both sexes in the category "very small" and "small" couldn't be referred any of the investigated mandibles.

Mandible height in symphysis (measurement 69 by Martin–Saller) — the investigated mandibles are remarkable for comparatively "small" height in symphysis. In female gender there are cases, which come under the limits of the category "very small". Concerning this feature we have observed the biggest sexual differences in the percentage distribution by categories.

Mandible branch height (measurement 70 by Martin–Saller) — in male gender the majority of cases comes into the category "large", followed by the category "medium". For females the percentage distribution in these two categories is conversely.

Mandible branch smallest width (measurement 71a by Martin-Saller) — for both genders highest is the per cent for the category "small". Concerning the bones of males there are established cases, which come underneath the limits of the category "very small".

Mandibular angle (measurement 79 by Martin–Saller) — in both sexes highest is the percentage frequency of bones, belonging to the category "medium". Concerning the distribution in the rest categories, big distinctions are observed.

Profile angle of mandible (measurement $79_{(1)}$ by Martin–Saller) — for this angle the mean values for both genders are very close. This fact gives us reason to suppose that as the mandible front width, so the profile angle shows a great variability. The percentage distribution for that feature is not discussed in the present work, since Alekseev–Debetz did not give categories about this angle.

Conclusion

1. All linear features have higher absolute values of mandible bones in individuals from the male gender, which is a natural biological regularity. Concerning both measured angles the priority is for females.
2. The sexual differences are biggest for the branch height and slightest for the profile angle.
3. Mandible front width and profile angle vary within wide limits in the separate individuals and these features do not depend on the sexual appurtenance.
4. According to the categories of Alekseev-Debetz, the mandible bones in individuals from the male gender are distinguished for: "medium" width, comparatively "large" projectional length, "small" height in symphysis, "large" height but comparatively "small" width of the branch. The mandibles of females have also "medium" width and comparatively "large" projectional length. In contrast to males, the bones in females have "medium" height in symphysis and "medium" branch height. For both genders highest is the percentage frequency of the mandibles that have "medium" value of the mandibular angle.

References

1. Jordanov, J., M. Botschev. Zusammenhang zwischen dem retromolaren Raum und den Massen des Unterkieferknochens beim Bulgaren. — Stomatol., **28**, 1978, 263—268.
2. Martin, R., K. Saller. Lehrbuch der Anthropologie in sistematischer Darstellung. Bd. I. Stuttgart, Gustav Fischer Verlag, 1957.
3. Wolanski, N. A symmetria ciala czlwieka i jet zmiennosc w swiette funkcji konczyn. — Przegl. Anthrop., **23**, 1957, 461-464
4. Алексеев, В., Г. Дебец. Краниометрия. Методика антропологических исследований. М., Наука, 1964.
5. Йорданов, Й., В. Бочев, Х. Папазян. Степента на асиметрия на долночелюстната кост у българина. — Стоматология, **59**, 1977, 6, 385—391.
6. Йорданов, Й. Антропология в стоматологията. С., Медицина и физкултура, 1981.
7. Йорданов, Й. Наръчник по антропология за медици и стоматолози. С., Университетско издателство „Св. Климент Охридски", 1997.

Institute of Experimental Morphology and Anthropology with Museum
Bulgarian Anatomical Society

Acta morphologica et anthropologica, 13
Sofia • 2008

Anthropological Characterization of the Nasal Region in Cranial Series from Medieval Necropolis in Drastar (9th-15th c. AD)

S. Nikolova, D. Toneva

Institute of Experimental Morphology and Anthropology with Museum, Bulgarian Academy of Sciences, Sofia

The aim of this investigation is to characterize the peculiarities in nasal region of the facial part of cranium in medieval population from Drastar, based on metric and scopic data for size, form and projection of nasal bones, nasal aperture and nasal' base. This craniological investigation was made on 69 crania of adult individuals (39 males and 30 females). The results show that the medieval population from Drastar was distinguished by a large nose size, as the nasal bones are strongly projected, symmetrical, long and wide. The form of the bone nose in profile is mainly straight and convex. In intersexual aspect was observed a tendency for *os nasale* in male crania to be relatively more high (convex) and narrower, compared to female crania.

Key words: nasal region, *os nasale, apertura piriformis.*

Introduction

The nasal region is one of the most characteristic parts of the human face, determining its aspect. The metric and scopic characterizations of the nasal region are important share of the data, necessary for the biological reconstruction of the investigated populations concerning the bone material from archaeological excavations [6].

Characterization of the nasal region complements the morphological notion for the facial part of cranium in buried individuals. The comparatively investigations of bone remains from different ages and areas gives an idea for specific morphological peculiarities of the human face.

The aim is to characterize the peculiarities in nasal region of the cranium's facial part in medieval population from Drastar, on the basis of metric and scopic data for the size and form, the projection of nasal bones, nasal aperture and nasal's base.

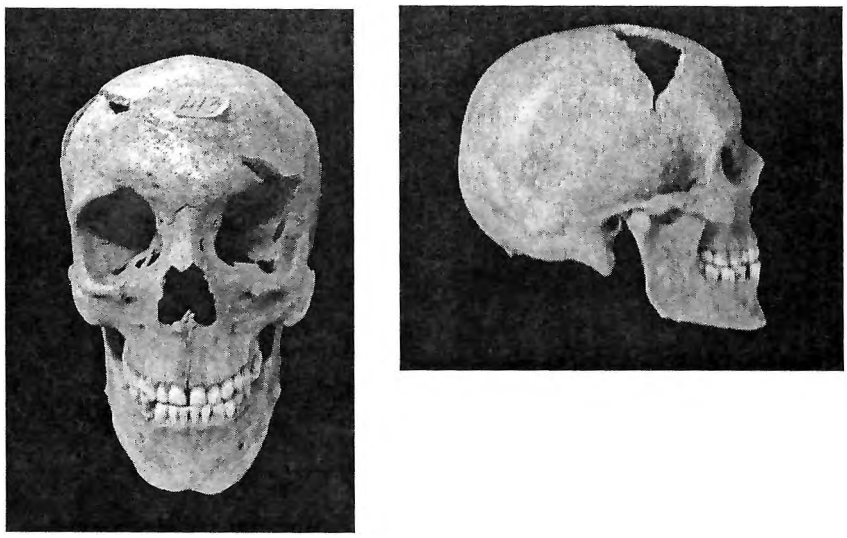

a *b*

Fig. 1. Male cranium of adult individual

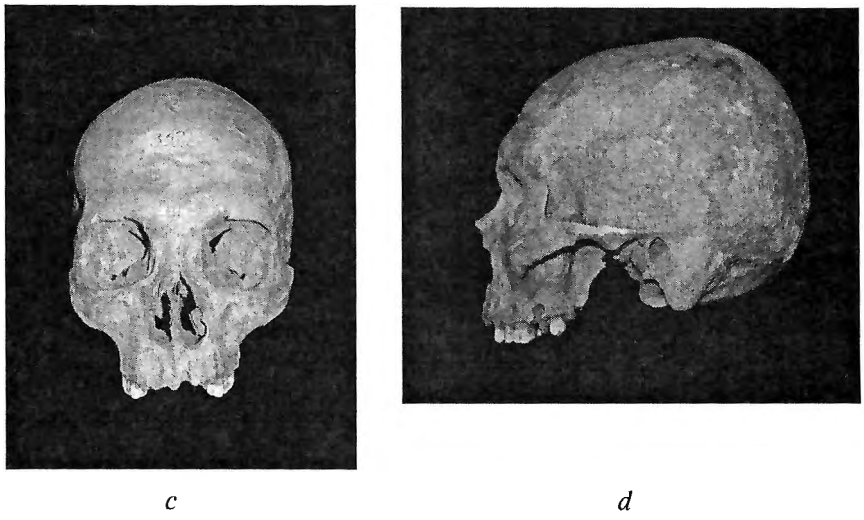

c *d*

Fig. 2. Male cranium of adult individual

Material and Methods

The craniological investigation was made on 69 crania of adult individuals (39 male and 38 female) from medieval necropolis in Silistra, dated 9th — 15th century AD (Figs. 1a, b; 2a, b) [5].

The sex of the investigated cranial series was determined on the basis of metric and scopic features by the methods of R. Martin — K. Saller; V. Pashkova; B. Nikityuk [2, 9, 8].

The physiological age of the individuals was determined by the obliteration's degree (G. Olivier) and by the degree of attrition of the chewing surfaces of the teeth (M. Gerasimov) [3, 7].

The metric characterization of the nasal region was made by the classic methods of R. Martin — K. Saller and B. Alekseev — G. Debetz [2, 4]. Nine linear and three angular features were measured and four indices were calculated. Five scopic features were investigated and described taking into consideration the corresponding grades and scales [7, 1, 2].

The data in this investigation were computed by variation and alternative analysis. The sexual differences in metric features were estimated through the U-test of Mann — Whitney.

Describing the results, the categories from the different features are defined according to theirs rubrics by R. Martin — K. Saller [2].

Results and Discussion

Metric characterization

The biostatistical results from this study are given in Table 1

Table 1. Biostatistical characterization of measurements and indices of the nasal region in male and female crania (osteological data)

No by Martin	Measurements and indices	Males						Females						U-value
		n	mean	min	max	SD	S_x	n	mean	min	max	SD	S_x	
54	Breadth of *aperture pirifomis*	37	24.80	21.00	30.00	2.29	0.38	30	23.25	20.00	27.00	2.08	0.38	0.012*
55	Height of *aperture pirifomis*	28	53.93	49.00	61.00	2.93	0.55	27	51.06	43.00	60.00	4.59	0.88	0.020*
49a	Dacrial height	20	22.88	20.00	27.00	2.30	0.52	15	21.23	18.00	25.00	2.08	0.54	0.053
50	Maxillo-frontal breadth	32	24.70	20.00	32.00	2.57	0.45	21	22.62	19.00	27.00	2.22	0.48	0.008*
57	Least breadth of *os nasale*	26	10.12	8.00	13.00	1.50	0.30	17	10.56	8.00	15.00	1.81	0.44	0.679
57_1	Greatest breadth of *os nasale*	17	18.18	11.00	25.00	2.96	0.72	12	17.13	14.00	20.00	1.69	0.49	0.160
49	Lacrimal breadth	4	23.50	20.00	27.00	2.89	1.44	8	24.25	20.00	27.00	2.36	0.83	0.808
DS	Dactial height	20	12.26	10.00	15.00	1.22	0.27	14	11.75	9.00	19.50	2.58	0.69	0.023*
SS	Simotic height	28	5.96	3.00	8.00	1.33	0.25	17	5.21	40.00	70.00	1.05	0.25	0.042*
73	Nose' profile angle	21	86.10	79.00	98.00	4.75	1.04	16	84.63	78.00	90.00	3.58	0.89	0.534
75	Profile angle of *os nasale*	10	53.40	44.00	65.00	6.13	1.94	9	54.67	43.00	73.00	8.62	2.87	0.905
75_1	Angle of projection of *os nasale*	8	31.63	26	38	3.74	1.32	8	31.50	25	42	5.76	2.04	0.792
54:55	Nasal index	27	46.38	37.07	57.69	4.74	0.91	24	46.21	35.71	55.81	5.43	1.11	-
$57:57_1$	Transversal index of *os nasale*	13	54.94	40.00	66.67	7.76	2.15	12	63.45	50.00	85.71	10.43	3.01	-
$DS:49_a$	Dacrial index	20	55.70	42.31	68.18	7.62	1.70	14	55.01	45.45	84.78	10.62	2.74	-
SS:57	Simotic index	26	58.00	34.78	77.78	12.62	2.47	16	49.73	33.33	63.64	8.62	2.15	-

* *Statistically significant differences at P<0,05.*

The least breadth of os nasale (57_1) and lacrimal breadth (49) are with greater mean values in the female crania from all measured breadth-wise features, as the difference is not statistically significant. All the rest breadth-wise features are greater in the male crania, as statistically significant differences (at $p<0,05$) display only the breadth of apertura pirifomis (54) and the maxillo-frontal breadth (50).

In the male crania all measured height-wise feature are with greater mean value, as all of them show statistically significant intersexual differences at $p<0,05$.

The nose' profile angle (73) is greater in the male crania as in both sexes predominate the crania with angle from the categories "orthognath" and "mesognath". The angle of projection of os nasale (75_1) is with almost equal mean values in both sexes, as the priority is for the male crania, while the profile angle of os nasale (75) is with greater value in the female ones. This expresses tendency, the nasal bones in female crania to be relatively more projecting.

Index characterization for form and proportionately

The nasal index (54:55) is an indicator for the relatively breadth towards height of apertura piriformis. The mean values in both sexes are almost equal, with small priority for male crania.

The transversal index of os nasale ($57:57_1$), indicates the relatively breadth of the nasal bones. The vastly less mean value in the male crania shows tendency for relatively more narrow os nasale at the male crania in comparison with female ones.

The dacrial index (DS:49a) gives idea for the relatively projective height towards breadth of the nasal' back. In the male crania this index has a greater value, which shows that the nasal' back in them is relatively more high (convex) and narrow, compared to female crania.

The simotic index (SS:57) is an indicator for the relatively projective height towards breadth of os nasale in their most narrow part. The vastly greater mean value in male crania express a tendency for nasal bone in their most narrow part to be relatively more high (convex) and narrow, compared with female crania.

Scopic characterization

The results from this study are given in Table 2

T a b l e 2. Distribution of the scopic features in both sexes (by total number and per cents)

Scopic fetures	Male		Female	
	n	%	*n*	%
1. Form of the bone nose in profile	**23**	**100**	**14**	**100**
straight	11	47.82	7	50
convex	10	43.48	4	28.57
concave	2	8.7	2	14.29
undulate	0	0	1	7.14
2. *Os nasale*	**25**	**100**	**14**	**100**
symmetrical, long, wide	13	52	7	50
symmetrical, long, narrow	2	8	1	7.14
symmetrical, short, wide	0	0	3	21.44
symmetrical, short, narrow	0	0	0	0
asymmetrical, long, wide	7	28	1	7.14
asymmetrical, long, narrow	3	12	1	7.14
asymmetrical, short, wide	0	0	1	7.14
asymmetrical, short, narrow	0	0	0	0
3. *Spina nasalis anterior* (1-5)	**23**	**100**	**22**	**100**
grade 1	0	0	0	0

grade 2	0	0	5	22,72
grade 3	11	47.82	13	59.09
grade 4	6	26.09	3	13.64
grade 5	6	26.09	1	4.55
4. Lower end of *apertura piriformis*	**39**	**100**	**29**	**100**
anthropina	23	58.97	17	58.62
infantilis	9	23.08	6	20.69
fossa praenasalis	4	10.26	1	3.45
sulcus praenasalis	3	7,69	5	17.24
5. Form of *apertura piriformis*	**26**	**100**	**20**	**100**
pear-shaped	22	84.62	13	65
triangle	3	11.54	5	25
heard-shaped	1	3.84	2	10

The bone nose in profile is predominantly convex and straight in male crania. The concave form is found more rarely, while the undulated one is not established. In the female crania are accounted all forms of the bone nose, as the convex and straight ones again are found in greatest per cent, while the concave and undulated form are found in less per cent [7].

In both sexes highest frequency has the symmetrical long and wide *os nasale.* Asymmetrical long and wide bones are found in a less per cent. At the female crania in few cases are found symmetrical short and wide, asymmetrical long and narrow, asymmetrical short and wide and asymmetrical long and narrow nasal bones [7].

Spina nasalis inferior is accounted by a 5 grades scale (1-5). Crania with grade 3 (middle development of the prick) are established at highest per cent in both sexes. Slightly developed prick (grade 2) in the male crania is absent, while in the female ones it is present. The grades 4 and 5 (strong developed nasal' prick) are found in equal per cent in male crania, while in female ones the 4 and 5 grades are more rarely established [1].

In both sexes according to the lower end of *apertura piriformis*, at highest frequency is the "*anthropina*" form (sharp ridge of *apertura piriformis*). The following by frequency is the "*infantilis*" form (blunt lower end). From all crania the "*fossae prenasales*" form (formed *fossae*) is established at lower frequency, while the "*sulcus praenasalis*" form (formed groove) is absent [2].

In both sexes the form of *apertura piriformis* is predominantly pear-shaped, as following by frequency is the triangle form, and the heard-shaped one is presented with lowest per cent [7].

Conclusion

The described results from the metric and scopic investigation of crania from medieval necropolis in D r a s t a r, characterize the morphological peculiarities in nasal region of the individuals. These results show that the medieval population from Drastar was distinguished by a large nose size, as the greatest superiority had the high and narrow *aperture piriformis* with lower end "*anthropina*" and well-developed *spina nasalis anterior.* The middle part of the face is "orthognathous", with relatively

high nasal's base. The nasal bones are strongly projecting, symmetrical, long and wide. The form of the bone nose is mainly straight and convex in profile and the nasal aperture is with pear-shaped form.

In intersexual aspect statistically significant differences are established in all measured height-wise features, as well as in two breadth-wise ones, which are with greater measurements in the male crania. The index characterization expresses tendency for *os nasale* in the male crania to be relatively more high (convex) and narrower, compared with female ones.

References

1. Broca, P. Instructions anthropologiques. Paris, 1875.
2. Martin, R., K. Saller. Lehrbuch der Anthropologie in sistematischer Darstellung., Band I. Stuttgart, 1957.
3. Olivier, G. Pratique anthropologique. Paris, 1960.
4. Алексеев, В. П., Г. Ф. Дебец. Краниометрия. М., 1964.
5. Ангелова, С т. Археологическото проучване на средновековния Дръстър /резултати и проучвания/. — В: Дуросторум — Дръстър — Силистра. Силистра, 1988, 32—52.
6. Боев, П., Н. Кондова, Сл. Чолаков. Биологична реконструкция на ранносредновековното население на българските земи. — Българска етнография, **2**, 1980, 15—27.
7. Герасимов, М. М. Восстановление лица по черепу. М., 1955.
8. Никитюк, Б. А. Определение пола по скелету и зубам человека. — Вопросы антропологии, **3**, 1960, 135—139.
9. Пашкова, В. Краниометрия как один из методов повышения достоверности определения пола по черепу. — Вопросы антропологии, **7**, 1961, 95—101.

Institute of Experimental Morphology and Anthropology with Museum
Bulgarian Anatomical Society

Acta morphologica et anthropologica, 13
Sofia • 2008

Anthropological Characterization of the *Scapula* in Bone Remains from Mediaeval Necropolis in Drastar (9th - 15th century AD)

D. Toneva, S. Nikolova

Institute of Experimental Morphology and Anthropology with Museum, Bulgarian Academy of Sciences, Sofia

In total, 41 males and 23 female scapulae were metrically and scopically investigated in detail. The results obtained show significant differences in size and form of the scapula in both sexes.

Key words: *scapula*, feature, sexual differences.

Introduction

The examination of human postcranial skeleton in bone remains from archaeological excavations, and in particular every bone of the skeleton, present an opening to give notion for sex and age, stature, proportionality and body massiveness of buried individuals and to trace back the physical development of differently ancient human populations.

The *scapula* as a whole is very rarely saved from archaeological excavation, and that's why the data of its detailed morphological description are too little.

The aim of this study is to make a detailed metric and scopic characterization of *scapula*, to establish the sexual differences of separate features and to determine these ones, which are of great significance for the sexual differentiation.

Material and Methods

The anthropological investigation was done on osteological material from archaeological excavations of mediaeval necropolis in the National Archaeological Reserve "Durostorum — Drastar — Silistra" [4]. In total, 41 males and 23 female scapulae, belonging to adult individuals, were investigated. The sex and age were determined by metric and scopic features of cranium and postcranial bones, described by R. Martin — K. Saller [1], V. P. Alekseev [3], B. A. Nikityuk [5], etc.

The anthropological investigation was done by the classical methods of R. Martin — K. Saller [1] and V.P. Alekseev [3]. Eleven metric features were measured, four indices were calculated and four scopic features were described through grades and scales after V. P. Alekseev [3].

The metric data were analyzed using SPSS version 13.0. The sexual differences were evaluated through the U-test of Mann-Whitney. The quantitative assessment of sexual differences was made by the Wolanski's index for inter-group comparisons (ISD) [2]:

$$ISD = \frac{2.(x_1 - x_2).100}{x_1 + x_2},$$

where x_1 is mean of the feature in males and x_2 is mean of the feature in females.

Results and Discussion

Metric characterization

The main biostatistical results of the study are given in Table 1.

Table 1. Biostatistical characterization of measurements and indices of human scapula, for individuals from both sexes (osteological data)

No by Martin	Features	Males						Females						ISD	U-value
		n	mean	min	max	SD	$s\bar{x}$	*n*	mean	min	max	SD	$s\bar{x}$		
1	Anatomical breadth	6	164.58	147	179	13.33	5.44	6	147.75	139	160	7.87	3.21	10.78	0.045*
2	Anatomical length	11	106.59	95	118	7.69	2.32	8	95.81	90	103	4.71	1.66	10.65	0.004*
3	Length of *margo lateralis*	18	140.17	128	155	7.24	1.71	13	126.23	115	140	8.41	2.33	10.47	0.000*
4	Length of *margo superior*	7	85.10	71	106	12.67	4.79	6	75.33	71	84	4.84	1.98	12.18	0.114
5a	Anatomical breadth of *fossa infraspinata*	9	119.06	106	137	8.93	2.98	7	111.00	100	120	8.37	3.16	7.01	0.124
6a	Anatomical breadth of *fossa supraspinata*	8	63.38	46	78	11.25	3.98	5	48.20	44	50	2.49	1.11	27.21	0.004*
7	Length of *spina scapulae*	13	141.42	123	157	10.83	3.00	7	126.93	120	138	7.09	2.68	10.80	0.008*
12	Length of *cavitas glenoidalis*	35	41.83	38	47	2.29	0.39	20	36.20	32	41	2.19	0.49	14.43	0.000*
13	Breadth of *cavitas glenoidalis*	35	29.69	23	35	2.11	0.36	23	25.02	23	30	1.63	0.34	17.07	0.000*
15	Breadth-wise - lengthwise angle	5	94.60	88	102	5.98	2.68	6	91.33	80	96	5.72	2.33	3.52	0.409
17	Axilo-glenoidal angle	5	139.00	130	152	8.00	3.58	6	140.00	131	151	7.77	3.17	-0.72	0.582
2:1	Scapular index	6	66.38	56.74	73.47	6.03	2.46	5	64.50	62.30	68.35	2.32	1.04	2.87	-
3:1	Marginal index	6	86.78	79.78	95.24	6.49	2.65	6	86.71	82.14	91.80	4.46	1.82	0.08	-
6a:5a	Index of spinal cavities b)	6	48.95	38.98	58.26	7.71	3.15	9	43.52	39.29	50.00	4.63	2.07	11.74	-
13:12	Lengthwise – breadth-wise index of *cavitas glenoidalis*	33	71.11	50.00	79.49	5.45	0.95	20	68.84	63.89	78.13	3.69	0.83	3.24	-

The basic metric features of ***scapula*** are **its anatomical breadth (1)** and **anatomical length (2)**. The measurements of both features are significantly greater ($P<0.05$) in male scapulae than in female ones. The difference is 16.83 mm for anatomical breadth and it is 10.78 mm for anatomical length.

The next two features characterize *fossa infraspinata* of the *scapula*. They are: **length of *margo lateralis* (3)** and **anatomical breadth of *fossa infraspinata* (5a)**. The means of both features are greater in male scapulae, but the sexual difference in

the first feature (13.94 mm) is statistically significant ($P<0.05$), whereas the difference for the second one (8.06 mm) is not significant.

The metric characterization of *fossa supraspinata* includes the following two features: **length of *margo superior* (4)** and **anatomical breadth of *fossa supraspinata* (6a)**. The measurements of these features are greater in male scapulae also, but only the second feature is statistically significant ($P<0.05$). The male-female difference is 9.77 mm for the length of *m. superior* and it is 15.18 mm for the anatomical breadth of *f. supraspinata*. The previous shows that this measurement is greater with a quarter in male scapulae than in female ones.

The ***spina scapulae*** is an important element for the anatomical structure of scapula and it is metric characterized through its **projection length (7)**. Its measurement is significantly greater ($P<0.05$) in male scapulae with 14.49 mm than in female ones.

The main features of ***cavitas glenoidalis*** are its length and breadth. The mean of the **length of *c.glenoidalis* (12)** is significantly greater ($P<0.05$) in male scapulae than the mean in female ones. The male-female difference is 5.63 mm. The **breadth of *c.glenoidalis* (13)** shows significant difference ($P<0.05$) between both sexes. It is greater in male scapulae with 4.67 mm.

In this study are read data for two angles: **breadth-wise - lengthwise angle (15)** and **axilo-glenoidal angle (17)**. The first angle is little greater than the right angle in both sexes — with 4.6° in male scapulae and with 1.3° in female ones. The second angle is an obtuse angle with almost equal values in both sexes — about 140°.

Index characterization about form and proportionality of scapula

The form and proportionality are determined computing following four indices:

The **scapular index (2:1)** is greater in the scapulae of male individuals at 1.88 %, than its value in these of females. The difference shows that male scapulae are relatively longer and narrower compared to female ones.

The **marginal index (3:1)** has very close values in scapula of males and females. This result shows that the scapulae in both sexes are with relatively almost equal length of *margo lateralis* towards anatomical breadth.

The **index of spinal cavities b) (6a:5a)** is greater in male scapulae at 5.43 %. That difference determines relatively larger breadth of *fossa supraspinata* in male scapulae compared to that in female ones.

The **lengthwise — breadth-wise index of *cavitas glenoidalis* (13:12)** is greater in male scapulae again at 2.27 %. This male-female difference shows that *cavitas glenoidalis* in males is relatively shorter and wider compared with the same one in females.

Comparative assessment of sexual differences by the data of ISD

The values of **index of sexual difference (ISD)** show that all measured features have priority for the male scapulae (with slightly exception for feature 17) (see Table 1). Highest value of ISD has the anatomical breadth of *fossa supraspinata*. Next by strength are the sexual differences for features characterizing *cavitas glenoidalis* — its breadth and length. Comparatively strong differences for both sexes display also the features that characterize the *scapula* as a whole, as well as its *fossa infraspinata*, *margo superior* and *spina scapulae*. Slightly sexual differences are found in the measured angles. Primary meaning for the assessment of sexual differences has the index of spinal cavities b) too. About other indices, the values of ISD show slight male-female differences.

Scopic characterization

The **form of *margo superior scapulae*** is reported in 11 male and 8 female scapulae. *Margo superior* is practically horizontal in 5 male and in 4 female scapulae. *Margo*

superior is inclined below 35° in other 5 male scapulae and in 3 female ones also. The incline of *margo superior* is above 35° in 1 male and 1 female scapula.

The **form of *incisura scapulae*** is determined in 23 male and in 11 female bones. The absence of *incisura scapulae* is registered in 2 males and 1 female scapula. A shallow incisura is recorded in 7 male and in 6 female bones. A deep *incisura scapulae* is observed in 13 male and in 4 female scapulae. An *incisura scapulae*, whose end almost shape a complete circle is met in 1 male bone only and it is not found among female scapulae. The form of *incisura scapulae* that is apertura is missing in both sexes.

The **form of *spina scapulae*** is determined in 27 male and in 16 female scapulae. The *spina scapulae* is thin, with small extension on the level of *incisura scapulae* in 14 male scapulae and in 13 female ones. The *spina scapulae* is thin in its basis and then get thick in 9 male and in 3 female scapulae. The *spina scapulae* is uniformly thin along its whole length in 2 male scapulae only, and the *spina* is sharply curved down after its basis in 2 bones, as well. The last two forms of *spina scapulae* are not recorded in female scapulae.

The **form of *cavitas glenoidalis*** is presented by a pear-shaped cavity in all 35 male and 22 female scapulae. An ovoid-shaped cavity is not observed.

Conclusions

All measured lengths and breadths of scapula are greater in males than in females.

According to the data of indices about form and proportionality, the male scapulae are relatively longer and narrower, with wider *fossa supraspinata* and with shorter and wider *cavitas glenoidalis*, compared to the female scapulae.

From scopic features the sexual differences are well pronounced in the form of *incisura scapulae*. It is predominantly deep in male scapulae, but it is mainly shallow in female ones.

The comparative assessment of sexual differences for all investigated metric features shows that male and female scapulae are differentiated at greatest about anatomical breadth of *fossa supraspinata* and about length and breadth of *cavitas glenoidalis*, which probably reflect the different development of the musculature in scapular region in both sexes.

The established sexual differences in the investigated anthropological features of scapula could be used to formulate the algorithms that determine or specify additionally the sexual affiliation of bone remains, when there are scarce or missing data for the sexual differentiation.

References

1. M a r t i n, R., K. S a l l e r. Lehrbuch der Anthropologie in systematischer Darstellung. Band I. Stuttgart, 1957.
2. W o l a n s k i, N. A symmetria ciala czlwieka i jet zmiennosc w swiette funkcji konczyn. — Przegl. Anthrop., **23**, 1957, 461-464.
3. А л е к с е е в, В. П. Остеометрия. М., Наука 1966.
4. А н г е л о в а, С т. Археологическото проучване на средновековния Дръстър (резултати и перспективи). — В: Дуросторум — Дръстър — Силистра. Силистра, 1988, 32—52.
5. Н и к и т ю к, Б. А. Определение пола по скелету и зубам человека. — Вопросы антропологии, 4, 1960, 135—139.

Institute of Experimental Morphology and Anthropology with Museum
Bulgarian Anatomical Society

Acta morphologica et anthropologica, 13
Sofia • 2008

Histomorphologic Changes in the Gingiva of Dogs with Different Periodontal Diseases

I. Borissov, D. Sivrev, D. Chaprazov, A. Sivreva***, N. Grozeva, E. Firkova****, I. Savov*****

Veterinary Faculty, Thracian University, Stara Zagora
**Medical Faculty, Thracian University, Stara Zagora*
***IPPS – Stara Zagora*
****Faculty of Dentistry, Medical University – Plovdiv*
*****ISP "Pirogov", Sofia*

We present histomorphologic changes in the gingiva of dogs with different periodontal diseases. Periodontal diseases in dogs show big variety when it concerns the clinical symptoms — from comparatively slight color changes (slight erythema) of the marginal and papillary tissues to severe ulcerations, necrosis and sequestrations. Histologic changes vary in accordance with the combination of the severity and the localization of the pathologic process — from vasodilation to deep ulcers, where some parts of the mucosa are lost.

Key words: mucosa, periodontal complex, gingivitis, inflammation, veterinary dentistry.

Introduction

The periodontal complex includes morphologically different tissues which are in a biologic and functional union [3, 11]. The diseases of this complex, both inflammatory like gingivitis and periodontitis, and the like are often spread in the clinical practice in people [1] and in animals [2, 8]. These diseases represent a serious challenge for the modern human and veterinary dentistry.

The main etiologic factor for the inflammatory periodontal diseases is the dental biofilm.

Still there are many unrevealed issues, connected with the initiation and progression of the inflammatory process in the periodontal tissues, the pathomorphologic changes and also the changes in the immune system [7].

The purpose of this study was to evaluate histomorphologic changes in the gingiva of dogs with different periodontal diseases. To solve the purpose we set 2 definite tasks:

1. To determine the clinical changes in dogs' periodontal complex.
2. To examine the histomorphologic changes in the periodontal tissues after the progression of an inflammatory reaction.

Material and Methods

For the purpose of our study we used 24 mongrel dogs, age between 3 and 5 years and weight between 12 to 16 kg. The dogs had clinical signs of generalized chronic periodontal disease. Clinical examination was performed by the Williams' periodontal probe. The main clinical parameters — pocket probing depth, gingival recession, clinical attachment level, were put in a special periodontal chart. We took a biopsy material from the free marginal edge and the attached gingiva in the left mandibular canine region. The material was processed followed the standard dying technique with hematoxillin — eosine.

After the fixation the slices were viewed by light microscope "Ampival" with magnification 4.0 × 0.10.

Results

1. Clinical results

The clinical signs were systematized in 4 groups according to the severity of the pathologic process:

Ist group — local gingival hyperemia without a swelling, bleeding on probing;

IInd group — bleeding on probing, swelling, pocket probing depth up to 3 mm;

IIIrd group — bleeding on probing, swelling, pocket probing depth more than 3 mm, tooth mobility grade 1 or 2;

IVth group — severe bleeding on probing, swelling, tooth mobility grade 3, pocket probing depth more than 3 mm and presence of pus in the pockets.

2. Histological results

Most of the samples showed acantosis — an overgrowth of stratum spinosum. At the same time tearing of the intercellular connections was obvious, together with initial invert micropapilomatosis and blood vessels dilatation (Fig. 1, 2, 3).

There also was in some cases an initial degree of keratosis of the cells in stratum corneum. The other mucosal layers were extended. A wide spread invert papilomatosis and hyperemia were obvious (Fig. 4).

The superficial mucosal layer was ulcerated in two of the dogs. A local acantosis, necrosis and sequestration of the tissue was seen (Fig. 5).

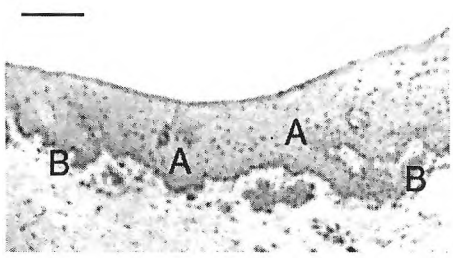

Fig. 1. Mucosa with acantosis (A), blood vessels enlargement and initial invert micro-papilomatosis (B). × 4

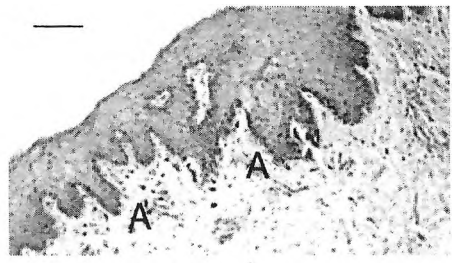

Fig. 2. Mucosa with initial invert Micropapilomatosis (A). × 4

Fig. 3. Mucosa with advanced invert Micropapilomatosis (A). × 4

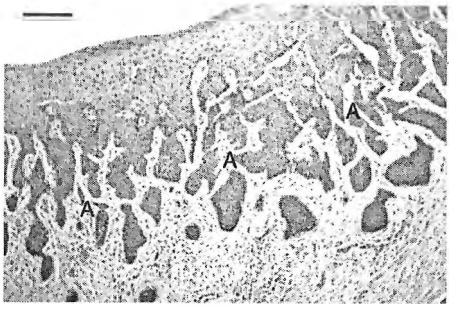

Fig. 4. Mucosa with wide spread invert micropapilomatosis (A). × 4

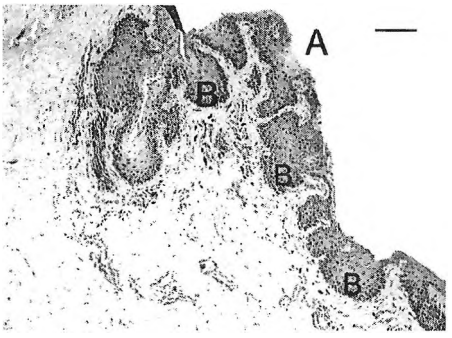

Fig. 5. Mucosa with ulceration (A) and focal acantosis (B). × 4

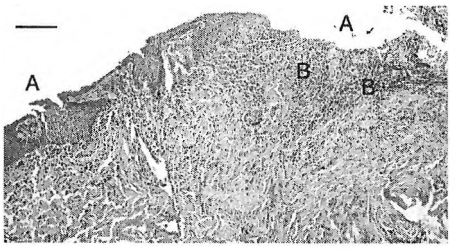

Fig. 6. Mucosa with ulceration (A) and diffuse deep nonspecific infiltrates (B). × 4

In the samples of one dog we found out severe granulocytes' infiltration with cariorexis of the nuclei in part of them. Some of the mucosa was necrotic and sequestrated. Thus ulcerations were formed, infiltrated with polymorphonuclear leucocytes and cellular debris (Fig. 6).

Duscussion

A variety of clinical signs were obvious. They characterized the severity of the disease, and also its type. The progression of the diseases is usually in both vertical and horizontal direction [4, 5].

The histologic changes in the initial stage are connected with cellular overgrowth in stratum spinosum (acantosis) and tearing of the intercellular connections. A pronounced micropapilomatosis was seen in the advanced stage of the disease.

The destruction of the epithelial cells and the desmosomes could be connected with a change of the interaction among them and also the expression of integrins [6]. This statement explains the possibility why in the advanced stage an ulceration, necrosis and sequestration of the tissue was seen in the superficial layer of the mucosa.

The progression of the disease is connected with lysis of collagen fibres of gingival connective tissue and an alveolar bone resorption. These processes lead to an increased tooth mobility. The pathologic changes in the periodontal tissues are also due to the cytotoxic activity of the involved root surface, damaged by the absorbed endotoxins and other inflammatory mediators [13]. Only one part of endotoxins' molecule — LIPID A — is with certain biologic activity, stimulates vascular permeability, activates the complement cascades, the production of interleukins and the involvement of the immune system [12].

Along with the destruction of the periodontal tissues a fibrosis and definite changes of the non-collagen ingredients is seen. These changes are different in the different clinical stages and the different periodontal disease in dogs [9, 10].

Conclusions

1. Periodontal diseases in dogs show big variety when it concerns the clinical symptoms — from comparatively slight color changes (slight erythema) of the marginal and papillary tissues to severe ulcerations, necrosis and sequestrations.
2. Histologic changes vary in accordance with the combination of the severity and the localization of the pathologic process — from vasodilation to deep ulcers, where some parts of the mucosa are lost.

References

1. Bartold, P., J. Laurence, A. Walsh, N. Sampath. Molecular and cell biology of gingival. — Periodontology, **24**, 2000, 28-55.
2. Boutoille, F., A. Dorizon, A. Navarro, J. Pelerin, M. Gauthier. Echocardiographic alterations and periodontal disease in dogs: a clinical study. — In: Proceeding of the 15th European Congress of Veterinary Dentistry, Cambridge, 2006, 63-65.
3. Camil, S., S. Hubert. Periodontal structure. — In: Stomatologie Veterinara. Cluj-Napoca, 2006, 16-37.
4. Gorel, C., Periodontal disease — prevention is the key? — EVDS, Forum, **10**, 2001, No1, 1-8.
5. Gorel, C., M. Gracis, Ph. Hennet, L. Verhaert. Disease types. — In: Periodontal disease in dogs. WALTHAM Focus, Aniwa Publishing, Special edition, 2003, 9-24.
6. Gurses, N., A. Thorup, J. Reibel, G. Carter, P. Holmstrup. Expression of VLA-integrins and their basement membrane ligands in gingival from patients of various periodontitis categories. — Journal of Clinical Periodontology, **26**, 1999, 217-224.
7. Jeusette, I., S. Fernandez, M. Compagnucci, L. Vilaseca, V. Romano, C. Torre. Effects of oral colostrums or whey on dental score, blood IGG and salivary IGA in cats following dental cleaning. — In: Proceeding of the 15th European Congress of Veterinary Dentistry. Cambridge, 2006, 107-108.
8. Lobprise, H. Canine periodontitis: Isolation and identification of periodontopathogens and initial evaluation of a bacteria. — In: Proceeding of the 15th European Congress of Veterinary Dentistry. Cambridge, 2006, 66-67.
9. Narayanan, A., R. Page. Connective tissue of the periodontium: a summary and current work. — Collagen Related Research., **3**, 1983, 33-64.
10. Schluger, S., R. Yuodelis, R. Page. Clinical stages. — In: Periodontal disease. Philadelphia, Lea & Febiger, 1990, 3-71.
11. Wiggs, R., H. Lobprise. Dental connection. — In: Veterinary Dentistry. Philadelphia, Lea & Febiger, 1997, 58-81.
12. Williams, K. Endotoxins. — In: Endotoxins, pyrogens, LAL testing and depyrogenation. Marcel Dekker, Inc., vol. 111, 2001.
13. Фиркова, Е., Обсъждане. — В: Обработка на кореновата повърхност при хроничен пародонтит (канд. дис.). София, 2005, 86—127.

Institute of Experimental Morphology and Anthropology with Museum
Bulgarian Anatomical Society

Acta morphologica et anthropologica, 13
Sofia • 2008

Anatomical Study of Rectal Fascia and Connective Tissue Structures Surrounding the Rectum

*D. Dardanov, E. Ivanov, N. Kovachev, T. Deliyski**

Department of Cytology, Histology and Anatomy, Medical University – Pleven
**Department of Surgical Oncology, University Hospital "Dr. Georgi Stranski" – Pleven*

The aim of the study is anatomical investigation of rectal fascia and its relation to perirectal connective tissue structures and spaces. Materials were from adult cadavers and human fetuses. They were dissected and examined histologically. The results show that rectal adventitia and rectal fascia are situated circularly around the extraperitoneal part of the rectum. Rectal fascia is bordered behind by retrorectal space, laterally is connected with pararectal pelvic space by lateral ligament and in front is part of recto-urogenital septum. There are collagen and single elastic fibres in the rectal fascia on histological sections. The rectum with rectal adventitia and fascia compose an integrated morphological compartment.

Key words: rectal fascia, rectal adventitia, pelvic fascias.

Introduction

Rectal fascia has the cardinal role among perirectal structures according to rectal cancer management. The first known description of rectal fascia has been given by Rumanian surgeon and anatomist T. Ionescu in 1890. He described "la gaine fibreuse du rectum" (fibrous envelope of the rectum), which circularly surround the extraperitoneal part of the rectum [2]. The review of contemporary publications shows that there are differences in description of rectal fascia. Because of that the aim of the study is macroscopic and histological investigation of rectal fascia and perirectal connective tissue structures and spaces.

Materials and Methods

We dissected precisely six embalmed with formaldehyde adult cadavers (three male and three female) without pelvic pathology. For histological investigations we used specimens from four fresh adult cadavers (two males and two females) without pelvic pathology. Samples after fixation were included in paraffin and cut at 4 μm. Sections were stained with Haematoxylin & Eosin, Azan, Van Gieson, Orcein and immunostaining with S-100 proteins (to present the nerve fibres). The same histologi-

cal methods were applied for specimens obtained from two (one male and one female) human fetuses with age 17 -19 weeks. On this fetal age the pelvic fascial structures are already developed and this gave us opportunity to investigate the precise topography and relations of perirectal fascias, ligaments and spaces [3].

Results

The rectal adventitia is situated round the muscular wall of the extraperitoneal part of the rectum between rectosigmoid and anorectal junctions (Fig. 1). It is composed of fat and loose connective tissue, branches of superior rectal artery, tributaries of superior rectal vein, perirectal lymph nodes and nerve fibres. The adventitia is the most developed dorsally, decreased laterally and is the thinnest anteriorly.

The rectal fascia is a thin sheet of connective tissue, intimately connected with underlying adventitia and has the same contour as the rectal adventitia. Its cranial beginning is situated just behind superior rectal artery. Rectal fascia is continuing and ending in subperitoneal connective tissue in peritoneal rectal walls. It is connected with longitudinal muscle layer of the anal canal. It is composed of collagen fibres intermingled with elastic fibres and fat tissue.

The retrorectal space is situated behind rectal fascia. There is loose connective tissue in it. The outer border of this space is inner layer of urogenital fascia (Fig. 2). Rectosacral fascia is a quadrangular sheet composed of collagen fibres, some elastic fibres and smooth muscles. It starts from the periosteum of fourth sacral vertebra and pass towards the rectal fascia in caudal and ventral direction (Fig. 3).

Rectal fascia is connected with pararectal pelvic space by lateral ligaments of the rectum, were autonomic nerves from inferior hypogastric plexus (rectal branches), small vessels and some collagen fibres are present.

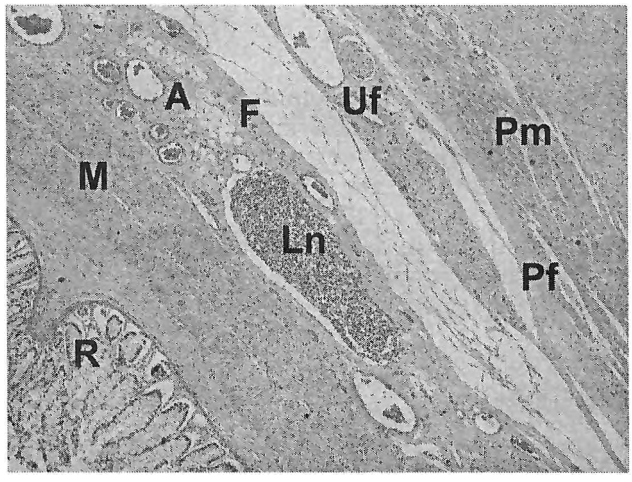

Fig. 1. Presenting of perirectal structures on histological section from human fetus (R — rectal mucosa, M — tunica muscularis, A — rectal adventitia, F — rectal fascia, Ln — perirectal lymph node, Uf — urogenital fascia, Pf — parietal fascia, Pm — m.piriformis). H&E staining, × 60

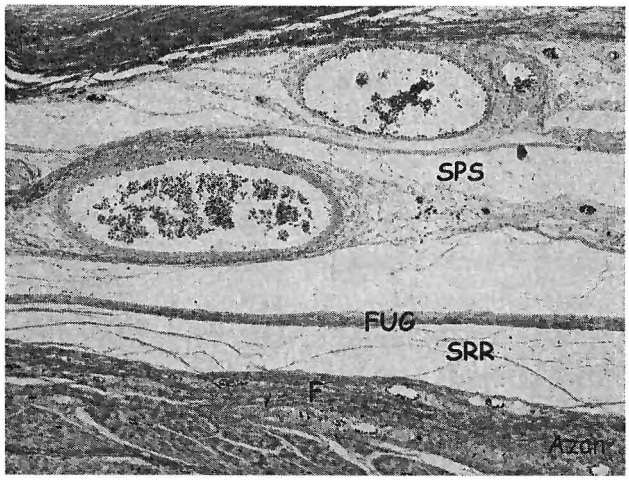

Fig. 2. Fascias and spaces behind the rectum on human fetus. (F — rectal fascia, SRR — retrorectal space, FUG —urogenital fascia, SRS —presacral space with venous plexus). Azan staining, × 100

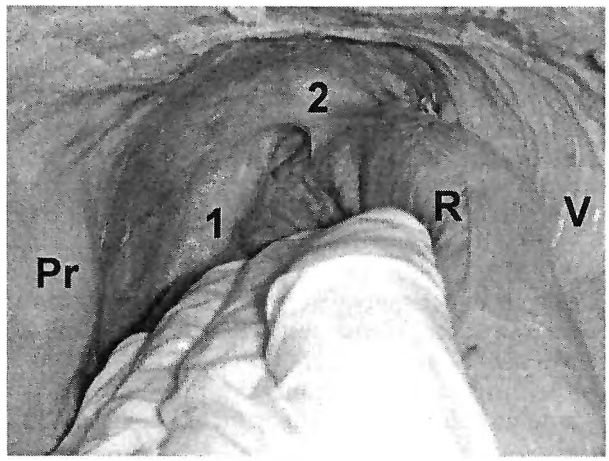

Fig. 3. Presenting of rectosacral fascia (1) and lateral ligament (2) on anatomical specimen from embalmed adult male cadaver (Pr — promontorium, R — rectum, V— urinary bladder)

Rectal fascia is a part of the recto-urogenital septum in front of the rectal wall. It is separated from peritoneoperineal fascia by prerectal space, filled with loose connective tissue. Peritoneoperineal fascia is structured by collagen and elastic fibres with longitudinal smooth muscle bundles and many nerves (Fig. 4).

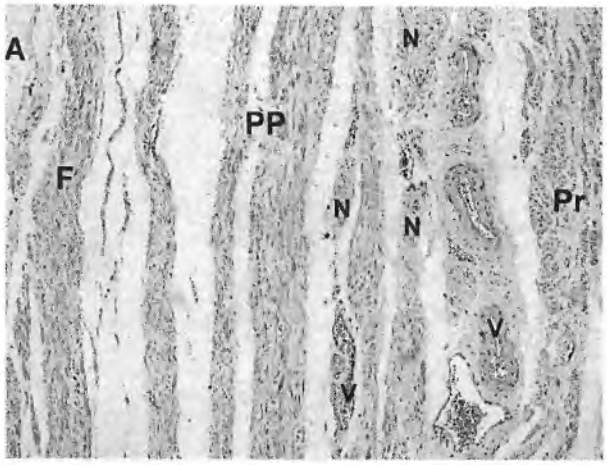

Fig. 4. Presentation of rectoprostatic septum in section from adult male cadaver (A — rectal adventitia, F — rectal fascia, PP — prostatoperitoneal fascia, Pr — prostate, N — nerve fibres, V — periprostatic blood vessels). H&E staining, × 60

Discussion

Our description of rectal adventitia and fascia is similar to this of H. Fritsch [3], and I. Bissett and coauthors [1]. On the other hand, we do not agree with R. Heald and B. Moran [4] who believe that rectal fascia is situated only behind the rectum. About urogenital fascia we agree principally with the descriptions of V. Muntean [7]. We share the view of T. Takahashi et al. [10] about lateral ligament's topography and structure, but we cannot accept the statement of O. Jones et al. [5] that lateral ligament do not exist really and is "artifact, produced during surgical technique". Our description of rectal and peritoneoperineal fascia in recto-urogenital septum coincide with this of I. Lindsey and coauthors [6]. However, we did not find two anatomical separate layers of peritoneoperineal fascia, as M. Nano et al. [8] presented. We believe that "posterior layer" of the peritoneoperineal fascia is in fact the rectal fascia; the statement is maintained by A. Ophoven and S. Roth [9] as well.

In conclusion we can state that rectum with rectal adventitia and rectal fascia composes an integrated morphological compartment, separate from other pelvic connective tissue.

References

1. Bissett, I., K. Chau, G. Hill. Extrafascial excision of the rectum-surgical anatomy of the fascia propria. — Dis. Colon Rectum, **43**, 2000, 903-910.
2. Chapius, P., L. Bokey, M. Fahrer, G. Sinclair, N. Bogduk. Mobilization of the rectum. — Anatomic concepts and the bookshelf revisited. — Dis. Colon Rectum., **45**, 2002, 1-8.
3. Fritsch, H. Topography and subdivision of the connective tissue in human fetuses and in the adult. — Surg. Radiol. Anat., **16**, 1994, 259-265.
4. Heald, R. and B. Moran. Embryology and anatomy of the rectum. — Semin. Surg. Oncol., **15**, 1998, 66-71.

5. Jones, O., N. Smeulders, O. Wiseman, R. Miller. Lateral ligaments of the rectum: an anatomical study. — Br. J. Surg., **86**, 1999, 487-489.
6. Lindsey, I., B. Warren, N. Mortensen. Denonvilliers' fascia lies anterior to the fascia propria and rectal dissection plane in total mesorectal excision. — Dis. Colon. Rectum., **48**, 2005, 37-42.
7. Muntean, V. The surgical anatomy of the fasciae and fascial spaces related to the rectum. — Surg. Radiol. Anat., **21**, 1999, 319-324.
8. Nano, M., A. Levi, F. Borghi, P. Bellora, F. Bogliatto, D. Garbossa, M. Bronda, G. Lanfranco, F. Moffa, J. Dorfl. Observations on surgical anatomy for rectal cancer surgery. — Hepato-Gastroenterol., **45**, 1998, 717-726.
9. Ophoven, A. and S. Roth. The anatomy and embryological origins of the fascia of Denonvilliers: a medico-historical debate. — J. Urol., **157**, 1997, 3-9.
10. Takahashi, T., M. Ueno, K. Azekura, H. Ohta. Lateral ligament: its anatomy and clinical importance. — Semin. Surgl. Oncol., **19**, 2000, 386-395.

Institute of Experimental Morphology and Anthropology with Museum
Bulgarian Anatomical Society

Acta morphologica et anthropologica, 13
Sofia • 2008

Is There a Place for Innovative Approaches in Learning Anatomy

R. Davidova, N. Narlieva

Department of Anatomy, Cytology and Histology, Medical University of Pleven

The increased exchange of medical professionals in the process of globalization pose a question of minimum requirements in medical education. The main recommendations of some international documents are moving towards more student-centered and self-directed learning, utilization the advances in computing and other technologies in delivering the material, early clinical contact and development of Clinical skills learning centers. We shear our experience of applying active learning approaches in teaching anatomy. The active learning methods are well accepted from students and the teaching staff. We steadily believe that there is a place for innovative approaches in learning anatomy. This is an appropriate way to overcome the gap between the basic sciences and clinic and will contribute to training good doctors who could be able to practice allover the world.

Key words: learning anatomy, active methods.

Introduction

The process of globalization led to increased free exchange of medical professionals. Our medical education needs conformation to the world standards. There are several international documents concerning main principles and educational goals that have to reach at 2010: "Global Essential Minimum Requirements for Medical Education" set of global minimum learning outcomes which students of medical schools must demonstrate at graduation; "Global standards for medical education and better health care" recommendations is the re-examination of the medical school educational strategy in reason the educational methods and the assessment to be confirmed with the new educational aims [12].

Applying the "Global standards" vary in different countries depending of specific health needs. To meet the challenges of increasing health needs permanent curriculum changes has inquired. Stress must be given to self-learning and early clinical contact which increases motivation and enriches pre-clinical education.

International experience

The answer of the basic question WHY will motivate students to study so bulky subject. In many medical schools a new approach of teaching and learning has searched.

Anatomy curriculum has structured to show examples of disordered structures because the most of symptoms have better accepted in the anatomy context [2].

Because of these pressures, anatomy experts have endeavored to implement several approaches of teaching and learning, such as self-directed learning [8], dissection repeated in the clinical year [7], case-based anatomy course and clinical anatomy with PBL [9].

The publication of "Tomorrow's Doctors" by the General Medical Council in 1993 has triggered a variety of responses from UK medical schools [1].

The recommendations are decrease the curriculum overloading, implementation the clinical aspects in teaching anatomy [3, 5], "vertical" and "horizontal" integration and early clinical contact for better understanding in the context of basic disciplines.

In UK different approaches are used. Integration is most appropriately achieved by a case-based or a problem-based approach (in Liverpool and Manchester) rather than a strictly system-based approach. In the University of Dundee the "spiral approach" has devised and is favoured — in the progression through the course (the same topic is visited several times in increasing level of complexity — through normal structure and function to abnormality and clinical practice).

In the University of Pretoria, South Africa, a clinical anatomy practicum for clinic is developed. It is conducted to prepare students for the inspection, palpation, percussion and auscultation of the cardiovascular, respiratory, abdominal and urogenital systems. Standardized patients, cadavers, skeletons, prosected specimens, plastinated specimens, X-ray, computed tomography, magnetic resonance images, multimedia programs and clinical case studies has used as resources [6].

Anatomy course has integrated in the curricula of many medical schools by implementing Clinical anatomy [4, 7, 8, 9, 10].

The human anatomy course in the Youngstown State University, US, is centered over a computer software program that presents detailed "step by step" cadaver dissections added with anatomy drawings, models and skeletons [11].

Our experience

From 1990/1991 academic year the anatomy curriculum in Medical University of Pleven includes 322 academic hours divided in three semesters. The restriction necessitated some changes in the curriculum. During the first semester the anatomy lectures was reduced to 8 hours — 4 hours basic knowledge about bones and 4 - about bone connections. This material is thought in details in osteology and artrology practicals and the student's knowledge is assessed in two colloquiums. The topograph anatomy course has removed from the regular lecture course and has proposed as facultative during dissections.

We implemented some active approaches in teaching anatomy by which we are trying to higher the quality of anatomy knowledge acquired. During first semester, we apply elements of self-studying in the courses of osteology and artrology. In a part of groups the students are "self-studied" — divided in subgroups they work with textbooks, atlases, anatomy preparations (bone and joint samples) and software and try to find and learn the objects. Assistants do not explain and show anything and only help the students. At the end of the practical different subgroups present some objects — bones or joints. The role of the assistant is to coordinate and to control the work and to support students when need to specify something. Thus, "the micro-lectures" about the simple anatomical objects, which students can see and fine easily

has avoided. Through a kind of "discovering", we want to stimulate the curiosity and to drive on the self-studying. The most positive in this stile of learning is the relatively individualization in studying process — the opportunity different subgroups to work with there owns speed and way convenient for students.

During the second semester when students do dissections and study internal organs we use so cold "clinical questions". The clinical questions are short (in few words) clinical cases with steadying learning organ or system. On this base, questions about macro and microscopic structure of organs were formulated to help students in answering the clinical question. For instance, to count the layers of the stomach destroyed by perforated stomach ulcus. To answer the clinical questions students have to do some independent self-preparing. At the beginning of the practical, they do a short incoming test to identify the level of self-preparing and to specify the main terms. The work continues with studying preparations from internal organs and observation the histological slides. At the end students try to answer the clinical question. These elements of active learning are very well accepted by the students. They are very interested and active in self-preparing and practical work.

During the dissections, other active learning activities are applied. Student group are divided in subgroups of 2-3 persons. Each subgroup is given so cold "clinical tasks" — short clinical case about a disease in particular aria or an organ in it. Students have to study the area (by self-preparing), to discuss between each other and with the assistant what must be done, to dissect the area and at the end to present it the other students. After that, the clinical case is discussed. This way of working and appearance stimulates the competition ("who will do the work best"). Self-assessment is provided.

There is a practice in our department that demonstrators develop interesting anatomy objects. These elaborations later become interdisciplinary and are the basic point for scientific researches.

The assessment in our department is current — test, self-assessment and peer-assessment; periodic — tests and colloquiums and final exam which includes test, practical exam and viva voice.

The interim results of active-learning groups do not differ significantly comparing with other students (results are higher with a few per cent). Studying the final exam results is imminent and future development in clinic. PBL-groups show significant higher results in the final exam (Table 1).

Conclusions

There is a common tendency to:

- reduce the anatomy curriculum;
- stress to active learning activities;
- look for alternatives in delivering information and learning — internet and special software.

T a b l e 1. Results from the final exam 2004 — 2006

Year	2003/04	2004/05	2005/06
Mean results	3.95	4.12	3.45
Active learning groups	4.35	4.28	3.63
Standard learning	3.44	3.94	3.38

Our proposals

• current optimizing of the basic anatomy course in three semesters by some program restructuring;

• implementation the active learning activities (PBL, active group learning and others) with including clinical aspects;

• try to find a way for some anatomy courses as modules in clinic — for instance CNS during studying neurology;

• short initiating anatomy courses for post-graduate trainers in sugary, orthopedics, radiology, obstetrics and others.

Our permanent goal is keeping traditions to enrich and modernize the anatomy teaching with new methods and approaches in reason to do it more attractive for students and post-graduate trainers, to help them in obtaining steady/stable knowledge for the human body which will be the base useful during there entire clinical practice.

References

1. Bullimore, W. Study skills and tomorrow doctors. WB Saunders Company Ltd, 1998. p. 170.
2. Eccles, S. Why anatomy should still be taught. — Student BMJ, **10**, 2002, 303-352.
3. Heylings, D. J. A. Anatomy 1999-2000: the curriculum, who teaches it and how? — Medical Education, **36**, 2002, No8, p. 702-710.
4. Kagan, I. I. Traditions and perspectives of clinical anatomy education in Russia. — Clin Anat., **15**, 2002, No2, 152-156.
5. Kennedy, D, M, Ip, N. Eizenberg, C. Adams. The text analysis object (TAO): Engaging students in active learning on the web. **www.ascilite.org.au/conferences/wollongong98/asc98-pdf**
6. Pabst, R. Gross anatomy: An outdated subject or an essential part of a modern medical curriculum? Results of a questionnaire circulated to final-year medical students. — Anat. Rac. **237**, 1993, 431-433.
7. Pepcac, S., D. A. Goodenough. Problem-Based Teaching and Learning as a Bridge from Basic Anatomy to clinical clerkships. — Surg. Radiologic, **20**, 1998, 203-207.
8. Peplow, P. V. Self-Directed Learning in Anatomy: Incorporation of case-based studies in to a conventional medical curriculum. — Medical Education, **24**, 1990, 425-432.
9. Rhoten, W. B. Guide to Gross Anatomy and Embryology. Joan C. Edwards School of Medicine, Marshall University, 2004, Huntington, WV.
10. Reidenberg, J. S., Laitman, J. T. The new face of gross anatomy. — Anat. Rec., **269**, 2002, No2, 81-89
11. Womble, D. Anatomy and computers: A new twist to teaching the oldest medical course. — Bioscene, **52**, 15-17. **www.ascilite.org.au/conferences/wollongong98/asc98-pdf**
12. Нарлиева, Н., В. Нишева, З. Радионова, С поглед към „Глобалните стандарти за медицинско образование и по-добра здравна помощ": перспективи и реалности но ВМИ — Плевен. 2003, ИЦ — „ВМИ — Плевен", 31—37.

Institute of Experimental Morphology and Anthropology with Museum
Bulgarian Anatomical Society

Acta morphologica et anthropologica, 13
Sofia • 2008

Glycogen and Collagen Fibres in Myocardium of Endurance Trained Rats Following Nandrolone Decanoate Treatment

S. Delchev, K. Georgieva, Y. Koeva, P. Atanassova*

Department of Anatomy, Histology and Embryology, Medical University, Plovdiv
**Department of Physiology, Medical University, Plovdiv*

The pattern of substrate use by the heart (fatty acids, lactate, and glucose) and its utilization varies according to the duration and intensity of workload and hormonal status. Sex hormones play a substantial role in regulating glycogen metabolism during exercise. The myocardial collagen matrix surrounds myocytes and functions as a medium between them and the circulatory system. This study investigates single and combine effect of endurance training and anabolic androgenic steroids (AAS) treatment on glycogen and collagen content in rat myocardium. AAS administration resulted in increased glycogen in cardiomyocytes and increased perivascular collagen fibres in sedentary rats. The training effects were not associated with alterations in either the glycogen or collagen content. Combining both factors - training and AAS, was manifested as a reduction in the glycogen amount in the cardiomyocytes and lack of changes in the collagen fibres around the vessels, as compared to the single effect of AAS.

Key words: glycogen, collagen, myocardium, endurance training, Nandrolone Decanoate.

It is known that glycogen stores, located primarily in the liver and skeletal muscles provide a ready source of energy for use during exercise. The pattern of substrate use by the heart (fatty acids, lactate, and glucose) and its utilization varies according to the duration and intensity of workload and hormonal status. To date, it is well documented that sex hormones like estrogens and testosterone play a substantial role in regulating glycogen metabolism during exercise [9]. Many athletes use supraphysiological doses of anabolic androgenic steroids (AAS) aiming to increase the glycogen content in tissues and improvement of their athletic performance [2].

Also, an increase in collagen concentration is observed as an integral part of extracellular matrix remodeling in myocardium in response to a variety of pathologies [8]. Little is known about the influence of AAS and exercise on the glycogen content and interstitial collagen in the myocardium.

The aim of the present study was to investigate single and combine effect of endurance training and AAS treatment on glycogen content and collagen fibers in rat myocardium.

Material and Methods

Forty male Wistar rats (initial body weight 200-220g) were randomly distributed into two main groups (n=20) - sedentary (S) and trained (T). The exercised rats trained on motor-driven treadmill with submaximal loading (70-75% VO_2 max) 5 days per week for 8 weeks. During the first 2 weeks the duration of the daily training session increased every second day. At the end of 2nd week the rats run 40 min daily and this loading was maintained to the end of the experiment. After second week from the beginning of the experiment half of the trained and sedentary rats received weekly either 10 mg·kg^{-1} Nandrolone Decanoate (ND) or Placebo (PL) i.m. for the last 6 weeks.

All the groups: S+Pl; S+ND; T+Pl; T+ND were subjected on submaximal running endurance (SRE) and VO_{2max} tests several times. The day after the last test was performed the animals were decapitated after thiopental anesthesia and material from the left heart ventricle of each animal was taken immediately. Samples of the middle third of the outer left ventricle wall were obtained and fixed in Bouin's fixative for twenty-four hours at room temperature and than embedded in paraffin. Part of paraffin sections (5 мm thick) was investigated histochemically for glycogen using PAS method (McManus, 1948) and the other part - for collagen using Azan method (Heidenhain, 1915).

The staining saturation of the PAS reaction and distribution of collagen were assessed by specialized software "DP-Soft" (Olympus, Japan) on 'Microphot' (Nikon, Japan) microscope, equipped with a Camedia-5050Z (Olympus, Japan) digital camera. Measurements were applied on longitudinal sections at equal magnification (×400).

Data was evaluated for statistically significant differences by two-way ANOVA followed by Games-Howell post hoc test. Significance was accepted at P<0.05. The results are presented as mean ± SEM.

Results and Discussion

In the sedentary control group PAS staining showed small amounts of glycogen in the cardiomyocytes. There was significant main effect of ND treatment on the glycogen content in comparison with placebo (15.75±0.42 vs. 9.19±0.42, P<0.001). Endurance training had significant main effect on myocardial glycogen (P<0.001). Trained rats presented lower glycogen than sedentary (10.39±0.42 vs. 14.55±0.42). There was significant interaction between training and AAS treatment (P<0.001).

ND treatment significantly increased glycogen content in cardiomyocytes of the sedentary animals compared with placebo (P<0.001) (Fig. 1). In the trained groups ND expressed similar effect on glycogen increasing it's content in T+ND group compared to training per se (P<0.01).

There was no significant difference between the trained (T+Pl) and control group (S+Pl). Combination of both factors resulted in an intermediate glycogen content, which in T+ND group compared to the steroid control was significantly lower (12.38±0.90 vs. 19.12±0.48, P<0.001).

Cardiomyocytes in the myocardium of the control group (S+Pl) were separated by small amounts of collagen in the interstitium (Fig. 2, A). In the perivascular areas collagen was slightly presented. There was no significant difference in the percentage of collagen fibres in the endomysium between all the groups (P>0.05)

An increase in the amount of collagen fibres surrounding the blood vessels of greater caliber was observed in the myocardium of untrained, ND-injected animals

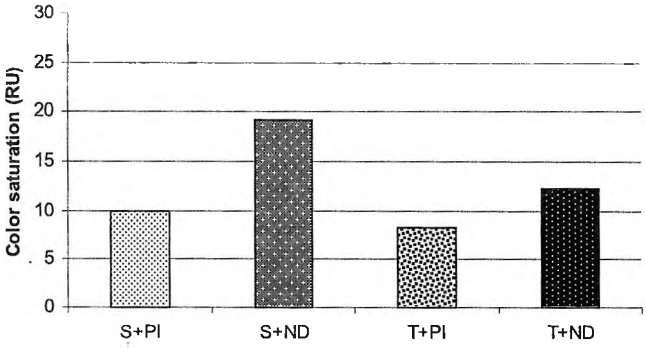

Fig. 1. Glycogen in the cardiomyocytes (in relative units)
*P<0.001, S+ND vs. S+Pl; **P<0.01, T+ND vs. T+Pl; #P<0.001, T+ND vs. S+ND

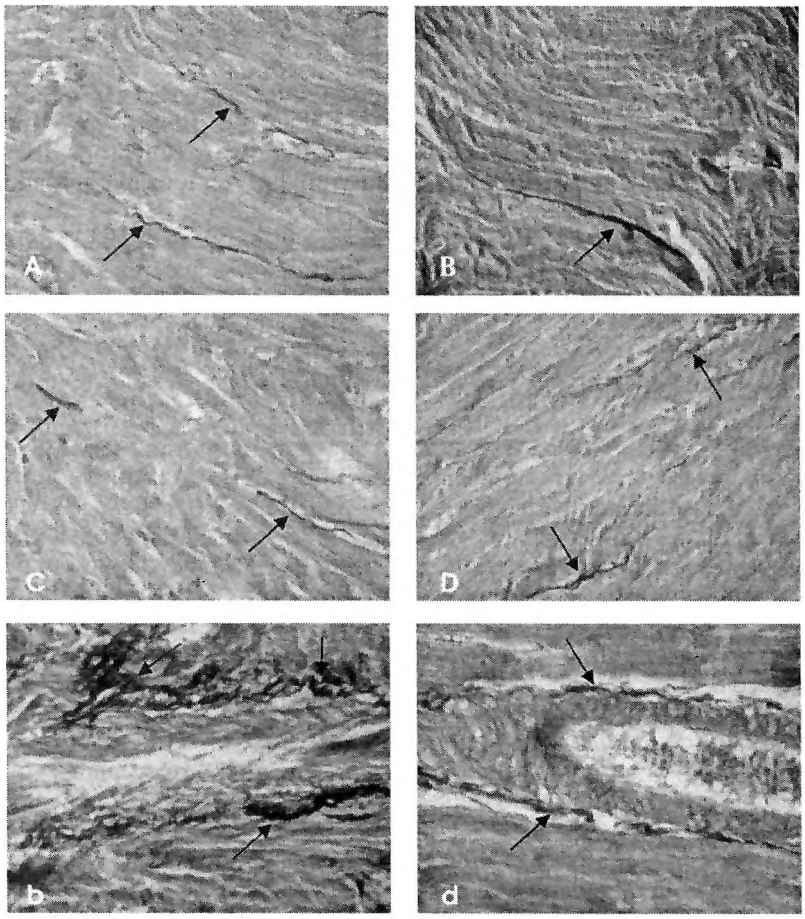

Fig. 2. Collagen fibres in the myocardium, Azan staining
A — sedentary+Placebo; **B, b** — sedentary+Nandrolone Decanoate; **C** — training+Placebo; **D, d** — training+Nandrolone Decanoate. Arrows indicate collagen fibres, × 400

(Fig. 2, b). In the myocardium of rats subjected to a submaximum training (T+Pl), no increase in the amount of collagen was observed - both around the vessels and in the intercellular spaces, as compared to the control (Fig. 2, d). Combining both factors did not alter the amount, neither of collagen in the interstitium, nor around the vessels, as compared to the control.

Endurance training did not lead to changes in the glycogen content in the cardiomyocytes. These results are consistent with the results obtained by other authors who also did not find any changes [2]. The content of connective tissue (mainly collagen) in the spaces between the cardiomyocytes also did not change. Similar results were reported by other research teams [6, 8, 10].

AAS treatment in untrained animals resulted in considerable glycogen increase in the cardiomyocytes. Being a derivative of testosterone (Ts), ND is capable of activating the processes of synthesis of enzymatic, structural, receptor and contractile proteins. Glycogenin, a protein that has been recently found in the muscles and the heart, is capable of initiating glycogen synthesis autocatalytically [1]. We hypothesize that ND influenced glycogenin activity in synthesizing a new glycogen. Another possible mechanism increasing glycogen content is the activation of lipoprotein lipase, as well as the predominant utilization of fats as a substrate [4]. On the other hand, glycogen accumulation could be interpreted as a pathologic tendency [5]. An increase of glycogen content in cardiomyocytes was found in left ventricle biopsies from patients, with coronary heart disease in the presence of areas with permanently reduced oxygen supply [3]. The increase in the collagen fibres in the perivascular areas is difficult to assess at this duration of AAS application. If this tendency is preserved with a more prolonged AAS treatment, this would definitely result in impairment of coronary blood flow and oxygen delivery.

On the other hand, endurance training led to decrease in Ts serum levels in the animals of the same experiment [7]. This fact could also account for the lack of changes in the glycogen and collagen content in the trained group.

Combining both factors — training and AAS — was manifested as a reduction in the glycogen amount in the cardiomyocytes, as compared to the single effect of AAS application. The levels remained higher, as compared to the independent effect of training. Similar results were obtained by Cunha et al. [2], but they found no glycogen increase in the myocardium of the steroid control. The lack of changes in the collagen content around the vessels in the group of trained animals that received an anabolic steroid (T+ND), is a sign of the beneficial influence of training, as compared to the single effect of AAS treatment.

References

1. Alonso, M. D., J. Lomako, W. M. Lomako, W. J. Whelan. A new look at the biogenesis of glycogen. — FASEB J., **9**, 1995, 1126-1137.
2. Cunha, T. S., A. P. Tanno, M. J. C. S. Moura, F. K. Marcondes. Influence of high-intensity exercise training and anabolic androgenic steroid treatment on rat tissue glycogen content. — Life sciences, **77**, 2005, 1030-1043.
3. Elsässer, A., M. Schlepper, W. Klövekorn et al. Hibernating myocardium. An incomplete adaptation to ischemia. — Circulation, **96**, 1997, 2920-2931.
4. Goodwin, G. W. and H. Taegtmeyer. Improved energy homeostasis of the heart in the metabolic state of exercise. — Am. J. Physiol. Heart. Circ. Physiol., **279**, 2000, H1490-H1501.
5. Kumar, V., R. S. Cotran, S. L. Robbins. — Robbins basic pathology. VII-th ed., Elsevier Science, Philadelphia, 2003.
6. Takala, T. E., P. Ramo, K. Kiviluoma et al. Effects of training and anabolic steroids on collagen synthesis in dog heart. — Eur. J. Appl. Physiol. Occup. Physiol., **62**, 1991, 1-6.

7. T e r z i e v a, D., K. G e o r g i e v a, P. P a v l o v. Changes in serum testosterone levels after nandrolone decanoate treatment and submaximal training in male rats. — Scientific researches of the Union of Scientists, Plovdiv, series G., Vol. III, 2004, 156-159.
8. T h o m a s, D. P., S. D. Z i m m e r m a n, T. R. H a n s e n et al. Collagen gene expression in rat left ventricle: interactive effect of age and exercise training. — J. Appl. Physiol., **89**, 2000, 1462-1468.
9. V a n B r e d a, E., H. A. K e i z e r, P. G e u r t e n et al. Modulation of glycogen metabolism of rat skeletal muscles by endurance training and testosterone treatment. — Pflugers Arch., **424**, 1993, 294-300.
10. W o o d i w i s s, A. J., B. T r i f u n o v i c, M. P h i l i p p i d e s, G. R. N o r t o n. Effects of an androgenic steroid on exercise-induced cardiac remodeling in rats. — J. Appl. Physiol., **88**, 2000, 409-415.

Institute of Experimental Morphology and Anthropology with Museum
Bulgarian Anatomical Society

Acta morphologica et anthropologica, 13
Sofia • 2008

Some Morphometrics Features on Mast Cells in Feline Pelvic Urethra

R. Dimitrov, A. Vodenicharov, G. Kostadinov, H. Hristov

Department of Veterinary Anatomy, Histology and Embryology, Faculty of Veterinary Medicine, Trakia University, Stara Zagora

The dense, shape and dimensions of mast cells in the pelvic urethra of 9 sexually mature clinically healthy male European shorthair cats were investigated following euthanasia.

The material was fixed in Carnoy's fixative, dehydrated, embedded in paraffin and stained with 0.1% toluidine blue.

The light microscopy revealed that most mast cells were present in the propria of pelvic urethra. Mast cells were also present in the urethral musculature and the intermuscular stroma. A relatively high concentration of mast cells was observed in the internal longitudinal smooth muscle layer. The observations on mast cells' shape and dimensions showed that they were the most elongated in the circular muscular layer. The mast cells in the musculature had a fusiform shape, those in the prostate lobules — oval and in the propria — oval and elongated. The morphometric data were statistically processed.

Key words: mast cells, pelvic urethra, tomcat.

Introduction

It is known that the anatomy of feline pelvic urethra has a number of specific features [11].

The studies about the localization, number and distribution of mast cells of tryptase-containing mast cells in human testes with either normal or abnormal spermatogenesis [14]. In cases with abnormal spermatogenesis, the number of mast cells was increased and their shape was rounded or elongated, indicating their degranulation. The results evidenced that mast cells and their secretory products were involved in the thickening of the wall of convoluted seminiferous tubules and other changes, observed in sterile testes.

Human testicular mast cells are divided into interstitial and peritubular. In impaired spermatogenesis, the number of interstitial mast cells was higher than that of peritubular ones. The mast cells in testes were considerably more numerous in sterility unlike their lower number in inflammations or neoplasms [1, 4].

The density of mast cells in the ventral part of prostate in the rat was high and decreased with age [3].

The number of mast cells was higher following castration in the connective tissue of the ventral prostate in gerbils [9].

Few mast cells were observed in the testicular interstitium of healthy boars. In boars with unilateral abdominal cryptorchism, mast cells were few whereas in bilateral cryptorchids, there were numerous mast cells [7].

The mast cells in the testicular interstitium of mice were found to be considerably more dense in the intact testis after transperitoneal unilateral torsion of the other testis [8].

The lack of data about the density, the shape and dimensions of mast cells in the pelvic urethra of male cats motivated the present study in order to elucidate their role in the function of male urethra in this animal species.

Material and Methods

Pelvic urethras of 9 clinically healthy, sexually mature male European shorthair cats, weighing 2.8-4 kg were studied. The cats were euthanized i.v. with 200 mg Thiopental (Biochemie, Austria).

The material was fixed in Carnoy's fixative for 4 hours, then put in 70° ethanol for 12 hours, dehydrated in an ascending alcohol series, cleared in xylene and embedded in paraffin.

The cross -sections (5-7 μm) were stained with 0.1% solution of toluidine blue in McIvane's buffer, pH 3 [6].

The density of mast cells (number, in mm^2) and dimensions (in μm) were measured with an eyepiece micrometer and shape were determined via light microscopy and their

The data were statistically processed (Data analysis, StatMost for Windows).

Results and Discussion

The total area of studied histological sections was 572 mm^2, with the greatest share of the external smooth muscle layer (165 mm^2 — 28.8%), followed by the middle circular layer, the propria with the erectile tissue and the internal longitudinal layer, whereas the disseminate prostate area was the lowest one — 36 mm^2 (6.3%). Of a total of 4060 mast cells studied, the greatest number were observed in the propria - 1100 (27.3%), followed by the middle circular, internal and external longitudinal muscle layers and the lowest - in the disseminate prostate - 33 (0.9%). The greatest density of these cells per mm^2 was observed in the propria — 9.41 ± 0.68, followed by the internal, the circular and the external muscular layer. The lowest density was that in disseminate prostate - 0.92 ± 0.24. Mast cells were the longest in the circular muscle layer - 16,36 ± 0,33 mm, the shortest - in disseminate prostate - 7.36 ± 1.69 mm, the thickest - in the propria - 8,22 ± 0,27 mm, and the thinnest - in disseminate prostate - 4.23 ± 0,98 mm (Table 1).

The light microscopic study showed that the most significant density of mast cells occurred in the propria of pelvic urethra. Significantly higher mast cell density was observed in the internal longitudinal smooth muscle layer followed by the middle and the external layer. The studies on the shape and dimensions of mast cells showed that they were relatively elongated (fusiform) in the circular muscle layer followed by the other two muscle layers and the propria and they were oval in disseminate prostate (Fig. 1).

T a b l e 1. Area (mm^2) of studied pelvic urethra regions with number and dimensions (μm) of mast cells within

Parameter	EM	MM	IM	PE	DP	Total
Area	165	143	110	118	36	572
%	28.8	25	19.2	20.7	6.3	100
Number	936	1033	948	1100	33	4060
%	23.1	25.4	23.3	27.3	0.9	100
Number — mm^2	5.67±0.36	7.22±0.34	8.62±0.61	9.41±0.68	0.92±0.24	6.97±1.5
Min — max	3.6-8.6	5.5-11.2	5.9-13.4	6.1-14.5	0-3.3	0.92-9.41
SD	1.59	1.43	2.57	2.88	1.03	3.36
Length	12.25±0.65	16.36±0.33	11.26±0.34	12.84±0.46	7.36±1.69	12.01±1.45
Min — max	7.9-17	13.6-19	9.5-15	10.2-16.3	10.2-18.7	7.36-16.36
SD	2.74	1.41	1.45	1.95	7.19	3.23
Thickness	6.97±0.34	6.3±0.37	6.17±0.31	8.22±0.27	4.23±0.98	6.37±0.65
Min — max	4.5-9.5	3.4-6.8	4.8-8.5	6.8-10.2	6.8-11.9	4.23-8.22
SD	1.44	1.56	1.32	1.15	4.14	1.45

EM — external longitudinal muscle layer; DP — disseminate prostate; MM — middle circular muscle layer; PE — propria and erectile tissue; IM — internal longitudinal muscle layer

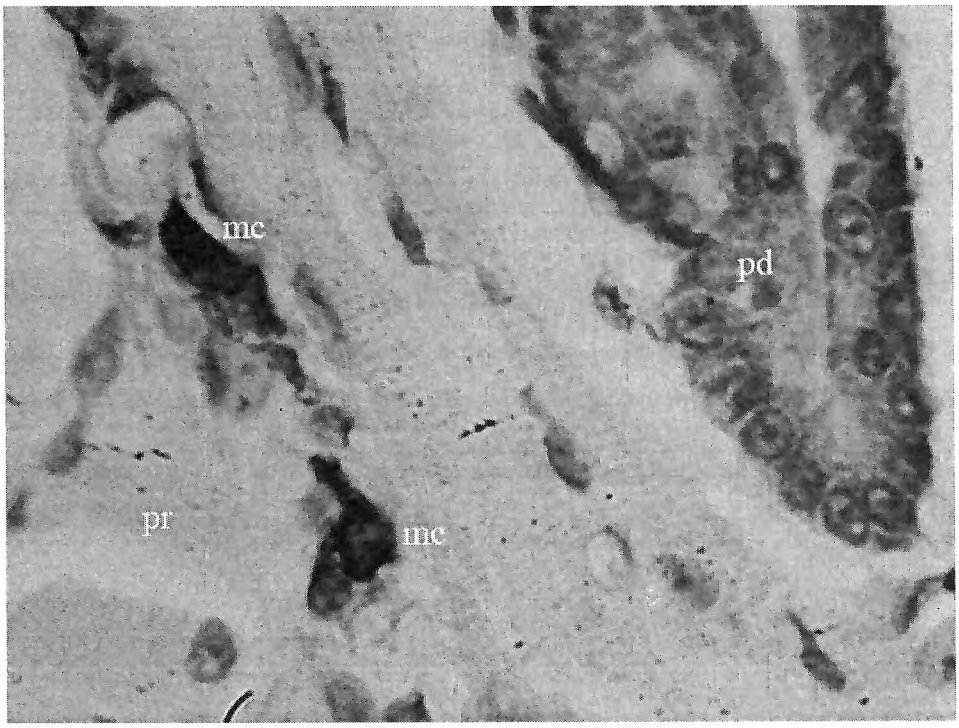

Fig. 1. Mast cells (mc), located in the propria (pr) of pelvic urethra and in vicinity of lobules of disseminate prostate (pd). × 400

The present study describes for the first time mast cells in feline pelvic urethra, observing a considerable predilectional, connective tissue presence. The obtained data added to the knowledge about these cells' distribution in the interstitial tissue of male genitals in rats, mice, boars, gerbils and humans [2, 3, 7, 13, 8, 9].

The data allowed us to support the assumption about the dominating affinity of mast cells towards the fibroelastic elements of pelvic urethra [11], corresponding to their known localization in the testicular interstitium in rats, mice and men [1, 3, 5, 8].

The considerably higher number of mast cells in the propria of pelvic urethra (9.41) and the muscle layers (from 5.67 at the external longitudinal to 8.62 at the internal layer) vs their density in disseminate prostate (0.92) suggested their role in the motility of fibromuscular elements, the regulation of vascular tonus and the microcirculation similarly to that described in the ureter of domestic pigs [10].

In our opinion, the fact that mast cells in the middle circular layer were with the most elongated shape compared to the other two longitudinal layers, deserves attention. It allowed us to assume that the marked elongation of cells was due to the high contractile amplitude of the circular layer.

In conclusion, the results of our study showed convincingly that the relatively higher dimensions (length and thickness) of mast cells in the propria vs those into the disseminate prostate, were indicative about their more active involvement in the connective tissue of feline pelvic urethra.

References

1. Appa, D. D., S. Cayan, A. Polart, E. Akbay. Mast cells and fibrosis on testicular biopsies in male infertility. — Arch. Androl., **48**, 2002, No5, 337-344.
2. Galli, S. J. New Concepts about the mast cell. — The New England Journal of Medicine, **328**, 1993, No4, 257-265.
3. Hammel, I., P. Roizman, R. Massas, A. Abramovic. Ontogeny of mast cells in the ventral prostate of the rat. — Int. Arch. Allergy Appl. Immunology, **93**, 1990, No2-3, 212-215.
4. Kollur, S. M., V. L. Pattankar, IA. Hag. Mast cells in testicular lesions. — Ups. J. Med. Sci., **109**, 2004, No3, 239-245.
5. Meineke, V., M. B. Frungieri, B. Jessberger, H. Vogt, A. Mayerhofer. Human testicular mast cells contain tryptase : increased mast cell number and altered distribution in the testes of infertile men. — Fertil. Steril., **74**, 2000, No2, 23-244.
6. Pearce, A. — In: Histochemistry, 2nd ed. London, J. & Churchill Ltd, 1960. 692 p.
7. Pinart, E., S. Bonet, M. Briz, S. Sancho, N. Garcia, E. Badia. Cytology of the interstitial tissue in scrotal and abdominal testes of post-puberal boars. — Tissue Cell., **33**, 2001, No1, 8-24.
8. Qo, S. Mast cell induction to the mouse testicular interstitium. — Nippon Hinyokika Gakkai Zasshi, **85**, 1994, 5, 747-752.
9. Sales, N. The effect of castration on the mast cells of the ventral gland of male gerbils (Meriones unguiculatus, Gerbillidae). — C. R. Seances Soc. Biol. Fil., **169**, 1975, No4, 856-862.
10. Vodenicharov, A., R. Leiser, M. Gulubova, T. Vlaykova. Morphologica and immunocytochemical investigations on mast cells in porcine ureter. — Anat. Histol. Embryol., **34**, 2005, 343-349.
11. Wrobel, K. Male Reproductive System. — In: Textbook of Veterinary Histology (Ed. H. Dellman, and J. Eurel). Fifth Edition. Philadelphia, Williams & Wilkins, 1998, 238-244.

Institute of Experimental Morphology and Anthropology with Museum
Bulgarian Anatomical Society

Acta morphologica et anthropologica, 13
Sofia • 2008

Some Radiographic Peculiarities in the Wrist Joint Complex with Hamatolunate Joint

S. Dyankova

Department Anatomy, Histology and Embryology, Varna Medical University "Prof. Dr Paraskev Stoyanov", Varna

The data from the literature sources show variation of the occurrence of the hamatolunate joint (HLJ) in the wrist joint between 26.7% to 73% due to the different research methods. Three methods were applied on one and the same material in the current study. The aim of this study was to evaluate the degree and the circumstances in which these methods can determine the presence of the HLJ. Twenty cadaver wrist joint complexes were studied for the presence of HLJ. The methods applied were radiological, dissection and macerated bones. In 3 cases the radiological method shows no sign of a HLJ, even though such a joint was detected by the two other methods. The radiological method cannot verify the presence of a HLJ in the cases where the width of the medial facet of the os lunatum for the os hanatum was less than 3mm.

Key words: wrist joint complex, types of lunate bone, hamatolunate joint, X-ray study morphometry.

Introduction

Recent studies on the presence of the HLJ and the types of the lunate bone that lead to the presence or the absence of such a joint show significant difference in the frequency of that variation in the wrist joint complex [6, 18]. The radiological study of D h a r a p et al. [5] shows that the *os lunatum* type II (with additional medial facet for *os hamatum*) [16] determines the presence of the HLJ and can be found in 26.7% of the studied cases. According to V i e g a s et al. [17] the same type *os lunatum* can be found in 73% of the cases using the wrist dissection (Table 1). In our opinion that significant difference is due to the abilities of the applied methods for visual detection of the medial facet of *os lunatum* — scopical observation of the macerated bones, cadaver wrist dissection, radiological, arthroscopical, and MRI images. S a g e r m a n et al. [12] estimated that the accuracy of the radiological determination of the different types of *os lunatum* vary between 64% to 72%. The aim of this study was to evaluate the degree and the circumstances in which any of the three methods can fail to detect cases with HLJ (e.g. *os lunatum* type II). The three methods applied on same material were radiological, dissection, and scopical observation of macerated bones with present morphometrics (Table 1).

Table 1.

Method of examination	Authors, year	os lunatum type I - %	os lunatum type II - %
Macerated bones	Dyankova, S. [6]	34 %	66 %
Dissection of wrists	Dyankova, S. [18]	44 %	56 %
	Viegas, S. F. [15]	39.3 %	60.7%
	Viegas, S. F. et al. [16]	34.5 %	65.5%
	Viegas, S. F. et al. [17]	27 %	73 %
	Arai T. [1]	42.5%	57.5%
Roentgenography of wrists	Aufauvre, B. et al. [2]	44 %	56 %
	Viegas, S. F. et al. [16]	46.1%	53.9%
	Tsude, S., Nakamura, R. [14]		
	■ Contralateral unaffected wrists of patients with trauma	42%	42%
	■ Contralateral unaffected wrists of patients with Kienböck's disease	37%	37%
	■ Bilateral wrists of volunteers	35%	35%
	Dharap, A. S. et al. [4]	61.2%	38.8%
	Dharap, A. S. et al. [5]	73.3%	26.7%
Arthroscopy	Dautel, G., Merle M. [3]	44.9%	55.1%
	Thurston, A. J., Stanley J. K. [13]	50%	50%
MRI and arthroscopy	Malik, A. M. et al. [7]	42.5 %	57.5 %
MRI and arthrography	Pfirrmann, C. W. A. et al. [11]	50%	50%

Material and Methods

Twenty cadaver wrist joints from the collection of the Department of Anatomy, Histology and Embryology at the Medical University — Varna, Bulgaria, were studied following all the ethical rules of work on cadaver material. The methods applied were antero-posterior radiography with PA-1-3 (60 κV, 10 mA, 1,2 mAXS, 100cm FFA); dissection of the wrist joints with measurement of the joint surfaces; scopical observation for the number of the joint facets on the distal and the proximal surface, and anthropometrical measurement [8] of the macerated bones.

Results and Discussion

The X-ray image of the wrist joint complex without a HLJ presents a continuous oval in the mediocarpal joint (Fig. 1, 3—A), while the wrist complex with a HLJ presents an interrupted oval (Fig. 2, 3—B).

Fig. 1. Wrist joint complex without a HLJ

Fig. 2. Wrist joint complex with a HLJ

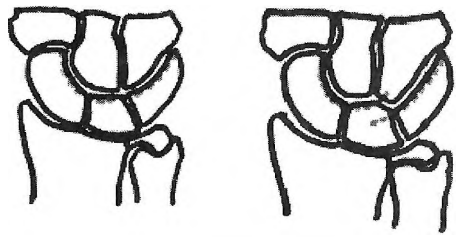

Fig. 3 *A* — Wrist joint complex without a HLJ - ontinuous oval in *art. mediocarpalis*; *B* — Wrist joint complex with a HLJ - interrupted oval in *articilatio mediocarpalis*

Table 2

Method of examination	Without a HLJ	With a HLJ
X-ray images	13	7
Cadaver wrist joints	10	10
Macerated bones	10	10

Fig. 4. X-ray image without visibility of the medial facet

Fig. 5. Cadaver wrist joints of the same wrist. The width of the medial facet is 1.8 mm

The data obtained through X-ray indicated a presence of the HLJ in 7 wrist joint complexes while the scopical observation on cadaver material and macerated bones revealed such a joint in 10 cases (Table 2).

Three X-ray images indicated no presence of a HLJ while the scopical observation showed its existence (Figs. 4, 5).

The morphometric measurements of the width of the joint facet of *os lunatum* for *os hamatum* on the wrist material was 1.8 mm, 2.1 mm, 2.8 mm correspondingly while on the macerated bones - 1.7 mm, 1.8 mm и 2.5 mm (Table 3).

Table 3

X-ray visibility of the medial facet	Cadaver wrist joints	Macerated bones
Cases without visibility	1.8 mm 2.1 mm 2.8 mm	1.7 mm 1.8 mm 2.5 mm;
Cases with visibility	3.2 mm и 5.6 mm	3 mm и 5.4 mm

The absolute measurements of the joint surfaces for *os capitatum* and *os hamatum* in case of *os lunatum* type II and their biomechanical and clinical significance are often discussed by different authors. According to V i e g a s et al. [16] the width of the facet for *os hamatum*, measured on cadaver material falls mainly in the 2-3 mm range; according to P f i r r m a n n et al. [11], who used the MRI method, the mean size is 4.5mm. The data of the current study suggests that facets smaller than 3mm cannot always be detected by X-rays which would result in a classification of such wrist joint complexes as ones without a HLJ. This can explain the differences in the data of the various studies, especially the data obtained through X-rays.

This fact deserves attention by the clinical practice for two reasons. The literature proves that *os lunatum* type II can be accompanied by frequent deep erosions of the cartilage in the proximal pole of *os hamatum* [1, 3, 9, 11, 14, 16]. Secondly, the presence of the medial joint facet has a significance for the development of the Kienböck's disease [10, 13, 18].

Therefore, we paid special attention to other factors that could help us in detecting the presence or absence of the HLJ using an X-ray image. Among these factors is the distance from the proximal pole of *os hamatum* to the medial end of the distal surface of *os lunatum*. The current study indicated that this distance was greater when *os lunatum* type II was present.

Conclusion

Wrists without a HLJ present a continuous oval in the midcarpal joint while wrists with present HLJ present an interrupted oval. The X-ray detection of the medial facet is problematic when the facet width is smaller than 3mm. Wrists without a HLJ have greater hamato-lunate distance in comparison to wrists with a HLJ.

References

1. A r a i, T. Roentgenographical and anatomical study of the midcarpal joint — morphology and degenerative change of ulnar side. — Nippon Seikeigeka Gakkai Zasshi., **67**, 1993, 1114-1121.
2. A u f a u v r e, B., G. H e r z b e r g, J. G a r r e t, E. B e r t h o n n e a u d, J. D i m n e t. A new radiographic method for evaluation of the position of the carpus in the coronal plane: results in normal subjects. — Surg. Radiol. Anat., **21**, 1999, 383-385.
3. D a u t e l, G., M. M e r l e. Chondral lesions of the midcarpal joint. — Arthroscopy, **13**, 1997, 97-102.
4. D h a r a p, A. S., H. A l - H a s h i m i, S. K a s s a b, M. F. A b u - H i j l e h. The hamate facet of the lunate: a radiographic study in an Arab population from Bahrain. — Surg. Radiol. Anat., **28**, 2006, 185-188.
5. D h a r a p, A. S., I. L u t f i, M. F. A b u - H i j l e h. Population variation in the incidence of the medial (hamate) facet of the carpal bone lunate. — Anthropol. Anz., **64**, 2006, 59-65.
6. D y a n k o v a, S. Lunate bone — types and morphological characteristic. — Acta Morphol. Anthropol., **10**, 2005, 304-308.
7. M a l i k, A. M., M. E. S c h w e i t z e r, R. W. C l u p, L. A. O s t e r m a n, G. M a n t o n. MR imaging of the type II lunate bone: frequency, extent, and associated findings. — Am. J. Roentgenol., **173**, 1999, 335-338.
8. M a r t i n, R., K. S a l l e r. Lehrbuch der Anthropologie. Bd.I, 1957, Bd.II, 1958, Stuttgart, G. Fischer Verl.
9. N a k a m u r a, K., R. M. P a t t e r s o n, H. M o r i t o m o, S. F. V i e g a s. Type I versus type II lunates: Ligament anatomy and presence of arthrosis. — J Hand Surg., **26A**, 2001, 428-436.
10. N a k a m u r a, K., M. B e p p u, K. M a t s u s h i t a, H. A o k i, T. I d e. Biomechanical analysis of force transmission across the midcarpal joint in Kienböck's Disease. — In 7th congress of the International Federation of Societies for surgery of the hand — Vancouver, Canada, May 24-28, 1998, 473-477.

11. Pfirrmann, C. W. A., N. H. Theumann, C. B. Chung, D. J. Trudell, D. Resnick. The hamatolunate facet: characterization and association with cartilage lesions — magnetic resonance arthrography and anatomic correlation in cadaveric wrists. — Skeletal Radiol., **31**, 2002, 451-456.
12. Sagerman, S. D., R. M. Hauk, A. K. Palmer AK. Lunate morphology: can it be predicted with routine x-ray films? — *J Hand Surg.*, **20**A, 1995, 38-41.
13. Thurston, A. J., J. K. Stanley. Hamato-lunate impingement: an uncommon cause of ulnar-sides wrist pain. — Arthroscopy, **16**, 2000, 540-544.
14. Tsuge, S., R. Nakamura. Anatomical risk factors for Kienböck's disease. — J. Hand Surg., **18**B, 1993, 70-75.
15. Viegas, S. The lunatohamate articulation of the midcarpal joint.— Arthroscopy, **6**, 1990a, 5-10.
16. Viegas, S. F., K. Wagner, R. Patterson, P. Peterson. Medial (hamate) facet of the lunate. — J. Hand Surg., **15**, 1990b, 564-571.
17. Viegas, S. F, R. M. Patterson, J. A. Hokanson, J. Davis. Wrist anatomy: incidence, distribution, and correlation of anatomic variations, tears, and arthrosis. — J. Hand Surg., **18**, 1993, 463-475.
18. Д я н к о в а, С. Морфология на китковия ставен комплекс и васкуларна анатомия на предмишничните кости с оглед някои проблеми на развитието и лечението на болестта на Kienböck. Дис. труд за „Доктор". Варна, 2005. 59 с.

Institute of Experimental Morphology and Anthropology with Museum
Bulgarian Anatomical Society

Acta morphologica et anthropologica, 13
Sofia • 2008

Anatomical Relationships at the Distal Radius and Ulna and the Articular Disc in the Wrist Joint Complex

S. Dyankova, G. Marinov

Department of Anatomy, Histology and Embryology, Varna Medical University "Prof. Dr. Paraskev Stoyanov", Varna

The present study aims at examining the extent to which the morphological characteristics of the distal *radius* and *ulna* and *discus articularis* are influenced by the different variations of the wrist joint complexes (the types and subtypes of the lunate bone and the ulna variant). Twenty cadaver complexes were studied for the type and subtype of *os lunatum* and the ulna variant and 106 macerated radial and 102 elbow bones (20 of them were taken from the studied joint complexes) were investigated for the morphological characteristics of the distal *radius* and *ulna* and *discus articularis*. It was found out that *crista transversa* was developed better at *os lunatum* subtype (+) and minus and neutral ulna variant, whereas changes in *discus articularis* were more dependent on *os lunatum* subtype (+) and ulna plus variant. The geometrical proportions of the surfaces of *radius* and *ulna* in *articulatio radioulnaris distalis* are also described.

Key words: Distal radius and ulna, discus articularis, os lunatum- types and subtypes, ulna variant.

Introduction

The interest in the morphological characteristics of the bone skeleton of the wrist joint complex (WJC) and its variations was greatly increased in the last decade [16]. Particularization of this knowledge has great practical importance for the correct interpretation of the results given by modern methods of image diagnostics, which are rapidly coming into use, and non-invasive methods for studying of carpal kinematics [1, 3, 8] as well as for dealing with numerous unclear problems of the biomechanics and pathology of the hand in the wrist area. Distal ends of the *radius* and *ulna* and of *discus articularis* (DA) are an important component of this complex. The goal of the present study is to clarify the following:

1. How does the type [17] and subtypes [4] of *os lunatum* and the ulna variant correlate with the morphological particulars of *facies articularis carpi radii* and of DA [2, 10, 14, 15, 18]?

2. What is the geometrical ratio in the joint surfaces of *radius* and *ulna* in *articulatio radioulnaris distalis* [5, 9, 10]?

Material and Methods

20 WJC from cadavers were studied scopically for:

a. Type and subtype of *os lunatum*; **b.** Ulna variant; **c.** Openings and erosions of DA.

The distal ends of 106 macerated radial 102 macerated ulnar bones (20 of them were from the studied joint complexes) were scopically studied for:

1. Presence and expressiveness of *crista transversa* [7], dividing *facies articularis carpi radii* on two fosses — radial (*fossa scaphoidea*) and ulnar (*fossa lunata*) [11] by an own scale: **a.** absent; **b.** partially present and **c.** fully present (the latter is qualified as low, average and high).

2. Geometrical rating of the angles between:

a. *facies articularis carpi radii* and *incisura ulnaris radii*;

b. *caput ulnae* and *circumferentia articularis ulnae* which were acute, right, obtuse.

Results and Discussion

In the 20 cadaver WJC 10 cases of *os lunatum* type I and 10 cases with *os lunatum* type II were detected. Only four of WJC with *os lunatum* type I had just one facet on their proximal joint surface i.e. with *os lunatum* subtype (—). The remaining 16 cases were with *os lunatum* subtype (+). 10 cases were with ulna neutral, 5 - with ulna minus and the remaining 5 — ulna plus variant. There were 6 WJC with changes in the DA.

The degree of development (Figs. 1, 2, 3) of *crista transversa* of the 106 radial bones is presented in fig 4.

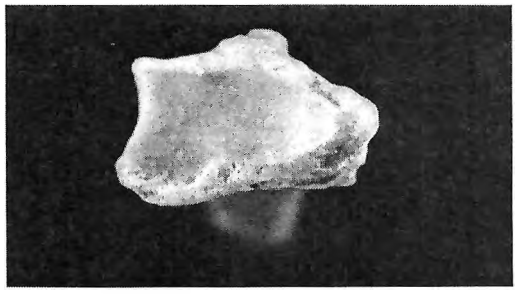

Fig. 1. Absent *crista transversa*

Fig. 2. Partially present *crista transversa*

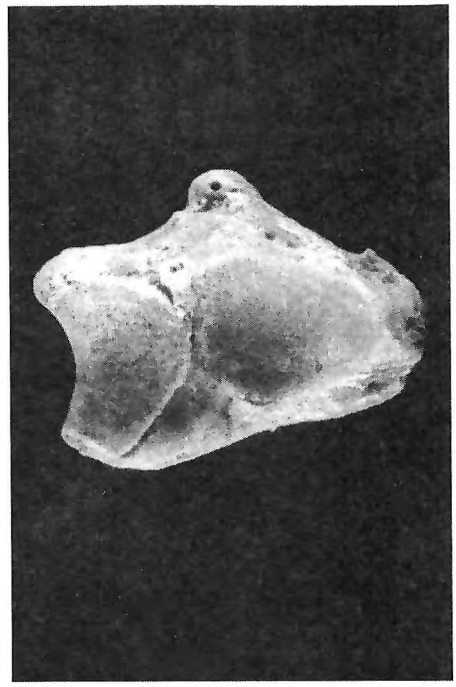

Fig. 3. Fully present *crista transversa*

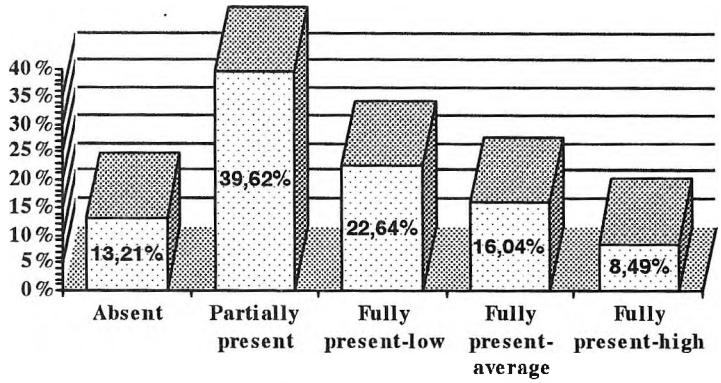

Fig. 4. Degree of development of crista transversa on facies articulairs carpi radii (n=106)

The results concerning the presence and development of *crista transversa* depending on the type and subtype of *os lunatum* and the ulna variant of the study of the 20 radial bones which are from the studied WJC, are presented in Figs. 5, 6 and 7.

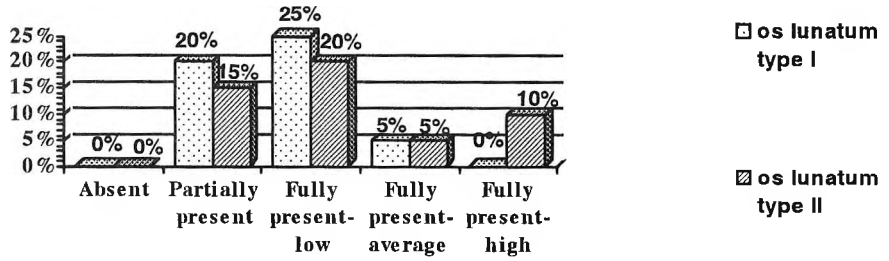

Fig. 5. Degree of development of crista transversa on facies articulairs carpi radii depending on the type of os lunatum (n=20)

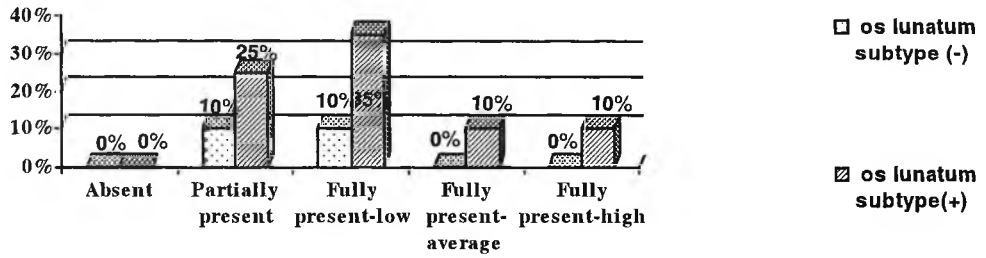

Fig. 6. Degree of development of crista transversa on facies articulairs carpi radii depending on the subtype of os lunatum (n=20)

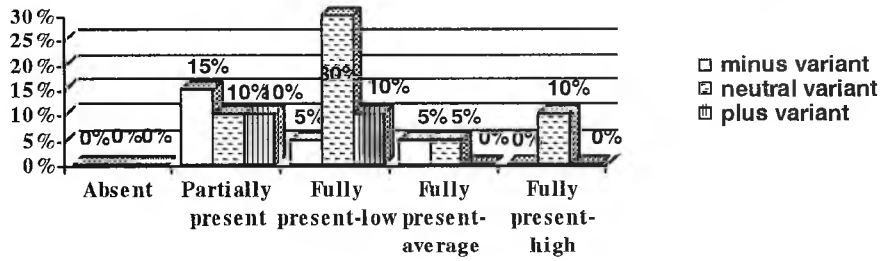

Fig. 7. Dependence of the presence of crista transversa and its development on the ulna variant

The analysis of the results showed that the presence and development of *crista transversa* is not influenced by the type of *os lunatum* but depended considerably on the subtype (+) as well as ulna neutral and minus variant [14]. Whether the cause of the presence and the height of *crista transversa* was the presence of a second facet on the proximal surface of *os lunatum* and the shorter *ulna,* or the second facet was formed because of the shorter *ulna*, is hard to tell but it is obvious that the applying of pressure in this part of the radiocarpal joint in these cases is greater.

The changes in DA depend on various factors [6, 12, 13] — ulna plus variant and a thinner DA [10], avascular central zone of DA [11]. This study detected changes in DA in joints with ulna neutral (60%) and ulna plus variant (40%) and in joints with *os lunatum* subtype (+) in 37.5% where in 87.5% of the latter erosions of the ulnar section of the proximal joint surface of *os lunatum* were observed [6, 13].

The angle between *circumferentia articularis ulnae* and the distal surface of its head is obtuse in 75 cases, right - in 26 cases and acute only in one case (Fig. 8.), whereas the angle between *facies articularis carpi radii* and *incisura ulnaris radii* is most often right - in 51 cases, obtuse - in 38 cases and acute - in 17 cases.

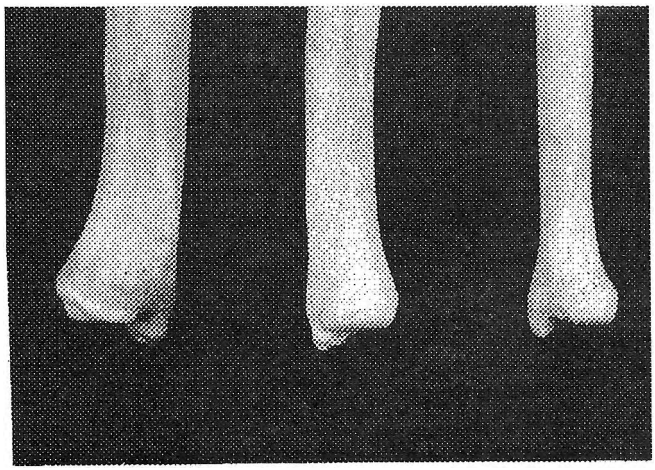

Fig. 8. Obtuse (1 and 2) and right angle (3) between *circumferentia articularis* and the distal surface of *caput ulnae*

Table 1. Dependence of the configuration of the distal ends of *radius* and *ulna* on the ulna variant.

Angle on		Cases, %	Ulna variant.		
ulna	*radius*		neutral *n*=10	plus *n*=5	minus *n*=5
obtuse	right	14 (70%)	6 (43%)	4(28,5%)	4(28,5%)
obtuse	right to obtuse	4 (20%)	2 (50%)	1 (25%)	1 (25%)
right to obtuse	right to acute	1 (5%)	1 (100%)	-	-
right to obtuse	right	1 (5%)	1 (100%)	-	-

The results of the present study on 20 pairs matching *ulna* and *radius* for the geometrical rating of the angles in their distal end depending on the ulna variant are presented in Table 1.

The joint surfaces described above are cylindrical in ulna neutral or plus variant whereas in ulna minus variant their configuration is conical [9, 10]. Schuurman [15] describes three types of relationships between these joint surfaces in the sagittal plane and four types in the transverse plane. The significance of these anatomical variations for the biomechanics and the pathology of the wrist is still poorly explored.

References

1. Camus, E., F. Millot, J. Lariviere, S. Raoult, M. Rtaimate. Kinematics of the wrist using 2D and 3D analysis: biomechanical and clinical deductions. — Surg. Radiol. Anat., **26**, 2004, 399-410.
2. Cerezal, L., F. Pinal, F. Abascal, R. Garcia-Valtuille, T. Pereda, A. Canda. Imaging Findings in Ulnar-sided Wrist Impaction Syndromes. — Radiographics, **22**, 2002, 105-121.
3. Crisco, J. J. S., W. Wolfe, C. P. Neu, S. Pike. Advances in the in vivo measurement of normal and abnormal carpal kinematics. — Orthop. Clin. North America, **30**, 2001, 219-231.
4. Dyankova, S. Lunate bone — types and morphological characteristic. — Acta morphologica et anthropologica, **10**, 2005, 304-308.
5. Ekenstam, F., C. G. Hagert. Anatomical studies on the geometry and stability of the distal radioulnar joint. — Scand. J. Plast. Reconstr. Surg., **19**, 1985, 17-25.
6. Jeffries, A. O., M. A. Craigen, J. K. Stanley. Wear patterns of the articular cartilage and triangular fibrocartilaginous complex of the wrist: a cadaveric study. — J. Hand Surg., **19B**, 1994, 306-309.
7. Kapandji, A. Biomechanik des Carpus und des Handgelenkes. — Orthopäde, **15**, 1986; 60-73.
8. Kaufmann, R., J. Pfaeffle, B. Blankenhorn, K. Stabile, D. Robertson, R. Goitz. Kinematics of the midcarpal and radiocarpal joints in radioulnar deviation: an in vitro study. — J. Hand Surg., **30A**, 2005, 937-942.
9. Koebke, J. Anatomical and clinical aspects of the wrist joint area. — Scr. Sci. Med. (Varna), **36**, 2004, suppl. 1, p.24.
10. Linscheid, R. L. Kinematic considerations of the wrist. — Clinical Orthop. Related Research, **202**, 1986, 27-39.
11. Mikic, Z. The blood supply of the human distal radioulnar joint and the microvasculature of its articular disc. — Clin. Orthop., **257**, 1992, 19-28.
12. Palmer, A. K. Triangular fibrocartilage disorders: injury patterns and treatment. — Arthroscopy, **6**, 1990, 125-132.
13. Palmer, A. K., F. W. Werner. The triangular fibrocartilage complex of the wrist — Anatomy and function. — J. Hand Surg., **6A**, 1981, 153-162.
14. Schuurman, A. H., M. Maas, P. F. Dijkstra, J. M. G. Kauer. Ulnar Variance and the Shape of the Lunate Bone. A Radiological Investigation. — Acta Orthop. Belgica, **67**, 2001, 464-467.
15. Schuurman, A. H. The ulnocarpal Region of the Wrist: Morphological, Biomechanical Radiological and Surgical Considerations. Utrecht, 2002. 128 p.
16. Viegas, S. F. Advances in the skeletal anatomy of the wrist. — Hand Clin., **1**, 2001, 1-11.
17. Viegas, S. F., K. Wagner, R. Patterson, P. Peterson. Medial (hamate) facet of the lunate. — J. Hand Surg., **15A**, 1990, 564-571.
18. Werner, F. W., A. K. Palmer, M. D. Fortino, W. H. Short. Force transmission through the distal ulna: effect of ulnar variance, lunate fossa angulation, and radial and palmar tilt of the distal radius. — J. Hand Surg., **17A**, 1992, 423-428.

Institute of Experimental Morphology and Anthropology with Museum
Bulgarian Anatomical Society

Acta morphologica et anthropologica, 13
Sofia • 2008

Variations of the Hypothenar Muscles

G. P. Georgiev, L. Jelev, L. Surchev

Department of Anatomy, Histology and Embryology, Medical University of Sofia

During routine anatomical dissections, in two hands, a number of variations of the hypothenar muscles were observed. In the first case, an absence of the flexor digiti minimi brevis muscle (FDMB) and short muscular bundle between the pisiform bone and the flexor retinaculum were found. In the second case, an additional lateral origin of the FDMB and unknown variant muscle, located deep to abductor digiti minimi (ADM) and FDMB, were described. Some of the present variant structures may be considered as possible entrapment site for the ulnar nerve at the wrist and must be borne in mind by the clinicians.

Key words: hypothenar muscles, variations, ulnar nerve compression, human.

Introduction

Anatomical variations of the hypothenar muscles are common. The knowledge of these anomalous muscles is important for the clinical practice because some of them may provoke symptomatic compression of the ulnar nerve at the wrist [1, 5].

In this paper, we describe some interesting variations of the hypothenar muscles found during anatomical dissections in formol-carbol fixed human cadavers from the autopsy material available at the Department of Anatomy, Histology and Embryology at the Medical University of Sofia.

Results

In case A (Fig. 1), in a right hand, an unusual arrangement of the hypothenar muscles was found. After removing the palmar aponeurosis and the palmaris brevis muscle, only two hypothenar muscles were observed. The medial well-defined muscle arose from the pisiform bone and from the tendon of the flexor carpi ulnaris muscle and inserted into the ulnar side of the base of the fifth finger. Lateral and deep to the medial muscle, the fibers of the opponens digiti minimi (ODM) were discovered, indicating the obvious absence of flexor digiti minimi brevis muscle (FDMB). In addition, an unusual muscular bundle originated from the pisiform bone, crossed in lateral and distal direction under the ulnar artery and nerve and

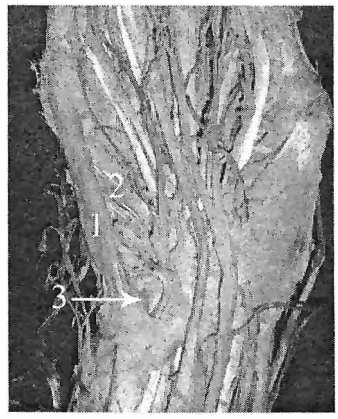

Fig. 1. Photograph of the variant findings, described in case A
1 — ADM; 2 — ODM; 3 — variant slip extending between the pisiform bone and the flexor retinaculum

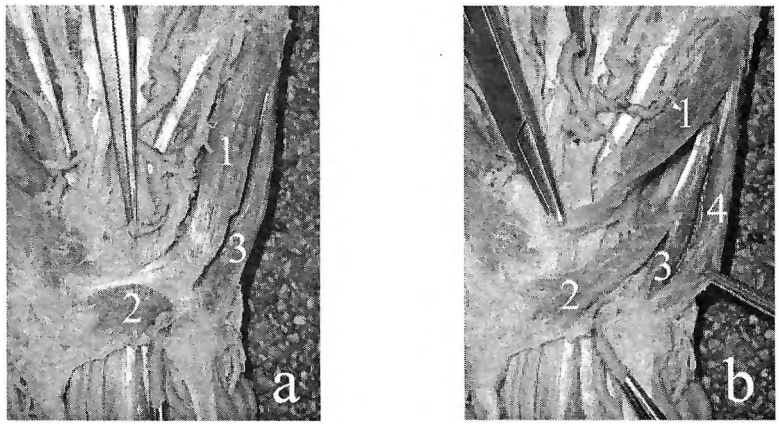

Fig. 2. Photograph of the variant findings, described in case B
a: 1 — FDMB; 2 — lateral belly of the deep aberrant muscle; 3 — ADM. **b**: 1 — FDMB; 2 — lateral belly of the deep aberrant muscle; 3 — medial belly of the deep aberrant muscle; 4 — ADM

inserted into the flexor retinaculum. The deep branch of the ulnar nerve innervated the medial hypothenar muscle and then pierced the ODM.

In case B (Fig. 2 a, b), in the left hand, a number of variations were observed. The FDMB (Fig.2 a) showed two proximal tendons - medial short one originating from the hamulus of the hamate bone and additional lateral tendon originating from the flexor retinaculum. The latter tendon, located between the ulnar artery and nerve, arched over the attachment of an aberrant muscle. The aberrant muscle (Fig. 2 b) located deep to the FDMB and ADM was composed of two well-defined muscular bellies - the lateral one arose from the lateral part of the flexor retinaculum and the medial one from the hamulus of the hamate bone. The lateral belly crossed ob-

liquely the ulnar nerve over the flexor retinaculum and passed in the same direction as the FDMB. The aberrant muscle was attached to the antero-lateral surface of the base of the fifth proximal phalanx. The deep branch of the ulnar nerve innervated the two bellies of the aberrant muscle.

Discussion

The aforementioned variant muscular structures seem to be related to the FDMB and ADM and therefore we review the reported variations of these two muscles.

The variations of the ADM are the most frequently described among the hypothenar muscles [4]. M a c a l i s t e r [7] reported three origins, second head, fusion with the FDMB, origin only from the pisiform bone and even absence. Other authors [2, 3, 5, 6] described an origin from the fascia of the forearm, palmaris longus, fascia of the flexor carpi radialis, intermuscular fascia, flexor carpi ulnaris and flexor retinaculum and dividing into two or three fascicles.

Compared to the ADM, the variations concerning the FDMB seem to occur less frequently [5]. M a c a l i s t e r [7] reported its absence, presence of an accessory palmaris slip joined to the FDMB, an unciform origin, presence of a slip to the metacarpal bone, union to the abductor. L e D o u b l e [6] reported an origin from the antebrachial fascia and fusion of the ODM and ADM.

In the cases of variations of the hypothenar muscles different relations to the ulnar artery and nerve might be observed [3, 8]. These relations define the role of the hypothenar muscle variations for the ulnar nerve compression [1, 5]. Additionally to nerve compression, an aberrant muscle may be also associated with thrombosis of the ulnar artery [9].

The variant muscles described in our report, have a close relation to the palmar branch of the ulnar nerve and possibly could cause nerve compression, presented by motor and sensory dysfunction. Therefore, the existence of such muscular variations should be taken in consideration by the clinicians.

References

1. A l - Q a t t a n, M. M. Ulnar nerve compression at the wrist by the accessory abductor digiti minimi muscle: wrist trauma as a precipitating factor. — Hand Surg., **9**, 2004, 79-82.
2. B e r g m a n, R. A., A. K. A f i f i, R. M i y a u c h i. Part I: Muscular system. In: Illustrated encyclopedia of human anatomic variations. 2004. http://www.anatomyatlases.org/AnatomicVariants/Anatomy HP.shtml
3. G l o o b e, H., P. P e c k e t. An anomalous muscle in the canal of Guyon (A possible ulnar nerve compression). — Ant. Anz., **133**, 1973, 477-479.
4. H a r v i e, P., N. P a t e l, S. J. O s t l e r e. Prevalence and epidemiological variation of anomalous muscles at Guyon's canal. — J. Hand Surg., **29B**, 2004, 26-29.
5. J e f f e r y, A. K. Compression of the deep palmar branch of the ulnar nerve by an anomalous muscle. Case report and review. — J. Bone Joint Surg., **53B**, 1971, 718-723.
6. L e D o u b l e, A. Muscles de la main. — In: Traité des variations du système musculaire de l'homme. Paris, Schleicher Frères, 1897, 153-218.
7. M a c a l i s t e r, A. Additional observations on muscular anomalies in human anatomy (third series), with a catalogue of the principal muscular variations hitherto published. — Trans Roy. Irish Acad., 1875, 1-130.
8. M u r a t a, K., M. T a m a i, A. G u p t a. Anatomic study of variations of hypothenar muscles and arborization patterns of the ulnar nerve in the hand. — J. Hand Surg., **29A**, 2004, 500-509.
9. P r i b y l, C. R., M. S. M o n e i m. Anomalous hand muscle found in the Guyon's canal at exploration for ulnar artery thrombosis. A case report. — Clin. Orthop. Relat. Res., **306**, 1994, 120-123.

Institute of Experimental Morphology and Anthropology with Museum
Bulgarian Anatomical Society

Acta morphologica et anthropologica, 13
Sofia • 2008

Senescent Changes of the Rat Aortic Endothelium Studied *en face*

L. Jelev, L. Surchev

Department of Anatomy, Histology and Embryology, Medical University of Sofia

In order to study the senescent changes of the rat aortic endothelium, this study examines on *en face* preparations the common morphology of the endothelial cells and the distribution of the mononuclear cells, adherent to the endothelium, in four age groups. The endothelium of the young, puberty and adult animals was composed of an even layer of elongated endothelial cells with one oval nucleus and small number of mononuclear cells. The most prominent findings in old endothelium were the presence of giant multinucleated endothelial cells and the larger number of the mononuclear cells adherent to the endothelium. The observations found and their literature explanations are discussed.

Key words: senescence, aortic endothelium, rat.

Introduction

There are number of studies examining the *en face* morphology of the endothelial cells of the rat aorta in experimental models of different pathologic conditions [4, 5, 10]. However, the information about the normal senescent of the rat endothelium is scarce. Because the *en face* method of studying the endothelium allows to observe a large amount of cells, we used it to examine the common morphology of the rat aortic endothelium in different age groups and to describe the characteristics of the aortic endothelium in old animals.

Materials and Methods

Male Wistar rats, bred in our laboratory, 1, 3, 6 and 18-month-old, were used for this study. Under deep pentobarbital anesthesia, a perfusion fixation with 10% phosphate buffered formalin was provided. The aortas were carefully dissected, opened longitudinally, then removed, pinned out flat on polyethylene strips and stored in formalin. Impregnation of the cell borders and haematoxylin staining of the nuclei, as described by J o n e s et al. [3] visualized the endothelial cells. The *en face* preparations were made according to the method of J o r i s et al. [5].

Results

The endothelium of the aortas of the animals from different ages showed differences of endothelial cell morphology and arrangement. The presence of the mononuclear cells, adherent to the endothelium, also differed between age groups.

The endothelium of the young animals (1-month-old) (Fig. 1) was composed of an even layer of small spindle-shaped endothelial cells with their long axes aligned parallel to the direction of the blood flow. The cells had one oval nucleus. Only few mononuclear cells throughout the endothelium were observed.

The endothelium of the puberty (3-month-old) (Fig. 2) and adult animals (6-month-old) (Fig. 3) was presented by an even layer of larger than in young animals cells with one oval nucleus. The number of the mononuclear cells, adherent to the endothelium, was greater than in young animals.

The endothelium of the old animals (18-month-old) showed areas of similar in size endothelial cells and also areas of differently sized endothelial cells (Figs. 4, 5). Most of the cells showed one oval nucleus, but also a small number of giant multinucleated (with two or more nuclei) endothelial cells was observed (Fig. 4). The number of the mononuclear cells, adherent to the endothelium, was larger than in adult group. In some areas these cells were detected either scattered throughout the endothelium or in small groups (Fig. 5).

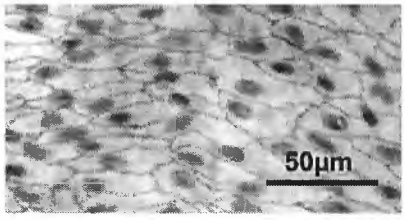

Fig. 1. *En face* preparation of the aorta of 1-month-old rat

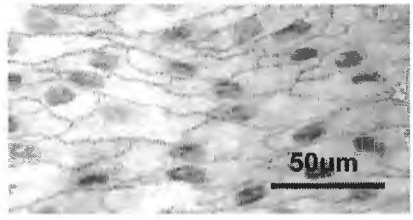

Fig. 2. *En face* preparation of the aorta of 3-month-old rat

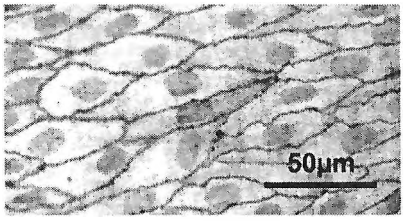

Fig. 3. *En face* preparation of the aorta of 6-month-old rat

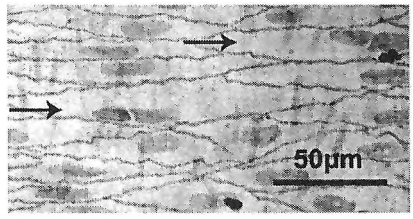

Fig. 4. *En face* preparation of the aorta of 18-month-old. Arrows indicate the giant multinucleated endothelial cells

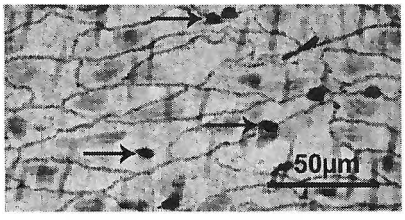

Fig. 5. *En face* preparation of the aorta of 18-month-old. Arrows indicate the mononuclear cells adherent to the endothelium

Discussion

The differences in the morphology of the endothelium among the rats from different ages represent the normal senescent process of the endothelial cells. In young animals the endothelium is composed of cells of nearly equal size that gradually become larger in puberty and adult animals. The differences in the endothelium composition of the old rats are due to the increased mean generation time of the endothelial cells [9]. Such long generation times diminish the ability to replace desquamated cells resulting in gradual loss of endothelial cells and presence of giant endothelial cells. In our study, in young, puberty and adult animals, the endothelial cells have only one nucleus, while in old animals, additionally to the usual cells with one nucleus, a small number of giant multinucleated cells is present. According to some authors [2] the multinucleated endothelial cells are prominent in newborn and adult animals (up to 10% of the cell population) and the increasing number of these cells is a characteristic of the aging mammalian and human endothelium [6]. The multinucleated endothelial cells are also known to be prevalent in atherosclerotic lesions of human [1, 7] and present in the rabbit aorta in experimental hypercholesterolemia [8].

Interesting findings presented in our study and most prominent in advanced age group were the mononuclear cells adherent to the endothelium. These mononuclear cells are variously reported as lymphocytes, macrophages and monocytes [4]. They have been observed singly or in small clusters on the endothelium of "normal" laboratory animals and suggested a minimal pathologic event [4]. Compared to the young animals, the endothelium of the old animals showed an increased number of the mononuclear cells.

Even comprising only four age groups, this *en face* study depicts the main changes of the rat aortic endothelium during the postnatal period. To present a more detailed information on this topic, a future study is necessary.

References

1. Cotton, R., W. B. Wartman. Endothelial patterns in human arteries. — Arch. Pathol., **71**, 1961, 3-12.
2. Gansburgsky, A. N., A. V. Pavlov. Cytological mechanism of postnatal growth of aortic endothelium. — Ontogenez, **25**, 1994, 33-39 (in Russian)
3. Jones, G. T., B. M. Martin, W. E. Stehbens. Endothelium and elastic tissue tears in the afferent arteries of the experimental arteriovenous fistulae in rabbits. — Int. J. Exp. Path., **73**, 1992, 405-416.
4. Joris, I., T. Zand, J. J. Nunnari, F J. Krolikowski, G. Majno. Studies on the pathogenesis of atherosclerosis. I. Adhesion and emigration of mononuclear cells in the aorta of the hypercholesterolemic rats. — Am. J. Pathol., **113**, 1983, 341-358.
5. Joris, I., T. Zand, G. Majno. Hydrodynamic injury of the endothelium in acute aortic stenosis. — Am. J. Pathol., **106**, 1982, 394-408.
6. Kamenskaia, N. L. Data on histogenesis of the human aorta. — Arkh. Anat. Gistol. Embriol., **36**, 1959, 61-66 (in Russian).
7. Repin, V. S., V. V. Dolgov, O. E. Zaikina, I. D. Novikov, A. S. Antonov, M. A. Nikolaeva, V. N. Smirnov. Heterogeneity of endothelium in human aorta. A quantitative analysis by scanning electron microscopy. — Atherosclerosis, **50**, 1984, 35-52.
8. Silkworth, J. B., B. McLean, W. E. Stehbens. The effect of hypercholesterolemia on aortic endothelium studied en face. — Atherosclerosis, **22**, 1975, 335-348.
9. Wagner, R. C. Endothelial cell embryology and growth. — In: Vascular endothelium and basement membranes (Ed. B. M. Altura). Basel, S. Karger, 1980, 45-75.
10. Zand, T., J. J. Nunnari, A. H. Hoffman, B. J. Savilonis, B. Macwilliams, G. Majno, I. Joris. Endotheial adaptation in aortic stenosis. Correlation with flow parameters. — Am. J. Pathol., **133**, 1988, 407-418.

Institute of Experimental Morphology and Anthropology with Museum
Bulgarian Anatomical Society

Acta morphologica et anthropologica, 13
Sofia • 2008

En face Study of the Internal Thoracic Artery in Human

*L. Jelev, L. Surchev, G. Milanov**

Department of Anatomy, Histology and Embryology,
**University Hospital of Cardiovascular Surgery "St. Ekaterina" Medical University of Sofia*

This study presents for the first time *en face* observation on the endothelium of the human internal thoracic artery. The normal and some pathologic findings reported correspond to the routine histology descriptions of the internal thoracic artery wall. Despite the arterial endothelium of the adult individuals frequently showed inflammatory cells infiltration, some lipid accumulations were found in only few arteries. The present findings and the method of observation of the arterial endothelium could be used in future studies and may help in investigating the causes of the internal thoracic artery graft failure.

Key words: internal thoracic artery, endothelium, human.

Introduction

The internal thoracic artery is widely used as arterial graft for the coronary system. This artery is relative rarely affected by atherosclerotic changes [1] and showed a long-term patency rate [5]. Nevertheless, in some cases, the arterial grafts developed some obstruction [2] thus compromising the heart blood supply. Therefore, the detailed knowledge on the normal and pathologic histology of the internal thoracic artery may help in improving the patency time. Up to now, light microscopically, the morphology of the internal thoracic artery has been investigated on routine transverse sections [1, 5, 6] and some authors used very oblique sections of the vessel wall [8]. These methods are good for the vessel wall investigations but they are not proper for studying of an important for the graft functioning structure - the arterial endothelium.

In order to demonstrate the characteristics of the endothelium of the internal thoracic artery and to describe the distribution of the possible lipid accumulations, we present here our *en face* study on this artery in humans of different ages and note the normal findings and some pathological observations.

Materials and Methods

The arterial specimens from 19 humans (14 men and 5 women), aged from 20 to 91 years, were examined. Parts from the internal thoracic artery were obtained from necropsies, within 8-24 hours of death, carried out in the Department of Forensic Medicine at the Medical University of Sofia. The arterial specimens were cut longitudinally, washed with normal saline, pinned out flat on polyethylene strips and fixed in 10% phosphate buffered formalin. Impregnation of the cell borders or haematoxylin staining of the nuclei visualized the endothelial cells. A combination of Sudan IV and haematoxylin staining was also provided. The *en face* preparations were made thereafter.

Results

On the *en face* preparations were observed the endothelial cells arrangement, the presence of different populations of inflammatory cells, and rarely lipids accumulations.

The normal or non-affected endothelium was seen primarily in the arteries of the young individuals (Figs. 1, 2). It was composed of an even layer of endothelial cells aligned parallel to the direction of the blood flow. Only few mononuclear cells throughout the endothelium were observed. No lipid accumulations were detected on Sudan IV — haematoxylin stained preparations.

Fig. 1. *En face* preparation of ITA of 20-year-old woman. Haematoxylin

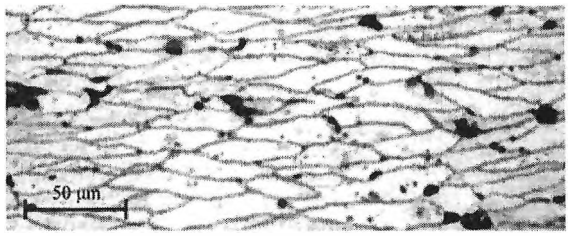

Fig. 2. *En face* preparation of ITA of 29-year-old man. Silver impregnation

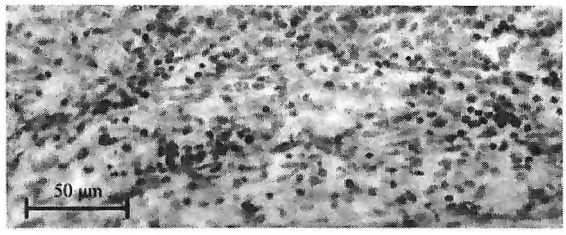

Fig. 3. *En face* preparation of ITA of 73-year-old woman. Haematoxylin

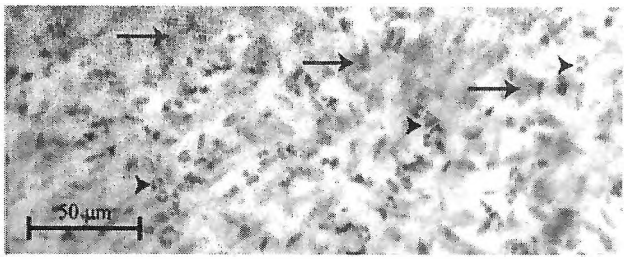

Fig. 4. *En face* preparation of ITA of 54-year-old man. Sudan IV — haematoxylin. Arrowheads indicate the nuclei of the polymorphonuclear leukocytes. Arrows show the lipid accumulations

In the endothelium of some of the older individuals, an increased number of mononuclear cells (Fig. 3), areas rich in polymorphonuclear leukocytes and small areas of lipid accumulations were detected (Fig. 4).

Discussion

Our study presents for the first time the light microscopic *en face* structure of the endothelium of the human internal thoracic artery. Up to now, the *en face* observation of the internal thoracic artery was presented in only one paper, but this was a bovine artery [7]. The *en face* observations of the internal thoracic artery correspond to the findings described on routine histologic sections [1, 6]. Even rich in different types of inflammatory cells adherent to the endothelium, the atherosclerotic changes of the internal thoracic artery seem to be minimal, even in older individuals. The great advantage of the *en face* method of observations is due to the possibility not only to detect pathologic changes, but also to present clearly the localization of the inflammatory cells and lipid accumulations throughout the endothelium.

The data present here, concerning the endothelium of non-processed to surgical procedure arteries may help in studying the sometimes reported failure of the internal thoracic artery grafts [2]. As seems, even prior to graft suture, some of the harvested internal thoracic arteries showed acute lesions concerning the endothelium and the subendothelial layer [4]. Such changes could be caused by the surgical dissection technique [3] and in future studies could be examined and compared to the *en face* findings presented here.

References

1. Arciniegas, E., E. Fermin, F. Tortoledo, J. R. Vasquez, A. Bello. Characterization of the atherosclerotic plaque in the internal mammary artery. — Cathet. Cardiovasc. Diagn., **43**, 1998, 413-420.
2. Bezon, E., A. Karaterki, J. A. Barra. Failure of coronary artery bypass with the internal thoracic artery. Does extended use of the internal thoracic artery affect the patency of the coronary artery. — Arch. Mal. Coeur Vaiss., **91**, 1998, 1139-1144.
3. Gottlob, R., G.F. Gestring, R. Rauhs. Die endothelschonende Operationsmetode. Ihre Bedeutung für die Venenchirurgie. — Langenbeck's Arch. Surg., **345**, 1977, p. 653.
4. Kanellaki-Kyparissi, M., K. Kouzi-Koliakou, G. Marinov, V. Knyazev. Histological study of arterial and venous grafts before their use in aortocoronary bypass surgery. — Hellenic J. Cardiol., **46**, 2005, 21-30.

5. Ojha, M., R. L. Leask, K. W. Johnston, T. E. David, J. Butany. Histology and morphology of 59 internal thoracic artery grafts and their distal anastomoses. — Ann. Thorac. Surg., **70**, 2000, 1338-1344.
6. Ruengsakulrach, P., R. Sinclair, M. Komeda, J. Raman, I. Gordon, B. Buxton. Comparative histopathology of radial artery versus internal thoracic artery and risk factors for development of intimal hyperplasia and atherosclerosis. — Circulation 100, 1999, Suppl., 19, 139-144.
7. Schaeffer, U., B. Tanner, T. Strohschneider, A. Stadtmuller, A. Hanneku m. Damage to arterial and venous endothelial cells in bypass grafts induced by several solutions used in bypass surgery. — Thorac. Cardiovasc. Surg., **45**, 1997, 168-171.
8. Sims, F. H. The initiation of intimal thickening in human arteries. — Pathology, **32**, 2000, 171-175.

Institute of Experimental Morphology and Anthropology with Museum
Bulgarian Anatomical Society

Acta morphologica et anthropologica, 13
Sofia • 2008

Distribution of Mast Cells in the Pelvic Urethra in Boars

G. Kostadinov, A. Vodenicharov, R. Dimitrov, P. Yonkova, H. Hristov

Department of Veterinary Anatomy, Histology and Embryology, Faculty of Veterinary Medicine, Trakia University, Stara Zagora

The localization and the histochemical features of mast cells in the urogenital system and especially in male genitals in domestic animals are not yet adequately investigated. Until now, the occurrence of mast cells in the kidney and the epididymis of domestic pigs are described.

The aim of the present study was to determine the localization and some histochemical particularities of mast cells in pelvic urethra, in the disseminate part of prostate and in the urethral muscle.

The data of our studies showed that the main part of mast cells were located in the connective tissue between glandular lobules and at the boundary between the pelvic urethra and the urethral muscle. A considerable amount of mast cells were also present adjacently to the epithelium of pelvic urethra. Mast cells with an obviously fusiform shape were observed both intraepithelially and near the basal membrane of epithelial cells.

Key words: mast cells, urethra pelvina, boar.

Introduction

It is known that the granules of mast cells contain ligands with a significant biological importance. This is the reason for the continuous interest to species-related, organ-, histo- and immunocytochemical features of mast cells during more than thirty years.

The localization and the histochemical features of mast cells in the urogenital system and especially in male genitals in domestic animals are not yet adequately investigated. The available literature data are mainly in humans and experimental animals [1, 2, 3, 4]. Until now, the occurrence of mast cells in the kidney and the epididymis of domestic boars are described [1, 5, 6, 7, 8].

There is a lot of evidence that the visualization of mast cells depends both on the type of used fixative and the staining technique [2, 9]. The animal species, subject of the studies, is also important.

The aim of the present study was to determine the localization and some histochemical particularities of mast cells in pelvic urethra, in the disseminate part of prostate and in the urethral muscle.

Material and Methods

The material was obtained from a slaughterhouse from 12 boars at the age of 6-12 months from the Danubian White and Landrace breeds. The specimens were fixed in Carnoi's fixative for 4 hours, then put in 70° ethanol for 12 hours, then dehydrated in an ascending alcohol series, cleared in xylene and embedded in paraffin. The cross-sections (6-8 μm) were stained with 0.1% solution of toluidine blue in McIvane's buffer, pH 3.

Results and Discussion

The data of performed investigations showed a various distribution of mast cells in the pelvic urethra and the disseminate part of prostate in healthy boars.

The principal part of mast cells were observed in the connective tissue among the glandular lobules, in the prostate part of pelvic urethra (Fig. 1). Mast cells were with a various shape) oval, elongated and irregular) with a clear γ — metachromasia. Some of them appeared with a high degree of activity (looked like "spilled"). A considerable amount of mast cells were observed in the connective tissue at the boundary between pelvic urethra and the urethral muscle that embraced it ventrally and laterally. The mast cells located among the muscle cells of the urethral muscle were significantly few and exhibited a marked fusiform shape. A relatively lower number

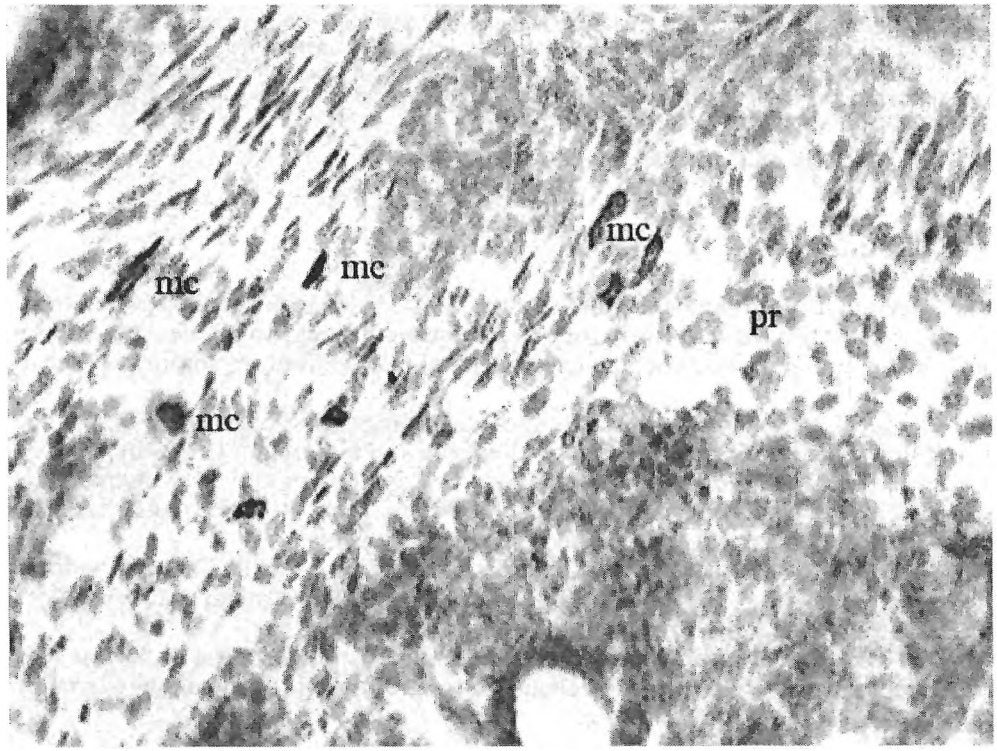

Fig. 1. Mast cells (mc) situated in the propria (pr) among the glandular lobules

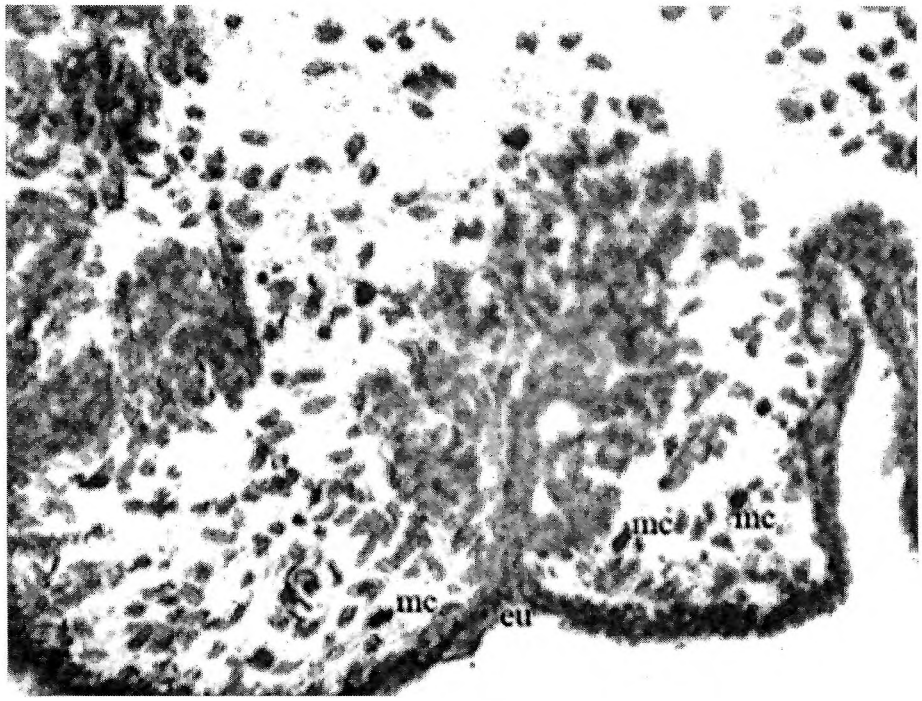

Fig. 2. Mast cells (mc) in a close vicinity to the epithelium of the urethra (eu)

Fig. 3. Mast cells (mc) with a fusiform shape in the epithelium of the urethra (eu)

of mast cells was observed in the propria among the end glandular tubulous and tubulo-acinous tops of parenchyma in the disseminate part of the prostate. Single mast cells were observed near the small and medium-size blood vessels of the interstitium of pelvic urethra. Part of them were situated in the adventitia of arterioles and venules, and single mast cells were located at its boundary with the media.

A considerable number of mast cells with oval and elongated shape were observed in a close vicinity with pelvic urethra epithelium. Single cells with a markedly fusiform shape were observed both intraepithelially and near the basal membrane of epithelial cells (Figs. 2, 3).

On the basis of results of previous studies of ours upon the distribution of mast cells in the penile urethra and the present data, the following comparisons could be made: near the epithelium of penile urethra, single mast cells were observed whereas within the epithelial, they were absent. Unlike that, a significant amount of these cells were discovered in the epithelium of pelvic urethra.

References

1. Anton, F., C. Morales, R. Agullar, C. Bellido, E. Agullar, F. Gaytan. A comparative study of mast cells and eosinophil leukocytes in the mammalian testis. — Zentralbl Veterinarmed A., **45**, 1998, 209-218.
2. Ghanem, N. S., E. S. Assem, K. B. Leung, F. L. Pearce. Guinea-pig mast cells: comparative study on morphology, fixation and staining properties. — Int. Arch. Allergy Appl. Immunology, **85**, 1988, 351-357.
3. Ghanem, N. S., E. S. Assem, K. B. Leung, F. L. Pearce. Cardiac and renal mast cells: morphology, distribution, fixation and staining properties in the guinea pig and preliminary comparison with human. — Agents Actions, **23**, 1988, 223-226.
4. Nistal, M., L. Santamaria, R. Paniagua. Mast cells in the human testis and epididymis from birth to adulthood. — Acta Anatomica, **119**, 1984, 155-160.
5. Pabst, R., W. Beil. Mast cells heterogeneity in the small intestine of normal, gnotobiotic and parasitized pigs. — Int. Arch. Allergy Appl. Immunology, **88**, 1989, 363-366.
6. Pinat, E., S. Bonet, M. Bryz, S. Sancho, N. Garcia, E. Badia. Cytology of the intestinal tissue in scrotal and abdominal testes of post-puberal boars. — Tissue Cell, **33**, 2001, 8-24.
7. Vodenicharov, A., C. Chouchkov. Morphological study of mast cells localization in the wall of the proximal tubule in the domestic swine kidney. — Anatomia Histologia Embryologia, **28**, 1999, 85-88.
8. Xu, L. R., M. M. Carr, A. P. Bland, G. A. Hall. Histochemistry and morphology of porcine mast cells. — Histochemistry Journal, **25**, 1993, 516-522.
9. Barret, K. E., M. Ennis, F. L. Pearce. Mast cells isolated from guinea-pig lung: characterization and studies on histamine secretion. — Agents Actions, **13**, 1983, 122-126.

Institute of Experimental Morphology and Anthropology with Museum
Bulgarian Anatomical Society

Acta morphologica et anthropologica, 13
Sofia • 2008

Age Related Changes in the Cells of Intervertebral Cartilage End Plates

B. Landzhov

Department of Anatomy and Histology, Medical University, Sofia

The intact human lumbar intervertebral discs were obtained and examined histologically the changes that occur with the cells in cartilage end plate (CEP). The objectives of the study were to examine the morphologic features of the CEP at different ages. Hematoxylin-Eosin and Masson-stained slides were observed with light-microscopic technique. The material from cadavers and surgical specimens was obtained. With ageing the numbers of chondrocytes was changed and apoptosis increased parallel with decreasing of the cell density. The quantity of apoptotic cells is greater in old CEP than in younger. Different types of cells, thickness and calcification were found.

Key words: age-related changes, human intervertebral discs, cartilage end plate.

Introduction

Cartilage end plates are parts of intervertebral disc, which lies between the vertebral body and annulus fibrosus. They are thin hyaline cartilage plates and form the anatomical and physiogical boundary of the disc which facilitates the diffusion of nutritients from the vertebra into the disc. Nutrients and metabolites that supply disc cells pass through the cartilage endplate [10, 12, 13]. The cells of the CEP are change with ageing [5]. Age-related changes concern all structural components, cells death, density and proliferation [4]. With our study we can contribute to the understanding of the changes that occur in CEP with ageing.

Material and Methods

Cartilage end plates were examined by routine light-microscopic technique. The obtained cadaver and surgical material from IVD of humans at different ages (between 20 and 60 years old) was fixed in 10 % formalin. Paraffin-embedded material was cut on 7 μm sections and stained with Hematoxylin-eosin and Masson.

Results and Discussion

The changes, the localization and the number of the cells were observed in order to determine the age-related changes. CEPs decrease in thickness and disappeared with aging (Fig. 1). Apoptosis increased with ageing and cell density decrease [1, 2, 3, 6, 7, 8]. Parallel with this increased the degenerative changes in all parts of the disc. Clusters of cells proliferation were formed and concentric tears appeared. The quantity of apoptotic cells is greater in old CEP than in younger (Figs. 2, 3). Boos et al. [4] described degenerative changes in the morphology of young age. They observed some very mild cleft formation.

CEPs, avascular in adults and vascular in degenerative discs play a key role in the metabolism of the IVD [9, 10]. Decreasing in permeability of the CEP is the main cause of degeneration of the disc and depends on the morphologic state of the CEP [11, 12, 13] This hypothesis is not clear. With ageing also can be seen a cleft formation and fissures within the CEP (Fig. 4).

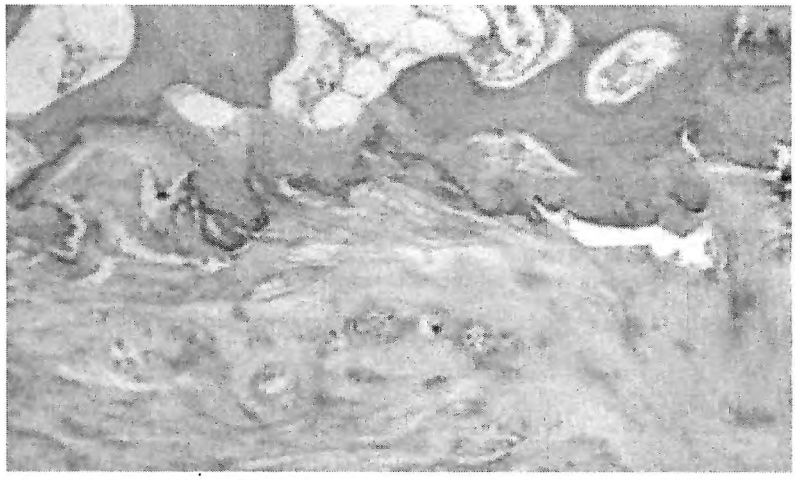

Fig. 1. 60 years old (HE, × 250)

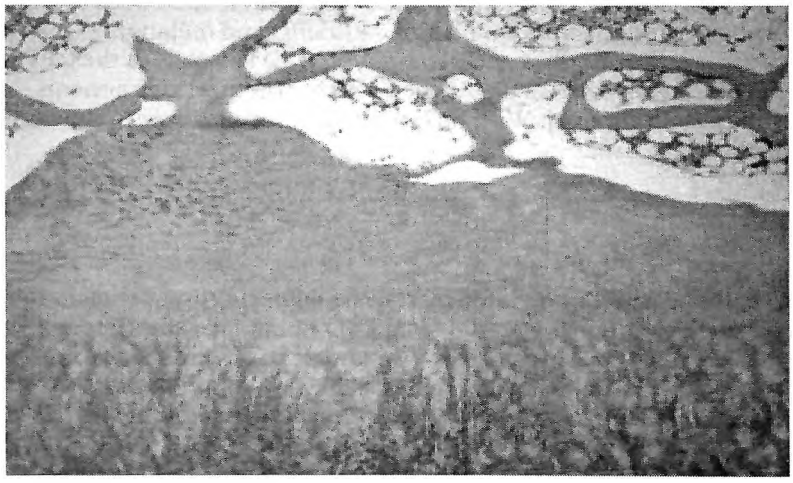

Fig. 2. 30 years old (HE, × 150)

Fig. 3. 25 years old (HE, × 200)

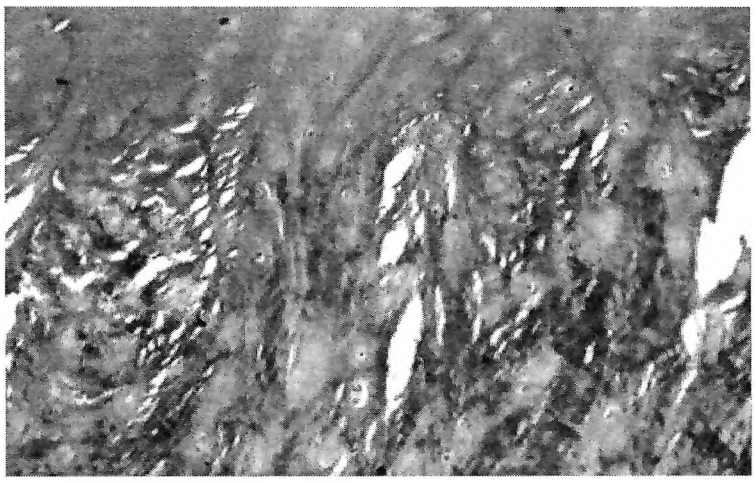

Fig. 4. 40 years old (Masson, × 250)

Conclusion

It is not enough known the process that occur within CEP with ageing. Cluster formations and new blood vessels appear with cell proliferation and degeneration. CEP decreases in thickness, disappears with aging and the chondrocytes change. These changes are very important in order to be understood the problems which occur in the disc.

References

1. Adams, M. A., D. S. McNally, P. Dolan. Stress distributions inside intervertebral discs: The effects of age and degeneration. — J. Bone Joint Surg., **78**, 1996, 965-72.
2. Antoniou, J., T. Steffen, F. Nelson, N. Winterbottom, A. P. Hollander, R. A. Poole, M., Aebi, M. Alini. The human lumbar intervertebral disc: evidence for

changes in the biosynthesis and denaturation of the extracellular matrix with growth, maturation, ageing, and degeneration. — J. Clin Invest., **98**, 1996, 996-1003.
3. Ariga, K., S. Miyamoto, T. Nakase, S. Okuda, W. Meng, K. Yonenobu, H. Yoshikawa. The relationship between apoptosis of endplate chondrocytes and aging and degeneration of the intervertebral disc. — Spine, **26**, 2001, No22, 2414-20.
4. Boos, N., S. Weissbach, H. Rohrbach, C. Weiler, K. F. Spratt, A. G. Nerlich. Classification of age-related changes in lumbar intervertebral discs: 2002 Volvo Award in basic science. — Spine, **27**, 2002, 2631-2644.
5. Chelberg, M. K., G. M. Banks, D. F. Geiger, T. R. Oegema. Identification of heterogeneous cell populations in normal human intervertebral disc. — J. Anat., **186**, 1995, 43-53.
6. Grignon, B., Y. Grignon, D. Mainard, M. Braun, P. Netter, J. Roland. The structure of the cartilaginous end-plates in elder people. — Surg Radiol Anat., **22**, 2000, No1, 13-9.
7. Gruber, H. E., E. N. Hanley. Analysis of aging and degeneration of the human intervertebral disc. Comparison of surgical specimens with normal controls. — Spine, **23**, 1998, 751-757.
8. Holm, S., A. K. Holm, L. Ekstrom, A. Karladani, T. Hansson. Experimental disc degeneration due to endplate injury. — J. Spinal Disord. Tech., **17**, 2004, No1, 64-71.
9. Moore, R. J. The vertebral end-plate: what do we know? — Eur. Spine J., **9**, 2000, No2, 92-6.
10. Nachemson, A., T. Lewin, A. Maroudas, M. A. Freeman. *In vitro* diffusion of dye through the end-plates and annulus fibrosus of human lumbar intervertebral discs. — Acta Orthop. Scand., **41**, 1970, 589—607.
11. Roberts, S., J. Menage, J. P. G. Urban. Biochemical and structural properties of the cartilage end-plate and its relation to the intervertebral disc. — Spine, **14**, 1989, 166-174.
12. Urban, J. P., S. Smith, J. Fairbank, C. Nutrition of the intervertebral disc. — Spine, **29**, 2004, No23, 2700-9.
13. Whalen, J. L., W. W. Parke, J. M. Mazur, E. S. Stauffer. The intrinsic vasculature of developing vertebral end plates and its nutritive significance to the intervertebral discs. — J. Pediatr. Orthop., **5**, 1985, No4, 403-10.

Institute of Experimental Morphology and Anthropology with Museum
Bulgarian Anatomical Society

Acta morphologica et anthropologica, 13
Sofia • 2008

Degenerative Changes in the Human Intervertebral Discs. Histochemical Study

B. Landzhov, L. Stokov, B. Vladimirov*, A. Bozhilova-Pastirova, W. Ovtscharoff*

Department of Anatomy and Histology,Medical University, Sofia
**Department of Orthopaedy and Traumatology, Medical University, Sofia*

The object of this study was to examine histochemically some of the causes leading to disc degeneration. Our results suggest that nicotinamide adenine dinucleotide phosphate-diaphorase (NADPH-d), which is a marker for nitric oxide synthase (NOS) and an indirect marker for nitric oxide (NO), is linked with the degenerative changes in the intervertebral disc (IVD).

Key words: intervertebral disc, degeneration, NADPH-d.

Introduction

NO is a messenger molecule that is synthesized from l-arginine. It is a result from the metabolism of the cells and activates many pathways by diffusing across membranes. It is synthesized from three different enzymes: inducible (iNOS), endothelial (eNOS) and neuronal (nNOS).

Materials and Methods

The obtained material was from individuals between 21 and 70 years old. We examined 10 controls from cadavers and 12 surgical specimens from patients with disc disease. Our histochemical study was to demonstrate histochemically the NADPH-d.

Results and Discussion

Our findings suggest that NADPH-d reactivity cells were more over in the discs with degenerative changes than normal. The lamellas in annulus fibrosus (AF) get more disorganized, and the connection between AF and cartilage and plates (CEP) disrupts. Many authors report that there is a correlation between proinflammatory mediators and the production of NO [1, 2, 4, 5, 6, 7, 10].

The quantity of the positive NADPH-d cells increase with the increase of degenerative changes in the disc. It is not clear enough this relationship. NADPH-d expression is strongest in the chondrocytes in 50-65 years old individuals (Fig. 1). Differences between expressions of NADPH-d positive cells in different parts of the disc are viewed. The quantity of these chondrocytes in the outer AF (Fig. 2) is greater than those in the inner region (Fig. 3). It is not clear whether this is a result of degeneration or it is a process of normal chondrocyte maturation [11]. On the other hand, many NADPH-d positive cells are observed on the border of the vascular canals (Fig. 4). This NO may come basely from endothelium. The basely production of NO comes from newly formed blood capillaries and granulate tissue around them [3].

The number of positive cells increases with ageing and degeneration respectively. The quantity of NO depends on the types of degenerative diseases [12].

Fig. 1. Old IVD, outer AF (× 250)

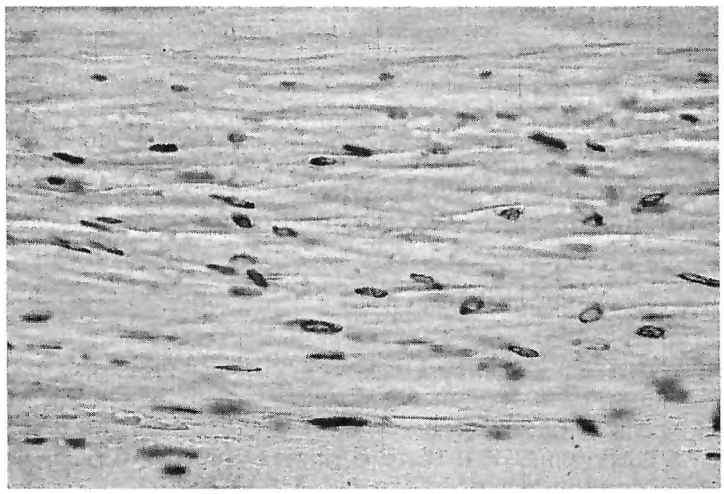

Fig. 2. Old IVD, outer AF (× 500)

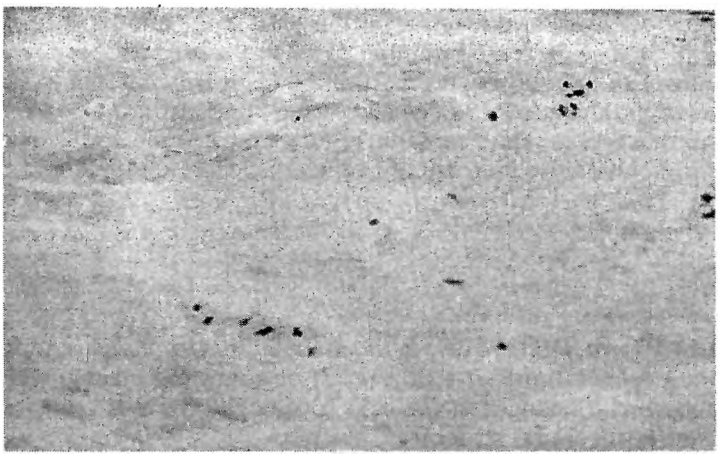

Fig. 3. Old IVD, inner AF (× 250)

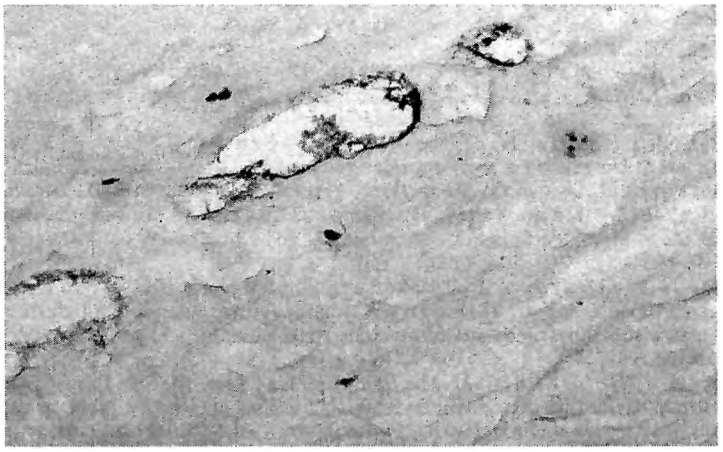

Fig. 4. Old IVD, outer AF (× 500)

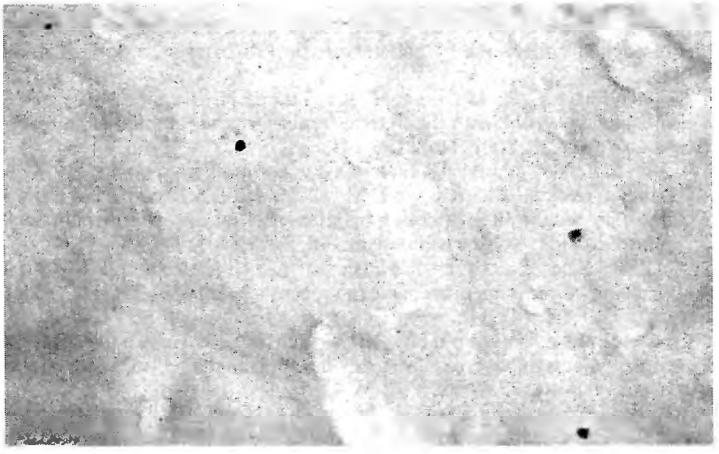

Fig. 5. Young IVD, AF (× 500)

The number of NADPH-d reactivity cell is least in the groups of 25-35 years old individuals (Fig. 5). The increased number of NOS-positive chondrocytes in young individual is a result of chondrocytes maturation [11]. The material from degenerative discs showed greater number of positive cells than normal control discs. With this we confirm that NO is a molecule that regulate the cell metabolism and increase its quantity parallel with the increase of cyclic tensile stretch [8, 9] and disc degeneration.

Conclusion

Degenerative changes in IVD are one of the main factors for appearance of low back pain. Often the degeneration starts as a result of abnormal mechanical load. This strength is related with changes in the cells, proteoglycans and collagen fibers, all intercellular and extracellular structures.

References

1. Burke, J. G., R. W. Watson, D. Conhyea, D. McCormack, F. E. Dowling, M. G. Walsh, J. M. Fitzpatrick. Human nucleus pulposis can respond to a pro-inflammatory stimulus. — Spine, **28**, 2003, No24, 2685-2693.
2. Furusawa, N., H. Baba, N. Miyoshi, Y. Maezawa, K. Uchida, Y. Kokubo, M. Fukuda. Herniation of cervical intervertebral disc: immunohistochemical examination and measurement of nitric oxide production. — Spine, **26**, 2001, No10, 1110-1116.
3. Hashizume, H., M. Kawakami, H. Nishi, T. Tamaki. Histochemical demonstration of nitric oxide in herniated lumbar discs. A clinical and animal model study. — Spine, **22**, 1997, No10, 1080-1084.
4. Kang, J. D., H. I. Georgescu, L. McIntyre-Larkin, M. Stefanovic-Racic, W. F. Donaldson 3rd, C. H. Evans. Herniated lumbar intervertebral discs spontaneously produce matrix metalloproteinases, nitric oxide, interleukin-6, and prostaglandin E2. — Spine, **21**, 1996, No3, 271-277.
5. Kang, J. D., H. I. Georgescu, L. McIntyre-Larkin, M. Stefanovic-Racic, C. H. Evans. Herniated cervical intervertebral discs spontaneously produce matrix metalloproteinases, nitric oxide, interleukin-6, and prostaglandin E2. — Spine, **20**, 1995, No22, 2373-2378.
6. Kang, J. D., M. Stefanovic-Racic, L. A. McIntyre, H. I. Georgescu, C. H. Evans. Toward a biochemical understanding of human intervertebral disc degeneration and herniation. Contributions of nitric oxide, interleukins, prostaglandin E2, and matrix metalloproteinases. — Spine, **22**, 1065-1073, No10.
7. Kohyama, K., R. Saura, M. Doita, K. Mizuno. Intervertebral disc cell apoptosis by nitric oxide: biological understanding of intervertebral disc degeneration. — Kobe J. Med. Sci., **46**, 2000, No6, 283-295.
8. Liu, G. Z., H. Ishihara, R. Osada, T. Kimura, H. Tsuji. Nitric oxide mediates the change of proteoglycan synthesis in the human lumbar intervertebral disc in response to hydrostatic pressure. — Spine, **26**, 2001, No2, 134-141.
9. Rannou, F., P. Richette, M. Benallaoua, M. Francois, V. Genries, C. Korwin-Zmijowska, M. Revel, M. Corvol, S. Poiraudeau. Cyclic tensile stretch modulates proteoglycan production by intervertebral disc annulus fibrosus cells through production of nitrite oxide. — J. Cell Biochem., **90**, 2003, No1, 148-157.
10. Taskiran, D., M. Stefanovic-Racic, H. Georgescu, C. Evans. Nitric oxide mediates suppression of cartilage proteoglycan synthesis by interleu-kin-1. — Biochem. Biophys. Res. Commun., **200**, 1994, 142-148.
11. Teixeira, C. C., H. Ischiropoulos, P. S. Leboy, S. L. Adams, I. M. Shapiro. Nitric oxide-nitric oxide synthase regulates key maturational events during chondrocyte terminal differentiation. — Bone, **37**, 2005, No1, 37-45.
12. Watanabe, T., S. Kato, K. Sato, K. Nagata. Nitric oxide regulation system in degenerative lumbar disease. — Kurume Med J., **52**, 2005, No1-2, 39-47.

Institute of Experimental Morphology and Anthropology with Museum
Bulgarian Anatomical Society

Acta morphologica et anthropologica, 13
Sofia • 2008

Microvascular Mechanisms of Chronic Venous Insufficiency

M. Minkov

Department of Anatomy, Histology and Embryology, Prof. Paraskev Stoyanov
Medical University of Varna

The study covered a material of 152 affluents of the saphenous veins as well as an operative material of 60 patients. The considerable number of the direct and indirect affluents without any valves in the outfall allows us to consider that there is a possibility for a blood reflux into the *vasa vasorum* of the saphenous veins not from the lumen of this vein itself but from the lumen of the affluents that do not possess any valves in their outfalls. In case of hypertension in the principal trunk and its affluents certain conditions for the development of reflux to the dermal pool, too, are created which results in oedema, microangiopathies and skin ulcerations.

Key words: saphenous vein, valves, *vasa vasorum*, varicosis.

Introduction

Chronic venous insufficiency of the lower extremity is a widely disseminated disease that, according to some authors' opinion, affects up to and over 50% of the examined populations. There exists a united concept in the literature available that the venous hypertension and the stasis related to it represent the first clinical symptom of the chronic venous insufficiency. C r o t t y [2, 3, 4] accepts that the development of the varicose process is related with the blood reflux into the *vasa vasorum* of the venous wall from the lumen of the vein. According to V a n c o v [12, 13] and M a r i n o v [14], a direct drainage of the *vasa vasorum* into the lumen of the saphenous veins can be observed as an exception only.

Based on our own investigations of the valvular apparatus of the superficial affluents of the saphenous veins as well as on the studies of the *vasa vasorum* of the valvular sinus wall of the varicose veins we defined our purpose to clarify the microcirculatory mechanisms that control the chronic venous insufficiency.

Material and Methods

The study covered 152 affluents of the saphenous veins, i.e. 61 direct and 91 indirect ones. The investigation of the valvular sinus wall was carried out on an operative material taken from 60 patients.

The provision with valves of the superficial affluents and the localization of the valves in it underwent an examination by means of a stereomicroscope. The material for the light-microscopic observation of the valvular sinus wall was fixed in a combination of different fixers. Stainings with hematoxylin-eosin (HE), orcein, Azan and after the methods of Mallory and of Van Gieson were made use of. The histological sections were examined under OLYMPUS BX-500 microscope and filmed by a video-camera.

Results and Discussion

Our study demonstrated that the provision with valves of the affluents of the saphenous veins, and especially of the indirect affluents places them into an unfavourable situation towards the venous hypertension in case of disturbed venous outflow from the lower extremities (Fig. 1).

The 'valvular index' after V a n c o v [12] concerning the direct affluents amounts to 2,06 while that concerning the indirect ones — to 1,28. The great number of the direct and indirect affluents without any valves in the outfall allows us to consider that there is a possibility for a blood reflux into the *vasa vasorum* of the saphenous veins not from the lumen of this vein itself but from the lumen of the affluents that do not possess any valves in their outfalls. In case of hypertension in the principal trunk and its affluents certain conditions for the development of a reflux to the dermal pool, too, are created which causes oedema, microangiopathies and skin ulceration. According to the present understanding of the topic, the pathological alterations in chronic venous insufficiency result from a preliminarily programmed

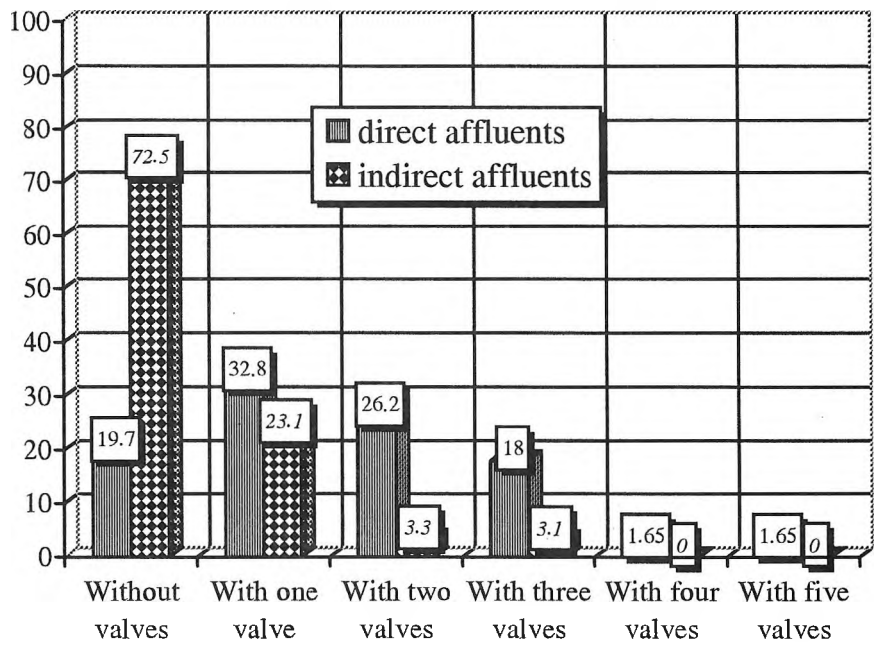

Fig. 1. Percentage distribution of the number of valves in the single affluents

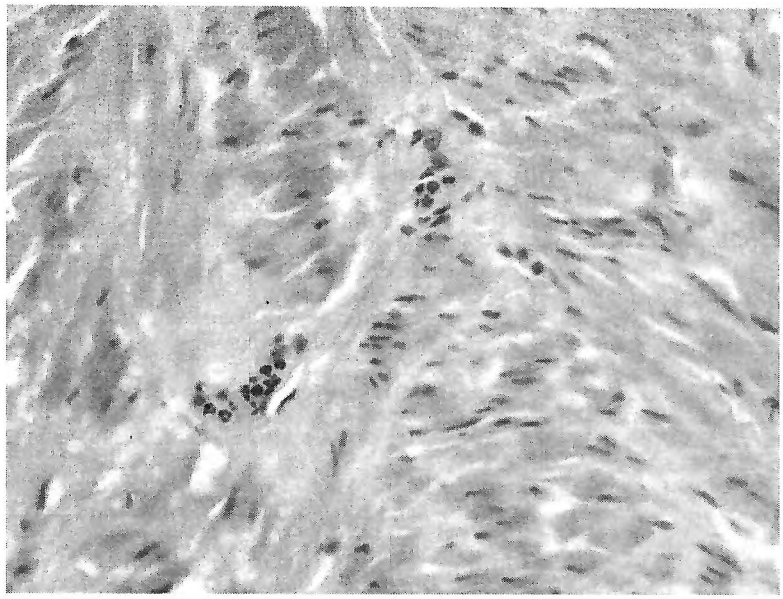

Fig. 2. Vena saphena magna. Vasa vasorum in the valvular sinus wall. HE, × 400

cascade of reactions with numerous signs of inflammation [1, 5, 6, 8]. The venous hypertension, blood stasis and hypoxia activate the endothelial cells and leukocytes towards an increased expression of adhesive molecules into their membranes through which an adhesion of the leukocytes on the endothelial surface and their penetration into the venous wall is accomplished (Fig. 2).

The enhancement of the tissue compression on the intramural vessels in the venous wall blocks the blood circulation in them which, on its part, leads to hypoxia of the venous wall. Besides the other source of oxygen provision of the venous wall, i.e. the blood stored in the lumen, presents with a lowered oxygen concentration.

Under the conditions of hypoxia, the endothelial and smooth muscle cells of the venous wall modify their physiological activity as some active substances such as growth factors and matrix metal proteinases are produced and thus the elimination of NO is suppressed [1, 7, 9, 10, 11]. In aggregate and by definite sequence of incorporation, these processes realize a venous wall remodeling. At the level of the principal subcutaneous veins and their affluents they manifest themselves with varicosities of the veins while at the level of the microcirculatory part of their pool - with skin alterations, including even with varicose ulcers.

References

1. Coleridge-Smith, P., J. Bergman. Inflammation in Venous Disease. — In: Molecular Basis for Microcirculatory Disorders (Eds. G. W. Schmid-Schönbein, D. N. Granger). Paris etc., Springer-Verlag, 2003, 489-500.
2. Crotty, T. The roles of turbulence and vasa vasorum in the aetiology of varicose veins. — *Med. Hypotheses,* **34**, 1991, 41-48.
3. Crotty, T. An investigation of the vasa venarum in a canine vein using radial reflux perfusion. — *Phlebology*, **10**, 1995, 12-18.

4. Crotty, T. The corrupted feedback hypothesis. — *Med. Hypotheses*, **61**, 2003, 605-616.
5. Jünger, M., S. Braun. Microvascular mechanisms controlling CVI. — In: Molecular Basis for Microcirculatory Disorders (Eds. G. W. Schmid-Schönbein, D. N. Granger). Paris etc., Springer-Verlag, 2003, 501-513.
6. Michiels, C. Role of the respiratory activity of vascular endothelial mitochondria in the pathophysiology of CVI. — *Phlebolymphology*, **39**, 2003, 105-112.
7. Nicolaides, A. Pathophysiology of chronic venous insufficiency. — *Medicographia*, **26**, 2004, 2, 128-132.
8. Schmid-Schönbein, G., Ph. Faha. Inflammation and the pathophysiology of chronic venous insufficiency. — *Phlebolymphology*, **39**, 2002, 95-104.
9. Schmid-Schönbein, G., S. Takase, J. Bergan. New advances in the understanding of the pathophysiology of chronic venous insufficiency. — *Angiology*, **52**, 2001, 27-34.
10. Takase, S., J. Bergan, S. Schmid-Schönbein. Expression of adhesion molecules and cytokines on saphenous veins in chronic venous insufficiency. — *Ann. Vasc. Surg.*, **14**, 2000, 427-435.
11. Weber, C. Novel mechanistic concepts for the control of leukocyte transmigration: specialization of integrins, chemokines, and junctional molecules. — *J. Mol. Med.*, **81**, 2003, 4-19.
12. Ванков, В. Строение и васкуляризация стенки вен и их клапанов (канд. дис.). Ленинград — Варна, 1968.
13. Ванков, В. Морфология на вените. София, Мед. и физк., 1989, 208 с.
14. Маринов, Г. Строеж и васкуларизация на вените на подбедрицата и задколянната яма (канд. дис.). Варна, 1969.

Institute of Experimental Morphology and Anthropology with Museum
Bulgarian Anatomical Society

Acta morphologica et anthropologica, 13
Sofia • 2008

Case of High Origin of the Common Peroneal Nerve Accompanied by Variation in the Sacral Plexus and the Piriformis Muscle

S. Pavlov

Department of Anatomy, Histology and Embryology,
University of Medicine "Prof. Dr. Paraskev Stoyanov", Varna

During routine tutorial in gross anatomy, we encountered a case (female, older than 60 years) of altered gross anatomy of the sacral plexus and the piriformis muscle, and altered passage and distribution of the superior and inferior gluteal arteries and their branches. From the lumbosacral trunk and the ventral division of S_2 arise branches, which form a second plate. This plate is situated behind the sacral plexus and passes through the piriformis muscle dividing it into two separate parts. It separates the superior gluteal nerve and the common peroneal nerve. The latter leave the pelvis between the two parts of the piriformis muscle. The anterior plate of the sacral plexus divides into the inferior gluteal nerve, the pudendal nerve and the tibial nerve. The posterior cutaneous femoral nerve begins with two roots arising from the two plates of the sacral plexus. The superior gluteal artery has large diameter and its descending branch takes over the blood supply of the gluteus maximus muscle. The inferior gluteal artery and the obturator artery arise from a common trunk originating from the posterior branch of the internal iliac artery. The inferior gluteal artery leaves the pelvis through the infrapiriform opening. It passes behind the tendon of the internal obturator muscle and splits into several branches providing blood supply for the latter muscle, the gemmeli muscles and partially for the head of the femur and the capsule of the hip joint.

Key words: high origin of the common peroneal nerve, piriformis muscle variation, sacral plexus variation, piriformis entrapment syndrome.

The gluteal region is subject to a vast number of serious surgical interventions. Any unexpected variation in its anatomical organization and in the spatial relationship between its main blood vessels and nerves can obstruct the work of the inexperienced surgeon. Even more, some of the anatomical variations in the gluteal region and the pelvis could be manifested clinically through peripheral entrapment syndromes like sciatica syndrome of unknown origin, piriformis entrapment syndrome etc.

Material and Methods

During a routine tutorial in regional anatomy of the lower limb we discovered a case (female, older than 60 years) of complex variation, which includes altered gross anatomy of the sacral plexus and the piriformis muscle, and altered passage and distribution of the superior and inferior gluteal arteries and some of their branches.

Results and Discussion

Normally the sacral plexus represents a triangular plate that is formed by the lumbosacral trunk, the anterior division of the S1, and portions of the anterior divisions of S2 and S3 nerves and is placed in front of the piriformis muscle pointing with its apex towards the infrapiriform foramen. The superior gluteal artery passes between the lumbosacral trunk and the anterior division of S2, and the inferior gluteal artery passes between the ventral divisions of S2 and S3. The apex of the plate points towards the infrapiriform foramen, where it continues into the sciatic nerve. The latter passes into the gluteal region between the piriformis muscle and the gemellus superior muscle and laterally to the inferior gluteal nerve and artery [10].

In our case from the lumbosacral trunk and the ventral division of S2 begin branches, which form a second plate. This plate is located behind the sacral plexus and passes through the piriformis muscle dividing it in two parts. It separates the inferior gluteal nerve and the common peroneal nerve (Fig. 1). The latter leave the pelvis between the two parts of the piriformis muscle. The anterior plate of the sac-

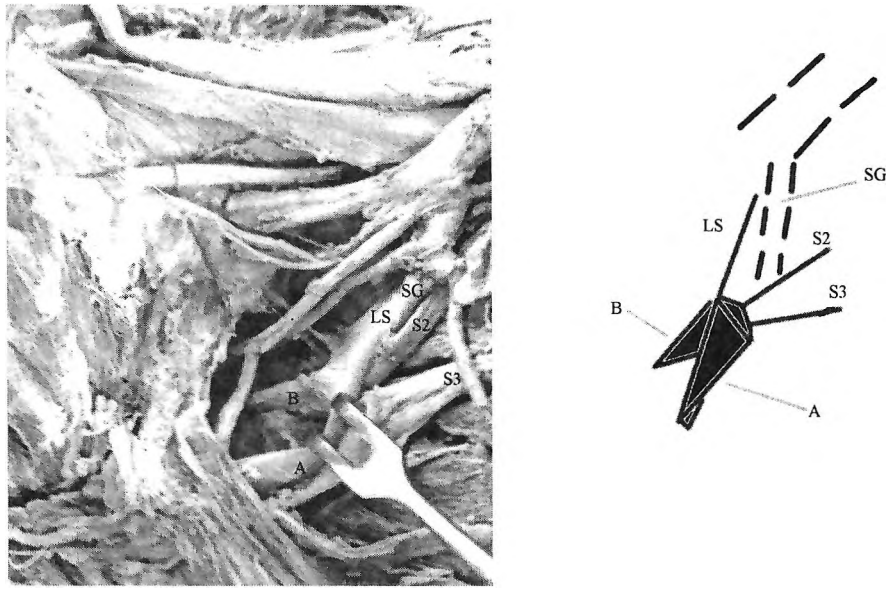

Fig. 1. Pelvic cavity. Sacral plexus
A — anterior plate; B — posterior plate; LS — lumbosacral trunk; SG — superior gluteal artery

ral plexus divides into the pudendal nerve and the tibial nerve. The posterior cutaneous femoral nerve begins from both plates of the sacral plexus with two roots forming a loop, which covers posteriorly the inferior part of the piriformis muscle. The superior and the inferior gluteal artery begin with a common trunk which exits the

Fig. 2. Posterior view of the piriformis muscle
GM — gluteus maximus muscle; PM — piriformis muscle; CP — common peroneal nerve; TN — tibial nerve; IGA — inferior gluteal artery (superficial branch of the superior gluteal artery); IGN — inferior gluteal nerve; CFP — posterior cutaneous femoral nerve

pelvis through the suprapiriform foramen and divides in the two gluteal arteries outside the pelvis so, that the inferior gluteal artery resembles in position and direction the superficial branch of the normal superior gluteal artery. In the described case this branch is very large in diameter and anastomoses with the lateral circumflex femoral artery (Fig. 2). Through the infrapiriform opening passes a small artery beginning in a common trunk with the obturator artery. In the gluteal region it passes behind the gemellus superior and the tendon of the obturator internus muscle and splits into several branches providing blood supply for the surroundings.

In the literature there is no information about the incidence of similar complex variation. The incidence of some of the described anomalies is as follows:

- superior and inferior gluteal artery rising in common trunk that divides outside the pelvis - about 3,5% (B r a i t h w a i t e, 1952) [2];

- high origin of the peroneal nerve passing through a divided piriformis muscle — about 14.3% (P o k o r n y et al. 2006) [9].

However, similar complex variations in the gluteal region are described often [3, 5, 7]. The variations of the branches of the sacral plexus and the muscles of the gluteal region are widely discussed in the literature mostly in connection to the diagnosis and treatment of the peripheral entrapment syndromes [1, 4, 6, 8]. Unfortunately, in our case there is no data whether the patient has expressed symptoms of entrapment of the common peroneal nerve and/or the inferior gluteal nerve. However, considering the literature it is very likely.

Another aspect of the described variation is the modification of the arterial bed of the inferior and superior gluteal artery, which leads to altered collateral network around the hip joint. Since the hip joint is subject to elevated surgical interest, the possibilities for such alteration must be taken into consideration prior to a surgical intervention in the gluteal region.

The structure of human body, although based upon common principles, differs from one individual to another. Thus inside the human population exist multiple variants of the human anatomical structure. The most common variant is known as "normal anatomy". The variants, distinctly deviating from this "normal" variant, are labelled "anatomical variation". In fact if one summarizes the incidence of all anatomical variations, one will realize that anatomical variations are occurring in the human population at least as often as the normal anatomical variant. That is why the healthcare provider must be familiar to the "normal" anatomy and to the anatomical variations as well.

References

1. B e n z o n, H. T., J. A. K a t z, H. A. B e n z o n, M. S. I q b a l. Piriformis syndrome.Anatomic considerations, a new injection technique, and a review of the literature. — Anesthesiology, **98**, 2003, 1442-1448.
2. B e r g m a n, R. A., A. K. A f i f i, R. M i y a u c h i. Illustrated Encyclopedia of Human Anatomic Variation, <http://www.anatomyatlases.org/AnatomicVariants/AnatomyHP.shtml>, January 1996 — January 2006.
3. G a b r i e l l i, C., E. O l a v e, E. M a n d i o l a. Inferior gluteal nerve course associated to the high division of the sciatic nerve. — Rev. chil. anat., **15**, 1997, No1, 79-83.
4. K o s u k e g a w a, I., M. Y o s h i m o t o, S. I s o g a i, S. N o n a k a, T. Y a m a s h i t a. Piriformis syndrome resulting from a rare anatomic variation. — Spine, 31, No8, E664-E666.
5. M a s, N., P. O z e k s i, B. O z d e m i r, S. K a p a k i n, M. F. S a r g o n, H. H. C e l i k, N. Y e n e r. A case of bilateral high division of the sciatic nerves, together with a unilateral unusual course of the tibial nerve. — Neuroanatomy, **2**, 2003, 13-15.
6. P a r k, H. W., J. S. J a h n g, W. H. L e e. Piriformis Syndrome. A case report. — Yonsei Med. J., **32**, 1999, No1, 164-68.

7. P a v a l, J., S. N a y a k A case of bilateral high division of sciatic nerve with a variant inferior gluteal nerve. — Neuroanatomy, **5**, 2006, 33-34.
8. P e c i n a, M. Contribution to the etiological explanation of the piriformis syndrome. — Acta Anat. (Basel), **105**, 1979, No2, 181-187.
9. P o k o r n y, D., D. J a h o d a, D. V e i g l, V. P i n s k e r o v a, A. S o s n a. Topographic variations of the relationship of the sciatic nerve and the piriformis muscle and its relevance to palsy after total hip arthroplasty. — Surg. Radiol. Anat., **28**, 2006, No1, 88-91.
10. S t a n d r i n g, S. Gray's Anatomy. 39th edition, London. Churchill Livingstone, 2004.

Institute of Experimental Morphology and Anthropology with Museum
Bulgarian Anatomical Society

Acta morphologica et anthropologica, 13
Sofia • 2008

Quantitative Intima-Media Relations in the Wall of the Major Leg Arteries and Veins During Childhood and Adolescence

S. Pavlov, S. Kirilova, G. Marinov

Departament of Anatomy, Histology and Embryology,
University of Medicine "Prof. Dr. Paraskev Stoyanov", Varna

The goal of current study is to evaluate the dynamic quantitative changes in the wall of the main vessels (arteries, superficial and deep veins) of the leg during the childhood and adolescence. Transverse sections of isolated vessels taken from the leg of 26 cadavers (0 to 19 years). The sections, stained with hemalaun-eosin and orcein, were measured via ocular micrometer/object micrometer system. Data was analyzed by means of descriptive statistics, ANOVA, correlation and graphical analysis. The increment of the intima thickness of the superficial veins correlates stronger with the age (r ~ 0,91) while in the arteries and deep veins the intima thickness correlates only moderately to considerably with age (r ~ 0,61). The relationships are opposite when the media thickness is observed. Generally, the intima is more uneven along the circularity of the investigated vessel. This is established through the large differences between minimum and maximum values of the intimal thickness of the same vessel. The media in the three vessel types shows only weak irregularity during the entire investigated age span.

Key words: arterial wall, venous wall, remodelling, quantitative relationship, intima, media.

The quantitative relationships in the wall of the blood vessels deliver valuable information needed for the prediction, the recognition and the prognosis of the variable heavy pathology of the vessel wall. Recently several advanced noninvasive methods for the precise estimation of these relationships were developed through successful combination of contemporary imaging techniques and advanced digital image analysis — multicontrast MRI with multispectral analysis, duplex ultrasound imaging with pixel distribution analysis etc. [1, 2, 3, 5, 10, 14, 15]. The correct assessment of the results is impossible without the data on the normal quantitative relationships in the vessel wall. The data although rich is currently insufficient, which lowers the reliability of these new methods and hinders their universal appliance in the diagnosis of arterial and venous diseases [6, 7, 8, 9, 11, 12, 17, 19, 20, 21].

Aim. This study is part of a project to establish the quantitative relationships in the wall of the blood vessels of the lower limb during pre- and postnatal development, in health and disease and to compare them to the qualitative differences in the

structure of the investigated vessels [13, 18, 23]. The current goal is to describe the dynamic quantitative changes in the wall of the leg arteries and veins during the childhood and adolescence.

Materials and Methods

For data collection were used transverse sections of isolated:

— main arteries of the leg: *a. tibialis anterior, a. tibialis posterior, a. peronea;*
— superficial veins of the leg: *v. saphena magna, v. saphena parva* ;
— deep veins of the leg: *v. tibialis posterior,*

taken from the middle and, in some cases, the proximal and distal third of the leg of 26 cadavers in the age of 0 to 19 years. The sections, stained with hemalaun-eosin and orcein, were measured via ocular micrometer/object micrometer system mounted on microscope Zeiss. Data was analyzed by means of descriptive statistics, ANOVA, correlation and graphical analysis [4, 16, 22].

Results and Discussion

Our findings are demonstrated in Figs. 1—5.

The first chart (Fig. 1) shows the age dependent variance of the mean intimal thickness for the three investigated vessel groups. The data forms rare elongated clouds, which are only loosely grouped around the linear trend lines. The trend lines for arteries and deep veins show moderate to considerable tendency of the mean intimal thickness to increase with age. The intima of the superficial veins, however, shows clear tendency to rise with age — its trend line is steeper and the data is more closely packed around it. The trend lines for the arteries and deep veins are almost parallel, which means that the speeds of increment of the intimal thickness are almost equal in both vessel groups. The steeper trend line of the superficial veins data stands for higher speed of age dependent intimal thickening.

The data in the second chart (Fig. 2) is tightly grouped around the linear trend lines, which are more steep then the ones in chart 1. This distribution characterizes stronger tendency of the mean media thickness of the three vessel groups to increase with age. The media of the three vessel groups increases with similar speeds as can be seen from the trend lines (almost parallel).

In fig. 3, displaying the age dependent variance in the intima/media index, the data seems ungrouped especially in the age between 0 and 13 years. In the rightmost parts of the chart (18-19 years) a slight tendency for grouping around the trendlines for arteries and deep veins is denoted. This is not enough for conclusion, however it is perhaps a sign of a developing trend, which will become visible in the adult age. The intima/media index of the superficial veins shows clearer tendency for age dependent increment.

The correlation coefficients (Table 1) illustrate moderate to considerable correlation between age and intima (r_{intima}) and strong to very strong correlation between age and media (r_{media}) for the arteries and the deep veins. The superficial veins show opposite relationship — very strong age correlation of the intima and moderate to considerable correlation of the media. The intima/media index correlates only weakly with age (r_{index}).

Figures 4 and 5 illustrate the individual variance of the minimal and maximal

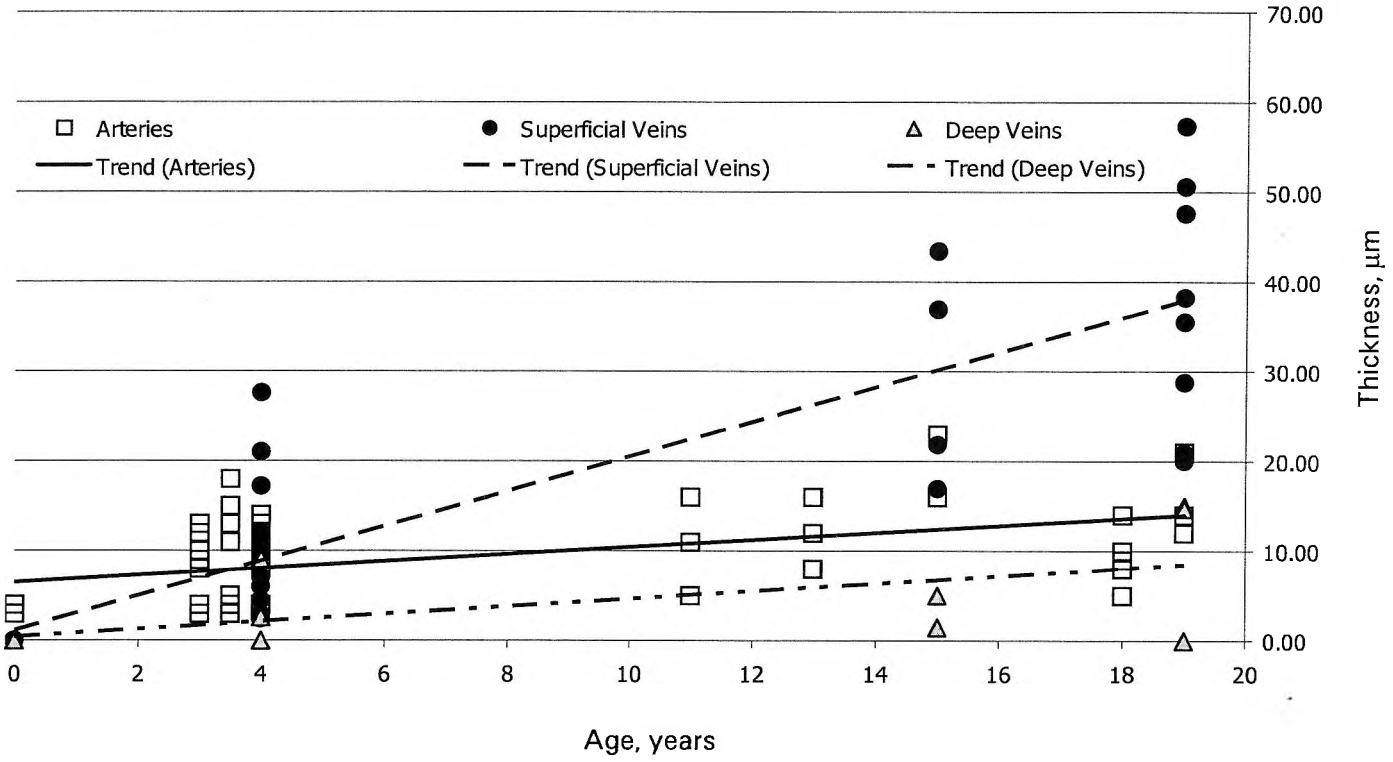

Fig. 1. Age dependent distribution of the intimal thickness. Explanations in text

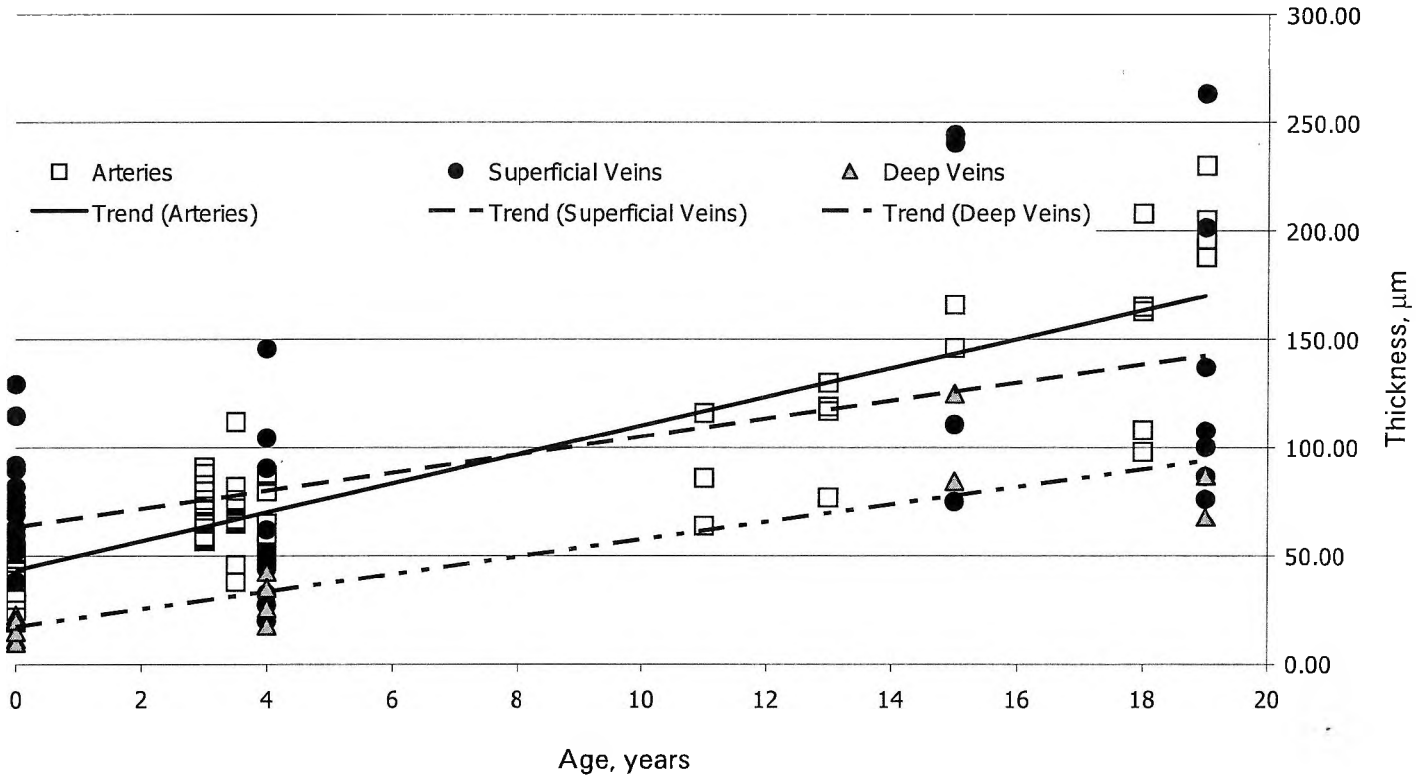

Fig. 2. Age dependent distribution of the media thickness. Explanations in text

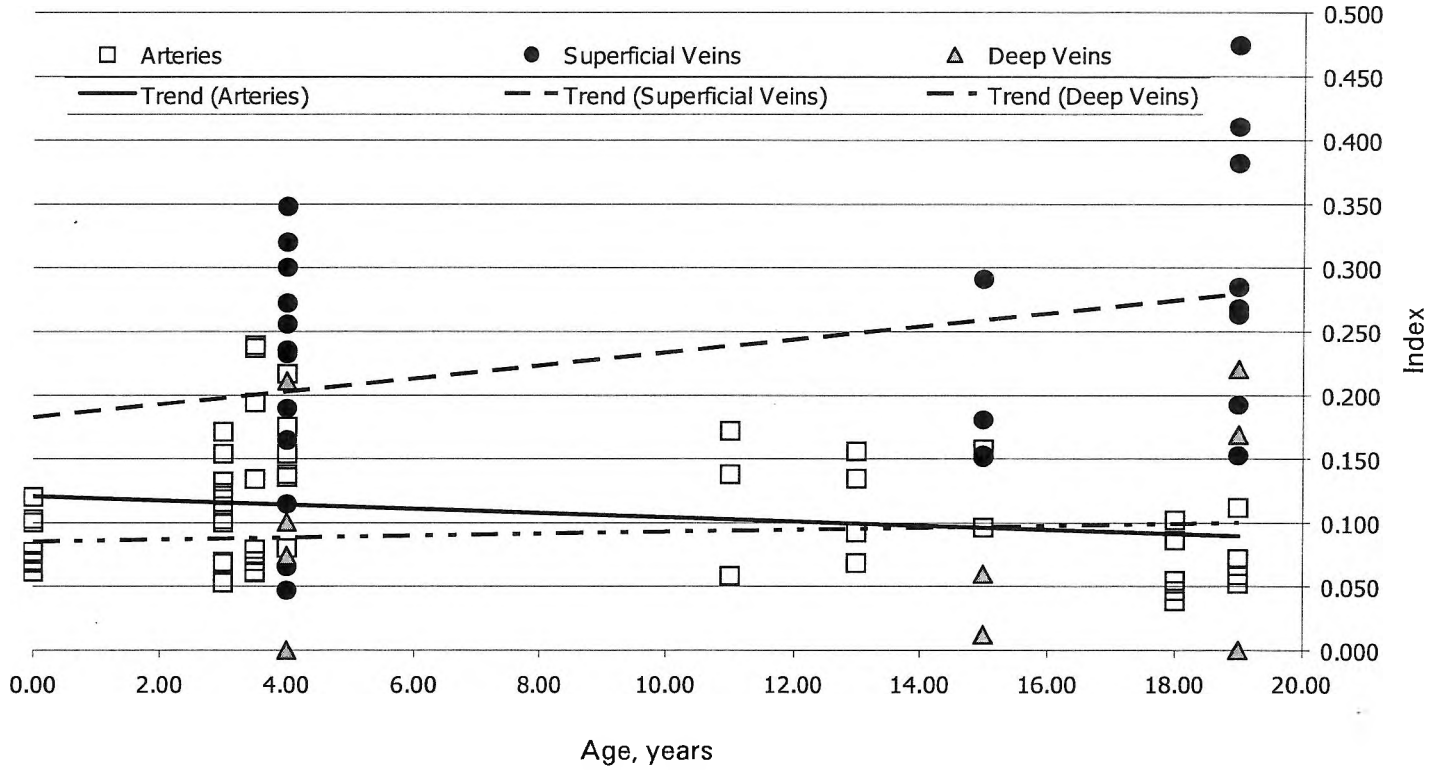

Fig. 3. Age dependent distribution of the intima/media index. Explanations in text

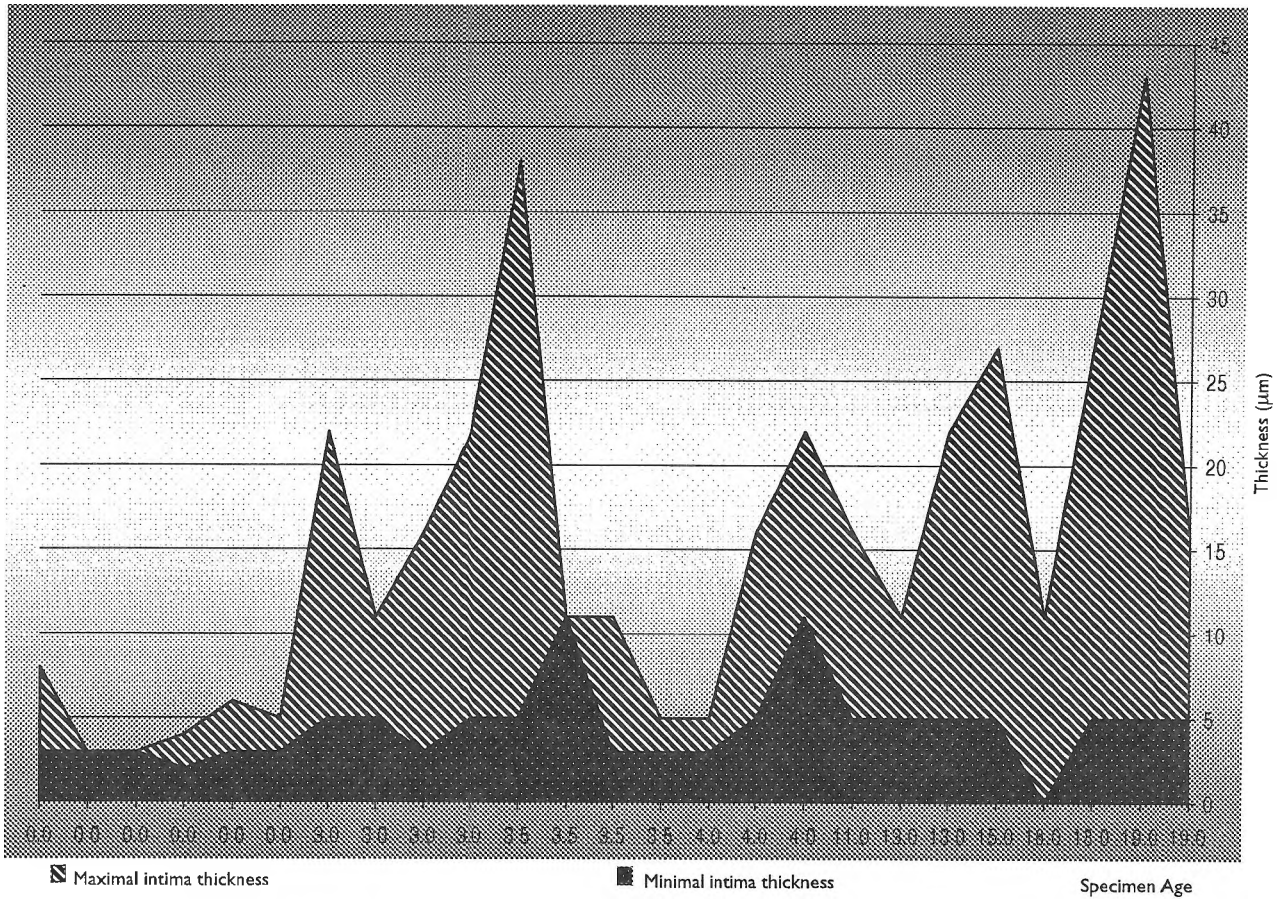

Fig. 4. Individual variance of the maximal and minimal intimal thickness. Explanations in text

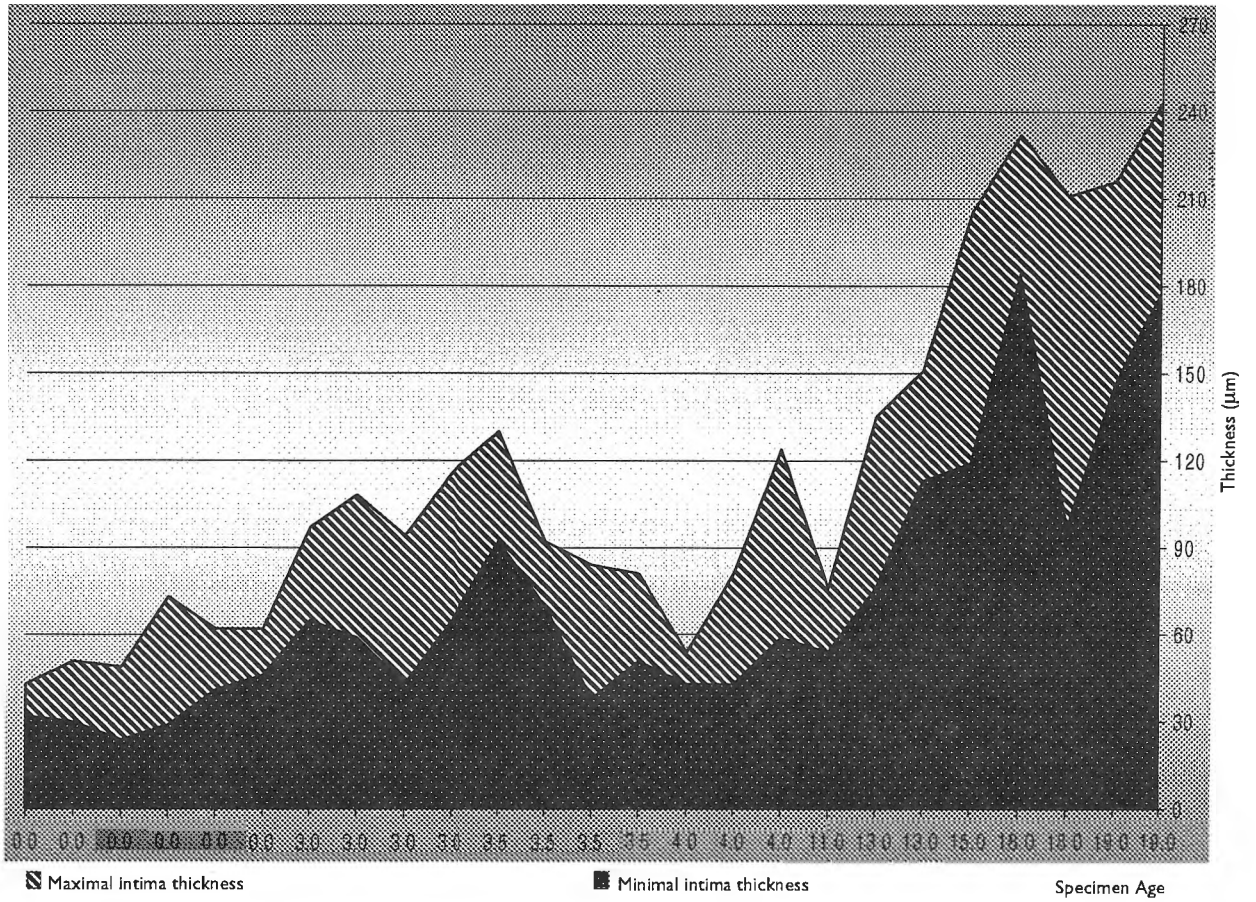

Fig. 5. Individual variance of the maximal and minimal media thickness. Explanations in text

Table 1. Correlation of intima, media and intima/media index with age

	r_{intima}	r_{media}	r_{index}
Arteries	0.51	0.88	- 0.22
Deep Veins	0.64	0.90	0.06
Superficial Veins	0.88	0.56	0.35

thickness of intima and media in arteries. As the minimal and maximal values were measured on different regions of the same transverse section, their variance characterizes the irregularity of the corresponding part of the vessel wall. Similar graphical analysis reveals almost the same relationships of the individual variance of the maximum and minimum values of the intima and media of deep and superficial veins.The minimal intima thickness remains thin throughout the entire age period. With increasing age in some regions of the intima appear sites of about 5 to 9 times thicker than the minimal intima. This is illustrated by the difference between the dotted and striped area and especially by the striped peeks in Fig. 5. The difference becomes greater with increasing age. Evenmore when comparing the variance of the maximal and minimal intimal thickness with the variance of the mean intimal thickness, it becomes clear that the age dependent increment in the mean thickness is a result of the increment in the maximal values.While these values are sign of irregularity of the intima along the arterial circumference, one draws the conclusion that these irregular places increase with age not only in thickness but also transversly, alias the irregularities spread over increasing portion of the vessel circumference.

Unlike the intima, the variances in the minimal and maximal medial thickness are almost parallel to each other, which creates the impression of regular, determined increase of the media thickness. The difference between maximal and minimal values is relatively small. Thus the conclusion can be drawn that the media thickness changes little and gradually along the vessel wall circumference. Similar graphical analysis reveals almost the same relationships of the individual variance of the maximum and minimum values of the intima and media of deep and superficial veins.

Whether this conclusions are true and what is the exact morphology of these irregularities in the arterial wall, remains to be established through a qualitative histological examination of the described material.

References

1. Bendick, P. J., G. B. Zelenock, P. G. Bove, G. W. Long, C. J. Shanley, O. W. Brown. Duplex ultrasound imaging with an ultrasound contrast agent: the economic alternative to CT angiography for aortic stent graft surveillance. — Vasc. Endovascular Surg., **37**, 2003, No3, 165-170.
2. Blebea, J., N. Volteas, M. Neumyer, J. Ingraham, K. Dawson, S. Assadnia, K. M. Anderson, R. G. Atnip. Contrast enhanced duplex ultrasound imaging of the mesenteric arteries. — Ann. Vasc. Surg., **16**, 2002, No1, 77-83.
3. Clarke, S. E., R. R. Hammond, J. R. Mitchell, B. K. Rutt. Quantitative assessment of carotid plaque composition using multicontrast MRI and registered histology. — Magn. Reson. Med., **50**, 2003, No6, 1199-1208.
4. Feinstein Alvan, R. Principles of Medical Statistics. London New York Washington, Chapman & Hall/CRC Boca Raton, 2002.
5. Gardner, D. J., B. B. Gosink, C. E. Kallman. Internal carotid artery dissections: duplex ultrasound imaging. — J. Ultrasound Med., **10**, 1991, No11, 607-614.
6. Kocova, J. Development of the vascular wall in the human limb. — Folia Morphol. (Praha), **20**, 1972, No3, 265-267.
7. Kocova, J. Histogenesis of the vascular wall in the limbs. — Folia Morphol. (Praha), **26**, 1978, No 2, 194-196.

8. Kocova, J., Z. Tesar. The development of the vascular system in man. — Cor. Vasa, **21**, 1979, No2, 124-127.
9. Kocova-Pechakova, J. Development of the venous wall in the extremities of sheep. — Pilzen Lek. Sborn., **33**, 1970, 5-13.
10. Lal, B. K., R. W. Hobson 2nd, M. Hameed, P. J. Pappas, F. T. PadbergJr, Z. Jamil, W. N. Duran. Noninvasive identification of the unstable carotid plaque. — Ann. Vasc. Surg., **20**, 2006, No2, 167-174.
11. Marinov, G., V. Vancov. Early changes of the smooth muscle cells (SMC) and extracellular matrix in the wall of the varicose veins. — Verh. Anat. Ges., **84**, Anat. Anz. (Jena), Suppl., **168**, 1991, 99-100.
12. Marinov, G. R., T. Tabakov. Medial and medio-intimal thickening and atherosclerosis. A light microscopical study on the lower limb arteries. — Verh. Anat. Ges., **76**, 1982, 291-292.
13. Pavlov, S., G. Marinov. Prenatal morphogenesis and remodeling of the wall of the main arteries of the leg and foot. — Acta Morphol. Anthropol., **10**, 2005, 110-113.
14. Zhang, S., J. Cai, Y. Luo, C. Han, N. L. Polissar, T. S. Hatsukami, C. Yuan. Measurement of carotid wall volume and maximum area with contrast-enhanced 3D MR imaging: initial observations. — Radiology, **228**, 2003, No1, 200-205.
15. Zhang, S., T. S. Hatsukami, N. L. Polissar, C. Han, C. Yuan. Comparison of carotid vessel wall area measurements using three different contrast-weighed black blood MR imaging techniques. — Magn. Reson. Imaging, **19**, 2001, No6, 795-802.
16. Автандилов, Г. Г. Морфометрия в патологии. — Москва, Медицина, 1973.
17. Ванков, В. Морфология на вените. — София, Медицина и физкултура, 1989.
18. Кирилова, С., С. Павлов, Г. Маринов. Ремоделиране на стената на магистралните вени на подбедрицата и ходилото в пренаталната онтогенеза. — Известия на съюза на Учените — Варна, **2003/2, 2004/1**, №1, 3—8.
19. Маринов, Г. Възрастови особености в структурата на стената на магистралните артерии на долния крайник. — Медико-биологични проблеми, МА, София, **V**, 1977, 49—57.
20. Маринов, Г., Т. Табаков. Структура и локализация на ранните интимални разрастванията в стените на магистралните артерии на долния крайник в пренаталната онтогенеза. — Медико-биологични проблеми, МА, София, **VIII**, 1980, 42—50.
21. Маринов, Г. Ранни задебеления на артериалната стена — класификация и роля в развитието на артеросклеротичния процес. — В: Научни доклади на „X Юбилейна сесия на ВМИ— Варна, 31 X 1981, Варна". Варна, 1982, 31—34.
22. Сепетлиев, Д. Медицинска статистика. София, Медицина и Физкултура, 1976.
23. Ставрев, Д., Г. Маринов, В. Княжев. Ремоделиране на стената на vena saphena magna при облитериращa атеросклероза на долния крайник. — Ангиология и съдова хирургия, **IV**, 2003, №1, 30—39.

Institute of Experimental Morphology and Anthropology with Museum
Bulgarian Anatomical Society

Acta morphologica et anthropologica, 13
Sofia • 2008

Histological Verification of the Biological Active Points Characteristics (BAP)

D. Sivrev, A. Georgieva, N. Dimitrov

Department of Anatomy, Medical Faculty, Thracian University, Stara Zagora

We tried to find some histological indications for existence of BAP. Usually there is a small skin pit covered with thin epithelium in point areas (HE). The connective tissue under the BAP is thinner compared with the areas outside of them (Mallory trichrome), and we established small quantity and a specific position of the collagen fibers, as well as increased number of blood vessels and nerve terminals ($AgNO_3$).

Key words: acupuncture, Mallory, connective tissue, epithelium, active points.

Introduction

The Biological Active Points and the energy channels are used in ancient China even at the time of the Chan dynasty (16^{th}- 11^{th} c. BC) [9, 10, 11, 12]. The modern science is trying to prove their existence using objective methods and analysis [1]. Most of the explorers use physic approaches (measuring the changes in the skin resistance) [4, 12], or merely the description of the clinical effect due to the stimulation of particular BAP [3, 7]. Many authors touch the pain as a big medical problem [2, 5, 6, 11] or describe alternative curative methods [8]. Publications concerning the special features of the tissue structure are rare. We didn't find any material about acupuncture point structure.

The object of this study is to estimate the presence of histological differences between the BAP and the tissues next to them. For the fulfillment of this object we selected a few major goals:

1. Estimation of the distinction between the structure and the thickness of the epithelial layer.

2. Proving the differences in the structure of the dermal connective tissue.

3. Comparative observation of the quantity of vascular and nerve elements in BAP and the tissues next to them.

Material and Methods

The research is made on a not conserved human corpse, as the samples were taken from the regions of the Sanjiao (Qihai RN6; Tienshu ST25) and Dazhui DU14. We used the Mallory's trichrome colouring and haematoxilin-eosin after an including in paraffin block, and the silver method of Bodian after the slicing with the freezing microtome.

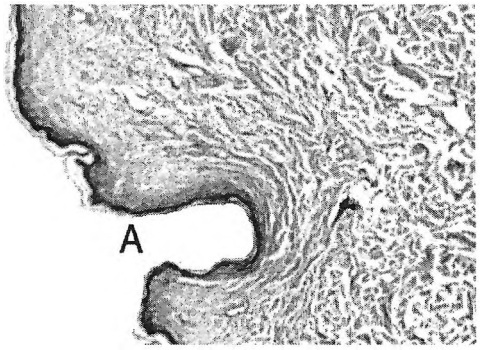

Fig. 1. HE colouring — Experimental group. × 50

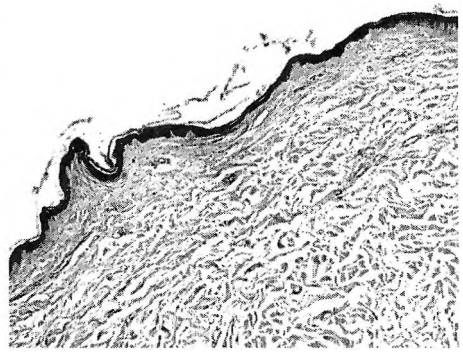

Fig. 2. HE colouring — Control group. × 50

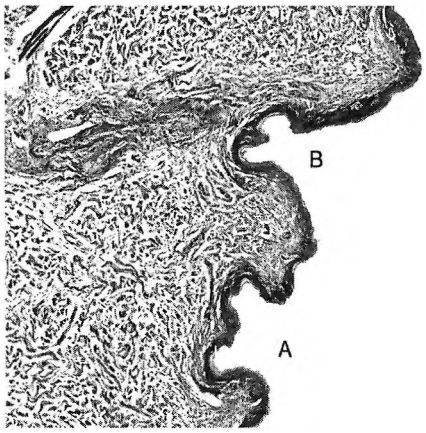

Fig. 3. Mallory trichrome colouring — Experimental group. × 50

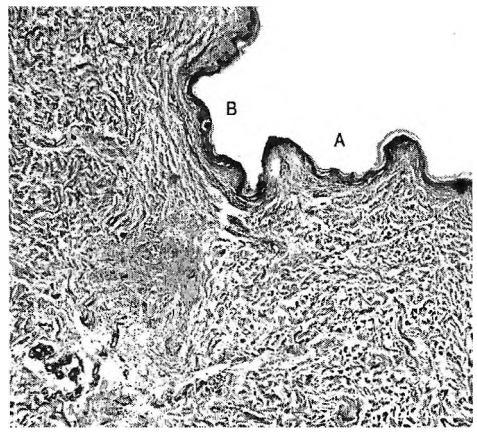

Fig. 4. Mallory trichrome colouring — Control group. × 50

Fig. 5. Bodian colouring — Experimental group. × 50

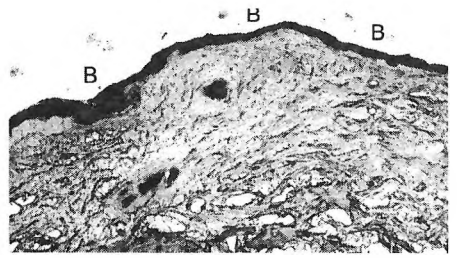

Fig. 6. Bodian colouring — Control group. × 50

Results

In the area of the BAP a small pit (A) covered with thinner epithelium is seen, although the difference in the thickness comparing with the controls is not significant and could be found in other areas of the preparation (Fig. 1). Similar pits are seen in the controls without any connection with the BAP (Fig. 2). However, the connective tissue under the BAP is several times thinner compared with the areas outside of them.

On the material treated by the Mallory's trichrome method on the experimental preparations we established a specific position of the collagen fibers (A, A) compared with the controls (B, B), as well as increased number of blood vessels (Figs. 3, 4).

Since BAP are not painful during puncture, we expected that free non capsulated receptors responsible for the sensing of the pain (A) would not be present in this part of the skin. There was no difference compared with the controls (B) (Figs. 5, 6).

Discussion

Some authors have described the presence of pits in the area of BAP [8], but it is not typical only for them. Our opinion is that the smaller thickness of the epithelium is caused by the reduction of stratum corneum, and the thinner stratum papillare determines the thickness of the dermal connective tissue. Using trichrome coloring difference in the quantity and the position of the collagen fibers was observed, which added to the reduction of the stratum corneum could be the reason for the lower impedance at the BAP.

Conclusions

1. Histomorphological differences between the BAP and the tissue areas around them are present.
2. The histological differences are mainly concentrated in stratum corneum of the epidermis, stratum papillare and in some measure in stratum reticulare of the derma.
3. Combined histological and physiological examination of a significant number of BAP, from most of the channels is needed to establish out of doubt the characteristics of the tissue elements in it, compared with areas without BAP.

References

1. Campbell, A. Point specificity of acupuncture in the light of recent clinical and imaging studies. — Acupuncture Medicine, **24**, 2006, No3, 118-122.
2. Donnellan, C. Acupuncture for central pain affecting the ribcage following traumatic brain injury and rib fractures — a case report. — Acupuncture Medicine, **24**, 2006, No3, 129-133.
3. McLean T., K. Kemper. Lifestyle, biomechanical, and bioenergetic complementary therapies in pediatric oncology. — Journal of Social Integrated Oncology, **4**, 2006, No4, 187-193.
4. Poon, C., T. Choy. Frequency dispersions of human skin dielectrics. — Journal of Biophysics, **34**, 1981, No1, 135-147.
5. Ratcliffe, J., K. Thomas, H. Mac, J. Brazier. A randomised controlled trial of acupuncture care for persistent low back pain: cost effectiveness analysis. — BMJ, **333**, 2006, No7569, 626-629.
6. Thomas, K., H. MacPherson, L. Thorpe, J. Brazier, M. Fitter, M. Campbell, M. Roman, S. Walters, J. Nicholl. Randomized controlled trial of a short course of traditional acupuncture compared with usual care for persistent non-specific low back pain. — BMJ, **333**, 2006, No7569, 623-626.
7. White, A. Electronic publishing and Acupuncture in Medicine. — Acupuncture Medicine, **24**, 2006, No3, 123-128.
8. Горанова, З. АНМО — Китайски лечебен масаж. София, Изд. НСА, 1994, 7—43.
9. Горанова, З. Развитие на китайската традиционна медицина. — В: Теоретичната система на китайската традиционна медицина. София, Изд. НСА Прес, 2001, 11—28.
10. Гуторанов, Г. Исторически преглед. — В: Козметичен и лечебен точков масаж. София, Изд. ГиС, 1997, 7-36.
11. Гуторанов, Г. Анатомични и патофизиологични основи на болката. — В: Болката. София, Изд. ГиС, 2004, 16—20.
12. Гойденко, В., Т. Норкина. Врата на облака или убежище на душата. — В: Метаморфозите на вълшебната игла. София, Медицина и физкултура, 1989, 3—11.

Institute of Experimental Morphology and Anthropology with Museum
Bulgarian Anatomical Society

Acta morphologica et anthropologica, 13
Sofia • 2008

Quantitative Intima-Media Correlations in the Vessel Wall of the Lower Limb at Patients with Chronic Arterial Insufficiency of the Lower Limb

D. Stavrev, G. Marinov

Department of Anatomy, Histology and Embryology Medical University "Prof. P. Stoyanov", Varna

In the present study a comparison is made between quantitative parameters of the walls of different vessels in the lower limb. It is a point of discussion how much the way and degree of remodelling of the venous wall influences the outcome of the auto transplantation procedure. We decide to use I/M index as a criterion with high authenticity about changes in the vessel wall. For the assessment we used diagram of dispersing and correlative analysis. The results of quantitative analysis show that this index has well expressed correlative dependence with the intimal thickness.

Key words: chronic arterial insufficiency of the lower limb, vessel wall, remodelling.

Introduction

Chronic arterial insufficiency of the lower limb induces changes in the vessel walls marked with the term remodelling. It is a point of discussion how much the way and degree of this remodelling influence the outcome of the autotransplantation procedure. In all cases the objective assessment of vessel wall condition needs qualitative analysis as well as quantitative one. It is possible for the both layers - intima and media. In the present study a comparison is made between quantitative parameters of the walls of different vessels in the lower limb.

Materials and Methods

A biopsy material from 9 a. femoralis, respectively a.poplitea, 6 v. femoralis and 16 v. saphena magna taken intraoperatively in the Clinic of Vascular Surgery at Medical University of Varna from patients with chronic arterial insufficiency of the lower limb II-III or III-IV degree at the moment of reconstruction with the help of autograft saphena bypass from the same limb and III-IV or IV degree, which has led to

gangrene and amputation, was studied. The biopsy material was fixed in 10% formalin and was soaked through paraffin and histovax. Histological sections were prepared with 5 μm thickness, colored by hematoxiline-eosine, with Orcein, Azan and by the methods of Van Gieson and Mallory. They were studied and photographed under Microscope Olympus BX50, equipped with video camera. The thickness of intima and media in the arterial and venous walls were measured upon digital images with the help of the program Image tool Version 3.00 (The University of Texas health Sciences Center in San Antonio.) The transversal dimensions (thickness) were measured in radial direction on regular intervals along the vessel circumference. On the next stage the proportion intima-media was calculated.

In all stages of the study the ethical standards of work with biopsy and necropsy materials were kept.

Results

The results from measurement of intimal and media thickness in the three kinds of vessels were put in tables. The average arithmetical value, standard deviation and the proportion of the thickness intima-media were calculated. The results were graphically presented.

The diagram of dispersing (Scatter plot) about gathering of the points, visually presents the availability, types and the intensity of the existing correlations. The presented diagrams of the three vessel types illustrated the positive correlation between intima-media and intimal thickness (Fig. 1). At the same presentation towards media arbitrarily dispersing of points shows lack of correlation (Fig. 2).

On the next stage as resumed index of the correlation degree we used the correlative coefficient of Pearson-R

The assessment of the result was made in both most used for this type correlative analysis scales:

$$Correl(X,Y) = \frac{\sum (x-\bar{x})(y-\bar{y})}{\sqrt{\sum (x-\bar{x})^2 \sum (y-\bar{y})^2}}.$$

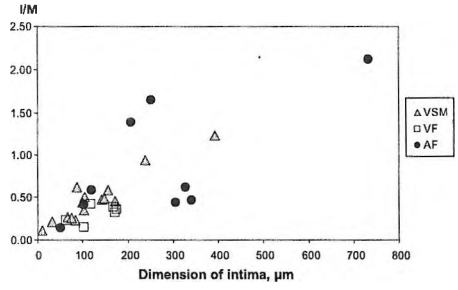

Fig. 1. Diagram of dispersing of intima

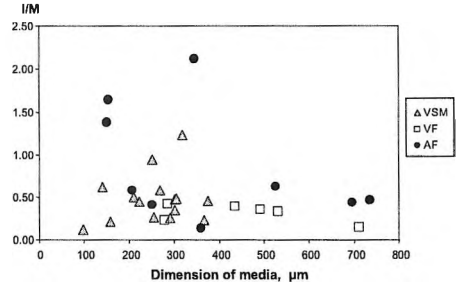

Fig. 2. Diagram of dispersing of media

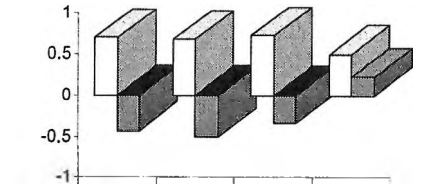

	average	min	max	σ
intima	0,690073	0,678515	0,730161	0,503048
media	-0,43618	-0,5104	-0,33666	0,222119

Fig. 3. Index of correlation Pearson Af

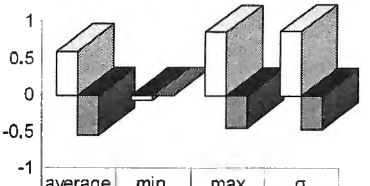

	average	min	max	σ
intima	0,59452	-0,0626	0,85881	0,87193
media	-0,5383	0,00341	-0,4331	-0,4538

Fig. 4. Index of correlation Pearson VF

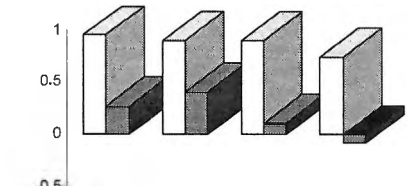

	average	min	max	σ
intima	0,9538317	0,8996544	0,9059028	0,7450992
media	0,2651402	0,3987556	0,1059973	-0,0793952

Fig. 5. Index of correlation Pearson VSM

I	II
0<R<0,3 - slight correlation	0-0,2 - slight correlation
0,3<R<0,5- moderate correlation	0,2-0,4 - moderate correlation
0,5<R<0,7 - significant correlation	0,4-0,6 - significant correlation
0,7<R<0,9 - high correlation	0,6-0,8 - high correlation
0,9<R<1,0 - very high correlation	0,8-1,0 - very high correlation

In arterial vessels R presents significant correlation in I^{-st} scale and high correlation in the II^{-nd} scale of I/M index with the intimal thickness. The results about the media show respectively moderate negative correlation in I^{-st} scale and significant negative correlation in the II^{-nd} scale (Fig. 3). About deep veins of the lower limb R presents significant and high correlation in the I^{-st} scale and high correlation in the II^{-nd} about I/M index with intimal thickness. About the media the results show respectively moderate negative correlation in the I^{-st} scale and moderate and significant negative correlation in the II^{-nd} scale (Fig. 4). About superficial veins of the lower limb R presents very high correlation in I^{-st} scale and very high correlation in the II^{-nd} scale of the I/M index with the intimal thickness. About the media results show respectively slight correlation in both scales (Fig. 5).

Discussion

The presented analysis aims unification of method of assessment of the lower limbs vessel conditions under the effect of chronic arterial insufficiency of the lower limb. It is obvious that using of absolute quantities in cases of clinical and laboratory researches is imprecise because of individual, age, sex, races and other peculiarities of every patient. With such motivation we decide to use I/M index as a criterion with high authenticity about changes in the vessel wall. The results of quantitative analysis show that this index has well expressed correlative dependence with the intimal thickness. Vessel media of the three groups presents slight or negative correlation with I/M index. We think it's due to the fact media is more stable to ischemia and even in cases with severe damages intima and adventitia keeps its structures.

Changes in I/M index correlate directly with intimal changes and can serve for assessment of vessel wall conditions.

References

1. Egan, T.J., A. Nur, M.C. Anderson, M. Corcoran, J. O'Driscoll. Preoperative evaluation of saphenous vein suitability as an arterial graft. — Vasc. Surg., **2**, 1984, 229-233.
2. Langes, K., W. Hort. Intimal fibrosis (phlebosclerosis) in the saphenous vein of the lower limb: a quantitative analysis. — Virchows Archiv A Pathol. Anat., **421**, 1992, 127-131.
3. Kanellaki-Kyparissi, M., K. Kouzi-Koliakou, G. Marinov, V. Knyazev. Histological study of arterial and venous grafts before their use in aortocoronary bypass surgery. — Hellenic J. Cardiol., **46**, 2005,21-30.
4. Marinov, G., V. Knyazhev, M. Trosheva. Some morphological peculiarities of the long saphenous vein with obliterating diseases of the lower limb. — Scripta Scientifica Medica, **24**, 1987, 30-35.
5. Stavrev, D., V. Knyazhev, G. Marinov. Intimal remodeling of the great saphenous vein in patients with chronic arterial insufficiency of the lower limb — comparisson with intimal remodeling of femoral artery. — Anatomical Collection, 2003, 84-86.
6. Stavrev, D., G. Marinov, V. Knyazhev. Femoral Vein Wall Remodeling in Chronic Arterial Insufficiency of the Lower Limb. — Acta Morphologica et Anthropologica, **10**, 2004, 78-82.
7. Taute, B.M., M. Schoenmetzler, R. Taute, K. Haensgen, G. Keyszer, C. Tiroch, H. Podhaisky. Common carotid intima-media thickness in peripheral arterial disease. — Int. J. Angiology, **13**, 2004, 27-30.
8. Ставрев, Д., В. Княжев, Г. Маринов. Ремоделиране на медията и адвентицията на голямата подкожна вена при пациенти с хронична артериална недостатъчност на долния крайник — съпоставка с ремоделирането на бедрената артерия. — Известия на Съюза на Учените—Варна, секция „Медицина и екология", 2001/2—2002/1, 10—15.

Institute of Experimental Morphology and Anthropology with Museum
Bulgarian Anatomical Society

Acta morphologica et anthropologica, 13
Sofia • 2008

Morphological Investigation on Mast Cells in Canine Anal Canal

I. S. Stefanov, A. Vodenicharov

Department of Veterinary Anatomy, Histology and Embryology Faculty of Veterinary Medicine, Trakia University, Stara Zagora

Light microscopic investigations upon mast cell localization in the wall of the anal canal were performed in healthy mongrel male dogs at the age of 3-4 years. It was found out that mast cells were situated in the three zones of the anal canal. In the columnar and intermediate zones, they were observed in the propria of the mucous coat, near the capillaries and the small blood vessels. In the mucous coat epithelium, mast cells were not found out. Mast cells were also present near the anal glands and their outlet ducts. In the smooth musculature of the anal canal, the mast cells were located among the smooth muscle bundles and around the smooth muscle cells, whereas in the external anal sphincter - in the peri- and the endomisium.

In the cutaneous zone, mast cells were discovered in the derma, near the sebaceous glands and their outlet ducts, near the sweat gland tubules, around the hairs and hepatoid circumanal glands (HCG). Mast cells were also present in the wall of perianal sinuses and their outlet duct.

The data of these studies allowed assuming that mast cells of anal canal's wall were involved in the local homeostasis and the function of musculature in this part of the intestinal canal.

Key words: mast cells, anal canal, dog.

Introduction

The anal canal of the dog has some specific structural features that are related both to the behaviour and communication of animals as well as to the pathogenesis of a number of pathological states [2, 3, 4, 6, 8]. The data about the presence of mast cells in the intestinal wall in animals are relatively few. These cells were described by single authors in the propria and the submucosa of the jejunum in swine [1].

The scarce data about the presence of mast cells in the anal canal of the dog motivated the present study aiming to elucidate their functional role on structures of the distal part of the gastrointestinal tract in this animal species.

Material and Methods

The material for the investigations was obtained from the wall of the anal canals of six mongrel healthy male dogs at the age of 3-4 years. The animals were euthanized with 5% thiopental solution. Pieces of 1 cm from all parts of the canal's wall were fixed in Carnoy's fixative for 4 hours at room temperature. Then they were dehydrated in ascending ethanol series, cleared in xylene and embedded in paraffin. From them, longitudinal and transverse cross sections of 6 μm, stained with 0.1% aqueous solution of toluidine blue (pH 3) were prepared.

Results and Discussion

During the light microscopic studies of specimens from the anal canal's wall, mast cells were discovered along and across in almost all its parts.

In the columnar and the intermediate zones, the relatively most regular distribution of mast cells was observed in the propria of the mucous coat and near the capillaries. Such cells were present also under the epithelium of the mucosa, and some of them were situated immediately near the basal membrane. Single mast cells were located both around the small blood vessels (in the propria and the submucosa) and in the vascular adventitia. Mast cells were detected in the subepithelial connective tissue around the anal sinuses and crypts as well. In the interstitium around the anal glands and their outlet ducts, a characteristic group of 3-4, less frequently of more cells, was observed (Fig. 1). Also, single mast cells were observed immediately

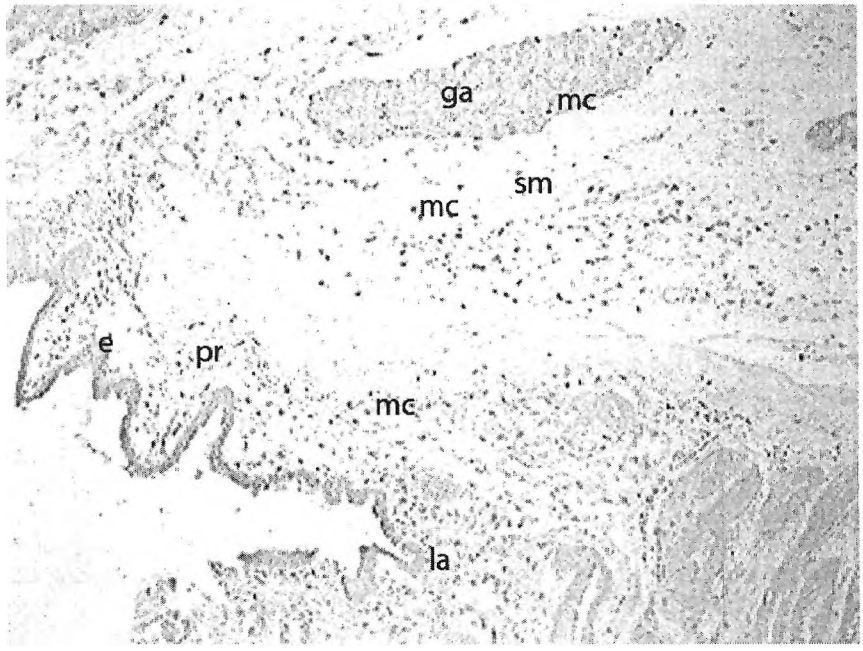

Fig. 1. Mast cells (mc) located in the propria (pr), beneath the epithelium (e), in the submucosa (sm) and around the anal glands (ga): la — linea anorectalis. × 100

near the epithelial basal membrane of glandular alveoli. Similar clusters were discovered in the connective tissue around the lymphatic follicles. The mast cells in the muscle layer of the wall were situated in the connective tissue stroma among the smooth muscle cells and bundles of the internal anal sphincter and of the longitudinal muscle layer. In the external anal sphincter, they were predominantly located in the perimisium whereas single cells could be also found more deeply.

In the cutaneous zone, mast cells were located mostly in the derma, adjacently to sebaceous and sweat glands as well as around the hair follicles. These findings confirmed the observation of other investigators, who described a similar localization in dogs too [5, 7]. In our studies however, mast cells located near the epithelial basal membranes of the glandular acini and sweat gland tubules were found out; moreover, single cells were observed even intraepithelially. Also, it was shown for the first time that the major part of mast cells in hairs was located in their connective tissue sheath and only some of them — in the epithelial sheath.

In the epithelial layer of the mucosa of all three zones of the canal, mast cells were not discovered. The absence of intraepithelially located mast cells in the intestinal wall was reported in swine [1].

In the layer with CHG, mast cells were found out in the vicinity with some of glandular lobes, and also in the interlobular connective tissue. It should be noted that although less frequently, they were observed in the wall of glandular cysts, a similar localization being unknown until now.

In the wall of the outlet duct of perianal sinuses, mast cells were distributed relatively regularly in the connective tissue, located between the basal membrane of the covering epithelium and the sebaceous glands. Also, single cells were observed

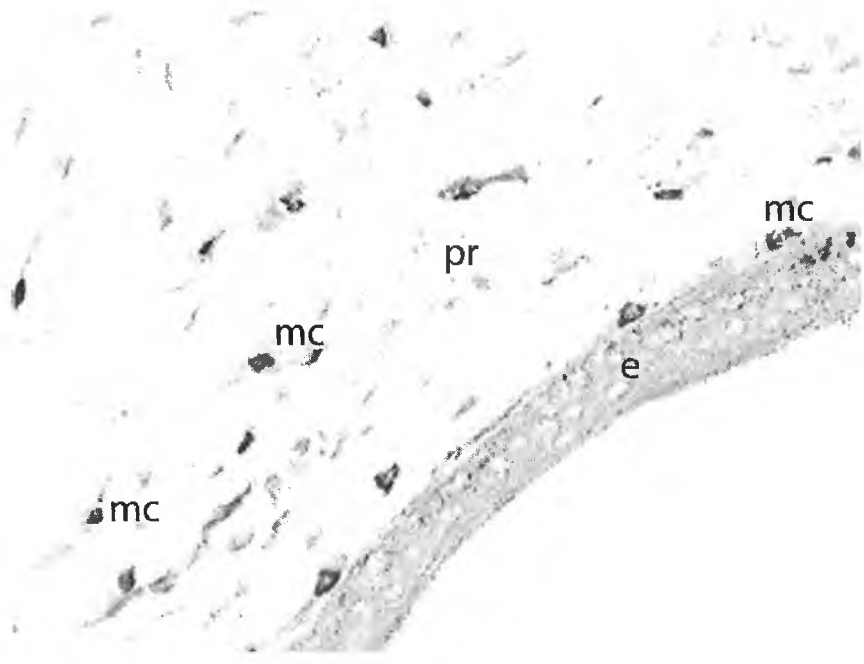

Fig. 2. Mast cells (mc) beneath the epithelium (e), in the propria (pr) of the wall of perianal sinuses. Single mast cells are situated near the basal membrane and intraepithelially. × 400

near the epithelial basal membrane of the aforementioned structures. A similar localization of mast cells was observed in the wall of sinuses too, the difference being that the respective glands were apocrine. In the muscle layer, the localization of mast cells was both in the perimisium and the endomisium. In some instances, an intraepithelial localization of mast cells in the covering epithelium was detected (Fig. 2). A similar position was also observed among the epithelial cells of some of glandular tubules, in the surrounding area of which, clusters of 3-4 mast cells were encountered and a localization immediately near the basal membrane could be frequently seen too.

In this study, along with confirming the known data, the localization of mast cells in some parts of the anal canal in the dog was described for the first time. The presence of these, undoubtedly important cells in the terminal part of the gastrointestinal tract in the dog, was certainly related to their barrier functions and mediating role in inflammations, as well as to the motor function of the striated and smooth musculature in the wall.

References

1. Ashraf, M., J. Urban, T. Lee, C. Lee. Characterizacion of isolated porcine intestinal mucosal mast cells following infection with Ascaris suum. — Veterinary Parasitology, **29**, 1998, 143-158.
2. Budsberg, S., T. Spurgeon. Microscopic Anatomy and Enzime Histochemistry of the canine Anal Canal. — Anatomia, Histologia Embryologia, **12**, 1983, 295-316.
3. Budsberg, S., T. Spurgeon, H. Liggitt Anatomic predisposition to perianal fistulae formation in the German Shepherd Dog. — American Journal of Veterinary Research, **46**, 1985, 1468-1472.
4. Donovan, C. Canine anal glands and chemical signals (pheromones). — Journal of the American Veterinary Medical Association, **155**, No12, 1969, 1995—1996.
5. Emerson, J., R. Cross. The distribution of Mast Cells in Normal Canine Skin. — American Journal of Veterinary Research, **26**, 1965, 1379-1382.
6. Isitor. G. Comparative ultrastructural study of normal, adenomatous, carcinomatous, and hyperplastic cells of canine hepatoid circumanal gland. — American Journal of Veterinary Research, **44**, 1983, 463-474.
7. Myles, A., R. Halliwell, B. Ballauf, H. Miller. Mast cell tryptase levels in normal canine tissues. — Veterinary Immunology and immunopathology, **46**, 1995, 223-235.
8. Nielsen, S. Glands of the canine skin. Morphology and distribution. — American Journal of Veterinary Research, **14**, 1953, 448-454.

Institute of Experimental Morphology and Anthropology with Museum
Bulgarian Anatomical Society

Acta morphologica et anthropologica, 13
Sofia • 2008

Variant Short Muscles of the Dorsum of the Hand — Extensor Digitorum Brevis Manus Muscle

L. Surchev, G. P. Georgiev, L. Jelev

Department of Anatomy, Histology and Embryology, Medical University of Sofia

The extensor digitorum brevis manus muscle (EDBM) is an additional muscle in the dorsum of the human hand presented in different forms. Here, we report three cases of this variant muscle found during routine anatomical dissections. In the first case, a short extensor to the second and third finger and an aberrant tendon of the extensor indicis were noted. In the other two cases, well-defined short extensors to the index finger were detected. The previously reported variations of the EDBM are reviewed and their possible clinical significance is discussed.

Key words: extensor muscles, hand, variations, clinical significance, human.

Introduction

The "extensor digitorum brevis manus" (EDBM) is a common name of group of variant muscles, originating from the dorsal wrist region and inserting to one or more tendons of the extensor digitorum muscle. Thus, sometimes described "extensor indicis brevis", "extensor digiti medii brevis" and "extensor brevis digiti indicis vel medii" should be regarded as forms of the EDBM [8]. Despite the presence of numerous reports of this muscle [4, 6, 9], it is still less known by the clinicians and is frequently misdiagnosed as a dorsal wrist ganglion [9].

In this paper, we describe three cases of EDBM, found during anatomical dissections in formol-carbol fixed upper extremities from the autopsy material available at the Department of Anatomy, Histology and Embryology at the Medical University of Sofia.

Results

Different forms of the EDBM were observed in three right hands dissected.

In case A (Fig. 1), the EDBM was located under the tendon of the extensor digitorum to the middle finger and between it and the extensor indicis tendon. The variant muscle has a flat spindle-shaped muscular body originating from the dorsal radiocarpal ligament. A small tendinous slip from the extensor indicis was attached

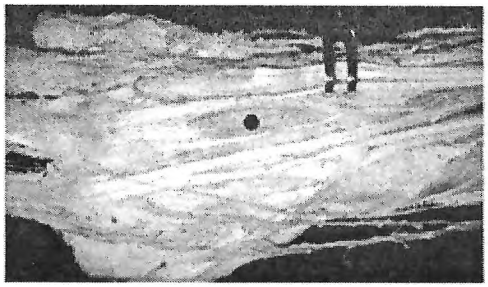

Fig. 1. Photograph of the extensor digitorum brevis manus (black dot) described in case A

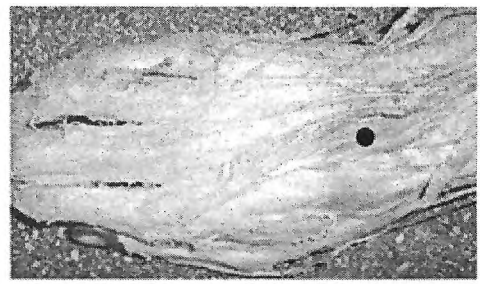

Fig. 2. Photograph of the extensor digitorum brevis manus (black dot) described in case B

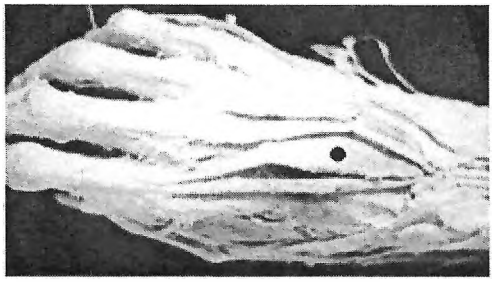

Fig. 3. Photograph of the extensor digitorum brevis manus (black dot) described in case C

to the lateral side of the EDBM. Distally, the variant muscle inserted to the extensor indicis tendon and to the middle finger tendon of the extensor digitorum.

In case B (Fig. 2), the EDBM was found lateral to the extensor digitorum tendon. In this case, the variant muscle replaced the usual extensor indicis. It arose from the wrist joint capsule and was attached to the index finger tendon of the extensor digitorum. A muscle with the same attachment points and location, but having stronger muscular body was found in case C (Fig. 3).

In all three cases, a branch of the posterior interosseus nerve from the radial nerve innervated the variant muscles.

Discussion

In 1734, Albinus first described the EDBM [6]. It is also known as muscle "mannieaux" [3, 4] and was studied during anatomical dissections [1, 4, 6, 8] and in living individuals [8, 9]. In the literature, different variations of the EDBM have been described. M a c a l i s t e r [6] and L e D o u b l e [4] reported different insertions of this muscle - to the middle finger; to the second and third fingers; to the ulnar side of the middle and ring finger; one to the middle and two slips to the fifth finger; to the second, third and fourth fingers. R o d r í g u e z - N i e d e n f ü h r et al. [8] reviewed the literature and stated that the most common insertion was into the index finger, followed by this into the middle, and those into the index and middle fingers. Variant origins have also been reported - distal end of the radius, dorsal radiocarpal ligament and wrist joint capsule [7, 8].

The muscular belly of the EDBM lies distal to the distal edge of the extensor retinaculum, so, a physical examination could reveal an elongated swelling in the

proximal part of the dorsum of the hand, usually between the middle and index finger extensor tendons. Due to this location, the variant muscle is frequently misdiagnosed as a dorsal wrist ganglion [5]. A close physical examination and the consideration that the EDBM becomes more prominent with active extension of the wrist and fingers, whereas a ganglion becomes more prominent with wrist flexion, may help in diagnosis [2]. In addition, a differential diagnosis with an exostosis, tendon sheath cyst, tenosynovitis of extensor tendons, hemangioma, rheumatoid tenosynovitis or benign soft tissue tumor could be made [8].

Some authors [7] noted that the EDBM might cause little or no pain. According to other authors [9], however, an existing EDBM may cause pain and swelling of the dorsum of the hand during a heavy manual work. In all these cases, the good knowledge of the muscular variations, presented in our report, may help clinicians in differential diagnosis with many pathological conditions in the dorsum of the hand.

References

1. Cigali, B. S., T. Kutoglu, S. Cikmaz. Musculus extensor digiti medii proprius and musculus extensor digitorum brevis manus — a case report of a rare variation. — Anat. Histol. Embryol., **31**, 2002, 126-127.
2. Fernandez Vázquez, J. M., R. L. Lischeid. Anomalous extensor muscle simulating dorsal wrist ganglion. — Clin. Orthop., **83**, 1972, 84-86.
3. Fontes, V. Note sur le muscle manieux. — C. R. Assoc. Anat., **28**, 1933, 289-294.
4. Le Double, A. F. Traite des variations du Systeme Musculaire de l'Homme et leur Signification au Point de Vue de l'Anthropologie Zoologique. Paris, Schleicher Freres, 1897, 203-217
5. Lehrberger, K., C. Tizian. Der musculus extensor indicis brevis-klinisch oft ganglion verkannt. — Chirurg., **55**, 1984, 768-769.
6. Macalister, A. Additional observations on muscular anomalies in human anatomy (third series), with a catalogue of the principal muscular variations hitherto published. Trans. Roy. Irish Acad., 1875, 1-130.
7. Ogura, T., H. Inoue, G. Tanabe. Anatomic and clinical studies of the extensor digitorum manus brevis. — J. Hand Surg., **14A**, 1987, 100-107.
8. Rodríguez-Niedenführ, M., T. Vazquez, P. Golanó, I. Parkin, J. R. Sañudo. Extensor digitorum brevis manus: anatomical, radiological and clinical relevance. — Clin. Anat., **15**, 2002, 286-292.
9. Ross, J. A., C. A. Troy. The clinical significance of the extensor digitorum brevis manus. — J. Bone Joint Surg., **51B**, 1969, 473-478.

Institute of Experimental Morphology and Anthropology with Museum
Bulgarian Anatomical Society

Acta morphologica et anthropologica, 13
Sofia • 2008

Durable Preservation of Feline Cardiac Structures Via Plastination Methods

D. Vladova, D. Sivrev, R. Dimitrov**, D. Kostov**, H. Hristov***

Department of Animals Morphology, Agricultural Faculty, Thracian University, Stara Zagora
**Department of Anatomy, Medical Faculty, Thracian University, Stara Zagora*
***Department of Anatomy, Veterinary Faculty, Thracian University, Stara Zagora*

Plastinated semi-transparent slices of cat cardiac structures were obtained. The slices processed according to the E12 plastination technique, are with dark-yellow to light-brown colour, whereas those plastinated with Biodur S10 — light-yellow with clear details. P40 plates are nearly completely transparent, but with a light yellowish taint.

Key words: plastination, Biodur, sheet, slices, heart.

Introduction

This experiment is part of a complex research of cardiac structures in the cat and represent a coordination approach for comparison and control of the correct interpretation of data obtained by other experimental techniques. Plastination is a method for a preservation of perishable biological specimens — whole organs or parts of them [8, 9]. These techniques use silicone Biodur S10 for plastination of whole organs [3, 4], epoxy resin Biodur E12 for preparation of body slices [1, 6, 7, 11] and polyester resin P40 — for brain sheet plastination [2, 5, 10] to obtain durable preparations that are safe for human health and are practically permanent [8].

The **aim** of the study was the visualization of cardiac structures by means of plastination technologies. The following **tasks** were performed with regard to achieve our aim: **1.** To specify the type of necessary anatomical structures; **2.** To determine the plastination method for processing of anatomical specimens; **3.** To select the protective material that should be used for obtaining durable results.

Material and Methods

The experiment was performed with four male cats conforming to all animal welfare regulations. After perfusion with 10% formalin and freezing at –35°C, the thorax of

animals was sectioned with a band saw to 0.6-0.8 mm thick slices (transverse sections). The slices were dehydrated and impregnated according to S10, E12 and P40 techniques.

Results

After the processing and the gas-curing phase of plastination, elastic semi-transparent slices with a thickness of 0.6-0.8 mm were obtained. The slices processed according to the E12 plastination technique, are with dark-yellow to light-brown colour (Fig. 1), whereas those plastinated with Biodur S10 — light-yellow with clear details (Fig. 2). P40 plates are nearly completely transparent, but with a light yellowish taint (Fig. 3).

Discussion

The analysis of this three plastination methods (Table 1) showed that the best optical results were obtained by the P40 plastination technique. These anatomical preparations are completely transparent and give the most complete image for anatomical

Fig. 1. A E12 plastination technique slice

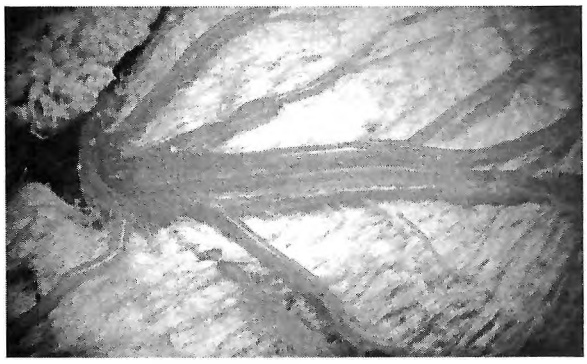

Fig. 2. A S10 plastination technique slice

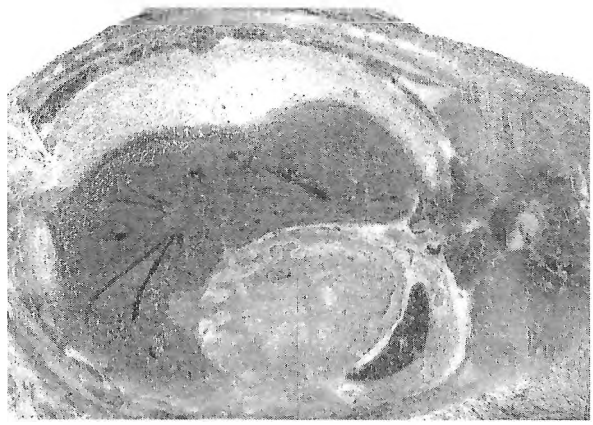

Fig. 3. A P40 plastination technique slice

T a b l e 1. Differences in the quality of anatomical preparations, obtained via three plastination techniques (using a 5-grade score system)

E12	Transparency ++	Elasticity +	Rigidity +++++	Strengths ++++	Durability +++++
S10	Transparency +++	Elasticity ++++	Rigidity +	Strengths ++++	Durability +++++
P40	Transparency ++++	Elasticity +	Rigidity +++++	Strengths ++++	Durability +++++

Strengths = tensile and compressive strengths.

details simultaneously with an adequate strength of preparations. They are suitable for study of fine cardiac details for a long time without risk of slice damage.

The slices prepared by the E12 plastination technique are with the least transparency and altered colour (the protective medium is dark-yellow to light-brown and the cardiac structures are dark brown that reduces the potential for observation of their structure). These slices are harder and stronger, but less elastic. They are appropriate for observation under any conditions, and the time of their use decreased under mechanical stress.

The S10 preparations are with the greatest elasticity, but are less transparent than both E12 and P40 slices. Relatively fewer details could be observed on them, they endure sharp mechanical stresses, for instance, falling on the floor, but are not resistant to tension — they are easily sheared at excessive stretching. Absolutely, they are the least expensive — from points of view of equipment and technology, but their relatively low mechanical strength and low durability makes them relatively costly.

Conclusions

1. Human and animal morphological preparations, made by plastination techniques, provide a very accurate view about the anatomical structure of processed organs. **2.** Depending on the applied plastination method, the optical and mechanical properties of preparations are different. **3.** The choice of a plastination method is determined by the purpose of ready preparations, the mode of their use and the

resources of the respective plastination laboratory. **4.** Plastination technologies are very promising in the field of morphology as an alternative for elaboration of durable anatomical preparations.

References

1. Cook, P. Epoxy and polyester sheet plastination. — Surgery, Radiology, Anatomy, **27** (Special Issue), 2005, 118-119.
2. Genser-Strobl, B, M. Sora. Potential of P40 plastination for morphometric hip measurements. — Surgery, Radiology, Anatomy, **27**, 2005, No2, 147-151.
3. Henry, R., Plastination of an integral heart-lung specimen. — Journal of International Society on Plastination. **1**, 1987, No2, 20-24.
4. Henry, R., P. Nel. Forced impregnation for the standard S10 method. — Journal of International Society on Plastination. **7**, 1993, No1, 27-31.
5. Latorre, R., A. Arencibia, F. Gil, M. Rivero, G. Ramirez, J. Vaquez-Auton, R. Henry. P40 and S10 Plastinated Slices: An Aid to Interpreting MR-images of the Equine Tarsus. — Journal of International Society on Plastination, **18**, 2003, 14-22.
6. Latorre, R., R. Reed, F. Gil, O. Lopez-Albors, M. Ayala, F. Martinez-Gomariz, R. Henry. Epoxy Impregnation without Hardener: To Decrease Yellowing, to Delay Casting and to Aid Bubble Removal. — Journal of International Society on Plastination, **17**, 2002, 17-22.
7. Probst, A, S. Kneissl, E. Polsterer, M. Sora, H. Konig. Cross-section anatomy — a necessary method for clinical examination with modern diagnostic imaging. — Wiener Tierärztliche Monatsschrift, **92**, 2005, No4, 100-106.
8. Von Hagens, G. Introduction to plastination. — In: Heidelberg Plastination Folder. Heidelberg, Universität Heidelberg (Second Edition), 1986, 1-9.
9. Von Hagens, G., K. Tiedmann, W. Kriz. The current potential of plastination. — Anatomy and Embryology, **175**, 1987, 411-421.
10. Weber, W., R. Henry. Sheet plastination of the brain — P35 technique, filling method. — Journal of International Society on Plastination. **6**, 1992, No1, 29-33.
11. Zhang, M. Scientific potential of plastination: tissue patterning and sheet plastination. — Surgery, Radiology, Anatomy, **27** (Special Issue), 2005, 119-120.

Institute of Experimental Morphology and Anthropology with Museum
Bulgarian Anatomical Society

Acta morphologica et anthropologica, 13
Sofia • 2008

Modern Trends and Scientific Contributions of IEMAM—BAS to Modelling of the Life Processes *in Vitro*

K. Baleva-Ivanova, M. Ivanova*

**Institute of Experimental Morphology and Anthropology with Museum, Bulgarian Academy of Sciences, Sofia*
MTF, Sofia

The article presents the history and the development of the ideas in the field of the modelling of the life processes in vitro during the last 68 years in the Institute of Experimental Morphology and Anthropology with Museum (IEMAM) — Bulgarian Academy of Sciences in Sofia.The aim of the authors is to systematise, analyze and discuss the modern trends and scientific contributions published in the scientific works in the IEMAM—BAS. In Bulgaria the method of tissue cultures was introduced by academician A. I. Hadjioloff in 1938. Later his Bulgarian scientific morphological school created many original methods and obtained important results for the theory and practice.

Key words: tissue cultures, growth factors, monoclonal antibodies, biotechnology.

The modelling of the life processes in vitro is an important and actual medico-biological problem. In the Institute of Experimental Morphology and Anthropology with Museum in Bulgarian Academy of Sciences (IEMAM — BAS) these investigations have nearly 68 years history.

The aim of the present study is to systematize, analyze and discuss the modern trends and scientific contribution in the field of the modelling of the life processes in vitro, published in the scientific works in the IEMAM — BAS during the last 68 years.

In our research the development of these conceptions and ideas were arbitrary divided into four periods: The first period is period of origin of the ideas —since 1938 till 1965. The method of tissue cultures was introduced in Bulgaria by academician A. I. Hadjioloff in 1938 [7]. In 1955 professor J.Jordanov suggested a new method for using the vitelline membrane as a sole for cultivation of tissue fragments and tumor cells. He has first used the yolk membrane of hen egg and other artificial semi-permeable membranes (collodion) in tissue cultures. In 1959 professor J. Jordanov developed a new original method for preparation of nutritional media based upon yolk dalysates [8, 9]. In the first period academician A. I. Hadjioloff and his Bulgarian scientific morphological school created many original methods and obtained important for the theory and practice results.

Second period is empirical — since 1966 till 1976. In 1966 Professor J. Jordanov developed an original modification of New's method, using celoidin membranes.

Later Professor J. Jordanov and P. Angelova applied in 1974 agar organ cultures upon celoidin membranes. They studied the impact of drugs upon the differentiation of bird and mammalian gonads in vitro. The scientific investigations and contributions of Dr. P. Angelova, Dr. L. Kancheva, professor J. Jordanov, Y. Martinova, professor M. Anastasova-Kristeva and academician A. Hadjioloff concern the morpho-functional differentiation of avian and mammalian embryonic, pubertal and adult gonads, in vivo and in vitro. Their works in the field of tissue culture are related especially to the mechanisms of regulation of the gonado- and gametogenesis [1, 10].

The third period is biotechnological - since 1977 till 1992. Professor J. Jordanov, P. Angelova, A. Boyadjieva. M. Kristeva cultured in vitro mammalian gametes and zygotes. They showed the important and original criteria of viability of the oocytes and zygotes for the in vitro fertilization and after cryoconservation. P. Angelova and M. Davidoff demonstrated the cellular localization of substance P and neuron-specific enolase-like immunoreactivity of mammalian Leydig cells in tissue sections and cell cultures. They observed that substance P has a modulatory effect on steroid production by foetal, immature and mature gonads of both sexes. A comparison of these results with data obtained in vivo and in vitro suggests that Leydig cells may be related to the APUD — or the diffuse neuroendocrine system [2].

Professor I. Goranov, E. Nikolova, M. Bratanov and A. Rusinova introduced in IEMAM—BAS the hybridoma biotechnology for production of monoclonal antibodies [12, 14]. They developed the methods for production of monoclonal antibodies against certain viruses and ricketsiae that caused the tick encephalomyelitis and yellow fever. The authors generated monoclonal antibodies against lymphocyte membrane markers involved in the recognition and presentation of the cells of the immune system.

M. Christova and E. Zaprianova investigated myelination and demyelination in tissue cultures. Their comprehensive studies into the same brain structures in vivo and in vitro suggest that myelinogenesis in tissue cultures has one of the same duration and periodicity as in vitro. Tissue cultures from the central nervous system are suitable model for studying the pathogenesis of demyelinating diseases and the important problems of neurobiology [5].

The last period is period of intensive development and broad application of in vitro biotechnology in biology and medicine - since 1993 and during 21st century. A. Rusinova, L. Kancheva, N. Atanassova generated new monoclonai antibodies against rat testicular antigens. They showed that the synthesis and cell specificity of antigens depend on the testicular development [3, 16]. L. Kancheva et al. demonstrated the expression of different proteins from cultured Sertoli cells of the mammals during different stages of the prepubertal period [11]. The effect of the vasoconstrictive peptide endothelin — 1 (ET-1) synthesized by and release from porcine granulosa cells on the ovarian steroidogenesis (progesterone production) was examined in vitro by R. Denkova et al. The authors elucidated the putative role of the neuropeptide in the regulation of the steroid secretion. Their findings suggested that ET-1, present in the follicular fluid may play an important role in the local regulation of progesterone production [6]. E.Yaneva et al. showed that ET-1 suppressed basal and FSH-stimulated progesterone production by ovarian granulosa cells, but this effect is not mediated by prostanoids [19]. K. Baleva - Ivanova et al. investigated the direct toxic effect of the Lindane on embryonic chick gonads during ontogenesis in organ culture [4].

D. Kadiysky et al. showed original results for in vitro cellular interrelationships between nervous and immune system [20].

Prof. E. Nikolova et al. studied the development of the systemic and mucosal

immune systems and the morphogenesis of the digestive tract in organ and cell cultures with application of milks' liquid and cellular factors [13].

V. Ogneva et al. established that the biologically active substances: fibroblast growth factor, epidermal growth factor, cholecystokinine stimulated the proliferation of the epithelial pancreatic cells during embryonic and postnatal development [15].

E. Zvetkova et al. determined the influence of haematopoietic growth factors and biologically active substances stimulating the formation of bone marrow colonies [18]. E. Nikolova, E. Zvetkova et al. reported an enhanced cell activation and basal cell proliferation of human and mouse peripheral blood T-lymphocytes in vitro and in vivo by using Vietnamese Crinum latifolium (L.) extracts [17].

During the last 68 years the most outstanding Bulgarian morphologists worked in IEMAM-BAS with their wide interests, original ideas and international recognition in the filed of modeling the life processes *in vitro*.

References

1. Angelova, P., J. Jordanov. Meiosis-inducing and meiosis-preventing effects of sex steroid hormones on hamster fetal ovaries in organ culture. — Archives d'Anatomie microscopique, **75**, 1986-1987, No 3, 149-159.
2. Angelova, P., M. Davidoff, K. Baleva, M, Staykova. Substance P and neuron-specific enolase-like immunoreactivity of rodent Leidig cells in tissue section and cell culture. — Acta histochem., **91**, 1991, 131-139.
3. Atanassova, N., A. Rusinova, L. Kancheva, C. Valkova. Stage — specific nuclear antigen is expressed in rat male germm cells during early meiotic prophase. — Mol. Reprod. Dev., **56**, 2000, No1, 45-50.
4. Baleva-Ivanova, K., P. Angelova. Effect of Lindane on the differentiation of embryonic chick gonads in culture. — Acta cytoliologica et morphologica, 1993, No3, 19-24.
5. Christova, M., E. Zaprianova. Myelination in tissue cultures from medulla oblongata and cerebellum. — Compt. Rend. Acad. bulg. Sci., **38**, 1985, No3, 385-387.
6. Denkova, R., E. Yaneva, K. Baleva, B. Nikolov, V. Bourneva. The influence of endothelin a1 on progesterone production by porcine granulosa cells. — Macedonian J. Reproduction, **5**, 1999, 181-185.
7. Hadjiolov, A. Comportement des enclaves lipidiques et des cellules des cultures vis-a vis des liposolvants. — Compt. Rend. Sci. Soc. Biol., **128**, 1938, 1098-1100.
8 Jordanov, J. Tissue cultivation experiments on eggyolk surface through vitelline membrane. — Compt. Rend. Acad. Bulg. Sci., **9**, 1956, No3, 57-60.
9. Jordanov, J. Cultivation of Chick Embryo Tissues in Egg Yolk Dialysates. — Sonderdruck aus. — Acta biologica et medica germanica, **4**, 1960, No3, 233-246.
10. Jordanov, J., M. Anastassova-Kristeva, A. Hadjioloff, A. Boyadjieva-Michailova. Zur Biologie des Sexualgewebes. II. In vitro — Zuchtung des Sexualgewebes von Huhnerembryonen. — Acta morph., Acad. Sci. Hung., **14**, 1966, No3-4, 211-226.
11. Kancheva, L., Y. Martinova, V. Georgiev. Prepubertal rat Sertoli cells secrete a mitogenic factor(s) that stimulates germ and somatic cell proliferation. — Mol. Cell. Endocrinol., **69**, 1990, 121-127.
12. Nikolova, E. Three anti-HLA-DR monoclonal antibodies antigen presentation and MLC in human systems. — Resume of Ph. D. Thesis, Szeged, 1985, 1-11,
13. Nikolova, E., M. Staykova, D. Raicheva, A. Neronov, I. Ivanov, I. Goranov. IL production by human colostral cells after in vitro mitogen stimulation. — Amer. J. Reprod. Immunol., **23**, 1990, 104-106.
14. Nikolova, E., E. Zvetkova. Monoclonal antibody reactive with human monocytes. — Comp. Rend, Acad. Bulg. Sci., **44**, 2002, No12, 109-111.
15. Ogneva, V., Y. Martinova. The effect of in vitro fibroblast growth factors on cell proliferation in pancreas from normal and streptozoticin-treated rats. — Diabetes Research and Clinical Practice, **57**, 2002, №1, 11-16.
16. Rusinova, A., N. Atanassova, L. Kancheva. Isolation and immunocytochemical characterization of a library of monoclonal antibodies directed against rat testicular antigens. — Endocr. Regul., **34**, 2000, No3, 135-143.

17. Tram, N., E. Zvetkova, E. Nikolova, E. Katzarova, G. Kostov, I. Yanchev, O. Baicheva. A novel in vitro and in vivo T-lymphocyte activating factor in crinium latifolium (L.) aqueous extracts. — Experimental pathology and parasitology, 1999, No3, 21-26.
18. Zvetkova, E., E. Janeva, E. Nikolova, G. Milchev, A. Dikov, I. Tsenov, N. Bojilova, A. Hadjioloff. Hemopoietic colony-stimulating activity of ranopterines in murine bone marrow agar cultures. — Compt. Rend. Acad. bulg. Sci., **44**, 1991, No2, 91-94.
19. Yaneva, E., R. Denkova, V. Bourneva, E. Zvetkova, K. Baleva, B. Nikolov. Involvement of prostanoids in the inhibitory effect of endothelin. — 1 on progesterone production of ovarian granulosa cells. — Methods Find. Exp. Clin. Pharmacol., **25**, 2003, No6, 437—439.
20. Кадийски, Д., М. Светославова, И. Христов, Б. Лосев. Взаимоотношения клеток нервной и иммунной систем *in vitro*. — Морфология, **119**, 2001, No2, 29—32.

С финансовата подкрепа на

ТП „Зентива Интернешънъл“ АД и ФОТ Лимитед

ZENTIVA

Вашият партньор в третото хилядолетие!

FOT LTD